USE OF WOLLASTONITE MICRO FIBERS IN REHABILITATION OF PQC ROADS

PH.D. THESIS

by

Shashi Kant Sharma

DEPARTMENT OF CIVIL ENGINEERING
INDIAN INSTITUTE OF TECHNOLOGY ROORKEE
ROORKEE – 247667 (INDIA)
OCTOBER, 2014

USE OF WOLLASTONITE MICRO FIBERS IN REHABILITATION OF PQC ROADS

A THESIS

Submitted in partial fulfilment of the requirements for the award of the degree of

DOCTOR OF PHILOSOPHY

in

CIVIL ENGINEERING

by

Shashi Kant Sharma

DEPARTMENT OF CIVIL ENGINEERING
INDIAN INSTITUTE OF TECHNOLOGY ROORKEE
ROORKEE – 247667 (INDIA)
OCTOBER, 2014

INDIAN INSTITUTE OF TECHNOLOGY ROORKEE
ROORKEE

CANDIDATE'S DECLARATION

I hereby certify that the work which is being presented in this thesis entitled **"USE OF WOLLASTONITE MICRO FIBERS IN REHABILITATION OF PQC ROADS"** in partial fulfilment of the requirements for the award of the degree of Doctorate of Philosophy and submitted in the Department of Civil Engineering of the Indian Institute of Technology Roorkee is an authentic record of my own work carried out during the period from July, 2011 to October, 2014 under the supervision of Dr. G.D. Ransinchung R.N., Associate Professor, and Dr. Praveen Kumar, Professor, Civil Engineering Department, Indian Institute of Technology Roorkee.

The matter presented in this thesis has not been submitted by me for the award of any other degree of this or any other institute.

(SHASHI KANT SHARMA)

This is to certify that the above statement made by the candidate is correct to the best of our knowledge.

(PRAVEEN KUMAR)
Supervisor

(G.D.RANSINCHUNG R.N.)
Supervisor

Date:

ABSTRACT

Self compacting concrete (SCC) is a concrete that has three specific rheological properties: flowability, passability and segregation resistance. These properties enable a concrete mix to flow, pass the obstructions as a whole unit, and compact fully under its own weight. SCC was primarily invented in Japan in the late 1980's because of the need of such concrete, which could fill the spaces in heavily reinforced structures resisting earthquakes. Over the past several years, it has gained popularity due to its commercial benefits in terms of ease of placement, no requirement of external vibration and above all improved durability.

Mix composition and fresh state properties of self compacting concrete are clearly different from that of ordinary concrete. The higher content of powder materials (cement, flyash, silica fume, fine aggregates passing 0.125 micron etc.) and lower content of coarse aggregates, improves the rheological properties, change the granular skeleton and microstructure of the self compacting concrete. As a result of which, the hardened properties of SCC and its durability properties are significantly affected.

The ultimate aim of concrete mix designer is to produce good concrete. The good concrete has to be satisfactory in its fresh state and hardened state. The requirements in the fresh state are that the consistency of the mix be such that it can be compacted by the means desired without excessive effort, and also that the mix is cohesive enough for the methods of transporting and placing used so as not to produce segregation with a consequent lack of homogeneity of the finished product. The primary requirements of a good concrete in its hardened state are a satisfactory compressive strength and an adequate durability. India has drawn up an ambitious plan to achieve a network of 4.4 million kms by 2021 at a projected financial outlay of Rs. 30, 92, 636 million. The rate of traffic growth that stood traditionally at 7.5% is about 10.16% per annum for the past 10 years. Considering the magnitude of road construction, improvement and strengthening, the demand of asphalt has grown many folds against supply constraints. Simultaneously, the cement production has increased substantially and the demands of pavement quality concrete (rigid pavements) are fast growing due to inherent advantages over bituminous flexible pavements. They have much longer life, lower maintenance cost, are more fuel efficient due to the hard surface, good riding quality, increased load carrying capacity for heavy vehicles, permeability to water and speedy construction over flexible pavements. Considering the above advantages possessed by PQC and scarcity of asphalt and rising prices of asphalt, it has become prudent to consider PQC (rigid pavement), a

far better alternatives to flexible pavement. The initial cost of PQC roads is about 25% to 30% more than that of bituminous roads which strongly suggests that efforts towards economizing the initial cost should be actively pursued. If we consider the life cycle cost, PQC has proved to be more economical over flexible pavements. One of the possible ways to offset the initial cost of PQC is to reduce the quantity of cement in the concrete. Therefore, there is an urgent need to economize the initial cost of pavement quality concrete (PQC) using low cost and abundantly available materials, capable of producing matching strength with better durability. All pavements deteriorate with time. The rate of deterioration of concrete pavement is comparatively much slower than the flexible pavement. Distresses in PQC (concrete pavements) are either structural or functional. Structural distresses primarily affect the pavement's ability to carry traffic load. Functional distresses mainly affect the riding quality and safety of the traffic. Understanding the causes of pavement distress is essential for providing appropriate effective repair and developing maintenance strategies. Repair techniques can be broadly classified into two categories i.e. preventive techniques and corrective techniques. For concrete roads in operation, the cost of repair and lane closure is two important considerations in deciding the type of repair to be undertaken. Repairs are only intended only to ensure that concrete pavements perform till design service life. The strategies for repair of older pavements could thus be different than those of new pavements. Decision is based on a trade-off between the "cost" of repair and the "remaining" life of the pavement. Full depth repair is recommended, if weak concrete is identified or suspected or the pavement had multiple type of distresses such as cracking, ravelling, large pop-outs/potholes and compression failure as blow-ups etc. Repair of full depth transverse cracks always requires new dowel bars to be placed and one new joint constructed. The large cracked slab is thus replaced by two smaller slabs with lower curl and warping stresses. The total distressed and surrounding areas (to be repaired) are marked on the pavement in rectangular form with sides parallel and perpendicular to the centre line by ensuring not less than 50 mm cutting beyond unsound concrete. This rectangular marked simplify saw cutting and concrete removal. A great care is taken to achieve stable patches and provided adequate room in the pit for dowel hole drill rigs and compaction. Normally, newly cut joint faces are scrabbled with a chisel or sand blasted to create roughness for better bond between old and new concrete. A precise and effective way to do is, before concreting the bottom and sides of the pit shall be kept wet for few hours (not less than 4 hours). The condition of surface shall be Saturated Surface Dry (SSD) and cement: sand 1:1 slurry with water-cement ratio not more than 0.62 shall be employed to coat the sides and bottom of pit to ensure better keying for the repair work. The unfortunate part is most of the

contractors seldom adopt such techniques as it demands high meticulousness and requires good nos. of skill labourers; therefore considered a lengthy process to them. Moreover, low and medium slump concrete mix could not evenly distributed across the cut portion and achieve desired level of compaction particularly in the corners, along the patch perimeter and around the dowel bars. As a result of which poor bonding at the interface of old and new concrete exhibits and leaves undulations in the surface. Thus, the repaired slab doesn't lasts for a long period of time, indeed the spot became more sensitive zone. In such dire circumstances, a concrete like SCC is a boon, which could easily fill the entire cut portions of the slabs by virtue of its high flowability and passability properties and thus imparts excellent bonding action at the interface of old concrete pavements & new concrete. Taking note of shortcomings of normal concrete mix and advantage of SCC mix in mind for old concrete pavement rehabilitation, the present research work is directed towards the use of wollastonite microfiber in SCC which is found abundantly in Rajasthan, Tamil Nadu, Uttarakhand and Chattisgarh in contact metamorphic zones, in some schists, gneisses and limestone inclusions in volcanic rocks for repairing of old concrete pavements. The wollastonite microfiber used in the present research work was obtained from Udaipur, Rajasthan. Chemically it comprises of 45.60% CaO and 48% SiO_2 which was confirmed by the presence of these oxides in large magnitude from the XRD study.

Many researchers have worked on concrete by part replacing cement by flyash and microsilica and their influence and performance were judged against the standard of concrete containing only Portland cement. It has been reported that they are promising materials for production of high performance concrete and save energy and conserve resources. Flyash and microsilica are well-established pozzolans; a concrete mix containing flyash is cohesive and has a reduced bleeding capacity. The mix can be suitable for pumping and for slip forming; finishing operations of flyash concrete are made easier. This is linked to the shape of the flyash particles. Flyash is a by-product of burning pulverised coal to generate electric power and variability of the material is very large, even the same power station will produce flyash with varying properties if the coal used is non-uniform in the short or long term. The flyash used in the present investigation was obtained from National Thermal Power Corporation, Ghaziabad, Uttar Pradesh. On the other hand, microsilica is a by-product of the manufacture of silicon and ferrosilicon alloys from high-purity quartz and coal in a submerged-arc electric furnace. Microsilica in the form of glass (amorphous) is highly reactive, and the smallness of the particles speeds up the reaction with calcium hydroxide produced by the hydration of Portland cement to produce additional calcium silicate hydrates. The microfine particles of microsilica

can enter the space between the particles of cement, and thus improve packing. The microsilica used in the present study was procured from a factory at Ludhiana. Considering the benefits offered by flyash and microsilica in high performance concrete, these cementitious materials were chosen for admixing jointly with wollastonite microfiber or alone in cement for observing performance of the self-compacting concrete for a set target flexural strength of 4.5 MPa at 28 days moist curing.

Initially, physical and chemical properties of the three cementitious materials were investigated including Portland cement in order to appreciate better their influences in PQC mix as well as SCC. The wollastonite microfiber used in the present research work was acicular in structure and possessed needle like structures under SEM images. It has average length of 0.03mm and mean size of 1.83 microns revealed from SEM study and particle size analysis. Whereas, the mean sizes of cement, flyash and microsilica are 20.05, 25.69 and 0.145 microns respectively. This analysis clearly suggested that microsilica has finest particles followed by wollastonite microfiber, flyash and cement respectively. Highest specific surface area is reported for microsilica (18000 m^2/kg) followed by wollastonite microfiber (827m^2/kg), flyash (380m^2/kg) and Portland cement (298m^2/kg) respectively.

The pastes were investigated for consistency, setting times, soundness and compatibility for various mixture proportions. XRD analysis and SEM images were analysed to determine the presence of different oxides and hydrated products respectively. Compatibility test was conducted using naphthalene formaldehyde sulphonate (NFS) and poly carboxylate ether (PCE) based superplasticizer. Then, wollastonite microfiber admixed cement mortars were prepared by part replacing cement with different amount of wollastonite (10%, 20% & 30%). Similarly, flyash admixed mortars were prepared by part replacing cement with different amount of flyash (10%, 20% & 30%). Another separate twelve mix proportions were prepared keeping flyash content constant @ 10%, 20% & 30% for different percentage microsilica content starting from 2.5% at an equal interval upto 10%. Similar, twelve mix proportions were prepared for wollastonite microfiber & microsilica admixed mortars by maintaining wollastonite content constant @ 10%, 20% & 30%. Lastly, fourteen admixed mortars were prepared containing all the three cementitious materials jointly in different quantities. Compressive strength, flexural strength, splitting tensile strength and modulus of elasticity of hardened mortar of the aforementioned mixes were ascertained to correlate better with the hardened concrete parameters. Further, efforts have also been made to evaluate the durability properties of these mixes by conducting rate of water absorption & sorptivity and abrasion resistance. Admixing of WMF improves flexural strength & modulus of elasticity of SCC significantly. This

improvement is continuous with days of moist curing. The improvement in flexural strength is even better on admixing of microsilica in the range of 5% -7.5% by weight of cement. In contrary, flyash admixed SCC improves compressive and splitting tensile strength irrespective of replacement levels and days of moist curing. Irrespective of amount and types of admixtures used, modulus of elasticity (E) was found to be lower in value in comparison to normal concrete. Higher abrasion resistance was offered by mortar containing WMF in presence of microsilica regardless of their content. From the statistical analysis, it is learnt that good correlation exhibits between abrasion resistance and compressive strength of mortar regardless of types of cementitious content.

To arrive at the SCC mix, the pre-requisite was to initially establish design mix in accordance with IRC: 44-2008 "Tentative Guidelines for Cement Concrete Mix Design for Pavements" published by Indian Roads Congress (IRC). The normal PQC mix was first derived and subsequently modification was made by incorporating cementitious materials to achieve ideal SCC mix. Several trial mixes were carried out in the laboratory by examining on the rheological properties of SCC in its fresh state. Tests like flowability, passability, segregation resistance through Abram's cone, V-funnel, J ring & probe test were conducted in the laboratory to judge the rheological properties of SCC and results were compared with European Federation for Specialist Construction Chemicals and Concrete Systems (EFNARC) specifications. Flyash addition improves the flow ability and passability of SCC mixes irrespective of part replacement level with or without microsilica. Segregation resistance of SCC mix improves considerably with an increase in flyash content. However, inclusion of flyash alone into the normal SCC was not possible to achieve ideal SCC mix on account of this, it is necessary to incorporate cohesivity inducing admixture like microsilica. Higher contents of flyash is possible for achieving ideal SCC provided the ratio of flyash to microsilica be maintained in the range of 4:1 to 3:1. Alike fly ash, inclusion of WMF at higher dosage affect the rheological properties of SCC mix considerably. The maximum part replaceable level of WMF in presence of microsilica and VMA is 20% by weight of cement. For achieving good flowability and passability of the SCC, about 5 -7.5% microsilica inclusion would be essential. Admixing of WMF modifies the gel pores and density of the SCC mix significantly. Part substitution of cement by both WMF and flyash together in presence of microsilica doesn't impart significant impact on the rheological properties of SCC. Effect of WMF in reducing the flow is more prominent than flyash. The right amount to add WMF and flyash together in presence of 5% microsilica is 15% for achieving ideal SCC mix.

The results from the tests conducted, showed that WMF with silica fume could act as a cement replacer in providing an economical SCC mix having good rheological, mechanical and durability properties. Overall there was an increment in flexural strength of all the WMF-silica fume admixed mixes by a value of 3.5%, whereas flyash-silica fume and combined mixes had a decrement of 17% and 8.5%, respectively. Modulus of elasticity had decreased for all the mixes, such that it had decreased by 17.3%, 44.3% and 45.3% for WMF-silica fume, flyash-silica fume and combined mixes, respectively. Talking about durability, the permeability of these mixes decreased by 82%, 74% and 61.5% respectively for WMF-silica fume, flyash-silica fume and combined mixes, respectively. Importantly, drying shrinkage reduced by 49% and 36.6% for WMF-silica fume and combined mixes, whereas it showed an increment of 1.25% for flyash-silica fume mixes.

Therefore, it was concluded that, WMF-silica fume mixes have an overall advantageous effect on the properties of SCC. The best WMF-silica fume mix named, CWS6 was chosen for further testing in the rehabilitation program.

A prototype was prepared in the laboratory, having its design done for axle load distribution specified in IRC 58-2011. A 100 mm thick DLC was laid on properly compacted subgrade layer and above it, 300 mm thick PQC was laid having a contraction joint between two panels of size 1.8 × 1.8 sq.m. each. After 28 days, the pavement was tested for deflections, obtained through plate loading at three locations i.e. corner, edge and interior. The deflections were recorded from the predetermined locations i.e. near both ends of the dowel bars in the two panels, approximately 300 mm from the panel division. This was done for three cases, normal PQC, normal PQC rehabilitated and WMF-silica fume reinforced SCC rehabilitated pavements. The load transfer efficiency was ascertained for all the cases. Afterwards the validation of finite element model of the prototype, designed on ABAQUS, was done by comparing the deflections at edge location for all the three cases. The model was validated for non-rehabilitated pavement and subsequently for WMF-silica fume reinforced SCC rehabilitated pavement. The validated model was used for determining the flexural stresses in the PQC under a specified set of loadings taken on the basis of axle load distribution on the road, as specified in IRC 58-2011. From the modeling, the flexural stresses so obtained yielded fatigue life for the left two pavements, namely, non rehabilitated pavement and WMF-silica fume reinforced SCC rehabilitated pavement.

The fatigue life of pavement rehabilitated with WMF admixed SCC (CWS6) was higher than that of normal concrete rehabilitated pavement. Finally, cost comparisons between rehabilitated PQC without admixtures and pavement rehabilitated with admixed self-

compacting concretes were also made and found that wollastonite microfiber inclusion would not only enhance the life of pavement but also would be able to offset the cost of pavement rehabilitation considerably in comparison to conventional rehabilitation technique.

ACKNOWLEDGEMENT

I wish to express my sincere gratitude to my supervisors Dr. G.D. Ransinchung R.N., Associate Professor, and Dr. Praveen Kumar Professor, Department of Civil Engineering, Indian Institute of Technology, Roorkee, for their invaluable, inspiring and untiring guidance and help in all the matters during my research work. I also gratefully acknowledge and admire their generosity and infinite patience shown by them with my lapses in all matters. I also wish to thank them for personal care and affection shown to me, which made my experience a memorable one.

The cooperation and help extended by the Head and faculty members of Civil Engineering Department is gratefully acknowledged. I also want to thank my research committee members for providing insightful and constructive comments. I express my special thanks to Prof. Umesh Sharma and Prof. Pradeep Bhargav for providing me permission, to perform the tests timely and with sophisticated equipments, useful in the present research work.

I am highly obliged to the lab personnel of transportation engineering laboratory who provided me continuous help in performing the testing work at the Pavement Testing Hall, specially the construction of pavement prototypes. Without their help it was an uphill task for me. I even express my obligations to the lab personnel of Structural Engineering Laboratory, without whose help and kind support, I would not have been able to work on the required instruments timely.

I thankfully acknowledge Ministry of human resource and Development, Govt. of India, for providing me financial assistance under the MHRD fellowship program, to perform research at IIT Roorkee. I offer my thanks to the staff of Departmental Library, Civil Engineering Department , Central Library and Computer Centre of IIT Roorkee.

Invaluable co-operation of the laboratory in charges Mr. Pradeep Singh, Mr. Surendra Sharma and Mr. Parveen Ahuja is gratefully acknowledged. The help of laboratory staff Mr. Manish, Mr. Rakesh, Mr. Bhopal Singh, Mr. Rajpal, Mr. Mukesh, Mr. Pushpendra, Mr. Gyanendra, Mr. Mishra and Mr. Dal Singh is key factor in conducting this experimental work. I also offer my thanks to the staff of Chemical Engineering Department Laboratory and Institute Instrumentation Centre for providing me help in conducting special tests related with my experimental work.

The most difficult hurdles seem easy and simple, when friends with their mere presence lead you across. Mr. Manish Kumar Rathore, Mr. Heaven Singh and Mr. Bibekananda Mandal will be remembered for their companionship and frequent encouragement during my difficult days.

In the end, I express my deep sense of gratitude to my parents for their blessing and endeavour to keep my moral high throughout the period of my work. Thanks to them, as they have made it possible for me, to reach where I am today. It is a pleasure to acknowledge my brother, sister in law and sister for their motivation and support which encouraged me at every moment.

I wish to take this opportunity to express my gratitude to all my teachers who are responsible for my personality development and career, specially Dr. Praveen Kumar who stood by me as a father and infused in me the habit of doing hard work with full perseverance and honesty.

Finally, last but not the least, I am grateful to God for bringing this day in my life.

(Shashi Kant Sharma)

CONTENTS

LIST OF TABLES

LIST OF FIGURES

LIST OF PLATES

1. INTRODUCTION

1.1 GENERAL

Cement can be described as a material with both adhesive and cohesive properties, which helps it in bonding minerals and their large fragments into a whole unit. It is the most widely used construction material in the world. It is composed mainly of calcareous and silicious minerals with some traces of aluminates. Portland cement which is used normally, consists mainly of CH, silica, alumina and iron oxide. These minerals diffuse and combine with each other to yield chemical compounds namely; tri calcium silicate (C_3S), di calcium silicate (C_2S), tri calcium aluminate (C_3A) and tetra calcium alumino ferrite (C_4AF). These compounds have different rates of hydration and strength development, thus it the percentage composition of these compounds which determine the strength and durability of cement composites. The hydration process of cement is not uniform; also it does not change uniformly. It keeps on varying and mostly has three peaks representing highest rates of hydration locally. When cement is mixed with water, then CH is released which leaves an outer layer of C_3S about 10 nm thick, thereby decreasing the hydration rate afterwards. During this time C_3A is also released into solution and starts forming tri calcium aluminate hydrate which leads to flash setting. Hence gypsum is added to cement to control flash set which subsequently reacts with C_3A to produce ettringite (calcium aluminate tri-sulphate hydrate) thereby decreasing the reaction rate. Thus, follows a dormant period, also called as an induction period. This period last for two hours during which the cement paste is workable. Eventually the surface layer of C_3S is broken either by the osmotic pressure or the crystals of calcium hydroxide. The rate of hydration again increases and hydration products come into contact with one another causing setting of cement. Heat evolution reaches its second peak after nearly 10 hours, thereafter the rate of hydration slows down over a long period because of the slow diffusion through the pores in the products of hydration. The peak is associated with the renewed reaction of the C_3A after the exhaustion of gypsum.

Depending upon the performance requirements, various types of cements could be developed by altering the quantities of these compounds in the cement. This is done either in the development stage of the cement to post developed stage. The post developed changes

are made by addition of mineral admixtures like flyash, microsilica and blast furnace slag etc. in the fine cement particles. The performance requirements are mainly concerned either with achieving flow, strength and durability; or altogether.

1.1.1 Mineral admixtures

The mineral admixtures can be classified into two categories i.e. natural and artificial. Few of them are also called as pozzolanas because of the same property shown on hydration. The natural pozzolanas include diatomaceous earth, volcanic glass and volcanic tuff, whereas artificial pozzolanas include flyash (FA), microsilica (SF), ground granulated blast furnace slag (GGBFS), rice husk ash (RHA), Metakaolin etc. the name mineral admixture is attributed to the main component present in them, which are mineral oxides. They are mainly silicious in nature. Some of them do contain high amount of aluminates with respect to ordinary Portland cement (OPC). These admixtures do not themselves act in the primary hydration process, but they act as converters, which convert primary hydration products such as CH and ettringite into calcium silicate hydrate (C-S-H) and calcium aluminate mono sulphate hydrate ($C\overline{A}\overline{S}\overline{H}$), thereby causing gel pores' refinement. Franco Massazza [94] states that heat of hydration decreases whilst the rate of clinker hydration increases, paste porosity increases and permeability decreases, both portlandite (CH) content and Ca/Si ratio in C-S-H decrease and the C-S-H content increases with the use of pozzolanas. The low basicity and permeability caused by the presence of pozzolanas increase the resistance of the concrete to CH leaching, sulphate and sea water attacks and chloride penetration. Even carbonation depth is practically unaffected by their use. They avoid expansion induced by alkali silica reaction. The freezing and thawing effect remains practically unaffected as the air entrained is not affected by the presence of pozzolans in concrete. D.M. Roy [146] suggested, that various cementitious materials affect the progress of hydration in consequence of their chemical composition, reactivity, particle size distribution, and particle shape. Also the combination rate depends upon the specific surface of the pozzolana and the temperature. The active phases mainly constitute of glassy and amorphous silicious minerals, with the glassy state having more reactivity than amorphous. Crystalline state is the most inert state. Class C fly ash, which has a high lime content, reacts, to some extent, direct with water; in particular, some C_2S may be present in the fly ash, and this compound reacts to form C-S-H. Also crystalline C_3A and other aluminates in flyash are reactive [146]. In addition, as with Class F fly ash, there is a reaction of silica with calcium hydroxide, produced by the hydration of Portland cement. Thus, Class C fly ash

reacts earlier than Class F fly ash, but some Class C fly ashes do not show a long term increase in strength [2]. Typically about one half of the particles in fly ash are smaller than 10 micrometre, but there may be wide variations. It is particles of that size, which are most reactive [102]. The reactivity is very high when the median diameter of the fly ash particles is smaller than 5 microns or even 2.5 microns.

The improvement in workability by fly ash is ascribed to its spherical shaped particles. This happens due to the modification in the flocculation of cement with a resulting reduction in the water demand [146]. The changed dispersion of cement particles is reflected in the microstructure of the hydrated cement paste, mainly its pore size distribution, the median pore size being smaller, and consequently the permeability being lower [144].

With respect to the resistance to sulphate attack, it should be noted that alumina and lime in the fly ash may contribute to the sulphate reactions. Specifically when present in the glass part of the fly ash, alumina and lime provide a long term source of material which can react with sulphates to form expansive ettringite [168]. A high silica/alumina ratio probably reduces the vulnerability to sulphate attack but no reliable generalization is possible. Because of the reduced permeability of mature concrete containing fly ash, the chloride ingress into such concrete is reduced. Even when the content of Class F fly ash is as high as 60 percent by mass of cementitious material, the passivation of steel embedded in mortar and the risk of corrosion were found to be unimpaired [25]. This was confirmed by other tests on concrete with high fly ash contents (58 percent of the total cementitious material) and water/cement ratios between 0.27 and 0.39, which have shown a very good resistance to chloride penetration [25]. The reaction of Class F fly ash requires a high alkalinity of the pore water. This alkalinity is reduced, when microsilica or GGBS are present in the mix. In consequence, the reactivity of fly ash in such mixes is reduced [40].

Microsilica greatly reduces or even eliminates bleeding. One consequence of the high early reactivity of the microsilica is that the mix water is rapidly used up; in other words, self dessication takes place [56]. At the same time the dense microstructure of the hydrated cement paste makes it difficult for water from outside, if available, to penetrate towards the unhydrated remnants of Portland cement or microsilica particles. In consequence strength development ceases much earlier i.e. until 56 days, than with Portland cement alone [56]. The contribution of microsilica to the early strength development (up to about 7 days) is probably through improvement in packing, that is, action as a filler and

improvement of the interface zone with the aggregate [18]. The bond of the hydrated cement paste with the aggregate, especially the larger particles, is greatly improved, allowing the aggregate better to participate in stress transfer [29]. Table 1 gives the estimated quantities of mineral admixtures available in India and worldwide along with their pozzolanic reactivity [135].

Table 1.1 Availability and pozzolanic reactivity of mineral admixtures

Mineral admixture	Annual availability (million ton)		Pozzolanic reactivity (mg of CH consumed per g of pozzolana)
	In India	World wide	
Coal ash	200 (India and China)	650	-
FA	82	370	875
Blast furnace slag	50 (India and China)	100	-
GGBFS	6.5	35	40
SF	-	2	427
RHA	3.8	20	-
Metakaolin	-	Equal to SF	1050

Source: [99, 61, 135]

FA is a finely divided spherical residue, which is produced from the combustion of pulverised coal in the boilers of thermal power or industrial plants. During their heating, the volcanic matter and carbon are burned off and mineral impurities i.e. clays, quartz and feldspar melt at high temperature and further solidify into spherical glassy particles. Some portion of this gets settled into the boilers whereas other portion fly with gases and is called as FA. Bottom ash settled in boilers comprise of coarser and angular particles with porous surface and hence does not have good pozzolanic properties. Characteristics of the FA finally depends upon geological features of coal deposits, combustion conditions and type of collection devices. ASTM C 618-84 classifies the FA into Class C (high calcium FA) and Class F (Low calcium FA) categories. FA of lignite and sub-bituminous coal, which contains 15-35% CaO is of Class C type, whereas bituminous and anthracite coal produces flyash of Class F, which contains less than 10% CaO. High calcium FA is in general more reactive and has both cementitious and pozzolanic properties [103, 4]. FA comprises 60-85% glassy particles, 10-30% crystalline compound, and upto 10% of unburnt carbon. SF is a by product of metallic silicon or ferro silicon alloys in electric arc furnace. When quartz is reduced into silicon at 2000°C, SiO_2 vapours are produced, which oxidise and condense in low temperature zone to tiny spherical particles consisting of non crystalline silica. Then SF is obtained as filtrate from outgoing gases trapped into the bags, and thus called as

condensed microsilica. It contains more than 85% silicon dioxide (SiO_2) in amorphous form. Microsilica has very fine spherical particles whose sizes and specific surfaces are smaller than cement particles by about 1000 and 60 times respectively. Its extreme fineness and high silica content makes it a highly effective pozzolanic material. Even though the rate of pozzolanic activity of microsilica is higher than flyash, but it's overall pozzolanic activity is lower because it has lesser number of active phases (mostly amorphous) than flyash. It was first used in the middle of the twentieth century at Oslo by the Norwegian institute of Technology for construction of a tunnel. Presently, it is used for the construction of high strength concrete. Cost of shipping and handling of SF is quite high owing to its fine particle size and low bulk density. The reactivity of high calcium flyash (ASTM Class C) is much more higher than Class F flyash. A higher alkalinity of pore water is required for Class F flyash to react. This alkalinity get reduced due to the presence of microsilica in the mix which absorbs the calcium ions from the pore solution. Flyash increases the workability of the mix due to the presence of the sulphate ions. It gets adsorbed on the cement grains and creates a negative charge on them, thereby deflocculating and dispersing them. Microsilica has higher reactivity due to its very high surface area. For a same admixture (same chemical composition and reactivity) the final strength achieved would be equal irrespective of difference in the particle shape, distribution and surface area. The final strength achieved for different admixtures may be equal or greater than control cement. In this way they ultimately remove the deficiency in the strength caused by the substitution of cement, though the reaction rate of different admixtures is different and initially they may not be providing comparable strength to cement.

The strength improvement in the concrete is not only provided by the pozzolanic activity of mineral admixtures, but due to the ability of very small particles to fit in between the cement particles and fill the capillary pores. This is called as packing effect. Apart from this the admixtures rearrange the oriented crystals of CH and ettringite due to packing and reduce the voids in between. This is called as grain size refinement. It is not clear, as to what effect these refinements leave on the rheological properties of concrete but it is clear that there is a considerable improvement in the durability of concrete.

1.1.2 Chemical admixtures

Chemical admixtures perform various functions in concrete. ASTM C 494-92 classify them on the basis of their functions as: water reducers, retarders, accelerators, water

reducers & retarders, water reducers & accelerators, and high range water reducers (super plasticizers). Super plasticizers are water soluble organic polymers which have to be synthesized using a complex polymerisation process to produce long molecules of high molecular mass, which makes them relatively expensive from water reducers. They have been classified into four main categories: sulphonated melamine-formaldehyde condensates; sulphonated napthalene-formaldehyde condensates; modified lignosulphates; and sulphonic-acid esters and carbohydrate esters. They may be used in solid or liquid state. The effectiveness of any admixture depends upon its dosage in the mix which in turn depends upon the properties of cement, water to cement ratio of the mix, type of aggregates, presence of air entraining agents or pozzolans, as well as the temperature of the mix. Water reducing admixtures and superplasticizers both work on the same basis. They create negative charge on the cement particles, as a result of which the cement particles repel each other and deflocculate. The deflocculation of cement particles makes the entrapped water available for unhydrated cement grains leading to an increase in hydration rate. The negative electrostatic charge on the cement particles attract the water molecules which form a thin layer around each cement particle, thereby increasing the dispersion and workability of the mix. High range water reducers consist of complex molecules which wrap themselves over the cement particles, creating a high negative charge and thus better deflocculation and dispersion of cement particles took place. Hence a superplasticizer causes an increment in setting time, strength and workability of the mix without any segregation and bleeding of mix.

The changes in the water content of the mix causes a corresponding change in the requirement of super plasticizers. The increment in water content either by direct addition increases the dispersion of cement grains before super plasticizer addition, thereby reducing the percentage decrement in water for the same increment in workability.

It is very important to know, when to add a super plasticizer to the mix. Super plasticizers containing sulphate groups get fixed by C_3A present in the cement, thus rendering the action of super plasticizers ineffective. The gypsum added to cement to control C_3A comes to rescue, but then it should be known when gypsum would act. This depends upon the ratio of aluminates to the gypsum present in the cement and is thus different for different cements. This defines the compatibilty of a super plasticizer with certain cement.

It was earlier thought that mineral admixtures do not affect the compatibility of cement mixes with super plasticizers, because the flocculation effect was held responsible for the increment in water demand, but studies have proved that though solid particles other than cement don't need dispersion but they need to be stabilized of their charges. Microsilica for example, originally having negative charge, exhibits positive charge in the alkaline pore solution due to adsorption of Calcium ions. This positive charge interferes with the working of super plasticizers and consumes their negative charge for its neutralization. In this way the dosage of super plasticizers becomes insufficient for the cement paste. Flyash too, contain negative charge originally due to the presence of sulphate ions adsorbed on its surface and thus may lead to adsorption of Calcium ions alike microsilica. Hence pozzolans mainly interfere with the acting tendency of the super plasticizers. The behaviour of pozzolans without super plasticizers is completely dependent upon their deflocculating tendency of cement grains as well as their surface area, such that the deflocculating tendency depends upon the charge carried by them and water consumption on the surface area. Hence, flyash particles lead to reduction in water demand of the cement mixes without super plasticizers. This defines the compatibility of a super plasticizer with a certain cement mix.

1.1.3 Aggregates

Aggregates are inert granular materials such as sand, gravel or crushed stone, that along with water and Portland cement, are an essential ingredient in concrete.

For a good concrete mix, aggregates need to be clean, hard, strong particles, free of absorbed chemicals and other fine material that could cause the deterioration of concrete.

Atleast three-quarters of the volume of concrete is occupied by aggregate and properties of aggregate greatly affect the durability and structural performance of concrete. Aggregate is cheaper than cement and it is, therefore, economical to put into the mix as much of the former and as little of the latter as possible.

Aggregates are used in concrete mixes to provide bulk to the concrete. Because of their higher compressive strength and modulus of elasticity they may provide the same properties to the concrete, provided the bond between the aggregates and mortar is strong. Because of the inherent non homogeneity, i.e. the difference in shape, coefficient of friction, modulus of elasticity (E), poisson ratio (μ) and coefficient of thermal expansion between aggregates and mortar, the mortar paste is not able to bind them properly and a transition

interface exist between these two phases. The interface is called as interfacial transition zone (ITZ), which consist mainly of early hydrated CH & ettringite, and very lesser quantity of C-S-H. The crystals of CH and ettringite neither provide good packing, nor are they able to bind the aggregates. This happens due to their shapes (CH-hexagonal platy, ettringite- platy long needles) and lesser adhesive power of their surfaces. If the ITZ is somehow made of C-S-H mostly, then cement mortar and aggregates would act as a single strong unit.

During shrinkage of concrete the mortar shrinks but aggregates do not and pose resistance to the movement of mortar, thereby developing tensile stresses in it. As a result of which very minute flaws are created in the mortar along the ITZ. On further exposure to environmental and loading conditions, the flaws grow into micro cracks which ultimately turn into macro cracks and cause strength failure. The development of cracks along the ITZ has been explained in the later paragraph.

Apart from strength failure there is also a danger of reduction in the durability of concrete mix due to the presence of micro cracks. The mortar volume along the ITZ mainly consist of one third of the total concrete volume and thus, may also act as a single continuous path for the transference of water. The water along with soluble carbon, chlorides and sulphates may cause deterioration of concrete and reinforcement and also cause problems of seepage. This is not acceptable and therefore improvement in the ITZ is required not only for improving the strength but also for the durability of concrete.

1.1.4 Concrete and Fibers

Cement composites are mainly made up of three components; cement paste, cement mortar and cement concrete. All these composites have same deficiencies; weak tensile strength (brittleness) and limited deformation capacity in the presence of cracking (lesser toughening strength). Once cracks are originated these composites fail in a brittle manner with little warning due to limited deformation capacity. Fig. 1 shows the stress strain curve for concrete, hardened cement paste and aggregates which explains the weak tensile strength and limited deformation capacity of cement composites. From the curves it is clear that aggregates have maximum tensile strength whereas hardened cement paste has minimum. Both aggregates and hardened cement paste show linear stress strain behaviour and lesser toughening strength. Their combination concrete shows somewhat different properties. It has medium tensile strength. It shows non linear stress strain behaviour and thus has more

toughening strength. The possible reason for this, is non homogeneity; the constituents of concrete have different elastic modulus and poisson's ratio, which leads to anisotropic and unequal distribution of stresses and strains between cement paste and aggregates.

Non homogeneity also leads to one more trouble. The interface between aggregates and cement paste called as interfacial transition zone (ITZ) acts as a major weak zone for distribution of stresses. If weak, strains grow at a larger rate in this zone, which leads to crack formation and finally failure of concrete mix. Hence, finally the strength of concrete mix depends upon interfacial bonding of aggregates and paste. If ITZ is weak, then concrete acts more as cement paste whereas if it is strong then it acts more as aggregates.

When load is first applied to the cement concrete, areas of stress concentration develop at the tips of the initial flaws. With additional loading, microcracks form (or initially present) and grow in the frontal process zones ahead of the flaw tips. It is assumed that the initial flaw will extend into the microcracked region when the microcracking has reached a saturated level [111]. Afterwards, they coalesce and turn into macro cracks. A reinforcing material is therefore required which may provide strength to the concrete before cracking, and cause delay in the propagation of cracks once they are formed.

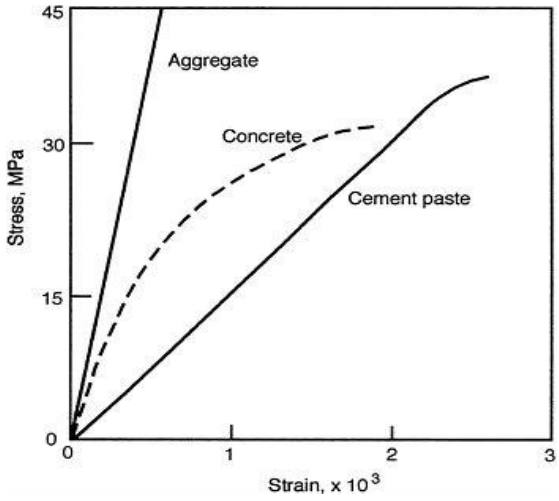

Fig.1.1 Stress strain curve under tension for cement paste, concrete & aggregate

The need of special reinforcing is fulfilled by the introduction of fibers in concrete. With proper incorporation of fibers, the failure mode of cement composites can change from brittle to quasi-ductile [86, 87, 83]. The toughness of the material (measured, for example,

from the area under a complete load-displacement curve) can also be significantly increased. An investigation into the reinforcing behaviour of fibers in various cement composites laid five stages of composite damage. They are: Zone I, linear-elastic behaviour; Zone II, nonlinear deformation; Zone III, stable growth of the failure crack; Zone IV, unstable growth of the failure crack; and Zone V, fiber bridging of the crack.

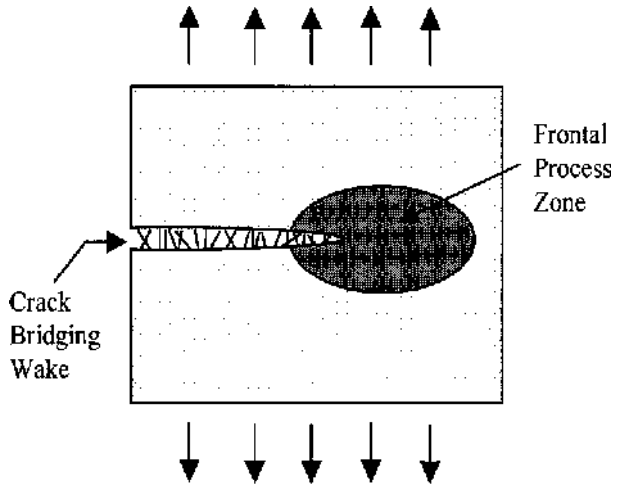

Fig. 1.2 Schematic of composite frontal process zone (FPZ) and crack bridging wake

In all the composites, fibers influence the fracture processes ahead of the crack tip in the frontal process zone (FPZ) (Stage I to IV) by introducing ductility, and behind the crack tip in the crack bridging wake (Stage V) by crack bridging, as is shown in Fig. 2. Improvement in ductility is mainly influenced by the stiffness (modulus of elasticity), volume fraction and bond properties of the fibers whereas crack width is strongly influenced by the yield strength, volume fraction, and bond properties of the fibers. Depending upon the type of fibers and their geometry, the level of improvement at each stage (out of five) is different for different composites.

For a thin sheet fiber reinforced cement concrete having initial flaw of approximately 60 μm, fibers with diameter <30 μm will be deemed micro fibers. Generally microfibers are fine fibers with lengths less than 10 mm and diameters <40μm. With their high specific surface areas (>200 cm^2/g), they provide a large number of fibers in a given section of the composites and thus furnish more effective reinforcing mechanisms at the microcracking level in the frontal process zone. Macro fibers have either their diameter greater than 40 μm or lengths larger than 10 mm, which facilitate the crack bridging effect [82]. Since concrete has already higher tensile strength than paste and mortars, therefore the effect of microfibers

is not much coherent in the concrete mixes. But nevertheless there is improvement in those concrete mixes where the tensile strength gets reduced by the reduction of cement content due to its substitution. Though macro fibers are effective in all cement composites, but with respect to micro fibers they are more effective in concrete mixes.

Examples of fibers are steel fibers, carbon fibers, PVA fibers, polypropylene fibers and wollastonite micro fiber. Steel fibers have high yield strength (nearly 1100 MPa) and possess lesser bond strength with the concrete. Owing to ductility of the steel, it could be easily processed into fiber form. Steel fibers are thus expensive, and even find their use in refractory appliances and electrical conduits. These fibers have special problem in mixing and there is difficulty in extrusion of steel fiber reinforced concrete. Furthermore, higher quantities of steel fibers start making lumps into the concrete and thus are not dispersed into matrix. These lumps act as a region of discontinuity with an otherwise homogenous composite, which affects the strength and durability of concrete. This fiber phenomenon is called as balling effect.

Carbon fibers or graphite fibers are thin fibers about 5-10μm in diameter. These are composed mainly of carbon atoms bonded together in crystals that are parallel aligned to the longer axis of the fiber. This alignment of carbon atoms in the crystal gives the fiber high strength to volume ratio. Carbon fibers have very high stiffness, low weight, high tensile strength, high chemical resistance, high temperature tolerance and thus low thermal expansion. Hence it has found its use in aerospace, military and motorsports apart from civil engineering infrastructure. Due to its processing complications and varied use in high end works, it has higher cost. Carbon fibers a have good electrical conductivity; this has made their use essential in high terrains, where the snow from the road surface could be removed by creating a high voltage difference along both the edges of the road. The current produced raises the temperature of the surface and melts the snow. These fibers are brittle, hence they are not much beneficial in the post cracking stage, where the fiber elongates under stresses.

Polyvinylalcohol (PVA) fiber is an organic fiber, produced about 75 years ago. Dr. Sakurda's research group at Kyoto Imperial University developed it and by 1950, its production and sale at large scale started [57]. It has high tenacity and modulus of elasticity in comparison with other organic fibers. The main advantage of these fibers is their high bonding with the cement matrix. Even, the bonding strength could be controlled by surface treatment of fibers (by converting a single fiber into thin multi ended fibrous mass). Apart

from improving the strength, these fibers also improve the durability of the cement composites. These fibers were originally developed for making cement composites but now they have found their use in making fishing nets, ropes, hoses, belts, tires codes, paper making felts, etc.

Polypropylene fiber (PP) is a thermoplastic polymer which is tough and flexible. It is often opaque and could be coloured. It has good resistance to fatigue and is even neutral to acid attack. Under the exposure to sunlight or UV rays, the degradation of PP fibers starts which is mainly a type of chain reaction. The tertiary carbon atom oxidise and produce a free radical which further reacts with oxygen, followed by chain scission to yield aldehydes and carboxylic acids. These fibers are very light in weight and can even float on water, hence they could be beneficially used for making light weight cement composites. These fibers have found their use in manufacture of various industrial and house hold products like cups, cutlery, caps, house wares and automotive parts.

Table 1.2 gives the properties of various kinds of fibers which have been used in cementitious composites during the last century and are still being used.

Table 1.2 Properties of reinforcing fibers for cement composites

Fiber type	Tensile strength (MPa)	Young's Modulus (GPa)	Fiber elongation (%)	Density (g/cu.cm.)	Remarks
PVA fiber	880-1600	25-40	6-10	1.30	-
PP	600	5	25	0.91	Floats in water
Nylon	750-900	3.4-4.9	13-25	1.10	-
Polyethylene	250-700	1.4-2.2	10-15	0.95	-
High performance polyethylene	2700	120	5	0.97	Expensive
Steel	1200	200	3-4	7.85	Heavy, rusts
Alkali resistant glass fiber	2200	80	0-4	2.78	Weak in alkali
Asbestos	620	160	-	2.55	Health risk

Source: [57]

Apart from these fibers, a new mineral fiber called as Wollastonite micro fiber (WMF) has found its application in manufacture of cement composites. Wollastonite microfiber is a naturally occurring mineral; chemically it is calcium meta silicate ($CaSiO_2$). It is inert, acicular, white silicate mineral of high modulus of elasticity and occurs in contact metamorphic zones, in some schists and gneisses and limestone inclusions in volcanic rocks [65].

In India, this rock is abundantly available in Rajasthan, Tamil Nadu, Uttarakhand and Andhra Pradesh as a low cost material. For the present work, Wollastonite micro fiber was obtained from the mine of Khera Tarla in Udaipur belt of Rajasthan.

The present level of extraction of wollastonite as per estimates is 2,50,000 MT/year from the mine of Khera Tarla and Bellea Pahar. Wollastonite micro fiber is cheaper in cost in comparison to other fibers like, steel and carbon micro fibers. when considered in terms of ASTM C 681-2008b, wollastonite micro fiber may be classified as Class C pozzolana.

It is classified in different grades depending upon the aspect ratio of length to diameter. In natural state, it is available in different shapes like –rock type, and lumps type. These mined rocks are broken down to 12 to 15 inches size and further crushed to about 1 inch and then ground to fine powder, and is already finding applications in paint, dental care, and ceramic tiles to name a few.

Its composition of nearly equal proportions of CH and silica having fine particle size were favourable indicators for its admixing in concrete by partial replacement of cement. In itself, wollastonite does not possess binding properties like cement, but, in presence of microsilica, it improves the properties of admixed concrete by fine packing of inert

1.1.5 Concrete pavement and its preservation

Portland cement concrete (PCC) consists of Portland cement, coarse and fine aggregates, water, chemical and mineral admixtures, and may or may not contain entrained air. Flexural strength of concrete is a direct input into the design process.

Concrete pavements have been used for highways, airports, streets, local roads, parking lots, industrial facilities, and other types of infrastructure. When properly designed and built out of durable materials, concrete pavements can provide many decades of service with little or no maintenance. Concrete pavements also known as pavement quality concrete

or rigid pavements have a long service life. Hence, with mega projects like National Highway Development Project (NHDP) AND Pradhan Mantri Gram Sadak Yojana (PMGSY) the pace of concrete pavement construction has increased recently.

All pavements deteriorate with time. There could be situations, where one or more repair techniques may be required to be used together to mitigate distresses. In some cases, where more than one repair technique is required to rectify the defects/distresses, these shall be executed in a proper sequence to ensure the effectiveness of such repairs. Distresses in concrete pavement are either structural or functional. Structural distresses primarily affect the pavement's ability to carry traffic load. Functional distresses mainly affect the riding quality and safety of the traffic.

All cracks are not structural cracks. structural cracking is often caused due to excessive loading, long joint spacing, and shallow or late sawing of joints, restraint at base or edge, due to joint lock up, inadequate thickness, material related problems etc. Structural cracks unless repaired effectively reduce the load carrying capacity of the pavement and adversely impact the design of service life of the pavement.

Concrete pavement in the real situations suffers from one distress or many times with a combination of distresses. The actual selection of the particular repair technique depends upon various factors. Full depth repair is recommended, if weak concrete is identified or suspected or the pavement had multiple types of distresses. Repair of full depth transverse cracks always requires new dowel bars to be placed and one new joint constructed. The large cracked slab is thus replaced by the two smaller slabs with lower curling and warping stresses.

Preservation of concrete pavements can be broadly classified into three categories:

(i) Concrete pavement restoration (CPR) techniques

(ii) Rehabilitation

(iii) Reconstruction

Concrete pavement restoration includes repair and maintenance operations without any overlay. Overlay options come under the head of rehabilitation, and reconstruction is undertaken after the end of service life or due to faulty design/construction. Full depth repair is also known as ultimate repair treatment. Full depth repair may be considered as the preferred repair option in the following situations:

(i) Partial depth repair has failed

(ii) The cross stitched longitudinal joint has again failed

(iii) The crack which was less than D/2 has propagated more than D/2 or full depth and the slabs across the crack are rocking

(iv) The slab has shattered and can no longer support the load of traffic.

(v) The spalling along the joint or crack is more than 505 depth of slab thickness

(vi) The corner break is down to down to full depth

(vii) Failure of pavement due to dowel bar locking and serious cracking along the joint

(viii) Blow up at expansion joint

Full depth repair entails removing and replacing atleast a portion of a slab down up to the bottom of the concrete.

1.1.6 Self Compacting Concrete

The definition of self compacting concrete (SCC) as described by the European concrete platform is expressed as follows:

"Self compacting concrete is an innovative concrete that does not require vibration for placing and compaction. It is able to flow under its own weight, completely filling formwork and achieving full compaction, even in the presence of congested reinforcement" (European Concrete Platform, 2012).

With regard to its composition, SCC consists of the same components as conventionally vibrated normal concrete, i.e., cement, aggregates, water, additives or admixtures. However, the high dosage of super-plasticizer used for reduction of the liquid limit and for better workability, the high powder content as 'lubricant' for the coarse aggregates, as well as the use of viscosity-agents to increase the viscosity of the concrete have to be taken into account. Super plasticizer enhances deformability and with the reduction of water/powder ratio, segregation resistance is increased. High deformability and high segregation resistance is obtained by limiting the amount of coarse aggregate.

The methodology followed to formulate the mix composition is mainly based on the following three steps: (i) the proportions of each aggregate on the final granular skeleton are determined; (ii) the proportions of the constituent materials of the binder paste are defined;

(iii) binder paste and granular skeleton are mixed in distinct proportions until self-compacting requirements in terms of spread ability, correct flow velocity, filling ability, blockage, and segregation resistance are assured, allowing the determination of the optimum paste content in concrete. Figure 3 shows the configuration of a normal concrete mix, thus explaining the powdery constituents and SP as separate entities.

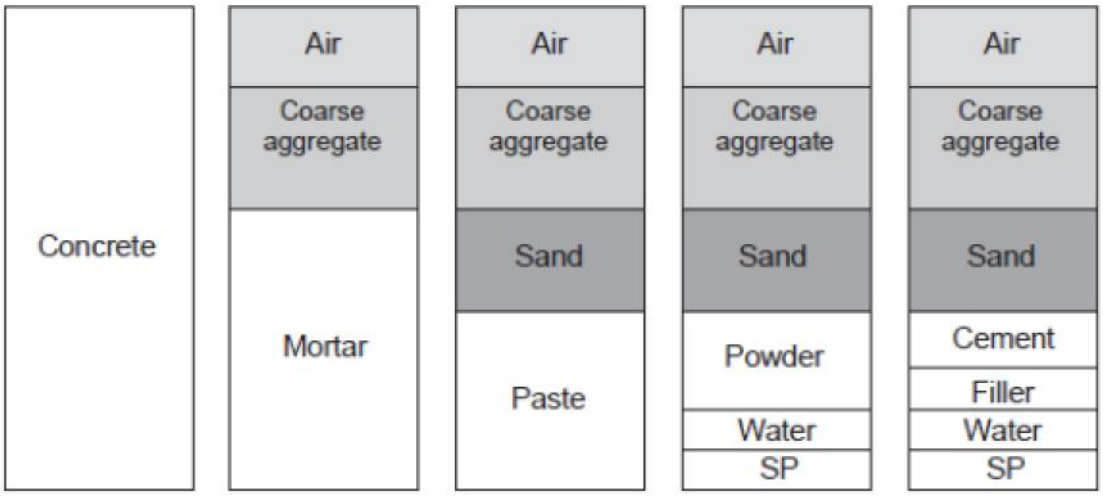

Fig.1.3 Various components of a design mix for concrete

Filler, cement and fine sand (passing 0.125mm) altogether constitute powder material. Filler material acts as viscosity modifier, shrinkage crack reducer and provides consistency & cohesiveness to the mix, thus making coarse aggregates to float as suspended particles in mix, thereby providing good flowability and avoiding segregation. Coarse sand and coarse aggregates provide bulk and weight to the mix required for self compaction, abrasion resistance and compression strength. Quantity and maximum size of coarse aggregates (MSA) need to be controlled to provide good passability and segregation resistance. More coarse aggregates could be used for their lesser MSA. Coarse sand fills the voids between paste and coarse aggregates. Water/cement ratio controls the strength, fluidity, passability and segregation resistance. Superplasticizers acting as surface tension reducers are added to powder paste, to maintain flow whereas viscosity modifying admixtures are required to prevent segregation, but their addition need to be controlled to provide good flow and passability to the mix.

The European Federation for Specialist Construction Chemicals [35, 36], states , that following guidelines are to be pursued for mix design of SCC:

(i) Total powder content: 160 to 240 liters (400-600 kg) per cubic meter.

(ii) Coarse aggregate content normally 28 to 35 per cent by volume of the mix. In terms of ratio, fine aggregate to coarse aggregate ratio lies between 50- 57% by volume. Fine aggregates are generally 40-50% by mortar volume.

(iii) Water: cement ratio is selected based on strength requirements. Typically water content does not exceed 200 liter/m^3.

(iv) Maximum size of aggregate (MSA) could be up to 20mm preferably.

1.2 OBJECTIVES OF THE INVESTIGATION

Realizing the difficulty, lack of uniformity & bonding, and complete compaction of conventional concrete by vibration while retrofitting dowel bars and full depth repairing of PQC; the present research work aimed at designing a suitable self-compacting concrete mix containing wollastonite micro fibers with or without flyash and microsilica. Following are the sub-objectives framed to accomplish the above cited objectives:

(i) To study the physical and chemical properties of OPC, wollastonite micro fiber and flyash

(ii) To study the cement paste and mortar properties with and without WMF and FA so as to compare with the SCC mix properties.

(iii) Production of control concrete mix and determination of the requisite changes to be made in control mix proportions for achieving an ideal SCC mix (qualifying workability and strength criteria).

(iv) To find the maximum substitution level of WMF with and without FA and microsilica in SCC mix. Accordingly, to find out the maximum possible fine aggregates to coarse aggregate ratio corresponding to the admixed paste.

(v) To study the mechanical and durability properties of control mix and SCC mix containing WMF, FA and SF.

(vi) In order to simulate the field conditions, a prototype of PQC slab to be constructed in the pavement testing hall and on which full depth repairing to be executed after ascertaining its fatigue life so that a fair comparison can be made with the fatigue life accrued after rehabilitation for a given constant loading condition.

1.3 SCOPE AND LIMITATIONS

In brief the scope of the present study could be listed as:

(i) The present study is concentrated on SCC for PQC slab's full depth repairing.

(ii) Specific grades of cement, WMF, and chemical admixtures were used. FA was obtained from National Thermal Power Corporation site at Ghaziabad.

(iii) Coarse and fine aggregates locally available conforming to IS: 383 and IS: 2386 codal specifications were used.

(iv) All concreting works done at specific cement content and water cement ratio of 0.37.

Following paragraph entails the list of activities performed during the present research work in order to achieve the objectives:

The testing program aimed at, sequentially finding out the ambiguities related with the use of admixtures and wollastonite micro fiber in self compacting concrete. For this one control mix and 45 cement substituted mixes were prepared. The mixes were classified into binary, ternary and combined mixes. Binary mixes were made by substituting cement with Flyash and Wollastonite (up to 30% replacement of cement with each respectively), in intervals of 10%. For ternary combinations, the mixes were prepared such that Wollastonite and Flyash had same replacement levels and Microsilica was added maximally up to 10% in addition for each mix, at intervals of 2.5% respectively. Then testing was performed on 12 ternary mixes of C-F-S as well as C-W-S.

Combined mixes were produced in such a way, that the quantity of Flyash and Wollastonite was varied in intervals of 5%, with maximum substitution level of 10%, and Microsilica was added in intervals of 2.5% (maximum up to 5%). Hence the maximum cement substitution level was put at 30% and fourteen mixes were achieved.

Tests were conducted on powder materials; pastes; mortars; control concrete; and WMF & pozzolana admixed SCC. Powder materials were tested for physical properties such as surface area, particle size distribution, specific gravity; and chemical composition. Pastes were tested for normal consistency, initial setting time, final setting time, pictorial (SEM image analysis) and quantitative analysis (XRD analysis) of hydrated compounds after 7 days and 14 days of hydration, respectively. Mortars were tested for mechanical properties and durability. Under mechanical properties, tests for compressive strength, flexural strength, splitting tensile strength and dynamic modulus of elasticity were conducted.

Cylinder (150ϕ×300mm) were used to determine compressive strength, splitting tensile strength and dynamic modulus of elasticity, whereas beams (500×100×100mm) were used to determine flexural strength. Rate of water absorption (sorptivity) test and abrasion resistance test were conducted on mortars for finding out their durability. Cylindrical discs (100ϕ×50mm) were used to determine sorptivity and cubes (100×100×100mm) were used for abrasion resistance, respectively. The testing was performed after 28 days of curing.

A control concrete mix was developed in accordance with Indian Roads Congress specification- IRC 44 for a flexural strength of 45 Kg/sq. cm. and then tested for workability, mechanical properties and durability. Flow trials were conducted to achieve SCC by changing the binder content of the control concrete mix (by admixing); then correspondingly changing the fine aggregate to coarse aggregate ratio along with superplasticizer content at a constant water to cementitious material ratio of 0.37. Superplasticizer was added to fulfil the water demand for creating self-compacting conditions. Like control concrete, SCC testing was performed in two forms: fresh and dry. In the fresh state, Abrams flow, V funnel, J ring, probe ring tests were conducted on the SCC trial mixes, whereas control concrete was subjected to only Abrams flow test. Concrete volume of 6 litres was used for Abrams flow test and J ring test, whereas 12 litres of concrete volume was used for V funnel test. Probe ring test was conducted by pouring concrete in cylindrical moulds (150ϕ×300mm). The trial mixes passing the fresh state tests were subjected to dry state tests. The specimen details of mortar and concrete are similar for mechanical testing. Chloride ion penetration test, permeability test and restrained shrinkage test were conducted to find out the durability of all concrete mixes. For chloride ion penetration cubicle specimen of (200×200×200mm) were used, whereas permeability test was conducted on cubes (150×150×150mm). Restrained shrinkage test was conducted on cylindrical concentric hollow rings apparatus.

Finally the best cost effective mix showing good mechanical properties, durability and lesser shrinkage was tested for rehabilitation work in the constructed prototype. The prototype was constructed with about 6 ton of concrete (DLC 100mm+ PQC 300mm), and contained a contraction joint, with dowel bars of 38 mm for load transference. The rehabilitation work was tested for load transfer efficacy and fatigue life.

1.4 ORGANISATION OF THE THESIS

The entire thesis is divided into six chapters. First chapter gives an introduction about cement, its hydration process, admixtures: mineral and chemical, aggregates, cement composites and fibers, pavement quality concrete and its rehabilitation, and finally the self compacting concrete. Later on it describes the objectives and scope of the investigation. Finally, the organisation of the thesis is presented.

The second chapter presents the literature review. The literature review has been divided into two groups; first one regarding the literature review of the normal cement composites, and the second one about SCC. Available literature review on various aspects of normal cement composites has been presented. This involves use of admixtures/fibers and their effects on the properties of normal cement composites. The effect of fiber type, geometry, volume, inclination and yield strength has been included to give an insight of the properties of various fibers on the normal cement composites. Literature review about admixtures like flyash and microsilica has been presented too. The literature review about SCC also presents the same parametric studies, along with procedure for proportioning of SCC mix and examples of SCC mix design.

The third chapter presents the detailed experimental program and results obtained there from.

The fourth chapter deals with the analysis of the results. Observations and results were analysed to obtain effect of superplasticizers, coarse aggregates, fine aggregates, mineral admixtures: flyash and microsilica, WMF on the workability, mechanical strength and durability of normal and admixed cement composites. The effect of curing time has also been studied to fine the changes brought by admixtures and WMF after longer durations. An effort has also been made to find the relationship between various properties of SCC, separately for each additive. Finally, the effect of mortar on the SCC has been presented in form of correlation coefficient between them.

The fifth chapter deals with the results obtained from the load transfer test conducted on the prototype of a rigid pavement, having a contraction joint. It presents the difference in the load transfer efficacy between the normal PQC pavement and normal concrete rehabilitated pavement; between the normal and WMF-microsilica admixed SCC

rehabilitated pavement. It also covers the validation of the model and finally presents the fatigue life of the WMF-microsilica rehabilitated pavement.

The sixth chapter presents the main conclusions of the study and identifies the scope for the future research.

The list of references is given at the end of the thesis.

2. LITERATURE REVIEW

2.1 Normal Cement Composites

Literature on normal cement composites has been divided into two categories: first category dealing with the cement admixed with mineral admixtures, and the second one dealing with fiber reinforced cement composites. The second category is further divided into four groups, each one of which discuss the studies conducted to find out the effect of fibers on mechanical properties; specific studies conducted to find the effect at pre crack and post crack stage; and shrinkage of composites respectively.

2.1.1 Effect of Admixtures on Cement Composites

Thomas et al. [167] investigated the use of ternary mixed concrete containing cement, flyash and microsilica. It was found that very high proportions of high lime flyash is required to control alkali silica reactivity (ASR) of concrete whereas low lime flyashes are durable and are able to control ASR and sulphate attack. The combinations of high lime flyash and small amounts of microsilica (3-6%) are very effective in reducing expansion caused due to ASR and resisting the sulphate attack. Also flyash was found to improve the workability which was reduced by microsilica, whereas microsilica led to early strength gain. Diffusion rate of ternary mixes was also less which reduced with time to a larger extent.

Langan et al. [78] studied the effect of microsilica and flyash addition at various W/CM (0.35, 0.4, and 0.5). For normal cement, the acceleration period started at 1.5-2 hours and ended at 7.5 hours. There was little effect of water to cementitious material ratio (W/CM) on its hydration activity. In case of microsilica (10% by binder) addition at W/CM of 0.35, the dormant period prolonged and the acceleration started at 2-2.5 hours. Further the rate of hydration was lower than normal cement until 7.5 hours. Afterwards the heat of hydration was higher. For higher ratios W/CM, microsilica effect was different. There was reduction in dormant period 1.5-2 hours, and the heat of hydration passed that of normal cement hydration at 6-7 hours. Afterwards it remained unaffected as it was for lower W/CM

ratio. This shows that microsilica retards hydration in mainly dormant and acceleration state at low W/CM ratios, whereas at higher ratios there is an overall increment in hydration rates at all ages.

For flyash addition (30-40%) at W/CM of 0.35, there was prolonged dormant period (until 3 hours), followed by acceleration period which ends up at 9 hours such that heat of hydration surpasses that of cement at 8 hours. There was a decrement in dormant period (until 2.5 hours) but the acceleration period prolonged until 9.5 hour such that the heat of hydration surpasses that of normal cement at 9 hours. At all ratios, the overall heat of hydration between 2-8 hours reduced. When SF and FA are incorporated together in cement, the hydration of the cement is significantly retarded, the heat of hydration is decreased and the early reactivity of the SF is hampered. Also the accelerating effect of the SF is delayed.

F.H. Wittman [174] studied the effect of addition of admixtures like flyash and microsilica, on the plastic shrinkage of mortar. It was demonstrated that plastic shrinkage occurs due to the build-up of capillary tension in the mixing water, present in the fresh concrete after the surface becomes dry. The plastic shrinkage for flyash (40% of total binder) which was coarser than cement was found to be lesser than normal cement, whereas for microsilica it was more. Though flyash delayed the shrinkage cracking at initial stages by providing excess water, but once the shrinkage of flyash admixed concrete started, the shrinkage occurred with higher rate. This is due to the reduction in the rate of tensile strength growth in its mixes. Microsilica (8% of binder) on the other hand increased the rate of tensile strength production, but it led to early plastic shrinkage, as at that time the hydration of microsilica had not started. It was also found; that mortars containing both flyash and microsilica (20% and 4% respectively) offset each other's shortcomings and prove to better crack resisting mix than normal cement. Mortars containing low water to cementitious ratio (W/CM) has lesser water, which becomes the sole factor controlling the plastic shrinkage. Flyash only reduced the tensile strength production whereas for microsilica the shrinkage stresses were higher than tensile strength production for low W/CM. Hence for low W/CM, the rate of shrinkage was high for both flyash and microsilica admixed mortars. Therefore it was concluded that both surface area and W/CM are factors affecting shrinkage.

Both flyash (20-40 %) and microsilica (8%) at the same W/CM reduced the chloride ion penetration by filling the pores in the cement grains of the concrete mixes. The effect of flyash was lower in the first 28 days, beyond which it was significant, and vice versa for microsilica case. But, flyash admixed concrete had lesser penetration values than normal concrete after 28 days. This is due to high reactivity of microsilica and low reactivity of flyash. Microsilica fills the voids with hydrated products early, whereas flyash being coarser fills them slowly. In both of the admixed cases the chloride ion penetration was lesser than the normal concrete. Drying shrinkage was also affected by both of the admixtures in the same way; such that both microsilica and flyash admixed concrete had lesser drying shrinkage than normal concrete after 120 days. But the 28 days value of drying shrinkage was higher for flyash concrete with respect to normal concrete. This is due to the fact that both admixtures reduce the voids in concrete which lowers the permeability of water vapours.

1 day and 90 days values of compressive strength of concrete were studied to find out the effect of microsilica and flyash at early stage and later stage. It was found that compressive strength for microsilica admixed concrete after 1 day was similar to normal concrete, whereas flyash admixed concrete had lower compressive strength. After 90 days, flyash admixed concrete had the highest compressive strength followed by microsilica admixed concrete. Even for a concrete containing both flyash and microsilica, the effect of microsilica after 1 day was apparent, but it diminished at 28 days. Flyash effect dominated at later ages of concrete.

2.1.2 Effect of Fibers on Cement Composites

The effect of fiber reinforcement has been studied by taking into consideration, the effect of their introduction at pre crack and post crack stages, along with the improvement in the quality of cement composites in terms of strength and durability.

2.1.2.1 Improvement in mechanical properties

Chen & Carson [26] designed an investigation to measure the influence of the length of randomly oriented wire fibers (38.2, 25.4, 12.7 mm) on the compressive strength, tensile

strength and flexural strength of FRC. The compressive and tensile strength, increased 60% for the 12.7 mm long fiber at 0.75% volume fraction in the mortar.

The compressive, tensile and flexural strength tests were carried out on mortar specimens reinforced with different lengths and volume fractions of steel and glass fibers by Naaman & Shah [109]. No significant increase in the stresses and strains at first crack were obtained. However, extensive micro cracking was observed on the surface of the failed flexural specimens indicating a significant contribution of the matrix even after first cracking.

Paillere & Serrano [124] reported improvements in bleeding strength ranging from 10 to 50 percent for straight fibers in lightweight concrete as against 10 to 37 percent for conventional concrete. In case of hooked fibers, this difference was much more (92 to 204 percent with conventional concrete having 1percent volume fraction of straight fibers).

Khan et al. [66] investigated the behaviour of fiber reinforced concrete under compression, indirect tension and pure flexure. The strengths were found to increase linearly with increasing fiber factor, defined as the product of fiber aspect ratio and volume fraction ($V_f \times l_f/d_f$).

The compression test results on normal and fiber reinforced concrete cylinders subjected to three different strain rates were presented by Otter and Naaman [121]. A 10 % increase in strength and 15% increase in toughness were reported when the strain rate was increased from 100 μ/s to 30000 μ/s. The influence of fiber addition to normal concrete was found to be comparable to that of confinement.

Kukreja & Chawla [75] investigated the various aspects of flexural behaviour of fiber reinforced concrete. The effect of various fiber shapes and volume factions on the flexural strength was studied. Three types of fibers (straight, bent and crimped) were used at volume percentages of 0.5, 1.0 and 1.5. all the fibers had an aspect ratio of 80. The flexural stiffness of fibrous concrete was reported to be higher than that of ordinary concrete. there was no significant variation in the strain and curvature distribution with different shapes of fibers. However, concrete reinforced with crimped fibers showed a lower flexural strength

than that with straight fibers. But the crimped fiber improved the control on cracking and associated properties.

Ramakrishnan [136] revised the recent advancements in fiber reinforced concrete composites. The following conclusions were drawn.

1. The increase in compressive strength due to addition of fibers varied from 0 to 20 percent, though there was a significant increase in the ductility and toughness. The compressive toughness index increased up to 300 percent due to addition of the fibers.
2. The flexural behavior of fiber reinforced concrete beams was almost linear up to the first crack. The toughness index of beams with hooked fibers was three times greater than that for beams reinforced with straight fibers.

Krishnamoorthy & Kumar [74] showed that the effect of steel fibers on the compressive strength of concrete was not significant. Increase in the compressive strength of concrete varied from 0-20%, but the workability was adversely affected with the addition of fiber volume exceeding 2%. The peak strain in compression increased substantially and the post cracking behaviour significantly improved with the addition of fibers. The presence of steel fibers significantly improved the post cracking behaviour of normal and reinforced concrete specimens in flexure. Crimped fibers, surface deformed fibers and fibers with end anchorages showed better performance than smooth fibers for the same volume concentration.

Singhal et al. [157] reported a reduced deflection of the fiber reinforced concrete beams after the initiation of the first crack. The concrete used was of M20 grade and the beams (150×150×1000 mm) had equal reinforcement on both the faces and the steel fibers (diameter=0.4mm, aspect ratio=75) were distributed in three different zones (entire cross section, tension zone only and tension combined with shear span). The gain in ultimate strength was the maximum for beams with fibers in tension zone only and the least in beams with fibers distributed throughout the depth of the beam compared to beams without fibers. Addition of steel fibers improved the toughness of the concrete beams. The maximum increase was observed for beams with fibers distributed throughout the cross section.

Sasturkar & Kaushik [150] reported that the ultimate strength of steel fiber reinforced beams increased with an increase in the fiber volume fraction. The maximum increase in strength was 63% for 1% of steel fiber addition. The corresponding increase in cracking strength was 25%. It was reported that crack spacing in fibrous beams was reduced upto 25% whereas the maximum reduction in crack width was 72% and 56% for design and ultimate load stages respectively for beams with 1.5% fiber content. The ultimate strains in fibrous beams were higher than that in non fibrous beam sections.

Kaushik et al. [64] presented the results of an investigation to study the properties of fresh and hardened fiber reinforced concrete. The basic parameters were fiber volume fraction (0.5, 1.0, 1.25 and 1.5%), maximum aggregate sizes (10mm and 20mm) and fiber types (straight and hooked steel fibers). The workability of the concrete (slump and compaction factor) decreased with an increase in the volume fraction of fibers upto 1.5% for maximum coarse aggregate size of 20 and 10 mm. Ramakrishnan [136] obtained similar results. Zero slump was recorded for a fiber volume fraction of 1% and a coarse aggregate size of 10 mm, whereas the slump recorded for 1.25% fiber content and a coarse aggregate size of 20 mm was about 10mm. The compaction factor and the flow Table spread decreased by 5-6% and 10-20% respectively when coarse aggregate of 20mm nominal size and hooked end fibers were used. The compressive strength of concrete with straight fibers increased by 9-21% when 10mm coarse aggregate was used and the same was 11 to 27.5% when coarse aggregate of 20mm size was used. For a fiber volume fraction of 1.5% the tensile strength of fibrous concrete increased by 50% and 34% for a coarse aggregate size of 10mm and 20 mm respectively as compared to normal concrete. The increase in flexural strength was found to vary from 57.5% to 62%. The ductility was increased upto 20 times when a fiber volume fraction of 1.25% was used with 20mm size coarse aggregate.

Krishnamoorthy & Ahmad [73] reported the results of an experimental program to study the behaviour of steel fiber reinforced flexural members. Black annealed mild steel wire with diameter of 0.46 mm was used as steel fiber. The aspect ratio of fibers varied from 60 to 100. The load at first crack increased by about 25% and the deflection at service load decreased by about 15%. The ultimate concrete strain at failure increased by three to four

times i.e. 0.0105 to 0.0140. The ductility ratio of flexural members increased significantly due to addition of fibers.

Pendyala et al. [128] carried out tests on flexural members made with high strength and compared the results with that of normal strength concrete. It was found that though high strength concrete was a more brittle material, flexural members made with high strength concrete exhibited greater ductility.

An overview of the properties of cement concrete composites reinforced with high volume fraction of carbon, steel and propylene micro-fibers was presented by Banthia et al. [13]. It was found that steel fibers provided better strengthening and stiffening and carbon fibers provided better ductility. The polypropylene fibers provided better toughness at larger crack openings. Two types of steel fibers, i.e. straight cylindrical fibers of 5 mm length and 0.25 mm diameter and cylindrical hooked fibers of 25 mm length and 0.3mm diameter were used in the investigation. The respective volume percentages of the fibers used were 5% by volume of 5 mm long fibers and 2% by volume of 25 mm long fiber. The compressive strength, Young's modulus and flexural strength were 19MPa, 50 GPa and 4 MPa respectively. It was reported that the use of a mix of shorter and longer fibers was useful to get a ductile and hardening post cracking behaviour in the cement composite with a very high tensile strength.

Ramalingam et al. [137] presented the results of an experimental programme to investigate the results of an experimental programme to investigate the strain- hardening of fiber reinforced mortar under flexural loading. The micromechanical parameters (fiber, matrix, fiber/matrix interface properties) were controlled through proper selection of reinforcing fibers (polyvinyl alcohol micro fibers and steel fibers), water to binder ratio and percentage of cement replacement by flyash. Flexural tests on specimens (300 75 20 mm) with 240 mm span were carried out under third point loading. The test results showed, that strain hardening behaviour with multiple cracking could be achieved by optimizing the volume fraction of hybrid fibers, water to binder ratio and percentage of flyash replacement.

Ghugal [46] reported the effects of crimped filers on the properties of fresh and hardened concrete. the workability of the mixes reduced as the aspect ratio and volume fraction of the

fibers increased. The 28 days strength of M20 concrete increased upto a maximum of 9.56% at 1% fiber content with a fiber aspect ratio of 38, while with a fiber aspect ratio of 50 it increased upto 12.69%. but the strength decreased at 1.5% and 2.0% fiber content. The test results showed that the incorporation of steel fibers with an aspect ratio of 38, gave a higher flexural strength than that with an aspect ratio of 50, for the same volume fraction of fiber in M20 grade of concrete. but for M35 grade concrete, the trend was found to reverse. The maximum increase in split tensile strength was obtained for 2% fiber content. For M20 grade concrete, the increase in shear strength for 1.5% fiber content was 38.7%, but the shear strength decreased at 2% fiber content for both the aspect ratios 38 and 50. For M35 grade concrete, the shear strength upto 2% fiber content (38.65%) for both the aspect ratios 38 and 50.

2.1.2.2 Pre Crack Reinforcement

Wu H.C. [177] and Pierre P. et al. [133] in their comparison studies found the difference in the role of fibers in cement paste and mortar. They concluded that for brittle materials, the magnitudes of the fracture toughness or the sizes of the existing flaws of the materials primarily determine their tensile strengths. Typically, a mortar has higher fracture toughness than that of a cement paste. Hence, a mortar is usually stronger in tension than a paste when a similar size of flaws is present in both materials. When fiber reinforcement is used, the composite can become tougher and stronger, resulting from the additional increase in fracture toughness due to the toughening effect of the fibers in front of the crack tip and the bridging effect of the fibers behind the crack tip. Therefore, the tensile strength of the cement-paste composites showing pseudo strain-hardening increases with the fiber contents, as found by the authors [177]. However, increasing fiber content inevitably induces higher air content.

It is very possible that high air content may also induce high air voids around the fibers. It is also possible that the high air content resulted from the entrapped air around the fibers. In either case, a weaker interfacial bond would exist due to less possible contact area of the fiber with the matrix. Thus, the increase in tensile strength at high fiber content 5% can be much less profound. Nevertheless, the tensile strength can possibly be increased if the interfacial bond can be improved by other means, such as the use of plasma treatment of

fibers [89]. The mortar composites still behave like a brittle material, because the air content increases with the sand-to-binder ratio and the microfiber content, and so possibly does the maximum flaw size of the composites, since it is likely a function of the air content, the sand-to-binder ratio, and the microfiber content [177]. The effect of increasing fracture toughness by addition of microfibers or sand on the tensile strength appears to be offset by the negative effect of the increasing flaw sizes; hence the tensile strength of the mortar composites is not significantly influenced by the sand-to-binder ratio or the microfiber content.

Bayasi and Zeng [16], who investigated the influence of reinforcing fibers on the compressive strength of fiber-reinforced normal-strength concrete, found that, concrete compressive strength increased by 15% when reinforced with 1.27-cm-long polypropylene fibers with a volumetric content of 0.1% and by 19% in the case of a volumetric content of 0.3%, whereas at a volumetric content of 0.50%, it decreased by 2.5%, compared with concrete having no reinforcing fibers.

2.1.2.3 Post Crack Reinforcement

The reinforcement efficiency, in terms of maximum crack bridging force and total energy absorption during fibre pullout, is a function of many parameters including the properties of fibre, matrix, and interface as well as fibre size, volume fraction, geometry, and distribution. Aveston et al. [8]; Li and Leung [86]; Li and Wu [87, 88] concluded , that when a composite is loaded beyond its tensile strength, a macroscopic crack is formed in the matrix. Subsequently, there are two possible scenarios. First, the composite load is large enough either to rupture the bridging fibres or to pull out the fibres, leading to rapidly or gradually declined post peak behaviour. This composite is still considered quasi-brittle. Secondly, the composite load can be shared by the bridging fibres. These fibres then transfer the load via their interface back into the matrix. If enough loads are transferred, the matrix may crack again and the process repeats until the matrix is broken by a series of sub parallel cracks. During the process of multiple cracking, the composite load can even rise and exceed the first cracking strength of the composite [176]. A critical fibre volume fraction, $V_{f,crit}$, has been defined as the minimum fibre quantity required for achieving multiple cracking. The exact magnitude of this quantity depends on fracture toughness of matrix,

fibre properties, and interfacial bonds [86]. Low fracture toughness of the matrix is in favour of low $V_{f,crit}$. Hence, a weak cement paste is expected relatively easy to achieve multiple cracking as compared with a mortar [176].

The crack bridging efficiency of a steel fibre depends on its length, radius, interfacial properties, and geometry as well as steel properties such as yield strength and ductility. An experimental study by Krishnadev et al. [72], showed that the strength of steel is more dominant than its ductility for the achievement of high pullout load and energy absorption. This is the reason that steel macrofibres are mostly used for providing post crack reinforcement in cement composites rather than ductile Poly Acrylic Nitrile (PAN) fibres. More specifically, among the fibres studied by Krishnadev et al. [72] the reinforcement efficiency increased with fibre strength. This conclusion, however, should be taken with caution as the experimental work is limited to the pullout of fibres lying perpendicular to the crack. This is a very rare situation in a real composite where fibres are distributed in a quasi-random manner.

As shown by Banthia and Trottier [12], the pullout behaviour of inclined fibres can be very different from that of perpendicular fibres. Results from perpendicular fibre pullout may therefore not be representative of crack bridging behaviour in the composite. For fibres inclined at an angle to the crack, a theoretical study by Leung and Chi [84] showed that there is an optimal range of fibre yield strength within which the best combination of peak pullout load and total energy absorption can be attained. Increasing the fibre yield strength beyond the optimal range will lead to excessive matrix local failure (near the fibre exit point) and hence a decrease in crack bridging efficiency. Banthia and Trottier [12] performed pullout tests on deformed fibres at various orientations. Due to matrix failure, which allows the fibre to relax, the pullout load for an inclined fibre increased at a much slower rate than that for a perpendicular fibre. In other words, for the inclined fibre to provide significant crack bridging force, a significantly larger crack opening is required. For most cases, the peak pullout load for the inclined fibre is also lower than that for the perpendicular case.

Banthia et al. [14] also performed pullout tests on straight micro steel fibres inclined at various angles. For microfibers, the relative peak load, defined as the ratio between the

peak loads of the angled and perpendicular cases, is less than unity for all inclination angles. This trend is different from that observed for macrofibers, e.g., Naaman and Shah [109], which showed an initial increase in relative peak load with inclination angle. This difference can be exnormaled in terms of matrix failure. For a microfiber, the embedment length is significantly shorter (3 mm versus 20 mm for the macrofiber). As matrix failure occurs, the microfiber will have a larger relative reduction in embedment length than the macrofiber. The reinforcement efficiency is therefore reduced to a higher extent. This is the reason that mostly macrofibers are favourable for providing post crack reinforcement in mortars and concrete mixes. In summary, matrix failure is widely observed when inclined fibres are pulled out of a cementitious matrix, whether straight fibre, deformed fibre, macrofiber, or microfiber is employed. Hence, it is favourable to use deformed inclined macro fibres for providing post crack reinforcement.

Lawler J.S. et al. [83] achieved a workable blend of microfibers and macrofibers in concrete. During the study, the flow of the wet mixture, mechanical performance, resistance to restrained ring shrinkage cracking and cracked permeability are all evaluated. In terms of ultimate strength, the steel hybrid mixture performance is comparable to the macrofiber while the Poly Vinyl Alcohol (PVA) hybrid exceeded it by a significant margin. The toughness of the PVA hybrid is greater than that of the macrofiber mixture in flexural displacements less than 0.5 mm but not superior at larger deformations. Beneficial effects of the microfiber in the flexural testing are seen up to and shortly after the peak. In this region of the materials' mechanical responses, the microfiber suppresses the process by which microcracks grow and coalesce to form macrocracks, the development of which signals a change in damage mechanism from crack development to crack opening and determines the strength of the composite.

The mixture containing the PVA microfiber hybrid showed retarded development of restrained ring shrinkage cracking as the microfibers again delayed the coalescence of cracks. However, at 44 days of age, the total crack width is approximately the same as that seen for the macrofiber specimen and much below that observed in the unreinforced concrete. The flow rate of water through cracked concrete is governed by the crack pattern. This is because for laminar flow conditions, flow rate is proportional to cube of crack width.

For a given deformation, a specimen with multiple cracks will display much less permeability than a similar specimen with only one crack. While crack tortuosity is increased through the use of hybrid reinforcement, resulting in a small but significant drop in permeability, the hybrid reinforced composite material is not able to carry a high enough post peak stress to cause additional cracks to develop [80]. Macrofiber reinforcement, on the other hand, resulted in multiple cracking and produced a lower permeability [82]. Contrary to the trends observed in mortar, when used in this higher strength concrete, the PVA microfiber hybrid reinforcement is less effective at improving mechanical performance and reducing the crack permeability than macrofiber-only reinforcement. While initial, first cracking strength is improved by the hybrid, this improvement is not maintained much past the peak load as it is in the mortar matrix. This may be exnormaled by the difference in the failure mechanism of the microfibers in the concrete compared to the mortar. The lower w/b in the concrete (less than 0.33 compared to 0.45 in mortar) produced a stronger matrix and stronger fiber-matrix bond and the microfibers broke instead of debonding and pulling out. This process consumed less energy so the microfibers are less effective at improving the composite toughness. In the dense concrete matrix, the microfibers increased the likelihood of macrofibers breaking. This type of macrofiber failure is much more likely to occur in the hybrid than in the concrete containing the macrofiber alone. This is clear evidence of interaction between the fiber types and this interaction may provide an opportunity for increasing the effectiveness of hybrid blends through modification of macrofibers as well as microfibers. Clearly, given the potential for improved performance through blending micro- and macrofibers, additional work is warranted in this field.

Singh & Madan [156] carried out an experimental study to predict the shear strength of steel fiber reinforced concrete in terms of direct shear strength and beam shear strength. It was found that addition of 1 percent steel fibers to the concrete beams increased the shear strength of the beams by about 63% and further increase of fiber volume did not increase the shear strength. The fiber reinforced concrete beams had a higher post cracking strength which can be useful in the design of beams. Direct shear strength increased to an extent of 70 percent for 1% fiber volume addition

2.1.2.4 Resistance to Shrinkage Cracking

Laboratory investigations by Saje et al. [149] into the time development of the shrinkage of polypropylene fiber-reinforced high-performance concrete analyzed this behaviour. The volumetric content of polypropylene fibers contained in the investigated concretes varied from 0 to 0.75%. Within this context, the influence of both dry and previously moistened polypropylene fibers added to the concrete on the shrinkage of the composites is examined. Electronic measurements conducted from the beginning of the hardening of the concrete also covered the early stage of autogenous shrinkage , that in high-performance composites, accounts for a significant part of total shrinkage. To compare the shrinkage of fiber-reinforced concrete with that of a comparable concrete without polypropylene fibers, the shrinkage of such a comparable concrete without fibers is also included in the measurements. The measurement results of the shrinkage of polypropylene fiber reinforced concrete and of a comparable concrete without polypropylene fibers showed that the autogenous as well as the total shrinkage of fiber-reinforced concrete is less than the shrinkage of a comparable concrete without fibers. By increasing the content of the fibers up to 0.5% of the volume of the composite, the shrinkage of the fiber-reinforced concrete is considerably reduced, whereas with further increasing of the fiber content, the shrinkage reduction rate became relatively insignificant. The concrete that had been reinforced by previously moistened polypropylene fibers, which served as an internal water reserve, exhibited a lesser degree of early autogenous shrinkage than the concrete that had been reinforced by dry polypropylene fibers. The drying shrinkage of high-performance concrete, reinforced by previously moistened polypropylene fibers, is, however, approximately twice as large as that of dry polypropylene fiber-reinforced high-performance concrete. In concretes, it is normally the cement gel or hardened cement paste that shrinks, whereas the aggregate grains from most of the rock materials do not shrink or even restrain the shrinkage of the cement gel [149]. For this reason, the shrinkage of a concrete made of an aggregate made with a higher-strength rock is less than in the case of an aggregate made with a lower-strength rock. Consequently, tensile stresses arise in the cement paste, which quickly reach the tensile strength of a young concrete. The additional internal stresses that occur during the period of hydration of the cement are further increased by the temperature gradient that results from the heat of hydration released during the concrete hardening process.

The occurrence of early cracks in concrete during its hardening is a consequence of these two physical phenomena mentioned. Reinforcing fibers added to the concrete restrain crack growth and increase the ductility of the composite, but they cannot replace the statically required reinforcement of structural elements [132].

Banthia and Gupta [10] found that polypropylene fiber reinforcement is very effective in limiting cracking in concrete. They suggested that polypropylene fibers generally result in a favourable decrease in the width and number of cracks. Thinner fibers are, according to them, more effective than thicker ones, and longer fibers are in turn more effective than shorter ones.

Kovler et al. [71] stated that the presence of polypropylene fibers results in a considerable decrease in the plastic shrinkage of fiber-reinforced concrete. With regard to the total shrinkage of fiber-reinforced concrete, they stated that the effect of polypropylene fiber reinforcement is virtually insignificant up to a volumetric content of 0.2%. According to their findings, crack width can be reduced by as much as 50% by increasing the volumetric content of polypropylene fibers. Swamy & Stavrides [164] also found that the drying shrinkage of polypropylene fiber-reinforced concrete is about 20% less than that of concrete without added fibers. Zollo [181] and Zollo et al. [182] have argued , that in the case of an appropriate quantity of added polypropylene fibers, the drying shrinkage of concrete can be reduced by as much as 75%.

Myers et al. [108], however, are of the opinion , that when added to concrete, polypropylene fibers exert a very small influence on shrinkage. Aly et al. [5] who studied the effect of polypropylene fibers on the shrinkage and cracking of normal strength concrete, concluded that, the shrinkage of test specimens made of fiber-reinforced concrete containing 0.50% by volume of polypropylene fibers increased by 15% after they are cured for 1 day and then exposed to a temperature of 23°C and a relative humidity of 50%, and by 22% after they had been cured for 7 days, when compared with the shrinkage of concrete containing no polypropylene fibers. At the same time, however, they stated that their results are in disagreement with those of several other authors. They justified their results with the increased porosity of fiber-reinforced concrete as compared with the porosity of concrete having no fibers and with the accelerated decrease of moisture in fiber-reinforced concrete.

From all the studies it is for sure that fibers' geometry bring certain change in the shrinkage of the cement composites.

Low & Beaudoin [91] investigated the factors that influence the flexural strength characteristics of the cement-water and the cement-microsilica-water systems reinforced with inorganic wollastonite micro-fibres are discussed. The effect of the wollastonite micro-fibres on matrix pore structure is investigated using mercury intrusion porosimetry and helium gas pycnometry. Fibre-matrix interaction is also examined using the conduction calorimetry method. Results from the study proved that incorporation of the wollastonite micro-fibres into cement and cement-microsilica matrices improves both the pre-peak and post-peak load-deflection response resulting in higher flexural strength and better ductility characteristics. It also modifies the microstructure of the cement based composite systems. Porosity, pore size distribution and solid density of the hydrated phases are significantly different in the cement-wollastonite and in the cement-microsilica-wollastonite composite systems. Wollastonite micro-fibres and microsilica addition appear to promote pore discontinuity in cement systems. It is suggested , that on the basis of conduction calorimetry measurements, there is no apparent chemical interaction between the wollastonite micro-fibres and the cement matrix during the hydration process.

In a similar study Ransinchung et al. [140] testified that up to 15% of wollastonite and 7.5% microsilica can be advantageously admixed with cement to significantly improve the water tightness of concrete, due to reduction in pore space and refinement of microstructure. In case of wollastonite and microsilica reinforced mortar investigation, Ransinchung & Kumar [139] concluded that mortar, which contains 82.5% cement, 10% wollastonite, and 7.5% microsilica, as cementitious material attains the highest compressive strength. The mortar, which contains 77.5% cement, 15% wollastonite, and 7.5% microsilica, as cementitious material achieves compressive strength higher than the conventional OPC mortar along with rendering maximum cement replacement for better economy of concrete work. It is observed that the compressive strength of mortar varied logarithmically with the days of moist curing and linearly with the proportion of admixing.

2.1.3 FIBERS' REINFORCED OVERLAYS

Repair works suffer from debonding and spalling of concrete layer. The major reasons often cited for debonding and spalling of repairs are differential thermal movements, elastic incompatibilities, shrinkage stresses, and occasional impact; rebar corrosion, substrate deficiencies, frost action, and poor workmanship [37, 42, 138). These same reasons are responsible for cracks in an otherwise, a simple concrete pavement topping. Given these reasons for spalling and debonding of repairs, durable thin repairs (less than 25 mm thick) are particularly difficult to achieve. For a durable repair, the desired characteristics of the repair material include low permeability, a high tensile strength, adequate impact resistance, sufficient deformability (ductility), high fracture toughness, low shrinkage, good dimensional stability, good abrasion resistance, and most of all, a strong tensile and shear bond with the base concrete. For thin repairs, however, the maximum dimensions of both the aggregate particles and the fibers have to be limited. Consequently, for thin repairs, the use of cements and mortars reinforced with very fine fibers (often called "microfibers") is conceivable.

Fwa & Paramasivam [44] employed one mortar mix with a water/cement ratio of 0.55:1 and one type of steel fibre to evaluate the feasibility of using thin steel fibre cement mortar overlay for the rehabilitation of surface-deteriorated concrete pavements, with improved resistance to surface abrasion, and a load-carrying capacity equal to or higher than the original design. The proportions of cement and sand used are 1:1.5 by weight. An accelerator is added at 1 litre per 22 kg of cement to give the desired high early strength. The steel fibres used are of the hook-end type, 30 mm long with an equivalent diameter of 0.4 mm.

Two surface abrasion tests are included in the preliminary phase. They are referred to as the polishing wheel test and the modified Dorry abrasion test. Flexural tests are conducted using prisms 500 mm long with cross-sections of 100 mm x 100 mm. Overlay thicknesses of 25 mm and 40 mm are studied. Flexural tests by means of third-point loadings are conducted for three cases as follows:

i. Tests producing tension in the bottom face of sound base concrete.

ii. Tests producing tension in the overlay which is cast on a sound base concrete.

iii. Tests producing tension in the overlay which is cast on a base concrete with a crack in its top surface. The base member is first loaded by third-point loading up to the peak resistance when a crack is formed close to the mid-span point. The crack usually measured between 0.04 mm and 0.20 mm in width, and extended to a depth between 50 and 75% of the thickness of the beam.

The test results suggested that 1% steel fibre cement mortar overlay would satisfactorily rehabilitate a surface-deteriorated concrete pavement, and that overlay 40 mm thick is preferable to overlay 25 mm thick.

Banthia and Dubeau [9] investigated the effect of addition of carbon and steel microfibers separately to the cement composites. It is concluded that more effective strengthening and toughening occurred due to carbon fibers as compared to steel fibers. At a low temperature of 50°C fibrous composites are stronger but more brittle than at a temperature of 22°C. In general, the peak loads in the case of carbon fiber-reinforced composites occur at greater displacements than those for composites containing steel fibers. Tensile bond strength too showed an increase at low temperatures compared to normal, which is apparently negligible.

Another fiber, Wollastonite, has found tremendous applicability in the improvement of repair works. Wollastonite is a naturally occurring, acicular, inert, white mineral (calcium meta silicate [ß - $CaO\text{-}SiO_2$]) of high modulus of elasticity, which is less costly than steel and carbon micro-fibers [89]. Prices for wollastonite range from $0.2/kg to $0.37/kg depending of its size, which is substantially cheaper than that of steel ($6.6/kg) [179], carbon ($11/kg) or glass ($2/kg) fibers [28]. It is formed due to interaction of lime-stone with silica in hot magmas. It is formed in nature by the reaction of calcium carbonate $CaCO_3$ with silica SiO_2 in hot magmas. Wollastonite is mined commercially for use in refractory ceramics and as a filler in paints. The processed granular material is of high purity, inexpensive, and readily available.

Available in abundance along the Udaipur belt of Rajasthan state of the Indian union as a low cost material, it may be ground to fine powder, and is already finding applications in

paint, dental care, ceramic tiles to name a few. Its composition of nearly equal proportions of lime and silica having fine particle size are favourable indicators for its admixing in concrete by partial replacement of cement. In itself, wollastonite does not possess binding properties like cement, but, in presence of microsilica, it improves the properties of admixed concrete by fine packing of inert material. Microsilica is a by-product of silicon metal or ferro-silicon alloy industries. Its high siliceous composition and very fine particle size are utilized beneficially in many works to improve the properties of fresh and hardened concrete. Reactivity of amorphous silica is directly proportional to the surface area.

Soliman and Nehdi [160] investigated the effect of incorporating wollastonite micro-fibers in ultra-high performance concrete (UHPC) on its early-age properties. Wollastonite micro-fibers were added at 0, 4, 8 and 12% as partial volume replacement for cement. Results showed that the early-age properties of UHPC mixtures incorporating wollastonite micro-fibers are highly affected by the micro-fibers content and aspect ratio. Increasing the wollastonite micro-fibers content resulted in compressive strength comparable to or higher than that of the control mixture without microfibers. Wollastonite micro-fibers reduced shrinkage strains and increased cracking resistance compared to that of the control mixture. However, no significant improvement in the flexural behaviour is achieved with the addition of wollastonite micro-fibers apparently due to a sudden rupture of micro-fibers within the matrix.

UHPC can be achieved through enhancing homogeneity (for instance by eliminating coarse aggregates) [27], producing stronger and higher packing density microstructure through using very low water to cement ratio (w/c) [151], and incorporating a high content of effective pozzolans. However, this unique mixture composition of UHPC increases its tendency to undergo early-age cracking [162]. Early-age cracking of cement based materials arises from the early rapid volume changes as a result of autogenous and drying shrinkage and thermal deformations [17]. Such volume changes induce tensile stresses within cement based materials. The tensile strength of such materials and its ability to resist tensile stresses increase with time [3]. Hence, a competition between the induced tensile stresses and the development of tensile strength of cement-based materials exists during early-ages. Once

tensile stresses exceeded the tensile strength, micro-cracking develops and propagates leading to visible shrinkage macro-cracking [3].

2.1.4 Conclusion on the Basis of the Studies

The following conclusions are drawn from the above literature review:

(1) When fiber reinforcement is used, the composite can become tougher and stronger, resulting from the additional increase in fracture toughness due to the toughening effect of the fibers in front of the crack tip and the bridging effect of the fibers behind the crack.

(2) Microfibers are more useful in pre crack reinforcement whereas macrofibers in post crack reinforcement because microfibers provide higher increase in tensile strength under lesser strains (micro cracks). On the other hand macrofibers only provide better bridging effect after the formation of critical crack due to their higher strength and larger embedment length. Thus they increase toughening strength only.

(3) For cement pastes the improvement can be induced at both stages and with both types of fibers, though generally microfiber reinforcement at pre crack stage is more required. Post crack reinforcement by toughening is provided in the form of stress transference from fibers to paste and vice versa, until multiple cracks appear. A critical fibre volume fraction, $V_{f,crit}$, defined as the minimum fibre quantity, is required for achieving multiple cracking in cement pastes. The exact magnitude of this quantity depends on fracture toughness of matrix, fibre properties, and interfacial bonds. Low fracture toughness of the matrix is in favour of low $V_{f,crit}$. Hence, a weak cement paste is expected relatively easy to achieve multiple cracking as compared with a mortar.

(4) Mortar and concrete mixes have higher tensile and toughening strength. Microfibers do not improve much of these properties. The effect of increasing fracture toughness and the tensile strength of mortars by addition of microfibers or sand appears to be offset by the negative effect of the increasing flaw sizes; hence the tensile strength of the mortar composites is not significantly influenced by the sand-to-binder ratio or the microfiber content. Therefore post crack toughening by macrofibers is more favourable in them.

(5) Micro and macro fiber hybrid reinforcement is best for strength enhancement and shrinkage reduction of cement mortars, whereas in concrete mixes macrofibers have been found to give better results. While initial, first cracking strength is improved by the hybrid, this improvement is not maintained much past the peak load, as it is in the mortar matrix case.

(6) For a concrete mix the crack bridging efficiency of a fibre depends on its length, radius, interfacial properties, and geometry as well as steel properties such as yield strength and ductility.

(7) As far as workability is concerned, bleeding water content increases by increase of the fiber volume fraction and fiber aspect ratio in the concrete mix. This is due to the increased non cohesiveness of the mix. The effect of increased water demand for lubrication of fiber precedes that of bleeding. Thus workability and tensile strength of mix decreases.

(8) Therefore tensile strength, fatigue strength and compression strength, all increase with increase in fiber content with the range lying in between 0-0.5% for most fibres, but decrease beyond high fiber content (5%). Also, there is an optimal range of fiber yield strength within which the best combination of peak pullout load and total energy absorption can be attained. Increasing the fibre yield strength beyond the optimal range will lead to excessive matrix local failure.

(9) Earlier it is found that it is not beneficial to use microfibers in concrete mixes but it has been determined that steel microfiber and wollastonite micro fiber reinforced mixes (either mortar or concrete mixes having maximum aggregate size 10mm) could beneficially be used as high strength overlays. As far as wollastonite is concerned, it increases flaw size definitely but workability and compressive strength increase for same cement content due to its fineness and class C pozzolanic action and; pore refinement of mix caused by it along with fiber action. The non cohesiveness caused by fiber addition can be mitigated by using smaller aggregate size, as are used for overlays. Thus macrofibers at higher contents too could be used for larger thickness pavements with smaller size aggregates, but then that would lead to strength reduction.

2.2 SELF COMPACTING CONCRETE

Self-compacting concrete (SCC), a new kind of high performance concrete (HPC) with excellent deformability and segregation resistance, is first developed in Japan in 1986. It is a special kind concrete that can flow through and fill the gaps of reinforcement and corners of molds without any need for vibration and compaction during the placing process. SCC is originally developed with the intention of simplifying casting operations in civil engineering construction of large dimensions, where a high percentage of reinforcement or complex geometries cause a difficult concrete flow. Soon it became clear, though, that the great productivity increase associated with SCC technology also habilitates it as a good solution for housing construction, precast industry, and other applications. The fresh SCC requirements are mainly resumed to the filling ability, the passing capacity, and the resistance to segregation. These properties are evaluated at the mix design stage, based on a series of tests in fresh samples. SCC has found special application in rigid pavements because of two main qualities: a) since it flows and compacts itself, therefore it binds the under layer normal concrete (in case of overlay) in a better manner, thus reducing chances of debonding and increasing better load transfer ability; b) reduces voids thus increasing solid space ratio, which reduces permeability and improves shear strength at interface of aggregates and hardened paste, finally increasing the durability and strength of concrete; c) there is better bonding of patch work with reinforcement and compaction doesn't need vibration.

2.2.1 Fundamental Aspects of Self Compacting Concrete

Self compacting concrete is clearly different from ordinary concrete in terms of mix composition and fresh state properties. Some important works relevant to the fundamental aspects of self compacting concrete are briefly discussed in this section.

Self compacting concrete was first developed in Japan in the late 1980's. The fundamental study on the workability of the concrete was carried out by Ozawa et al. [123] at the University of Tokyo.

Ouchi [122] reviewed the history of development and application of self compacting concrete in Japan. Two important criteria were mentioned for achieving self compactibility:

(1) Limited aggregate content and higher powder content
(2) Co existence of high deformability and high viscosity

The method is shown schematically in Fig 2.1

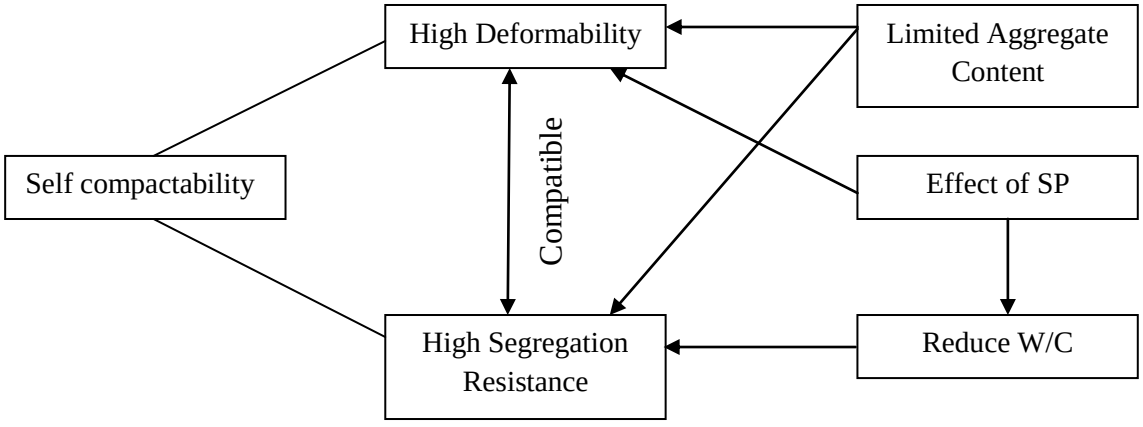

Fig. 2.1 Method of achieving self compactibility [122]

The main benefits of the self compacting concrete can be summarised as follows:

(1) Shortened construction period
(2) Assured compaction to the structure: confined zone in which vibration compaction is difficult
(3) Improved construction environment
(4) Less manpower requirement

Noguchi & Mori [115] reported on the evaluation of fresh properties of self compacting concrete. The principles for the test on flowability, adhesiveness, segregation resistance, passing ability and filling ability were discussed. Two different approaches were proposed for the final evaluation of the filling capacity of SCC in the target structure. The first approach was based on a mock up modelled after the target structure and placing the SCC with specified procedures.

The second approach was the estimation of filling capacity based on the work on the rheological properties of the SCC and mortar.

The Orimet test for the assessment of workability of flowing concrete was developed by Bartos [15]. The test is based on the principle of an orifice rheometer which is applied to fresh concrete. The Orimet consists of a vertical casting pipe fitted with an interchangeable conical orifice at its lower end. A trap door is used to close the orifice. The internal diameter reduces from 120 mm within the casting pipe to 80 mm at the end of the orifice. The Orimet is used for the determination of flow time. Flow times less than 5 seconds indicate good mixes.

The flowing ability, passing ability and resistance to segregation are the key properties of SCC. Flowing ability can be measured by slump flow test and V funnel test whereas L box test and U box test give an assessment of the passing ability and resistance to segregation of the concrete. But these give only an approximate estimation of different properties and cannot ensure that the concrete is indeed self compacting, fulfilling all the criteria for self compacting concrete. Rooney & Bartos [145] developed a settlement column segregation test for fresh self compacting concrete. In this test, a column of SCC with internal dimensions of 500mm × 150mm × 100mm is subjected to controlled jolting action followed by an undisturbed settlement period of 5 minutes. Samples are then collected from the top and bottom of the column and the mortar is washed out through a 5 mm sieve. A significantly higher mass of coarse aggregates in the bottom sample than in the top sample (represented in the form of mean segregation ratio which is ratio of aggregate mass in top and bottom sample) indicates the risk of segregation. Results from the tests on three different mixes (refer Table 2.1) are summarized in Table 2.2. The test results indicate that the apparatus can successfully detect the difference in segregation resistance between mix 1 and mix 2, and between mix 2 and mix 3.

Table 2.1 Mix design details, kg/cum [145]

Material	Mix 1	Mix 2	Mix 3
OPC	300	300	300
Limestone powder	248	248	248
Coarse aggregate	954	954	954
Fine Aggregate	700	700	700
Water	167	167	167
Viscocrete 2	4.66	9.32	13.97

Table 2.2 Settlement column segregation test results [145]

Mix	1	2	3
Mean Segregation Ratio	1.048	0.782	0.390
Standard Deviation	0.047	0.055	0.064
Coefficient of Variation (%)	4.44	7.03	16.52

Grunewald & Walraven [49] studied the effect of fibers on the workability of fiber reinforced mortar. They introduced a fiber factor ($V_f \times (L/D)$) as the product of the volumes fraction and the aspect ratio of the fibers. The effect of the fiber factor and the fiber volume fraction on the slump flow is shown in Figures 2.2, 2.3, 2.4.

It was concluded that at high flowability the effect of different types, contents and combinations of steel fibers could be described by the fiber factor. The rheological constants like yield value and plastic viscosity increased with an increase in the fiber factor.

Saak et al. [148] introduced a new segregation controlled design methodology for self compacting concrete (SCC). According to the theory the aggregate segregation is governed by the yield stress, viscosity and density of the cement paste matrix. A rheological self flow zone (SFZ) for concrete exists where the aggregate segregation is avoided without affecting workability. Following two equations govern the segregation of the particles in static and dynamic condition:

Static condition: $\left(\tau_y / \Delta\rho\right) \geq \frac{4gr_p}{3}$ (1.1)

Dynamic condition: $\nu = \left(\frac{8}{3}\right)\frac{\left(gr_p\Delta\rho\right)}{\sqrt{C_D\rho_m}}$ (1.2)

Where,

τ_y =yield stress

$\Delta\rho$ = density difference between the matrix and the segregation particle

ν = constant terminal falling velocity of the particle

C_D = drag coefficient, and ρ_m = density of matrix

Experiments were performed using a spherical glass aggregate and cement paste to verify the static segregation control theory. The new SCC design approach reveals that concrete will have the greatest fluidity at the lowest paste yield stress and viscosity, where segregation is absent. The segregation resistance is optimised at the highest yield stress and a viscosity that still produces flowable materials. This critical range of yield stress and viscosity where segregation is minimized, is known as self flow zone (SFZ).

Mac Donald & Lukkarila [93] reported that the binder composition or water/binder ratio can be changed to alter the strength, set and chemical shrinkage characteristics of the mixture without additional admixtures. Large dosage of the viscosity modifying agent did not affect the other plastic and hardened properties of the concrete.

Boel et al. [20] investigated the pore structure of seven self compacting mixes and one traditional concrete mix. cores of 14 mm diameter and 30 mm height were drilled out of the cubes 100×100×100 mm. These cubes were stored for 56 days at 20° ± 2° and 90% relative humidity. A computerized X ray micro tomography (CT), a radiological imaging technique was used to investigate the pore structure of concrete. It was found that the self compacting concretes had a different pore structure than the traditional concrete due to its changed material composition. The influenced the durability and more particularly the behaviour with respect to water. The main conclusion was that self compacting concretes absorbed less water than the traditional concrete and the absorption increased with an

increase in water cement ratio and decrease in cement content. The better behaviour of SCC may be attributed to the existence of more isolated pores.

Naphthalene sulphonate superplasticizer is often used in self compacting concretes to improve the fluidity of fresh concretes. The fluidity increases as the amount of adsorption increases. But, due to the addition of flyash, the relation between the fluidity, the dose of superplasticizer and the amount of adsorption of the superplasticizer changes due to the properties of the flyash. Termkhajornkit et al. [166] investigated this aspect of concrete with two types of flyash. They examined the relationship between the amount of adsorption of superplasticizer and the flow values of the paste by changing the replacement ratio of the flyash and the dose of the superplasticizer. The zeta potential of the powdered particles was also determined. It was reported that the fluidity of the paste was affected by the bulk solid volume of the flyash, and the flow value increased as the bulk solid volume increased. The adsorption of the naphthalene sulphonated superplasticizer to the surface of the particles changed the zeta potential of the surface to the negative side and changes the absolute value. As a result, the particles which had the same sign of zeta potential repelled each other and increased the fluidity.

Khayat et al. [68] investigated the effect of packing density of the fine particles on the workability of self consolidating concrete. Two aggregate combinations were taken. The first was discontinuously graded aggregate containing 0-4 mm sand and 7-16 mm coarse aggregate with a packing density of 0.8, whereas the second one was continuously graded with 0-2, 3-6 and 7-16 mm aggregate combinations with slightly lower packing density of 0.72-0.75. Thirty two mixes containing 420,480 and 550 Kg/cum of cement and limestone filler and water to powder ratios of 0.33, 0.40 and 0.50 were investigated. Concretes with the highest packing density had a low demand for the high range water reducer and developed lower viscosities. The effect was more for lower water to binder ratio. Concretes with a high packing density exhibited slightly better filling capacities. Higher resistance to surface settlement was obtained with the concrete having a higher fine content (<80 μm).

Mahesh & Santhanam [97] studied some simple test methods to characterize the rheology of self compacting concrete. The mixture proportions studied are given in Table 2.3. The slump flow values of the mixtures varied between 660 mm and 730 mm whereas

T_{50} slump flow time in seconds was between 2.6 to 4.5 seconds. The difference in level of concrete in the two limbs of the U box was found to be within the acceptable limits, 10 mm to 30 mm. The V- funnel flow times varied from 2.6 seconds to 14.5 seconds. These values were acceptable for self- compacting concrete. the mixtures: WG-100, WG-110 and HPS-90 did not fulfil the criteria for self compacting concrete. the blocking factors of the mixtures in the L-box test were in the range of 0.489 to 0.643 which were lower than the acceptable values of 0.80 to 1.00 as reported in published literature.

The investigation suggested a linear relationship between the V funnel flow time and the T50 slump flow. It was also observed that the viscosity of the SCC mixtures decreased with an increase in the water to powder ratio. It was concluded that the slump flow value and the U box test were reliable to characterize the SCC mixtures as acceptable or unacceptable.

Table 2.3 Mixture proportions of different SCC mixtures to compare their rheology [97]

Ingredients	WG-90	WG-100	WG-110	HPS-90	HPS-100	HPS-110
Water powder ratio (by volume)	0.9	1.0	1.1	0.9	1.0	1.1
Water content l	220	220	220	220	220	220
Cement Kg/ cum	360	360	360	360	360	360
Flyash Kg/ cum	291.5	236.8	192.0	291.5	236.8	192.0
Fine aggregate (FA), Kg/ cum	656	714	770	656	714	770
Coarse aggregate (CA), Kg/ cum	715	717	715	715	717	715
Superplasticizer (% by weight of cement)	1.0	0.8	0.7	1.0	0.8	0.7
VMA (percentage by weight of cement)	0.0225	0.025	0.0375	0.200	0.375	0.300

Kumar & Kaushik [77] proposed a new model for interfacial transition zone in SCC. significant features of the interfacial transition zone in normal concrete studied by various researchers are summarized in Table 2.4. A thin shell of CSH was found to be located about 10-15 micron away from the aggregate in the self compacting concrete. the transition zone lying between the aggregate surface and the CSH layer was rich in calcium hydroxide crystals. Unreacted grains of microsilica and flyash of size 1-2 μm were observed in this zone. the features of the transition zone in SCC and conventional concrete are summarized in Table 2.5.

Table 2.4 Model for interfacial transition zone in SCC

No.	Micro structural feature	Barnes et al. (1980)	Oliver grandet (1982)	Zimbelan	Montorio (1986)
1.	Presence of $Ca(OH)_2$ layer at aggregate surface	Yes continuous with preferred orientation	Yes, almost continuous	Yes, continuous	Yes, almost continuous
2.	CSH present in continuous form	Adjacent to CH layer, that is duplex film	Almost continuous	Not in continuous film form	Not in continuous film form
3.	Presence of partially hydrated cement grains (Hadley	Yes	-	-	Yes
4.	Ettringite in direct contact with aggregate/CH film	No	May be	Yes	Yes

Table 2.5 Comparison of interfacial transition zone in SCC and normal concrete

No.	Feature	Conventional concrete	Self compacting concrete (with flyash and micro silica)
1.	CH film at the aggregate surface	Yes	Yes
2.	Ettringite and/or mono sulphate in vicinity of aggregate surface	Yes	No
3.	CSH presence in ITZ	Yes but sparse	More; a distinct layer at some distance away from the aggregate surface
4.	Micro filter effect in ITZ	No	Yes
5.	Presence of partially reacted grains in ITZ	No cement	Yes flyash
6.	Qualitative dimensions	Porous	Less porous

2.2.2 Principles of SCC Mix design

The SCC is that concrete, which gets compacted due to its self weight and is deaerated (no entrapped air) almost completely while flowing in the form work. In densely reinforced structural members, it fills completely all the voids and gaps and maintains nearly horizontal concrete level after it is placed. With regard to its composition, SCC consists of the same components as conventionally vibrated normal concrete, i.e., cement, aggregates, water, additives or admixtures. However, the high dosage of super-plasticizer used for reduction of the liquid limit and for better workability, the high powder content as 'lubricant' for the coarse aggregates, as well as the use of viscosity-agents to increase the viscosity of the concrete have to be taken into account. Superplasticizer enhances deformability and with the reduction of water/powder segregation resistance is increased. High deformability and high segregation resistance is obtained by limiting the amount of coarse aggregate. These two properties of mortar and concrete in turn lead to self compactability limitation of coarse aggregate content. Nawa et al. [110] reviewed various aspects of the materials and design of self compacting concrete. self compacting concrete is classified into three types mentioned below:

(1) Powder type self compacting concrete in which a large amount of powder is used.

(2) Viscosity agent type self compacting concrete in which viscosity agent is added.

(3) Combined type self compacting concrete where both the powder and viscosity agent are combined to get self compacting properties. Self compacting concrete mainly consists of three types of material, powder, aggregate and admixture.

Powder: includes cement, flyash, micro silica, blast furnace slag powder and limestone powder. Aggregate: includes sand, crushed aggregate, gravel. Admixture: includes both superplasticizer and viscosity modifying agent. Some procedures like JSCE method and Okamura's method are proposed for proportioning self compacting concrete. JSCE method has been outlined in Fig. 2.2.

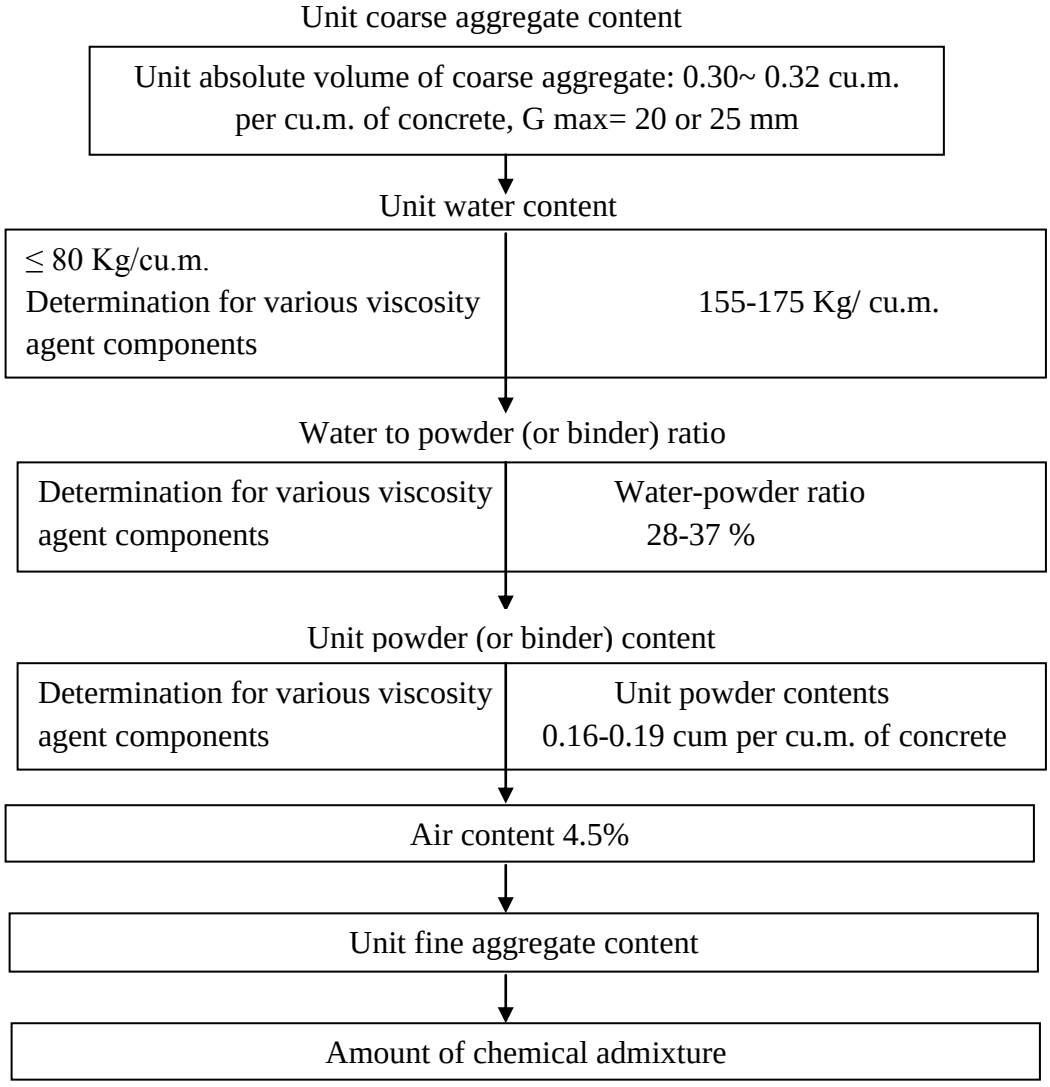

Fig 2.2 JSCE method (viscosity agent type) for mix proportioning of SCC [108]

The key for developing self compacting concrete is to find out suitable amounts of water and superplasticizer for given powder characteristics. Maeyama et al. [96] proposed a scientific model namely the water layer model for mix proportioning of self compacting concrete. If the particle size distribution of powder is given, the required amount of water can be determined by the model for making flowable and non segregating concrete. this limit amount of water does not contribute to the flowability of the paste. The thickness of the limit amount of water on a particle is uniform irrespective of the particle size. the water exceeding the limit amount of water contributes to the flowability of the paste. The applicability of the model was verified for paste, mortar and concrete with various kinds of powders.

An experimental study on the effects of the ambient temperatures and expansive additives on the self compacting concrete was made by Hori et al. [58]. High belite cement, ordinary Portland cement and fine limestone powder were used as powder materials. A calcium-sulpho-aluminate type expansive additive, a polycarboxylic acid based water reducing agent and a surfactant were used in the study. Sea sand and crushed stone were used as fine and coarse aggregates respectively. The specimen of self compacting concrete containing belite cement and ordinary Portland cement were called HB concrete and NP concrete, respectively.

It was revealed that the fluidity of the NP concrete was lowered and that of HB concrete was increased with an increase in the ambient temperature. The expansion of HB concrete was larger than that of NP concrete and the shrinkage of HB concrete was smaller than that of NP concrete at any ambient temperature.

The flowing time in the O-rote test was not affected by the addition of the expansive additive. The properties of self compacting concrete did not deteriorate due to the addition of the expansive additive. In fact, it was very effective in compensating the shrinkage of self compacting concrete.

The applicability of the already proposed water layer model was investigated by Midorikawa et al. [104] for different characteristics of the sand. The results of the investigation indicated that the Water Layer Model was effective in deciding the water content. The effect of water and superplasticizer could be exnormaled using the Water Layer Model.

Reknes [143] reported a particle matrix based design of self compacting concrete with lignosulfonate water reducer. The workability of the concrete was considered as a function of two phases of the material namely matrix phase and particle phase. The following definitions of the two phases are used in the particle matrix model:

1. The matrix consists of the water, chemical admixtures, cement, pozzolans and aggregate fines, that is, particles with diameter < 125μm.
2. The particles phase consists of aggregate particles with diameter ≥ 125μm.

Both the properties of particles and the matrix, affect the workability of the concrete. The particles properties dominate the workability of the concrete at a relatively low matrix volume, but the matrix properties dominate it at a high matrix volume. Test results confirmed this behaviour of the concrete. There was almost no effect of increasing the water cement ratio and lignosulphate dosage in the concrete with matrix volume of 350 l/m^3. The slump was only 150 mm at a water cement ratio of 0.52. To make the concrete really workable, the matrix volume had to be increased above 350 l/m^3. At this stage the matrix phase started to dominate the properties of the concrete over the particle phase and the effect of the improved matrix workability with increasing water-cement ratio and lignosulphonate dosage at a matrix volume of 370 l/m^3 or more.

Pedersen & Mortensen [127] characterized the matrix phase of the concrete and studied the effect of particle size distribution and the specific surface area of fillers on the rheological properties of the matrix. The viscosity and yield stress were measured on a FANN-viscometer. The results indicated that fillers, as a cement replacement, had a significant effect on the matrix rheology and thus the rheology of SCC. Using the knowledge of the effects of plasticizing agents, cement and filler on the rheology of the matrix, the right combinations of the materials can be chosen to produce low strength SCC.

Petersson [130] investigated the properties of self compacting concrete with limestone powder as filler. The limestone filler powder is normally positively charged and the aggregate is negatively charged. This hinders proper dispersion of the limestone particles during mixing. An investigation was carried out for different mixing order of the materials as shown in Table 2.6.

Table 2.6 Different mixing orders for SCC [130]

Mixing Number	Sequence of mixing materials
BL1	Aggregate + limestone, mixing, cement + water and ½ superplasticizer, AEA mixing, rest 1 minute and then rest of superplasticizer, mixing 1 minute
BL2	Aggregate + cement, mixing, limestone + water and ½ superplasticizer, AEA mixing, rest 1 minute and then rest of superplasticizer, mixing 1 minute
BL3	Aggregate + cement + water with ½ superplasticizer, AEA, limestone filler mixing, rest 1 minute and then the rest of superplasticizer, mixing 1 minute
BL4	Cement + limestone filler, mixing, aggregate + water and ½ superplasticizer and AEA, mixing, rest 1 minute and then rest of superplasticizer, mixing 1 minute

Thin section analysis of the hardened specimens showed that mixing alternative BL4 was best suited for dispersion of fine filler. Microscopic analysis showed that the worst mixing alternative was BL1. The mixing sequence BL2 and BL3 were a little better. It was also found that use of limestone filler in SCC resulted in high compressive strength which was dependent on the amount of cement, C_3A content of cement and the filler. The frost resistance was also investigated at different ages.

Marquardt et al. [100] reported a new method for the optimization of the mix design of self compacting concrete. The method was developed at the University of Rostock. The method is summarized as follows:

(a) The method is based on the volume fraction method which takes into account the water demand of the individual concrete constituents.

(b) The water demand of each concrete constituent was determined by measuring the power consumption of the mixer driver and the amount of total water added to the mix.

(c) The sum of the water demands of the individual components gives the optimum water requirement to produce flowable and non segregating SCC.

The experimental investigation verified the applicability of the method. All the SCC's designed on the basis of the above concept of determining water demand of the individual

components showed high degree of self compactibility (flow diameters were between 62 and 79 cm without segregation).

The development of medium and low grade SCC is necessary to increase the use of self compacting concrete for various construction works. Johansen & Busterud [62] reported the development of SCC with characteristic compressive strength varying from 15 to 65 MPa. The water content was in the range of 180 to 200 l/cum. Following aggregate fractions were used for making the SCC:

i) 0- 0.5 mm cyclone sand
ii) 0- 8 mm washed sand
iii) 4 – 8 mm natural gravel
iv) 8 – 16 mm crushed natural gravel

The different grades of SCC and their compositions are summarized in Table 2.7.

Table 2.7 Different grades of SCC and their compositions [62]

Cement grade- cement concrete composition	SCC15*	SCC25*	SCC35*	SCC55*
Cement content (kg/cum)	228	260	325	415
CSF (kg/cum)	22	20	15	20
Free water (kg/cum)	200	199	203	172
Water powder ratio	0.436	0.416	0.400	0.347
Air content (%)	2	2	2	5
Aggregate (kg/cum)	1863	1842	1782	1685

*Characteristics compressive strength after 28 days

The proportions varied slightly for different grades of cement. The SCC15 with characteristics compressive strength of 15 N/mm^2 at 28 days was suitable only upto a slump flow of 650 mm. The use of Norcem High Strength Cement resulted in a moderate need of matrix (348 l/cum excluding air). The matrix volume varied from 357 to 370 l/cum when other types of cement were used. The cost of the concrete increased moderately.

The frost experience of self compacting concrete in Argentina was reported by Fornasier et al. [41]. Two self compacting concrete mixtures, one with viscosity modifying admixture and the other with limestone filler, were studied. The admixture doses, the water powder ratio and the contents of fine aggregate and limestone filler were determined through

tests on paste and mortar. The mixture with limestone filler and very little content of viscosity enhancing admixture showed better performance than the mixture with viscosity enhancer only.

Ghezal & Khayat [45] reviewed the results of a factorial design carried out to mathematically model the influence of key parameters on various properties of self compacting concrete. An empirical statistical model was derived over a wide range of mixture proportioning. The model is valid for mixtures with 0.38 to 0.72 water to powder ratio, 250 to 400 kg/cum of cement, upto 120 kg/cum of fillers, and 0.12% to 0.75% of high range water reducing agents by mass of powder. Cement was replaced upto 20% by limestone filler. Mixtures with limestone filler of 100 kg/cum exhibited greater resistance to surface settlement at a particular slump flow compared to similar concrete with low content of limestone filler. The model can be used to optimize economical SCC mixtures with lower contents of cement and water reducers that meet the workability and strength requirement of SCC for residential and commercial applications.

Due to the use of high dosage of superplasticizers and a high volume of paste and powder, the cost of self compacting concrete is higher than that of the cost of normal concrete. In view of the fact that the strength of SCC is usually high, Ribeiro and Goncalves [144] studied the possibility of using lower content of cement and higher content of mineral admixtures to produce a low cost SCC. A low cost superplasticizer and a higher volume of water were used in the investigation. The optimization of the mixture was done considering the following points:

- Minimum cement content for a given strength
- Maximum flyash content to reduce the cement and superplasticizer contents
- Maximum limestone powder content to increase the paste volume, fluidification and reduction in segregation
- Maximum aggregate size lower than 16mm
- Limit the sand content that influences the strength
- Use of a low cost chemical admixture

Table 2.8 shows a comparison of costs of SCC and normal concrete. The results showed that SCC can be produced with costs similar to those of normal concrete.

Table 2.8 Costs of SCC and normal concrete [144]

Material	SCC (Kg/cum	Normal concrete (Kg/cum)	Unit cost (Euro)	SCC cost (Euro)	Normal concrete cost (Euro)
Coarse aggregate	786	1130	9.76/ ton	7.67	11.03
Fine aggregate	786	795	9.76/ton	7.67	7.76
Cement	205	240	68.35/ton	13.99	16.40
Flyash	102	80	19.53/ton	2.00	1.56
Limestone powder	256	-	15.14/ton	3.87	-
Total powder	563	320	-	-	-
Superplasticizer	5.6	-	0.68/l	3.85	-
Plasticizer	-	2.58	0.40/l	-	1.01
Water	195	160	0.01/l	1.90	1.56
Total				40.95	39.32
Water-powder ratio	0.346	0.500	-	-	-

Konig et al. [70] produced self compacting concrete using lignite flyashes. The water requirement was reduced by the addition of the lignite flyash. The setting time became shorter and the investigation on mortar showed satisfactory strength development. The compressive strength of SCC was 56 N/mm^2 at 28 days.

Skarp et al. [158] reported the use of modified colloidal silica (MCS) for mix proportioning of self compacting concrete. It is a synthetic, amorphous silica of primary particles. The particle size of the modified colloidal silica is less than 100 nm in a water solution. In concrete the MCS reacts with the calcium ions and forms calcium silicate hydrate (CSH). The reaction of MCS creates multiple particles of CSH gel that exhibit a filler capability and contributes to the stability of the concrete mix. The MCS has significant effect on plastic viscosity without changing the yield stress of the paste. Slightly higher dosages of superplasticizer (3- 35 kg/cum) was needed in the mix containing MCS. The MCS concrete gained a higher strength (5 N/mm sq) than the control concrete mix in the 16 hours, but the 28 days strength of the MCS concrete was lower than that of the control

concrete mix. A small dose of MCS can be used to produce cost effective SCC with lower binder and fines content.

An experimental work for the optimization of high strength self compacting concrete was carried out by Gomes et al. [47] assuming the concrete to be a two phase material consisting of paste and aggregate. The optimization process is outlined in Fig 2.3 where sf/c, sp/c and f/c denote, respectively, the microsilica dosage, the solid superplasticizer dosage and the inert filler dosage, all expressed by the weight of cement.

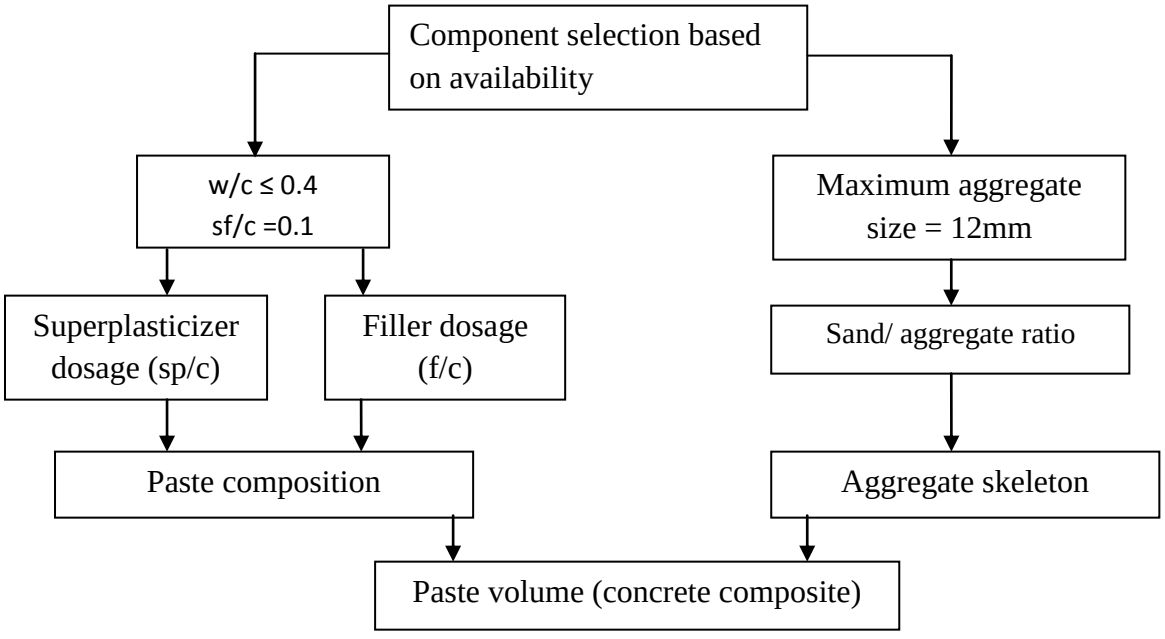

Fig 2.3 The optimization process [47]

High strength cement, microsilica, a copolymer based superplasticizer, and a limestone filler and aggregates were used in the mix. The marsh cone and mini slump tests were used for optimizing the superplasticizer dosage and filler content for the required paste fluidity. The concept of the minimum void content was used to determine the aggregate grading and the paste content was found after tests on concrete. The SCC had a 7 days compressive strength of 60 MPa for a water cement ratio of 0.4 and filler cement ratio of 0.3.

Self compacting concrete has usually higher powder content and higher than normal sand content. But in some applications high sand contents are not desirable. Daczko & Kurtz [32] reported the basic procedure for proportioning high volume coarse aggregate self

compacting concrete. A randomised block factorial statistical experiment was performed to identify the major factors to be considered in proportioning high volume coarse aggregate self compacting concrete. Self compacting concrete containing high volumes of coarse aggregates ranging from 365 to 425 litres per cum were developed in the investigation. The SCC with the highest volume of coarse aggregate content (425 litres) showed the greatest variation on flow properties. It was found that there was a maximum dose of viscosity modifying agents above which instability of the mixtures was observed.

Mueller et al. [106] reported the development of self compacting light weight concrete with weights ranging from 1350 to 1900 kg per cum. The unit weight of concrete was adjusted varying the types and amounts of fine and coarse lightweight aggregates. The tests on the hardened properties showed that the compressive strength and the modulus of elasticity of lightweight self compacting concrete were comparable to those of the ordinary structural lightweight concretes.

Bui et al. [23] introduced a new approach to the mix design of SCC. The criteria are minimum apparent viscosity, minimum flow and optimum flow-viscosity ratio. These criteria are related to the average aggregate diameter and aggregate spacing which can be computed from the paste volume (or aggregate volume), average diameter and void content of aggregate. The experimental results showed that the paste rheology model and criteria could be applied for different coarse to total aggregate ratios, different cement contents, different water to binder ratios, as well as different contents and types of flyash. Further minimum paste volume method was applied in designing cost effective self consolidating concrete. the compressive strength of SCC designed by this method varied from 70 to 105 MPa for a water to binder ratios between 0.3 to 0.35 and cement contents between 250 to 410 kg per cum. The 28 days compressive strength of a series of SCC containing milled limestone (water to binder ratio-0.37 to 0.45, cement content : 250 to 325 kg per cum, limestone content: 190 to 250 kg per cum) varied from 27 to 42 MPa.

Ravindrarajah et al. [142] showed that fine and coarse aggregate could be partially replaced with flyash in producing flowable, non segregating high strength self compacting concrete. It was also found that flyash in self compacting concrete helped to improve the later age strength beyond 28 days.

Kumar and Kaushik [76] developed eco friendly self compacting concretes using marginal materials like stone crusher dust. Stone crusher dust (< 4mm) and 2-6 mm size crushed aggregates were used to produce self compacting concretes with 28 days compressive strength of about 70 MPa. It was also reported that multi carboxylate ether based superplasticizers had an edge over SNF based superplasticizers in production of self compacting concrete (SCC). A typical mix proportion of high strength SCC is shown in Table 2.9.

Table 2.9 A typical mix proportion of high strength SCC [76]

Cement (kg per cum)	400	VMA (kg per cum)	3
Flyash (kg per cum)	273	Crusher dust (kg per cum)	725
Microsilica (kg per cum)	20	2-6 mm size aggregate (kg per cum)	290
Water (l per cum)	175	12 mm size aggregate (kg per cum)	505
Water/powder ratio	0.25	Slump flow (mm)	700
Superplasticizer (kg per cum)	12		

Dattatreya et al. [33] reported the development of SCC mixes with three water-binder ratios and incorporating high volumes of cement replacement materials. The mixes had cement replacement levels of the order of 45 to 55%. A water powder ratio slightly higher than that recommended by Okamura was used. This was due to the more rough texture of flyash and slag compared to those used by other investigators. The SCC's developed showed adequate self compactability and had good mechanical and durability properties. It was also observed that the use of high volumes of mineral admixtures resulted in a low chloride permeability even for a high binder content and lower aggregate volume fraction.

Vengala et al. [171] described a sequential procedure to develop self compacting concrete. fifteen mixes were investigated. The water cement ratio and the superplasticizer dosage were kept constant except for a few initial mixes. Flyash replacement of 5, 10, 15, 20 and 25 percent, respectively, of the coarse aggregate was adopted. To obtain adequate flowability in SCC, a viscosity modifier was used to stabilize the mixes. The investigation showed that SCC could be developed based in volume fraction changes with reference to a non superplasticized concrete. SCC was achieved when volume of paste was between 0.43

and 0.45. it was also observed that use of fine flyash resulted in an increase of the 28 day compressive strength of concrete by about 38 percent.

2.2.3 Effects of admixtures on SCC

Bouzoubaa and Lachemi [21] investigated the feasibility of producing SCC with high volumes of Class F flyash (40-60%). Nine SCC mixtures and one control concrete were studied at constant cement content (400 kg/m^3) and the water/cementitious material ratios ranged from 0.35 to 0.45. All mixtures were tested for fresh state properties i.e. viscosity and stability. The mechanical properties of hardened concretes such as compressive strength and drying shrinkage were also determined. 28 days compressive strength values ranged from 26-48 MPa which were quite lesser than normal concrete but it indicated that economical medium strength SCC could be made by substituting cement with high volumes of flyash. Lomboy et al. [90] investigated the differences in the strength and shrinkage properties of semi flowable self compacting concrete (SFSCC) and ordinary pavement concrete containing 20% Class F flyash. Compressive strength, splitting tensile strength, modulus of elasticity and fracture strength of both the concretes were evaluated at 1,3,7,14 and 28 days and were found to have negligible differences except modulus of elasticity, which reduced for SFSCC. Also shrinkage induced cracking was found higher in SCC.

Parra et al. [125] studied the effect of fine content on the SCC. Splitting tensile strength, modulus of elasticity and drying shrinkage were studied. It was made clear in the study that tensile strength evolves differently than compressive strength and factors like: mix design parameters and properties of additives greatly influence the behaviour of SCC. Since the splitting tensile strength mostly depends upon aggregate-paste bond, therefore any change brought in this field affected the tensile strength severely. At early ages, the lime formed at the interface of aggregates and paste is higher in number and thus decreases the splitting tensile strength of concrete. Lime produced by polycarboxylate based superplasticizer too decreased the tensile strength. With time the lime gets converted into CSH, depending upon the type of pozzolan. Even admixtures like lime fillers, increased the early age hydration by providing nucleating sites for formation of hydration products but they increase the surface area too which cause shrinkage cracks.

At early ages enough water is available for effective functioning of admixtures, and thus their positive effects mitigate the negative effects. Hence a very small difference (3.5%) was found between the tensile strength of normal concrete and SCC at 7 days. In normal concrete enough water is not available for the pozzolanic reactions at later ages, whereas SCC does contain it, due to delayed hydration caused by pozzolans. Therefore, whereas at 28 days the normal concrete reaches a tensile strength of between 13.7% and 30% greater than that of the SCC, at 90 days these differences are reduced to values of between 4.2% and 11.9%. For a normal concrete containing pozzolans, if it contains more water, then it will behave more like a SCC, but at lower water content, even though the tensile strength is higher at initial ages, yet its gain get diminished at later ages.

Modulus of elasticity (E) tests at 28 and 90 days showed that the paste volume and W/CM ratio control the modulus of elasticity to the highest extent. For SCC, the E values were lower, inspite of the fact that: a) SCC is denser and stronger at aggregate-paste interface; b) E values of corresponding pastes of SCC were higher than those of pastes corresponding to normal concrete. This is due to the higher paste volume of SCC. Higher fraction of paste lowers the stiffness of concrete. For the same paste volume if the W/CM ratio of the SCC is reduced by introducing filler material which occupies spaces in voids between cement grains, then it also stiffens the paste, apart from just increasing its interlocking with aggregates due to higher density. Hence, the reduction in E value of SCC can be mitigated by reducing the W/CM which directly affects the strength of concrete. Therefore high strength concretes have lesser differences in E values for normal and SCC, whereas lesser to medium strength concrete have higher.

Tests conducted to determine drying shrinkage yielded, that drying shrinkage does not depend upon the strength of the concrete: this is true either if the binder (cement+flyash) content and the W/CM ratio are constant or if the workability is kept constant by modifying the composition and thus the strengths. A substitution of 50% cement with flyash did not affect the drying shrinkage. It was confirmed that the addition of flyash maintained the same binder content, and increased water demand fulfilled by superplasticizer maintained the final W/CM ratio. This reduced the shrinkage, though there was a reduction in the strength of the concrete.

Turcry et al. [169] investigated the comparative behaviour of ordinary pumpable concrete (OC) and SCC made with the same ingredients at higher W/C ratios (0.47-0.6%). This study is different from other studies, because mostly mineral admixtures are being used to substitute cement in large volumes to increase the paste content, but here, only lime filler was used apart from other similar ingredients, to produce SCC. There was a difference in the volume of lime filler, water, superplasticizer as well as presence of very small volumes of viscosity enhancing agents, in the OC and SCC.

It was found that compressive strength and tensile strength of both the concretes are same, whereas E value was lower by 2-8% and drying shrinkage was higher by up to 16% in SCC with respect to ordinary pumpable concrete. The paste volume difference was 20% in OC and SCC. This proved that the difference in E values is not directly proportional to the difference in paste volumes. The final W/CM ratio obtained due to lime filler volumes was quite less in SCC (0.37-0.41) which was smaller than W/C ratios of OC (0.47-0.60). Larger volumes of cement in the SCC along with smaller value of W/CM resulted in no difference, in compressive and tensile strength. Modulus of elasticity got improved to some extent by this strength increment as the bond strength between the paste and aggregates improved. Hence the use of fine materials up to the extent of filling only the voids between cement grains could decrease the reduction in E value and improve the strength of SCC.

2.2.4 Effect of Fibers on SCC

SCC mixtures exhibit dense properties, finer binder and aggregate proportions (maximum aggregate size lesser than 20mm). Fine materials like flyash, microsilica and granulated blast furnace slag are added to increase the paste content, thus improving the flowability, self compacting ability and segregation resistance of SCC mix. Superplasticizers too improve these properties. Hence they shrink on water loss either due to surface evaporation or temperature gradient due to hydration (temperature difference in top and middle layers of mixes). Therefore fiber addition is brought into SCC mixes, as has already been described because of their beneficial effect. Various studies have been conducted to study the influence of fibres' addition on the SCC mixes along with the factors involved.

Hossain et al. [59] studied the influences of fiber types/size/dosages and fiber combinations (used in hybrid mixes) on fresh (slump flow, L-box passing ability, V-funnel flow time and segregation index - a measure of workability) and rheological (viscosity and yield stress at various time intervals ranging from 10 to 70 minutes) properties based on experimental results. The workability/rheological properties of concrete mixtures are found to depend on types/dosages/geometry of fiber and in case of hybrid mixtures; interaction and synergic properties between different fiber types also played a critical role. The maximum dosage of PVA is limited to 0.125% compared to 0.3% of metallic ones in developed FRSCC mixtures due to PVA's higher workability reduction/viscosity increase capability. Study indicated that a homogenous fiber distribution can be obtained up to a critical fiber content and once that is surpassed, a stiff structure of the granular skeleton make self compaction impossible as has been proved in the study by Grunewald & Walraven [49]. The optimization of fresh and rheological properties of FRSCC is essential in order to ensure better mechanical and durability characteristics in the hardened state. It is important for FRSCC to have low yield stress and optimal viscosity to ensure required flowability and to prevent segregation.

Following conclusions are drawn from the study:

i) In general, slump flow and L-box passing ability decreased and V-funnel time increased with the increase fiber volume in the developed concrete mixtures. PVA fiber showed distinguished higher influence on slump flow spread, V-funnel flow time and L-box passing ability (a measure of workability) compared to metallic ones for the same fiber dosage. With respect to control mix: (a) a maximum slump flow reduction of about 45% is observed with PVA compared to 19% of metallic ones, (b) a maximum V-funnel flow time increase of 132% is observed with PVA compared to 92% of metallic ones and (c) a maximum reduction of up to 61% is observed for L-box passing ability due to the addition fiber.
ii) The use of short metal fiber improved workability of concrete mixtures compared to longer ones. This is attributed to the fact that the longer fiber can have more detrimental interference with the aggregates and can obstruct the flow more than short fibers.

iii) At a constant fiber volume: (a) both PVA and metallic fibers produced lower plastic viscosity compared to control mix (no fiber), (b) metallic fiber produced higher (1.3 to 1.8 times) plastic viscosity compared to PVA at 10, 40 and 70 minutes, however, rate of increase decreases with time.

iv) Generally, the plastic viscosity/yield stress increases with the increase of PVA/metallic/hybrid fiber volume and elapsed time. Compared to control mix, yield value (at 10 minutes) of metallic fiber mixes significantly increased (97 times) with the increase of fiber volume of up to 0.3%. For the similar dosage, the increase in yield value for metallic fiber is also significantly higher (14 times) compared to PVA. Increase of viscosity due to increase of PVA fiber is higher compared to metallic ones. Long metallic fiber also produced higher (30 to 50%) viscosity compared to short metallic fiber.

v) Higher workability reduction/viscosity increase of PVA concrete mixtures compared to metallic ones limits the maximum dosage of PVA fiber to 0.125% compared with 0.3% of metallic fiber to achieve a FRSCC mixture. Both metallic and PVA fiber showed similar trend of variation.

Cunha et al. [31] presented and discussed experimental results of both straight and hooked-end steel fibers pullout tests on a self-compacting concrete medium. It is found that the maximum pullout load had an almost linear increase with the embedded length for both hooked and straight fibers. However, this increase is more significant on the straight fibers, since the pullout response of hooked fibers, regardless the fiber embedded length, is predominantly influenced by the mobilization and straightening of the fiber hooked-end. Regarding the effect of the fiber orientation angle, the maximum pullout load increased up to an inclination angle of 30° and then decreased for a 60° inclination angle. For both hooked and straight fibers the highest maximum pullout load is observed for an inclination angle of 30°.

Pareira et al. [129] prepared a steel fiber reinforced self compacting concrete (SFRSCC) mix and tested it for mechanical properties. Contradicting the design guidelines of normal SCC, more than 600 Kg/m^3 of powder content is used in the preparation of mix. Binder

powder preparation was considered first step in design mix steps followed by aggregate quantity determination and; mixing proportions of powder & aggregates was third step.

Kim et al. [69] experimentally investigated the properties of self-flowing concrete containing fly ash, in which flow was >600 mm and compared with those of ordinary concrete. It was found that volume ratio of coarse aggregate-to-concrete greatly influenced flowability and workability. Self-flowing concrete also had good mechanical properties at both early and late ages with compressive strength reaching as high as 40 MPa at 28 days, for maintained w/binder ratio (at different superplasticizer content). The creep of self-flowing concrete investigated was greater than that of ordinary concrete at early ages, and drying shrinkage was much higher.

2.2.5 Conclusion from the Studies

It was concluded from these studies that replacement of cement with fine material cause increase in creep and shrinkage since both of these depend upon the pore structure of hydrated mortar paste. Hence a material is required which could solve the purpose of filler as well as a fiber. As a fiber it would reduce shrinkage along with providing tensile strength & toughening. Both paste constitution and aggregate proportion ratio; and combination of both these materials in mix are important parameters controlling behaviour of SCC. Therefore care must be needed for attaining the optimum quantities of both.

3. EXPERIMENTAL PROGRAM AND TEST PROCEDURES

3.1 GENERAL

In order to achieve the set objectives of the present investigation, efforts have been made to conduct the laboratory tests systematically by dividing into six broad categories as explained below. This chapter entails about the sample preparation and testing procedure in addition to experimental program.

1. Investigation on ordinary Portland cements & mineral admixtures.
2. Investigation of mineral aggregates to judge their suitability for use in self compacting concrete (SCC).
3. Investigation of paste's properties with or without mineral admixtures.
4. Investigation of mortar matrix with or without mineral admixtures.
5. Investigation of self compacting concrete made with mineral admixtures and normal concrete.
6. The real potential of SCC has been analysed by constructing & testing on the prototype pavement in the laboratory

A. Investigation on OPC & mineral admixtures.

Following are the tests conducted in the laboratory:

(i) Fineness
(ii) Particle size analysis through Laser diffraction technique.
(iii) Surface area analysis using Blaine's and BET air permeability apparatus.
(iv) Consistency and setting time
(v) Soundness
(vi) Specific gravity
(vii) Chemical composition analysis using X ray fluorescence spectrometry

B. Investigation on mineral aggregates

Mineral aggregates collected from the local query were subjected to the following tests to judge its suitability for use in SCC:

(i) Aggregate gradation (particle size distribution)
(ii) Shape test
(iii) Aggregate impact value
(iv) Aggregate crushing value
(v) Los Angeles abrasion value
(vi) Specific gravity and water absorption

C. Investigation on paste properties with or without mineral admixtures

To understand the behaviour of concrete it is imperative to acquaint ourselves with the structure of hydrated hardened cement paste. Keeping the necessity of this study in mind, the following tests have been performed in the laboratory:

(i) Compatibility test between cement, mineral admixtures and superplasticizer
(ii) Quantitative phase analysis of hydrated paste using XRD technique
(iii) Surface morphology of hydrated paste using SEM

D. Investigation on mortar matrix with or without mineral admixtures

Realizing the important role of mortar matrix in the hardened concrete, efforts have also been made to conduct the following tests:

(i) Flow test
(ii) Compression test
(iii) Flexural test
(iv) Splitting tensile test
(v) Modulus of elasticity
(vi) Abrasion resistance test
(vii) Rate of water absorption

(viii) Coefficient of sorptivity

E. Investigation on normal concrete and self compacting concrete with admixtures

The following tests were conducted to study the behaviour of normal concrete and self compacting concrete with admixtures, in the fresh and hardened state:

(i) Slump flow test
(ii) V funnel test
(iii) J Ring test
(iv) Probe ring test
(v) Compression test
(vi) Splitting tensile strength test
(vii) Flexural strength test
(viii) Modulus of elasticity test
(ix) Restrained ring shrinkage test
(x) Chloride ion penetration test
(xi) Permeability test

F. The real potential of SCC has been analysed by constructing a prototype in the laboratory to simulate the rigid pavement field conditions. Plate load test was performed to compare the three prototypes, namely: non rehabilitated pavement, normal concrete rehabilitated pavement and fiber reinforced concrete rehabilitated pavement for the following parameters:

(i) Load transfer efficiency
(ii) Fatigue life
(iii) Cost analysis

Since the mechanical tests like compression strength test, flexural strength test, splitting tensile strength test and modulus of elasticity have the same procedure for mortar and concrete, therefore in order to avoid repetition, the tests on mortar and concrete have not been discussed separately under the individual headings of mortar and concrete. Instead, the tests have been discussed under the heading “mortar and concrete” altogether, and wherever

a test has been performed specifically for mortar and not concrete, then it has been mentioned on the heading itself.

3.2 MATERIALS USED

3.2.1 Cement

Ordinary Portland cement 43 grade conforming to IS: 8112 was used as a binder in presence of water. Cement used in the present study was further tested for ascertaining its physical properties such as, fineness, specific surface area, soundness, consistency, setting times, and specific gravity. IS: 4031 (Part 1) guidelines were followed for determining the fineness of cement by dry sieving. Also, fineness was measured for cement and other admixtures by laser particle diffraction technique. Ankersmid laser diffractometer was used for this purpose. The particle size analysis of cement is necessary to determine the reactive power of cement along with the pore size distribution of the matrix.

This study is based on the principle of Laser diffraction given by Fraunhofer, which states that the intensity of light scattered by a particle is directly proportional to the particle size. When a laser beam passes through a dispersed particulate matter, then it diffracts on collision with it. The angularity of diffraction depends upon the size of particle, if the size is bigger than the angle of diffraction relative to the beam is small, and vice versa. It measures particle sizes ranging from nanometres to millimetres in size. In this experiment laser made of He-Ne gas is passed through the particulate solution and later condensed by a lens, which refracts the light on sensors. The schematic diagram of laser diffraction and testing apparatus of Ankersmid Laser diffraction based particle size analyzer used in the present investigation are shown in Fig 3.1 (a) & (b) and Plate 3.1 respectively.

IS: 4031 (Part 2) guidelines were followed for determining the specific surface areas of cement by using Blaine’s air permeability apparatus. Plate3.2 shows the photograph of Blaine’s air permeability apparatus. Specific surface area is a measure of water adsorption tendency of a fine particle in the wet matrix. It also indicates the reactive power of the particle. The more is the specific surface, more is the tendency of a particle to react and vice versa. The specific surface is increased if the given mass of a particle is crushed to smaller size; it even increases with the porosity of the particles.

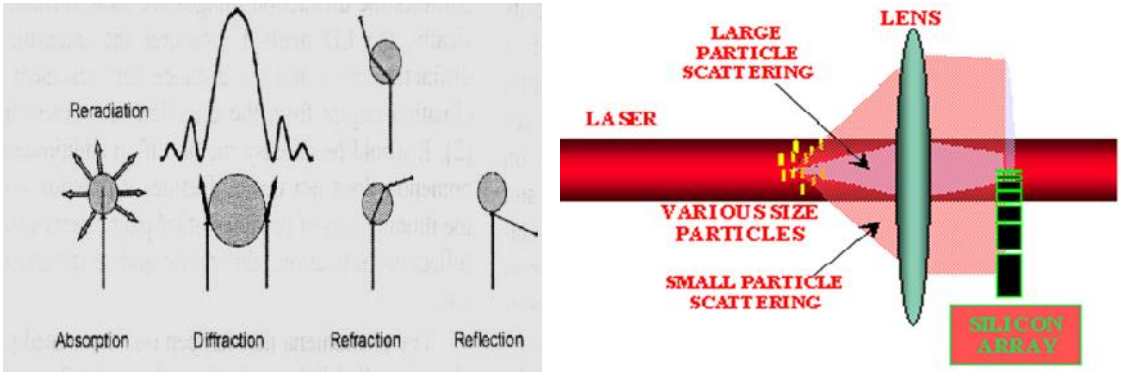

Fig 3.1 (a) Interaction forms of radiation with matter & (b) Schematic diagram of laser diffraction

Plate 3.1 Ankersmid laser diffraction based particle size analyzer used in the study

Plate 3.2 Blaine's air permeability apparatus

3.2.1.1 Normal consistency

The normal consistency test of cement gives a measure of the water requirement of the cement paste to achieve a workable consistency. IS: 4031 (Part 4) guidelines were followed for determining the normal consistency of cement. Further carrying over the testing part to the initial setting time and final setting time determination, IS 4031 (Part 5) guidelines were followed to perform the test for measuring the required properties. Vicat's apparatus having a movable weight of 300 gm was used for finding out the normal consistency, initial setting time & final setting time. A plunger as shown in Fig 3.2, is used for penetrating inside the pastes made of cement, with and without admixtures, whereas a needle of cross sectional area 1sq. mm is used for performing initial setting time test. Normal consistency is given by that water content, at which the Vicat's plunger of dimensions 10 mm diameter and 50 mm height, is just able to penetrate to a depth of 33-35 mm from the top of specimen. Initial setting time is that time when the needle is able to penetrate to the same from top in a time of 5 seconds, when released smoothly after being touched at the surface. For final setting time test an annular attachment having a needle at bottom and thicker diameter plunger at its top is used. This is shown in the form of enlarged view of needle, in Fig. 3.2. The final setting time is said to be achieved when the needle penetrates, but the plunger is able to make only an impression on the paste.

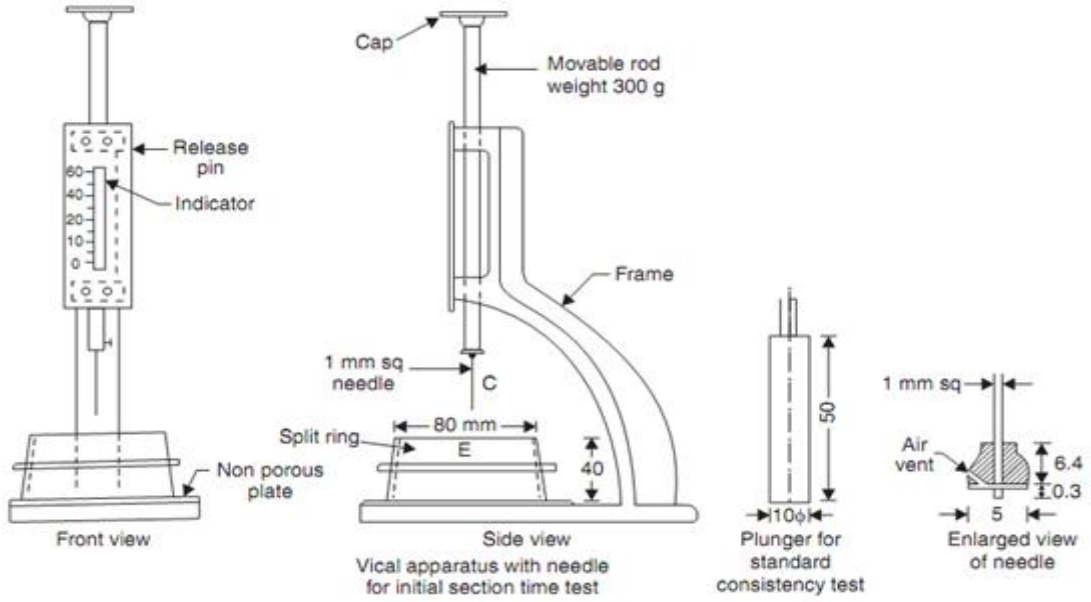

Fig. 3.2 Schematic diagram of Vicat apparatus showing attachments

Plate 3.3 Normal consistency test done on Vicat's apparatus

3.2.1.2 Setting times

Initial setting time gives an indication of the time when the cement starts losing its plasticity and the water content in the pore solution starts getting yield strength. Cement does not gain strength at this stage. Finals setting time is the time when cement has fully lost its plasticity and has acquired stiffness. At this stage cement starts gaining strength and beyond this stage the drying shrinkage of cement binder in mortar and concrete matrix starts. Hence finding out these values is very important.

3.2.1.3 Soundness test

Soundness of cement was determined by following the guidelines given in IS: 4031 (Part 3). It indicates the expansion tendency of cement due to the presence of free lime in it. The test is performed with Le Chateleir apparatus as is shown in Fig. 3.2. The apparatus consist of a small split cylinder of brass or other metal. It is 30mm in diameter and 30 mm in height. On the other two sides of split are attached two indicator arms 165mm long with pointed ends. Cement gauged with water at 0.78 times the normal consistency is filled into the mould and covered with glass Plates from both sides. The whole assembly is put inside the water, at a temperature of 27 degree celsius for 24 hours. After that the distance between the arms is noted. Later on the specimen with assembly is put inside boiling water for about

25-30 minutes and kept boiling for 3 hours. Then the mould is removed, cooled and the distance between arms is again noted. The soundness is then given by the difference in the distance between the arms before and after the boiling of the specimen. A soundness value less than 10 is desirable as per codal recommendations for a cement to be fit for construction purpose. This test is performed for atleast two samples of binder.

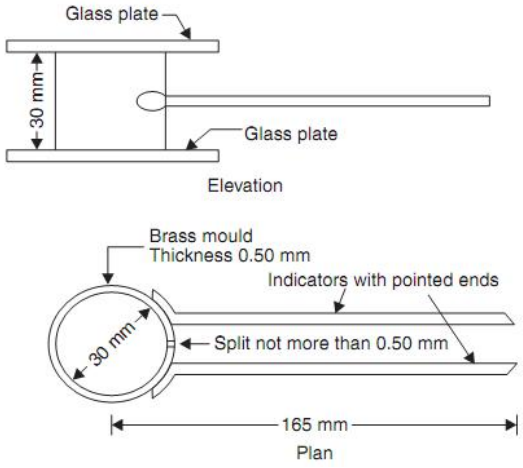

Fig. 3.3 Schematic diagram of le chatelier apparatus for measuring soundness

3.2.1.4 Specific gravity of cement

IS:4031 (Part 11) codal provisions were followed to find out the specific gravity of cement. A graduated apparatus was used, filled with kerosene and cement was used for finding out the rise in kerosene height. This enabled to determine the volume of cement for a given mass of cement. The specific gravity was thus determined by dividing the volume by mass of cement. Specific gravity of cement is necessary not only in the mix design of concrete but, it also helps in determining the flow of self compacting concrete. Fig. 3.4 shows the Le Chateleir apparatus used for conducting the test.

The experiment is conducted at a constant temperature of 27 degrees Celsius. The kerosene or other liquid which do not mix with cement is filled in the flask so that the level of liquid lies between 0 and 1 graduation. Afterwards the flask is put inside the water bath to maintain a constant temperature of liquid at 27 degrees Celsius. The flask is then taken out, and 64 gm cement is filled in it very neatly so that it does not touch the neck of the apparatus. After filling the cement, the level of liquid shall rise to graduations as marked in

the apparatus starting from 18 and forward. The flask is then again put inside the water bath until constant temperature of 27 degree Celsius is not achieved. The density is then evaluated as the ratio of mass of cement by the volume measured in terms of height difference between the graduations of the flask. Atleast two samples of the cement were taken to avoid errors evolved on basis of temperature difference or wrong filling technique.

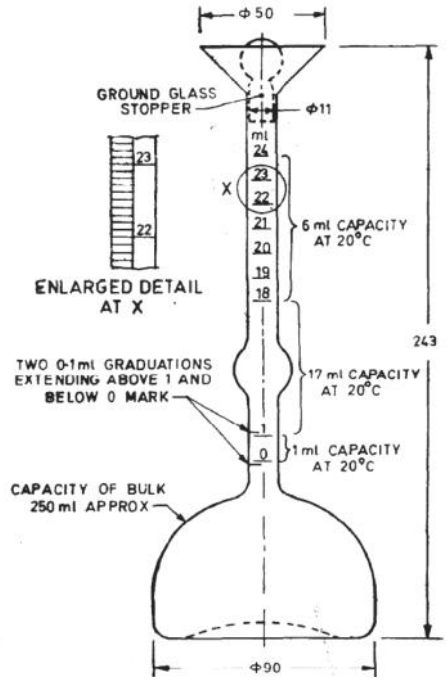

Fig. 3.4 Schematic diagram of le chatelier apparatus for measuring specific gravity

Efforts have been made to determine the chemical properties of all considered mineral admixtures including ordinary Portland cement. Chemical property of a material signifies the quantity of various kinds of chemical compounds present in a material. This test was performed for cement and admixtures used in the present study, as per the codal recommendations of IS: 12803: 1989, IS 4032 and IS 1727, using an X ray fluorescence spectrometer.

The formation of active and inert phases in a certain material depends upon the presence of chemically reactive compounds and it is the presence of active phases which enables the material to react during the hydration process. Generally, glassy and amorphous states are active while crystalline state is inert. All active phases are rich in silica. The crystalline state mainly consists of lime. Wollastonite which is calcium meta silicate is an

inert crystalline material containing nearly equal proportions of silica and lime. Hence, this strongly hinted that a certain state may show different chemical compounds bonded together to constitute amorphous, crystalline or glassy state.

Massazza F. [94] had also affirmed that the amount of combined slaked lime in the pore solution essentially depends on the following:

a) The nature of the active phases
b) Their content in the pozzolan
c) Their SiO_2 content
d) The slaked lime-pozzolan ratio of the mix

The first three points are related with the chemical composition of pozzolans. Another reason to study the chemical composition is the tendency of a pozzolan to prevent expansion caused by siliceous water absorbing and expanding gel caused by alkali silica reactivity. Though the present study has not measured the expansion of concrete, as expansion joints are provided in concrete pavements to take care of this factor, it is imperative to testify the role of chemical properties, whenever a new admixture is incorporated.

3.2.2 Admixtures

Wollastonite micro fiber (WMF) having average length of 0.03mm, diameter 1.82μ and thus an aspect ratio of 16.5 was selected and incorporated in concrete/mortar by part replacing the OPC to judge the potential of this material with respect to the cement. Its efficiency to impart flow to SCC was also checked, because of the fact that wollastonite micro fiber being treated as a fiber and a Class F pozzolana. Other than wollastoite micro fiber (WMF), flyash (F) and microsilica (S) were also considered in the present investigation to study the rheological characteristics in the fresh state and behavioural effect of SCC mix on admixing of these aforesaid pozzolans, when they are incorporated individually or in combination. Physical properties such as specific gravity, bulk density & fineness of F, WMF and S were determined in accordance with IS: 4031 Part (1-11). Specific surface area of F, WMF & S was measured using ASAP 2020 Micrometrics BET's surface area analyzer by the method of nitrogen adsorption. The instrument set up is shown in Plate 3.4.

Chemical analysis for oxide composition of OPC, WMF, FA and SF were determined in accordance with IS: 3032 and IS 1727, respectively.

Plate 3.4 BET air permeability apparatus

Also, particle size analysis was carried out using laser based particle size analyzer. The instrument set up is shown in Plate 3.1.

In addition to above studies mineralogical analysis of hydrated pastes was performed by X ray diffraction test. In an X ray diffraction measurement, a crystal is mounted on a goniometer and gradually rotated while being bombarded with X rays, thus producing a diffraction pattern. Every crystal has its own diffraction pattern, which depends upon diffracted X rays caused by the atomic spacing of different layers within it.

Bragg's law states that the wavelength of incident X rays is directly proportional to the d spacing (layers' atomic spacing) and angle of diffraction θ (theta) of the diffracted rays, where N is an integer.

$$N\lambda = 2d(\sin\theta)$$

Fig 3.5 shows the diffraction phenomenon with respect to d and θ, and Plate 3.5 shows the X ray diffraction test under progress in the laboratory.

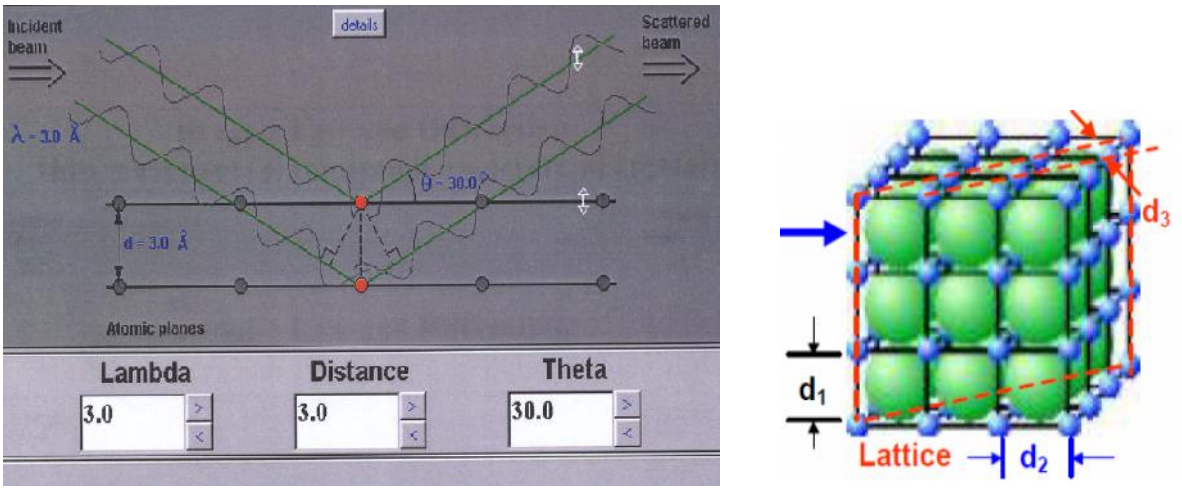

Fig 3.5 (a) Diffraction angle of x ray with respect to wavelength; (b) d spacing in a crystal

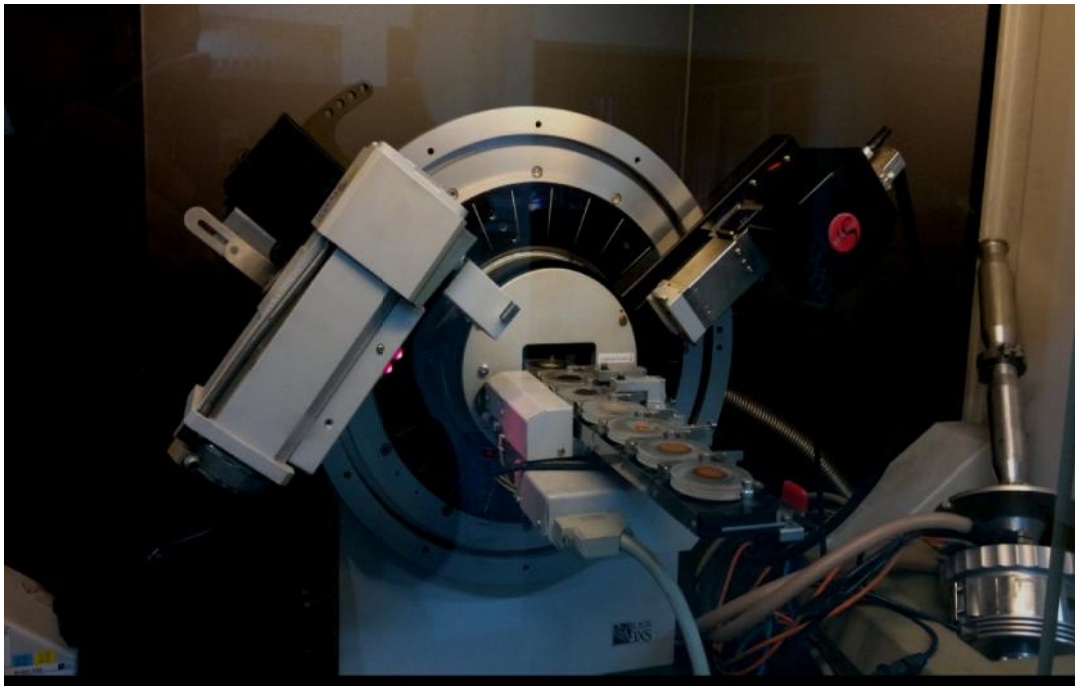

Plate 3.5 X-Ray diffraction test in progress at the laboratory

The diffraction pattern as well as its intensity helps in determining quantitatively, the minerals present in hydrated paste. Each compound has its own diffraction pattern. The quantitative analysis works by matching simultaneously the diffraction pattern of different possible hydration products with the observed pattern such that the combined correlation

coefficient of all matching is as least as possible. The program XPERT HIGHSCORE was used to do the quantitative analysis of processed profile.

Following steps were followed while conducting the quantitative analysis of minerals:

a) The first step is “intensity scale”, which finds the scale of intensity of different possible patterns, from the observed diffraction data.
b) In the second step, the background of prototype patterns and observed pattern is matched.
c) This is followed by zone shifting in which the patterns are matched for lateral shift in their peaks.
d) In the fourth step the peaks are matched for their shape parameters.
e) The fifth step consists of matching the peaks for their half width.

Generally peaks overlap after the fifth step. The coefficient of correlation for weighted profile (Rwp) has approached nearly to the possible coefficient of correlation (Rp) at this step, while descending down in each step. But still if the peaks do not overlap then there is possibility for other steps namely “z and w width”, “preferred orientation of peak” etc. In present analysis, the peaks overlapped after half width reduction.

Microstructural features of the hardened pastes were also studied using scanning electron microscope (SEM) technique. This test was performed to analyze the morphology of various hydration products formed at 7 days for paste mixes. The knowledge of crystal shape, intensity on grey scale and size helps in determining them. Six types of hydration products were analyzed and confirmed from the images which were obtained as a result of secondary electron emission, when an electron beam collides elastically with an atom of a compound. The electrons are generally absorbed at the inner face of a compound but are reflected from its surface. These electrons thus help in determining the topography of a compound, i.e. whether it is amorphous, platy, acicular, hexagonal, rhombohedral or prismatic in shape.

The six compounds analyzed are C-S-H (calcium silicate hydrate, which is mainly found in two types at this duration, poor fibrous structure and plane flaky structure), ettringite (calcium alumino tri sulphate hydrate found with fine needle structure), calcium

alumino mono sulphate hydrate (hexagonal di hydroxide double layered structure having greyish white colour), wollastonite micro fiber (calcium meta silicate having acicular or needle structure, with white colour intensity lesser than ettringite) and slaked lime (calcium hydroxide having hexagonal structure with high intensity white colour). Plate 3.6 shows the scanning electron microscope used for obtaining the images.

Plate 3.6 Scanning electron microscope used to obtain SEM images

The results obtained from the test were found to be in acceptance with results obtained from X-Ray diffraction test.

To evaluate the compatibility of cement & admixed slurries with superplazticizers, Marsh cone test was performed according to ASTM D 6910. The test measures the viscosity of slurry mix (946 ml) in the form of time (seconds) taken to flow from Marsh funnel into a graduated cup. Plate 3.7 shows the Marsh funnel/cone employed in the present investigation.

This test enables to ascertain the optimum dosage of a superplasticizer for cement slurry. The optimum dosage is that dosage of superplastcizer, beyond which there is no change in flow time of cement slurry when it is made to flow through a conical apparatus, with an aperture of 5 mm. Since a superplasticizer works mainly on the cement slurry, the predominance of supplementary cementitious materials on slurry flow at their higher content was expected and had to be checked.

Initially study was conducted for a water-cementitious material ratio of 0.35 as normal concrete mix for PQC was to be designed. Total 45 mixes were considered for compatibility study including control mix. Water- cementitious material ratios of 0.3 and 0.4 were chosen other than 0.35. Flow times for various mixtures were noted and graphical plots were drawn connecting Marsh cone time in seconds and dosages of superplasticizer.

The dose at which the Marsh cone time is lowest is considered a saturation point, the complete set up of Marsh cone apparatus and slurry mix preparation are shown in Plate 3.7 (a) & (b), respectively.

Plate 3.7 (a) Marsh cone test apparatus & (b) Slurry mix under preparation

3.2.3 Aggregates

Natural dolomite aggregates collected from Delta were used as coarse aggregates. River bed sand collected from the local basin was used as fine aggregate for preparing concrete.

The gradations of coarse aggregates and fine aggregates were carried out in accordance with IS: 383. Materials conforming to this particular codal specification were used in the present research work. In order to collect better information about these aggregates, it was imperative to conduct a few laboratory tests on these aggregates in the laboratory. Physical properties such as specific gravity, bulk density, water absorption, crushing value, aggregate impact value, shape parameters and moisture content etc. were determined in accordance with IS 2386 in relative parts. Shape tests were performed on the aggregates to find out their suitability for concrete work. Flaky aggregates led to non homogeneity in the mix and have

lesser strength. Elongated aggregates led to the accumulation of water below them, thus making the interfacial transition zone weaker and also may cause segregation.

In order to assess the mechanical and durability properties of aggregates, following studies were carried out:

(i) Aggregate impact test

(ii) Aggregate abrasion value test

(iii) Aggregate crushing value test

The tests related to mechanical properties of the aggregates were conducted in accordance with IS: 2386 (Part-4).

Desired combined gradation was established by blending different sizes of aggregates after using their respective individual gradations.

3.3 TRIAL MIXES

Since the number of mixes was more, they have been designated according to constituent material content. Binary mixes have been designated as CW1-CW3 for three percentage substitution (10%-30%) with wollastonite and flyash mixes as CF1-CF3 for three percent substitution with flyash. For ternary mixes the designations have been done in group of four mixes, having same wollastonite or flyash content. Thus wollastonite mixes have been designated as CWS1-CWS4, CWS5-CWS8 and CWS9-CWS12 for three percentage substitutions of wollastonite and four percentage substitutions of microsilica. Likewise, flyash ternary mixes have been designated as CFS1-CFS4, CFS5-CFS8, and CFS9-CFS12. In case of combined mixes the designations have been done on the basis of flyash or wollastonite content, which varies from 5%-10%. It was decided that the alphabet representing material of quantity 5% would be in lowercase and that for 10% would be in upper case. As the case in binary mixes, the microsilica content will decide the numeral suffix. For example; the mix with 5% wollastonite and 10% flyash and 2.5% microsilica is designated as CwFS1. In all subsequent testing this designated has been followed. Table 3.1 shows the various mixes, their designation, and the percentage of each material in the mix.

For ternary combinations studies the mixes were prepared in such a way that wollastonite and flyash had same replacement levels, but along with it microsilica was added maximally up to 10% in intervals of 2.5% respectively for both wollastonite and flyash. Hence testing was performed on 12 ternary mixes of C-F-S as well as C-W-S.

Combined mixes were made to judge two things: a) whether the flyash-wollasonite combination can produce self compacting concrete b) which combination would dominate F-S or W-F; or W-S in the strength, durability and water requirements of a SCC mix. The mixes were produced in such a way that in no case, the microsilica may exceed the quantity of either the flyash or the wollastonite in the mix. the quantity of flyash and wollastonite was varied in intervals of 5%, with maximum substitution level of 10%.

Table 3.1 Mixes chosen for the tests and their material composition

Mix	Percentage of material in mix				Paste Composition
Designation	Cement	Flyash	Wollastonite	Microsilica	C+F/WMF+S
C	100	-	-	-	100
W	-		100	-	100
F	-	100	-	-	100
M0	-	-	-	100	100
CW1	90	-	10	-	90+10
CW2	80	-	20	-	80+20
CW3	70	-	30	-	70+30
CWS1	87.5	-	10	2.5	87.5+10+2.5
CWS2	85	-	10	5	85+10+5
CWS3	82.5	-	10	7.5	82.5+10+7.5
CWS4	80	-	10	10	80+10+10
CWS5	77.5	-	20	2.5	77.5+20+2.5
CWS6	75	-	20	5	75+20+5
CWS7	72.5	-	20	7.5	72.5+20+7.5
CWS8	70	-	20	10	70+20+10
CWS9	67.5	-	30	2.5	67.5+30+2.5
CWS10	65	-	30	5	65+30+5
CWS11	62.5	-	30	7.5	62.5+30+7.5
CWS12	60	-	30	10	60+30+10
CF1	90	10	-	-	90+10
CF2	80	20	-	-	80+20
CF3	70	30	-	-	70+30
CFS1	87.5	10	-	2.5	87.5+10+2.5
CFS2	85	10	-	5	85+10+5
CFS3	82.5	10	-	7.5	82.5+10+7.5
CFS4	80	10	-	10	80+10+10
CFS5	77.5	20	-	2.5	77.5+20+2.5
CFS6	75	20	-	5	75+20+5
CFS7	72.5	20	-	7.5	72.5+20+7.5

CFS8	70	20	-	10	70+20+10
CFS9	67.5	30	-	2.5	67.5+30+2.5
CFS10	65	30	-	5	65+30+5
CFS11	62.5	30	-	7.5	62.5+30+7.5
CFS12	60	30	-	10	60+30+10
Cwf	90	5	5	-	90+5F+5W
CwfS1	87.5	5	5	2.5	87.5+5F+5W+2.5S
CwfS2	85	5	5	5	85+5F+5W+5S
CWf	85	5	10	-	85+5F+10W
CwF	85	10	5	-	85+10F+5W
CwFS1	82.5	10	5	2.5	82.5+10F+5W+2.5S
CWfS1	82.5	5	10	2.5	82.5+5F+10W+2.5S
CwFS2	80	10	5	5	80+10F+5W+5S
CWfS2	80	5	10	5	80+5F+10W+5S
CWF	80	10	10	-	80+10F+10W
CWFS1	77.5	10	10	2.5	77.5+10F+10W+2.5S
CWFS2	75	10	10	5	75+10F+10W+5S
CWFS3	72.5	10	10	7.5	72.5+10F+10W+7.5S
CWFS4	70	10	10	10	70+10F+10W+10S

3.4 MORTARS AND CONCRETE

Ordinary concrete requires external compaction work by internal or external vibrators for proper compaction, filling of the form work and covering of the reinforcement. Proper SCC fulfils atleast the same quality level but with no vibration work. SCC compacts itself automatically by its own weight, in order to achieve a very effective SCC, the friction between the particles has to be reduced at the same time as satisfying stability of the fresh concrete has to be maintained. Keeping these requirements in view, efforts were initially made to establish a referral normal concrete designed for a characteristics flexural strength of 4.5 MPa in accordance with IRC: 44-2008. From here on, numbers of trial mixes were established by changing the powder composition and accordingly reducing the coarse aggregates to fine aggregate ratio. To reduce the friction between the particles and thereby increase the deformability, high range water reducer, or so called superplasticizer was utilized. Also, to control the stability and avoid concrete segregation, very fine powder of WMF, flyash and microsilica was introduced by partly replacing the cement as well as sand. In order to increase the viscosity of the SCC mix, viscosity modifying agent (VMA) was also introduced. Table 3.2 entails the details of the concrete mix ingredients adopted for normal concrete for PQC slab.

Table 3.2 Mix design of normal PQC

Mix design for Normal M-40 concrete used to derive SCC for rehabilitation as per IRC 44				
Cement	Sand	Coarse aggregates	Water	Nominal MSA=16mm
450	711	1057	165	Superplasticizer 0.3% ~1.23lt/cu m.
1	1.58	2.35	0.36	
		20mm 10mm		CA:FA=60:40
		740 317		C.A :- 20mm:10mm=70:30
Assuming that 20% cement reduction takes place on addition of superplasticizer				

Several trials were made to achieve satisfactory SCC mix presented in Fig 3.6 below.

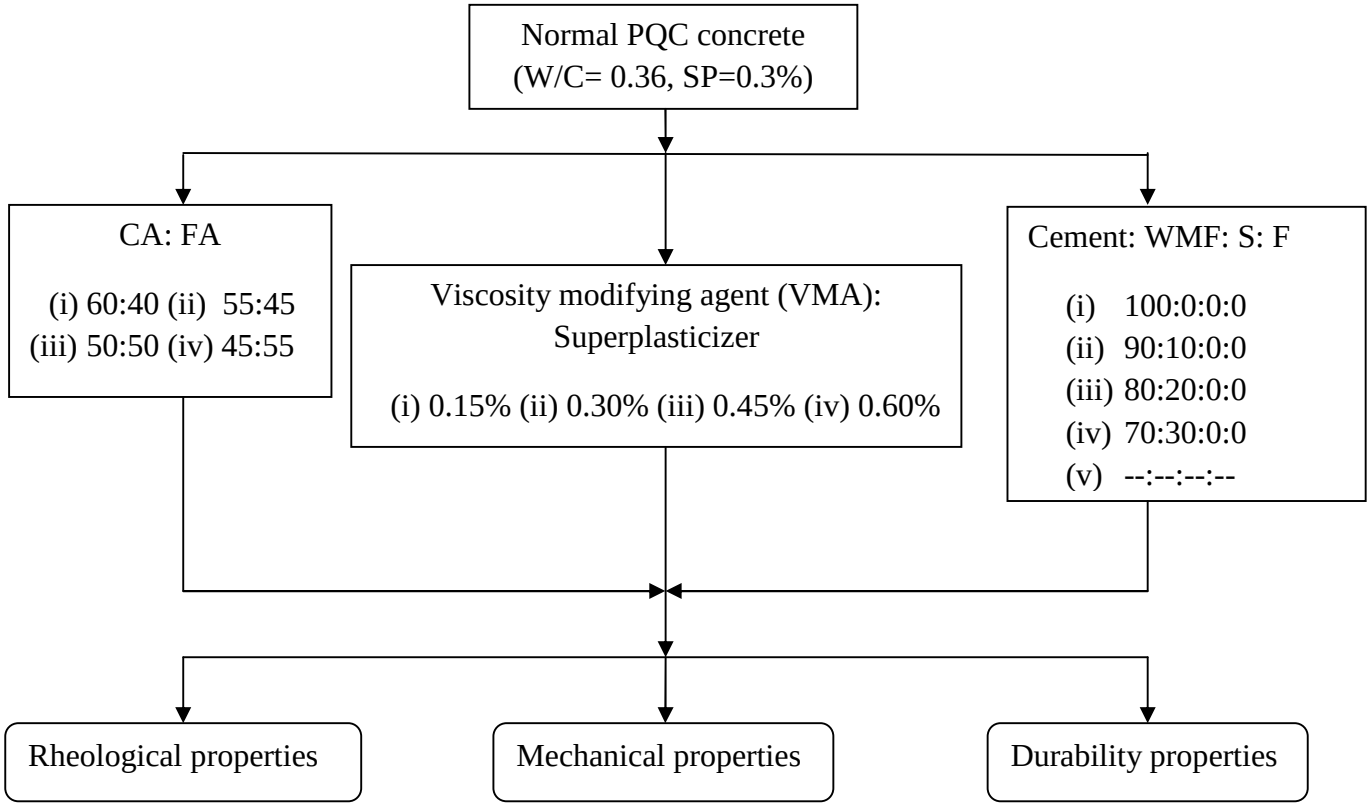

Fig. 3.6 Procedure followed to obtain SCC from normal pumpable PQC

Fig. 3.7 depicts how the constituent materials and their properties typically differ between SCC and conventional concrete. The main difference is that the amount of gravel in SCC is reduced due to their acquired increased amount of powder. The ratio between paste (i.e.

water, cement & powder) and aggregates (i.e. sand and gravel) is smaller for conventional concrete in comparison to SCC.

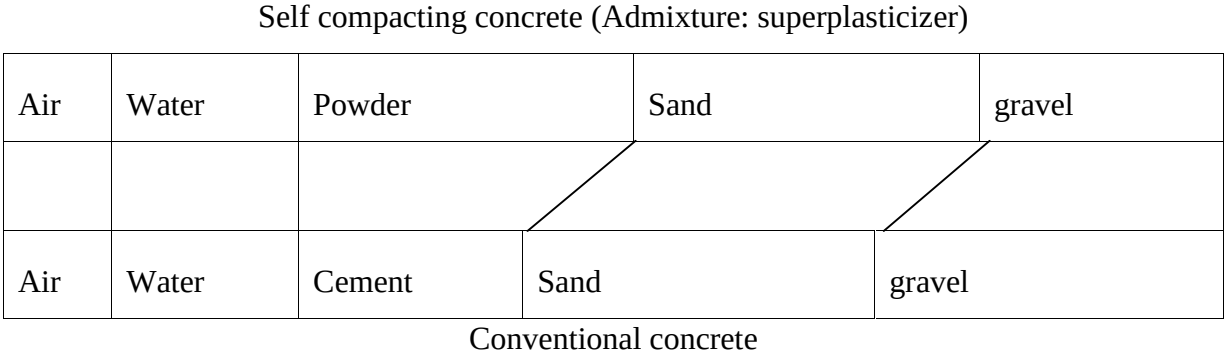

Fig 3.7 Proportions of constituent materials of SCC versus conventional concrete

3.4.1 Fresh State Tests

The fresh state tests are conducted on both mortar and concrete mixes. For mortar, specifically flow test is conducted, whereas in case of a self compacting concrete (SCC), fresh state tests like Abram's flow test, V funnel test, J ring test, L box test, U box test and Probe ring test are conducted to check the rheology of the mixes. In the present study only Abram's flow test, V funnel test, J ring test and Probe ring test have been performed. L box test and U box test measure the passability of SCC, which in present study has been checked through J ring test. Hence, these two tests have not been conducted.

Realizing the fact that shrinkage characteristics of the concrete are significant factors in the design of PQC mix as it affects the degree to which the concrete changes in volume over time, changes in dimensions of PQC slab due to shrinkage effect and temperature differential needs a careful examination to prevent from damage of PQC slab before design life.

The hardening of large and open areas of PQC causes cracks due to plastic and drying shrinkage. To some extent plastic shrinkage would be controlled by providing proper curing, whereas for drying shrinkage it may have to alter the morphology of the concrete matrix. In order to evaluate the shrinkage effect on admixing of WMF, F & S, restrained

shrinkage test has been adopted in the present investigation. The details of the test are presented in the forthcoming paragraphs under the heading of fresh state tests.

3.4.1.1 Flow test on mortar

After getting the knowledge regarding the flow of slurries with or without superplasticizers, the tests are conducted to find the interaction of sand in conjunction with paste, as far as the flow of mortar is considered. This is important because sand plays an important role to provide flow to the pastes, but excess sand in concrete may cause loss of homogeneity, and thus makes cohesion less concrete. Hence, this test has been conducted to find the optimum amount of sand for a given powder material. Normally, for a self compacting concrete, the volume of sand is nearly half of the volume of mortar, therefore, undermining the effect of sand on the behaviour of mortar would be a big mistake.

There are a lot of tests, mainly vibratory, to measure the rheological properties of the concrete mixtures quantitatively. These are; compaction test, power remoulding test, Vee Bee consistometer test, etc. These tests simulate more to the behaviour of mortar used in normal cement composite, where the compaction energy used is considerable. For a self compacting concrete, where the impact or vibration energy is negligible, a mortar having the tendency to flow with minimal effort (when superplasticizers are not added) must be designed. Hence for testing the rheological behaviour of mortar in this study, flow test is performed according to ASTM C 1437. The flow Table consist of a top disc, raised on a shaft such that it could be lifted to 0.5” and dropped when a pulley attached to the shaft is rotated. The top has a diameter of 10”. Both the shaft and the top are cast of rigid iron. A hollow cone is used to place the requisite mortar on the top, which is cast of bronze or brass. The cone has 2.75” and 4” as the dimensions of upper and lower diameters.

In this test the freshly mixed mortar mixes are placed inside the cone shaped mould in two layers. Afterwards, the mould is slowly removed and the vibrating table, over which the mould is placed, is dropped 25 times in 15 seconds. Flow F is then calculated as the average percentage increment of four diameters of the sample, such that the diameter is recorded in millimetres. For each mix two samples are tested. Plate 3.8 shows the lab moments when the test was conducted on mortar.

Plate 3.8 Flow test apparatus with mortar on disc top

3.4.1.2 Slump Flow Test for SCC

The basic equipment used is the same, as that for the conventional slump test. The only difference is, that the diameter of the spread of the 6 litres concrete sample is measured, i.e., a horizontal distance as against the vertical slump reading in the conventional test. While measuring the diameter of the spread, the time that the sample takes to reach a diameter of 500 mm (T50) is also sometimes measured. The slump flow test can give an indication about the filling ability of SCC and an experienced operator can also detect an extreme susceptibility of the mix to segregation. The diameters of upper and lower base of cone are 100mm and 200mm and their height difference is 300mm. Plate 3.9 shows the various images taken whilst the test was being conducted in the laboratory to check the flowability of SCC. For comparison purpose, the flow of normal concrete mix is also presented along the side of SCC mix.

Plate 3.9 Flow test on normal concrete (L.H.S.); and a trial mix (R.H.S)

3.4.1.3 V-funnel Test for SCC

The V-funnel test was developed in Japan and used by Ozawa, et al [123]. The equipment consists of a V-shaped funnel as shown in Fig 3.18. The funnel is filled with concrete (12 litre) and the time taken by it to flow through the apparatus is measured. This test gives account of the filling capacity (flowability). Segregation resistance for flow is measured as the time taken for flow of sample which is allowed to fall after five minutes of refilling the V funnel. The inverted cone shape shows any possibility of the concrete to block; is reflected in the result.

Plate 3.10 V Funnel used for checking the flow time and segregation resistance of SCC

3.4.1.4 J Ring Test for SCC

This test was developed in the University of Paisley. The main purpose of performing this test is to measure the passing ability of the SCC.

For this measurement, the ring consists of vertically aligned bars through which the concrete is supposed to flow. The bars act as a source of hindrance to the free flow of concrete. Hence the spacing between centre to centre of bars is most important factor controlling the flow, which is decided to be taken as three times the diameter of the maximum nominal size of aggregates present in the SCC.

The ring is 300 mm in diameter and the height of the ring due to vertical placement of bars is 100 mm. Plate 3.11 shows the various images taken during the performance of the J Ring test in the laboratory. Table 3.3 shows the guidelines suggested by EFNARC [36] to check the properties of SCC as per the test requirements.

The experiment for this test requires Abrams cone too. The Abrams cone is first placed inside the ring on a flat surface and 6 litres of SCC is filled in it. Afterwards the SCC is allowed to flow freely when the cone is slowly lifted up. The SCC flows through the bars' spacings, but owing to the hindrance imposed by bars a height difference is created in the SCC at the front and behind the bars. This height difference is an indicator of the passing ability of the SCC.

Table.3.3 EFNARC[36] specified requirements for mix design of SCC

	Method	Unit	Typical range of values	
			Minimum	maximum
1	Slump flow by Abram's cone	mm	650	800
2	T50 slump flow	sec	2	5
4	V funnel	sec	6	12
5	Time increase, V Funnel at t= 5min	sec	0	+3

Plate 3.11 J Ring test conducted in laboratory to check the passability of SCC

3.4.1.5 Probe test for SCC

The segregation probe, inspired by the penetration apparatus method, is a fast and effective method to measure the thickness of mortar/paste at the top of fresh SCC. A thicker layer of mortar/paste at the surface corresponds to a lower static stability. The results of the segregation probe method and the measured thickness of the mortar/paste layer in hardened concrete are found to be quite similar. The segregation probe is a 5 in. diameter ring connected with a 6 in. high rod marked with scale. Plate 3.12 shows the probe ring placed on the SCC and Fig. 3.8 shows the schematic diagram of the probe ring. The whole probe is made of 1/16 in. diameter steel wire. The total weight of the probe is about 18 g. Before the test, fresh concrete is cast into a 6 × 12 in. cylinder with one lift. The concrete is allowed to rest for 2 min. before the test, during which excessive disturbance is avoided. The

segregation probe is then placed gently on the concrete surface allowed to settle for 1 min. The penetration depth marked on the rod is used to determine the stability rating in accordance with the specifications presented in Table 3.4. The segregation probe test is simple and rapid and thus is suitable for quality control and other applications such as robustness measurement. Due to its high flowability, SCC is much more susceptible to stability problem than normal concrete. Small changes in moisture content of aggregates or dosage of admixtures may affect the fresh properties significantly. It is thus important to examine the robustness of SCC to ensure it is within the capabilities of the concrete producer.

Plate 3.12 Probe Ring test to check the segregation resistance of SCC

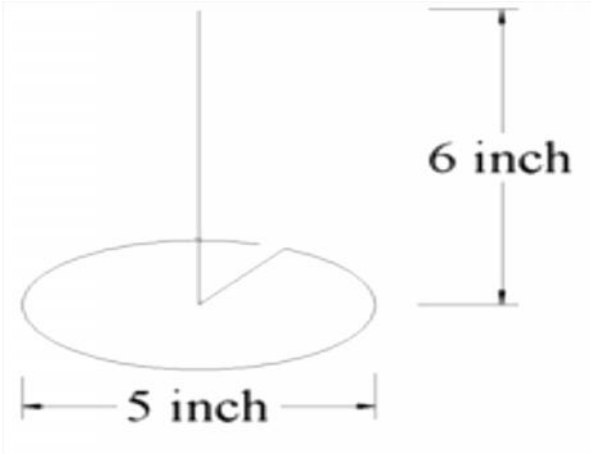

Fig 3.8 Schematic diagram of probe ring

Table.3.4 Stability rating for penetration probe method

Penetration depth (mm)	Rating	Corresponding rating in
<4	0 stable	0 stable
4~7	1 stable	1 stable
7~25	2 unstable	2 unstable
>25	3 unstable	3 unstable

3.4.1.6 Restrained ring shrinkage test for SCC

This test is carried out according to the specifications of ASTM C1581, using a 50 mm thick concrete specimen, 150 mm in height, cast around a steel ring of 25 mm thickness and 300 mm outside diameter. A sample of freshly mixed concrete is compacted in a circular mould around the steel ring.

The compressive strain developed in the steel ring caused by shrinkage of the mortar or concrete specimen is measured from the time of casting. Cracking of the test specimen is indicated by a sudden decrease in the steel ring strain. The age at cracking and the rate of tensile stress development in the test specimen are indicators of the material's resistance to cracking under restrained shrinkage.

Structural steel pipe with a wall thickness of 13 mm, an outside diameter of 330mm and a height of 150 mm are taken. Strain gauges are used to measure the strain development in the inner steel ring at an interval of not more than 30 minutes.

The specimen and ring are transported to an environmental chamber where conditions are maintained at 22°C and 50% RH. After bringing the test specimen to the testing environment, the bolts of the inner ring are loosened. After 2 minutes of loosening the bolts the strain gauge is connected to the data acquisition system. Daily visual inspection is conducted for each specimen. Fig. 3.9 depicts the ring and microscope setup & Plate 3.13 shows the test photographs accrued form the laboratory whilst the test was under progress. Two specimens are tested for each mix.

At the end of curing period, which is generally 24 hours or the time when final setting of the concrete has taken place, the outer ring is removed. The upper concentric space thickness of specimen is coated with epoxy substance so as to disallow evaporation of

water through it. The time when first strain reading is obtained after the coating procedure, is called as the time of initial strain. Then the cracking time is measured as the time duration between the time of initial strain and the time when there is a sudden decrease in the strain (beyond 30 microns). The cracking age or (elapsed time at cracking) is reported to the nearest 0.25 day. If a specimen does not fail in this duration, then the age of termination of the experiment is reported.

From the strain- time variation average strain rate is recoded which yields average stress rate by the equation 3.1 as follows:

$$£_{net} = \sim \times \sqrt{t} + k \qquad (3.1)$$

$£_{net}$ = net strain, m/m.

α = strain rate factor for each strain gage on the test specimen (m/m)/day$^{1/2}$

t = elapsed time, days, and

k = regression constant

The stress rate is calculated from the strain rate by the equation 3.2 as follows:

$$q = \frac{G \times \sim_{avg}}{2 \times \sqrt{t_r}} \qquad (3.2)$$

Where,

q = stress rate in each test specimen, MPa/day,

G = 72.2 GPa,

$| \sim_{avg} |$ = absolute value of the average strain rate factor for each test specimen, (m/m)/day$^{1/2}$

and, t_r = elapsed time at cracking or elapsed time when the test is terminated for each test specimen, in days.

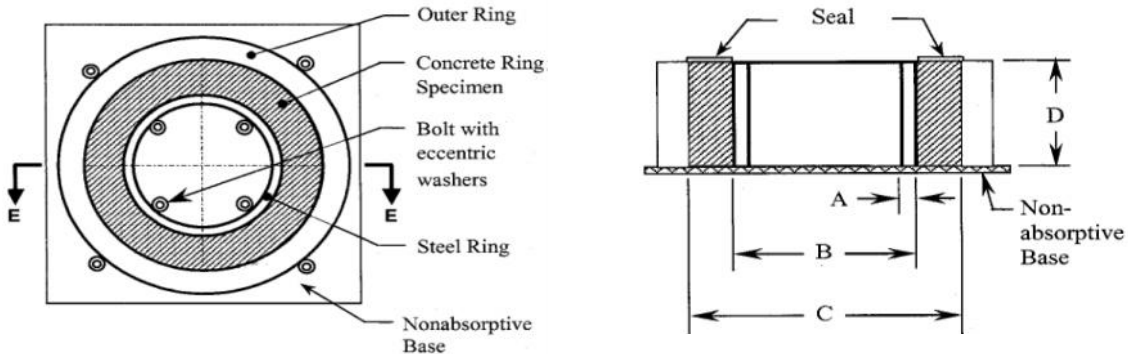

Fig.3.9 Schematic diagram of restrained ring shrinkage apparatus

Plate 3.13 Ring shrinkage test

3.4.2 Hardened State Tests

For hardened state, test specimens consist of 100×100×100 mm cubes, 150×150×150 mm cubes, 150×300 mm cylinders, 100×100×500 mm prisms, and 100×50 mm cylindrical discs. The cubes and cylinders are used for compressive, splitting tensile strength and abrasion resistance test respectively; the prisms are tested for flexural strength, and the cylindrical discs are used for water absorption tests. 100×100×100 mm cubes are used for testing mortar mixes whereas 150×150×150 mm cubes are used for concrete. Plate 3.14 shows the photographs of various types of specimens made for testing the mortar and concrete mixes. Compressive strength of mortar & concrete were determined by testing three cubes for each mix, after 7, 28, 60, 90 days of curing for concrete and 28 days of

curing for mortar. In case of splitting tensile strength test, three cylindrical specimens were tested for each mix, at 7, 28, 60, 90 days for concrete and 30 days for mortar. The flexural tensile strength test was performed with three prismatic specimens for each mix at durations of 7, 28, 60, 90 days for concrete, and 30 days for mortar. Modulus of elasticity for mortar was found out using three cubes for each mix, tested after 30 days for mortar, while modulus of elasticity for concrete was found out by testing two cylinders for each mix after the durations of 28 days. Abrasion resistance was determined, such that three cubic samples for each mix of mortar were available for testing at the age of 30 days.

Durability tests like rate of water absorption & sorptivity were conducted after 30 days in the present study. the duration of only 30 days was selected because after such duration the capillary voids in the cement composites get transformed into gel pores on account of continuous hydration process going on in the mixes. This results in very low values, and thus would require larger test durations and could generate error. For these tests, circular disc specimens were tested after 7, 28 and 60 days of curing. Permeability test was conducted after 30 days, with three cylindrical specimens for each mix of concrete. For chloride ion penetration test, two cuboidal specimens of size 100×100×300 mm were cast for each mix, and three specimens were extracted in the form of core from each cuboid, such , that in total six specimens were tested after 28, 60 and 90 days of curing in the chloride water.

Plate 3.14 Photographs of samples prepared in the laboratory for different tests

The prisms are cast using Plexiglas moulds. After casting, the specimens are stored at room temperature for 24 hr. They are covered with plastic sheets to minimize evaporation loss. After 24 hr, the specimens are removed from the moulds and cured for 7, 28, 60 and 90 days in a room maintained at 100 percent relative humidity and a temperature of 22°C. The various hardened state tests conducted on a cement composite are summarized below:

3.4.2.1 Compressive strength test

Compressive strength is the most accepted property of a cement composite to evaluate its quality, because most desirable characteristics of a cement composite are qualitatively related to its compressive strength. The compressive strength gives an idea regarding the compactness of a cement composite. If well compacted, a cement composite produces higher strength and resists aggressive environment in better way. Strength of a cement composite depends upon bond at aggregate-binder surface and in the binder itself. Presence of flyash, microsilica and fibers influence the compressive strength of a cement composite by changing the above mentioned factors.

Compressive strength of a cement composite can be measured by cubes or cylinders. Cubes are common in India and its testing is easier, while cylinders have true compaction zone, which is free from lateral effects of friction due to Platens. In addition to the size and shape of the specimens, rate of loading, thickness and attachment of Plates in the testing machine, plainness of end surfaces cylinder specimen, dryness of specimen etc. also affects the test results. During compression a linear compressive strain and a lateral tensile strain is developed in the specimens and a cement composite fails due to limiting strain in tension at circumference. In the present study all specimens are kept in air for small time before testing, to attain saturated surface dry condition.

In the laboratory compressive strength test was carried out on a hydraulically operated Amsler compressive testing machine of 200 ton capacity (Plate 3.15). Calibration of the machine was done at regular intervals by standard proving ring. This test was conducted as per the specifications of IS: 516:1959. Rate of loading equal to 140 kg per sq. cm. per minute is maintained in compression test. Cubes are tested after 30 days, 60 and 90 days of curing. Direction of loading is kept perpendicular to the casting surface of the cubes.

The maximum load is recorded and compressive strength is taken equal to maximum load divided by cross sectional area of the specimen.

Plate 3.15 Photographs of Compressive strength test accrued from the laboratory

3.4.2.2 Splitting tensile strength test

Pavement quality concrete is normally not designed to resist direct tension but the knowledge of tensile strength is of value in estimating the load under which the crack will develop. The absence of cracks is of considerable importance in maintaining the life of the structures especially in rigid pavements. An appreciation of the tensile strength of a cement composite helps in understanding the behaviour of dowel and tie bars' reinforced concrete, even though the actual design calculations do not take the tensile strength into account. A direct application of the pure tensile force, free from eccentricity is difficult. Therefore no standard test using direct tension is available. The most common and recommended indirect methods are split tensile strength test and flexural tensile strength test.

In this test a cement composite's cylinder is placed horizontally between the Platens of compressive testing machine and load is applied along the generatrix of cylinder. Every element on the vertical diameter of the cylinder is subjected to a vertical compressive stress and a horizontal tensile stress. Split tensile strength of the a cement composite is equal to horizontal tensile stress at the failure of the specimen. Due to development of high compressive stress at the top and bottom contact lines, a narrow strip of packing material is required between the cylinder and Platens. Testing without such packing reduces the observed strength for same a cement composite. the split tensile strength test is simple to perform and gives more uniform results, than other tension tests.

The strength determined in the split tensile strength test is believed to be closer to the tensile strength of a cement composite, than the modulus of the rupture. Slight rotation of Platens from a plane perpendicular to the axis of cylinder, affects the test results and should be avoided. The split tensile strength is carried out as per the specifications of IS 5816-1999 on the same compression testing machine (Plate 3.16). The cylindrical specimen is placed horizontally between two Platens, with care to avoid rotation of the Platens. Load is applied at a uniform rate of 0.2 kg per sq. mm. per minute. Split tensile strength of a cement composite is calculated from eq. 3.3 as:

$$\pm_{sp} = \frac{2P}{\circledR LD} \tag{3.3}$$

where P is failure load, L is the height of the cylinder and D is the diameter of the cylinder.

Plate 3.16 Splitting tensile strength test

3.4.2.3 Flexural strength test

Flexural tensile strength test is another indirect test method for tensile strength of a cement composite in which a prism of plain mortar/concrete is subjected to flexural loading. Modulus of rupture is the theoretical maximum tensile stress reached in the bottom fiber of the prism and calculated with the assumption of linear stress distribution on cross section of prism at failure, however actual stress distribution is parabolic. Hence, the modulus of rupture overestimates the tensile strength of a cement composite and gives higher value than would be obtained in splitting tension test. Another possible reason for higher value is, under split test entire section of the specimen is subjected to the maximum stress while in flexural test maximum stress is developed only at the bottom most layer.

The flexural strength test simulates the field condition of rigid pavements, where vehicular load along with stresses caused by temperature differentials in the pavement, cause maximum tensile stresses at the bottom of the pavement. Value of modulus of rupture of a cement composite is influenced by the dimensions of the prism, placing of beam with respect to its casting direction, and on arrangement of loading, like central point loading or third point loading. The third point loading gives lower and more accurate value in comparison to the central point loading arrangement.

Flexural strength test was conducted in the laboratory as per the specification of IS 516:1959 (Plate 3.17). Hydraulically operated universal testing machine of 10 ton capacity is used in the present study. Prism specimens of 100×100×500 cu.mm. size are tested at 400 mm c/c span, on two steel rollers of 38 mm diameter.

Third point loading method is adopted where two concentrated loads are placed at each third points of supporting span. Load without shocks is applied at uniform rate of 180 kg per minute, up to the failure. According to the distance of the crack from the support to the bottom face, the modulus of rupture of a cement composite is calculated either from Eq 3.4 or 3.5.

$$\pm_b = \frac{PL}{bd^2}, \text{ if a is greater than 13.3 cm} \qquad (3.4)$$

$\pm_b = \frac{3PL}{bd^2}$, if a is lesser than 13.3 cm but greater than 11 cm (3.5)

where P is failure load, l is the length of span, b is the width of prism, d is the depth of the prism and a is the distance between line of fracture and nearest support on the tension side.

Plate 3.17 Flexural tensile strength test conducted on prismatic specimens

3.4.2.4 Modulus of elasticity test

Non linear relation between stress and strain is well known for a cement concrete. In spite of non linearity, the elastic modulus of a cement concrete is considered in determination of stress and deflection. For a mortar, the modulus of elasticity has been

determined so as to check and compare the influence of aggregates on the modulus of elasticity of self compacting concrete (which contains lesser volume of aggregates).

Modulus of elasticity of a cement concrete is defined in a somewhat arbitrary manner. Under uni-axial compression, three modulus namely tangent modulus, secant modulus and chord modulus have been reported in literature. All these forms represent the static modulus of elasticity of a cement composite. There is an another type of modulus of elasticity, called as dynamic modulus of elasticity.

For testing the modulus of elasticity of mortar mixes in present study, the dynamic modulus of elasticity has been chosen which is generally higher than static modulus of elasticity obtained from loading of specimens. Equation 3.6 gives the relation between static and dynamic modulus of elasticity as follows:

$$E = 0.83E_d \tag{3.6}$$

The ultra sonic pulse velocity method is used for measuring the dynamic modulus of elasticity of mortar. In this test an ultrasonic pulse is generated by an electro-acoustical transducer. The pulse travels through the mortar and undergoes several reflections at the boundaries of the different material phases (air, mortar and aggregate) within the composite. Thus, a system of stress waves is developed which includes longitudinal (compressive), shear (transverse) and surface (Rayleigh) waves. The receiving transducer detects that longitudinal wave which is the fastest. Since the velocity of pulse does not depend upon the geometry of the material through which it passes, therefore pulse velocity method is advantageous in investigating structural composites. Plate 3.18 shows the photos of the test conducted at the laboratory on dry specimen. The dynamic modulus of elasticity is evaluated from the pulse velocity by the relationship as given in equation 3.7:

$$E = \frac{°(1+«)(1-2«)V^2}{(1-«)} \tag{3.7}$$

Where, E= dynamic Young's modulus of elasticity in MPa, P= density in kg/sq.m., V= pulse velocity in m/sec and μ = dynamic Poisson's ratio; its value varies from 0.20 to 0.35, with 0.24 as an average.

Plate 3.18 Laboratory procedure of determining static & dynamic modulus of elasticity

3.4.2.5 Abrasion test for mortar

Abrasion test was performed as per IS: 9284-1979. In this test an abrasive sand charge (4000g), passing 1mm and retained on 0.5 mm sieve is stroked with a 10 cm a cement composite cube specimen. A pneumatic hollow needle with an arrangement for striking charge from a height of 50 mm, with an air pressure of 0.14 N/mm^2 is used. Two impressions (at 2.5 cm each from edge) are made on a single face by rotating the sample at 180°. The abrasion resistance is measured as the inverse of loss in weight of sample. Plate

3.19 shows the various specimens tested in the laboratory for abrasion loss and the test being whilst being conducted at the laboratory.

Plate 3.19 Abrasion test conducted on cubical mortar specimens

3.4.2.6 Rate of water absorption and sorptivity coefficient test

Water absorption is defined as, the process whereby the concrete takes in a fluid to fill spaces within the materials. Effective porosity of the concrete is measured by water absorption.

For measurement of rate of water absorption ASTM C 1585-11 is to be followed. The standard test specimen is a 100 +/- 6 mm diameter disc, with a length of 50 +/- 3 mm.

Fig 3.10 shows schematic diagram of water absorption test apparatus and Plate 3.20 shows the photograph of the samples being submerged partially in the laboratory whilst the test was being conducted.

The average test results of at least 2 specimens constitute the test result. Test specimens after curing period of 7, 28 and 56 days, are placed in the environmental chamber at a temperature of 50 +/- 2°C and RH of 80 +/- 3 % for 3 days. Alternatively, test specimens are placed in a desiccators, inside an oven at a temperature of 50 +/- 2°C for 3 days. If the desiccator is used, relative humidity in the desiccator is controlled with a saturated solution of potassium bromide, but the test specimens are not allowed to contact the solution.

After 3 days, each specimen is placed inside a sealable container. A separate container is used for each specimen. Precautions must be taken to allow free flow of air around the specimen by ensuring minimal contact of the specimen with the walls of the container. The container is stored at 23 +/- 2°C for at least 15 days before the start of the absorption procedure.

The specimen is removed from the storage container and the mass of the conditioned specimen is recorded to the nearest 0.01 g before sealing of side surfaces. Mass of the sealed specimen is measured to the nearest 0.01 g and recorded as the initial mass for water absorption calculations. The support device is placed at the bottom of the pan and the pan is filled with tap water so that the water level is 1 to 3 mm above the top of the support device. The water level is maintained at 1 to 3 mm above the top of the support device for the duration of the tests.

The mass of the samples is to be recorded at start, after 1, 5, 10, 20, 30 and 60 minutes. The actual time shall be recorded to within +/-10 s. The measurements are to be continued every hour, +/- 5 min, up to 6 h, from the first contact of the specimen with water and the time to be recorded within +/-1 min. After the initial 6 h, measurements are taken once a day up to 3 days, followed by 3 measurements at least 24 h apart during days 4 to 7; a final measurement that is at least 24 h after the measurement at 7 days is taken. For each mass determination, the test specimen is removed from the pan, the timing device is stopped

if the contact time is less than 10 min, and any surface water is blotted off with a dampened paper towel or cloth. After blotting to remove excess water, the specimen is inverted so that the wet surface does not come in contact with the balance pan (to avoid having to dry the balance pan).Within 15 sec of removal from the pan, the mass is measured to the nearest 0.01 g. The specimen is immediately replaced on the support device and the timing device is started.

The absorption, I, is the change in mass divided by the product of the cross-sectional area of the test specimen and the density of water. For the purpose of this test, the temperature dependence of the density of water is neglected. The units of I are mm and is given by equation 3.8 as follows:

$$I = \frac{mt}{ad} \tag{3.8}$$

where:

I = the absorption, m = the change in specimen mass in grams, at the time t, a = the exposed area of the specimen, in mm^2, and d = the density of the water in g/mm^3.

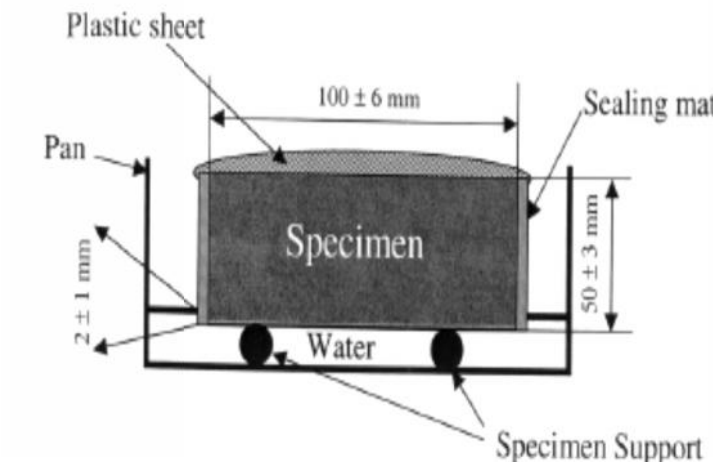

Fig. 3.10 Schematic diagram of water absorption test apparatus

Coefficient of water absorption is considered as a measure of permeability of a cement composite. This is measured by determining the rate of water uptake by drying a cement composite cylindrical specimen in a period of 1 h. The cement composite specimens

are preconditioned by drying in an oven at 105°C for seven days until constant weight is reached and then allowed to cool in a sealed container for three days. The sides of the specimen are coated with transparent epoxy resin, and placed partially immersed in water to a depth of 3 mm at one end, and at the other end a loosely attached plastic is secured with a rubber band. The quantity of water absorbed (Q) is calculated for about 5 days or until the specimen registers constant weight, which happens earlier.

In the present study the coefficient of water absorption (K) was calculated for 7, 28 and 56 days of moist curing and is determined using the equation 3.9 as follows:

$$K = \frac{I}{\sqrt{t}} \tag{3.9}$$

Where I is the water absorption as calculated before and t is the elapsed time after dipping of the specimen in water.

Plate 3.20 Water absorption test conducted at the laboratory

3.4.2.7 Permeability test

Permeability is defined as the flow property of a porous medium, which characterizes the ease with which a fluid will pass through it, under the action of a pressure differential. The movement of various kind of fluids through concrete takes place not only by the flow through the porous system but also by diffusion and absorption. Diffusion is the movement of fluid under a concentration gradient where as absorption is due to capillary suction.

The diffusion in this study has been measured by a test known as chloride ion penetration test; also absorption potential of concrete is found by rate of water absorption/sorptivity tests. These tests have been discussed also.

Micro cracking has its locus at the interface zone. Therefore it may not be absurd to consider the interface zone role in influencing the permeability of concrete. However, L.A. Larbi [77] found, that despite the higher porosity of the interface zone, the permeability of the concrete is controlled by the bulk of the hardened cement paste, which is the only continuous phase in the concrete. Support to the Larbi's view is lent by the fact , that the permeability of the hardened cement paste is not lesser than that of concrete made with a similar cement paste. Hence, in the present study, the permeability of concrete has only been found out, and has been supposed , that in any case the permeability of concrete would be equal to or higher than the permeability of corresponding mortar mixes..

The test has been carried out as per specifications of IS: 3085-1965 and has been discussed as follows:

The apparatus consists of permeability cells, water reservoirs and pressure lines. The water reservoir is filled with a graduated side arm gauge glass. Heavy duty armoured hose is used for high pressure connections. Each of the three reservoirs is calibrated under the operating pressure of 10 kg/sq cm. the specimens are thoroughly cleaned to remove all dirt. The end faces of the specimens are lightly chiselled. The specimen is placed at the centre of the cell, with the lower end resulting on the ledge. The annular space between the specimen and the cell is caulked to a depth of about 10 mm using a cotton cord soaked in molten wax. The rest of the space is filled with molten wax, levelled with the top of the specimen. Care is

taken to refill any drop in the level due to cooling of the wax. After this, the funnel is placed in the position and the cell assembly is connected to the water reservoir. The test setup is shown in Plate 3.21. The air bleeder valve, the valve between the reservoir and the cell, and the drain cock are opened and the water is allowed to enter the reservoir. The drain cock is closed when the water passed freely through it and the water reservoir is filled. The reservoir water inlet and air bleeder valves are then closed. Then the test pressure of 10 kg/sq cm is applied to the water reservoir and the initial reading of the gauge glass is recorded. Containers are placed under the cells to collect the water percolating through the specimens. In the beginning, the rate of water intake is larger than the rate of outflow. As the steady state is reached, the two rates became equal and the outflow stabilized. The test is continued for about 100 hours after the steady state is reached. The coefficient of permeability is calculated by equation 3.10 as follows:

$$K = \frac{Q}{AT\left(\frac{H}{L}\right)} \tag{3.10}$$

Where;

K = coefficient of permeability in cm/sec;

Q = quantity of water in millilitres percolating over the entire period of test after the steady state has been reached;

A = area of the specimen face in cm^2;

T = time in seconds over which Q is measured; and

H/L = ratio of the pressure head to thickness of specimen, both expressed in the same units

Plate 3.21 Permeability test being conducted at the laboratory

3.4.2.8 Chloride ion penetration test

Chloride ion penetration test determines the penetration of chloride ions into concrete from a solution of sodium chloride. Capillary absorption, diffusion and hydrostatic pressure are the factors which are responsible for the penetration of chloride ions into a concrete; but diffusion, which is the movement of chloride ions under a pressure gradient is the most suitable and easy method for testing the pore structure or thereby the durability of concrete. The rate of ingress of chloride ions into concrete depends upon its pore structure which is affected by various factors like materials, construction methods and age. Also pore structure is affected by water cement ratio and inclusion of supplementary materials. The ingress of chloride ions into concrete leads to its long term deterioration. As the chloride ions penetrate into the concrete the ph value (hydrogen ion concentration) of concrete decreases due to increment in acidic content, caused by absorption of hydrogen ions by chloride ones. A coating on the steel bars, which is strong under the basic environment, starts degrading due to transitioned acidic environment. This is called as depassivation of steel and causes the reinforcing bars to corrode under the effect of oxygen and moisture.

In this test, the specimens are kept in the solution fully immersed for the durations, for which the results are sought to provide better and uniform conditions for all specimens,

for the diffusion of chloride ions. ASTM C1543-10a guidelines have been followed for ponding procedure of the test specimens. Fig 3.11 shows the diagrammatic view of the ponding of a concrete specimen. Plate 3.22 shows a couple of images from the laboratory, when the test is being conducted. It shows the ponding of samples, extracted cores and their testing in laboratory with chemicals.

The test method given in IS 14959 Part-2 is followed to find out the water soluble chloride ions present in the concrete specimens. Three cores of equal diameter and length (diameter generally taken as 3 times the aggregate size) are taken out from three equilateral locations of the cuboidal specimens. These are later crushed & grounded after sieving off the aggregates from the crushed cores. The powder material (1 kg) is used and mixed with silver chloride (0.02N), and then titrated with ammonium thiocyanate (0.02N). The end point of titration is given the turning of white solution into faint reddish brown coloured solution. Generally the test results are more accurate if the samples are tested for a long duration i.e. 90 days.

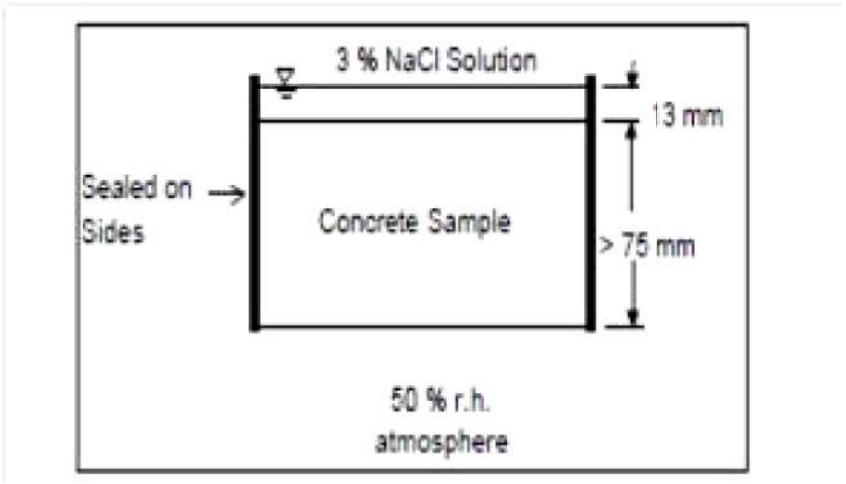

Fig 3.11 Schematic diagram of ponding of concrete specimens

Plate 3.22 Chloride ion penetration test conducted on grounded cylindrical specimens

3.5 PROTOTYPE CONSTRUCTION AND FEM MODELING

The Finite Element Method (FEM) analysis done in this study takes advantage from the fatigue life equation given in IRC 58, for various kinds of roads. This equation involves two independent variables: stress ratio and probability factor. For highways and expressways, the fatigue life has been suggested on the basis of these two variables, in the equation 3.11 and 3.12, and 3.13, as follows:

$$\text{Log}_{10} N_r = \left(\frac{0.9781 - SR}{0.0828}\right), \quad \text{For SR>0.55} \tag{3.11}$$

$$N = \left(\frac{4.2577}{SR - 0.4325}\right)^{3.268}, \quad \text{For SR between 0.45 and 0.55} \tag{3.12}$$

$$\text{Stress ratio SR} = \frac{\text{Stress caused at load level r}}{\text{Modulus of rupture of concrete}} \tag{3.13}$$

3.5.1 Prototype Construction

The prototype construction has been divided into following three steps:

(i) Mix design of the PQC as per IRC 44, for a standard load distribution as per IRC 58

(ii) Design of the dowel bars

(iii) Construction of DLC and PQC

(iv) Curing and sawing of PQC at joints during sawing window

3.5.1.1 Mix design for PQC

The mix design of PQC was done for a non pumpable condition. No superplasticizer or mineral admixture was incorporated to be a part of the mix design. The mix was designed as per IRC 44, for a 28 days target compressive strength evaluated on the basis of design flexural strength of 4.5 MPa. Table 3.5 shows the details of the mix, designed for the requisite flexural strength. Coarse aggregate to fine aggregate ratio was chosen to be approximately 60:40.

Table 3.5 Mix design of PQC

Mix design for Normal M-40 concrete used to derive SCC for rehabilitation as per IRC 44				
Cement	Sand	Coarse aggregates	Water	Nom. MSA=16mm
450	711	1057	165	Superplasticizer 0.3% ~1.23lt/cu m.
1	1.58	2.35	0.36	
		20mm 10mm		CA:FA=60:40
		740 317		C.A :- 20mm:10mm=70:30
Assuming that 20% cement reduction takes place on addition of superplasticizer				

After designing the mix, other details regarding the design of pavement and joints was taken over. Firstly, the pavement thickness was evaluated on the basis of an axle load distribution. The axle load distribution has been provided in Table 3.6. The pavement was designed as a four lane divided highway, with two lanes in each direction, and for a design life of 30 years. The lane width was taken as 3.5 m and transverse joint spacing of 4.5 m was chosen. A traffic of 2000 commercial vehicles per day in each direction, in the year of completion of construction was assumed. The percentage of front single axle, rear single axle and rear tandem axle was taken as 50%, 30% and 20% respectively. The percentage of commercial vehicles with spacing between the front axle and the first rear axle less than 4.5 m was taken as 50 percent. It was also assumed that both day time and night time traffic volumes are equal. Front (steering) axles were not included in the design and average number of axles per commercial vehicle were taken as 2.0. Apart from this, other design details used are as following:

(i) Modulus of elasticity of concrete, MPa: 30000
(ii) Thickness of dry lean concrete subbase, mm: 100
(iii) Effective modulus of subgrade reaction of foundation, MPa/m: 300
(iv) Unit weight of concrete, kN/cum: 24
(v) Radius of relative stiffness, m: 0.69265
(vi) Poisson’s ratio: 0.15
(vii) Shoulders tied condition: NO
(viii) Dowel bars in transverse joints: YES
(ix) Average annual rate of growth of commercial traffic: 0.075
(x) Load transfer efficiency factor: 0.66

Table 3.6 Axle load distribution taken for the design of pavement

Axle Load Spectrum Data								
Rear Single Axle			Rear Tandem Axle			Rear Tridem Axle		
Load Group (kN)	Load (kN)	Freq-uency (%)	Load Group (kN)	Load (kN)	Freq-uency (%)	Load Group (kN)	Load (kN)	Freq-uency (%)
185-195	190	0.64	380 - 400	390	2.14	530-560	545	0
175-185	180	0.8	360 - 380	370	2.14	500-530	515	0
165-175	170	0.8	340 - 360	350	2.14	470-500	485	0
155-165	160	2.58	320 - 340	330	2.14	440-470	455	0
145-155	150	2.58	300 - 320	310	4.28	410-440	425	0
135-145	140	5.8	280 - 300	290	4.28	380-410	395	0
125-135	130	5.8	260 - 280	270	12.86	350-380	365	0
115-125	120	11.82	240 - 260	250	12.86	320-350	335	0
105-115	110	11.82	220 - 240	230	10.72	290-320	305	0
95-105	100	12.9	200 - 220	210	10.72	260-290	275	0
85-95	90	12.16	180 - 200	190	7.14	230-260	245	0
< 85	80	32.3	< 180	170	28.58	< 230	215	0
		100			100			0
Front Single Axles and Rear Tridem axles not considered for bottom-up analysis								

3.5.1.2 Design of dowel bars

The arrangement of dowel bars, their diameter, spacing and loading location for performing Plate load test was decided on the basis of literature review; study done by Madasamy et al. [95] provides the detailing of bars, loading and pavement cross section.

The design of the dowel bars was determined for a slab thickness of 300mm, radius of relative stiffness of 0.693 and for bar diameter of 35 mm. load transfer efficiency of bars was taken as 40%. On the basis of these parameters, bar spacing of 250mm centre to centre, for each bar was determined, thus giving 7 no. bars. The corner spacing of the last bar was taken as 150mm.

3.5.1.3 Construction of DLC & PQC

About 6 ton of concrete was used in the construction of prototype. Plate 3.23-3.29 show the various stages of construction of a rigid pavement. Initially form work is done on a compacted subgrade. The subgrade was compacted at optimum moisture content which resulted in the value of effective modulus of subgrade reaction to be 300MPa/m. After one day of drying, the DLC was cast on the subgrade, as has been shown in Plate 3.24.

Plate 3.23 Compacted subgrade and installed form work

Plate 3.24 Finished DLC surface

After 7 days of casting of DLC, PQC was cast on the finished DLC subbase. But before, that U cage containing dowel bars spaced at 250 mm c/c was positioned on the finished DLC layer, such that the nearest edge of the slab was 150 mm away from the centre

of the nearest dowel bar. The DLC was laid in two compacted layers of 50 mm each, whereas PQC was laid in three layers of 100mm thickness each.

Plate 3.25 Positioning of Dowel Bars

Plate 3.26 Laying of PQC

Plate 3.27 Layer Wise Compaction Performed on Fresh PQC

Plate 3.28 Leveled PQC Surface

Plate 3.29 Finished Thickness of Rigid Pavement Prototype

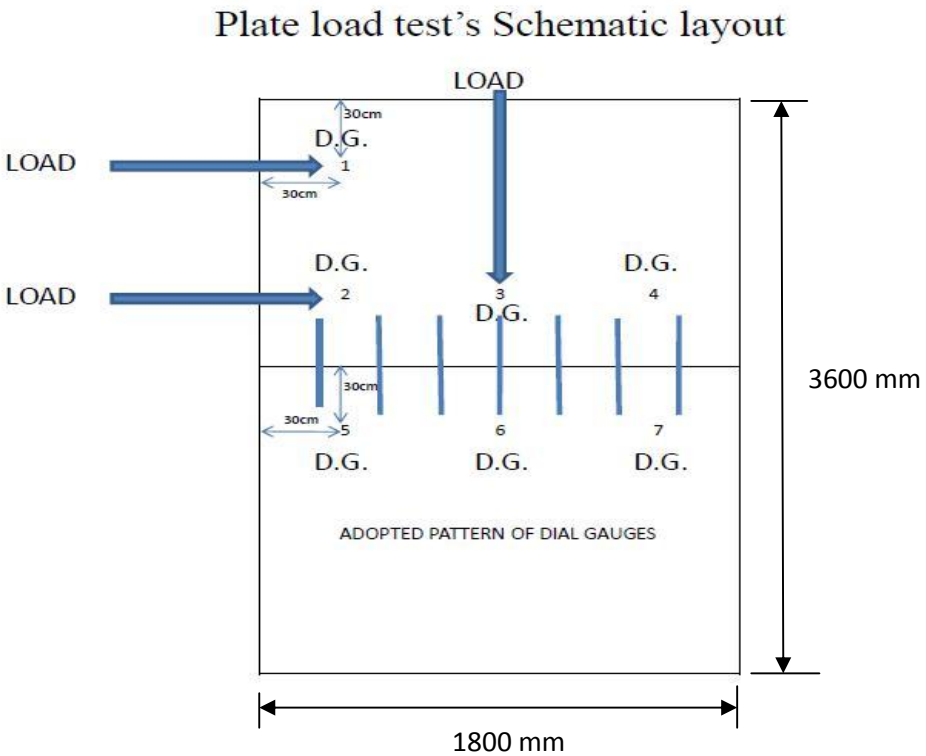

Fig 3.12 Schematic layout of Plate load test conducted in the laboratory

3.5.2 Comparison of Load Transfer Efficacy

Fig. 3.12 shows the loading points as well as the locations where the dial gauges were setup to find the deflections in the pavement. The dial gauges at location 1, 2, 3 & 4 were installed to observe the deflections on the loading side, whereas dial gauges 5, 6 & 7 were installed to find out the deflections on the adjacent side of loading, right near the end of dowel bars. Location 1, 3 and, 2 & 4 correspond to corner, centre, and edge conditions of loading, which are the three conditions for which the pavement design is checked.

With the given loading conditions, three cases of loading arise which are: edge loading, corner loading and centre loading. For these three loading cases, three deflection comparison cases were taken for each, i.e. comparison of 2-5, 3-5 and 4-7 deflection cases. These locations are present on both sides of contraction joint and therefore their percentage deflection difference gives an idea of the load transfer efficacy of the PQC. On the basis of load deflection equations (three in number for three deflection cases) for each loading case, a generalized load-deflection equation was obtained. Hence in all nine equations were available. A loading increment profile was then selected, and the deflection values were obtained at both ends of the bars, for loading at locations 2, 3, 4.

Afterwards, statistical analysis was made out to calculate a common probability of reduction in deflections at both ends of the bars. This probability value obtained for normal PQC and rehabilitated PQC, thus, gives an idea of the load transfer efficacy of the rehabilitated pavement.

3.5.3 Creation of FEM Model

A model of the rigid pavement having contraction joint was created with the help of 3D visualization and analysis application ABAQUS. The arrangement of dowel bars, their diameter, spacing and loading location for performing Plate load test was kept similar as in the prototype.

Boundary conditions to the model were assigned on the basis of actual working of rigid pavement. The top of the slab was fixed against movement in two horizontal directions. The bottom face of PQC was also restricted in the same manner to allow the

bending of the slab. The top and bottom face of the DLC was free to move in vertical direction and along the transverse direction but restricted in the vehicular direction. The top face of the subgrade was free to move in all directions but its bottom face was restricted in the vertical direction to simulate infinite subgrade behaviour. Then the model was analysed for deflections under similar unique loading profile and six deflections' gauging (2-5, 3-6, 4-7) locations as done in the prototype.

The model was then refigured for changed properties, owing to the changed material, caused by rehabilitation. The rehabilitation work required, the loading panel to be cut into two parts extending from centre of one panel to the joint. Half depth cutting of the panel was done with the help of cutter and driller. Then rehabilitation work was done with the selected fiber reinforced SCC mix. After 14 days of hydration this portion was also subjected to the same loading profile; deflections were obtained at all the six locations. Also bending stress was found for edge loading (location no.2), for both rehabilitated and non rehabilitated case, under the load of 10 tonnes, which were later used for finding out fatigue life of the pavement.

3.5.4 Validation of the Model

The validation of the model was done on the basis of deflections obtained under the same unique load increment profile which was chosen for prototype loading. The validation was done for both non rehabilitated and rehabilitated pavement.

The deflections values obtained for both model and prototype were tested for a chi square value, which gives a measure of the correlation between the observed and the expected values. The observed values in our study are those of model, and expected values relate to those of prototype's. If the chi square value (right tailed) comes to be lesser than that of critical chi square value, then the model will be assumed as validated.

After validation, bending stresses were found out at the bottom of the PQC for a maximum design single wheel load of 10 ton (axle load of 20 ton), under edge loading condition. The value of Modulus of rupture was taken from the laboratory tests conducted on various concrete mixes. Finally, the fatigue life of the pavement was found out, for both

rehabilitated and non rehabilitated case, with the help of stress ratio value obtained from bending stress and modulus of rupture.

4. RESULTS AND DISCUSSION

4.1 INVESTIGATION ON OPC AND MINERAL ADMIXTURES

The investigation on OPC and mineral admixtures was carried out with the aim to find their physical and chemical properties. These properties play a pivotal role in providing strength and durability to mortar, and concrete mixes. Efforts have been made to determine their fineness, particle size, surface area, specific gravity, chemical composition, consistency & setting time, and soundness etc.

4.1.1 Particle Size Analysis

Particle size analysis was performed for WMF, cement, fly ash and microsilica using Ankersmid laser based analyzer. Fig. 4.1 clearly illustrates that microsilica is finest among all considered powdery materials followed by WMF, fly ash and cement respectively. The peak of WMF lies exactly in between the peaks of microsilica and OPC. This interpretation clearly infers that WMF used was median size to both microsilica and OPC and hence, an excellent interlocking within these particles is anticipated physically. It is also clearly depicted that OPC used for the study, exhibits particle sizes comparable to flyash as revealed by the presence of secondary peak in Fig. 4.1. Peak patterns analysis suggests that fly ash and OPC have nearly same size range but from the prolonged post peak profile of fly ash, it is learnt that there are numerous fraction of flyash those are even larger in size than OPC particles.

Cumulative percentage sizes of OPC, flyash, wollastonite microfiber and microsilica are illustrated in Fig. 4.2. From this analysis, it is learnt that microsilica has particle size ranging from 0.01-0.5 microns and about 80 percent of WMF particles were in the range of 0.5-4.47 microns. About 80 percent of OPC and flyash particles are greater than 4.47 microns but if one precisely looks at particular size range i.e. upto 0.9 microns, OPC particle is much finer than flyash. Table 4.1 entails about the median size, mean size and various D sizes of microsilica, cement (OPC), flyash and WMF. The largest fraction found for

microsilica, OPC, flyash and WMF are 0.145, 20.055, 25.705 and 1.830 microns respectively. Microsilica used in the present work comprised more than 50 percent of particle size in the range of 0.087-.05 microns and 9.639 microns for flyash. From the particle size distribution patterns, it got to know that OPC offers maximum uniformity in size distribution followed by fly ash, WMF and microsilica respectively. The findings strongly suggested that larger fraction of flyash having size greater than OPC may retard the reaction rate as well as may lower density of mix. However, a fair chance for improvement on workability is speculated due to higher rate of dispersion of cement particles on account of high negative charge carried by their larger sizes. On other hand, ultra-fine nature of microsilica, WMF and fly ash would enhance the pore infilling capacity significantly.

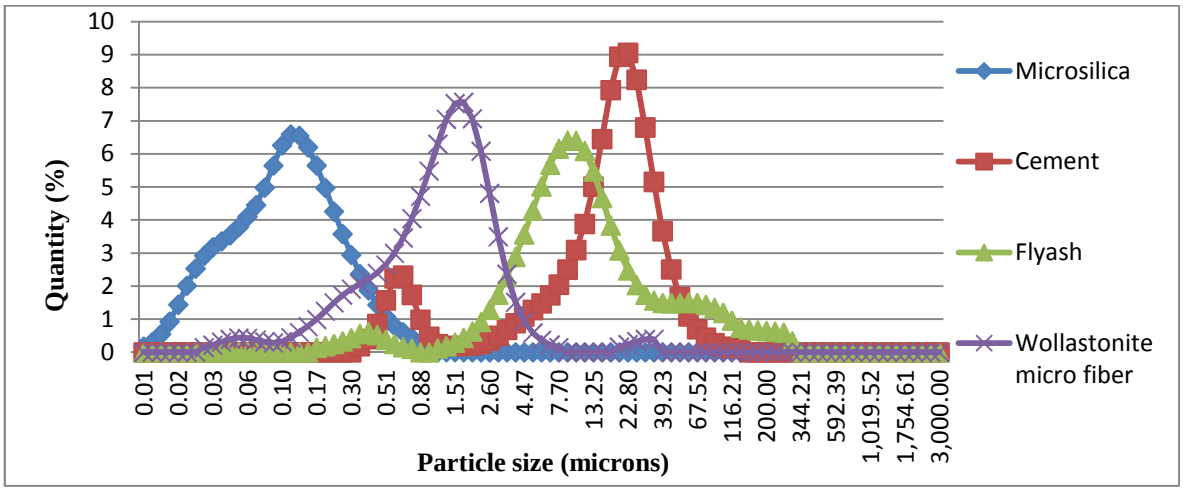

Fig 4.1 Percentage Sizes of various particles

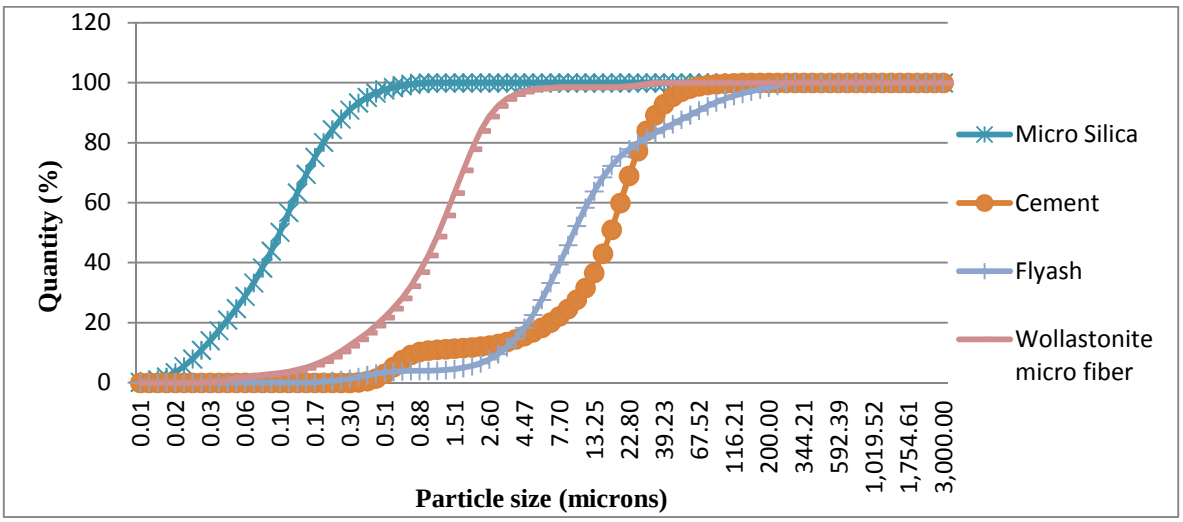

Fig 4.2 Cumulative percentage sizes of various particles

These observations are also verified from Table 4.1, which shows important size variation data for all powder materials.

Table 4.1 Cumulative percentage sizes of various particles

All sizes in micron	Microsilica	Cement	Flyash	WMF
Median Size	0.087	17.093	9.639	1.181
Mean Size	0.145	20.055	25.695	1.830
D10	0.029	0.843	3.056	0.409
D45	0.089	17.093	8.661	1.064
D90	0.284	35.298	63.146	2.723

4.1.2 Surface Area Analysis

Surface area is an important parameter which decides the reactivity and water adsorption tendency of a given volume of material. For two materials having similar volumes, the surface area could be different, which depends upon the degree of fineness of the particles of the material. A higher surface area means, a higher exposed area, which naturally would allow maximum reaction per unit volume of the particle. But the limitation is , that the exposed surface should have natural tendency to react, which depends upon the chemical composition and existing form of the surface crystal. If the crystal has higher silica content and glassy in nature, then naturally it would have higher reactivity. So the test results would obviously indicate the reacting tendency of an admixture, but not the true reacting power.

Table 4.2 provides the results obtained from Blaine's air permeability test on cement, and BET permeability test on WMF, flyash and microsilica. The results prove that microsilica is the finest among all, followed by WMF, flyash and OPC respectively. If one compares the degree of fineness of microsilica, WMF and fly ash with OPC, they are in the order of 60, 2.8 and 1.3 times finer than OPC respectively. Results strongly hinted that reactivity of microsilica would be prominently proactive in comparison to the rest as it has inherent ability to contribute strength development through their pozzolanic reactivity. BET's study result strongly suggests that WMF is fine enough to modify the properties of concrete in its fresh or hardened states. The inclusion of WMF would have significant

physical effect of modifying the flocculation of cement and the median particle size being smaller, presence of WMF would infill micro pores and voids of the cement system better as a result of which coefficient of permeability of cement matrix would reduce significantly. Fibrous mineral wollastonite micro-fiber has been used for development of high performance cement composites offering economic benefits over steel or carbon micro-fibers [91,92]. The fly ash used in the present study has specific surface area very close to OPC but the influence of fly ash on the properties of fresh concrete is linked to the shape of the fly ash particles. The reduction in water demand of concrete caused by the presence of fly ash is usually ascribed to their spherical shape, this being called a “ball-nearing effect”. The extend of packing depends both on the fly ash and on the cement used: better packing is achieved with coarser Portland cement and with finer fly ash [30]. One beneficial effect of packing on strength is a reduction in the volume of entrapped air in the concrete but the main contribution of packing lies in a reduction in the volume of large capillary pores. It is worth noting that the positive influence of the fineness of fly ash is coupled with its spherical shape.

Table 4.2 Specific surfaces of various materials used in the study

Material	Specific surface (sq. m/Kg)
OPC	298
WMF	827
Flyash	380
Microsilica	18000

4.1.3 Specific Gravity and Soundness

Table 4.3 shows the specific gravity of cementitious materials, tested using Le Chatelier flask. The results clearly show, that Microsilica offers the lowest value of specific gravity followed by fly ash, wollastonite micro-fiber and OPC respectively. As the specific gravity of a material is a good indication of heaviness of the material with respect to water, the present study connotes that microsilica is 2.05 times lighter than water. Likewise applies for Fly ash, WMF and OPC respectively. The specific gravity of admixtures affects the flowability of fresh concrete, along with their viscosity in the paste form. Hence, it could be

said that mixes prepared with microsilica would have tendency to achieve better flow, followed by flyash, WMF and plain OPC respectively.

Table 4.3 Specific gravity of various materials

Material	Specific Gravity
OPC	3.15
WMF	2.9
Flyash	2.52
Microsilica	2.05

As far as soundness test conducted on cement is concerned, it was found to expand by 7 mm. Test results infer , that there is not much free lime present in the cement which could cause expansion of cement by the formation of CH.

4.1.4 Chemical Composition

Table 4.4 shows the quantitative results of the amount of oxides present in cement and other admixtures, as has been found through X ray fluorescence spectrometer test when conducted in accordance with IS: 12803.

Table 4.4 Chemical properties of Cementitious materials including OPC

Compound	Cement	Flyash	WMF	Microsilica
SiO_2	20.2	35	48	92.9
Al_2O_3	5.2	26	1.4	0.9
Fe_2O_3	3	8.7	0.6	0.72
MgO	1.51	5	0.2	0.57
SO_3	2.2	3	-	0.16
Na_2O	0.08	1.5	-	0.32
Chloride	0.014	0.005	-	0.037
Loss on ignition	4.3	5	4	2.6
CaO	62.9	15.3	45.9	1.4
K_2O	0.6	0.5	-	0.4

The following are the few observations drawn from the study of chemical compositions:

(i) Fly ash used in the present study contains appreciable amount of silica and highest amount of alumina when compare to the rest of the materials. By the presence of substantial amount of lime in it, the aforesaid lime can be said to belong to the category of medium lime fly ash and would liberate moderate heat of hydration. Higher content of silica strongly indicates good potential to reduce formations of CH and ettringite.

(ii) WMF shares equal amounts of lime & silica, and traces of alumina. Their presence indicates that WMF has tendency for self cementation & moderate rate of reaction. Silica in WMF also makes it possible for the later to reduce ettringite and CH content of the mix. By virtue of its crystalline nature, WMF is more inert than been reactive and served as excellent pore filler.

(iii) Microsilica mainly consists of silica and rest other oxides are in meagre amount. In its amorphous state, microsilica is very fine particle and possesses higher surface areas. By virtue of its microfine nature, microsilica is a promising material for infilling micro pores and apt for reduction of hydrated cement compounds like CH and ettringite considerably.

4.1.5 Normal Consistency

Normal consistency is related with water requirement which could make the paste workable. For pure cement it depends upon the quantities of compounds responsible for the hydration, as well as the fineness of cement particles. Higher the rate of hydration of C_3A in cement, higher would be the formation of ettringite crystals; thus causing reduction in workability. With the introduction of admixtures, the fineness of binder powder further increases. This increase depends upon the particle size (surface area) as well as quantity of admixtures. The surface area of admixture particle, affects the water required for lubrication and adsorption at their surfaces', plus filling of pores between cement particles, thereby release of water. It has been amply demonstrated that admixing of mineral admixtures into the cement paste system facilitates the release of water and reduction in hydration of cement particles. As has been observed during the laboratory study, volume of admixtures brings a

complex change and affects the workability properties considerably. Notable release of water has been observed for admixtures taken in smaller quantities, but at higher volumes the behaviour of admixtures are different and it is being explained below in the sequential steps:

Let us assume that the admixtures are inactive or their performance is hindered because the water required for their performance is less, in comparison to the water present in the paste. In that case their migration into the voids of cement particles is reduced because the force of cohesion between cement particles is higher due to smaller thickness of water layer between them. This increases the content of admixtures outside the voids of cement particles. As a result, there is a non homogenous paste which has higher viscosity on account of increased adsorption of water by admixtures; increased viscous and frictional effect by thicker layers of admixtures, with no release of water at all. Hence, at lower water contents, with an increment in the mineral admixtures' quantity the water demand for achieving normal consistency will keep on increasing. There is generally no effect of high initial water content on admixtures' hydration rate. Apart from the discussion on normal consistency, it has been suggested that microsilica and flyash have same effect on water demand, but the effect on paste's hydration is different for flyash and microsilica & WMF. Microsilica & WMF increase the hydration rate and reduce the dormant period whereas flyash increase it, subsequently initial setting time increases. Langan et al. [78] & Soliman and Nehdi [160], explained the hydration potential of microslica & flyash, and WMF, respectively on the same basis.

Fig. 4.3 shows the general trend of normal consistencies of cement pastes with or without mineral admixtures for singular, binary and ternary mixes. The combined normal consistency trend is shown in Fig. 4.4.

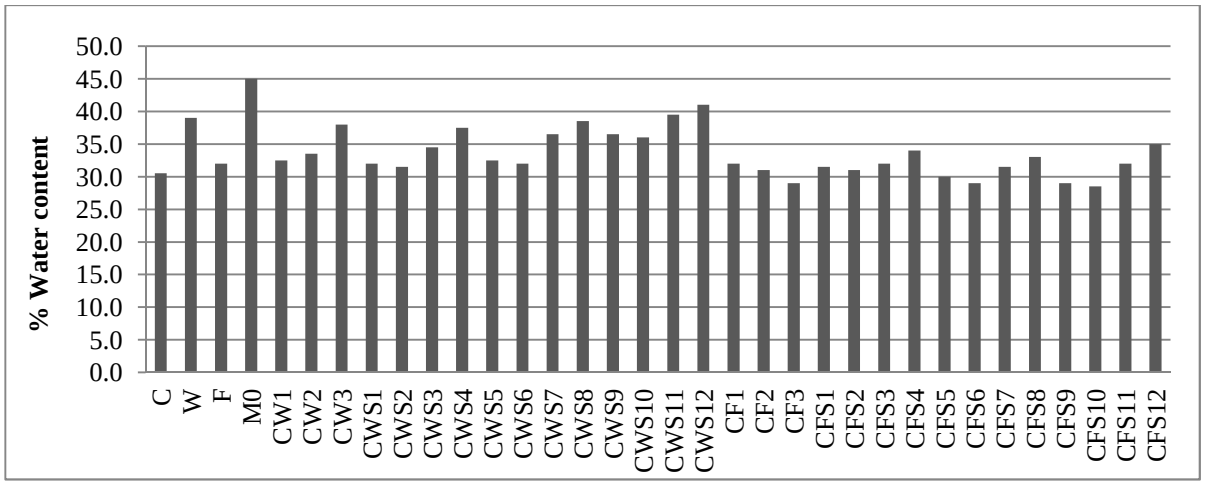

Fig 4.3 Normal consistency values for singular, binary and ternary mixes

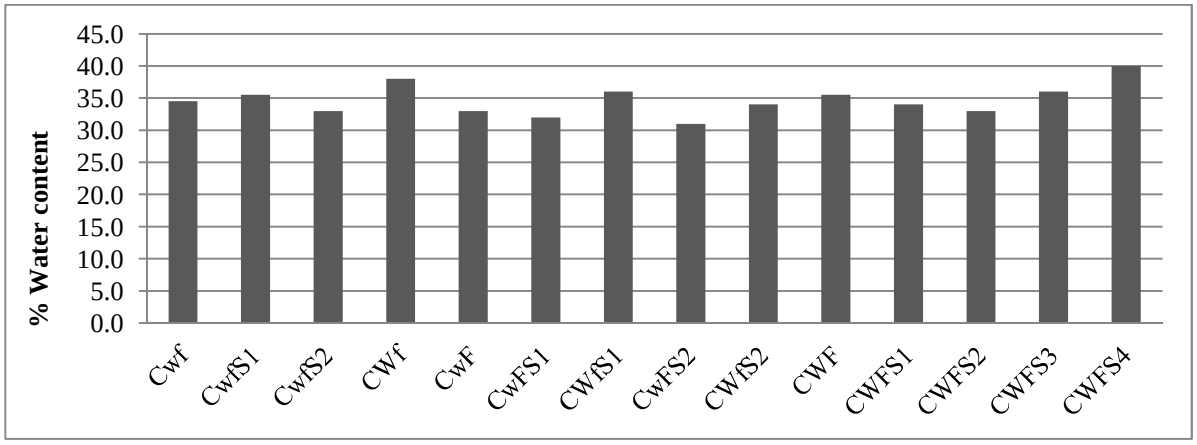

Fig 4.4 Normal consistency values for combined mixes

(i) Pastes of cement & admixtures

The results for grouts made of cement and admixtures are illustrated in Fig 4.3. It was found that WMF and microsilica demand more water for achieving normal consistency. Flyash grout took lesser water in comparison to rest of the admixtures, followed by cement's grout. The influence of surface area of the materials on normal consistency is conspicuously distinguished as can be seen from the Figs. 4.3 & 4.4. As expected, maximum normal consistency is being offered by 100 % microsilica mixture followed by 100% wollastonite, 100% fly ash and 100% cement respectively. Laboratory results strongly suggested having strong influence of surface area of materials on rheological properties of paste apart from chemical reaction. In general, it has been observed, that pastes containing both WMF and

Microsilica showed higher demand of water for achieving normal consistency. Flyash on the other hand decreased the water demand. But the rate of increment and decrement of normal consistency of pastes depend upon the type and amount of admixture used.

(ii) WMF

The addition of WMF in lower percentage irrespective of combinations (binary & ternary mixes) showed small increase in demand of water upto 20% WMF part replacement. However, beyond this replacement level, the increase in water demand has risen sharply (Figs. 4.3 & 4.4). This phenomenon is observed mainly due to excellent voids infilling capacity of WMF for being acicular in shape and micro fine size as a result of which WMF coated around the cement particles prevented from having ease flow. This frictional effect is more pronounced for higher percentage part replacement of cement by WMF. Notably, incorporation of WMF beyond 20% does not show any significant benefits in water release, indeed, it decreases.

WMF though, is a fine material and releases water by grain size refinement, but by virtue of its acicular structure, it showed tendency to increase the friction to flow. Water releasing tendency is more pronounce when cement was partly replaced by wollastonite in the range of 10 -20% by weight of cement. This tendency is more active in comparison to friction inducing tendency. Beyond 20% replacement level, water demand is substantial for achieving normal consistency. This is attributed to extra water absorbed by the WMF particles coating around the sphere of the cement grains.

(iii) Flyash

Flyash improves workability of concrete on account of two factors; firstly, due to the spherical shape of its particles (ball bearing effect), and secondly, due to the modification in the flocculation of cement, thereby resulting in the reduction in the water demand in consequence of electrical charges [144], the finer flyash particles get adsorbed on cement particles and thus the change in the dispersion of cement particles is reflected in the microstructure of the cement paste, mainly its pore size

distribution. The median pore size is reduced and thus permeability is also lowered. Roy D.M. [146]. For a constant workability, the water demand has been found to be reduced by 5 to 15% for a flyash admixed concrete, in comparison to plain cement concrete having the same cementitious material content [30]. Excessive amount of flyash would confer no further benefit with respect to water demand, and only 20% flyash has been found to work beneficially [54]. Figs. 4.3 & 4.4 entail, that incorporation of fly ash upto 20% by weight produced higher normal consistency values (32 & 31) in comparison to cement's consistency but at 30% part replacement level, this value (29) found to be even less than that of cement's consistency (30.5). The trend of reduction in normal consistency is approximately linear with the percentage flyash replacement level as can be seen from Fig. 4.3. The reduction in normal consistency is mainly contributed by the presence of bigger particle size of flyash and by virtue of its less moisture attraction characteristics. It may also be due to the presence of sulphate ions in flyash which carry a high negative charge as a result of which repulsive force developed between the particles and hence a larger distance exhibit between cement particles which is why larger fly ash particles could seep in it and occupied the open gap. In addition to the above reasons, investigators opined that the existence of fly ash fraction greater than 5 microns about 80% revealed by the particle size analyser might also be one of the reasons as this size matched with the average void size of cement particles leading to ease infilling of voids of cement particles.

(iv) Microsilica

Fig. 4.3 clearly illustrated that highest normal consistency is offered by microsilica followed by wollastonite microfiber and cement respectively. Reason is quite obvious and simple to say that microsilica and WMF possessed higher surface area than cement.

The water demand increases at a smaller rate up to 5% of Microsilica content and thereafter water demand is quite pronounced for higher microsilica content for achieving normal consistency.

For microsilica addition in the range of 0-5%, the ball bearing effect of microsilica small spherical particles tend to increase the workability of the mix by reducing the friction between cement particles. Also, the tendency for water release due to pore size and grain size refinement caused by microsilica, releases more water into the mix and reduces the friction respectively. But due to its larger surface area, microsilica beyond 5% starts making a thicker paste around cement particles and increases the viscosity at a higher rate. The increment in viscosity provided by the viscous paste of microsilica remains effective for a certain thickness beyond which there is not much effect of its increment. Hence at 10% microsilica it has been found , that for both flyash and WMF mixes there is not much increment in water demand for achieving normal consistency. In ternary mixes, at higher WMF or flyash content (20-30%), addition of microsilica above 7.5% does not bring much change in normal consistency since WMF/flyash also hinders the pore filling by microsilica due to its own filling effect.

4.1.6 Initial Setting Time and Final Setting Time

Initial setting time is the time when the paste starts loosing the plasticity. It is generally marked by the time when the acceleration of hydration starts after the dormant period. Hence the initial setting time is dependent upon the sum of initial hydration period and dormant period. Final setting time is the time when the paste has lost its plasticity and it starts hardening or gaining strength. It is marked by the end of the acceleration period. In this context, Langan et al. [78] have also conducted the study. In their study also, they have found that for plain cement, the acceleration period begins at approximately 1.5–2 hours after introduction of the water and ends approximately 5.5 hours later. Present study clearly revealed that incorporation of wollastonite microfiber into cement paste increased both initial and final setting times apart from consistency value increased. About 13.3%, 28.67% and 21.33% increment in initial setting time were observed when WMF was incorporated @ 10%, 20% & 30% by weight of cement respectively. The final setting time for the same replacement levels of WMF are 15.91%, 31.36% and 29.09% respectively. On further addition of microsilica along with WMF, there was a considerable increase in both initial as well as final setting times. For the pastes where WMF was kept constant @10% and for

varying percentage content of microsilica i.e. 2.5%, 5.0%,7.5% and 10%, the percentage increases in initial setting times were 40%, 72%, 110% and 159 % respectively and for the final setting time these values were 33.18%, 34.9%, 41.18% and 65.14% respectively. Further increasing of WMF content, to 20% from 10%, for same microsilica contents, further increased the initial setting times considerably, but final setting time decreases gradually. On further addition of WMF upto 30% for the same microsilica contents, a strong tendency of decreasing both initial and final setting times was observed indeed final setting times were even less than that of cement's setting times. These findings are in the line of study conducted by Soliman and Nehdi [160]; they found that incorporation of WMF into cement pastes increase both initial and final setting times by reducing the number of active sites for hydration products to form along with reducing the cement content by its replacement, which complements the reduction in hydration rate.

For flyash, at lower water/cement ratio, the retardation is less and vice versa. Microsilica according to literature prolongs hydration at both dormant and acceleration period, at lower water/cement ratios. At higher ratios it is found to decrease the dormant period and initiate the acceleration period at early stage, thereby reducing the time when acceleration period ends. Hence it could be assumed that microsilica reduces both of the setting times i.e. initial and final

Even though it increases the release of water but loss of hydration is large enough to reduce the initial setting times and final setting times of the paste. On contrary inclusion of flyash into the cement paste reduced final setting time but increases initial setting times. The increase in initial setting time is approximately linear with respect to flyash contents. The percentage increments are in very resemblance to that of WMF admixed pastes which are in the range of 10% to 28%. The only distinct difference noticed was, fly ash admixed pastes rendered smaller final setting time in comparison to their counterparts. Incorporation of microsilica increase both initial and final setting times. The final setting times are apparently higher than their counterpart pastes (cement: wollastonite microfiber: micosilica), whereas initial setting time decreases considerably. In overall, setting times tend to increase as the dosage of wollastonite microfiber increases for the same quantity microsilica contents.

But for quaternary mixes (cement: wollastonite: flyash: microsilica), the setting times tend to decrease. However, these values are always higher than that of 100% cement irrespective of WMF, fly ash and microsilica contents as can be seen from Table 4.5.

The present experimentation program also yielded the same results. The results have been provided in Table 4.5, and Fig 4.5 & 4.6.

Table 4.5 Setting times of various mixtures

Mix	Cement	Flyash	WMF	Microsilica	NC %	IST	FST
C	100	-	-	-	30.5	150	220
W	-		100	-	39.0	-	-
F	-	100	-	-	32.0	-	-
S	-	-	-	100	45.0	-	-
CW1	90	-	10	-	32.5	170	255
CW2	80	-	20	-	34.5	193	289
CW3	70	-	30	-	37.0	182	284
CWS1	87.5	-	10	2.5	34.0	211	293
CWS2	85	-	10	5	33.5	258	344
CWS3	82.5	-	10	7.5	36.0	315	408
CWS4	80	-	10	10	37.5	389	469
CWS5	77.5	-	20	2.5	35.0	247	347
CWS6	75	-	20	5	36.0	295	396
CWS7	72.5	-	20	7.5	38.0	367	468
CWS8	70	-	20	10	38.5	405	520
CWS9	67.5	-	30	2.5	38.0	224	312
CWS10	65	-	30	5	37.5	278	366
CWS11	62.5	-	30	7.5	39.5	351	437
CWS12	60	-	30	10	39.5	430	506
CF1	90	10	-	-	32.0	165	249
CF2	80	20	-	-	31.0	176	277
CF3	70	30	-	-	29.0	193	313
CFS1	87.5	10	-	2.5	31.5	204	290
CFS2	85	10	-	5	31.0	249	335
CFS3	82.5	10	-	7.5	32.0	310	425
CFS4	80	10	-	10	33.0	374	488
CFS5	77.5	20	-	2.5	30.5	213	319
CFS6	75	20	-	5	29.0	265	372

CFS7	72.5	20	-	7.5	30.0	327	461
CFS8	70	20	-	10	31.0	408	543
CFS9	67.5	30	-	2.5	29.0	237	358
CFS10	65	30	-	5	28.0	293	425
CFS11	62.5	30	-	7.5	30.0	360	530
CFS12	60	30	-	10	31.5	443	626
Cwf	90	5	5	-	34.5	162	243
CwfS1	87.5	5	5	2.5	35.5	201	297
CwfS2	85	5	5	5	38.5	240	321
CWf	85	5	10	-	38.0	167	253
CwF	85	10	5	-	37.5	162	257
CwFS1	82.5	10	5	2.5	38.0	222	329
CWfS1	82.5	5	10	2.5	39.0	229	349
CwFS2	80	10	5	5	39.0	294	388
CWfS2	80	5	10	5	40.0	300	393
CWF	80	10	10	-	38.5	174	270
CWFS1	77.5	10	10	2.5	39.0	250	391
CWFS2	75	10	10	5	39.5	349	444
CWFS3	72.5	10	10	7.5	40.0	458	597
CWFS4	70	10	10	10	42.0	610	721

General behaviour of the cement pastes with respect to the setting times with or without wollastonite microfiber, flyash and microsilica is discussed below in brief:

A. Initial setting time:

(i) The addition of all the admixtures resulted in an increment in the initial setting times of the cement pastes.

(ii) If comparison is made between the effect of WMF and flyash on initial setting times, then it shows that equal mass of flyash results in a higher increment in initial setting time, in comparison to WMF.

(iii) Microsilica has the highest power to increase the initial setting time of the pastes in comparison to WMF or flyash. Whether it is admixed along with WMF or flyash, approximately equal increment rates in initial setting times have been observed for a given percentage addition of microsilica at a given percentage mass of WMF or flyash.

(iv) Also it has been observed that for higher contents of both flyash and WMF, the addition of microsilica beyond 7.5% does not increase the initial setting time at the same rate, with which it had done initially, when varying from 0-7.5%.

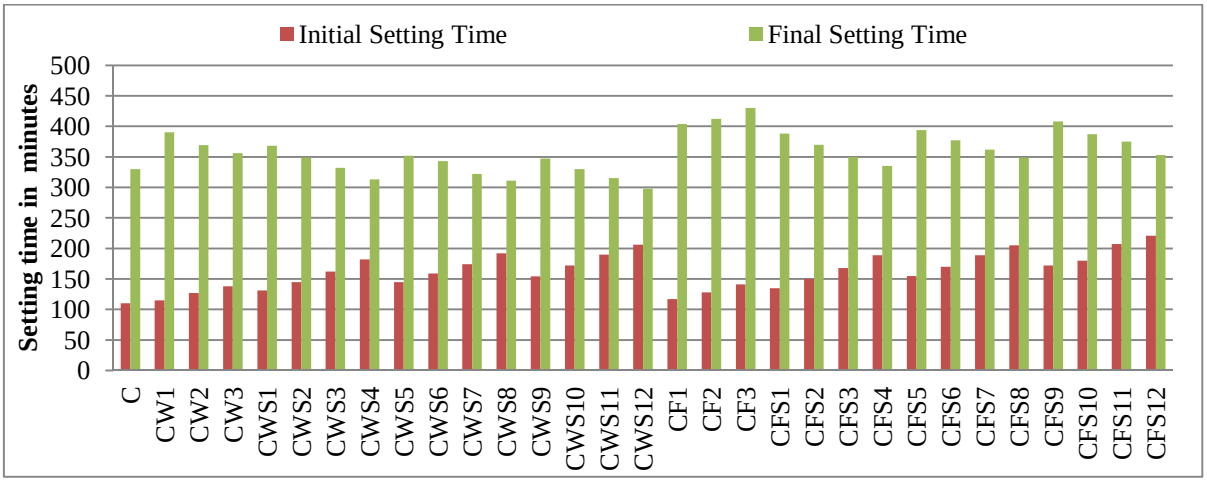

Fig 4.5 Setting Time of Singular, Binary and Ternary Mixes

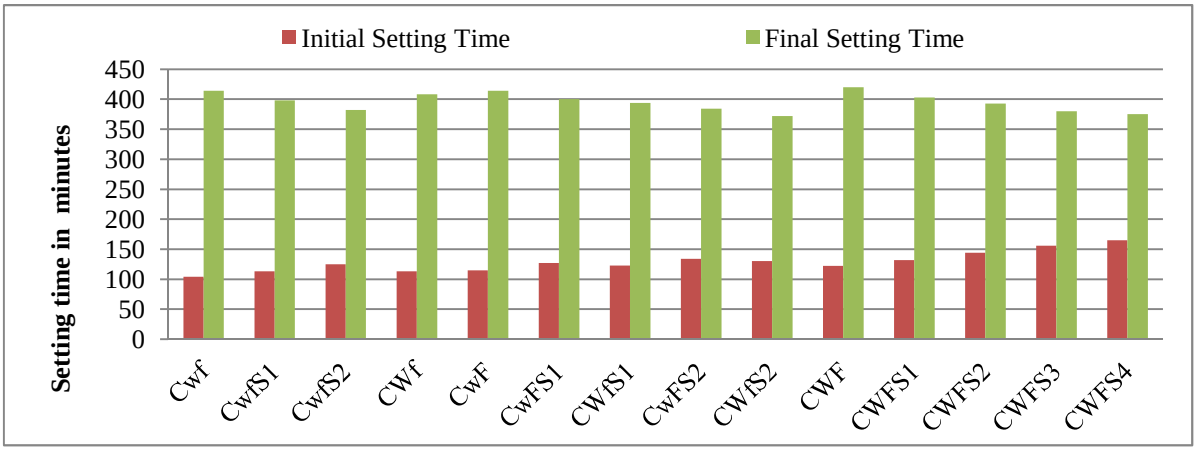

Fig 4.6 Setting Time of combined Mixes

B. Final setting time:

(i) The addition of both WMF and microsilica reduce the final setting times of the cement pastes, whereas flyash increases the final setting time of the pastes.

(ii) The rate of reduction/increment is highest for microsilica, followed by WMF and flyash when comparison is made for equal mass of these admixtures.

(iii) No special change in the decrement rate of final setting time has been observed in case of microsilica addition at higher contents (>7.5% by mass of cement replacement).

The findings of the present study are very much in the line of studies conducted by the earlier researchers and stated that all the admixtures prolong the dormant period, which obviously result in increment in initial setting times of the pastes. Microsilica is the finest, and thus it gets adsorbed more easily and completely over the cement particles, therefore microsilica reduces the hydration rate to the highest extent, and this trend is followed by WMF and flyash whose surface areas vary accordingly. All of the admixtures increase the dormant period because dormant period is influenced by the breaking of initially hydrated layer from the surface of cement particles, and if the adsorbed admixtures on the surface hinder it, then cement particles will not hydrate even if there is sufficient amount of water available for hydration to take place. When the content of microsilica is higher than 7.5%, there is a reduction in the increment rate of initial setting time. This is because, microsilica up to 7.5% by mass of mix is sufficient to cover the cement particles by adsorption. Over and above this percentage, microsilica would only increase the thickness of inter-crystal paste between cement particles which has minimal effect on the dissolution of cement crystals form its surface, though they indirectly reduce the spaces for hydration products to form and affects the final setting time to a higher extent. Hence after 7.5% of microsilica, there is reduction in the increment rate of initial setting time.

The final setting time corresponds to the time duration between the instant, the water was added and initial hydration started to the time when the acceleration period ended. Literature studies state that microsilica in presence of enough water reduces its retarding behaviour and the acceleration period ends early, whereas flyash increase its retardation at higher water contents. At the end of dormant period the water level of the mix is highest because of delayed hydration, and when the film of hydrates break on the cement particles then the admixtures start reacting with the lime so formed after hydration of new cement compounds. Microsilica has the highest reactivity followed by WMF and flyash because of their surface areas. Hence it is obvious that the acceleration period of microsilica would end earlier than WMF, followed by flyash. More is the admixture present more would be the reaction rate, but is has been observed that flyash increases the final setting times with the rise in its content. This is because flyash because of low surface area and lower potential to reduce lime (evident by XRD test) did not enter into the voids between cement particles fully. Though with the increment in its content the fraction lower than 5 microns increased inside

the cement voids but a simultaneous larger increment in fraction greater than 5 micron takes place in the paste which causes dilution of the cement. The increased secondary hydration by flyash due to its increased content in cement voids is much lesser than the reduction in hydration caused by the relative reduction of cement. For WMF and microsilica this is not so, because of their higher reaction rates. Microsilica and WMF have nearly 47.3 and 2.2 times more surface area than flyash which explains their higher hydration rate than the dilution caused by them.

4.2 INVESTIGATION ON MINERAL AGGREGATES

Fig. 4.7 shows the gradation of the coarse aggregates used in the present work. The curve is nearly S shaped with more than 70% of fraction lying between 10 mm and 20 mm. Since the aggregates in the middle most size range are quite high and rest size ranges have very small fraction of aggregates, this curve represents open graded aggregates. The voids are lesser which could be filled by fine aggregates and pastes, and with the decrease in the coarse aggregates to fine aggregate ratio of mix, the aggregate gradation in the small size range would increase thereby turning the gradation into well/dense graded. This condition was achieved in the trials when the ratio of coarse aggregates to fine aggregates was decreased. This finally resulted in an improved condition for achieving SCC.

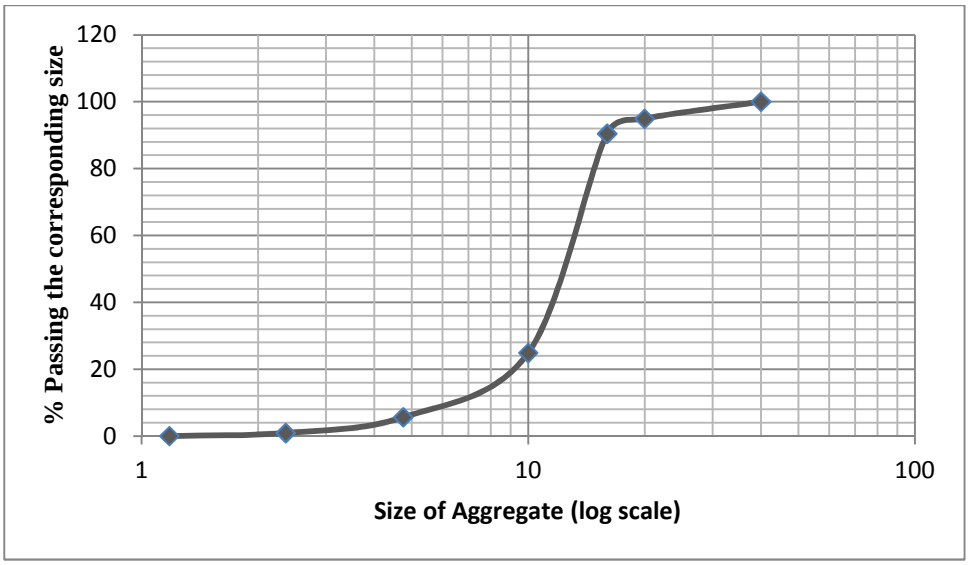

Fig. 4.7 Gradation of Coarse Aggregates

Referring to Table 4.6, in which, the cumulative percentage passing of aggregates was determined, it was found that more than 90% of particles are retained by 10mm IS sieve size whereas the next bigger sieve size having lesser than 10% aggregates retained on it is 16mm. Therefore the maximum size of aggregates (MSA) has been found to be 16mm. The spacing of bars in the ring test for passability of SCC mixes is based on this MSA. It is generally 3 times the MSA.

Table 4.6 Result of sieve analysis of coarse aggregates with MSA 16mm

IS Sieve Size (mm)	Weight retained (g)		Percentage weight retained		Cumulative Percentage weight retained		Percentage weight passing		Percentage of different fractions		Combined
	20mm	12.5mm	20mm	12.5mm	20mm	12.5mm	20mm	12.5mm	0.6	0.4	1
40	0	0	0	0	0	0	100	100	60	40	100
20	767	126	7.67	1.26	7.67	1.26	92.33	98.74	55.40	39.50	94.90
16	528	323	5.28	3.23	12.95	4.49	87.05	95.51	52.23	38.20	90.43
10	8172	4923	81.72	49.23	89.39	53.72	10.61	46.28	6.37	18.51	24.88
4.75	533	4008	5.33	40.08	94.72	93.8	5.28	6.2	3.17	2.48	5.65
2.36	-	390	-	3.9	-	97.7	-	2.3	-	0.92	0.92
1.18	-	230	-	2.3	-	100	-	0	-	0	0

Table 4.7 presents the values of physical, mechanical and durability tests performed on the coarse aggregates. The results show that the aggregates are mechanically fit, have good density, are durable and, are having good shape parameters.

Table 4.7 Results of various tests conducted on coarse aggregates

Test	Value
Aggregate Impact Value	15
Aggregate Abrasion Value	19
Aggregate Crushing Value	10.4
Specific Gravity	2.6
Water Absorption of Coarse Aggregate	0.4
Flakiness Index	21.16
Elongation Index	7.41
Angularity Number	5.01

Table 4.8 shows the particle size distribution of fine aggregates. The fineness modulus of fine aggregates as found from this tabular data, is 3.23. This suggests that the fine aggregates conform to grading zone-II in accordance with IS 383. The specific gravity of fine aggregates was found to be 2.58 which are quite near to that of coarse aggregates' specific gravity.

Table 4.8 Particle size distribution of fine aggregates

IS Sieve Size	Weight retained	Percent weight retained	Cumulative % weight retained	Percent weight passing
4.75	27	2.71	2.71	97.29
2.36	108	10.83	13.54	86.46
1.18	67	6.72	20.26	79.74
600	100	10.03	30.29	69.71
300	300	30.09	60.38	39.62
150	350	35.11	95.49	4.51
75	45	4.51	100.00	0.00
				FM= 3.23

4.3 INVESTIGATION ON PASTES WITH AND WITHOUT ADMIXTURES

4.3.1 XRD Study

The X-ray diffraction technique was employed to determine the behaviour of different paste mixes at initial stages of hydration. Samples were taken for test after allowing hydration for 14 days.

XRD patterns depicted in Figs. 4.8-4.52, respectively show the quantitative data obtained in the form of pi-chart from the XPERT High Score application. Besides quantitative data, labelled peak diagram has been shown for cement in Fig. 4.8. The labelled peak diagram of hydrated cement shows that a given peak may correspond to a peak occurring in the diffraction pattern of two or more hydration products. Therefore simultaneous matching of intensities of different compounds is necessary to find out the quantitative value of a given compound in the hydrated mix.

Table 4.9 provides the data compiled in a tabular form.

Table 4.9 X Ray Diffraction Data of Pastes

Mix	Percentage of constituting material	% Ettringite	% CH	% CSH	% C_3A
C	100C	2.3	9.8	37	5.5
CF1	90C+10F	2.8	8.9	38.7	5.8
CF2	80C+20F	2.7	6.4	40.2	6.5
CF3	70C+30F	3.2	2.8	42.4	6.7
CFS1	87.5C+10F+2.5M	2.5	10	39.4	5.8
CFS2	85C+10F+5M	2.9	10.6	40.1	5.8
CFS3	82.5C+10F+7.5M	3.6	7.7	41.3	6.2
CFS4	80C+10F+10M	4.1	4.6	45.9	6.2
CFS5	77.5C+20F+2.5M	2.8	7.2	41.4	5.9
CFS6	75C+20F+5M	2.9	8.6	42.2	6
CFS7	70C+20F+7.5M	3.4	6.2	46.6	6.1
CFS8	72.5C+20F+10M	3	5.6	46.9	6.1
CFS9	67.5C+30F+2.5M	2.4	6.3	44	5.8
CFS10	65C+30F+5M	3.4	4.1	45.1	6.6

CFS11	60C+30F+7.5M	3.1	4.5	47.4	7.1
CFS12	62.5C+30F+10M	2.8	6	50.4	6.9
CW1	90C+10W	2.5	10	39.9	5.8
CW2	80C+20W	5.4	5.4	41.9	5.1
CW3	70C+30W	10.2	4.2	39.8	6.3
CWS1	87.5C+10W+2.5M	6.2	2	39.3	5.7
CWS2	85C+10W+5M	9	4.1	40	5.9
CWS3	82.5C+10W+7.5M	2	2.1	40.5	5.9
CWS4	80C+10W+10M	7.1	5.8	43.2	5.7
CWS5	77.5C+20W+2.5M	2.9	5.6	46.2	6.3
CWS6	75C+20W+5M	4.9	4.4	47.4	6.4
CWS7	72.5C+20W+7.5M	5.8	2.9	50.2	6
CWS8	70C+20W+10M	4.4	2.5	55.4	6.2
CWS9	67.5C+30W+2.5M	2.8	8.6	40.7	5.4
CWS10	65C+30W+5M	7.5	5.6	44.1	4.7
CWS11	62.5C+30W+7.5M	5.3	5.8	45.9	6
CWS12	60C+30W+10M	4.9	6.1	46.3	5.5
Cwf	90C+5F+5W	2.9	8.8	41	5.8
CwfS1	87.5+5F+5W+2.5M	2.5	7.9	41.6	6
CwfS2	85+5F+5W+5M	3.1	7.6	46.3	6
CWf	85+5F+10W	2.2	10.1	40.2	5.9
CwF	85+10F+5W	2.3	12.7	40.2	5.1
CwFS1	82.5+10F+5W+2.5M	2.4	12.8	41.5	5.5
CWfS1	82.5+5F+10W+2.5M	2.3	3	36.7	5.5
CwFS2	80+10F+5W+5M	2.9	7.4	42.6	6
CWfS2	80+5F+10W+5M	3	7.2	48.4	5
CWF	80+10F+10W	3.7	4.5	45.3	6.3
CWFS1	77.5+10F+10W+2.5M	3.1	4.6	47.8	6.4
CWFS2	75+10F+10W+5M	4.5	6.1	46	8.6
CWFS3	72.5+10F+10W+7.5M	2.9	9.2	45.9	5.6
CWFS4	70+10F+10W+10M	3.6	7.1	46.4	5.8

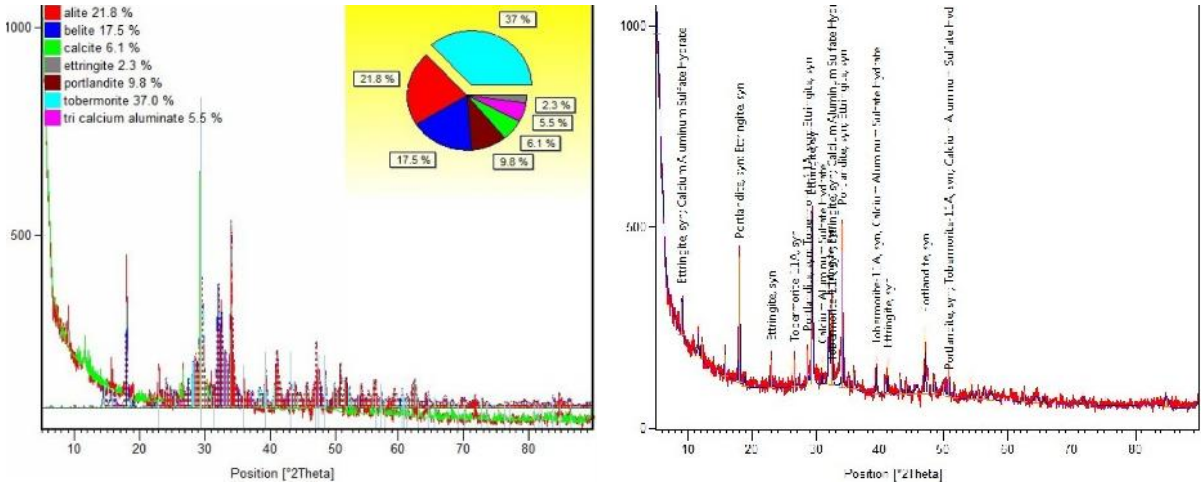

Fig. 4.8 XRD pattern: Hydrated cement mass (100% cement)

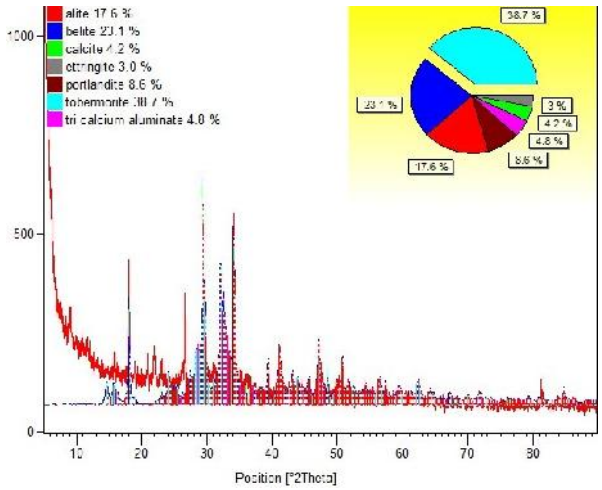

Fig. 4.9 XRD pattern: CF1 (C-90%, F-10%)

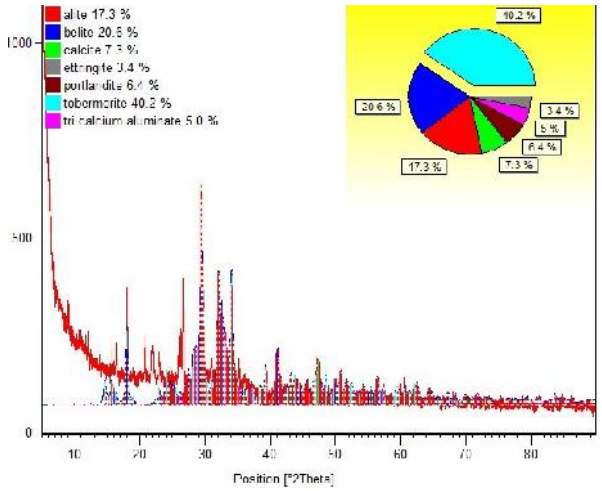

Fig. 4.10 XRD pattern: CF2 (C-80%, F-20%)

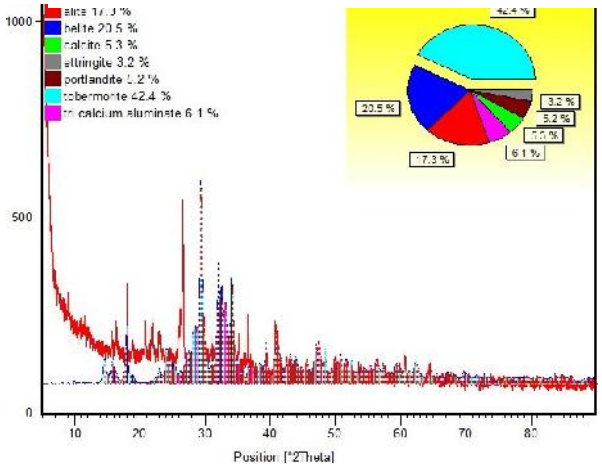

Fig. 4.11 XRD pattern: CF3 (C-70%, F-30%)

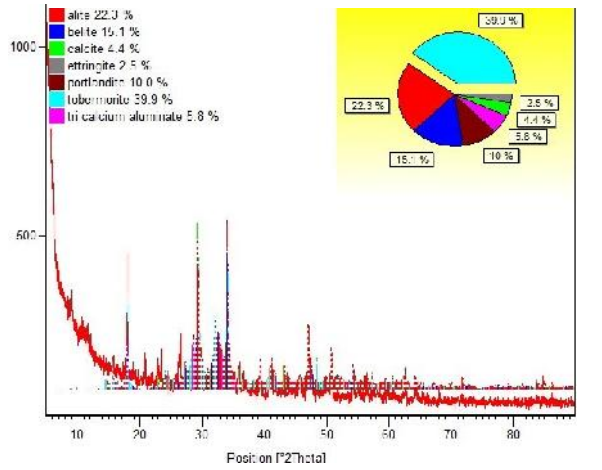

Fig. 4.12 XRD pattern: CW1 (C-90%, W-10%)

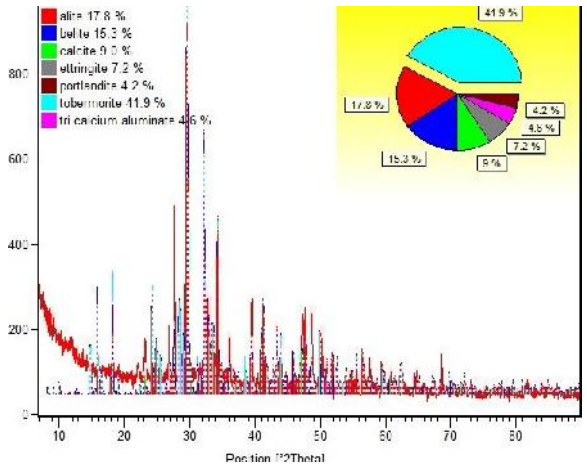

Fig. 4.13 XRD pattern: CW2 (C-90%, W-20%)

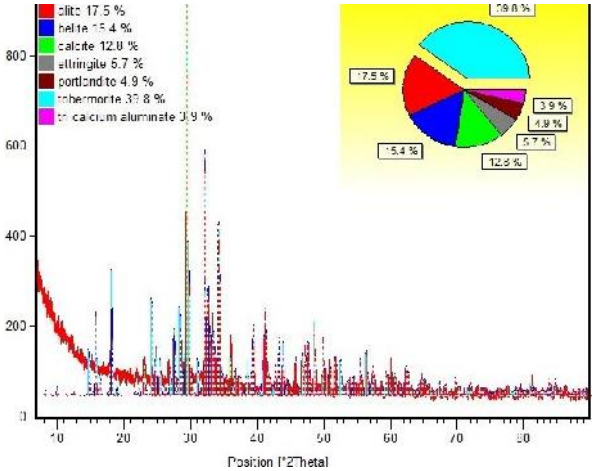

Fig. 4.14 XRD pattern: CW3 (C-90%, W-30%)

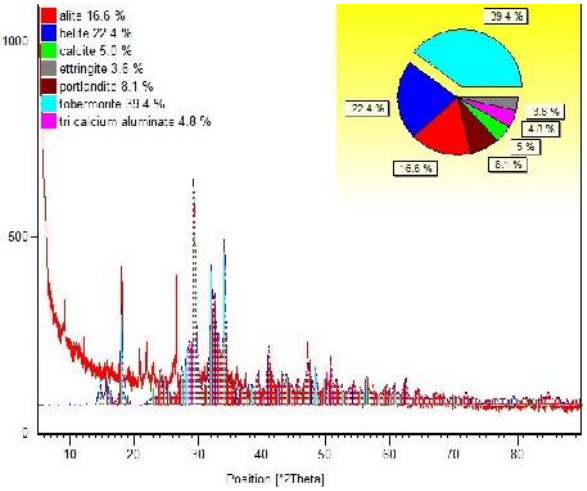

Fig. 4.15 XRD pattern: CFS1 (C-88.5%, F-10%, MS-2.5%)

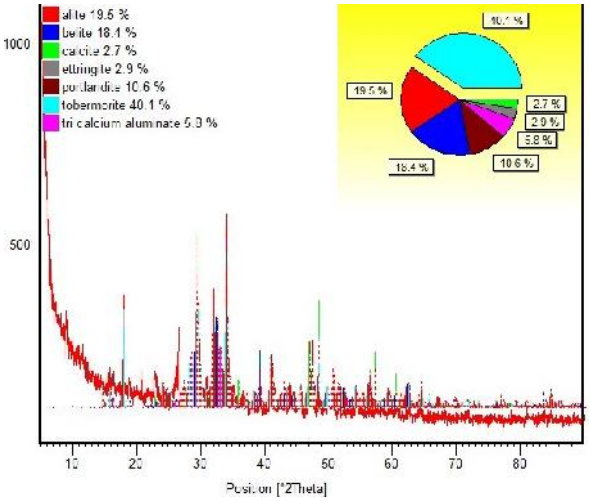

Fig. 4.16 XRD pattern: CFS2 (C-85%, F-10%, MS-5%)

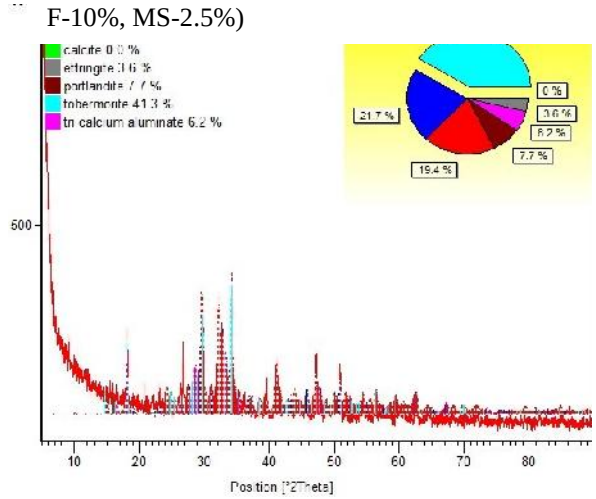

Fig. 4.17 XRD pattern: CFS3 (C-82.5%, F-10%, MS-7.5%)

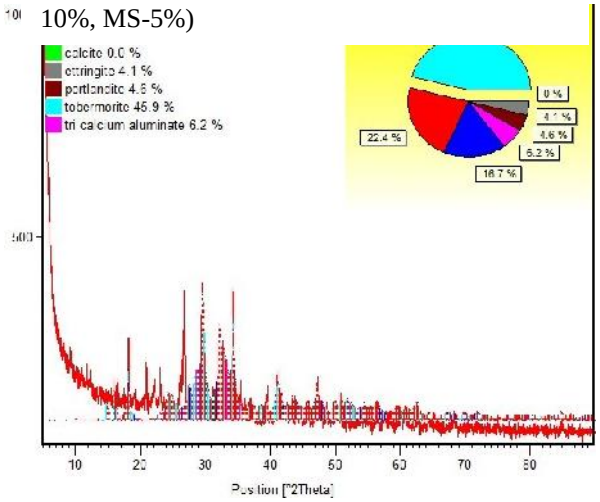

Fig. 4.18 XRD pattern: CFS4 (C-80%, F-10%, MS-10%)

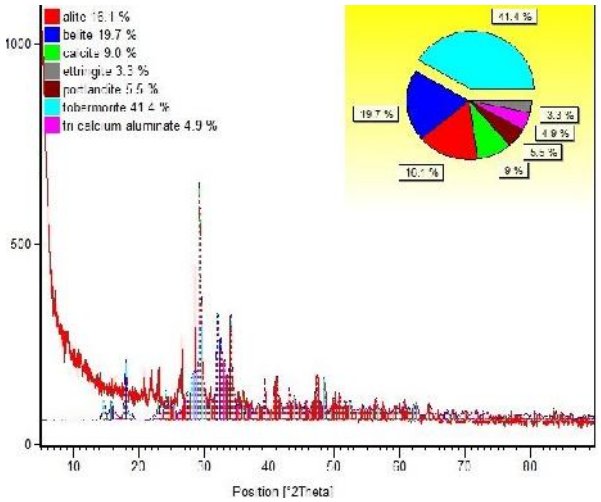

Fig. 4.19 XRD pattern: CFS5 (C-77.5%, F-20%, MS-2.5%)

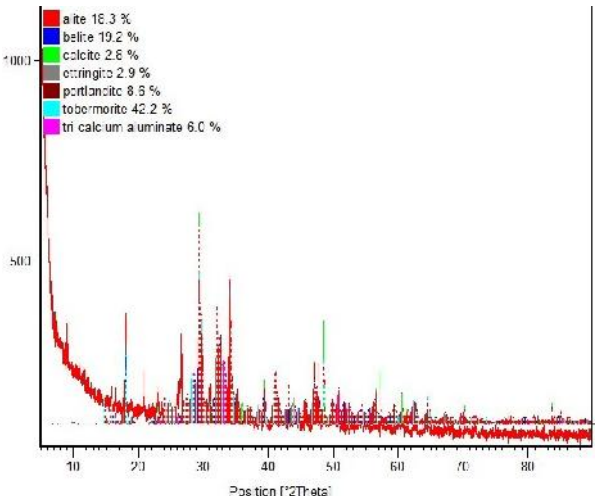

Fig. 4.20 XRD pattern: CFS6 (C-75%, F-20%, MS-5%)

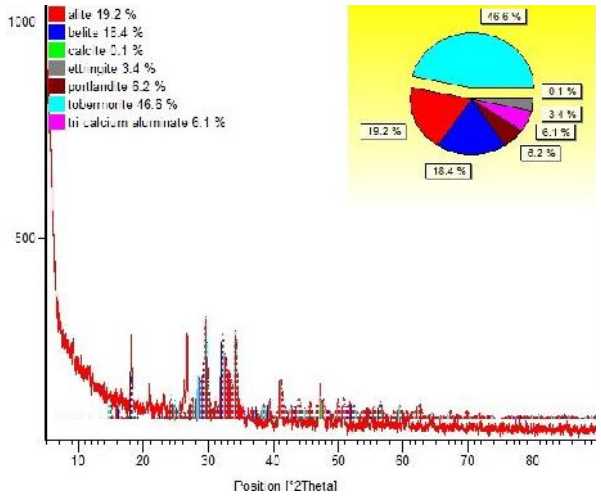

Fig. 4.21 XRD pattern: CFS7 (C-72.5%,F-20%,MS-7.5%)

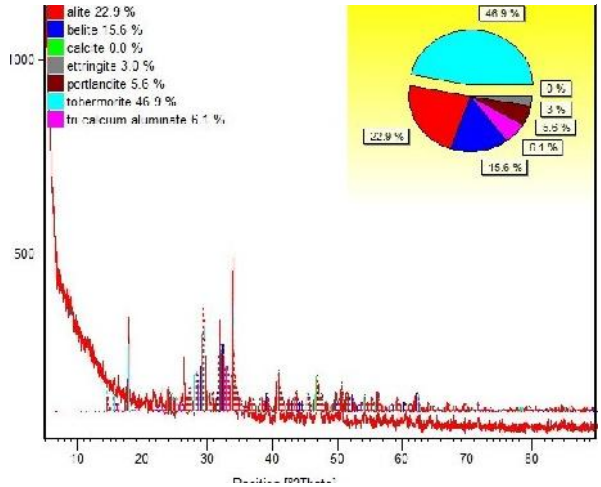

Fig. 4.22 XRD pattern: CFS8 (C-70%,F-20%,MS-10%)

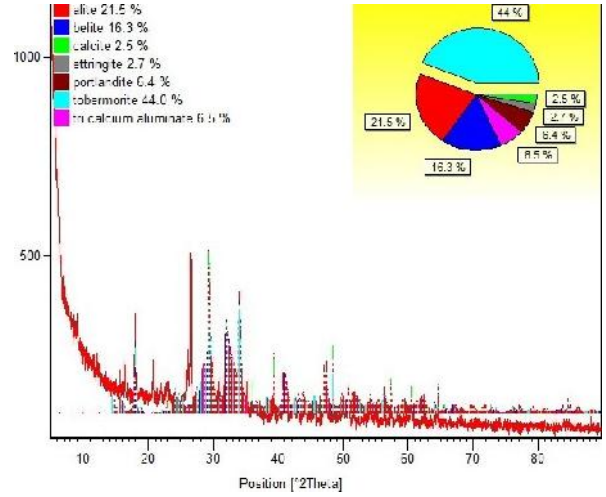

Fig. 4.23 XRD pattern: CFS9 (C-67.5%, F-30%, MS-2.5%)

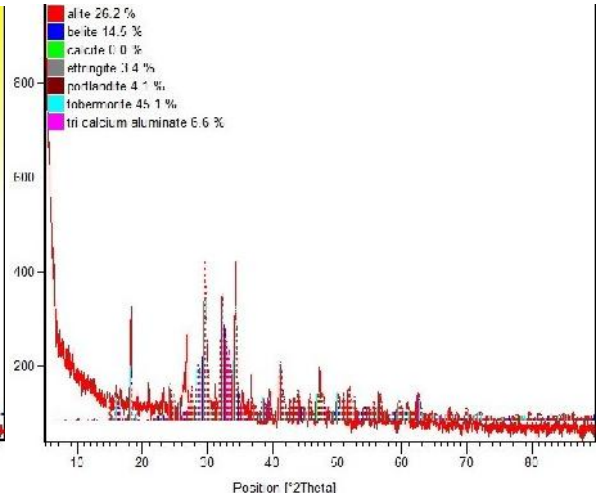

Fig. 4.24 XRD pattern: CFS10 (C-65%, F-30, MS-5%)

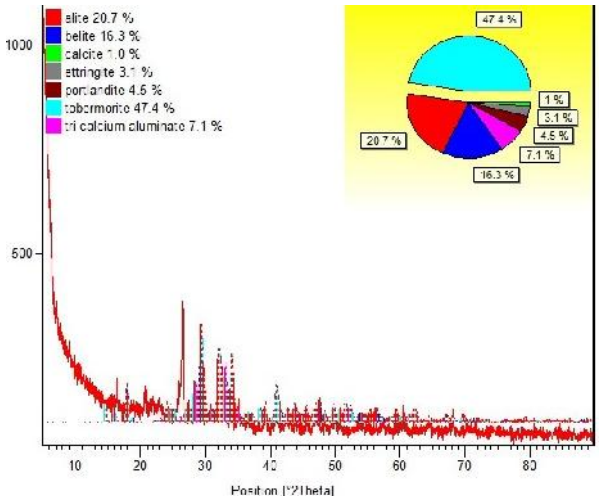

Fig. 4.25 XRD pattern: CFS11 (C-62.5%, F-30%, MS-7.5%)

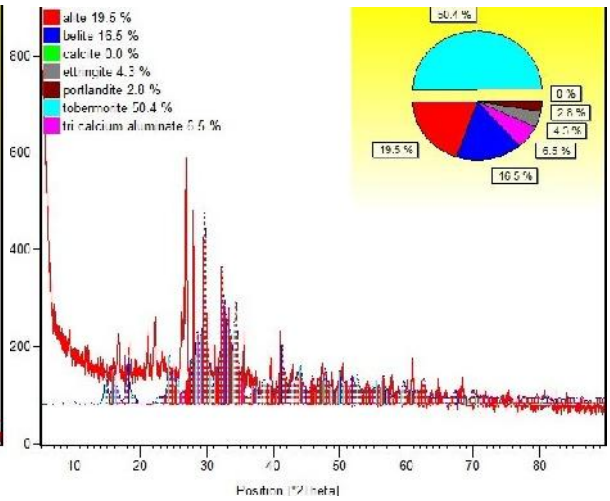

Fig. 4.26 XRD pattern: CFS12 (C-90%, F-30%, MS-10%)

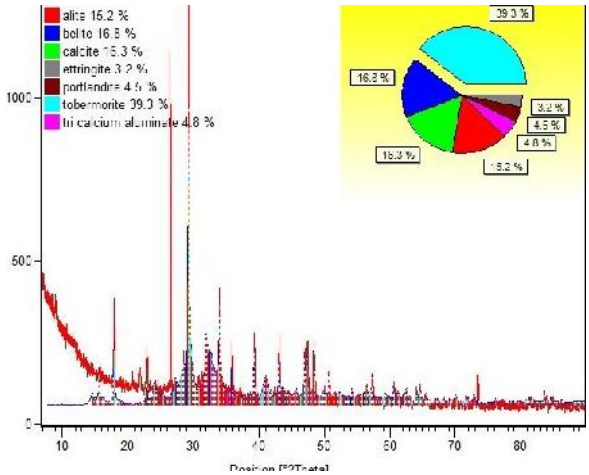

Fig. 4.27 XRD pattern: CWS1 (C-88.5%, W-10%, MS-2.5%)

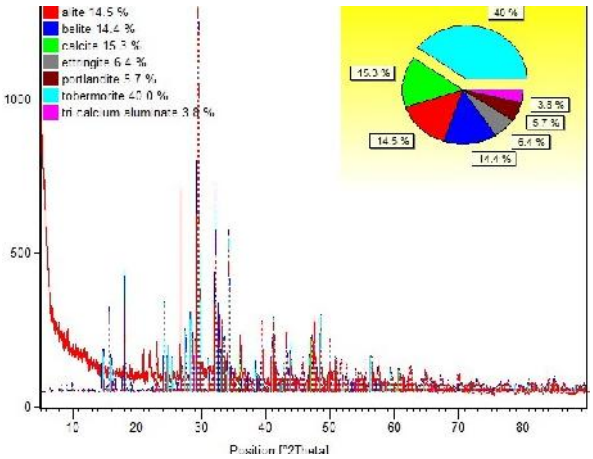

Fig. 4.28 XRD pattern: CWS2 (C-85%, W-10%, MS-5%)

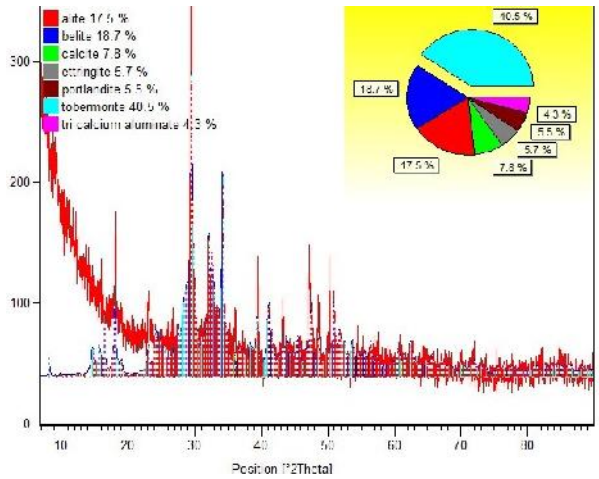

Fig. 4.29 XRD pattern: CWS3 (C-82.5%, W-10%, MS-7.5%)

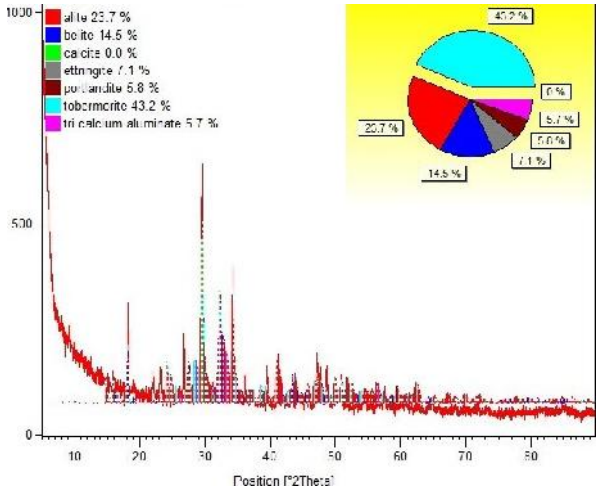

Fig. 4.30 XRD pattern: CWS4 (C-80%, W-10%, MS-10%)

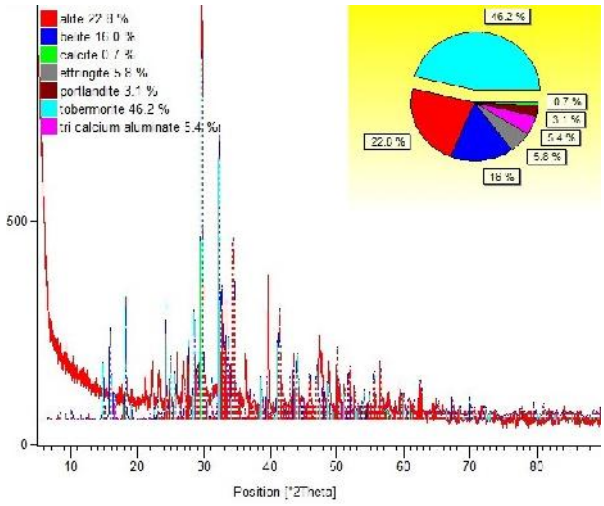

Fig. 4.31 XRD pattern: CWS5 (C-77.5%, W-20%, MS-2.5%)

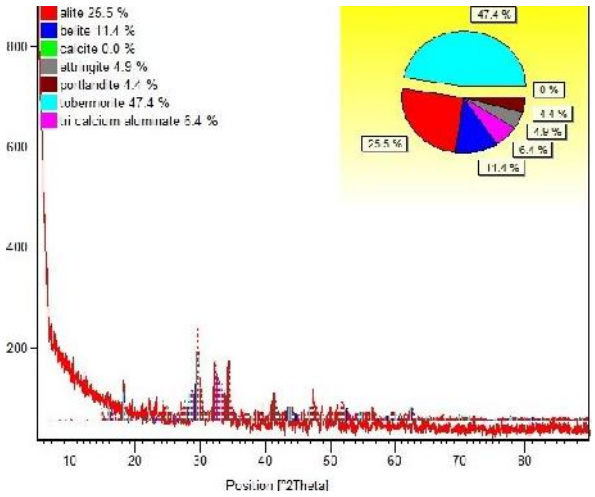

Fig. 4.32 XRD pattern: CWS6 (C-75%, W-20%, MS-5%)

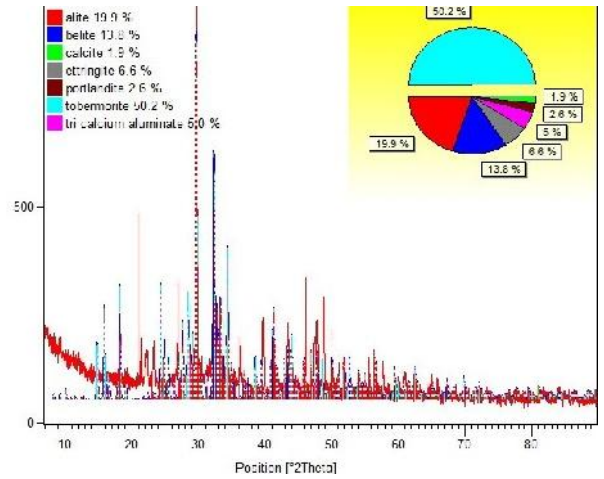

Fig. 4.33 XRD pattern: CWS7 (C-75%, W-20%, MS-7.5%)

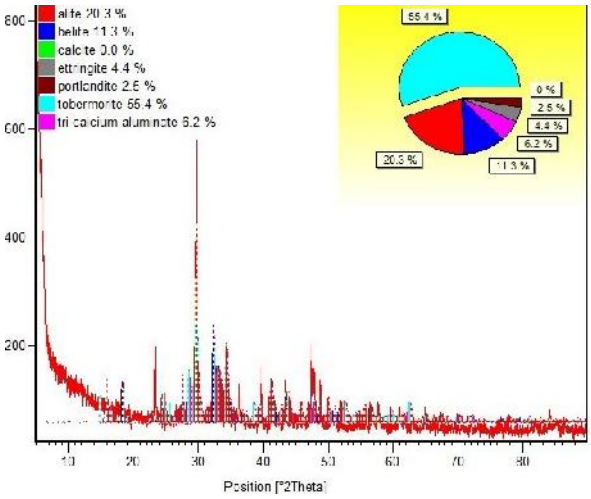

Fig. 4.34 XRD pattern: CWS8 (C-75%, W-20%, MS-10%)

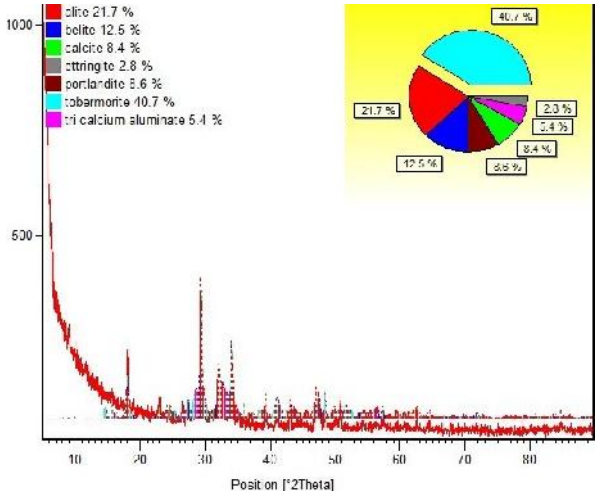

Fig. 4.35 XRD pattern: CWS9 (C-67.5%, W-30%, MS-2.5%)

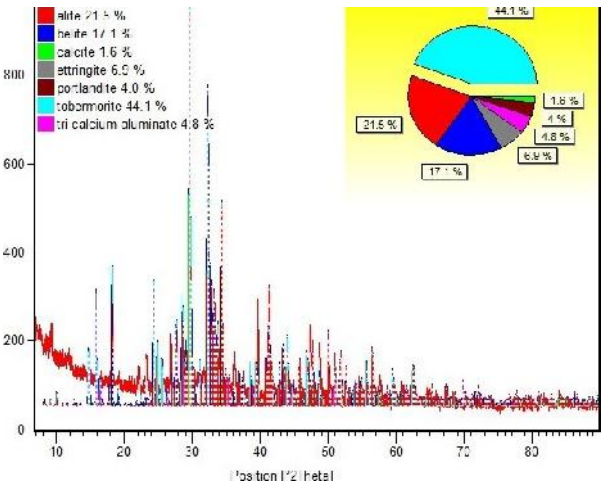

Fig. 4.36 XRD pattern: CWS10 (C-65%, W-30, MS-5%)

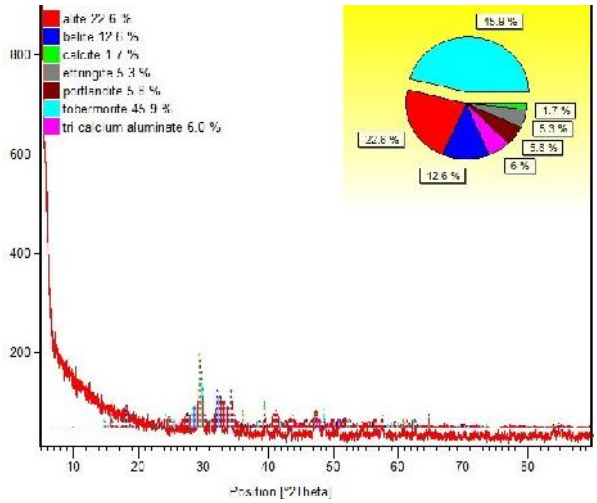

Fig. 4.37 XRD pattern: CWS11(C-62.5%, F-30%, MS-7.5%)

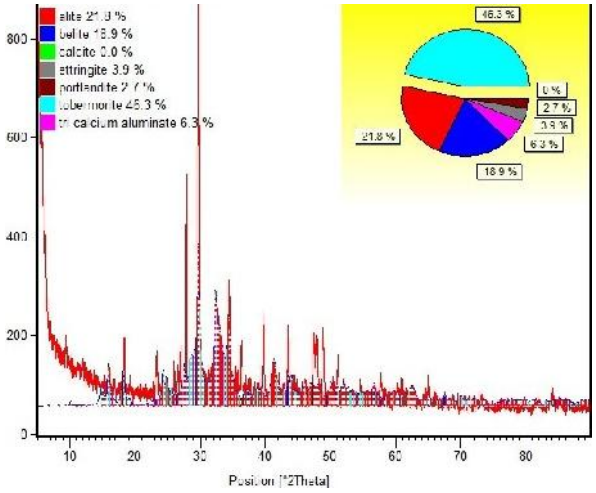

Fig. 4.38 XRD pattern: CWS12(C-90%, F-30%, MS-10%)

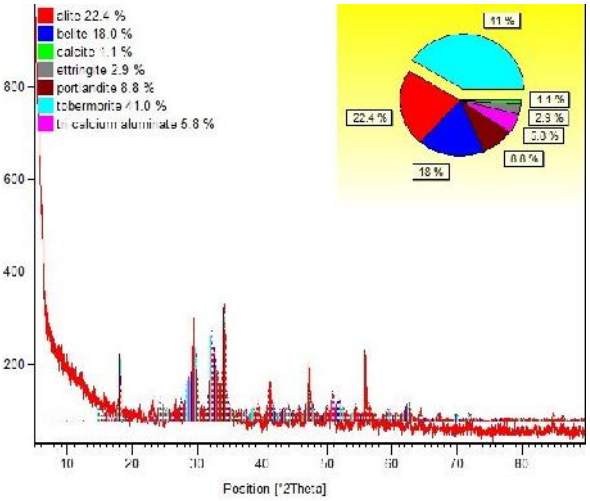

Fig. 4.39 XRD pattern: Cwf (C-90%, W-5%, F-5%)

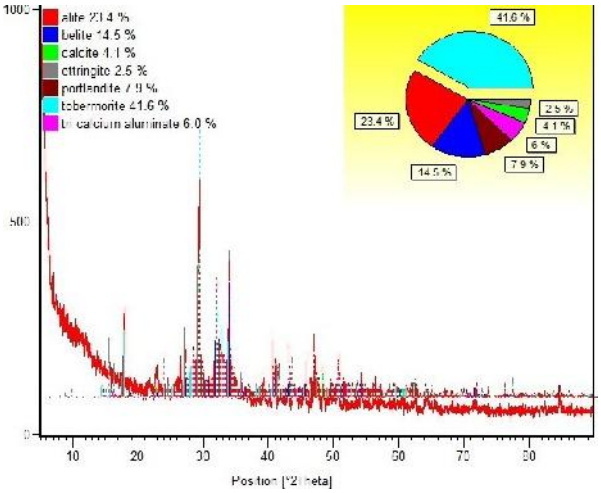

Fig. 4.40 XRD pattern: Cwf S1(C-90%, W-5%, F-5%, MS-2.5%)

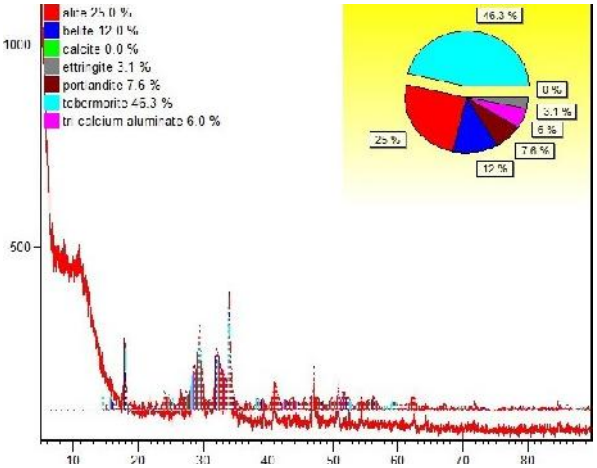

Fig. 4.41 XRD pattern: CwfS2 (C-85%,W-5%.F-5%.MS-5%)

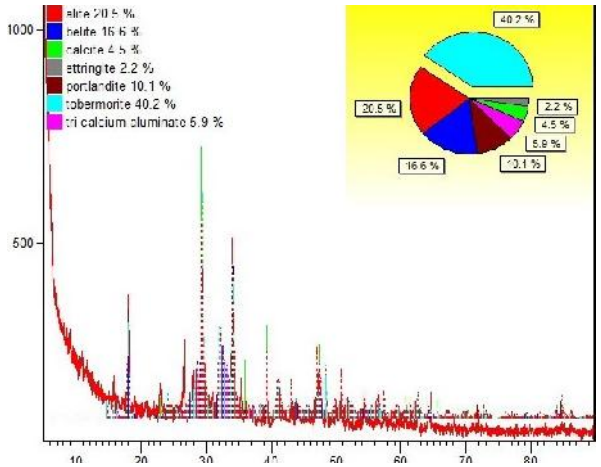

Fig. 4.42 XRD pattern: CWf (C-85%,W-10%.F-5%)

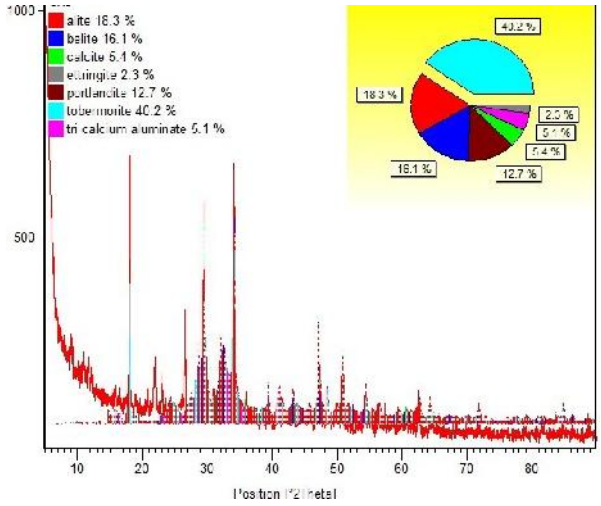

Fig. 4.43 XRD pattern: CwF (C-85%,W-5%,F-10%)

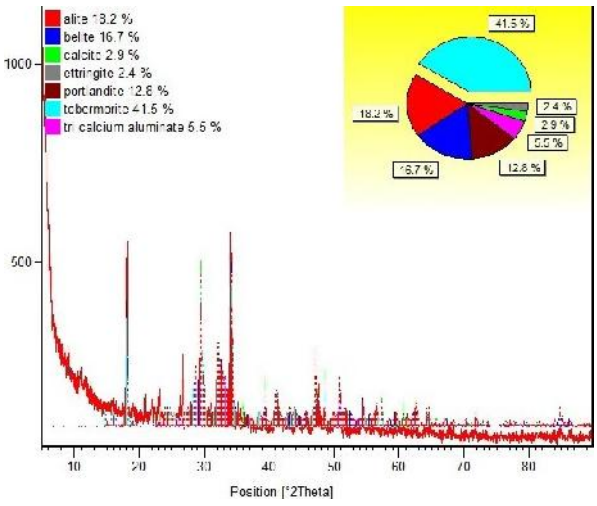

Fig. 4.44 XRD pattern: CwFS1 (C-82.5%,W-5%,F-10%,MS-2.5%)

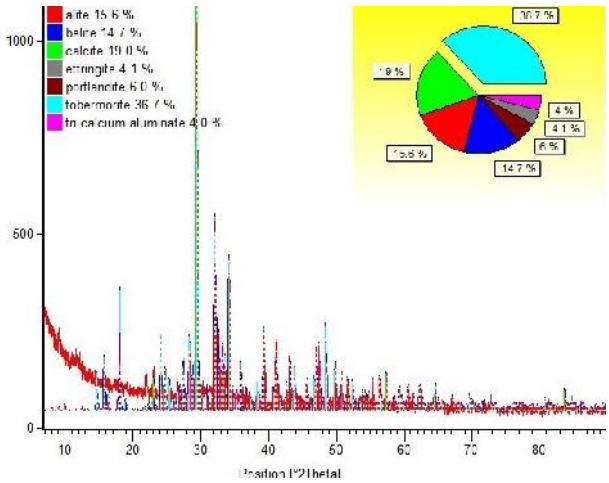

Fig. 4.45 XRD pattern: CWfS1 (C-82.5%,W-10%,F-5%,MS-2.5%)

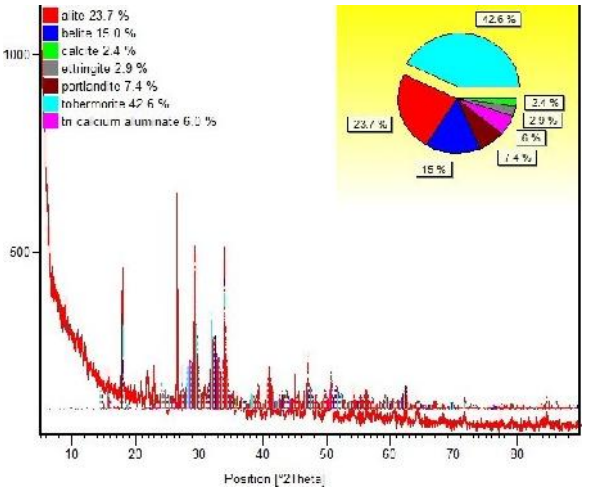

Fig. 4.46 XRD pattern: CwFS2 (C-80%,W-5%,F-10%,MS-5%)

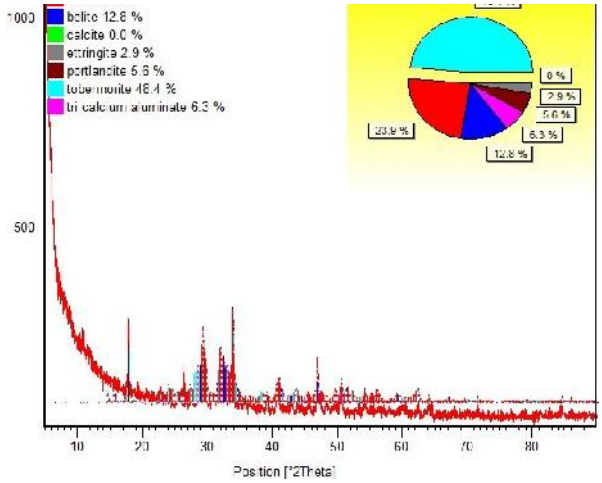

Fig. 4.47 XRD pattern: CWfS2 (C-80%,W-10%,F-5%,MS-5%)

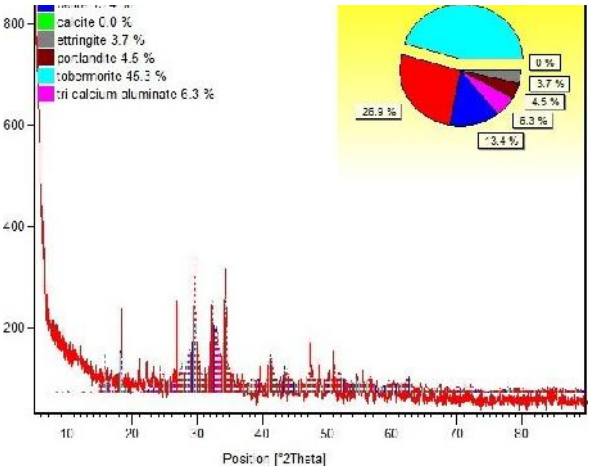

Fig. 4.48 XRD pattern: CWF (C-80%,W-10%,F-10%)

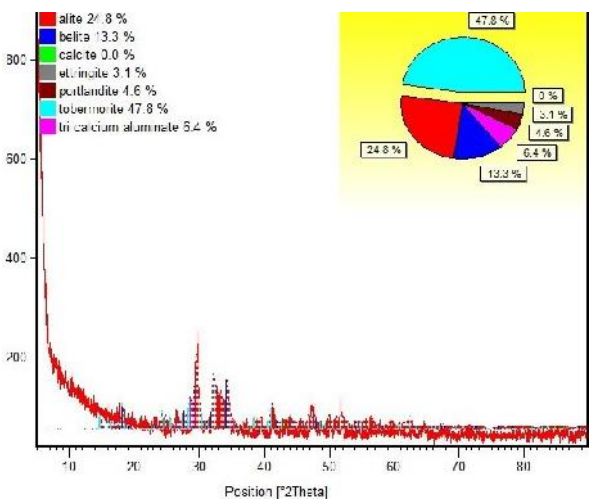

Fig. 4.49 XRD pattern: CWFS1 (C-77.5%, W-10%,F-10%,MS-2.5%)

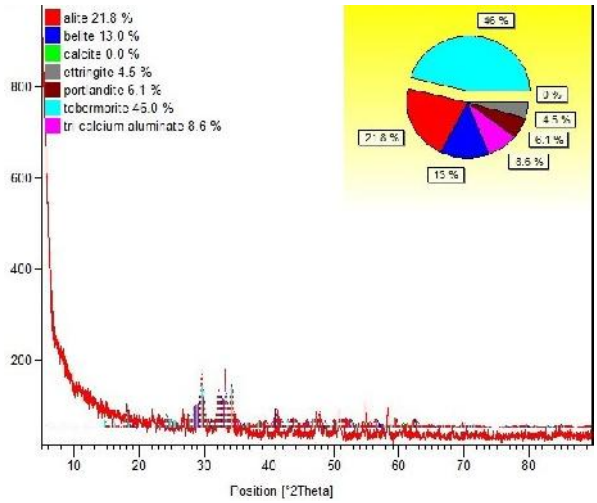

Fig. 4.50 XRD pattern: CWFS2 (C-75%, W-10,F-10%,MS-5%)

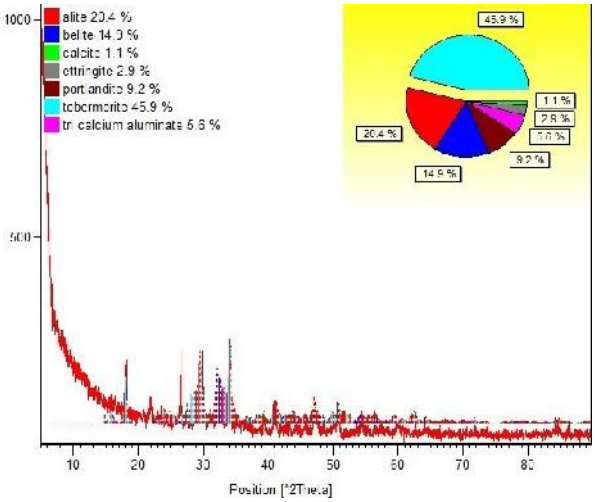

Fig. 4.51 XRD pattern: CWFS3 (C-72.5%, W-10%,F-10%,MS-7.5%)

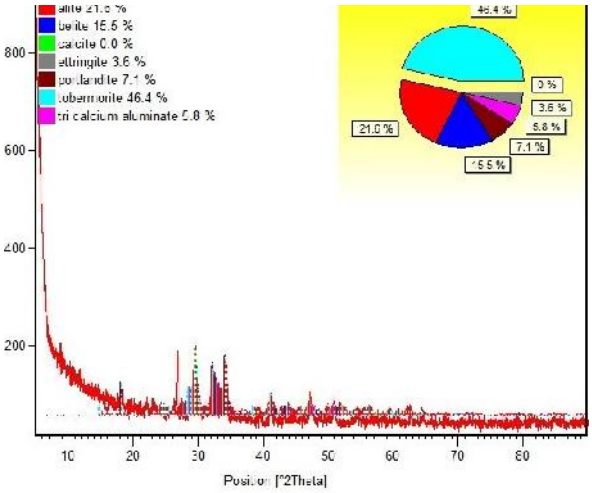

Fig. 4.52 XRD pattern: CWFS4 (C-70%, W-10%,F-10%, MS-10%)

Following observations are made from the XRD study:

(i) Influence of flyash & microsilica

With the increase in flyash content, the rate of chemical reaction tends to increase between 1-3 days. Formations of C-S-H gels increase with the increase of flyash inclusion and on the other hand, there is considerable reduction in CH formation. It has also been observed that inclusion of flyash slightly generates more C_3A and ettringite compounds as can be read from the Table 4.9. No significant improvement in the formation of C-S-H gel was observed for the ternary mixes when flyash content was maintained constant @ 10% and for varying content of microsilica i.e. 2.%% , 5.0%, 7.5% & 10% when compared to binary mixes (cement: flyash). The influence of flyash is rather more effective than microsilica content as far as formations of C-S-H gels are concerned. Higher formations of C-S-H gels on admixing of flyash is mainly due to presence of substantial amount of silica in flyash and when this component combines with the free calcium hydroxide, liberated during hydration of cement, reacted to form additional calcium-silicate –hydrate (C-S-H).

(ii) Influence of wollastonite microfiber and microsilica

WMF led to an increment in the water content by displacement of water from cement particles' voids and also hydration space, due to percolation effect. This favoured a high rate of reaction and thus more C-S-H content in the initial period of hydration. But this effect was limited up to only 20% WMF content, because beyond it, the dilution of cement prevailed which led to a decrement in the C-S-H gel formed.

WMF reduced lime content alike flyash, due to good amount of reactive silica present in it but only flyash was found to reduce ettringite from the hydrates due to higher amount of less reactive alumina, which went into solution slowly after ettringite formation and converted ettringite into calcium aluminate mono sulphate hydrate. Formations of C-S-H gels were almost equal to that of flyash admixed cement pastes irrespective of their contents. The rate of formation of C-S-H compounds gradually increased as the dosage of WMF increased for the same microsilica contents and subsequently CH compounds reduced. For binary mixes, maximum C-S-H compounds were observed from CF3 (70%C: 30% F) mix followed by CW2 (80%C: 20%W), CF2 (80%C:20%F), CW1 (90%C:10%W), CW3

(70%C: 30%W), and CF1 (90%C:10%W) respectively. Similarly for ternary mixes, maximum C-S-H compounds were produced by CWS8 (70%C: 20%W: 10%M), followed by CFS12 (62.5%C: 30%F: 10%S), CWS7 (72.5%C: 20%W: 7.5% S), CFS11 (60%C: 30%F: 7.5%S) & CWS6 (75%C:20%W:5%S), respectively. The most prominent mixes among the quaternary proportions which produced maximum C-S-H compounds are CWfS2 followed by CWFS1, CWFS4, CwfS2 and CWS12 respectively. Microsilica addition shortened the dormant period and increased the acceleration of hydration after dormant period. Therefore an increase in C-S-H content was found with increase in microsilica content both for flyash and WMF substitution. Microsilica increases the hydration rate and it reduces the lime content at a higher rate than other admixtures, but it cannot control growing ettringite because of its lower alumina content.

4.3.2 SEM Image Analysis

The structure of the calcium silicate hydrate was studied by Diamond [33]. It was found in the study, that calcium silicate hydrate exists in variety of forms, namely: fibrous, flattened, reticular and irregular grains. All these forms are difficult to define. The variation is due to the ratio of lime (CaO) to silicate (SiO_2) content in it. With age the ratio keeps on changing. At a given time in a paste, various forms may coexist due to presence of newly hydrated surfaces of cement particles along with old hydrated ones. In order to show this confusion and structural non uniformity, calcium silicate hydrates have their chemical composition being represented as C-S-H. The hashes within the C, S and H represent the changing ratio of their linkage. The C-S-H has its length in the range of 0.5 to 2 microns and it is lesser than 0.2 microns in thickness. CH exists in the form of distinguished thick hexagonal Plates of white colour, such that all Plates are inclined to a certain axes at similar angle. These platy crystals are much bigger in size than crystals of other hydration products. Ettringite exist in the form of thin elongated needles mainly occurring in small groups, having bright white colour, which enhance the stiffness of the concrete. Calcium aluminate mono sulphate exists in the form of greyish-black hexagonal crystals combined together in the form of a rosette structure. Due to low sulphur content, they are prone to sulphate attack.

Plate 4.1(1)-(45) show the SEM images of the paste, with or without mineral admixtures obtained after 7 days of curing.

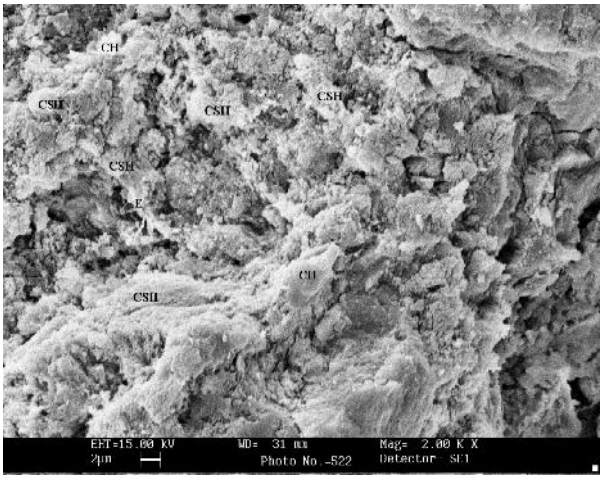

Plate 4.1 (1) Hydrated cement mass

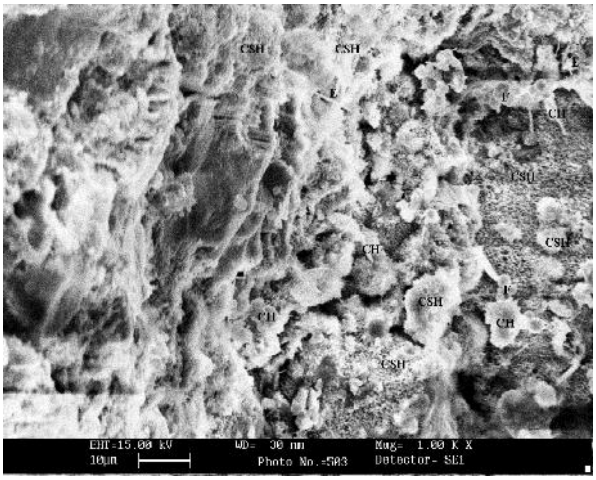

Plate 4.1 (2) CF1 (C-90%, F-10%)

Plate 4.1 (1) shows presence of C-S-H and CH in the ground mass. Plate 4.1 (2) depicts the presence of C-S-H and numerous CH in sample.

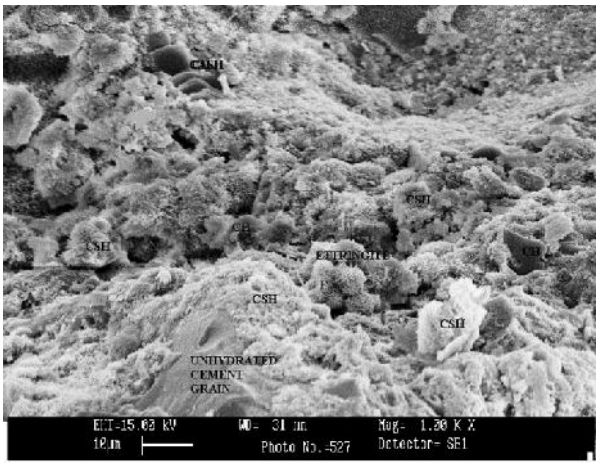

Plate 4.1 (3) CF2 (C-80%, F-20%)

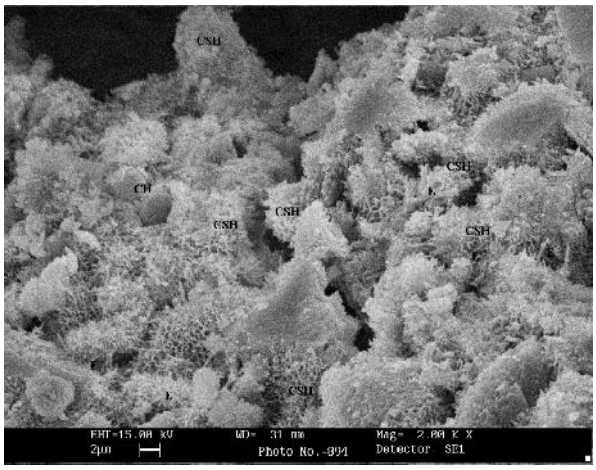

Plate 4.1 (4) CF3 (C-70%, F-30%)

Plate 4.1 (3) shows appreciable amount of C-S-H, and small quantities of CH compounds. The reduction in CH compounds is due to conversion of the same to C-S-H compounds under pozzolanic activity between silica and CH liberated during hydration of cement.

Plate 4.1 (4) shows the larger area of initially developed C-S-H in the Plate. This is due to higher amount of CH and ettringite being converted into C-S-H.

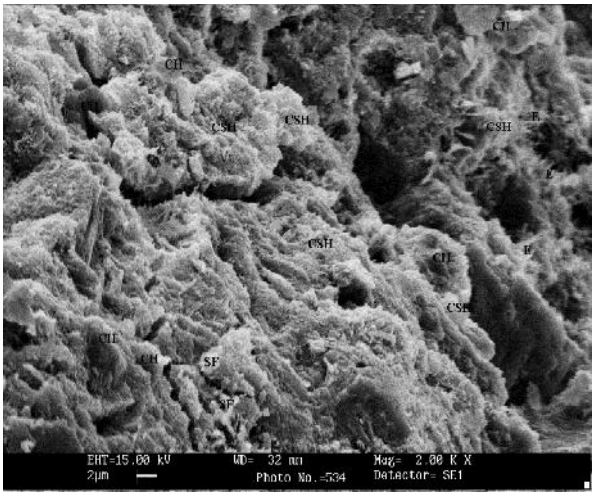

Plate4.1 (5) CFS1 (C-88.5%, F-10%, MS-2.5%)

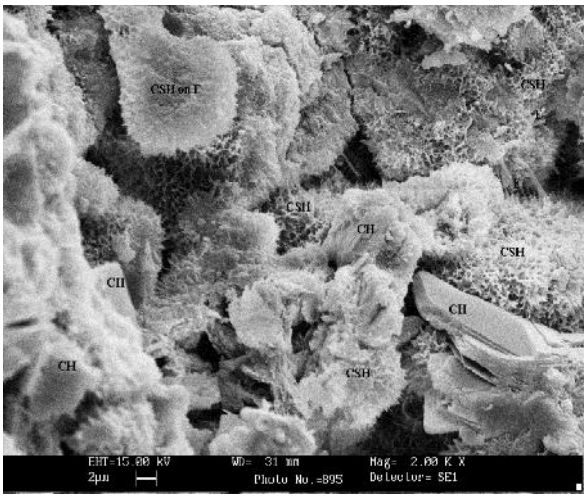

Plate 4.1 (6) CFS2 (C-85%, F-10%, MS-5%)

Presence of numerous air voids is visible in both plates 5 & 6. Both the groundmasses contain micro-cracks. Presence of few ettringites at the interface of coarse aggregates and hydrated cement paste are also distinctly observed. Both of these Plates show an improvement in grain refinement on account of microsilica plus flyash. The small and fibrous C-S-H nucleated on the surface of cement grains due to microsilica is clearly visible in Plate 4.1 (6). For even 5% microsilica, there is presence of CH in the mix. C-S-H is also seen nucleated on the bigger sized flyash particles.

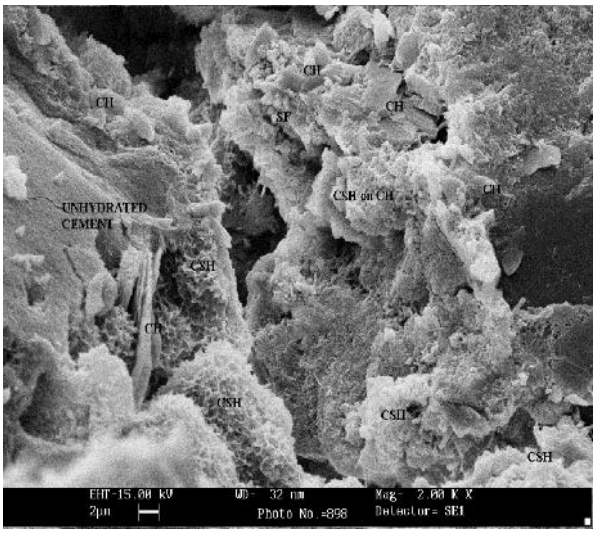

Plate 4.1 (7) CFS3 (C-82.5%, F-10%, MS-7.5%)

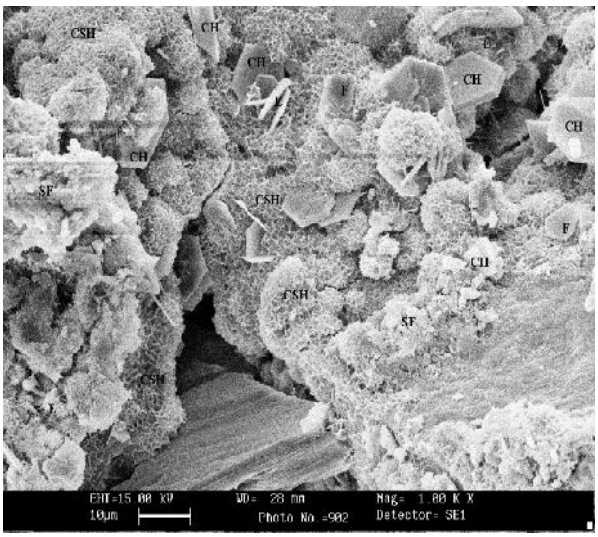

Plate 4.1(8) CFS4 (C-80%, F-10%, MS-10%)

Larger micro-cracks and air pockets are visible in Plate 4.1 (7). Few remnant cement grains & unhydrated microsilica are also clearly noticed from Plate 4.1 (7). Abundant

formations of C-S-H compounds are distinctly noticed from both the Plates 4.1 (7) & (8). However, denser matrix of C-S-H compounds & platy structures of CH compounds are more distinctly observed from Plate 4.1 (8). This proves that flyash at 10% content, in presence of high microsilica content, is still able to cause grain size refinement within the voids of cement particles though the pore size refinement is low.

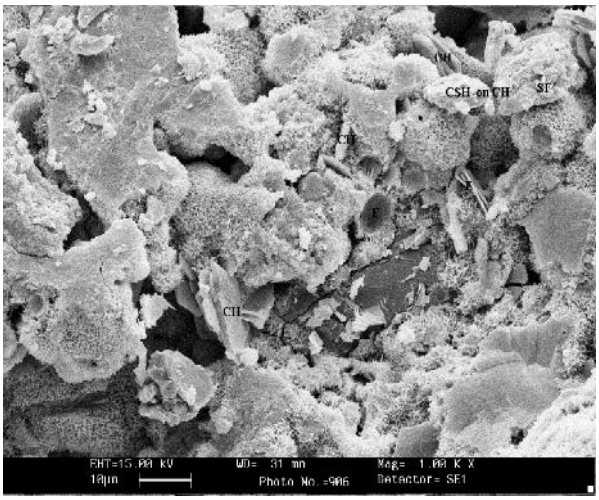

Plate 4.1 (9) CFS5 (C-77.5%, F-20%, MS-2.5%)

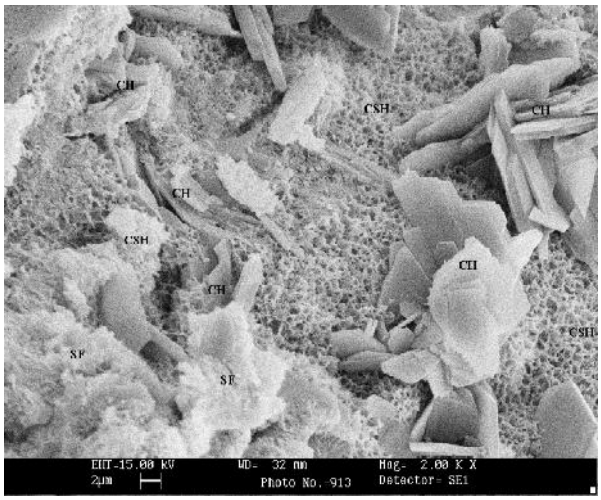

Plate 4.1 (10) CFS6 (C-75%, F-20%, MS-5%)

Due to lesser microsilica in CFS 5, it does not show enough C-S-H on the cement grains. In Plate 4.1 (10), there is very high amount of C-S-H nucleated on the cement grains surface due to hydration by microsilica. But along with this, CH is also visible, which proves that even for 20% flyash, CH is not being controlled.

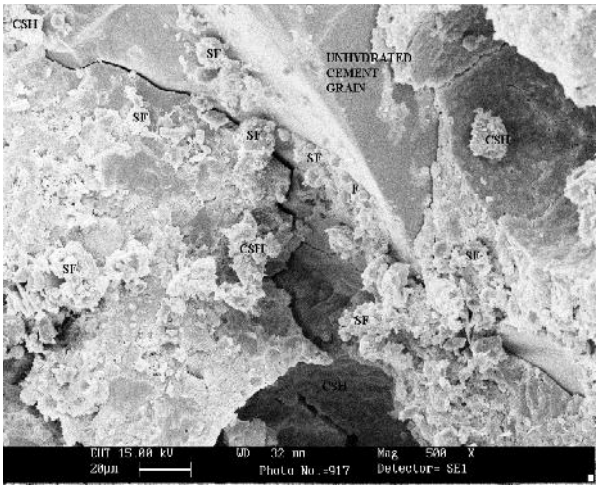

Plate 4.1 (11) CFS7 (C-72.5%,F-20%,MS-7.5%)

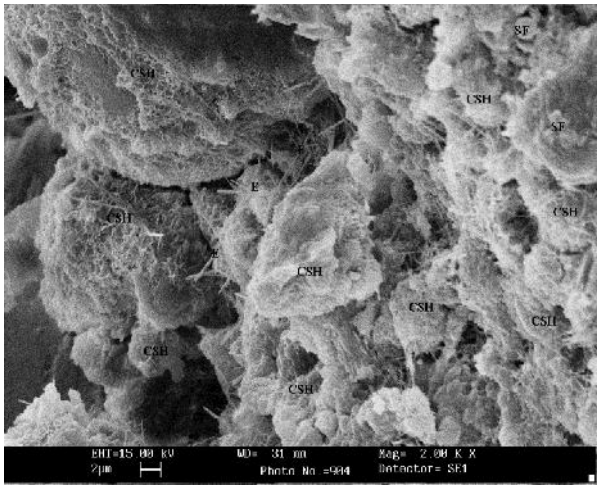

Plate 4.1 (12) CFS8 (C-70%,F-20%,MS-10%)

Plate 4.1 (11) & 4.1 (12) show the presence of ettringite at higher amounts of microsilica. This proves that the effect of microsilica hydration is more production of C-S-H by consumption of CH than ettringite. Though, flyash is present in considerable amount (20%) here, but due to lower rate of hydration it is not able to convert the CH and ettringite so quickly.

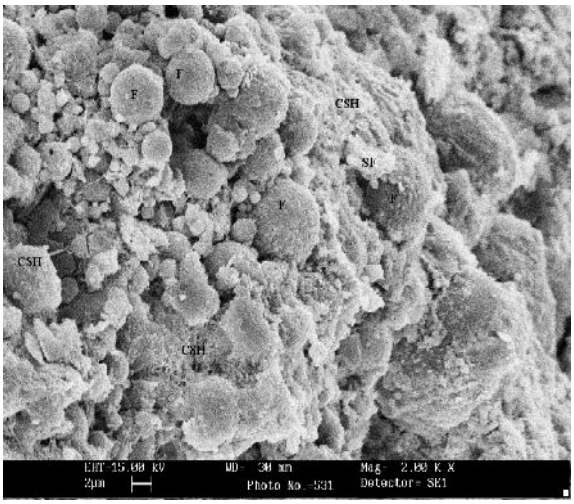

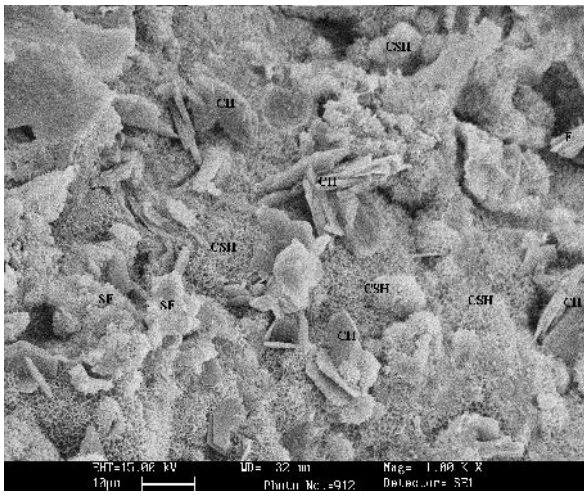

Plate 4.1 (13) CFS9 (C-67.5%, F-30%, MS-2.5%) **Plate 4.1 (14) CFS10** (C-65%, F-30, MS-5%)

In mix CFS9 and CFS 10, the flyash content is already too high, whereas the microsilica content is not so. Therefore a high volume of unhydrated flyash can be seen in Plate 4.1 (13) and 4.1 (14). The medium amount of microsilica though has been able to be adsorbed and hydrated on the flyash surface, thereby densifying the mix, as seen in Plate 4.1 (14).

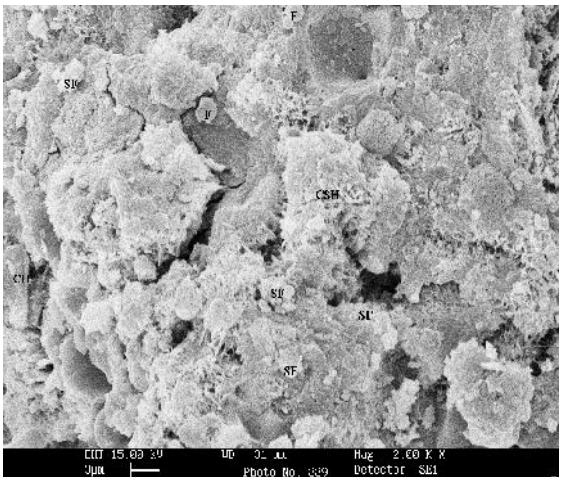

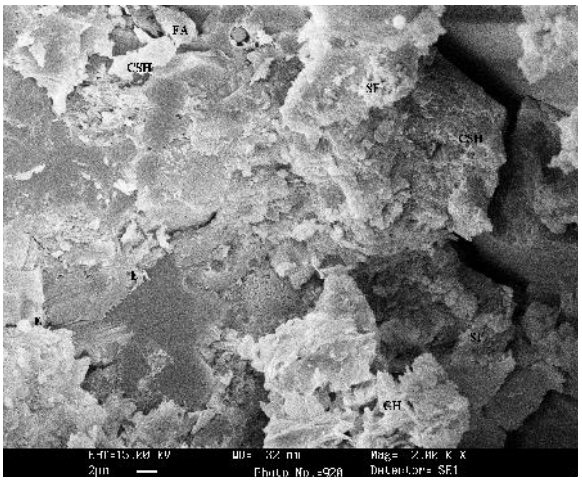

Plate 4.1 (15) CFS11 (C-62.5%, F-30%, MS-7.5%) **Plate 4.1 (16) CFS12** (C-90%, F-30%, MS-10%)

In Plate 4.1 (15) & (16), microsilica particles are seen on the surface of unhydrated cement particles. CFS 11 looks more dense and hydrated than CFS 12. Some trace of CH is also visible on the lower right corner of the mix CFS12. This shows the optimum amount of microsilica is around 7.5% in the mix containing more than 20% flyash.

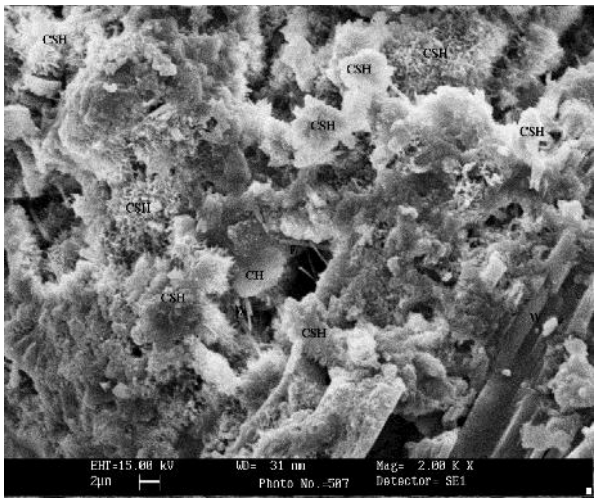

Plate 4.1 (17) CW1 (C-90%, W-10%)

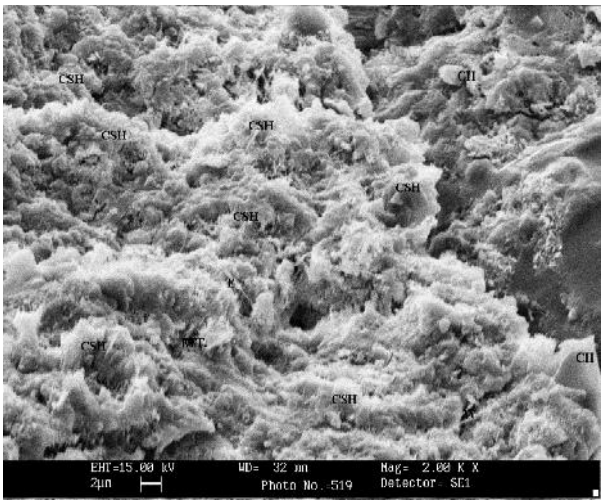

Plate 4.1 (18) CW2 (C-90%, W-20%)

The mix CW1 and CW2 in the Plate 4.1 (17) & (18) show no presence of unreacted WMF even at 20% of its content in the mix. This proves that WMF is not inert.

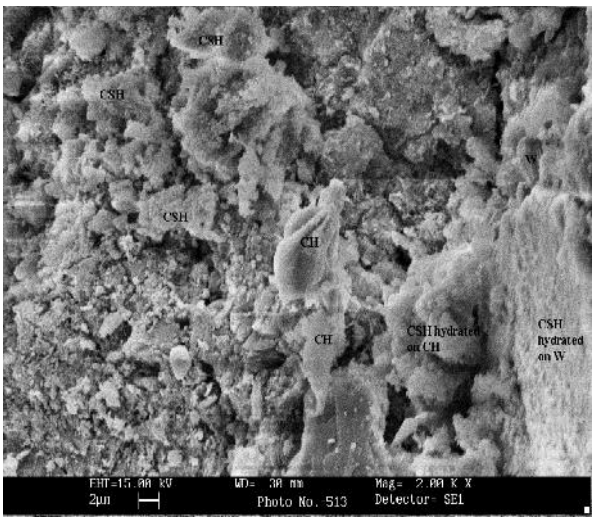

Plate 4.1 (19) CW3 (C-90%, W-30%)

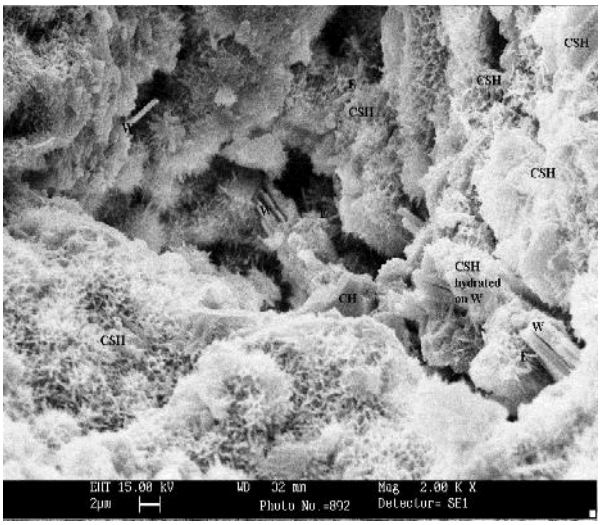

Plate 4.1 (20) CWS1 (C-88.5%, W-10%, MS-2.5%)

In Plate 4.1 (19) C-S-H along with small amount of CH is seen. But there is no sign of Ettringite. It could mean that WMF converted both CH and ettringite by its hydration, but XRD

tests do not comply with this view. Hence, it may happen that WMF caused more grain size refinement of ettringite and CH rather than pore size refinement. Plate 4.1 (20) shows, higher amount of C-S-H on cement particles, due to hydration by microsilica. The unhydrated WMF is also seen on the right hand side corner and in the interior of the Plate. This clearly represents that microsilica is highly reactive in the presence of WMF too, as flyash.

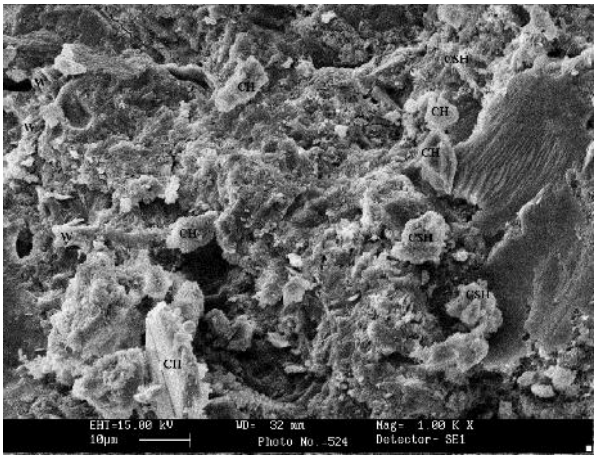

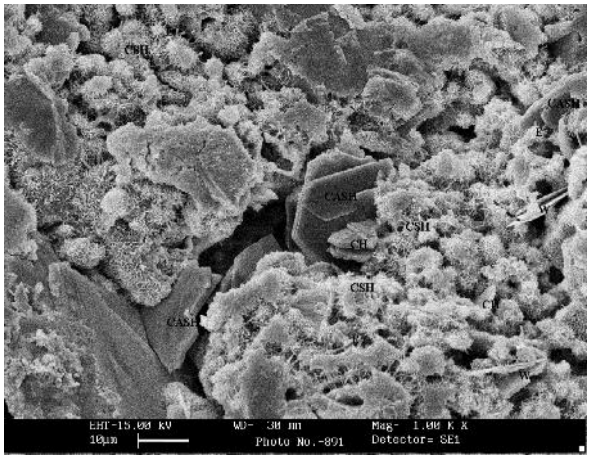

Plate 4.1 (21) CWS2 (C-85%, W-10%, MS-5%) **Plate 4.1 (22) CWS3** (C-82.5%, W-10%, MS-7.5%)

In both the mixes shown above in Plate 4.1 (21) & (22), the structure is dense with the presence of high surface area C-S-H. There is presence of ettringite as seen on the lower right hand side portion of Plate 4.1 (22) in mix CWS3. This proves that alike flyash-microsilica, WMF-microsilica are also not able to convert ettringite into mono sulphates to appreciable extent. Also greyish coloured hexagonal CASH is seen in the interior of this Plate, which proves that a little conversion activity of ettringite is though going on.

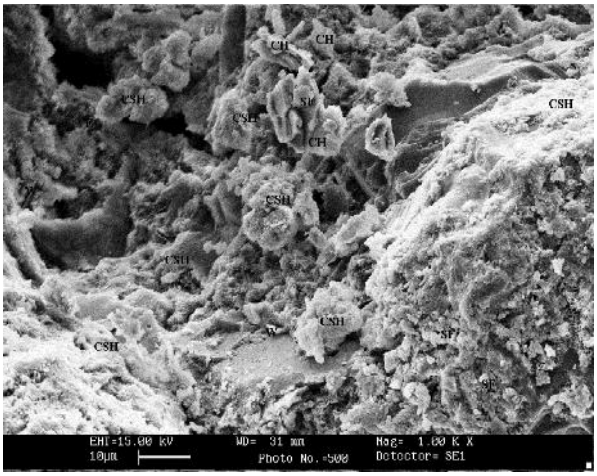

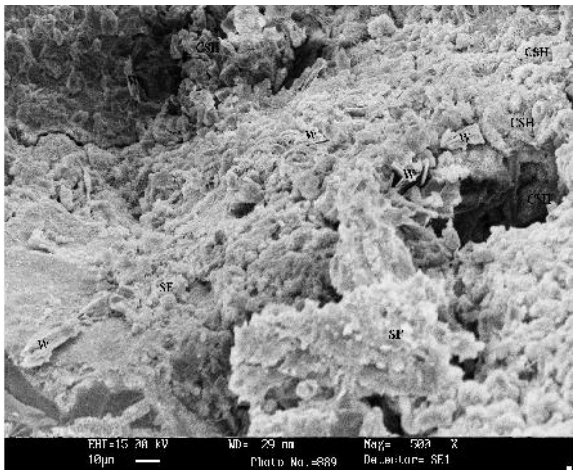

Plate 4.1 (23) CWS4 (C-80%, W-10%, MS-10%) **Plate 4.1(24) CWS5** (C-77.5%, W-20%, MS-2.5%)

Not much appreciable information is available from Plate 4.1 (23) & (24), which only shows that a thick and wide spreaded C-S-H layer is nucleated on the cement particles caused by the combined action of WMF and microsilica. Microsilica adsorbs fully on the cement particles and hydrate there. Further hydration makes large flakes on earlier produced small thin fibrous C-S-H produced by microsilica.

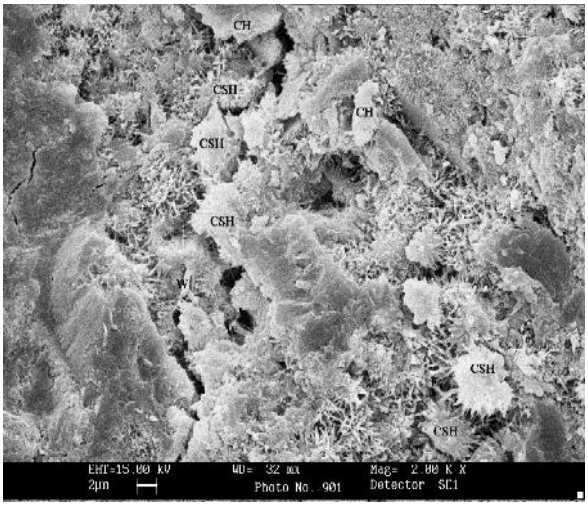

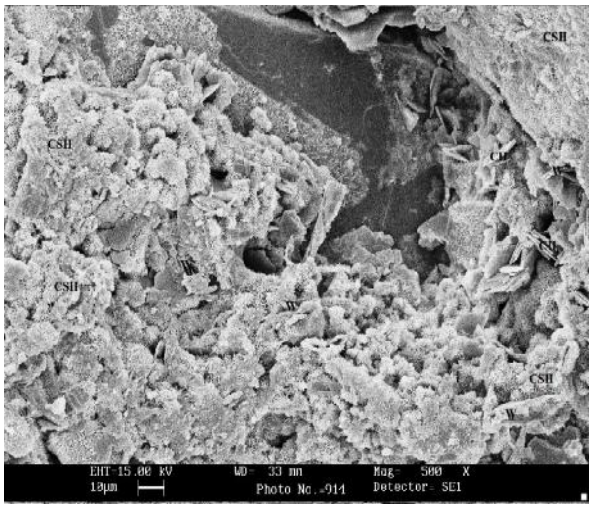

Plate 4.1(25) CWS6 (C-75%, W-20%, MS-5%)

Plate 4.1 (26) CWS7 (C-75%, W-20%, MS-7.5%)

Plate 4.1 (25) shows the presence of C-S-H and ettringite together, though the action of microsilica is apparently seen in the form of thin fibrous C-S-H layer on the cement grains. Very little presence of CH is seen. At high amount of microsilica (7.5%), WMF microsilica is seen nucleating on the particles of WMF in Plate 4.1 (26), having mix CWS7.

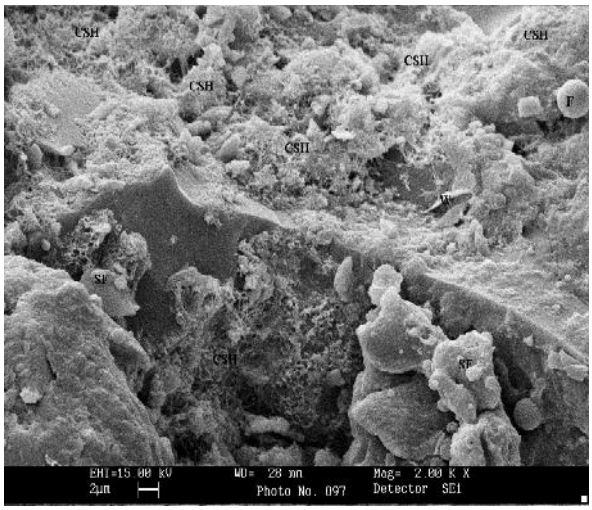

Plate 4.1 (27) CWS8 (C-75%, W-20%, MS-10%)

No trace at all of WMF is seen in Plate 4.1 (27) because of the presence of high microsilica, which nucleated on the particles of WMF too, along with cement, and thus bound them together. This also improves the strength. Presence of calcite is also seen in this Plate, which shows the effect of enough lime in the mix (probability of expansion).

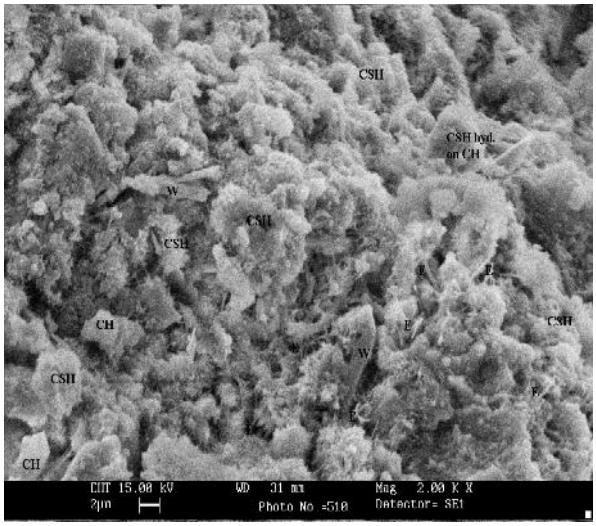

Plate 4.1(28) CWS9 (C-67.5%, W-30%, MS-2.5%)

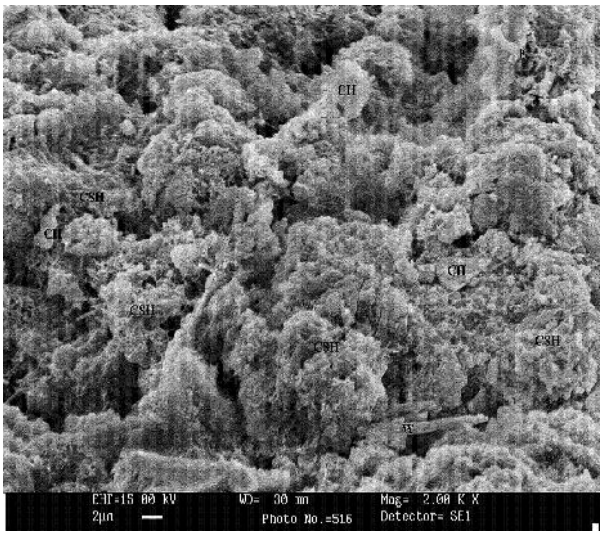

Plate 4.1 (29) CWS10 (C-65%, W-30, MS-5%)

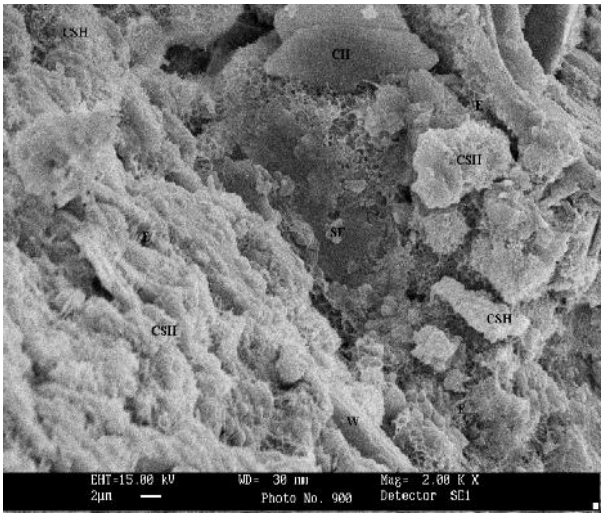

Plate 4.1 (30) CWS11(C-62.5%, F-30%, MS-7.5%)

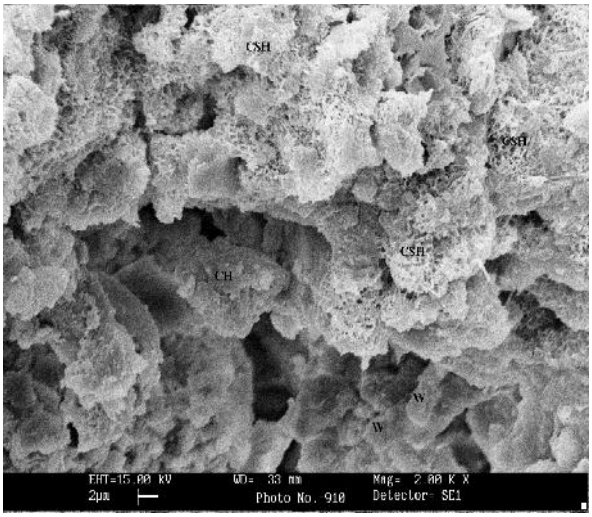

Plate 4.1 (31) CWS12(C-90%, F-30%, MS-10%)

The mixes in Plate 4.1 (28), (29), (30) and (31) show a very similar dense indistinguishable C-S-H layer on cement particles. A very small trace of CH is also seen but due to grain size refinement it looks disoriented. There are very less voids and even no presence of free WMF or microsilica is seen.

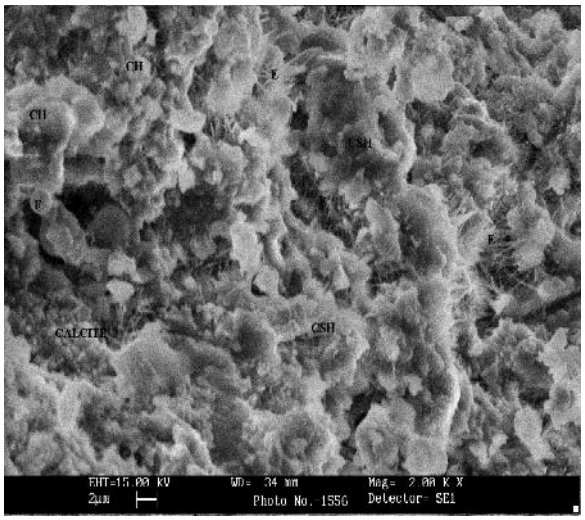

Plate 4.1 (32) Cwf (C-90%, W-5%, F-5%)

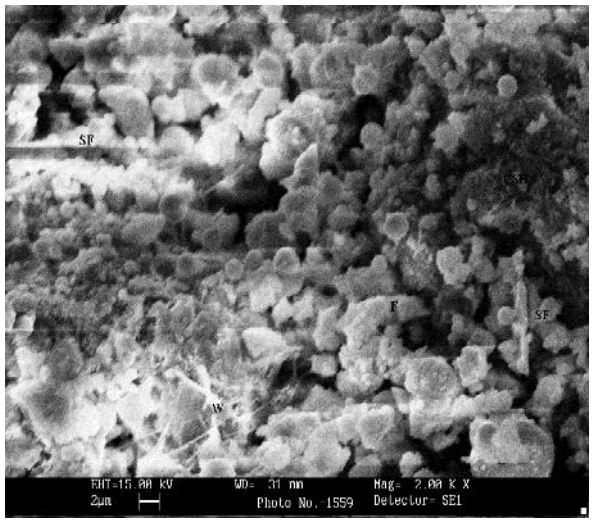

Plate 4.1 (33) CwfS1 (C-88.5%,W-5% F- 5%,MS-

The Plate 4.1 (32) & (33) shown above, represent a dense structure, which indicates more strength than same mass of other admixture combinations discussed earlier. But instead of C-S-H, there is presence of free flyash and hydrated product like calcite which do not provide strength. Hence these mixes may be impermeable on account of grain refinement but don't have equal proportions of strength increment.

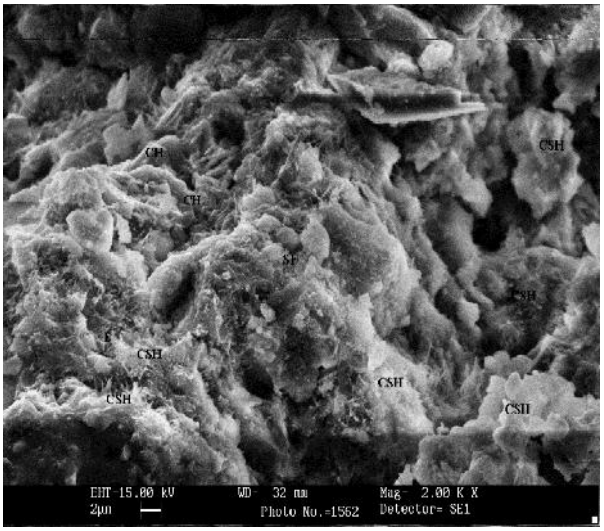

Plate 4.1 (34) CwfS2 (C-85%,W-5%,F-5%,MS-5%)

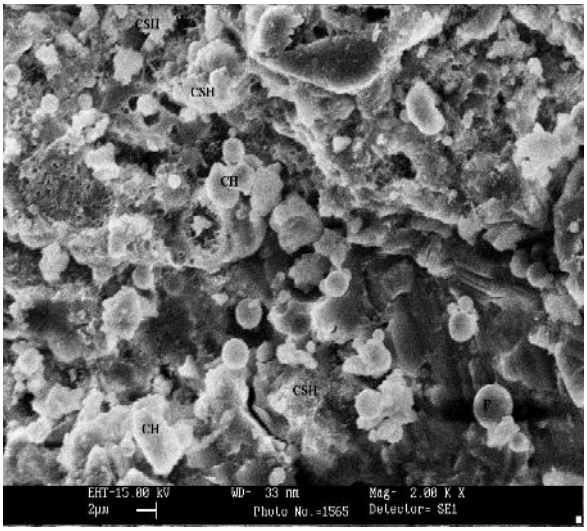

Plate 4.1 (35) CWf (C-85%,W-10%,F-5%)

Plate 4.1 (34) & (35) shown above indicate more dense structure and also more presence of C-S-H in comparison to Cwf and CwfS1. Still there is presence of free non reacted flyash on the hydrated products.

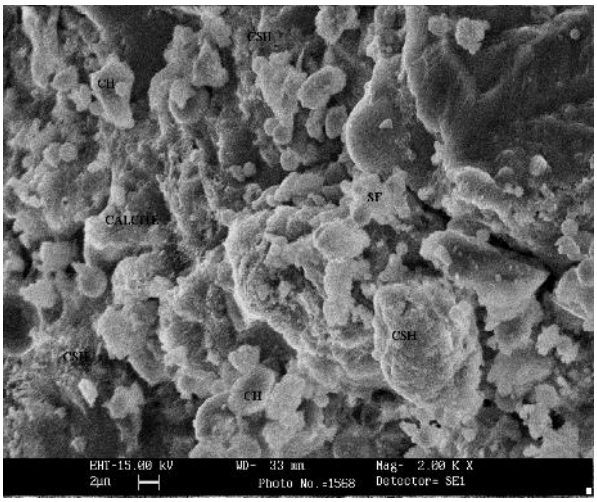

Plate 4.1 (36) CwF (C-85%,W-5%,F-10%)

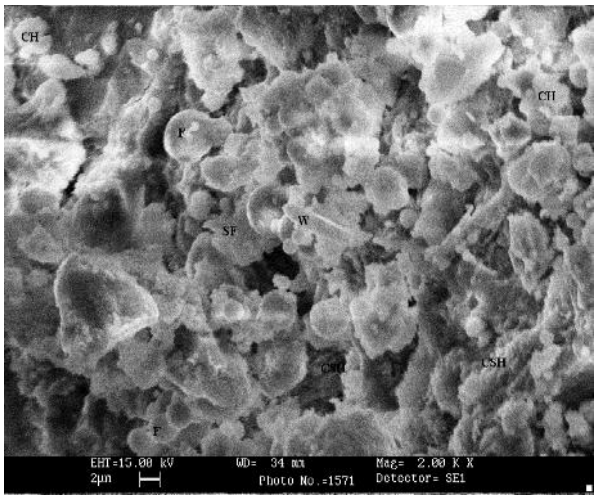

Plate 4.1 (37) CwFS1 (C-82.5%,W-5%,F-10%,MS-2.5%)

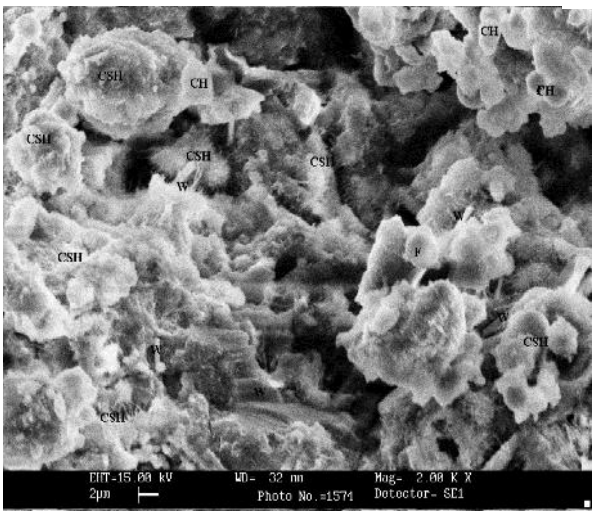

Plate 4.1 (38) CWfS1 (C-82.5%,W-10%,F-5%, MS-2.5%)

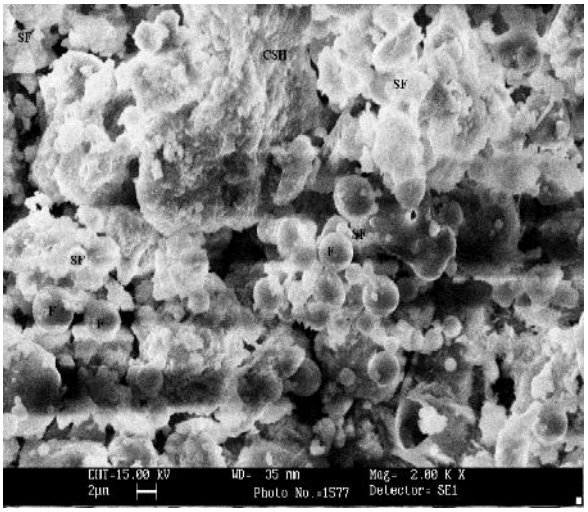

Plate 4.1 (39) CwFS2 (C-80%,W-5%,F-10%,MS-5%)

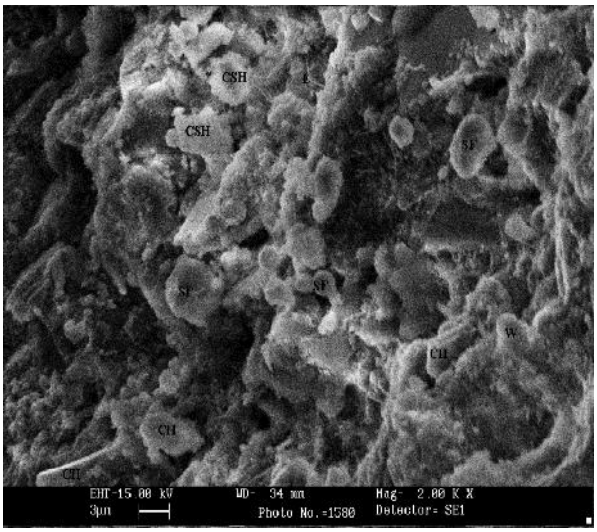

Plate 4.1 (40) CWfS2 (C-80%,W-10%,F-5%,MS-5%)

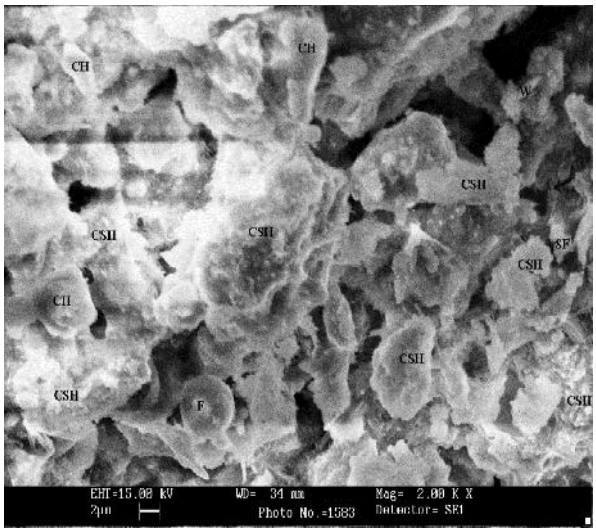

Plate 4.1 (41) CWF (C-80%,W-10%,F-10%)

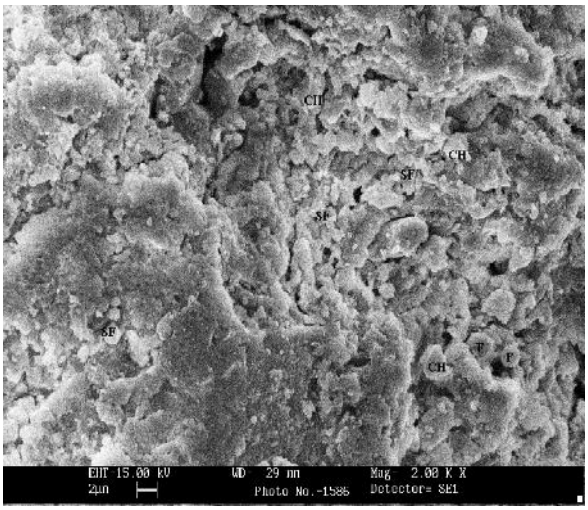

Plate 4.1 (42) CWFS1 (C-77.5%,W-10%,F-10%, MS-2.5%)

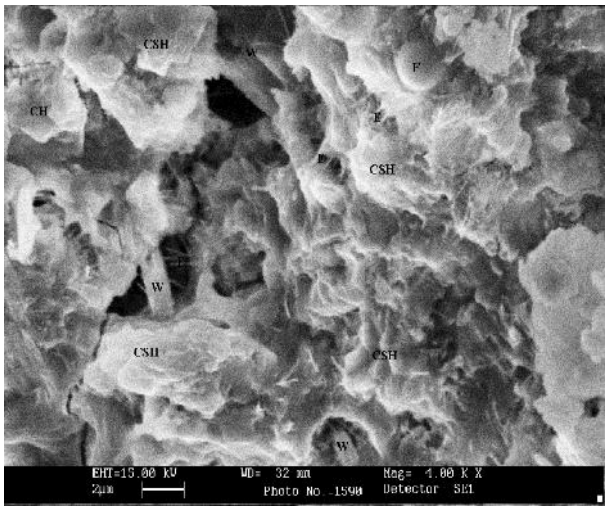

Plate 4.1 (43) CWFS2 (C-75%, W-10,F-10%,MS-5%)

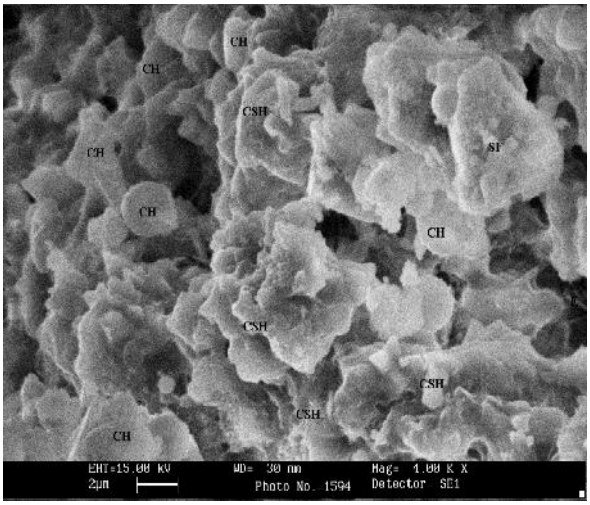

Plate 4.1 (44) CWFS3 (C-72.5%,W-10%,F-10%,MS-7.5%)

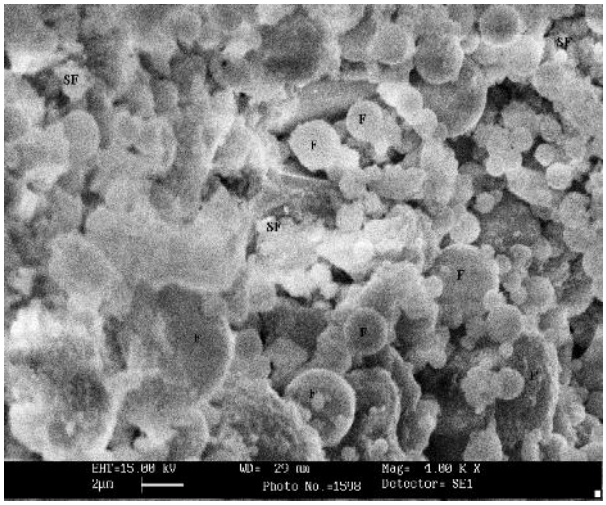

Plate 4.1 (45) CWFS4 (C-70%, W-10%,F-10%, MS-10%)

For the Plates 4.1 (36)-(45) shown above, one thing is clear, which is the presence of free flyash in all the combined mixes, as if it has not reacted on account of water utilisation by microsilica and WMF. The mixes CWFS1-CWFS4 are very dense and have good amount of C-S-H in them. This shows that these last four mixes have good strength as well as less permeability. It is not sure that whether the free flyash will have water to hydrate later, as is seen from the Plates, that they are densely bright and may contain no pore water.

4.3.3 Compatibility with Superplasticizer

Due to the necessary use of superplasticizer for making a medium strength self compacting concrete, it was necessary to check the compatibility of superplasticizer with cement pastes containing admixtures. The admixtures present in the paste led to a change in proportions of C_3A in the powder material.

As has been proved in the literature, that poly carboxylate ether (PCE) based superplasticizers act mainly on alite hydrated phases if no hydrated products of C_3A are available. Therefore the retardation of hydration to improve workability, by the use of PCE based superplasticizers depended mainly on the aluminate content of the cement and admixtures. The sulphate content too, has an effect on the early hydration of aluminates, but since it is mainly found in cement, and negligibly in the admixtures, therefore the effect of workability has been evaluated mainly on the basis of the aluminates content of the admixtures. Apart from this an obvious parameter is the size and surface area of admixtures. More is the surface area, more an admixture gets adsorbed on the cement particles and hence lesser work is required to be done by superplasticizers. Hence, in that case, superplasticizers are needed in lesser volumes. Highly fine admixtures realign the ettringite and lime crystals due to either packing or hydrating them. The first process is called as grain size refinement whereas later process is called as pore size refinement. The pore water consumed in the hydration of lime and ettringite causes reduction of flow. Hence surface area or reactivity, pore water availability, free lime content and C_3A content of admixture play an important role in ascertaining the compatibility of superplasticizer with a cement-admixture mix.

In the present study, NFS (Naphthalene formaldehyde sulphonate) and poly carboxylate ether (PCE) based superplasticizer were used at two mixing moments; first one at the time when water along with superplasticizer was mixed with the powder material and second one at the time when water was already mixed with the powder material. The NFS based superplasticizer was a total failure as very high content of this superplasticizer (more than 3% by mass of cement) at both introduction methods, was required by the various admixed pastes. The mixes containing microsilica required higher quantities of superplasticizers with respect to other admixtures. Even concrete trial samples were made to check the setting times of concrete.

It was observed that the samples did not start hardening even after 3 days for superplasticizer content higher than 3%, and thus they broke on demolding.

Therefore, next trials were conducted to study the effect of PCE based superplasticizers on pastes, with their two introduction methods. It was found, that whether PCE based superplasticizer is mixed initially or after mixing of water, there is no significant difference in the behaviour of PCE, which suggests, that cement contains good ratio of aluminates and sulphates in it. This is proved by the X ray fluorescence test, which gives the amount of aluminates and sulphates in the cement as 5.2 and 2.2 percent respectively. The flyash introduction, which contained 26 percent aluminates and 3% sulphates, also did not alter the superplasticizer behaviour. This suggests, that the aluminates present in flyash are not highly reactive and have a higher inert crystalline content. Tables 4.10 & 4.11 show the data obtained from testing of the pastes at different W/C ratios (0.3, 0.35 & 0.4), with different contents of superplasticizer added sequentially to the mixes, to check their flow.

Table 4.10 Flow time (seconds) variations of binary and combined slurry mixes

	Superplasticizer →				0.3	0.6	0.9	1.2	1.5	1.8	0.3	0.6	0.9	1.2	1.5	0.3	0.6	0.9	1.2	1.5
Mix	C	F	W	S	Flow at W/C=0.3						Flow at W/C= 0.35						Flow at W/C =0.4			
C	100	-	-	-	1920	938	358	235	200	184	1320	900	400	228	218	850	310	213	196	190
CW1	90	-	10	-	825	373	280	218	188	175	630	280	266	215	210	229	201	192	189	186
CW2	80	-	20	-	938	704	595	525	452	410	582	540	195	150	135	210	165	95	80	77
CW3	70	-	30	-	1286	878	736	611	531	485	756	588	525	441	433	270	210	189	183	180
CF1	90	10	-	-	565	316	220	186	160	147	513	344	254	216	208	190	120	93	90	89
CF2	80	20	-	-	512	248	189	149	125	114	438	264	228	180	172	180	110	87	83	80
CF3	70	30	-	-	461	222	165	127	114	107	428	278	233	197	188	176	105	85	80	78
Cwf	90	5	5	-	720	356	247	206	175	162	586	289	263	208	203	205	144	94	87	82
CwfS1	87.5	5	5	2.5	666	328	235	194	164	152	536	282	236	198	191	190	132	88	81	77
CwfS2	85	5	5	5	772	384	262	213	182	166	482	310	225	199	190	181	131	95	86	80
CWf	85	5	10	-	779	489	369	308	260	242	485	256	216	180	176	198	145	100	89	83
CwF	85	10	5	-	651	309	233	185	158	142	442	239	198	169	163	185	134	93	83	78
CwFS1	82.5	10	5	2.5	614	292	220	174	148	133	394	275	201	177	172	153	113	75	65	60
CWfS1	82.5	5	10	2.5	682	423	299	262	223	208	412	272	205	178	171	138	88	74	70	68
CwFS2	80	10	5	5	768	372	264	209	177	164	358	260	190	175	169	142	98	85	80	79
CWfS2	80	5	10	5	841	503	351	298	254	234	378	259	207	176	167	126	87	72	67	62
CWF	80	10	10	-	690	398	319	267	227	207	428	221	189	158	153	176	125	107	97	92
CWFS1	77.5	10	10	2.5	658	384	292	245	208	192	362	238	167	152	145	160	120	98	88	84
CWFS2	75	10	10	5	769	441	319	267	227	211	349	221	156	144	139	160	113	99	92	88
CWFS3	72.5	10	10	7.5	849	483	337	285	241	226	378	270	195	174	169	173	123	110	100	96
CWFS4	70	10	10	10	942	518	351	299	256	235	395	275	201	183	174	188	138	117	108	102

Table 4.11 Flow time (seconds) variations of ternary slurry mixes

	Superplasticizer→				0.3	0.6	0.9	1.2	1.5	1.8	0.3	0.6	0.9	1.2	1.5	0.3	0.6	0.9	1.2	1.5
Mix	C	F	W	S	Flow at W/C=0.3						Flow at W/C= 0.35					Flow at W/C =0.4				
CWS1	87.5	-	10	2.5	760	334	236	187	159	149	627	270	240	210	203	211	160	89	69	65
CWS2	85	-	10	5	815	351	240	185	158	149	575	532	182	144	137	201	183	185	181	173
CWS3	82.5	-	10	7.5	1103	466	299	233	198	184	936	592	346	328	318	309	240	128	100	92
CWS4	80	-	10	10	1182	500	298	231	195	182	1103	628	328	313	300	351	264	148	106	99
CWS5	77.5	-	20	2.5	821	549	413	359	307	290	562	231	189	152	148	196	181	184	175	168
CWS6	75	-	20	5	996	605	414	362	310	288	545	327	240	160	146	186	148	81	65	62
CWS7	72.5	-	20	7.5	1448	830	514	455	386	353	801	328	238	193	189	287	250	265	258	242
CWS8	70	-	20	10	1625	859	514	438	370	342	1158	470	305	250	246	309	274	289	269	249
CWS9	67.5	-	30	2.5	1277	806	612	511	441	406	735	525	415	354	345	250	177	152	136	130
CWS10	65	-	30	5	1469	872	625	516	447	404	830	550	403	341	336	207	150	131	122	119
CWS11	62.5	-	30	7.5	1599	931	612	509	438	395	1115	725	473	399	389	360	248	207	189	183
CWS12	60	-	30	10	1682	944	581	485	410	380	1235	767	452	391	374	412	279	232	203	193
CFS1	87.5	10	-	2.5	512	288	202	170	144	132	463	254	177	188	185	173	149	124	113	108
CFS2	85	10	-	5	511	313	219	187	158	147	446	229	159	171	169	143	120	93	83	77
CFS3	82.5	10	-	7.5	674	416	285	245	210	193	749	429	297	317	314	196	128	96	88	78
CFS4	80	10	-	10	749	458	309	264	229	215	801	476	334	353	346	258	192	162	102	69
CFS5	77.5	20	-	2.5	472	243	182	149	122	114	425	300	221	195	186	156	114	94	86	82
CFS6	75	20	-	5	492	274	208	167	139	128	386	267	196	171	164	129	104	90	84	80
CFS7	72.5	20	-	7.5	760	434	311	251	208	195	727	522	380	342	333	193	153	129	116	107
CFS8	70	20	-	10	923	535	381	307	257	237	824	597	438	394	387	230	143	95	79	75
CFS9	67.5	30	-	2.5	454	187	122	108	96	92	405	272	222	190	181	142	92	78	73	72
CFS10	65	30	-	5	624	206	133	116	103	98	394	246	203	175	163	119	89	83	79	77
CFS11	62.5	30	-	7.5	869	369	234	208	184	170	504	348	277	245	233	165	131	102	90	87
CFS12	60	30	-	10	916	406	263	224	195	184	571	405	322	286	278	188	145	110	93	85

In order to visualize the effect of increment in superplasticizer over the viscosity/flow time of the slurry mixes, Figs. 4.53-4.82 try to categorize the mixes as per the increment in the volume of admixture/fiber and provide variation of flow time for each water to cement ratio, respectively. Binary mixes constitute one set of figures, flyash and WMF ternary mixes constitute six sets of figures and combined mixes have been classified into three further sets. One set representing combination of flyash and WMF only; other set constituting flyash and WMF in equal mass ratios along with varying masses of microsilica; the last set constituting unequal ratios of flyash and WMF along with varying masses of microsilica. Hence, for each water to cement ratio, there are ten sets of figures, thereby constituting thirty figures for three sets of water to cement ratios. In each figure cement has been included for providing ease in acknowledging the effect of admixtures/fibers in the pure cement mixes.

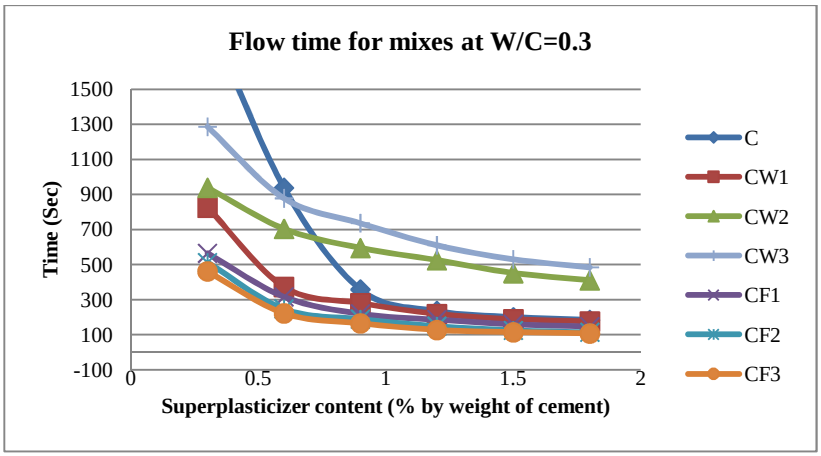

Fig. 4.53 Flow- time variation for binary mixes at W/CM = 0.3

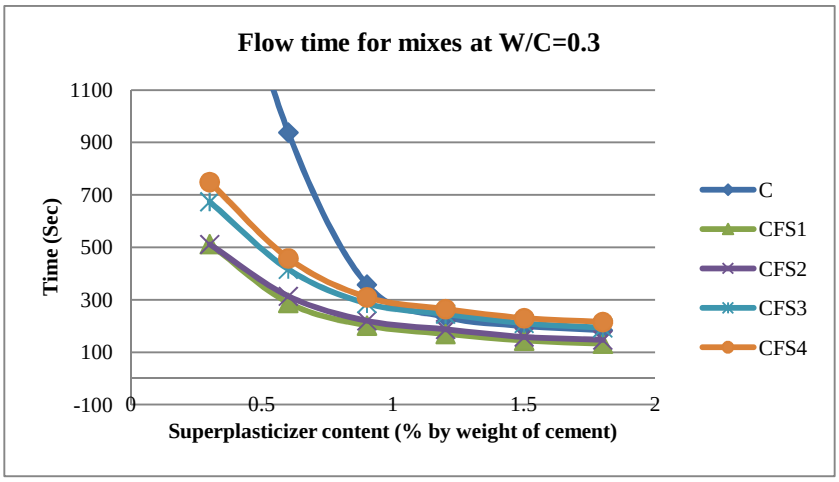

Fig. 4.54 Flow- time variation for ternary mixes containing 10% flyash at W/CM = 0.3

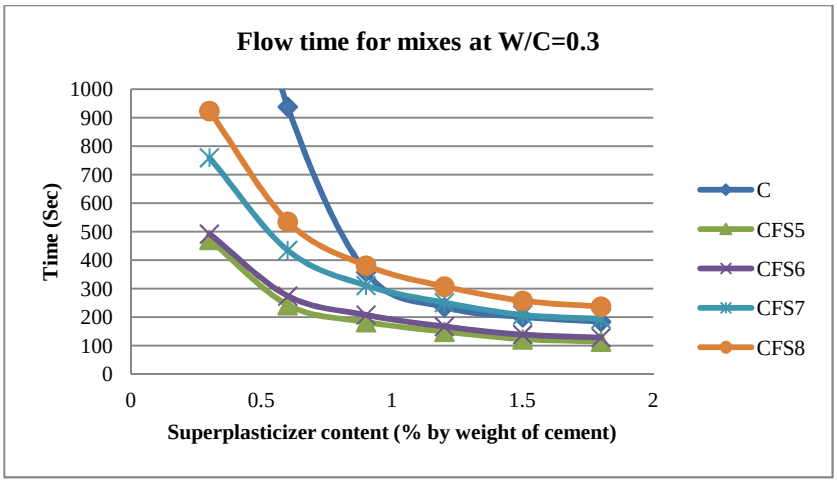

Fig. 4.55 Flow- time variation for ternary mixes containing 20% flyash at W/CM = 0.3

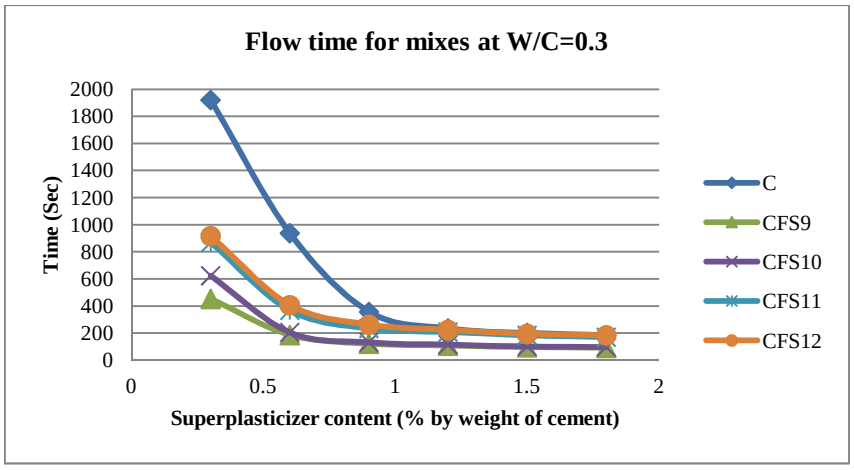

Fig. 4.56 Flow- time variation for ternary mixes containing 30% flyash at W/CM = 0.3

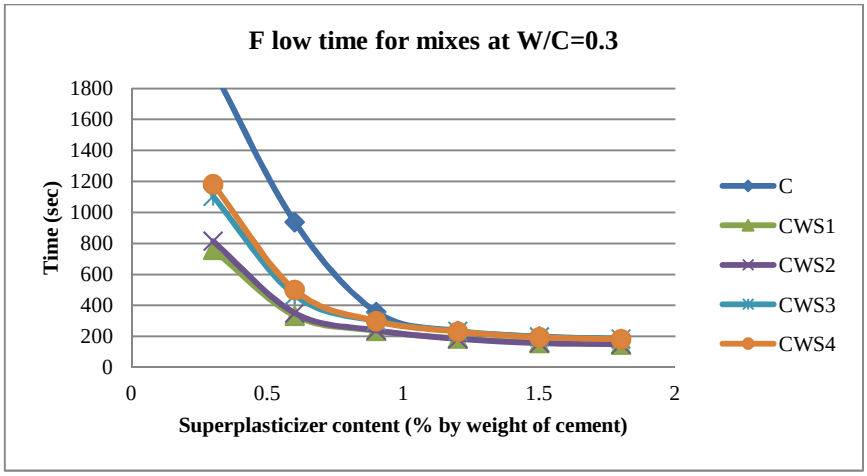

Fig. 4.57 Flow- time variation for ternary mixes containing 10% WMF at W/CM = 0.3

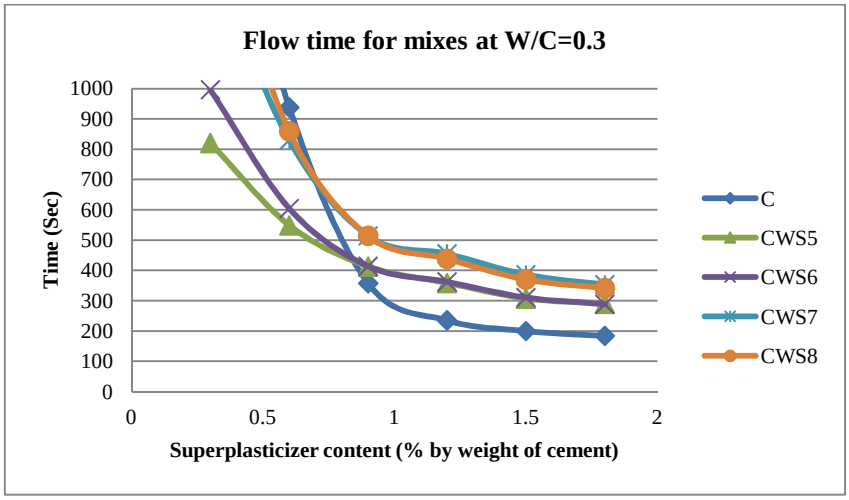

Fig. 4.58 Flow- time variation for ternary mixes containing 20% WMF at W/CM = 0.3

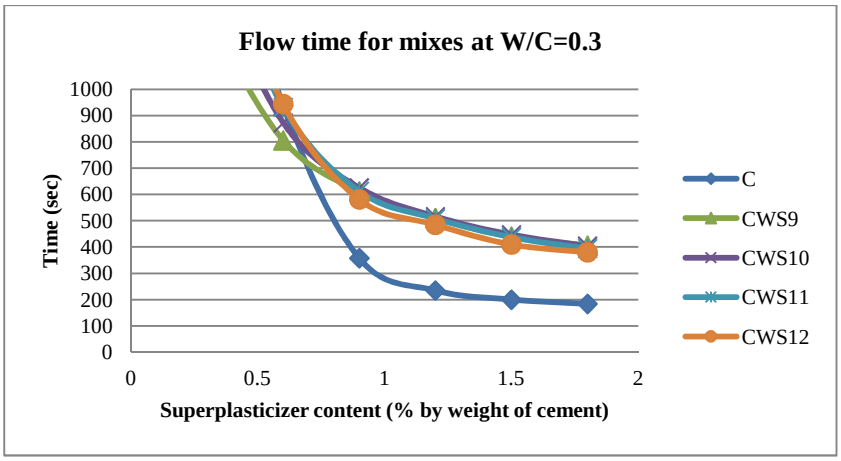

Fig. 4.59 Flow- time variation for ternary mixes containing 30% WMF at W/CM = 0.3

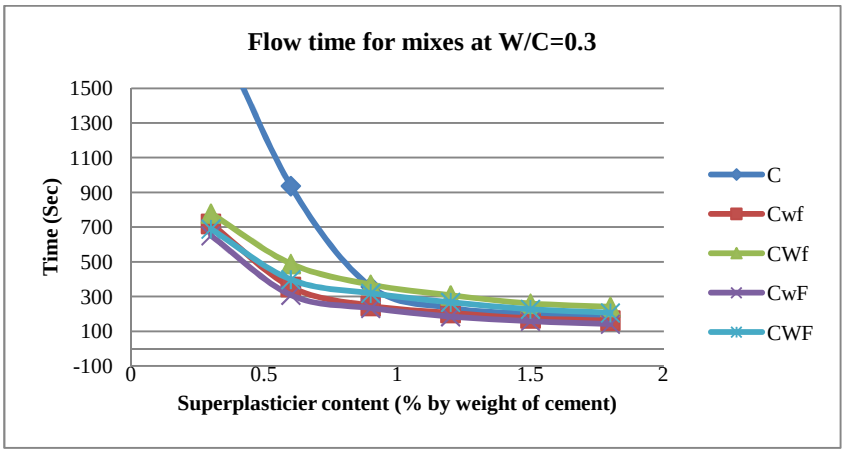

Fig. 4.60 Flow- time variation for combined mixes containing no microsilica at W/CM = 0.3

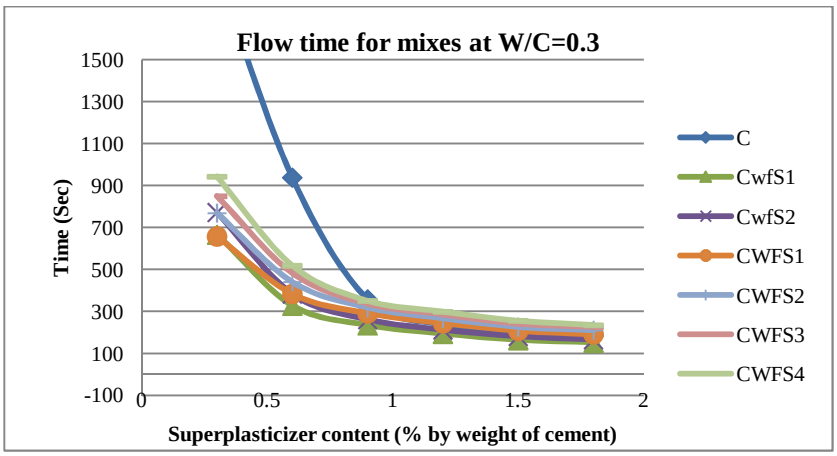

Fig. 4.61 Flow- time variation for combined mixes containing equal masses of flyash and WMF at W/CM = 0.3

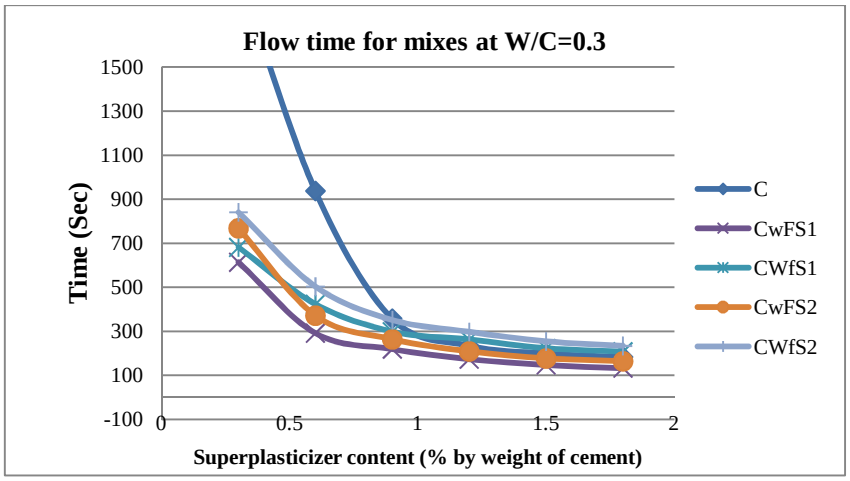

Fig. 4.62 Flow- time variation for combined mixes containing unequal masses of flyash and WMF at W/CM = 0.3

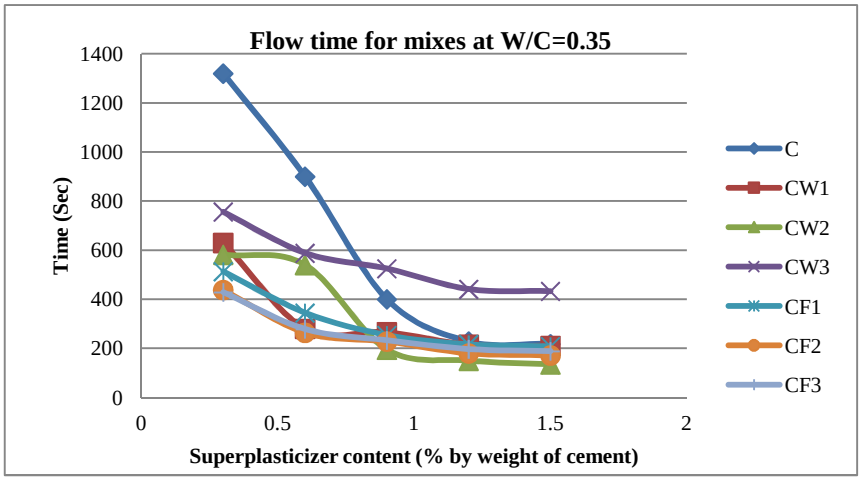

Fig. 4.63 Flow- time variation for binary mixes at W/CM= 0.35

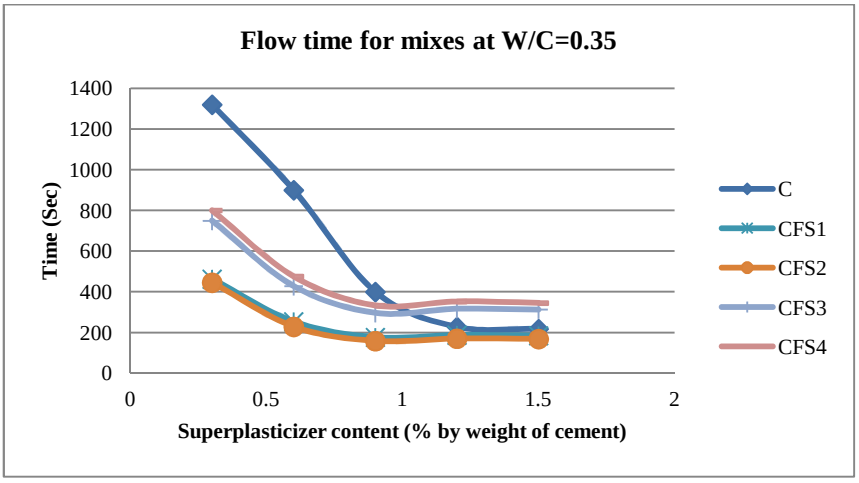

Fig. 4.64 Flow- time variation for ternary mixes containing 10% flyash at W/CM= 0.35

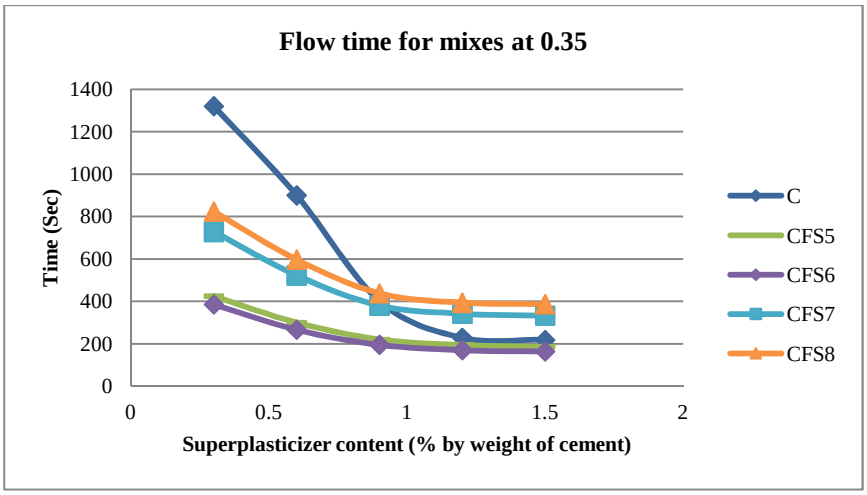

Fig. 4.65 Flow- time variation for ternary mixes containing 20% flyash at W/CM= 0.35

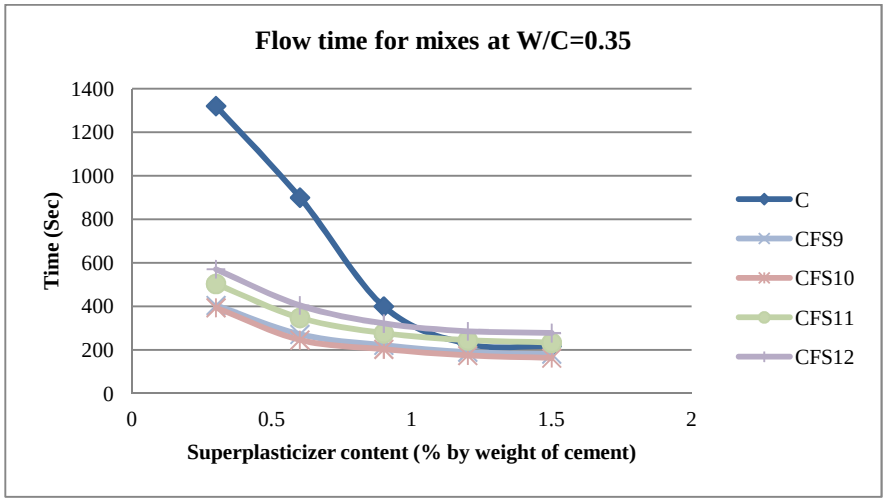

Fig. 4.66 Flow- time variation for ternary mixes containing 30% flyash at W/CM= 0.35

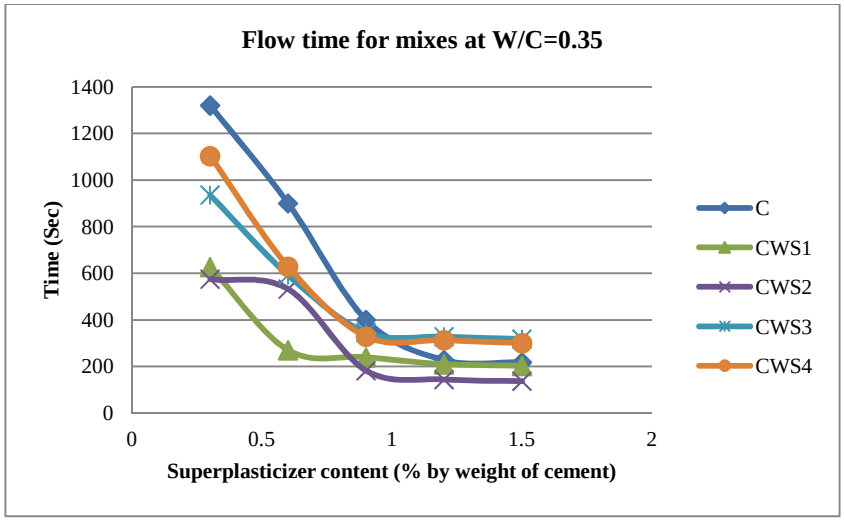

Fig. 4.67 Flow- time variation for ternary mixes containing 10% WMF at W/CM= 0.35

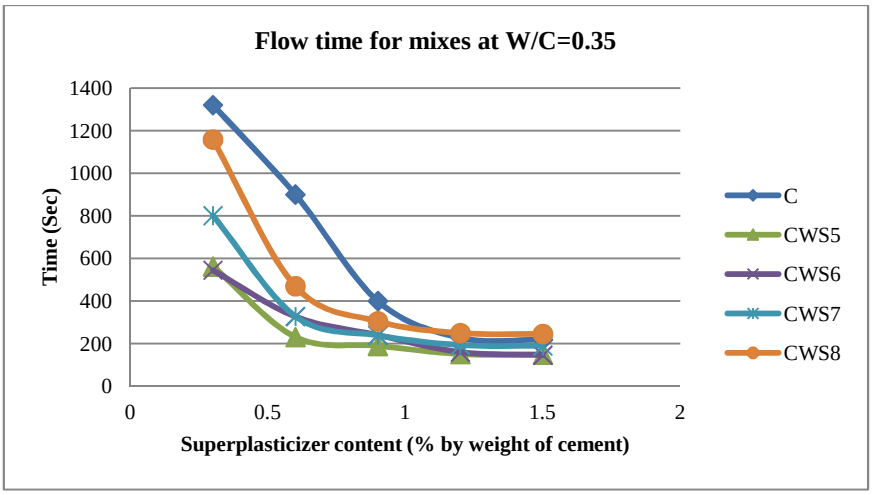

Fig. 4.68 Flow- time variation for ternary mixes containing 20% WMF at W/CM= 0.35

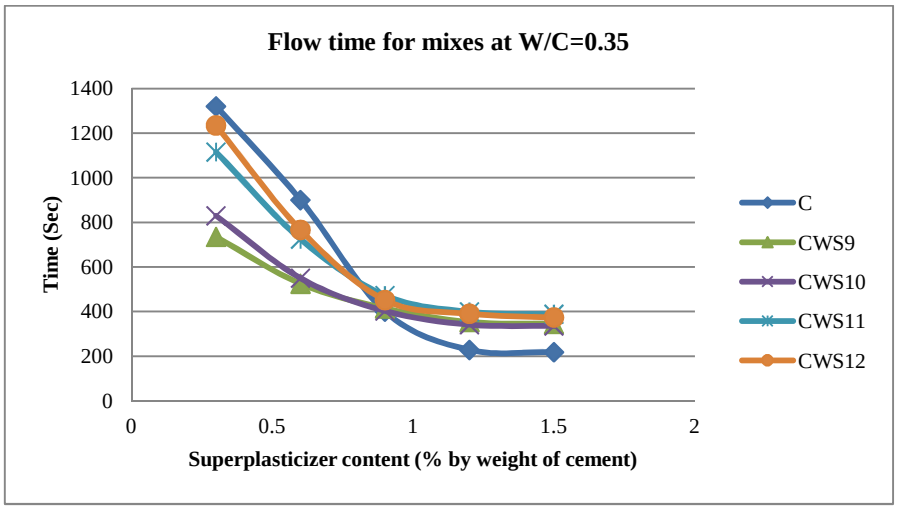

Fig. 4.69 Flow- time variation for ternary mixes containing 30% WMF at W/CM= 0.35

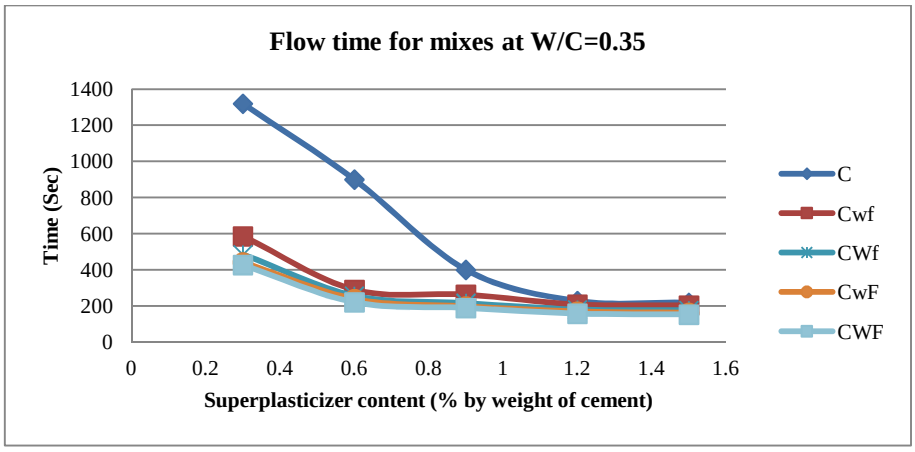

Fig. 4.70 Flow- time variation for combined mixes containing no microsilica at W/CM= 0.35

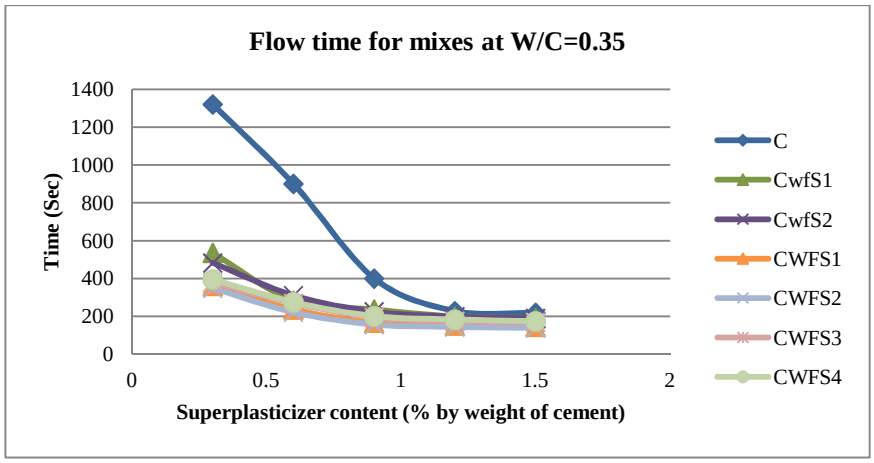

Fig. 4.71 Flow- Time variation for combined mixes containing equal masses of flyash and WMF at W/CM= 0.35

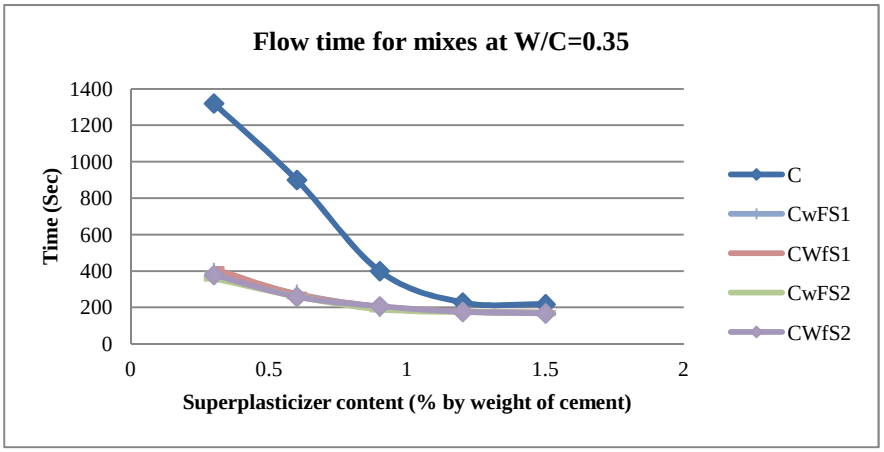

Fig. 4.72 Flow- time variation for combined mixes containing unequal masses of flyash and WMF at W/CM= 0.35

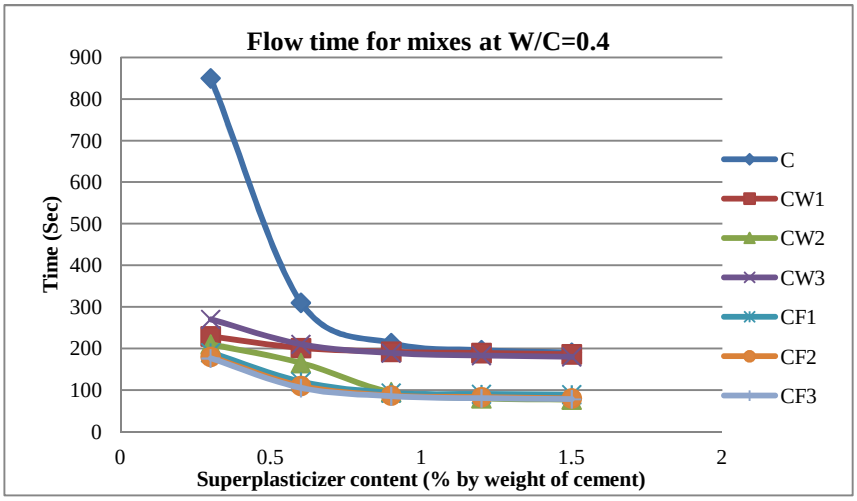

Fig. 4.73 Flow- Time variation for binary mixes at W/CM = 0.4

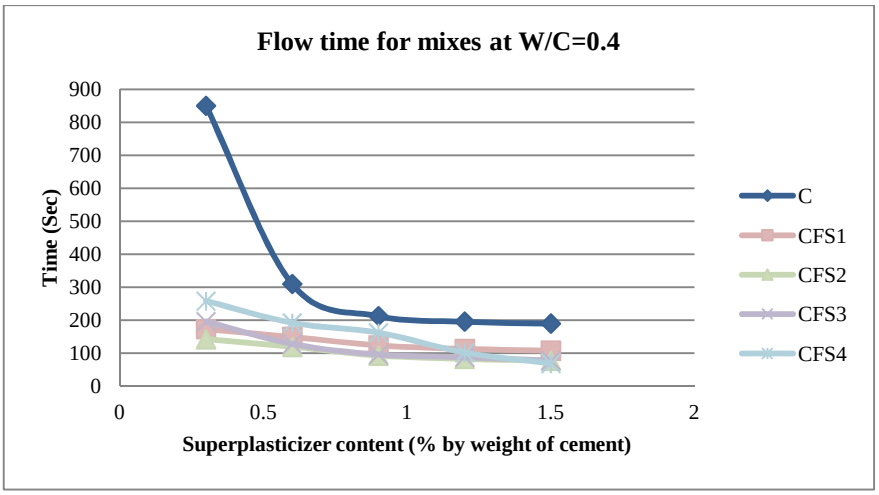

Fig. 4.74 Flow- time variation for ternary mixes containing 10% flyash at W/CM = 0.4

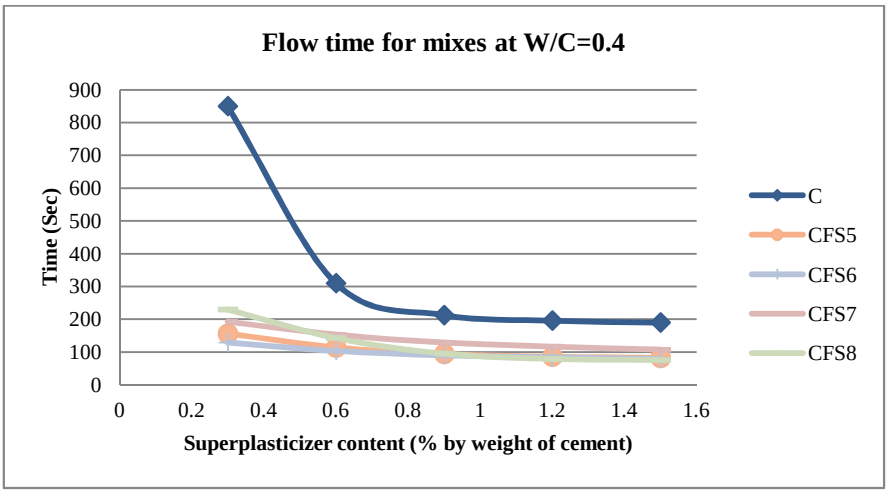

Fig. 4.75 Flow- time variation for ternary mixes containing 20% flyash at W/CM = 0.4

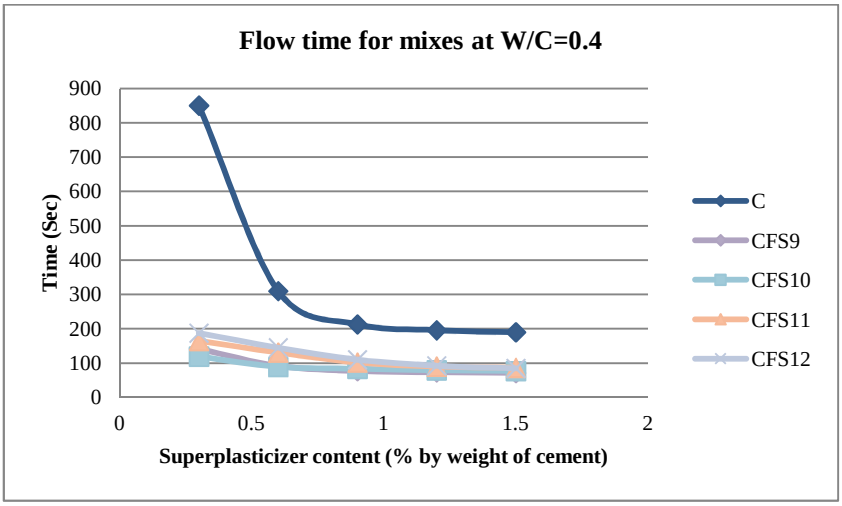

Fig. 4.76 Flow- time variation for ternary mixes containing 30% flyash at W/CM = 0.4

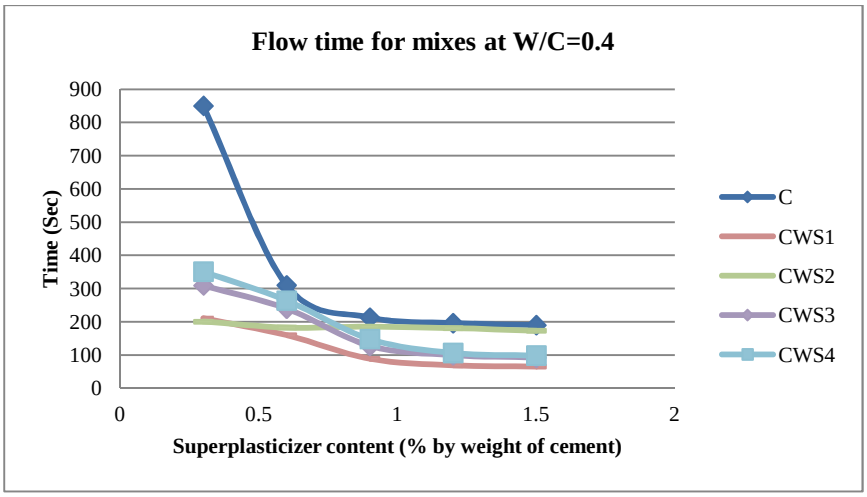

Fig. 4.77 Flow- time variation for ternary mixes containing 10% WMF at W/CM = 0.4

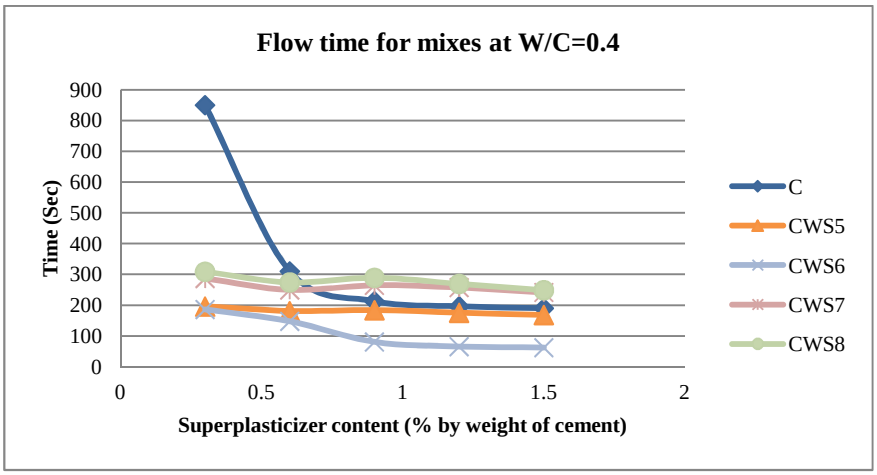

Fig. 4.78 Flow- time variation for ternary mixes containing 20% WMF at W/CM = 0.4

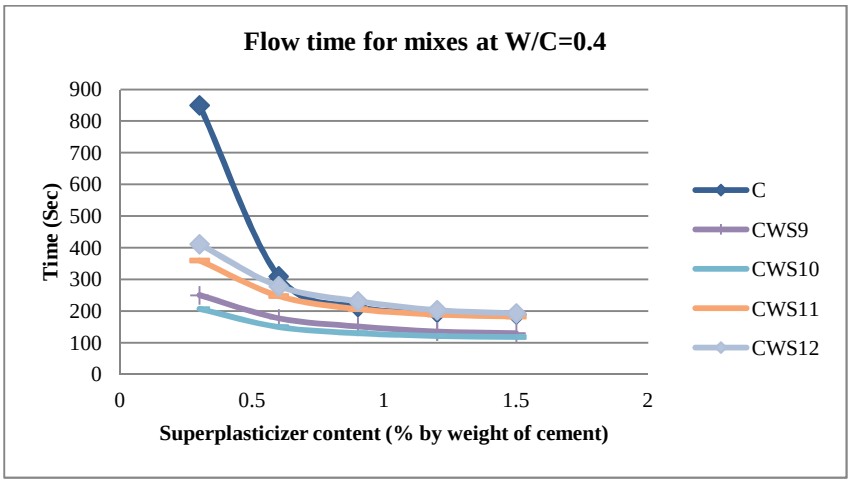

Fig. 4.79 Flow- time variation for ternary mixes containing 30% WMF at W/CM = 0.4

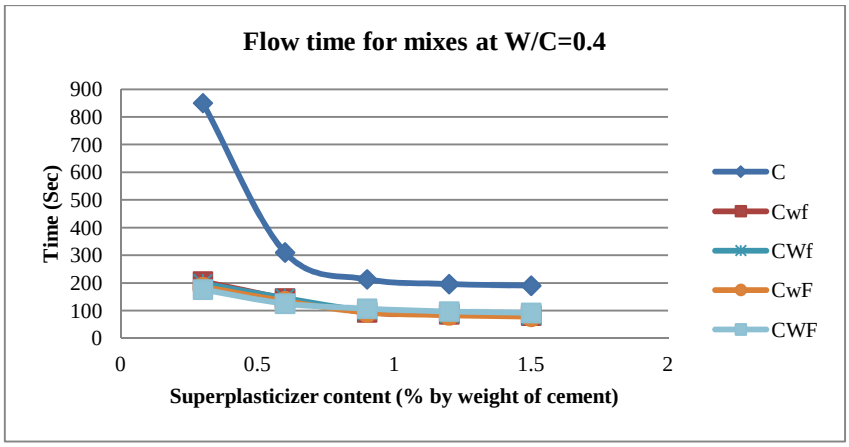

Fig. 4.80 Flow- time variation for combined mixes containing no microsilica at W/CM = 0.4

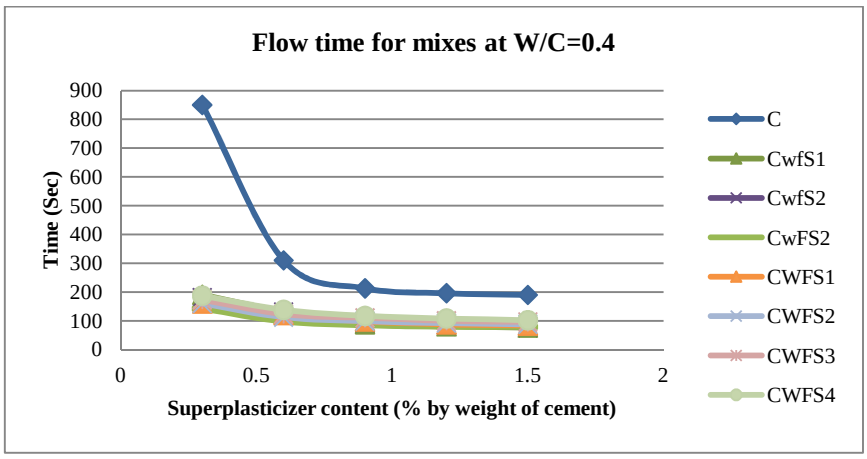

Fig. 4.81 Flow- time variation for combined mixes containing equal masses of flyash and WMF at W/CM = 0.4

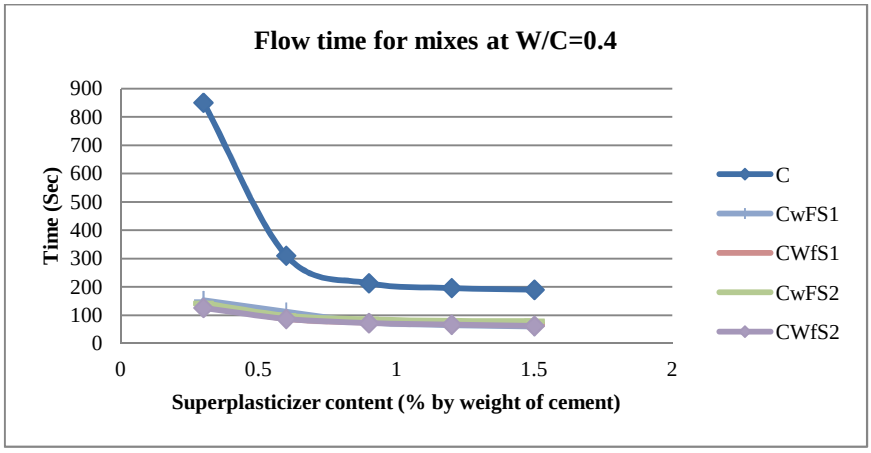

Fig. 4.82 Flow- time variation for combined mixes containing unequal masses of flyash and WMF at W/CM = 0.4

The following paragraphs entail the results obtained, when water was added along with superplasticizer into the powder material. The analysis has been done by observing the effect of admixture type and content on the flow time of pastes (shown in Figures 4.53-4.82) at different W/C ratios and superplasticizer content.

(i) At W/C=0.3

The water content is low and therefore the activity of microsilica and WMF is retarded. This retardation is not similar to the retardation in hydration caused by the admixtures at dormant period; it is related to time period just after the addition of water. This retardation effect is lower for lower contents of these admixtures and gets amplified at their larger contents. Therefore both microsilica and WMF at their lower content did not get adsorb on the cement particles, thereby showing a raised water demand. This demand kept on increasing with their higher contents due to retardation, and owing to more water consumption by their particles' surfaces. Hence, flow time shows a small increment with microsilica and WMF addition at their lower content, and at their higher contents, flow time shows a high increment.

Flyash mixes have normal consistency in this range because of the workability created by the repulsive forces of adsorbed particles of flyash carrying negatively charged sulphate ions, which repel the cement particles far apart, thus releasing more water. Therefore no retardation was observed in the effects of flyash, which kept on reducing the water demand at its increased content, by filling the voids in cement particles. The reason for continuous reduction in water demand by flyash is the low reaction tendency of flyash, even when its effect is not retarded, which necessitated higher contents of flyash to get adsorbed on the cement particles. The rest higher fraction of large sized flyash particles in the paste, further reduced the water demand due to dilution. The aluminates present in the flyash could have done two functions depending upon their reactivity: firstly they could have consumed the superplasticizer, and secondly, converted the ettringite and lime into monosulphates and C-S-H respectively. This somehow should have reduced the water content in pore solution. It is not sure that up to what extent the aluminates were reactive, but overall, there is a decrement in the flow time by the use of flyash.

As far as increment in superplasticizer is concerned, it has been observed that fine admixtures start behaving normally with an increment in effective water content caused by superplasticizer. Thus, for WMF and microsilica, flow time reduced up to 20% WMF and 5% microsilica content and thereafter it increases due to the water demand created by excess WMF and microsilica, as their further adsorption was not possible on cement particles beyond that content. No behaviour change was observed in the flyash mixes with an increment in superplasticizer because the behaviour of flyash did not vary much with a small increment in the effective water content of mix.

Initially whatever may be the effect of admixture but at higher superplasticizer contents there is enough water in the paste and the paste behaviour becomes independent of the behaviour of its constituents. This generally happens at superplasticizer contents above 1.5%, 1.2%, and 0.9% for water /cementitious material ratio of 0.3, 0.35, and 0.4, for both pure cement paste and admixed pastes.

(ii) At W/C=0.35

The water content is high for flyash admixed pastes, whereas it approaches normal consistency for pastes containing lower contents of WMF and microsilica.

Therefore flyash was observed to release entrapped water at a higher rate, at its lower contents and as the flyash content increased, the rate decreased abruptly due to no further increment in adsorption of flyash at cement particles' surfaces. Hence, at medium W/C ratios, flyash admixed pastes were observed to increase flow up to 20% content and then it remained constant.

WMF and microsilica acceleration effect was enhanced at this stage. WMF and microsilica mixes released more water at their lower content in comparison to their water consumption by adsorption of water at their respective surfaces. Hence they gave lower flow times. At higher content, WMF and microsilica were found to increase the flow time as their further adsorption on cement particles reduced. This increment in flow time was lower in comparison to same mixes at lower W/C ratio (0.3%), which is obvious. Hence, for pastes having higher content of WMF and microsilica, the W/C ratio of 0.35 is low, and they behave as being retarded.

(iii) At W/C=0.4

The water content is high enough for flyash admixed pastes, whereas it approaches normal consistency for WMF and microsilica admixed pastes, especially those containing higher content of WMF and microsilica. Same effect for flyash was observed at this W/C ratio as was observed at 0.35% W/C. For WMF-microsilica mixes the effect of WMF and microsilica was unhindered up to 20% content of WMF and up to 5% content of microsilica, after which it registered a small decrement. This happened because, even though the amount of water in the pore solution is higher for the free movement of WMF and microsilica particles, but there is a limit beyond which all the surfaces of cement particles get engulfed with admixtures and no further adsorption is possible.

Hence a water content of 0.35 % is favourable in this case for achieving flowable pastes. Since for a SCC, the volume of mortar is nearly two third of the volume of concrete, therefore a water content of nearly 0.35% would be better for achieving a SCC.

4.4 MORTARS

4.4.1 Flow of Mortar

(a) Observations

The first thing which was observed from the experimentation, conducted for finding out normal consistency is, that the water present at normal consistency (30-40%) ensures workability in terms of mixing and handling, but not flow. Second observation which was made from the tests on pastes for compatibility with superplasticizer is, that the presence of water acts directly as well as indirectly for increasing the flow of mix. Directly, it acts as medium for increasing flow, whereas indirectly it favours the retardation/acceleration of the working of admixtures. Hence, at a certain water content, the water which was earlier entrapped in the mix gets released by admixture action, and workability/flow of mix improves with respect to normal paste.

At normal consistency it is assumed that the behaviour of the admixtures in unhindered. This means that they have the tendency to migrate into the voids between the cement particles and release water. But the flow is only induced at the stage when, there is

no restriction to the movement of one layer of mix over the other. This could happen only if there is required thickness of non viscous pore solution present between two cement particles, which already have adsorbed admixtures on their surfaces. Otherwise the inter-particle frictional forces, along with viscous forces of the pore solution will not let the flow of cement to take place. If the admixture is in lower amounts, then the cement particles' voids are filled with them such that the cement particles are not far apart and there is high inter-particle friction. If water is added to reduce this friction then segregation takes place. In case, if the admixture is in excess, then the cement particles are dispersed far apart and there is large thickness of admixture layer between them. Hence, extra water is required to reduce the viscosity of the admixture layer for maintaining a required flow.

In case of flow test of mortars, the water was added on the basis of normal consistency of the pastes, (P/4+3) % by weight of mortar (P is the normal consistency of the paste). Hence there is unhindered migration of admixtures in the paste. Definitely at low admixture content there would be just filling of cement voids by the admixtures along with the adsorption of admixtures by cement particles. Hence, the thickness of inter-particle pore solution phase is very less and is not viscous (though its degree depends upon the type of admixture). At higher admixture contents, there would be larger interaction of admixtures with fine aggregates because a thick pore solution exists between cement-cement phase and cement-fine aggregate phase. Therefore at higher admixture content, the behaviour of mortar also depends upon its surface morphology apart from water content. Those admixtures which increase viscous or frictional forces would reduce the flow and vice versa. The specific gravity/weight of the admixtures complements the flow reducing properties by increasing the weight of obstruction producing materials.

At lower contents of admixtures, the behaviour would depend more upon the ability of the admixture to provide cohesion to the mix, because the excess water if added to induce flow would cause segregation (this was checked by adding more water for both lower and higher content of admixture). If the admixture is viscous then it will bring cohesiveness to the mix, which is beneficial for efficient flow of mortar.

Hence an admixture would be beneficial or hazardous for the flow of mortar, depending upon its quantity and surface morphology.

(a) Following paragraphs give the results regarding the use of each kind of admixture, for flow:

(i) Flyash addition

Replacement of cement with high volume flyash reduced the viscosity of the mix. The smooth flyash particles did not stick to other materials in the mortar, and being having lower specific gravity made the paste lighter which favoured good flow under impact. Hence flyash at its higher content improved the flow of mortar. At lower content it reduced the cohesiveness of the mix and thus reduced the flow of mortar.

(ii) WMF addition

WMF has higher specific gravity, which approaches that of cement particles. Its shape is acicular, which provides friction to flow, plus its very fine size makes the mortar viscous at its higher content. The presence of larger frictional forces under larger weight resists flow and there is no pro flow factor present.

Hence, at its higher content, WMF caused a reduction in the flow. At its lower content, the frictional force between the WMF layer and cement particles did not allow the paste to flow. Therefore, it reduced the flow at lower contents in comparison to flyash mixes.

(iii) Microsilica addition

Microsilica has the highest adhesion among used admixtures and its specific gravity is very low. At its lower content, silica was able to maintain the cohesiveness of mortar mixes due to its smooth and sticky surface, and thus it increased the flow of mortar. But at its higher content, the force of adhesion increased too much, so that even with its minimal weight, the resistance to flow was very high. Hence at higher content it reduced the flow of mortar maximally. Therefore the order of flow reduction at lower content of admixture is: microsilica> flyash> WMF. At higher contents the order is: flyash>WMF>microsilica.

Similar trend was observed for all admixtures in binary, ternary and combined mixes. Table 4.12, Figs.4.83 & 4.84 show the flow variation for mortar mixes containing pure binder material, binary, ternary and combined mixes.

Table 4.12 Flow of different mortar mixes obtained from test

Mix	Mix Composition	D	D'	D'-D	% Flow ((D'-D)/D)*100)
C	100	100	108	8	8
W	100	100	118	18	18
FA	100	100	127	27	27
SF	100	100	114	14	14
CF1	90+10	100	111	11	11
CF2	80+20	100	113	13	13
CF3	70+30	100	116	16	16
CW1	90+10	100	110	10	10
CW2	80+20	100	112	12	12
CW3	70+30	100	110	10	10
CFS1	87.5+10+2.5	100	112	12	12
CFS2	85+10+5	100	114	14	14
CFS3	82.5+10+7.5	100	111	11	11
CFS4	80+10+10	100	108	8	8
CFS5	77.5+20+2.5	100	114	14	14
CFS6	75+20+5	100	117	17	17
CFS7	72.5+20+7.5	100	114	14	14
CFS8	70+20+10	100	112	12	12
CFS9	67.5+30+2.5	100	117	17	17
CFS10	65+30+5	100	121	21	21
CFS11	62.5+30+7.5	100	118	18	18
CFS12	60+30+10	100	115	15	15
CWS1	87.5+10+2.5	100	113	13	13
CWS2	85+10+5	100	115	15	15
CWS3	82.5+10+7.5	100	110	10	10

CWS4	80+10+10	100	108	8	8
CWS5	77.5+20+2.5	100	114	14	14
CWS6	75+20+5	100	116	16	16
CWS7	72.5+20+7.5	100	112	12	12
CWS8	70+20+10	100	109	9	9
CWS9	67.5+30+2.5	100	112	12	12
CWS10	65+30+5	100	114	14	14
CWS11	62.5+30+7.5	100	110	10	10
CWS12	60+30+10	100	109	9	9
Cwf	90+5F+5W	100	110	10	10
CwfS1	87.5+5F+5W+2.5M	100	113	13	13
CwfS2	85+5F+5W+5M	100	116	16	16
CWf	85+5F+10W	100	109	9	9
CwF	85+10F+5W	100	112	12	12
CwFS1	82.5+10F+5W+2.5M	100	115	15	15
CWfS1	82.5+5F+10W+2.5M	100	111	11	11
CwFS2	80+10F+5W+5M	100	117	17	17
CWfS2	80+5F+10W+5M	100	114	14	14
CWF	80+10F+10W	100	110	10	10
CWFS1	77.5+10F+10W+2.5M	100	114	14	14
CWFS2	75+10F+10W+5M	100	116	16	16
CWFS3	72.5+10F+10W+7.5M	100	113	13	13
CWFS4	70+10F+10W+10M	100	110	10	10

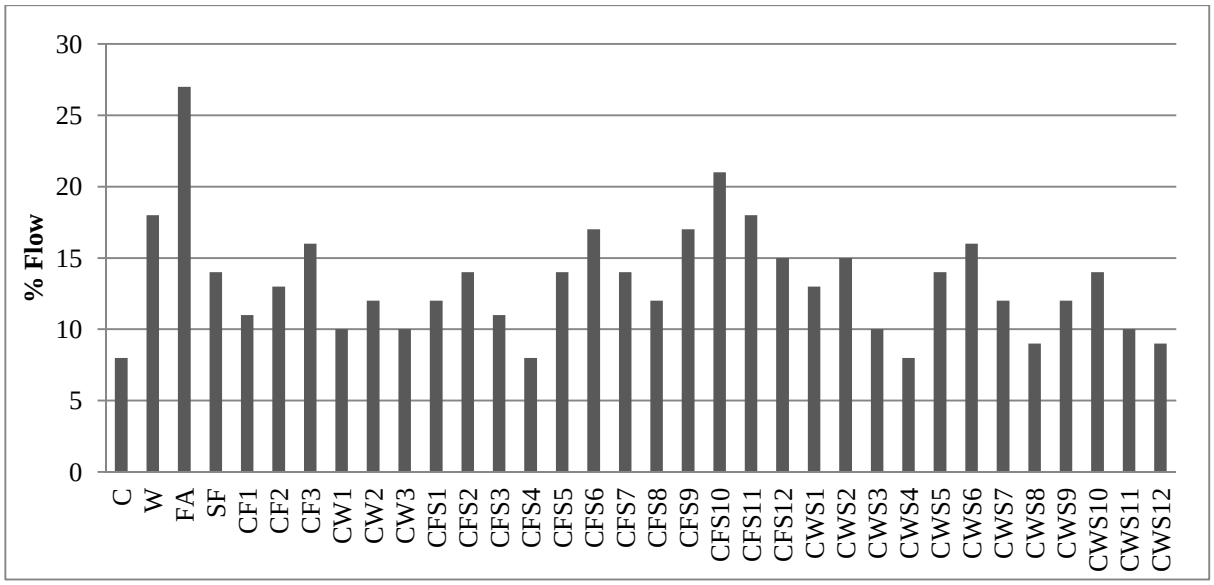

Fig 4.83 Flow of mortars containing pure binder, binary and ternary mortar mixes

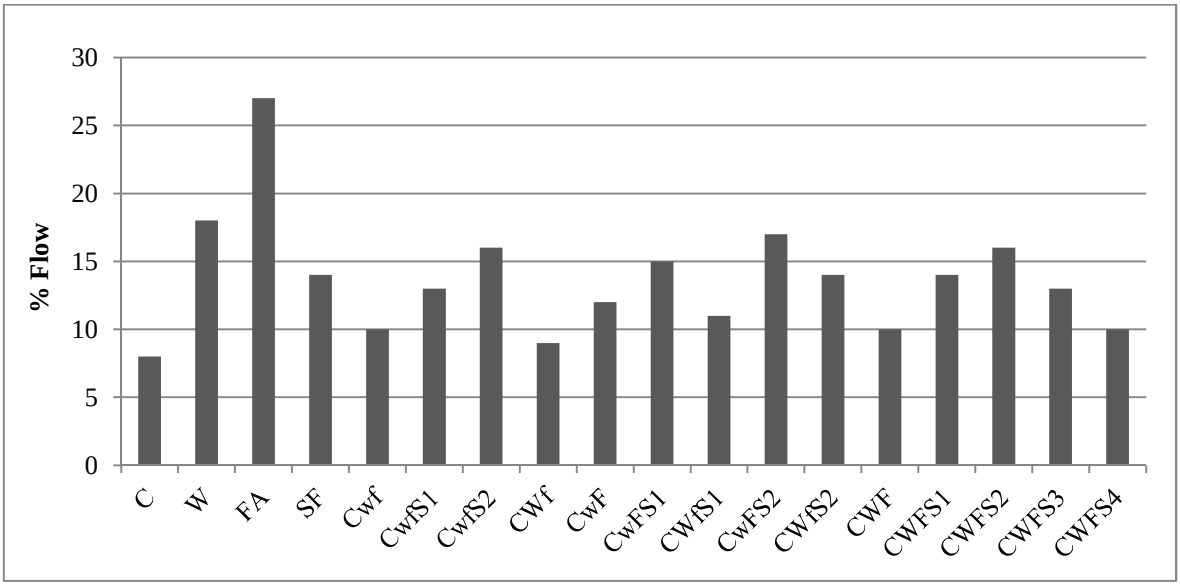

Fig. 4.84 Flow of pure binder & combined mortar mixes

The mechanical properties of mortar, such as compressive strength, flexural strength, splitting tensile strength have been discussed altogether with the corresponding mechanical properties of concrete. This is because, more or less; there exist a common effect of admixtures on mortar and concrete. The difference arising out of interfacial transition zone in concrete brings certain differences which could be explained in the same paragraph in which the mortar variation is explained.

4.4.2 Abrasion Resistance (Sand Blasting Method)

Abrasion resistance is directly proportional to the compressive strength of concrete. Literature studies prove that tests performed in arbitrary conditions, though may not provide equal results, but support the fact, that abrasion resistance is directly proportional to the compressive strength of the mix [159]. In case of SCC too, this relationship is valid, as has been confirmed in the present study. ACI 223-93 [1] suggests, that shrinkage compensating mixes have higher abrasion resistance. This is due to the absence of fine cracks in their matrix. Hence, it becomes imperative to find out the effect of shrinkage compensating admixtures on SCC. Also, previous studies conducted on use of pozzolans in concrete suggest, that there is negligible or very meagre improvement in abrasion resistance of concrete containing Class C or F flyash [85]. Microsilica cause a huge improvement in the abrasion resistance of concrete. This is due to the absence of bleeding, which causes reduction in weak top layer formation. Also better paste-paste and paste-aggregate bond cause reduction in wearing of concrete.

Table 4.13 shows the observations made in the laboratory regarding finding out of abrasion loss in the cubical samples of size 10×10×10 cu.cm., and has been explained for possible reasons in the following paragraph:

(i) WMF addition

The abrasion resistance studied after 28 days showed that flyash decreased abrasion resistance whereas WMF increased it. Excess of WMF imparts more packing in a given volume of paste by grain size and pore size refinement. Even though it densifies the mortar, which should increase the strength of mortar and its resistance against abrasion, but the dilution of cement in mortar, causes reduction in C-S-H formation too. Apart from this WMF reinforces the mortar too, due to its bonding with it. The bonding results on account of WMF getting adsorbed on cement particles and afterwards being hydrated there itself.

It was found, that up to twenty percent content of WMF, the strength loss due to loss in C-S-H formation caused by dilution, is nullified by packing and reinforcing effect. After 20% WMF content, the packing starts hindering further C-S-H formation, as a result of which the water content in the pore solution between cement particles diminishes and the

availability of nucleating surfaces for hydration products too decreases. This also affects the strength of interfacial transition zone where the mortar containing WMF binds aggregates. The overall effect was reduction in abrasion strength at WMF content greater than 20%. Figs 4.85 & 4.86 show clearly, the effect produced by admixtures on the abrasion resistance of mortars.

(ii) Flyash addition

Flyash addition has been found to reduce the 28-day abrasion resistance of mortar mixes. With an increment in the flyash content up to 30%, there was a corresponding uniform increment in weight loss of specimens due to abrasion.

The possible reasons for loss in abrasion resistance due to flyash are; loss in strength due to dilution, lesser packing effect of flyash, less strength enhancement due to lower rate of C-S-H formation by flyash. Even though the water liberation is more in case of flyash, but the dilution of cement and lesser hydration rate of flyash cause reduction in strength of mortar at 28 days.

(iii) Microsilica addition

Even in case of microsilica inclusion, WMF also interferes in the pore size refinement and grain size refinement done by microsilica. Though it is not able to get adsorbed on the cement particles' surface, because of its lesser tendency on account of its lower surface area. But, it totally affects the filling of spaces in cement particles' voids. This does not affect strength to a higher extent which seems to increase with the WMF content initially because of its reinforcing effect. But the reduced pore size refinement caused by filling of voids by acicular WMF has a straightaway effect on the density of hydration products and thus abrasion resistance. The density increases with the age and it is expected that after 90 days WMF too should give same abrasion resistance as that of WMF-microsilica mixes.

Hence for 28 days, it could be said that microsilica addition in WMF mixes only lead to moderate strength increment in comparison to flyash-microsilica mixes. Flyash-microsilica mixes have extra advantage of both strength increment and pore refinement, due to increment in hydration caused by microsilica in bigger sized flyash particles (approx same

size as cement particles) which provide more nucleating surfaces. Hence the rate of abrasion resistance is more in microsilica-flyash mixes in comparison to WMF-microsilica mixes, though overall WMF-microsilica mixes have highest abrasion resistance values.

Table 4.13 Weight loss due to abrasion of various mortar mixes tested after 28 days

Mix	W	W'	(W-W')/W*100	Mix	W	W'	(W-W')/W*100	Mix	W	W'	(W-W')/W*100
C	2192.0	2186.5	0.251	CF1	2176.0	2166.0	0.460	CW1	2241.0	2233.5	0.335
Cwf	2285.0	2276.5	0.372	CF2	2068.0	2053.5	0.701	CW2	2038.5	2032.57	0.291
CwfS1	2333.5	2327.0	0.279	CF3	2100.0	2081.3	0.892	CW3	2155.5	2149.12	0.296
CwfS2	2275.0	2269.2	0.254	CFS1	2074.0	2066.8	0.346	CWS1	2201.0	2193.93	0.321
CWf	2276.0	2270.2	0.254	CFS2	2154.5	2148.1	0.296	CWS2	2212.5	2206.24	0.283
CwF	2216.0	2208.0	0.361	CFS3	2116.5	2111.4	0.241	CWS3	2030.0	2024.76	0.258
CwFS1	2290.0	2282.7	0.320	CFS4	2102.0	2097.6	0.211	CWS4	2105.5	2100.24	0.250
CWfS1	2231.0	2225.8	0.231	CFS5	1854.0	1843.3	0.579	CWS5	2020.0	2014.49	0.273
CwFS2	2199.5	2193.1	0.290	CFS6	2145.0	2134.0	0.511	CWS6	2137.5	2132.26	0.245
CWfS2	2296.5	2291.4	0.224	CFS7	2114.0	2104.8	0.433	CWS7	2108.0	2103.21	0.227
CWF	2282.0	2275.0	0.307	CFS8	2123.5	2115.7	0.366	CWS8	2128.0	2123.11	0.230
CWFS1	2246.5	2240.3	0.274	CFS9	2149.5	2134.0	0.723	CWS9	2077.5	2071.7	0.279
CWFS2	2168.5	2162.9	0.259	CFS10	2052.0	2039.1	0.630	CWS10	2065.5	2060.38	0.248
CWFS3	2349.5	2343.5	0.255	CFS11	2093.5	2081.7	0.562	CWS11	2116.0	2111.07	0.233
CWFS4	2233.5	2227.4	0.274	CFS12	2126.5	2115.4	0.520	CWS12	2139.0	2133.89	0.239

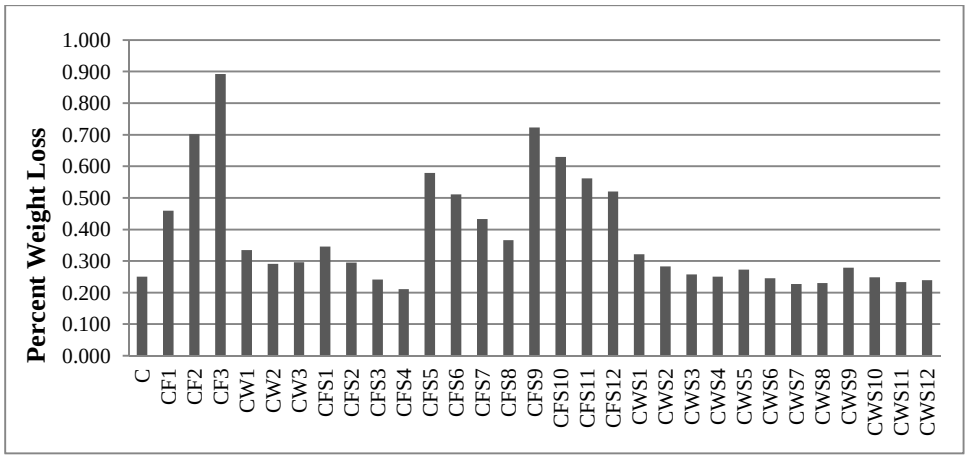

Fig 4.85 Abrasion resistance binary and ternary mortar mixes

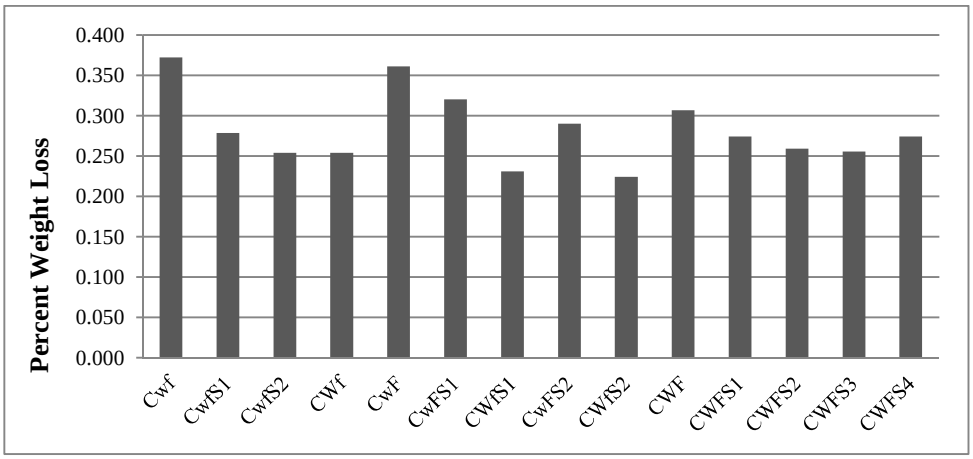

Fig. 4.86 Abrasion resistance of combined mortar mixes

4.4.3 Rate of Water Absorption and Sorptivity

Since the tabular form of representing the rate of water absorption is much space consuming, therefore curves in Figs. 4.87-4.95 have been used to show their variation with time. Tables 4.14, 4.15 and 4.16 show the initial and final sorptivity values for different concrete mixes. Figs 4.96-4.101 show the initial and final sorptivity variation of mixes with duration, in form of bar charts. As is clear from the figures on sorptivity values, both WMF and flyash binary mixes have registered reduction in water absorption values at all durations with respect to normal concrete but the secondary sorptivity of WMF admixed mortars is considerably low, and suggest that water absorption after 7 hours occurs at a very slow rate in these mortars. In other words, the voids are present on the surface, but are not interconnected in WMF admixed mortars. As far as the effect of microsilica is concerned, it

is seen that microsilica equally complements other admixtures in their resistance against water absorption. If duration is considered, then it is found that WMF registers greater loss in sorptivity values with age with respect to flyash. Also, if combined mixes are considered; it has been found that it is quite difficult to explain the random behaviour of mortar mixes with respect to the percentage of admixtures in them. But, it is apparent from the results , that when both WMF and flyash are together in the mortar, then it does not show any improvement with respect to mortars containing either WMF or flyash.

Obtaining a significant of microsilica in the combined mixes is negligible, as it has been seen in most of the mixes, that with the increment in microsilica percentage, an increment in sorptivity has been found. This may be due to self-desiccation caused by co-existence of many fine admixtures together, which reduces the water availability and hydration spaces. The freely available unreacted admixtures in SEM images of combined pastes mixes after 7 days prove this fact. Though it has been seen that permeability was reduced in combined mixes, but that happened on account of non-passability of water through very fine capillary voids where the water is under tension. Also the unreacted particles do block the easy flow of water through them due to filler effect.

The random inexplicable behaviour with respect to the combined presence of flyash and WMF is probably on account of hindered action of one admixture in presence of other, and due to creation of more capillary voids. One thing is quite apparent, which is the increment in sorptivity value with combined percentage increment in WMF+ flyash content. This may be due to increment in capillary voids caused by flyash, which WMF somehow is not able to fill when its quantity by mass is either low or equal to flyash, which is generally happening in the combined mortar mixes.

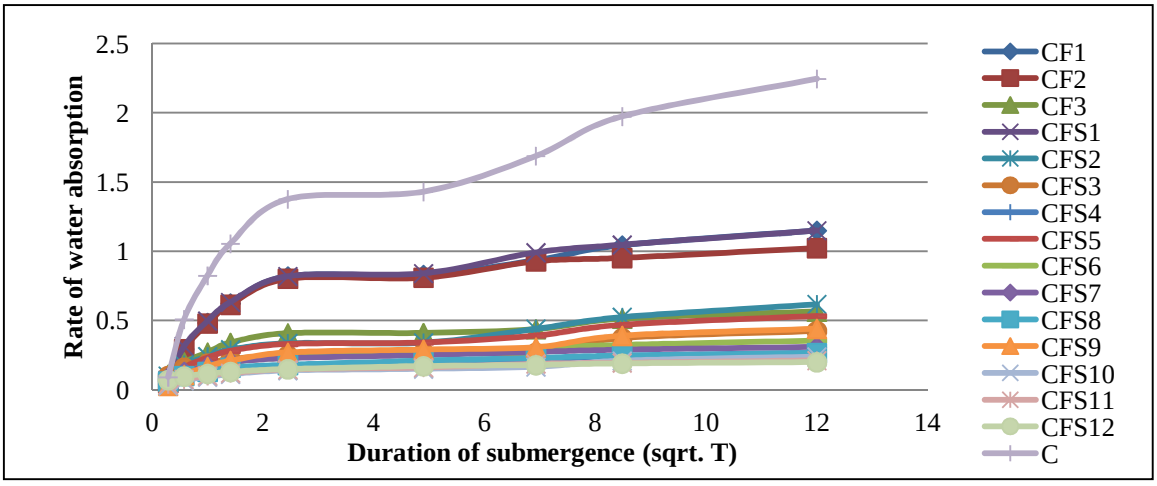

Fig 4.87 Rate of Water absorption of normal & flyash admixed mortars at 7 days

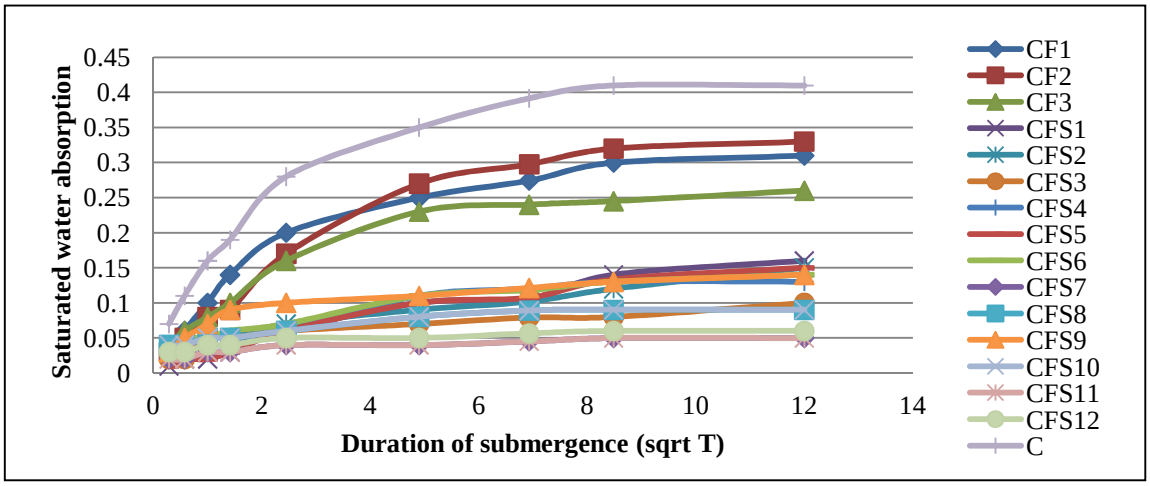

Fig 4.88 Rate of Water absorption of normal & flyash admixed mortars at 56 days

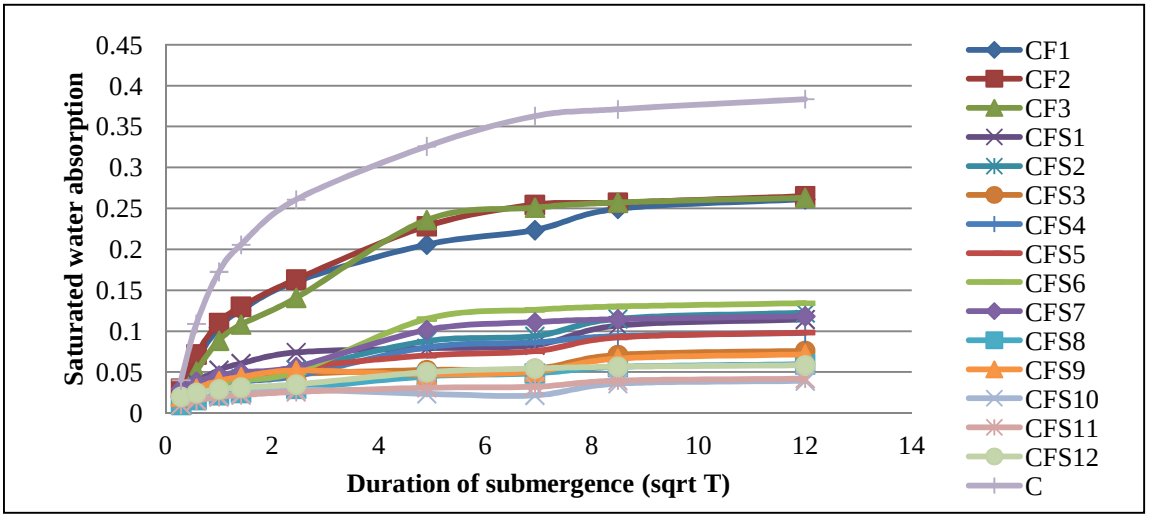

Fig 4.89 Rate of Water absorption of normal & flyash admixed mortars at 56 days

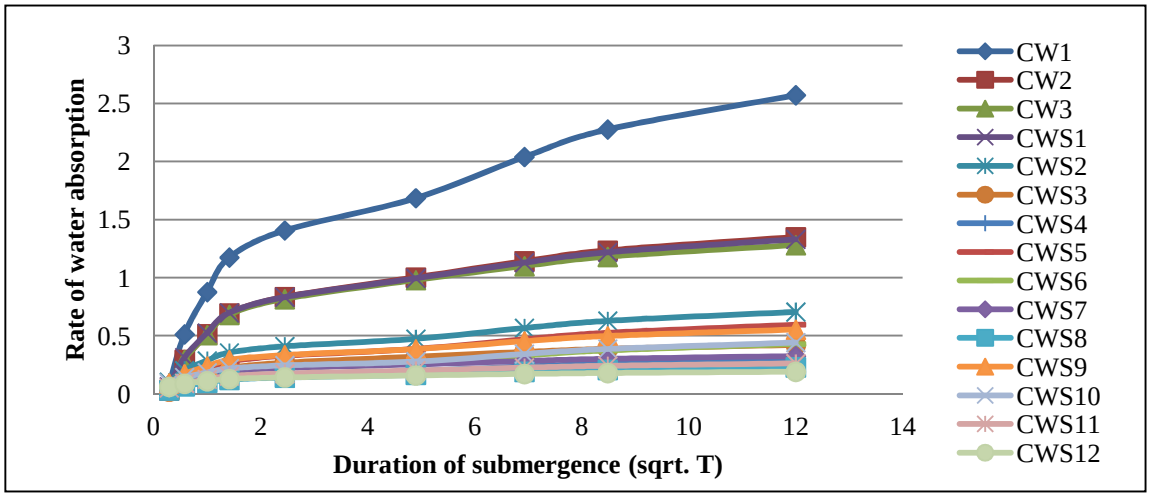

Fig 4.90 Rate of Water absorption of WMF admixed mortars at 7 days

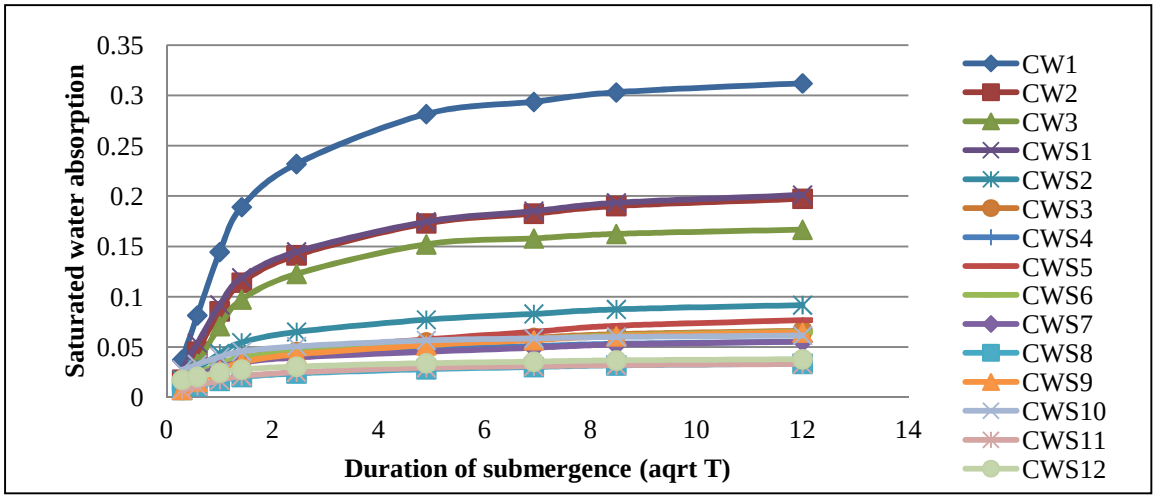

Fig 4.91 Rate of Water absorption of WMF admixed mortars at 56 days

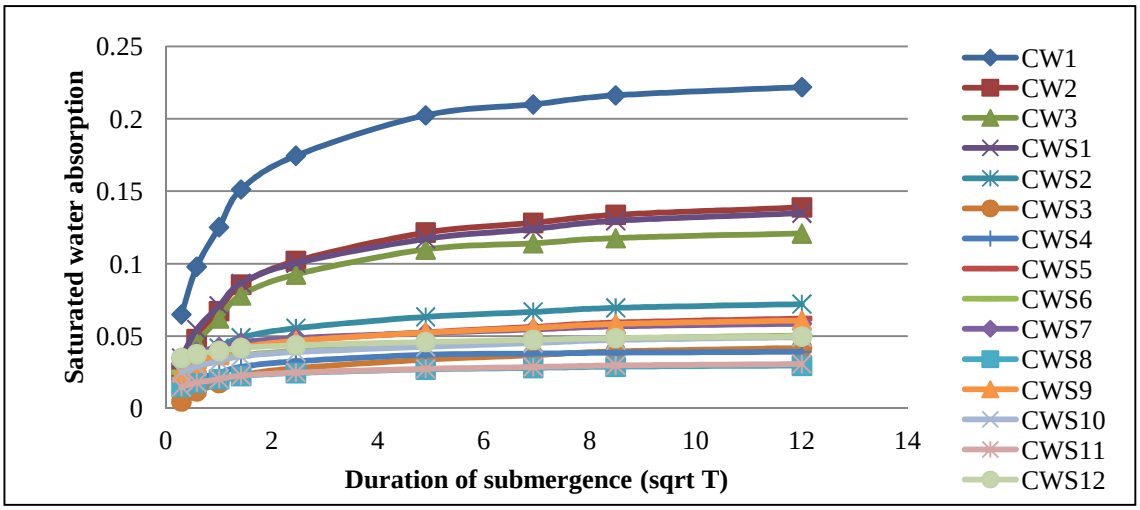

Fig 4.92 Rate of Water absorption of WMF admixed mortars at 56 days

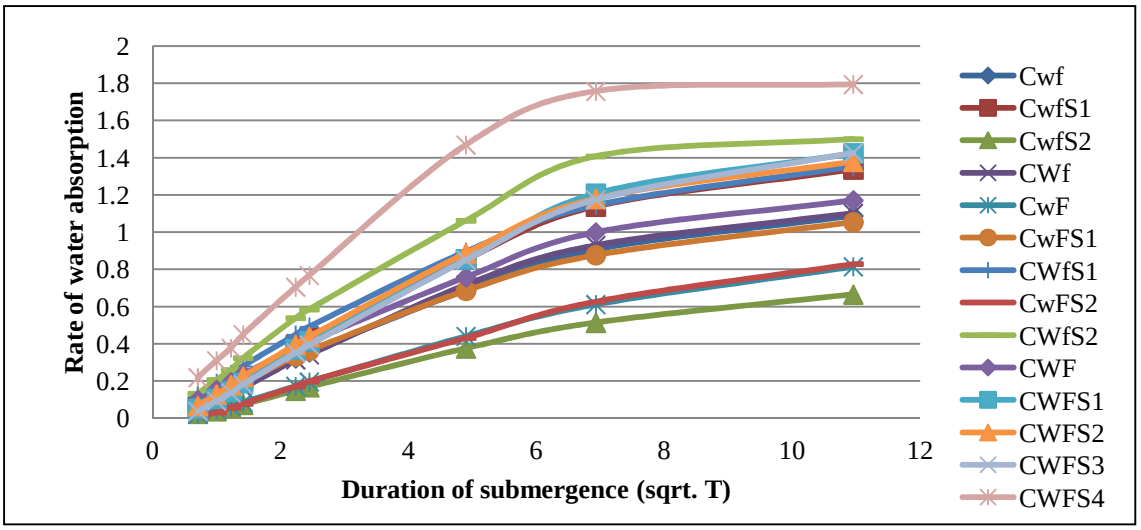

Fig 4.93 Rate of Water absorption of combined mortars at 7 days

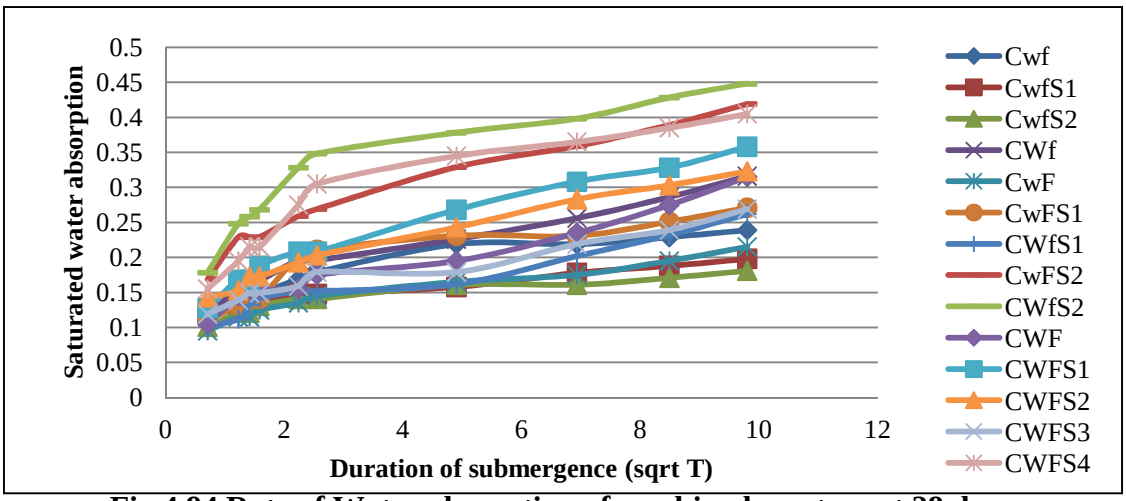

Fig 4.94 Rate of Water absorption of combined mortars at 28 days

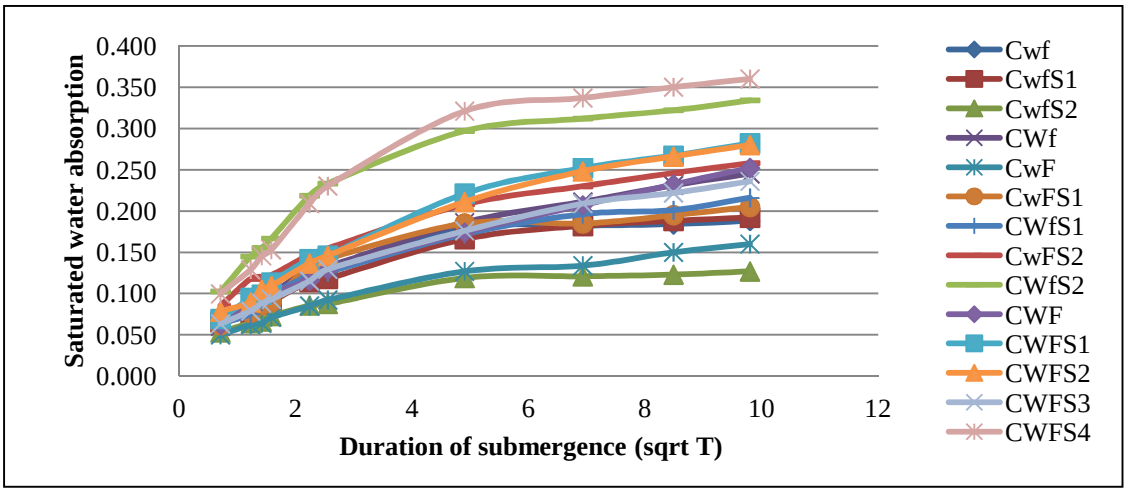

Fig 4.95 Rate of Water absorption of combined mortars at 56 days

Table 4.14 Sorptivity values at different durations for normal & flyash admixed mortars

Mix	Initial sorptivity (m/sec$^{1/2}$)			Secondary Sorptivity (m/sec$^{1/2}$)		
	7 Days	28 Days	56 Days	7 Days	28 Days	56 Days
CF1	6.01E-05	1.31E-05	1.08E-05	7.50E-06	1.41E-06	1.30E-06
CF2	5.80E-05	1.08E-05	1.03E-05	5.02E-06	1.41E-06	8.58E-07
CF3	2.30E-05	9.26E-06	1.01E-05	3.64E-06	7.04E-07	6.37E-07
CFS1	5.78E-05	3.86E-06	4.17E-06	7.26E-06	1.41E-06	8.28E-07
CFS2	1.82E-05	3.09E-06	3.30E-06	6.50E-06	1.41E-06	8.11E-07
CFS3	1.15E-05	3.09E-06	2.12E-06	3.62E-06	7.04E-07	5.51E-07
CFS4	9.66E-06	2.32E-06	1.94E-06	1.54E-06	4.69E-07	4.16E-07
CFS5	2.08E-05	3.86E-06	3.51E-06	4.51E-06	1.17E-06	6.57E-07
CFS6	1.24E-05	2.31E-06	3.09E-06	2.21E-06	7.04E-07	4.51E-07
CFS7	1.07E-05	1.54E-06	2.04E-06	1.39E-06	2.35E-07	3.95E-07
CFS8	9.25E-06	1.54E-06	1.53E-06	1.30E-06	2.35E-07	3.48E-07
CFS9	1.84E-05	5.40E-06	2.47E-06	3.54E-06	7.04E-07	5.78E-07
CFS10	8.37E-06	1.54E-06	1.43E-06	2.07E-06	2.35E-07	3.67E-07
CFS11	8.24E-06	1.54E-06	1.22E-06	1.21E-06	2.35E-07	2.62E-07
CFS12	6.06E-06	1.54E-06	1.15E-06	6.83E-07	2.35E-07	1.99E-07
C	9.92E-05	1.62E-05	1.70E-05	1.92E-05	1.41E-06	1.35E-06

Table 4.15 Sorptivity values at different durations for WMF admixed mortars

Mix	Initial sorptivity (m/sec$^{1/2}$)			Secondary Sorptivity (m/sec$^{1/2}$)		
	7 Days	28 Days	56 Days	7 Days	28 Days	56 Days
CW1	10.23E-05	1.50E-05	8.44E-06	2.08E-05	7.16E-07	4.57E-07
CW2	6.19E-05	9.55E-06	5.93E-06	8.16E-06	5.75E-07	4.08E-07
CW3	5.98E-05	8.88E-06	5.21E-06	7.07E-06	3.44E-07	2.60E-07
CWS1	5.96E-05	9.04E-06	5.04E-06	7.89E-06	6.23E-07	4.17E-07
CWS2	2.37E-05	3.67E-06	2.36E-06	5.46E-06	3.41E-07	2.08E-07
CWS3	1.90E-05	2.90E-06	1.77E-06	2.40E-06	2.69E-07	1.90E-07
CWS4	9.96E-06	1.87E-06	1.36E-06	2.25E-06	1.74E-07	4.77E-08
CWS5	2.14E-05	3.08E-06	1.70E-06	4.90E-06	4.50E-07	2.24E-07
CWS6	1.28E-05	2.17E-06	1.14E-06	3.94E-06	2.89E-07	1.62E-07
CWS7	1.10E-05	1.71E-06	1.06E-06	1.68E-06	2.40E-07	1.53E-07
CWS8	8.50E-06	1.26E-06	7.39E-07	1.51E-06	1.28E-07	6.02E-08
CWS9	1.87E-05	2.72E-06	1.69E-06	3.96E-06	3.01E-07	1.98E-07
CWS10	1.19E-05	1.79E-06	1.08E-06	3.85E-06	1.15E-07	1.58E-07
CWS11	9.53E-06	1.34E-06	7.65E-07	1.42E-06	8.59E-08	7.94E-08
CWS12	6.25E-06	1.01E-06	6.71E-07	7.43E-07	9.33E-08	9.02E-08

Table 4.16 Sorptivity values at different durations for combined mortars

Mix	Initial sorptivity (m/sec$^{1/2}$			Secondary Sorptivity (m/sec$^{1/2}$)		
Cwf	2.71E-05	4.52E-06	4.86E-06	1.10E-05	6.80E-07	3.06E-07
CwfS1	3.57E-05	2.71E-06	4.78E-06	1.33E-05	1.36E-06	8.85E-07
CwfS2	1.37E-05	3.62E-06	3.12E-06	7.98E-06	6.80E-07	2.72E-07
CWf	3.02E-05	7.24E-06	6.51E-06	1.06E-05	3.06E-06	2.01E-06
CwF	1.65E-05	4.52E-06	3.84E-06	1.03E-05	1.70E-06	1.12E-06
CwFS1	2.89E-05	9.05E-06	7.29E-06	1.01E-05	1.36E-06	6.80E-07
CWfS1	3.55E-05	4.52E-06	5.66E-06	1.26E-05	3.40E-06	1.50E-06
CwFS2	1.83E-05	9.05E-06	6.27E-06	1.09E-05	3.06E-06	1.70E-06
CWfS2	4.32E-05	1.54E-05	1.18E-05	1.21E-05	2.38E-06	1.26E-06
CWF	3E-05	6.33E-06	6.04E-06	1.13E-05	4.08E-06	2.65E-06
CWFS1	3.47E-05	7.24E-06	6.95E-06	1.57E-05	3.06E-06	2.08E-06
CWFS2	3.55E-05	5.43E-06	6.11E-06	1.35E-05	2.72E-06	2.35E-06
CWFS3	3.41E-05	5.43E-06	5.98E-06	1.59E-05	3.06E-06	2.04E-06
CWFS4	5.25E-05	1.36E-05	1.18E-05	8.95E-06	2.04E-06	1.33E-06

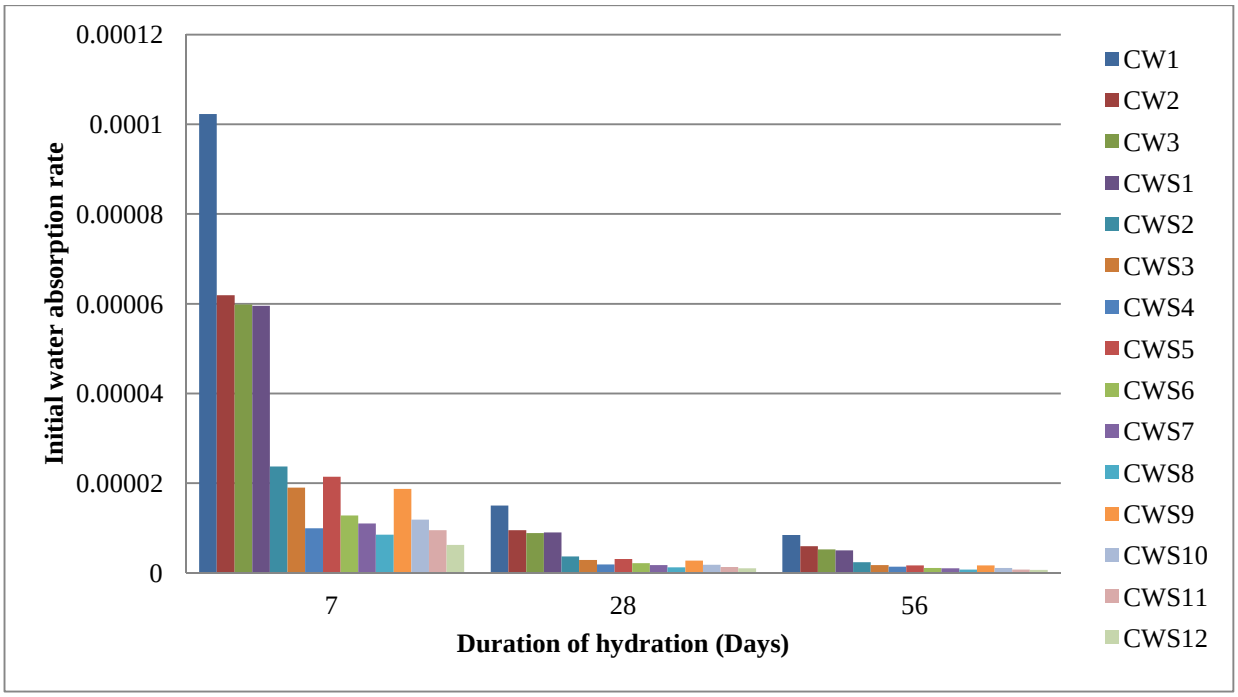

Fig. 4.96 Initial sorptivity for WMF admixed mortar mixes

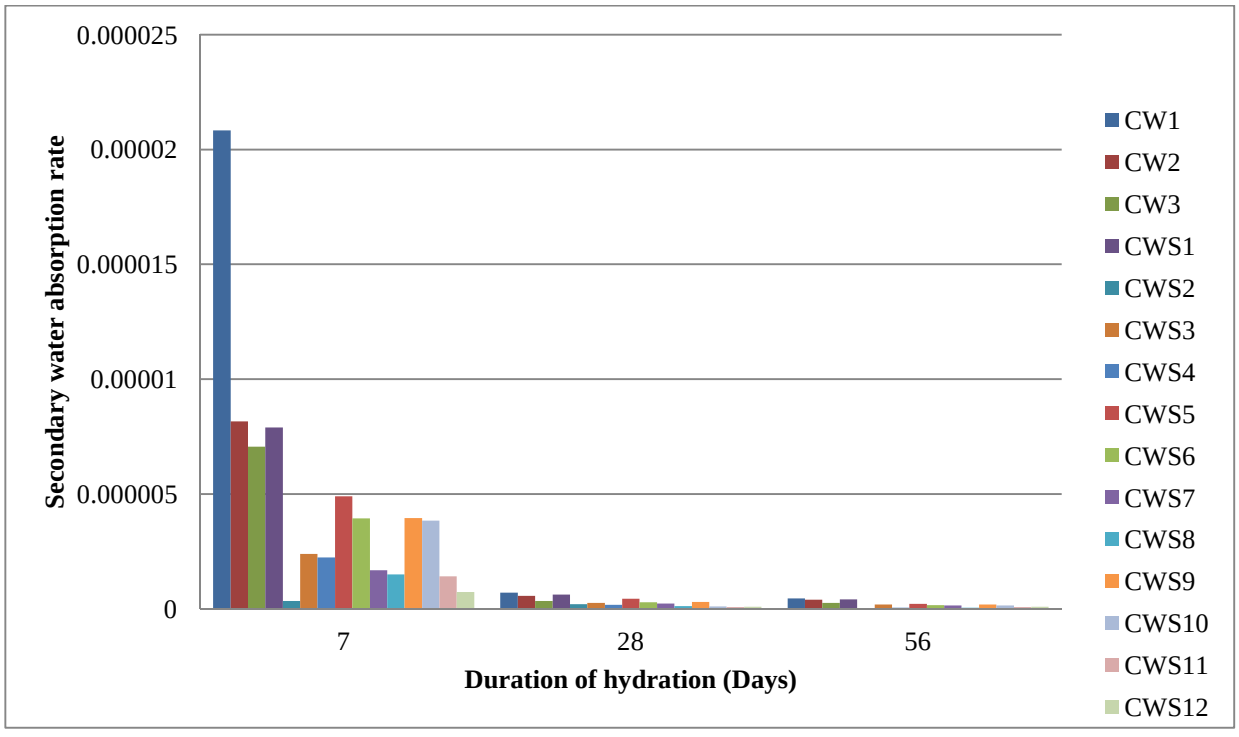

Fig. 4.97 Secondary sorptivity for WMF admixed mortar mixes

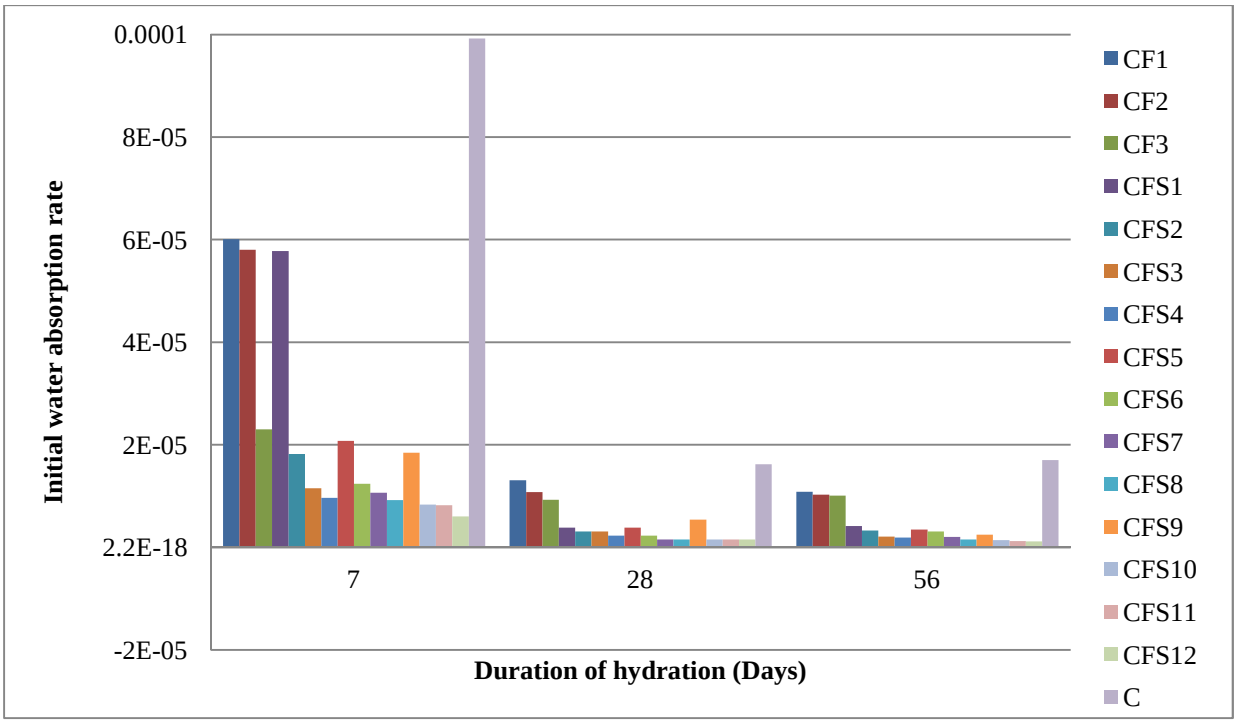

Fig. 4.98 Initial sorptivity for flyash admixed mortar mixes

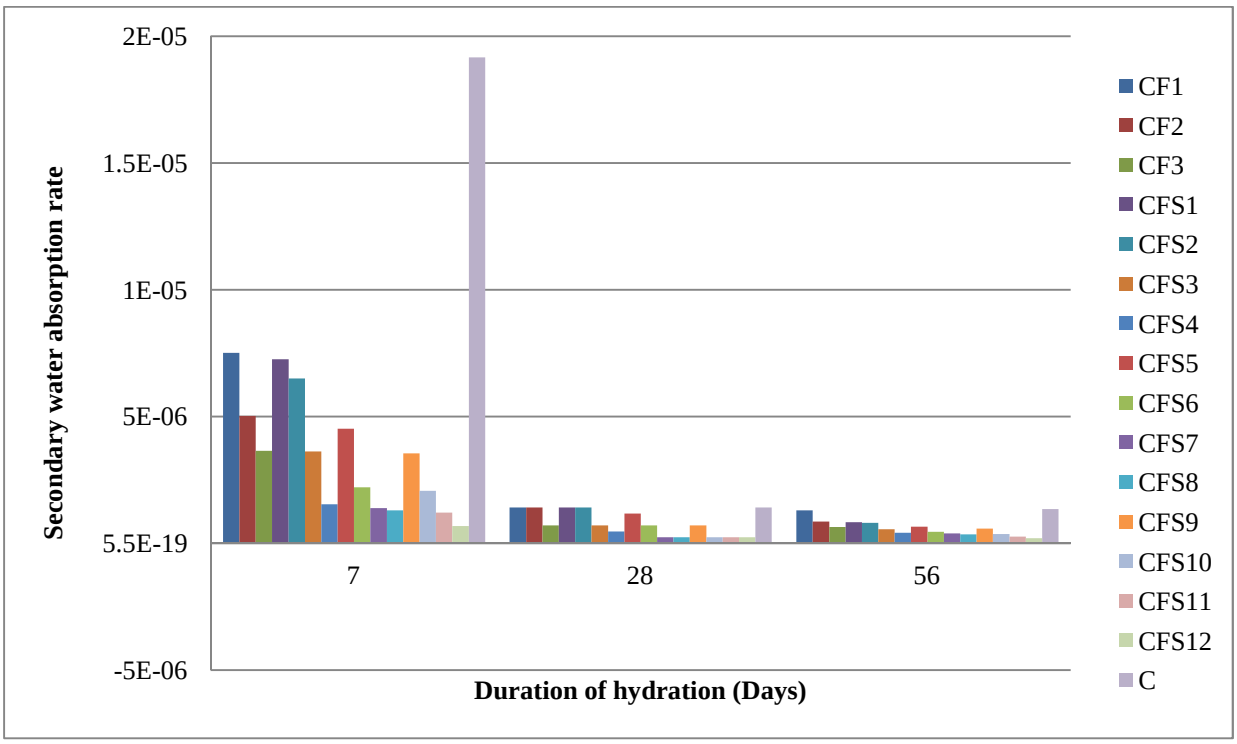

Fig. 4.99 Secondary sorptivity for flyash admixed mortar mixes

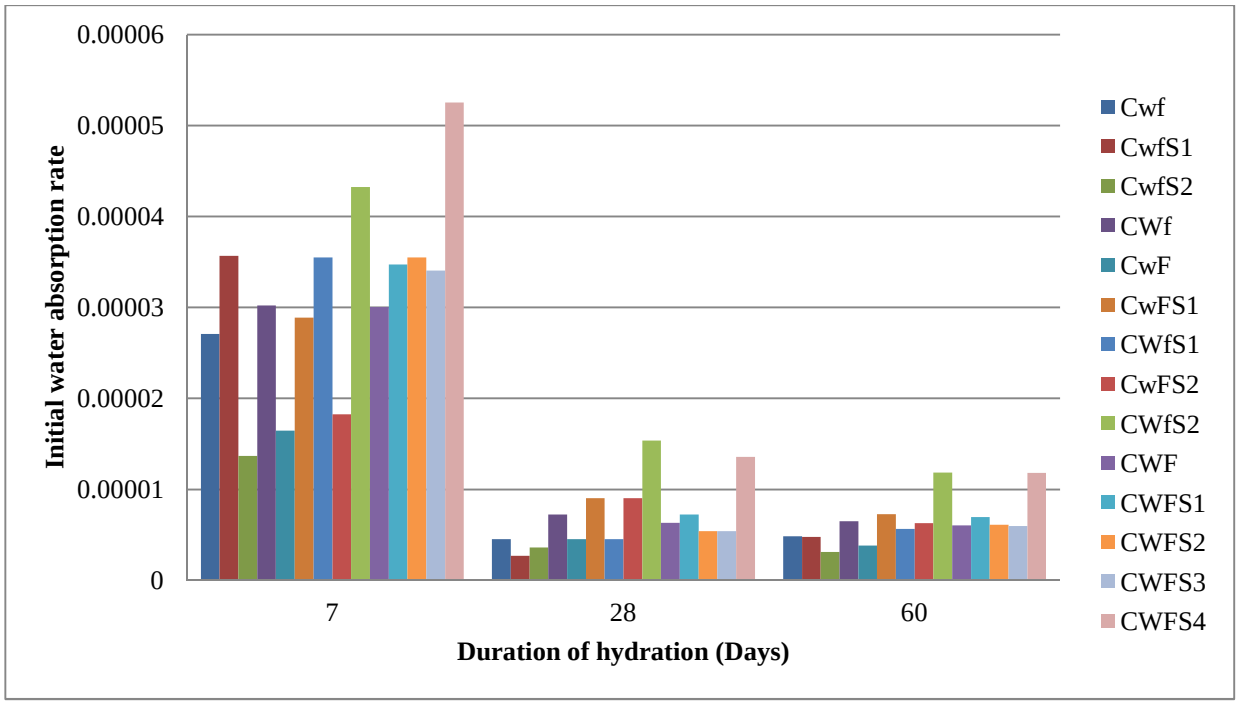

Fig. 4.100 Initial sorptivity for combined mortar mixes

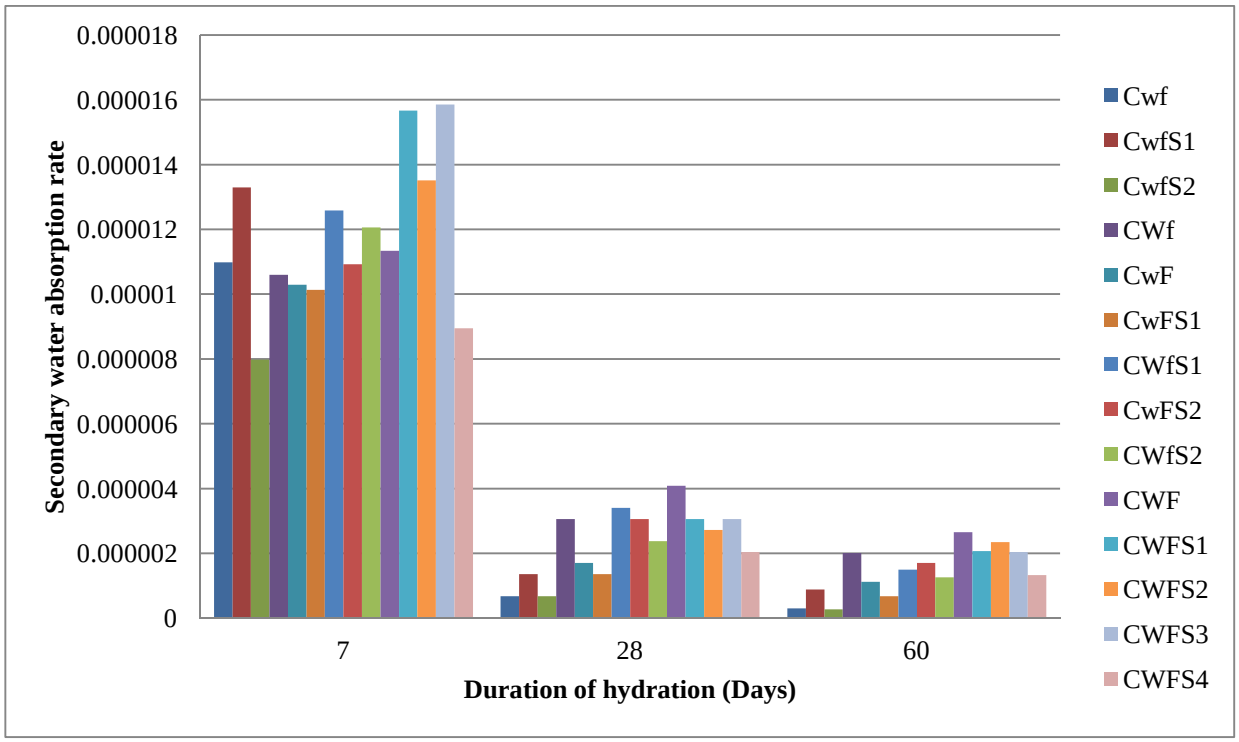

Fig. 4.101 Secondary sorptivity for combined mortar mixes

4.5 CONCRETE

4.5.1 Rheology of SCC

The rheological properties of SCC are measured in terms of flowability, passability and segregation resistance. The rheological tests were conducted in continuation of finding the optimum quantity of aggregates (coarse and fine) along with superplasticizers, for a given mass of binder. Since there were a lot of variables involved in the realization of SCC, trials were conducted for a given binder type, with continuously changing ratio of CA/FA. For each ratio, a set of trials were conducted with increasing dosages of superplasticizers, until the optimum content of superplasticizer is achieved, or the mix achieved the specified rheological properties of a SCC, or the mix showed segregation and thus, further superplasticizer could not be added. Since in this test for a given binder a certain CA: FA is first chosen and tested, hence, it is the CA: FA ratio, which is critical for a given binder content. The starting CA/FA ratio was obtained on basis of the mix design for highly workable pavement quality concrete.

(a) Observations

(i) It was found that for a given binder content, there is an optimum ratio of CA: FA. If the value of the ratio is higher than the optimum value, then the flow of the mix is reduced apparently. It was supposed that segregation too depends on the ratio of CA: FA, such that at higher ratio, segregation would be higher. But the assumption was wrong because at higher coarse aggregate content only flowability and passability were maximally affected. The possible reason is, that the binder material is sufficient for holding either the coarse or fine aggregates, provided the total volume of aggregates remain the same.

(ii) For a given total summed volume of coarse aggregates and fine aggregates, more is the content of fine aggregates, more would be the flow. But there is a limitation; the content of fine aggregates could not be increased beyond a certain value. After this value, the segregation of concrete occurs. This is because; the volume of binder was already lower in the concrete mix so as to hold the fine aggregates. This resulted in a lower cohesion & flowability of the mix. In order to increase the flow, if further superplasticizer is added, then the increased effective water content reduced the

viscosity of the paste to such an extent that laitance formation takes place. High viscosity of fresh cement paste component mitigate the downward movement of the heavier aggregate particles, mix with low water/cement ratios are less prone to segregation [19]. There are two forms of segregation; one form in which the separation of coarse aggregates occurs in very lean mixes containing higher specific gravity due to higher volume of aggregates, and other form in which there is reduction of cohesion on account of reduced surface tension caused by higher volumes of water, owing to separation of cement paste from the aggregates mass. This is called as laitance formation and is different from bleeding. With higher volume of fine aggregate this type of segregation occurs.

(iii) Hence, while addition of superplasticizers for a given binder mass, if segregation occurs, then fine aggregates need to be reduced or the superplasticizer content has exceeded. Since fine aggregates were increased sequentially and previous fine aggregate content had already failed the test, therefore it means that the self compacting condition is not achievable for a given binder content on basis of PQC mix design. In present study the last possible superplasticizer content has been reported and the corresponding flow parameters have been noted.

(iv) The maximum possible content of fine aggregates for a given binder content was found to be directly proportional to the average surface area of the binder. This means, that the increment in fine aggregate content over and above that of the mix design value, is directly proportional to the increment in surface area caused by the fraction of admixture in the paste.

(v) Binder content, CA/FA ratio and surface morphology; all effect the flow of SCC to big or small extent depending upon the property. Flowability and passability were found to be dependent more on the binder content and CA/FA ratio, whereas the segregation resistance depended more on the surface morphology of the binder material.

Table 4.17 below provides the measurements taken while performing the fresh state tests on SCC in the laboratory. The green coloured area indicates the passing of sample for a certain criteria associated with the property of SCC. If a mix passes all the criterion, then it is relied to be taken as a self compacting concrete (SCC). Also the Table provides the

amount of superplasticizer used, as well as the minimum possible ratio of coarse aggregates to fine aggregates which could be taken for the attainment of SCC for a specific powder material.

.

Table 4.17 Results obtained from the performance test conducted on SCC in the fresh state

Mix	Percentage of cementitious materials in Powder				CA:FA	Super plasticizer (ml/cu.m. of mix)	Abram's flow (600-750) (mm)	V Funnel time (6-12) (sec)	V Funnel time after 5 min (+3) (sec)	J Ring diff. (0-10) (mm)	Probe ring penetration (0-7) (mm)	Super plasticizer (% of cementitious materials)
	C	F	WMF	SF			Flowability	Flowability	Segregation Resistance	Passability	Segregation Resistance	
C	100	-	-	-	60:40	1227.3	360	17	24	24	2	0.30
CW1	90	-	10	-	55:45	1840.9	560	10	12	21	3	0.45
CW2	80	-	20	-	50:50	1840.9	580	8	10	19	5	0.45
CW3	70	-	30	-	50:50	2454.5	540	12	12	21	4	0.6
CWS1	87.5	-	10	2.5	55:45	1840.9	580	9	11	15	3	0.45
CWS2	85	-	10	5	50:50	1840.9	630	8	10	9	5	0.45
CWS3	82.5	-	10	7.5	50:50	1840.9	620	9	10	10	4	0.45
CWS4	80	-	10	10	50:50	1840.9	605	10	11	13	3	0.45
CWS5	77.5	-	20	2.5	50:50	1840.9	646	7	11	11	5	0.45
CWS6	75	-	20	5	50:50	2454.5	660	7	9	5	7	0.6
CWS7	72.5	-	20	7.5	50:50	2454.5	620	8	11	8	5	0.6

CWS8	70	-	20	10	50:50	2454.5	590	9	14	10	4	0.6
CWS9	67.5	-	30	2.5	50:50	2454.5	570	10	12	14	5	0.6
CWS10	65	-	30	5	45:55	2454.5	630	7	9	12	3	0.6
CWS11	62.5	-	30	7.5	45:55	1840.9	575	9	13	17	2	0.45
CWS12	60	-	30	10	45:55	1840.9	530	13	18	22	2	0.45
CF1	90	10	-	-	55:45	1227.3	570	10	16	15	5	0.3
CF2	80	20	-	-	55:45	1227.3	581	9	17	13	7	0.3
CF3	70	30	-	-	55:45	1227.3	604	7	18	11	9	0.3
CFS1	87.5	10	-	2.5	55:45	1840.9	585	9	16	12	5	0.45
CFS2	85	10	-	5	50:50	1840.9	615	8	14	11	8	0.45
CFS3	82.5	10	-	7.5	50:50	1840.9	600	9	10	15	6	0.45
CFS4	80	10	-	10	50:50	1840.9	573	10	12	18	3	0.45
CFS5	77.5	20	-	2.5	50:50	1840.9	625	7	9	9	7	0.45
CFS6	75	20	-	5	50:50	1840.9	650	6	9	8	9	0.45
CFS7	72.5	20	-	7.5	50:50	1840.9	618	8	9	10	6	0.45
CFS8	70	20	-	10	50:50	1840.9	587	10	11	13	6	0.45
CFS9	67.5	30	-	2.5	50:50	1840.9	633	6	15	11	10	0.45
CFS10	65	30	-	5	50:50	1227.3	663	5	17	8	12	0.3
CFS11	62.5	30	-	7.5	45:55	1227.3	623	7	17	13	9	0.3
CFS12	60	30	-	10	45:55	1227.3	594	8	21	15	7	0.3

Cwf	90	5	5	-	55:45	1840.9	560	11	11	10	4	0.45
CwfS1	87.5	5	5	2.5	55:45	1840.9	580	10	12	14	6	0.45
CwfS2	85	5	5	5	50:50	2454.5	605	8	11	10	7	0.6
CWf	85	5	10	-	50:50	1840.9	545	13	18	22	2	0.45
CwF	85	10	5	-	55:45	1840.9	585	10	12	15	5	0.45
CwFS1	82.5	10	5	2.5	55:45	1840.9	615	7	9	6	5	0.45
CWfS1	82.5	5	10	2.5	55:45	1840.9	580	11	12	15	3	0.45
CwFS2	80	10	5	5	50:50	1840.9	640	6	9	5	6	0.45
CWfS2	80	5	10	5	50:50	2454.5	610	8	10	8	4	0.6
CWF	80	10	10	-	50:50	1840.9	550	12	14	20	4	0.45
CWFS1	77.5	10	10	2.5	50:50	1840.9	575	11	12	14	5	0.45
CWFS2	75	10	10	5	50:50	1840.9	610	8	11	12	7	0.45
CWFS3	72.5	10	10	7.5	50:50	1840.9	580	10	11	13	5	0.45
CWFS4	70	10	10	10	50:50	2454.5	550	12	15	22	4	0.6

Figs. 4.102-4.113 show the results obtained from the test in form of bar charts. After recognizing the important points from these bar charts, following results have been suggested on the basis of role of each of the admixture in imparting flow to the SCC:

(i) WMF addition

Cohesion in small amounts is necessary for a good flow of mix because the mix flows homogeneously, together with minimal opposition caused by viscous forces. Passability also decreases with increased cohesion, because the mix try to remain altogether when the obstruction confronts it, but for a mix to show segregation resistance it should have higher cohesion. Apart from viscous forces in the pore solution, the inter-particle frictional forces tend to reduce the flowability and passability but enhance the segregation resistance of concrete mix.

WMF is acicular and it has high adsorption tendency as well as the tendency to be a part of pore solution at its higher contents. Hence it increases the inter-particle friction by producing friction between cement particles on which it get adsorbed, and it also increases the viscosity of pore solution at its higher contents.

Therefore it was observed that with WMF addition the flowability and passability of mix reduced, though up to 20% WMF its rate of reduction was less. Segregation resistance increased with increment in WMF content.

(ii) Microsilica addition

With microsilica addition at lower amount 0-5%, the flowability, passability and segregation resistance increased because microsilica has smooth texture and spherical shape, which induces a ball bearing effect between cement particles on whom it get adsorbed. The ball bearing effect does not allow the cement particles to move away though it allows them to roll or slide over each other on account of the sticky nature of microsilica. Khayat & Aitcin [67] also suggest, that presence of microsilica affects the properties of fresh concrete by inducing cohesivity and thus reducing the bleeding of concrete. Both of these factors work contradictory as far as shrinkage is concerned; on one hand cohesivity reduces shrinkage, whereas on other the reduced bleeding increases it. The increased cohesivity also

requires more slump for a given flow, with respect to a normal concrete. But it has one advantage which is homogeneity, and thus enables good passability and flowability, thereby enabling microsilica admixed concrete as a pumpable concrete [39].

Hence at higher amount of microsilica, the flowability and passability decreased but the segregation resistance increased, because the pore solution between the cement particles get thicker and more viscous due to increased microsilica content.

(iii) Flyash addition

Flyash at all contents improved the flowability and passability of mixes, but it decreased the segregation resistance of self compacting concrete. This phenomenon has already been explained when flow of mortars was discussed.

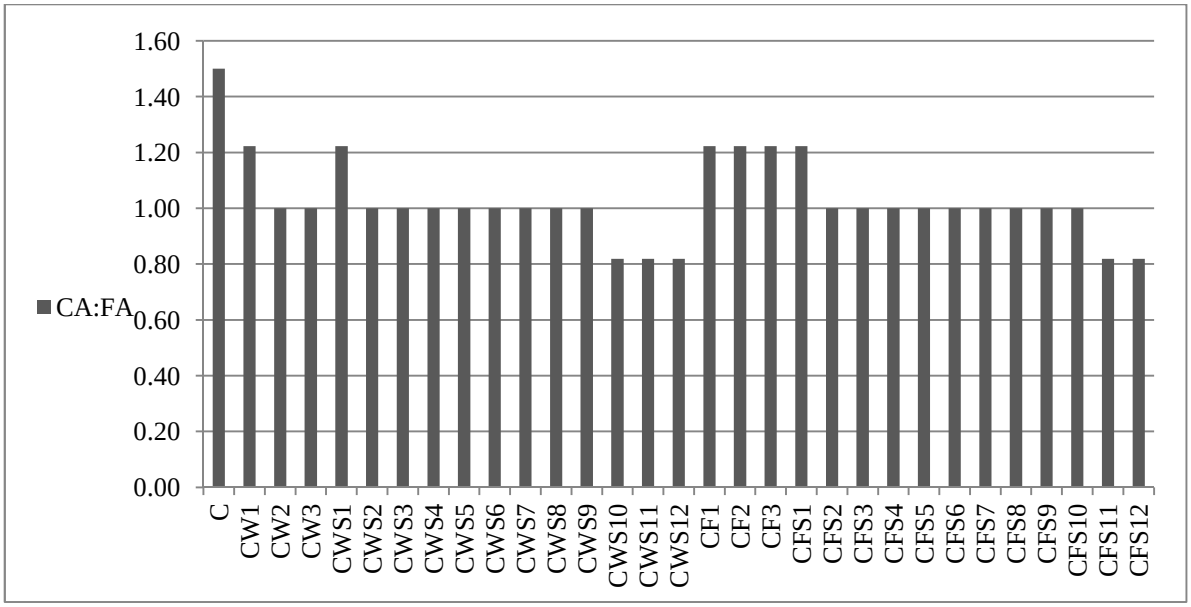

Fig 4.102 Optimum coarse aggregate to fine aggregate ratio for binary and ternary concrete mixes

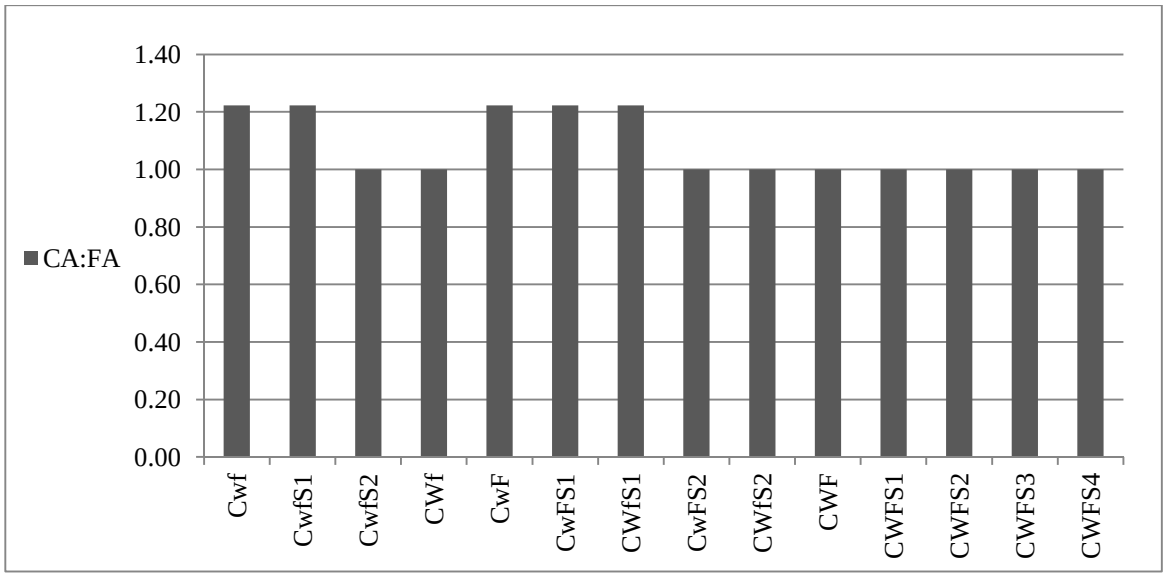

Fig 4.103 Optimum coarse aggregate to fine aggregate ratio for combined concrete mixes

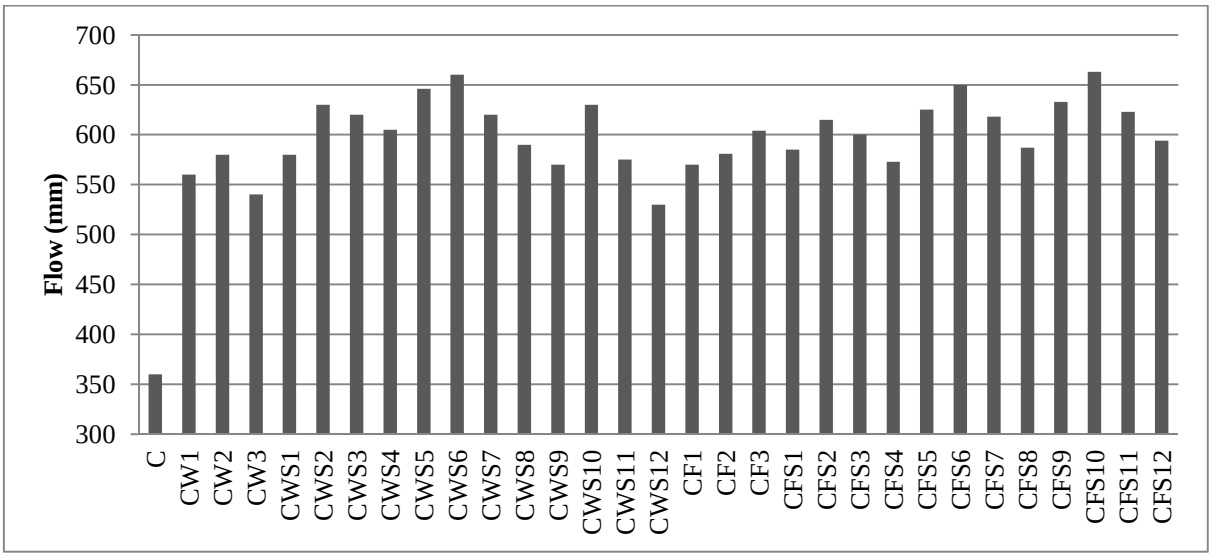

Fig 4.104 Flow of binary and ternary concrete mixes

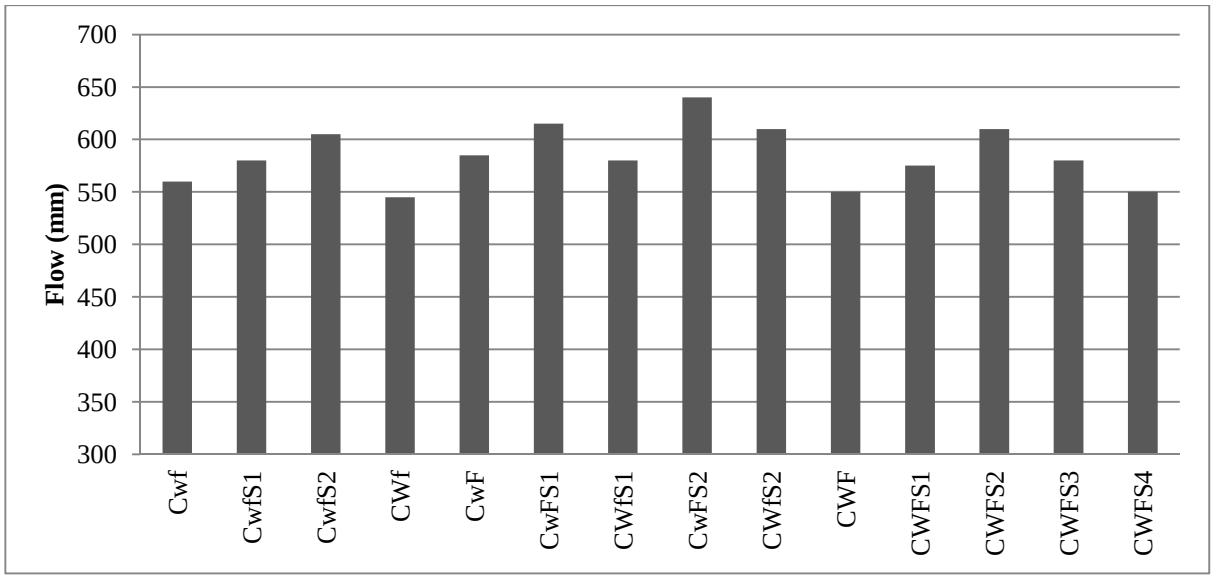

Fig 4.105 Flow of combined concrete mixes

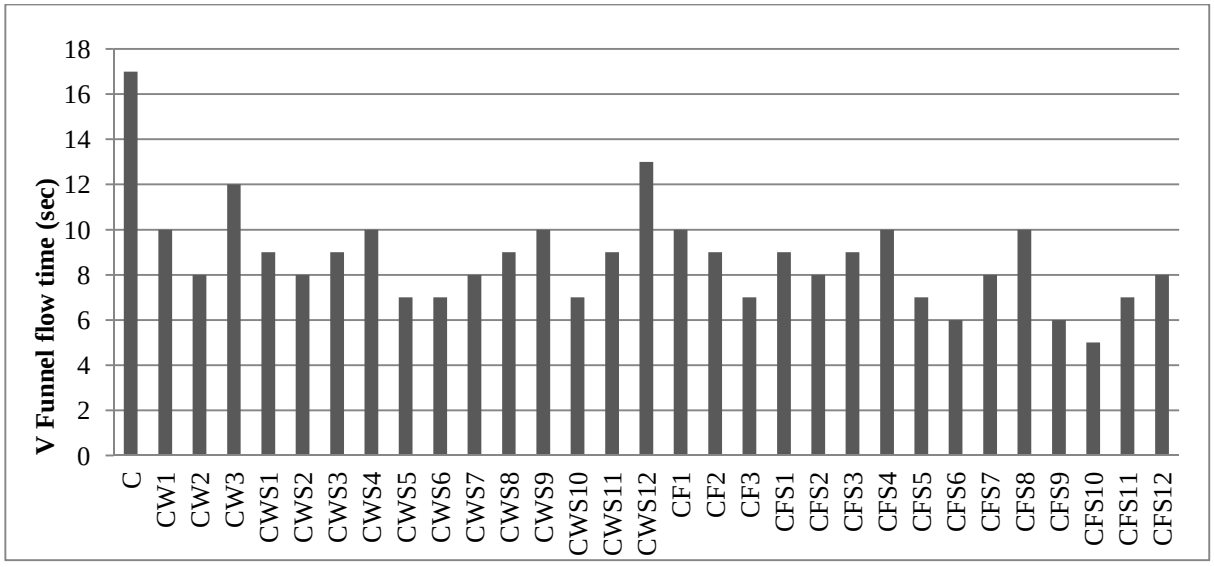

Fig 4.106 V funnel flow of binary and ternary concrete mixes

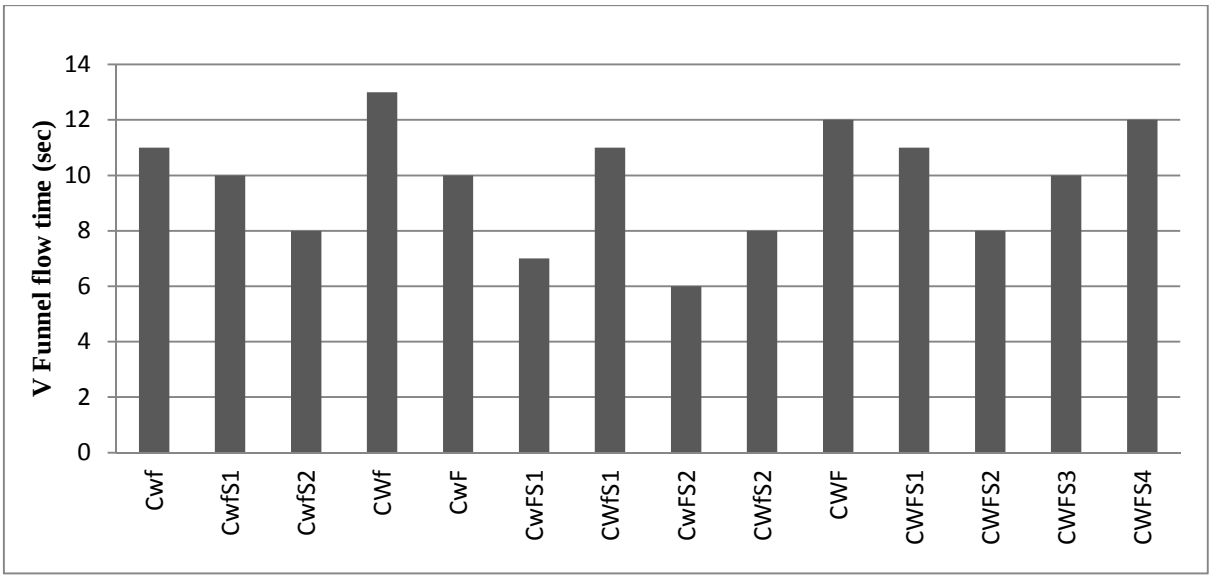

Fig 4.107 V funnel flow of combined concrete mixes

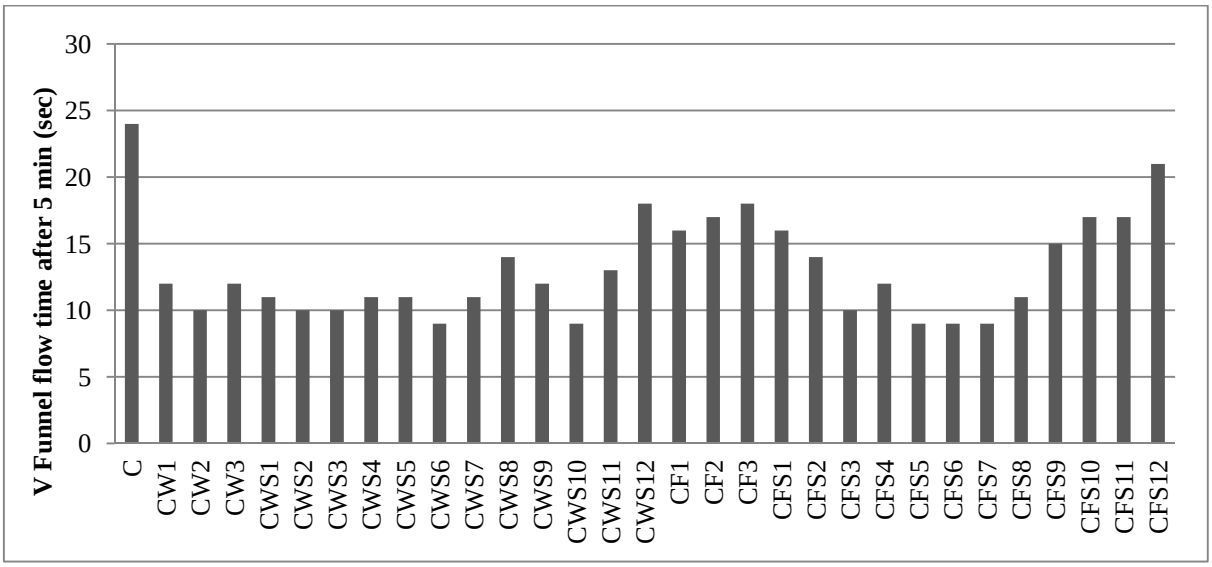

Fig 4.108 Segregation of binary and ternary concrete mixes from V funnel test

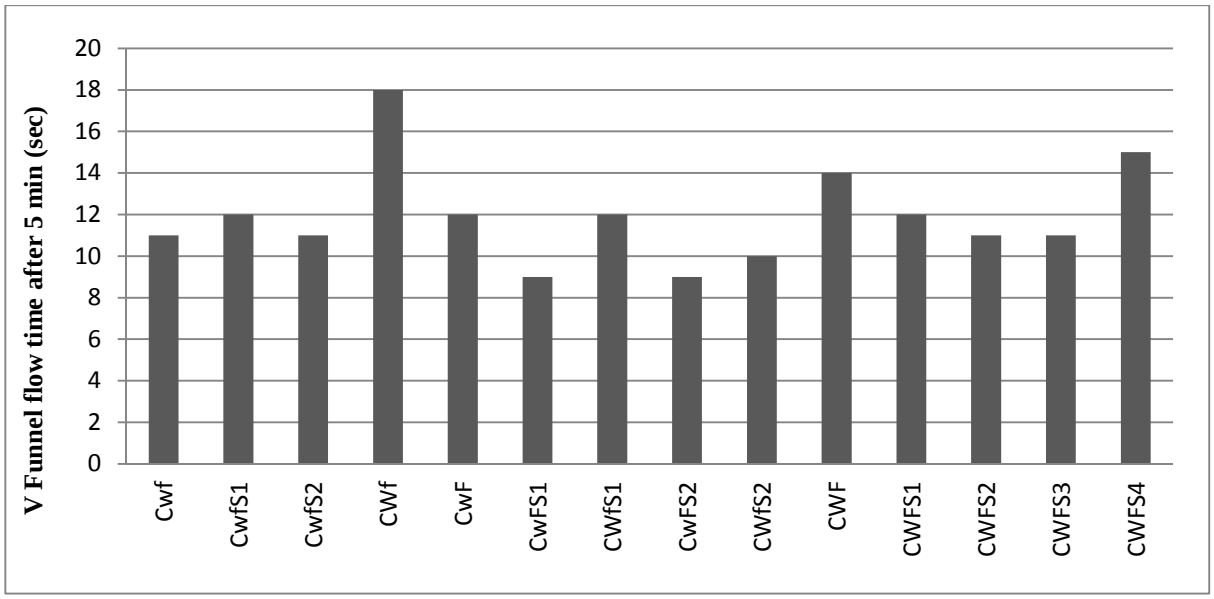

Fig 4.109 Segregation of combined concrete mixes from V funnel test

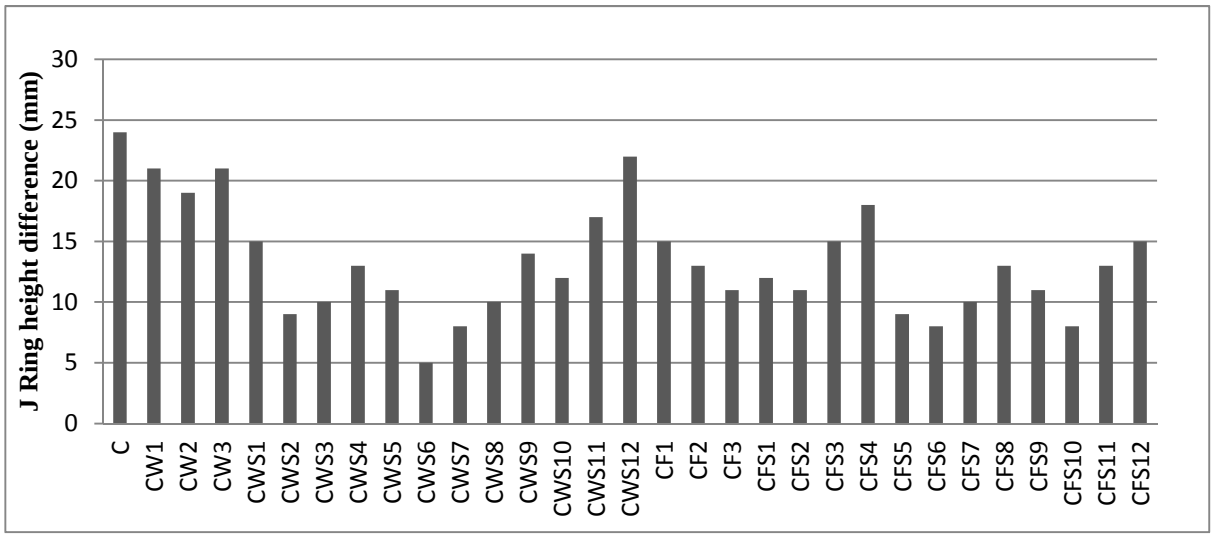

Fig 4.110 Passability of binary and ternary concrete mixes from J ring test

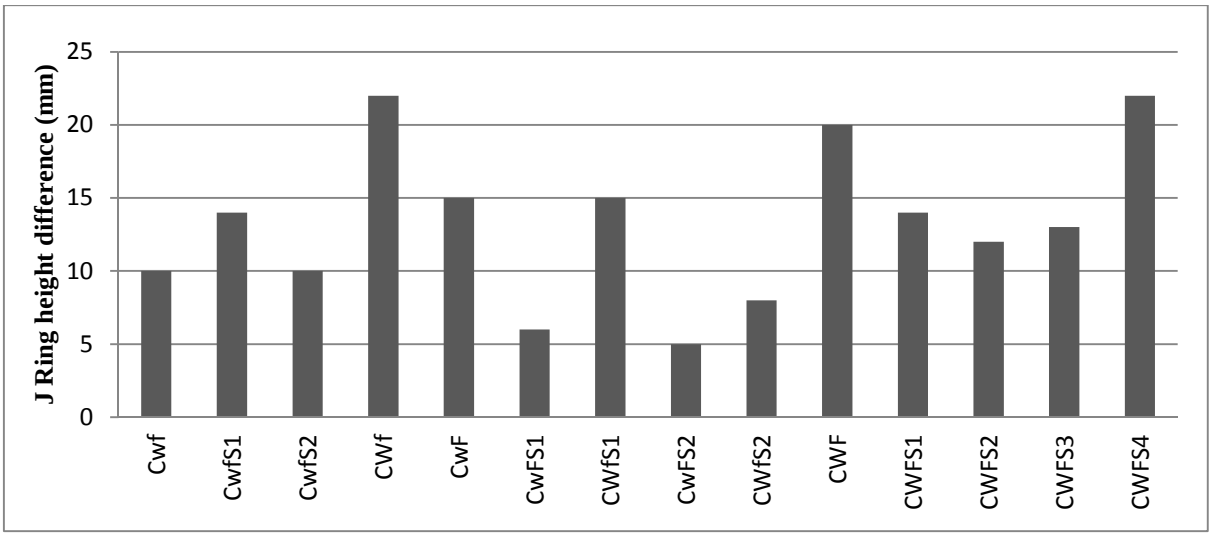

Fig 4.111 Passability of combined concrete mixes from J ring test

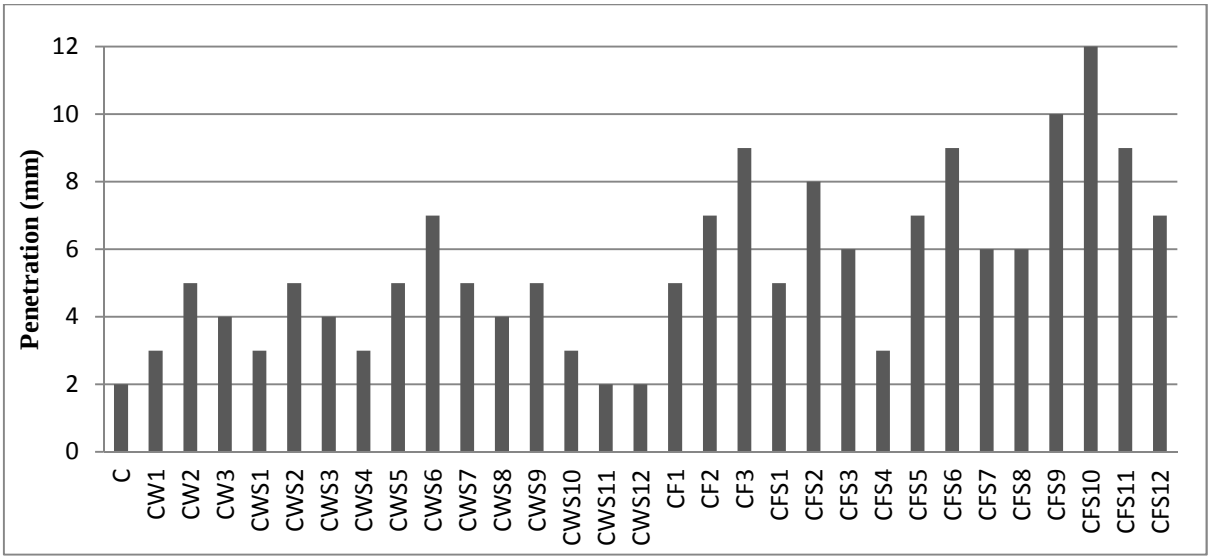

Fig 4.112 Segregation resistance of binary and ternary concrete mixes from Probe ring test

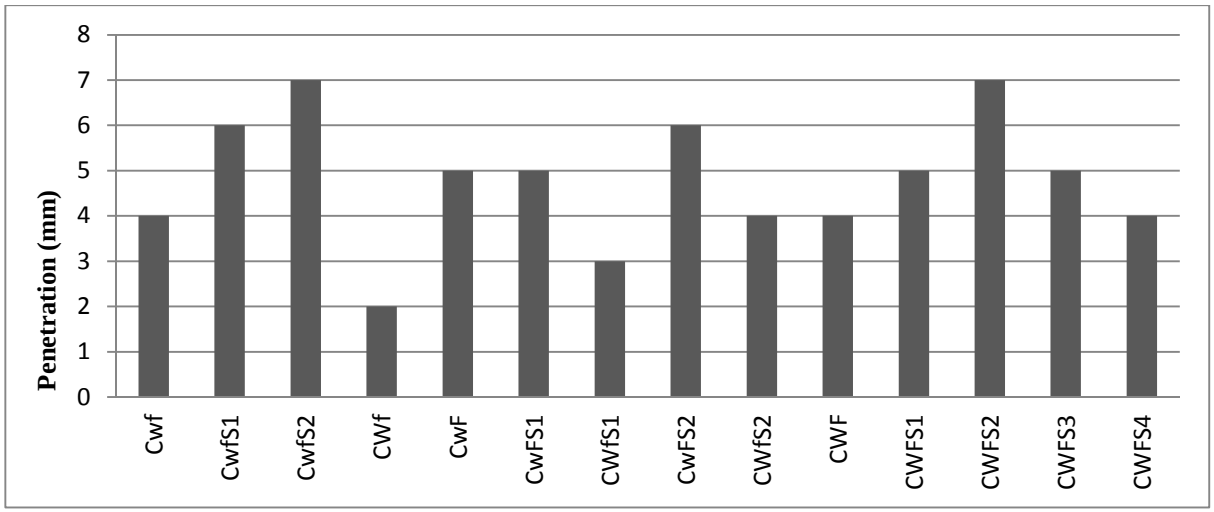

Fig 4.113 Segregation resistance of combined concrete mixes from Probe ring test

4.5.2 Compressive Strength

There is no doubt that porosity, defined as the total volume of the overall volume of pores larger than gel pores, expressed as a percentage of the overall volume of the hydrated cement paste, is a primary factor influencing the strength of the cement paste. The voids themselves need not act as flaws but the flaws may be cracks in the individual crystals associated with the voids [112, 113]. A linear relation between the strength and the porosity, within the range of the latter between 5 and 28 percent, was established by Odler & Rossler [118]. The effect of pores smaller than 20 nm in diameter was found to be negligible. Hence the filler effect of admixtures play a big role in enhancing the compressive strength of the concrete mixes.

This initial activity of the admixtures lay a founding stone of their future course of work and it is expected, that with some continuous reduction in their working efficiency with time, they would maintain the difference in the properties of concrete. The working of admixtures in bringing pore size and grain size refinement has already been discussed in the paragraph stated under normal consistency on page 124.

(a) Compressive strength variation in mixes

Tables 4.18 & 4.19 show the compressive strength data of mortar and concrete mixes respectively. Figs. 4.114, 4.115, 4.116 & 4.117 entails the compressive strength of normal,

binary, ternary & combined mortar mixes, respectively. Similarly, compressive strengths of respective concrete mixes have been entailed in Figs. 4.118, 4.119, 4.120 & 4.121, respectively.

Table 4.18 Compressive strength of mortar mixes after different durations

Mix	Comp. Str. (MPa)			Mix	Comp. Str. (MPa) in			Mix	Comp. Str. (MPa) in		
Days	7	28	60	Days	7	28	60	Days	7	28	60
C	22.0	32.0	37.5	CF1	21.8	27.0	33.5	CW1	22.4	31.3	36.2
Cwf	18.5	26.0	31.0	CF2	23.1	26.4	35.4	CW2	25.3	34.2	37.6
CwfS1	21.8	27.4	36.0	CF3	24.0	25.4	37.0	CW3	24.4	33.5	36.9
CwfS2	25.1	29.2	38.5	CFS1	23.1	27.7	34.3	CWS1	23.1	32.5	36.9
CWf	24.0	32.0	39.4	CFS2	24.1	29.0	35.6	CWS2	24.5	34.0	37.9
CwF	18.5	30.2	39.0	CFS3	25.5	30.3	36.7	CWS3	25.6	35.3	39.0
CwFS1	17.5	31.0	39.2	CFS4	26.7	31.2	38.0	CWS4	27.0	36.6	40.8
CWfS1	18.0	33.5	40.0	CFS5	23.9	26.9	36.1	CWS5	25.9	34.8	38.5
CwFS2	21.8	33.2	40.2	CFS6	25.5	27.7	37.5	CWS6	27.5	35.8	39.8
CWfS2	23.0	35.3	40.6	CFS7	26.5	29.0	39.0	CWS7	28.6	37.0	41.0
CWF	21.8	31.2	40.5	CFS8	28.0	30.4	39.8	CWS8	29.8	38.8	42.3
CWFS1	23.0	32.7	41.0	CFS9	24.7	26.3	37.7	CWS9	24.7	34.2	37.6
CWFS2	23.5	34.0	41.0	CFS10	25.9	27.2	39.0	CWS10	25.9	35.4	38.4
CWFS3	24.0	35.2	41.7	CFS11	27.4	28.5	40.2	CWS11	27.2	36.7	39.3
CWFS4	23.8	34.8	41.1	CFS12	28.6	29.7	41.1	CWS12	28.8	37.9	40.0

Table 4.19 Compressive strength of concrete mixes after different durations

Sr .No.	Mix	7 Days	28 Days	60 Days	90 Days
1	C	37.40	54.06	60.01	63.66
2	CF1	33.19	42.29	46.74	48.74
3	CF2	30.69	38.58	43.89	51.38
4	CF3	26.80	33.59	39.41	52.21
5	CW1	31.51	40.49	45.05	48.25
6	CW2	36.84	45.95	51.08	54.50
7	CW3	36.63	46.80	50.89	49.76
8	CFS1	37.32	46.37	51.27	51.30
9	CFS2	38.71	48.45	53.78	56.70
10	CFS3	41.47	51.45	56.47	60.20
11	CFS4	41.60	52.41	59.84	62.00
12	CFS5	32.06	40.83	45.67	50.01
13	CFS6	34.34	42.93	48.99	58.07
14	CFS7	35.76	45.09	54.92	64.94
15	CFS8	38.08	48.02	58.49	68.50
16	CFS9	28.73	36.20	41.33	49.10
17	CFS10	30.33	38.93	46.13	57.28
18	CFS11	32.30	40.54	48.26	67.75
19	CFS12	32.98	41.59	51.85	68.90
20	CWS1	34.29	42.92	48.51	55.35
21	CWS2	35.10	44.75	49.47	51.68
22	CWS3	37.71	47.30	52.62	56.37
23	CWS4	37.59	47.60	53.80	61.38
24	CWS5	37.28	47.33	53.66	61.99
25	CWS6	39.34	49.45	56.25	65.86
26	CWS7	39.96	53.00	58.22	66.10
27	CWS8	42.22	53.60	60.77	70.20
28	CWS9	38.10	47.69	53.90	61.50
29	CWS10	38.87	49.10	57.83	68.89
30	CWS11	39.85	51.30	61.99	76.59
31	CWS12	41.30	51.70	64.39	80.34
32	Cwf	29.17	44.06	49.41	54.59
33	CwfS1	30.25	45.85	50.89	53.99
34	CwfS2	36.61	46.65	52.44	58.52
35	CWf	32.86	47.50	53.44	59.89
36	CwF	25.20	42.71	47.87	52.79
37	CwFS1	28.96	44.40	49.58	53.91
38	CWfS1	29.49	49.20	54.70	58.45
39	CwFS2	28.89	45.80	51.23	56.09
40	CWfS2	33.35	51.29	57.38	62.82
41	CWF	30.14	47.10	52.79	58.22
42	CWFS1	28.67	48.60	54.27	59.01
43	CWFS2	30.43	50.20	56.06	60.95
44	CWFS3	33.84	51.70	59.07	70.39
45	CWFS4	30.55	53.60	59.71	64.29

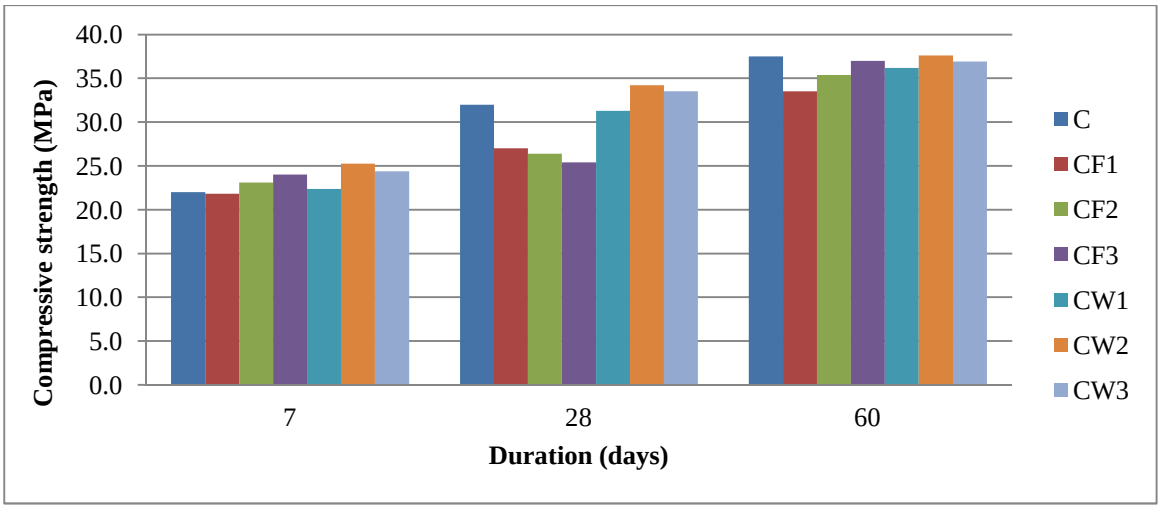

Fig 4.114 Compressive strength of normal and binary mortar mixes

In overall, it has been observed that with the use of admixtures, the strength of mortar falls on account of dilution (reduction in cement content) but there are some admixed mortars, which yield greater strength than normal mix, on account of improvements in the matrix.

Fig 4.114 clearly depicts incorporation of flyash & wollastonite @ 10% by wt. of cement into the cement matrix lowers the compressive strength of mortar at early age in comparison to normal cement mortar. The lower compressive strength is mainly due to reduction in cement content of mortar matrix system. But if we compare the strength development patterns within the admixed samples, we may find that there is an increment in compressive strength with increase of flyash replacement level particularly at the age of 7-day. This is attributed by the presence of appreciable quantity of micro fine particles of flyash which allows reorientation of the cement and flyash particles physically and simultaneously it also accelerates the rate of hydration of the matrix system. The strength enhancement at the early age of mortar may be due to higher rate of hydration contributed by flyash as manifested from the XRD and SEM studies. Whereas, at the age of 28-day, compressive strength starts declining with flyash content and these strength are almost comparable with the 7 days strength. This phenomenon is mainly due to greater dilution of cement and lower rate of hydration of matrix system directly influenced by the fly ash particles. However, the trend of increment of compressive strength conspicuously depicted that at 60 days, there is a significant increment in strength with the increment of flyash

content. The increase in compressive strength at the later age is mainly due to the formations of profuse amount of C-S-H gels generated from the chemical reaction between CH liberated during the hydration of cement and silica. Form the above analysis, it is learnt that prolonged curing has more impact on strength development for flyash admixed mortar.

For WMF admixed mortar, the mixes offered an increment in compressive strength at all ages, up to 20% WMF content, beyond which the strength development retards irrespective of days of curing. The increase in compressive strength due to admixing of WMF is on account of its excellent water expelling capacity from the voids of the cement particles by virtue of its micro fine size which is also termed as filler effect. Soliman and Nehdi [160] also, suggest the same reason for the WMF's effect. Apart from this effect, WMF imparts excellent reinforcing effect and pore refinement. Incorporation of WMF beyond 20% does not provide additional advantage on strength development, because at this replacement level there is enough dilution of cement, and overlapping of WMF exhibit within the mortar matrix, hence no significant strength enhancement can be achieved.

The compressive strength of normal mortar at 60 days is found to be approximately equal to mixes containing 30% flyash, and 20% WMF, whereas at 28 days, the mixes containing more than 20% WMF offered higher compressive strength than normal mortar mixes.

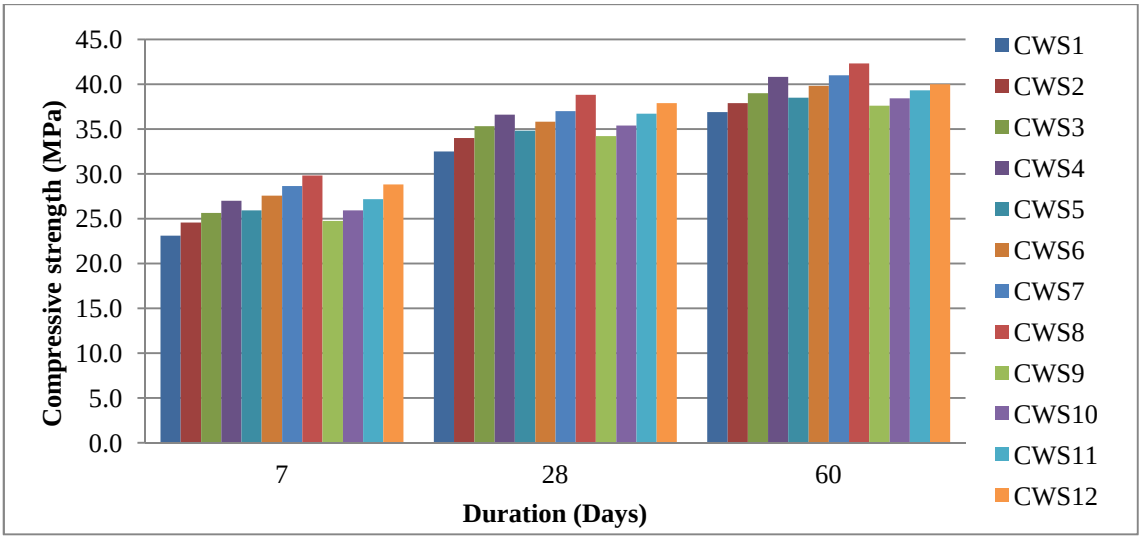

Fig 4.115 Compressive strength of WMF admixed ternary mortar mixes

The trend of compressive strength development for ternary mixes is very similar to that of binary mixes irrespective days of curing as depicted in Fig. 4.115. Inclusion of microsilica along with wollastonite microfiber imparts better strength development in comparison to mortar mixes containing only cement & WMF. Laboratory results demonstrated that microsilica has better potential to elevate compressive strength of mortar in comparison to other two admixtures as can be seen from Fig.4.115.

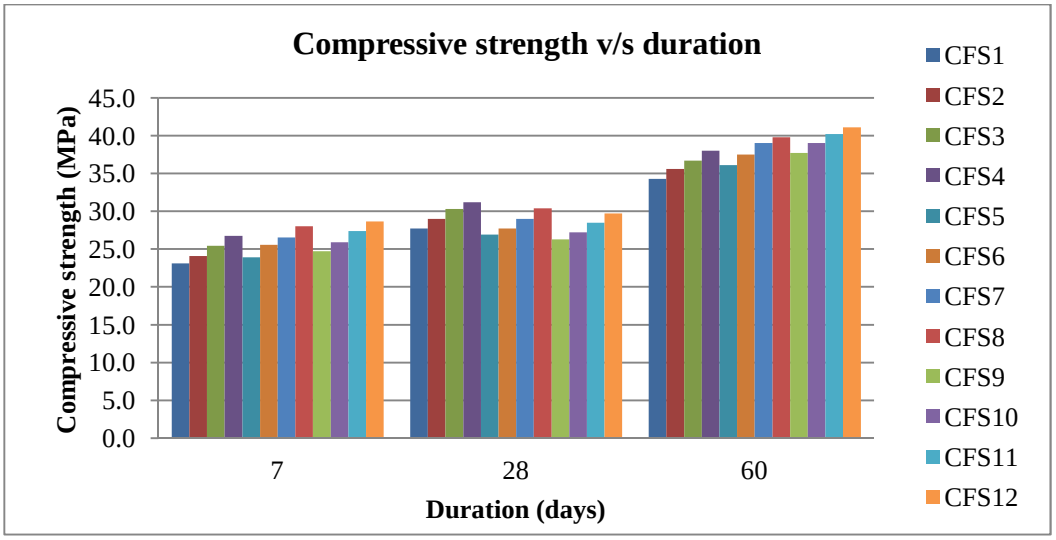

Fig 4.116 Compressive strength of flyash admixed ternary mortar mixes

Microsilica perform in improving the compressive strength of the mortar mixes, in a similar way as it did for WMF admixed mortars. The individual effect of flyash (as shown in Fig. 4.116) with time is the same as it was in the case of binary mixes.

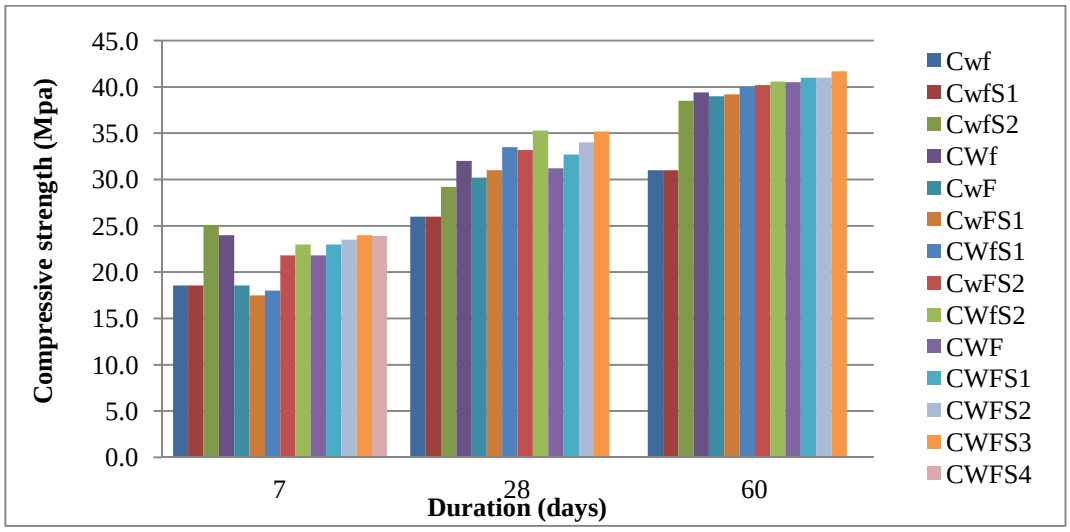

Fig 4.117 Compressive strength of combined mortar mixes

The trend of development of compressive strength of combined mortar matrix is very much similar to those binary and ternary mixes except for a few mixes particularly CwFS1 & CWfS1. One of the reasons for having such anomalies results may be due to improper mixing of powdery materials at the time sample preparation. In overall, results have demonstrated that WMF has better efficacy to improve compressive strength than flyash irrespective days of curing as can be read from Fig.4.117. If we look at the performance of compressive strength development after inclusion of WMF, fly ash and microsilica, highest compressive strength is being offered by CwFS2 at 7 days moist curing, CWFS3 & CWfS2 at 28 days moist curing and CWFS3 at 60 days moist curing. The main reasons for offering appreciable compressive strength of mortar is due to the formation of substantial amount of C-S-H gels for the aforementioned mixes as manifested from the XRD and SEM studies. For mixes having total WMF and flyash content lesser than 20%, microsilica was found to be effective to boost the compressive strength at its contents of 5%. Microsilica content less than 5.0% does not contribute appreciable improvement on strength.

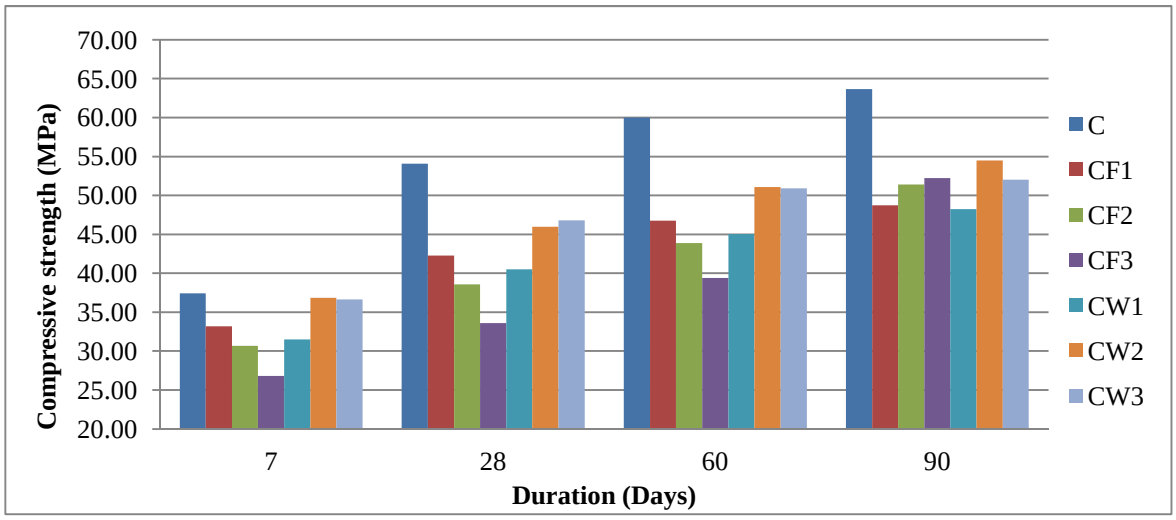

Fig. 4.118 Compressive strength of normal and binary concrete mixes

For concrete mixes, inclusion of fly ash leads to a reduction in compressive strength whereas WMF improves the compressive strength up to its 20% content, alike mortar. Unlike mortars, incorporation of flyash continued to decrease the compressive strength upto 60 days. But the concrete cured beyond 60 days showed considerable improvement in compressive strength as can be seen from Fig.4.118. The trend of improvement of

compressive strength clearly depicted that prolonged curing is more beneficial for admixed concrete as far as strength improvement is concerned.

For WMF admixed concretes, compressive strength increases with the increase of WMF percentage inclusion levels. Irrespective of days of moist curing, concrete mix containing 20% WMF produced better compressive strength than rest of the combinations. If we look at the strength development pattern obtained at 60 days moist curing, concrete mixes containing 20% WMF and 30% WMF produced same compressive strength but at 90 days moist curing, lower compressive strength was offered by the mix containing 30% WMF. Such phenomenon observed mainly due to slower rate of hydration of cementitious system on account of significant amount of cement content reduction and on other hand presence of WMF particles at the interface of aggregate more than the necessity as a result of which additional advantage could not be drawn for being adding extra amount of WMF into the concrete system. Considerable improvement in compressive strength of WMF admixed concrete upto 20% is primarily due to its excellent voids infilling capacity by virtue of its microfine size and secondarily, being siliceous material, its imparts better pozzolanic action particularly when silica from WMF comes in contact with CH liberated during the hydration of cement particles as a result of which additional C-S-H compounds produces. As in the case of flyash admixed concrete, prolonged curing plays a significant role in the compressive development for WMF admixed concrete too.

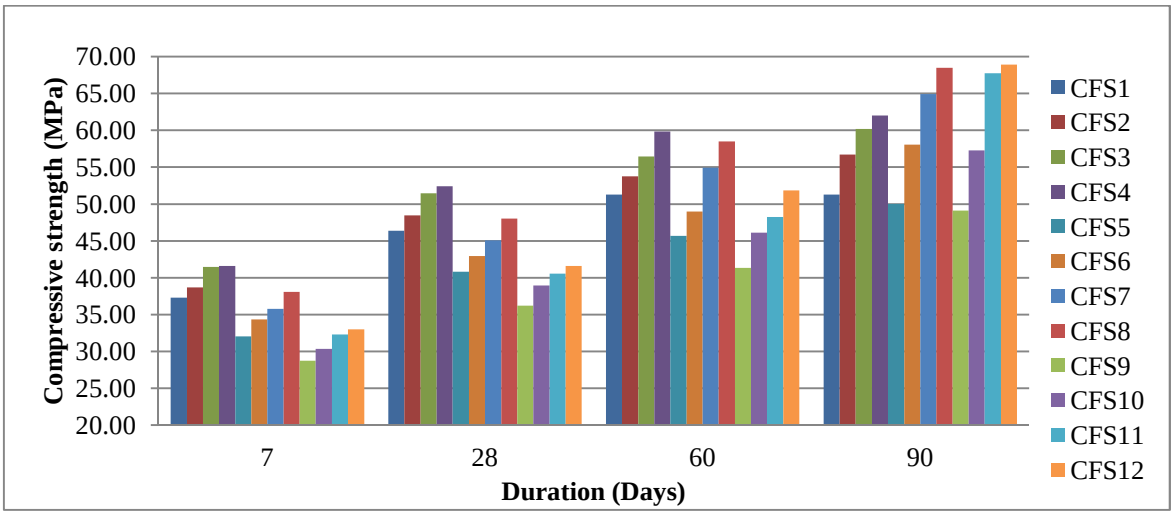

Fig 4.119 Compressive strength of flyash admixed ternary concrete mixes

As the duration of curing period increases, there is an increment in compressive strength values of mixes with an increment in microsilica content. The rate of increase is quite significant for those mixes, which have flyash content equal to or greater than 20% and microsilica content equal to or greater than 7.5%. This is because of the extra nucleation spaces provided by flyash to microsilica with enough water, which otherwise would left very less within the hydrated pore solutions adjoining the cement particles.

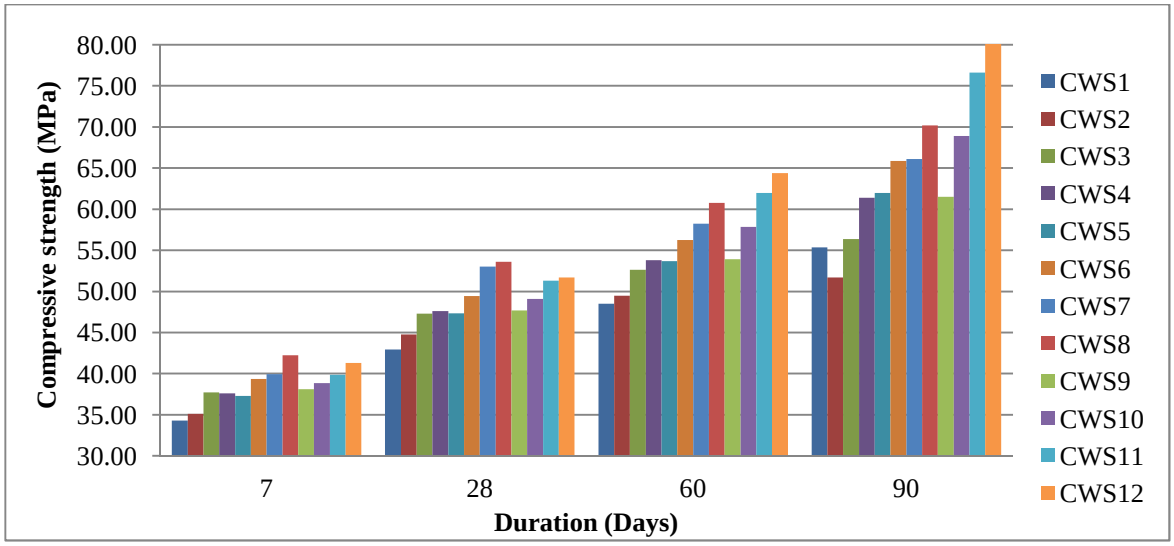

Fig. 4.120 Compressive strength of WMF admixed ternary concrete mixes

The trend of increase of compressive strength for WMF admixed ternary concrete mixes quite resembles to that of binary concrete mixes. However, in the case of WMF admixed ternary concrete mixes, CWS12 offered the maximum compressive strength followed by CWS11, CWS8, CWS10, CWS7, CWS6, CWS9,CWS5,CWS4,CWS3,CWS1 and CWS2 respectively at 90 days moist curing. Very similar trend of increase of compressive strength is observed at 60 days moist curing. Whereas, at 7 & 28 days moist curing, compressive strength development pattern is slightly abrupt. Highest compressive strength is being offered by CWS8 at the age of 7 & 28 days but in the long run, this particular mix designation fail to prove to be highest ones. Such a phenomenon strongly inferred that for concrete mix containing WMF and WMF & microsilica together, compressive strength obtained either at 60 or 90 days moist curing should be considered for the design of pavement to draw the maximum possible advantage as their efficacy is being strongly influenced by the prolonged curing.

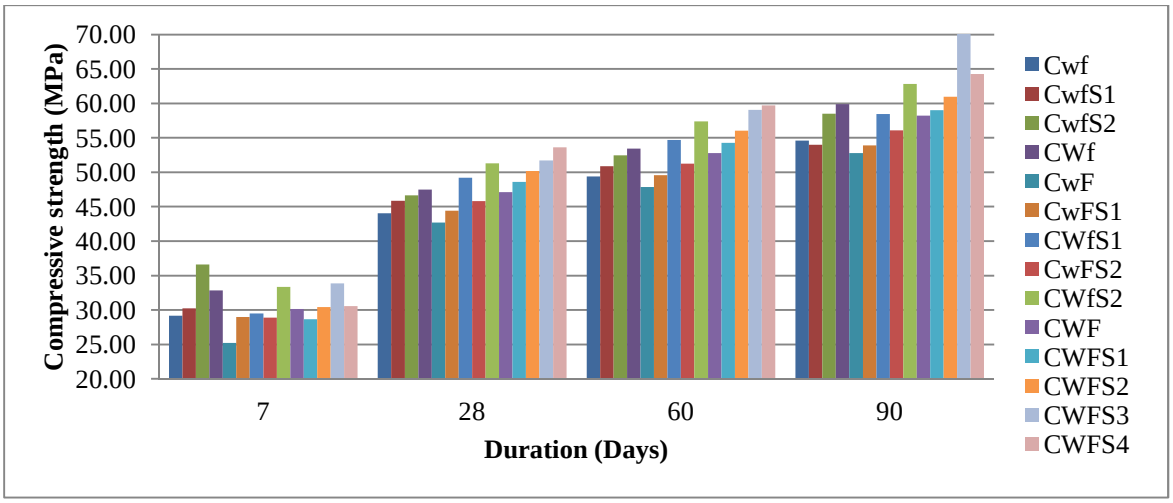

Fig. 4.121 Compressive strength of combined concrete mixes

Fig.4.121 clearly illustrates the trend of compressive strength development of the total fourteen concrete mixes considered in the present study. By and large after having examined in details about the effect of admixtures inclusion on compressive strength development, it is learnt that inclusion of microsilica upto 5% is highly beneficial for mixes containing combined WMF-flyash together of 15% and for mixes containing WMF-flyash together of 20%, higher dosage of microsilica upto 7.5% is essential to boost the compressive strength of concrete.

(b) Influence of admixtures on concrete strength

According to the chemical requirements suggested in ASTMC 618, WMF used in the present study is conforming to Class F Pozzolana. Potential to produce additional C-S-H compounds on admixing of WMF has already been reported from the SEM images obtained at an age of 7 days and 14 days XRD analysis in the present study. A more formal definition of ASTM C 618 -94a describes pozzolana as a siliceous or siliceous and aluminous material which in itself possesses little or no cementitious value but will, in finely divided form and in the presence of moisture, chemically react with calcium hydroxide at ordinary temperatures to form compounds possessing cementitious properties. It is essential that pozzolana be in a finely divided state as it is only then that silica can combine with calcium hydroxide in the presence of water to form stable calcium silicates which have cementitious properties. The results of 7 & 14 days were acquired deliberately to facilitate continuous analysis of their behaviour from the initial stage of hydration. Admixing of WMF reduced

lime content to a higher extent than fly ash as a result of which better pore and grain size refinement is expected and at the same time there is high possibility to improving the interfacial transition zone (ITZ). Also, WMF being fibrous in nature, it impart better reinforcing effect in mortar portion as well as at ITZ as a result of which double benefits could be drawn by admixing WMF into normal concrete mix. Because of these factors, WMF admixed concrete produced less shrinkage effect which mitigates no. of flaws and therefore mortar got toughened and got strongly bound with aggregate that overall resulted in the compressive improvement.

Flyash, overall, is a low reactive pozzolana. The strength improvement due to flyash is due to its pozzolanicity and filler effect. The flyash particles fits into the voids of cement particles, and later on after hydration, nucleate hydrated products over its surface, thereby reducing the capillary voids or porosity, which imparts strength [30]. It is only during the first two-three days, that its reactivity is a bit higher because of small quantity of reactive silica present in it (confirmed from chemical analysis done through X Ray fluorescence), but owing to its bigger size this reactive silica is not able to hydrate lime into C-S-H at the same rate as WMF. It does not have any fiber effect because of its spherical smooth particle shape. The increment in hydration because of flyash is on the account of water released due to its dispersion effect, the presence of poorly reactive aluminates which slowly convert the ettringite into hydrated aluminates, and the bigger sized particles which adsorb less water and provide nucleating surfaces for other admixtures like microsilica to hydrate owing to its smooth surface. Even though flyash is a low reactive material, but it does maintained continuous reactivity and hence more densifying took placed in presence of extra fine pozzolanic which finally resulted in improvement of mortar paste to a greater extent.

In the above paragraphs , an attempt has been made to explain the behaviour of concrete mixes when flyash and WMF were incorporated independently. This paragraph aims at explaining their behaviour change with time. Inclusion of WMF & flyash together seems to be ineffective in comparison to the performance of concrete that containing both WMF & microsilica together irrespective of their contents. This ineffectiveness in chemical reaction may be due to presence of substantial amount of larger particle of flyash as a result of which initial chemical reaction has been retarded. As a consequence of this, till 28 days ternary

mixes containing both WMF and flyash showed nearly equal rate of increment in compressive strength per unit fraction of microsilica added.

After 28 days, the reactivity of microsilica drops down due to depleting moisture content. Both WMF and flyash, are able to hold moisture effectively at 30% & 20% and higher levels, respectively. Microsilica which was earlier adsorbed onto cement particles, and being reactive goes inside this pore solution which lies in the vicinity of these admixtures, due to the potential gradient developed on account of concentration difference. It starts hydrating on the nucleating surfaces provided by these admixtures. The hydration rate of microsilica is higher in this case due to lesser competition for moisture with respect to the situation when microsilica was competing with cement particles for moisture. The hydration done on these admixtures at their respective contents, caused an additional improvement. WMF gave exceptional high improvement at 30% due to its fiber action on the hydrated paste bound to it.

4.5.3 Splitting Tensile Strength

Splitting tensile strength and flexural strength are dependent both on aggregate-paste and paste-paste interaction. Splitting tensile strength development depends more on the aggregate-paste bond strength developed in the initial stages of hydration of a normal concrete, whereas flexural strength depends more upon paste-paste interaction, which goes on developing at all ages as the hydration process goes on infinitely.

Strength in tension depends upon the load distribution which depends upon the type of composite and the specimen shape. Griffith [48] explained the discrepancy on account of flaws. The flaws lead to high stress concentration in the certain areas of material sample and the failure of that area under loading initiates the deterioration cycle and other areas fail rapidly. A.M. Neville [112] suggested, that flaws are more in concrete containing more voids, but the voids themselves do not act as flaws and the latter are just the cracks associated at the interface of voids and concrete. Alford et al. [6] proved, that voids at this interface are not only responsible for loss in tensile strength and, also the voids are distributed randomly in concrete [113]. Hence only voids are not responsible, but the ITZ too. The ITZ is weak due to the loose packing and bonding of cement paste with aggregate

mass on account of heterogeneity. This is called as wall effect. There is thus less cement paste to hydrate and fill the original voids. Consequently the ITZ has higher porosity than hydrated cement paste further away from the coarse aggregates [152]. It is on the account of crack propagation during flexural strength testing, where the maximum stress arises at the extreme bottom fiber and propagates towards the neutral axis, beyond which the compressive bending stresses do not allow the aggregate paste interface to fail and provide internal frictional resistance. Hence flexural strength depends more upon the strength of paste rather than aggregate-paste interface. Neville am. In case of splitting tensile strength test, the bending stresses along the whole section below the platens, is subjected equally to tensile bending stresses, the failure of which depends more upon the aggregate paste interface [53].

L.A. Larbi [79] suggested that the aggregate paste interface consist of duplex layer; the inner one of thickness 0.5 micron consisting of oriented elongated crystalline lime, and the outer one consisting of C-S-H of same thickness. Apart from this duplex film there is a thick interface layer (50 micron thick) which consists of products of hydration (C-S-H, ettringite and completely hydrated aluminates). For the interfacial transition zone to improve, porosity of both the duplex film and outer thick layer need to be low. This means that firstly the lime in duplex film needs to be controlled and, secondly the thick interface should contain lesser amount of ettringite. Both these factors are thus important for a high splitting tensile strength. For paste-paste interface to be strong hydrated products should not leave capillary pores of sizes greater than 20 micron, which would only be possible if the grain size refinement between cement particles have taken place. Following paragraphs provides the general results and the explanation for the performance of certain type of SCC on basis of this theory:

(i) Addition of flyash and WMF

The initial development of interface zone is the advantage factor associated with flyash. In case of flyash addition, the ettringite and lime content in the initially developed interface zone decreases with an increment in flyash content. Flyash at the interface during the time of mixing of concrete and up to three days is reactive enough to cause both grain

size and pore size refinement; though in the paste-paste interface the grain size refinement was not conspicuous due to comparable sizes of flyash and cement.

In case of WMF admixed SCC, the rate of hydration is fast in initial days, and more C-S-H is produced, but along with it more ettringite and lime are produced. WMF has shown reactivity with lime (verified from XRD test) and thus reduces lime content by forming low lime C-S-H gel. This may be due to the presence of highly reactive silica in WMF, even though it is lesser in quantity than microsilica. It also leads to grain size refinement by nucleating lime and C-S-H on its well distributed particles across the whole mix. Though the fiber-paste bond does not play much role in increasing splitting tensile strength; yet it is confirmed, that the bond between fiber and paste does not develop much strength uptil 28 days. The extra amount of ettringite produced with respect to flyash admixed SCC, causes a reduction in splitting tensile strength in WMF admixed SCC. Splitting tensile strength increases with an increment in both flyash's and WMF's content, but for flyash it is comparatively higher.

The discussion above made, was in reference to the behaviour of flyash and WMF admixed SCC up to 28 days. For binary mixes, this difference in their strength remained same for all ages. But in case of microsilica combined ternary SCC mixes, after 28 days, both the mixes showed nearly same values of splitting tensile strength inspite of the fact that WMF is more reactive than flyash. This is attributed to the interference provided by microsilica, which has been discussed already while explaining the behaviour of compressive strength with time. Both were found ineffective, but their effectiveness is more pronounced for prolonged curing and their higher contents

(ii) Microsilica addition

In case of microsilica reinforced SCC, the highest initial hydration rate and pore size plus grain size refinement done by microsilica is very effective in increasing the splitting tensile strength of concrete. Though microsilica does not reduce ettringite but higher C-S-H formation in the thin 0.5 micron interface next to aggregate provides more binding strength and thus develops the interfacial transition zone to a greater extent, irrespective of WMF and flyash content. Microsilica not only improves the early strength and lowers penetrability, but

also improves the ITZ, by forming a thin sticky layer of hydrated products on the surface of aggregates, by converting the lime present in that zone. Hence, it breaks the wall effect of aggregates, which prevents bigger cement particles to pack tightly against the aggregate particles. Microsilica content in the range of 10% has generally been found to cover the aggregate fully and excess of it, does not contribute to improvement in ITZ [152]. In presence of WMF, therefore lesser microsilica may do this purpose

In the present study, effort was also made to correlate and compare the behaviour of mortar and hardened properties of concrete with or without admixtures. But study on mortar was limited to only 28 days whereas for concrete mixes, studies have been conducted considering 7, 28, 60 and 90 days.

This has been done for flexural strength test and modulus of elasticity test also. Tables 4.20 and 4.21 provided below show the data pertaining to splitting tensile strength of mortar and concrete mixes respectively. Figs. 4.122-4.127 show the splitting tensile strength comparison in the form of bar charts for better comparison.

Table 4.20 Splitting tensile strength of various mortar mixes after 28 days

Mix	Splitting Tensile. St. (N/mm^2)	Mix	Splitting Tensile. St. (N/mm^2)	Mix	Splitting Tensile. St. (N/mm^2)
C	4.88	CF1	4.88	CW1	4.88
Cwf	4.95	CF2	4.95	CW2	5.10
CwfS1	5.10	CF3	4.95	CW3	5.24
CwfS2	5.31	CFS1	4.88	CWS1	5.10
CWf	5.31	CFS2	5.10	CWS2	5.31
CwF	5.10	CFS3	5.31	CWS3	5.38
CwFS1	5.24	CFS4	5.31	CWS4	5.52
CWfS1	5.38	CFS5	5.10	CWS5	5.24
CwFS2	5.38	CFS6	5.24	CWS6	5.38
CWfS2	5.66	CFS7	5.38	CWS7	5.52
CWF	5.52	CFS8	5.52	CWS8	5.52
CWFS1	5.66	CFS9	5.24	CWS9	5.52
CWFS2	5.73	CFS10	5.38	CWS10	5.73
CWFS3	5.80	CFS11	5.52	CWS11	5.80
CWFS4	5.52	CFS12	5.52	CWS12	5.73

Table 4.21 Splitting tensile strength of concrete mixes after different durations

Sr .No.	Mix	7 Days	28 Days	60 Days	90 Days
1	C	1.97	5.52	5.95	6.22
2	CF1	1.84	4.53	4.74	4.81
3	CF2	1.97	4.78	5.13	5.33
4	CF3	2.10	5.10	5.58	5.93
5	CW1	1.78	4.42	4.64	4.72
6	CW2	1.88	4.53	4.81	4.96
7	CW3	1.88	4.64	4.82	4.85
8	CFS1	1.97	4.73	5.00	5.12
9	CFS2	2.05	4.95	5.28	5.46
10	CFS3	2.14	5.14	5.44	5.59
11	CFS4	2.14	5.21	5.78	6.23
12	CFS5	1.98	4.87	5.15	5.28
13	CFS6	2.10	5.08	5.53	5.83
14	CFS7	2.15	5.24	6.17	7.05
15	CFS8	2.14	5.21	6.17	7.10
16	CFS9	2.13	5.18	5.54	5.75
17	CFS10	2.14	5.31	5.97	6.51
18	CFS11	2.26	5.48	6.22	6.85
19	CFS12	2.23	5.44	6.52	7.59
20	CWS1	1.91	4.61	4.96	5.18
21	CWS2	1.95	4.81	5.07	5.18
22	CWS3	2.08	5.05	5.39	5.58
23	CWS4	2.21	5.42	5.89	6.21
24	CWS5	1.89	4.63	5.05	5.34
25	CWS6	1.98	4.81	5.29	5.64
26	CWS7	1.96	5.04	5.36	5.53
27	CWS8	2.14	5.25	5.80	6.21
28	CWS9	1.94	4.70	5.11	5.39
29	CWS10	2.03	4.95	5.66	6.28
30	CWS11	2.07	5.15	6.09	6.99
31	CWS12	2.09	5.05	6.19	7.36
32	Cwf	1.54	4.50	4.81	4.99
33	CwfS1	1.59	4.67	4.95	5.09
34	CwfS2	1.99	4.91	5.29	5.53
35	CWf	1.64	4.57	4.94	5.18
36	CwF	1.41	4.63	4.93	5.09
37	CwFS1	1.60	4.74	5.05	5.21
38	CWfS1	1.45	4.69	5.01	5.20
39	CwFS2	1.60	4.90	5.24	5.44
40	CWfS2	1.66	4.93	5.33	5.59
41	CWF	1.57	4.74	5.10	5.32
42	CWFS1	1.48	4.85	5.21	5.43
43	CWFS2	1.57	5.01	5.40	5.64
44	CWFS3	1.73	5.12	5.69	6.12
45	CWFS4	1.49	5.07	5.48	5.75

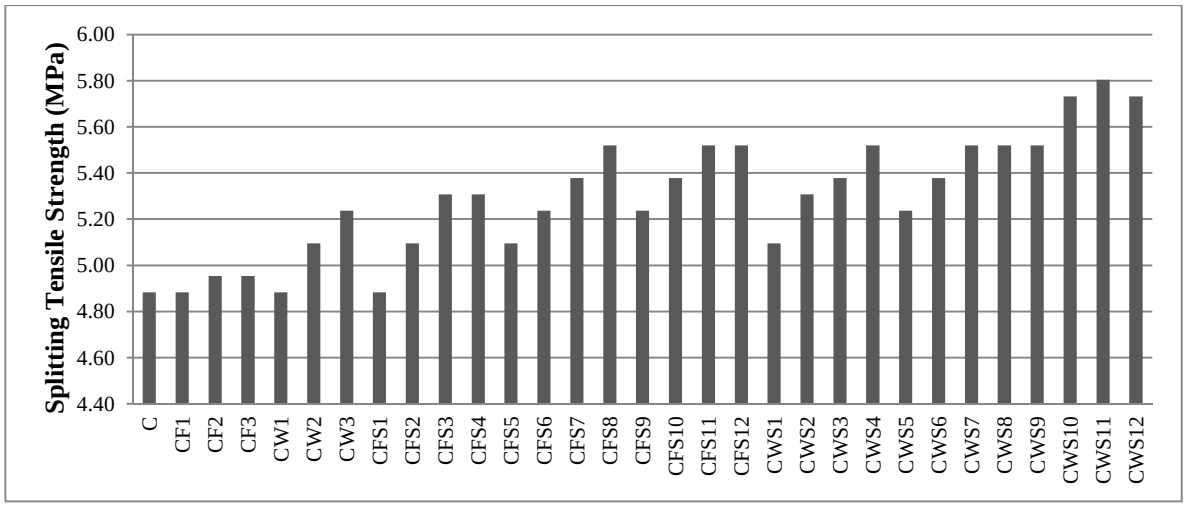

Fig. 4.122 Splitting tensile strength of normal, binary and ternary mortar mixes

Splitting tensile strength is influenced more by the strength of interfacial zone and to some extent by the strength of paste. In case of mortar it is only the strength of paste which is the main controlling factor and WMF apart from causing grain and pore size refinement; it reinforces the paste matrix too. Therefore with WMF, more increment in the splitting strength takes place. Splitting strength decreased with flyash content exceeding 20% and with microsilica content greater than 7.5% because, both of these materials at their higher content make the mortar more brittle, though they increase the compressive strength. A brittle structure fails very early in tension, which is why splitting tensile strength decreases. Flyash content higher than 20% also increases the porosity of the mix further, due to its bigger size.

WMF does not make the structure brittle, even though the modulus of elasticity of WMF is high. As its being acicular in structure and fibrous in nature, it reinforced betters the cement paste consequently strengthened the ITZ and hence sustains better tensile stresses. When the tensile stress in the critical failure plane reaches the strength of concrete in tension, it does not fail because of the bond with fiber. The fiber takes the further load until it fails and then the stress is transferred to adjoining location. The other location also takes also takes time to fail. In this way the behaviour of paste and mortar becomes more of a ductile one than brittle.

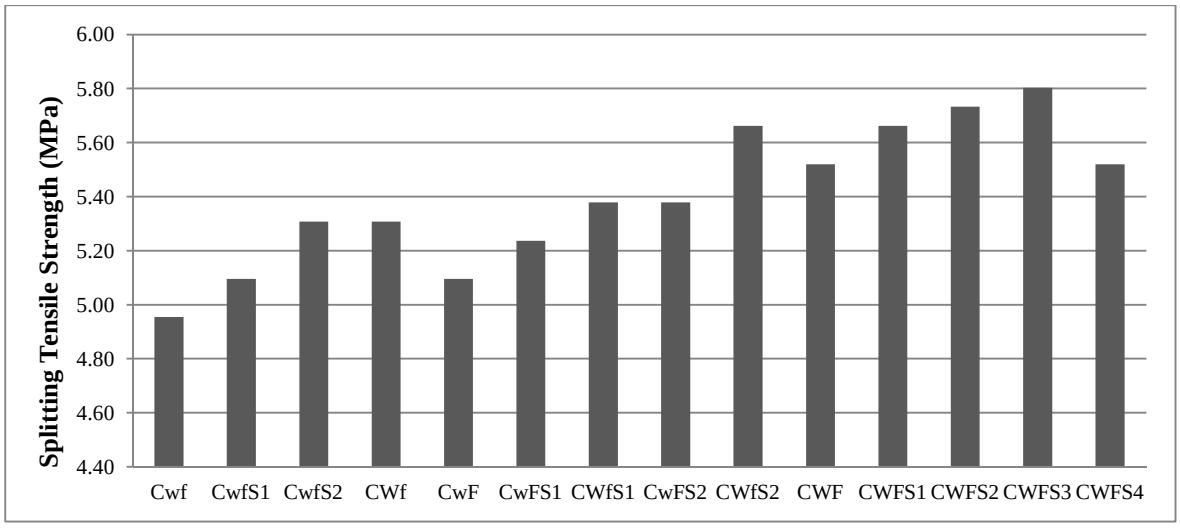

Fig 4.123 Splitting tensile strength of combined mortar mixes

This behaviour is quite simple, as it could be seen, that with the increment in WMF and flyash, the splitting tensile strength increases with respect to normal mortar. Even microsilica also shows the same behaviour. But the higher contents of microsilica have shown loss in splitting tensile strength in the mix CWFS4. In all the combined mixes the flyash content is not greater than 10%. Hence, no decrement in splitting tensile strength with an increment in flyash content has been observed.

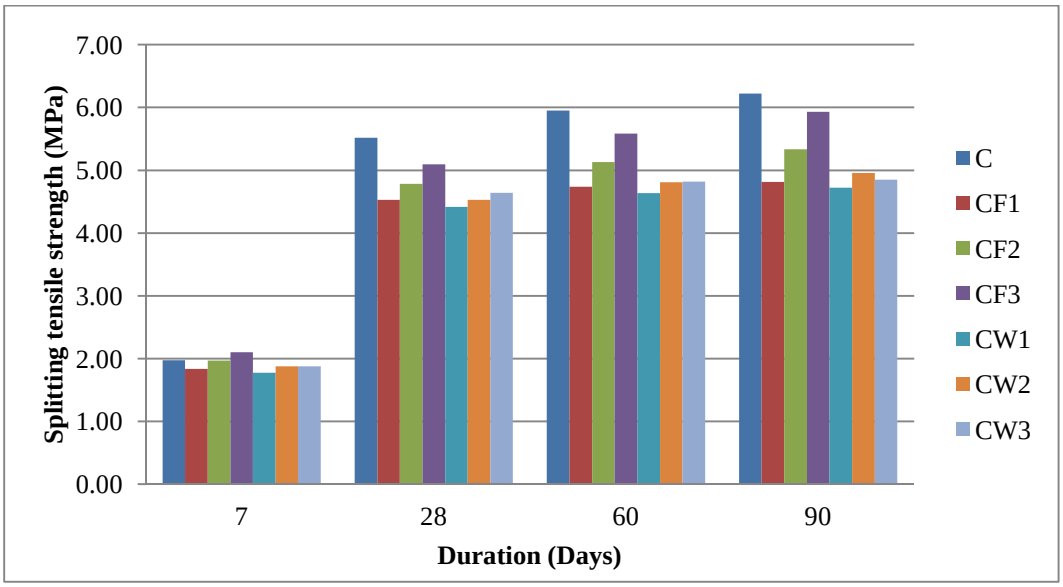

Fig. 4.124 Splitting tensile strength of normal and binary concrete mixes

For concrete mixes, both flyash and WMF have shown improvement in flexural strength with an increment in their content, in the mix. The increment is relative to their contents, and not with respect to the normal concrete with respect to which there is a reduction in this strength. It's because of the dilution effect of these admixtures.

There is more improvement with an increment in flyash content in comparison to WMF because, unlike mortar where there is no ITZ, here flyash is improving the ITZ more than WMF. The deficiency in improvement of ITZ is a bit compensated by the reinforcing effect of WMF. Porosity caused by higher contents of flyash highly affects the compressive strength, but as far as splitting tensile strength is concerned; its effect is not that significant because, the load distribution mechanism is not similar. Hence, the improvement in bond strength at ITZ makes it possible for even higher contents of flyash, to increase the splitting tensile strength.

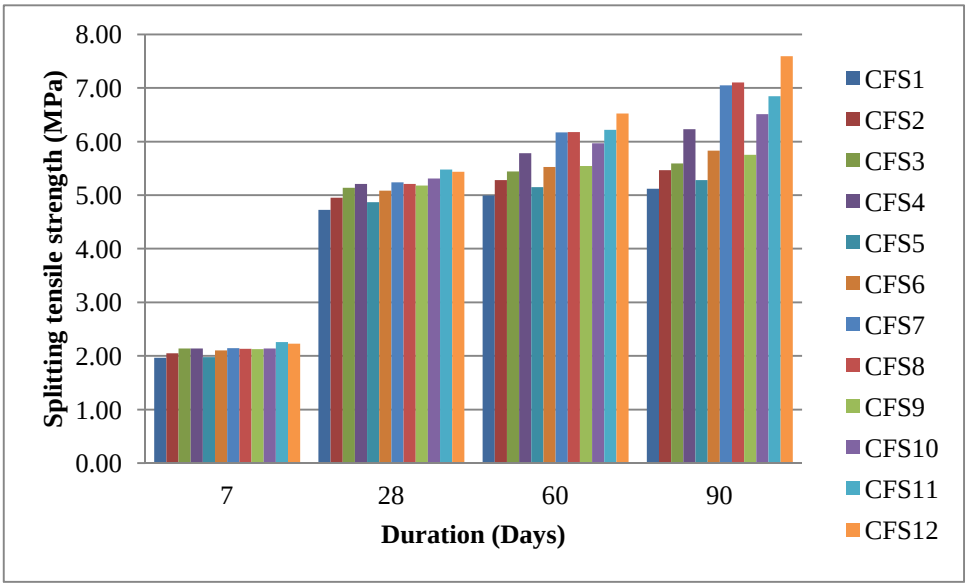

Fig 4.125 Splitting tensile strength of flyash admixed ternary concrete mixes

In the case of flyash admixed concretes, the brittleness caused by combined flyash and microsilica does not affect the splitting tensile strength significantly, as it did in mortars. Because, the stiffness of mortar portion of concrete holds no value against those of aggregates. If the ITZ is stronger than the tensile stresses would be taken by the aggregates first, as aggregates have generally higher tensile strength than concrete. Hence, stiffness of paste has nothing to do with the tensile strength if the ITZ is stronger, the present case falls

in the same line. Therefore there is difference behaviour for concrete from mortar. At 7 and 28 days, the microsilica in the mixes is equally effective, irrespective of flyash content. Hence, for all mixes, it could be seen , that the splitting tensile strength is equal, but these splitting tensile strength are higher than that of normal concrete. Further addition of microsilica improves the tensile strength to a greater extent, when the duration of hydration is high (> 60 days). This is because at this duration, the hydration of cement has reduced negligibly, but the high surface area bearing microsilica further reacts if sufficient pore water is available. This pore water is highly available with higher Content of flyash as it has better potential to retain water. The phenomenon observed is depicted in Fig. 4.125.

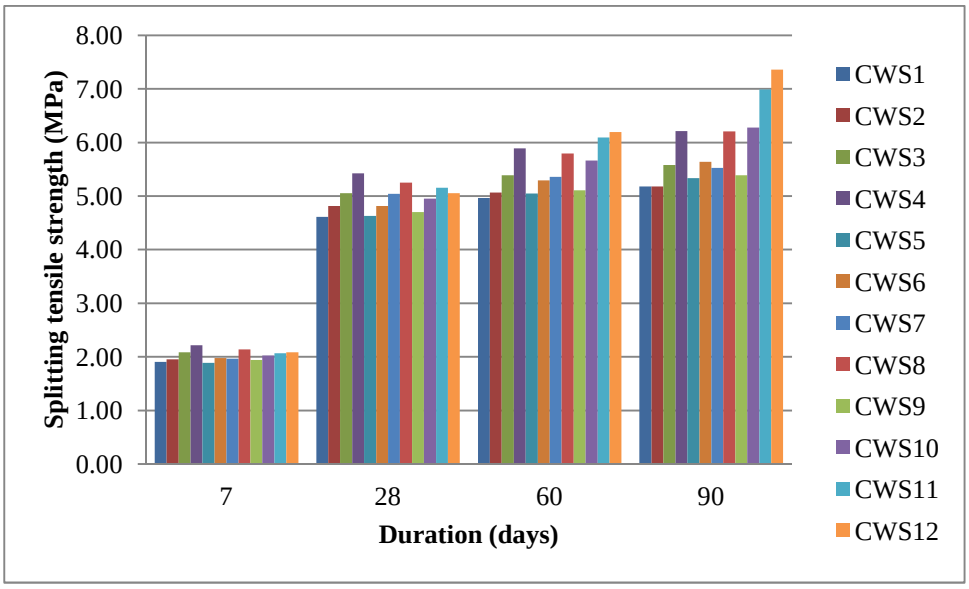

Fig. 4.126 Splitting tensile strength of WMF admixed ternary concrete mixes

In case of WMF admixed ternary mixes, there is also equal splitting tensile strength between the mixes at 7 and 28 days. At 60 days and above, the tensile strength is affected more by the presence of microsilica and the pore water made available to it by either flyash or WMF. Since WMF is finer than flyash, accordingly water absorption rate would also be more in comparison to flyash. If we compare the degree of reactivity between flyash, WMF and microsilica, microsilica has better potential than the aforesaid admixtures. WMF being such material which has excellent water holding capacity in comparison to flyash. Amount of water adsorbed and absorbed by WMF imparts additional water for further hydration process of the cementitious system particularly for microsilica. Microsilica being microfine

in nature, it could easily seep inside the gel pores with WMF particles and in such a way by each fraction of WMF enough water would be made available to microsilica for further hydration process as a result of which microsilica content upto 7.5% could achieve proper hydration even in the case of prolonged curing (i.e. beyond 28days). Due to this special effect, appreciable increase in splitting tensile strength is observed for WMF & microsilica admixed concretes as can be seen from Figs.4.126. & 4.127.

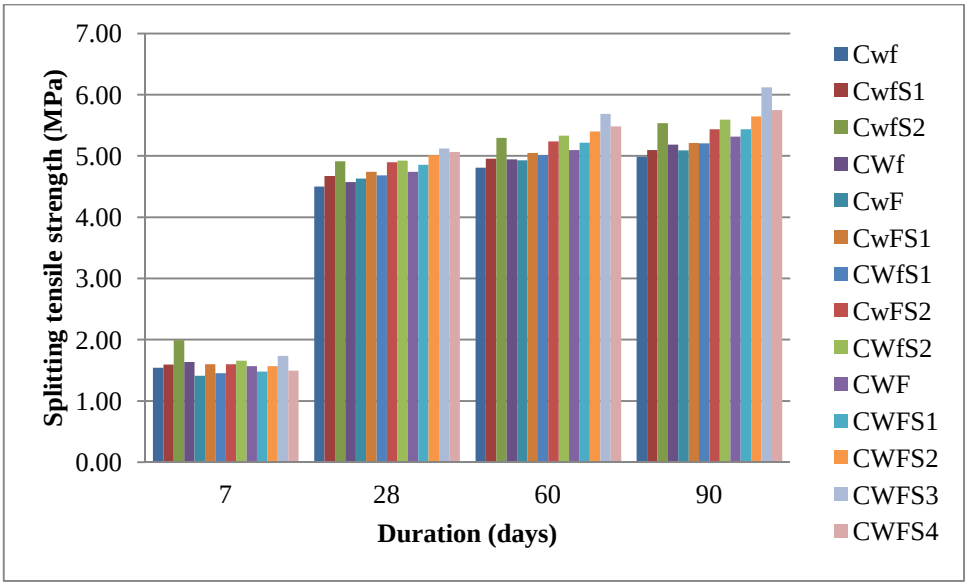

Fig 4.127 Splitting tensile strength of combined concrete mixes

As it has already been suggested , that the use of both flyash and WMF increase the splitting tensile strength of concrete. Also, flyash does this more efficiently than WMF. Microsilica complements WMF, greater than flyash. These three observations totally explained the behaviour of combined mixes also. Due to dense matrix of these mixes, the water availability is a big issue even at seven days. Therefore, even at this duration, it has been seen , that higher contents of microsilica (5% or higher) are able to work under higher contents of admixtures (combined admixture content (greater than 15% or so). Very high microsilica contents (10%) are seen to decrease the splitting tensile strength at all durations because, this content leads to self desiccation even with higher contents of other admixtures.

4.5.4 Flexural Strength

The results from the flexural strength test are presented in the Tables 4.22 & 4.23 for mortar and concrete respectively. Figs. 4.128- 4.133 show the flexural strength comparison in the form of bar charts for better comparison.

Table 4.22 Modulus of rupture of various mortar mixes after 28 days

Mix	Flex. St. (kg/cm^2)	Mix	Flex. St. (kg/cm^2)	Mix	Flex. St. (kg/cm^2)
C	48.0	CF1	44.0	CW1	44.0
Cwf	48.0	CF2	40.0	CW2	52.0
CwfS1	52.0	CF3	40.0	CW3	56.0
CwfS2	56.0	CFS1	48.0	CWS1	48.0
CWf	52.0	CFS2	48.0	CWS2	52.0
CwF	52.0	CFS3	52.0	CWS3	52.0
CwFS1	56.0	CFS4	56.0	CWS4	56.0
CWfS1	56.0	CFS5	44.0	CWS5	56.0
CwFS2	56.0	CFS6	44.0	CWS6	56.0
CWfS2	60.0	CFS7	48.0	CWS7	60.0
CWF	60.0	CFS8	48.0	CWS8	64.0
CWFS1	60.0	CFS9	40.0	CWS9	56.0
CWFS2	64.0	CFS10	44.0	CWS10	60.0
CWFS3	68.0	CFS11	44.0	CWS11	64.0
CWFS4	56.0	CFS12	44.0	CWS12	68.0

Table 4.23 Modulus of rupture of concrete mixes after different durations

Sr .No.	Mix	7 Days	28 Days	60 Days	90 Days
1	C	3.80	4.87	5.32	5.54
2	CF1	3.28	4.32	4.71	4.90
3	CF2	2.83	3.73	4.09	4.33
4	CF3	2.32	3.06	3.38	3.65
5	CW1	3.44	4.51	4.93	5.15
6	CW2	3.64	4.81	5.25	5.48
7	CW3	3.71	4.88	5.30	5.46
8	CFS1	3.27	4.32	4.71	4.90
9	CFS2	3.45	4.55	4.97	5.19
10	CFS3	3.62	4.79	5.22	5.40
11	CFS4	3.63	4.79	5.26	5.58
12	CFS5	2.93	3.85	4.21	4.41
13	CFS6	3.06	4.04	4.44	4.71
14	CFS7	3.25	4.28	4.76	5.25
15	CFS8	3.31	4.36	4.85	5.34
16	CFS9	2.38	3.14	3.45	3.66
17	CFS10	2.57	3.37	3.73	4.05
18	CFS11	2.71	3.57	3.96	4.30
19	CFS12	2.62	3.45	3.86	4.32
20	CWS1	3.51	4.63	5.08	5.35
21	CWS2	3.61	4.75	5.18	5.39
22	CWS3	3.72	4.91	5.36	5.60
23	CWS4	3.76	4.94	5.42	5.71
24	CWS5	3.76	4.94	5.42	5.73
25	CWS6	3.87	5.10	5.60	5.93
26	CWS7	4.03	5.26	5.73	5.94
27	CWS8	3.94	5.18	5.68	6.00
28	CWS9	3.78	4.98	5.46	5.76
29	CWS10	3.90	5.14	5.68	6.14
30	CWS11	4.04	5.30	5.89	6.46
31	CWS12	3.96	5.22	5.83	6.52
32	Cwf	3.46	4.39	4.81	5.05
33	CwfS1	3.52	4.47	4.89	5.10
34	CwfS2	3.49	4.59	5.03	5.28
35	CWf	3.46	4.43	4.86	5.11
36	CwF	3.32	4.12	4.51	4.73
37	CwFS1	3.31	4.20	4.59	4.81
38	CWfS1	3.69	4.59	5.02	5.24
39	CwFS2	3.43	4.32	4.72	4.95
40	CWfS2	3.75	4.75	5.19	5.44
41	CWF	3.39	4.28	4.68	4.91
42	CWFS1	3.57	4.43	4.85	5.08
43	CWFS2	3.65	4.55	4.98	5.21
44	CWFS3	3.68	4.67	5.13	5.44
45	CWFS4	3.72	4.59	5.02	5.25

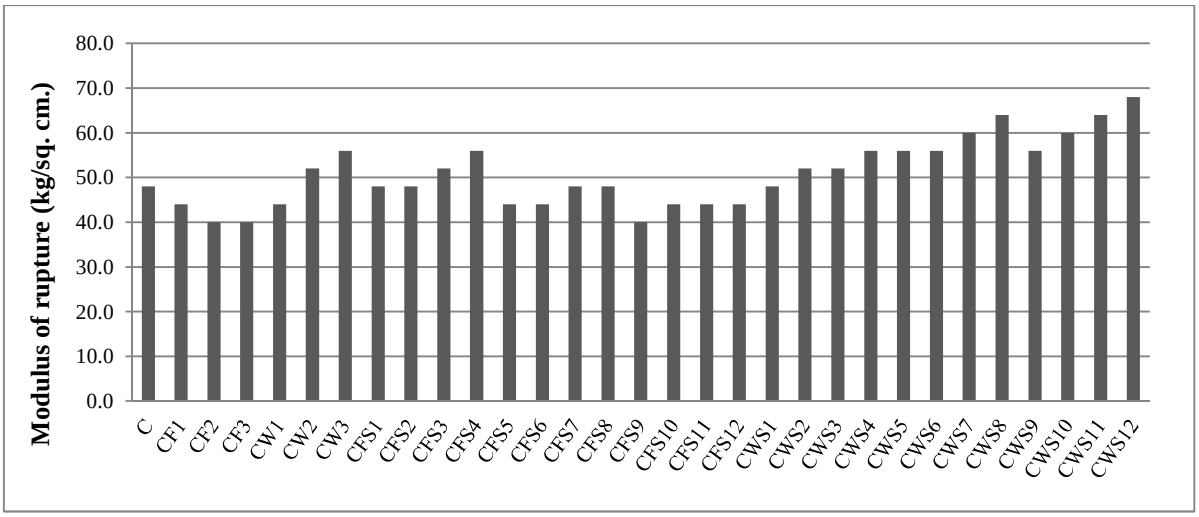

Fig 4.128 Flexural strength of normal, binary and ternary mortar mixes

The flexural strength of concrete is of interest in the design of pavement slabs. Flexural strength. Based on the extensive research conducted by the researchers, it was found that flexural strength of concrete is about 8 to 11 percent of the compressive strength for higher ranges of concrete strength (greater than 25 MPa) and 9 to 12.8 percent for lower ranges of concrete strength (less than 25 MPa). But for SCC mix, the literature available in this regard is scanty and over and above that the present study dealt with the use of different admixtures in SCC mixes for cement concrete pavement rehabilitation work, hence, it is imperative to check the effects of these admixtures on rheological properties of fresh SCC concrete mix and mechanical properties of hardened concrete.

As we know that flexural strength of concrete is mainly affected by the ITZ and ITZ is considered as the strength-limiting phase in concrete. It is because of the presence of ITZ that concrete fails at a considerable lower stress level than the strength of either of the two main components. Because it does not take very high energy levels to extend the cracks already existing in the interfacial transition zone. In the composite material, the interfacial transition zone serves as a bridge between the two components: the mortar matrix and the coarse aggregate particles. On admixing of WMF improves the ITZ considerably. The rate of improvement is more pronounced for higher part replacement of cement by WMF upto 30%. Beyond this replacement level, no significant improvement was observed. Similarly admixing of flyash showed some improvements, but if we look at paste interface

development, no significant improvement has been observed. This is mainly attributed to the decrease in the rate of hydration of cementitious material upto 28 days moist curing as a result of which appreciable improvement in flexural strength of mortar was not observed (Fig. 4.128), may be in the long run under pozzolanic action, strength might improve. For combined mixes wherein WMF, flyash & microsilica were admixed together in combination of cement, highest flexural strength is being offered by CWFS3 followed by CWFS2, (CWFS1, CWF, CWfS2), (CwFS2, CWFS4, CWfS1,CwFS1, CwfS2), (CwF, CWf,CwfS1), and Cwf respectively. Microsilica complements both flyash and WMF in flexural strength improvement considerably (Fig. 4.129). However, inclusion of microsilica upto 10% with flyash content of 20% decreases flexural strength in comparison to rest of the combinations. This is attributed to the self-desiccation caused by presence of excessive amount of microsilica than the required. It is also conspicuously noticed from the Fig. 4.54, that flexural strength does not affect much due to contents of WMF and flyash between replacement levels of 5-10% by weight of cement.

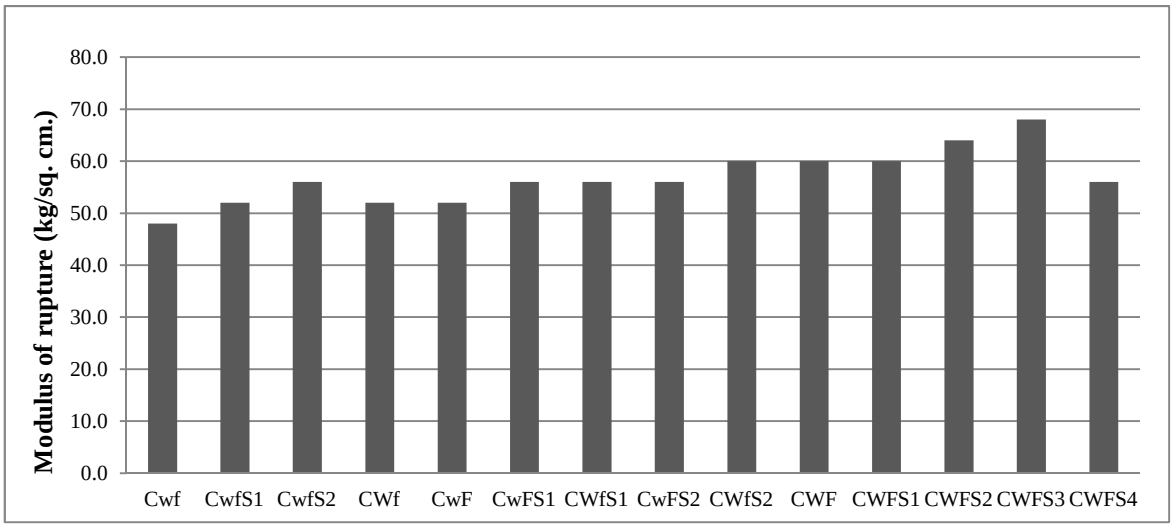

Fig 4.129 Flexural strength of combined mortar mixes

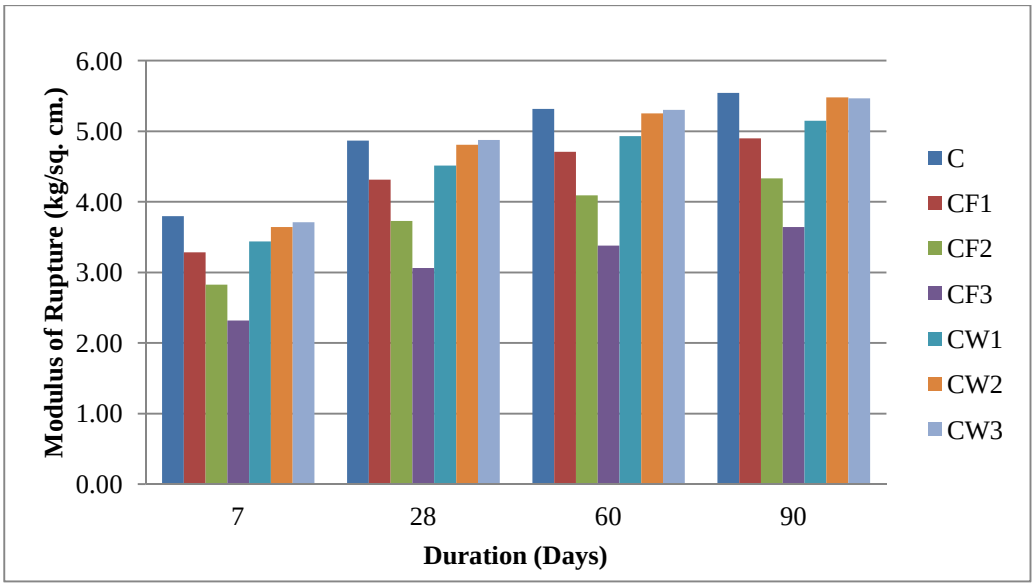

Fig 4.130 Flexural strength of normal and binary concrete mixes

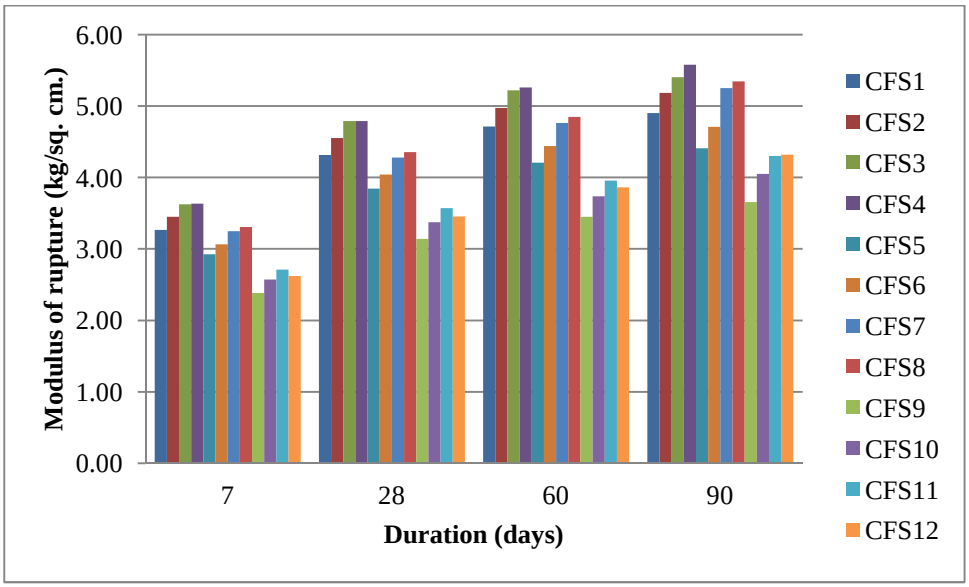

Fig 4.131 Flexural strength of flyash admixed ternary concrete mixes

Fig. 4.131 clearly illustrates that flexural strength increases with the increase of flyash content. This increment is more pronounced for prolonged curing. Significant improvement in flexural strength of concrete was observed on admixing of microsilica irrespective of days of moist curing but for concrete that contains flyash 30% and 10% microsilica do not showed any improvement in the flexural strength (Fig.4.132).

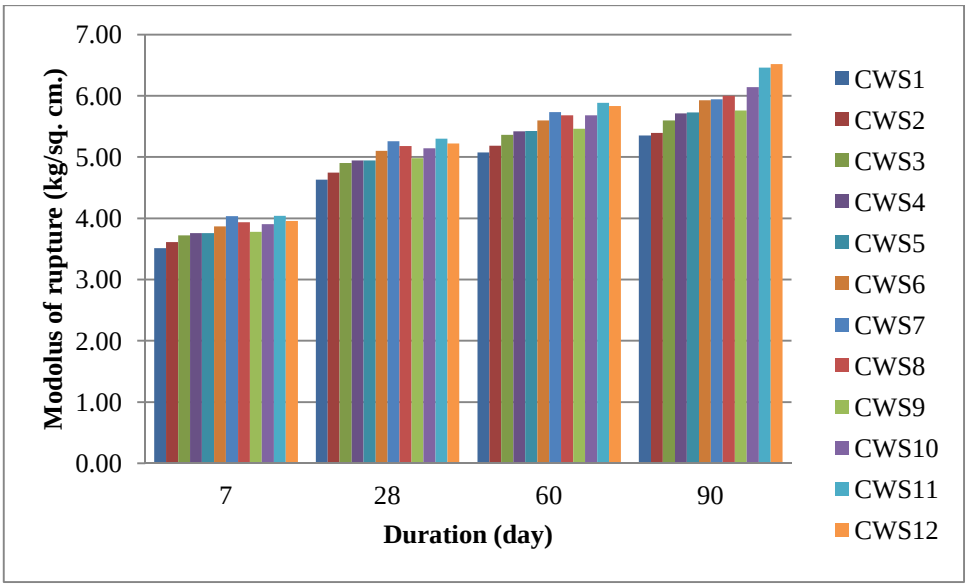

Fig 4.132 Flexural strength of WMF admixed ternary concrete mixes

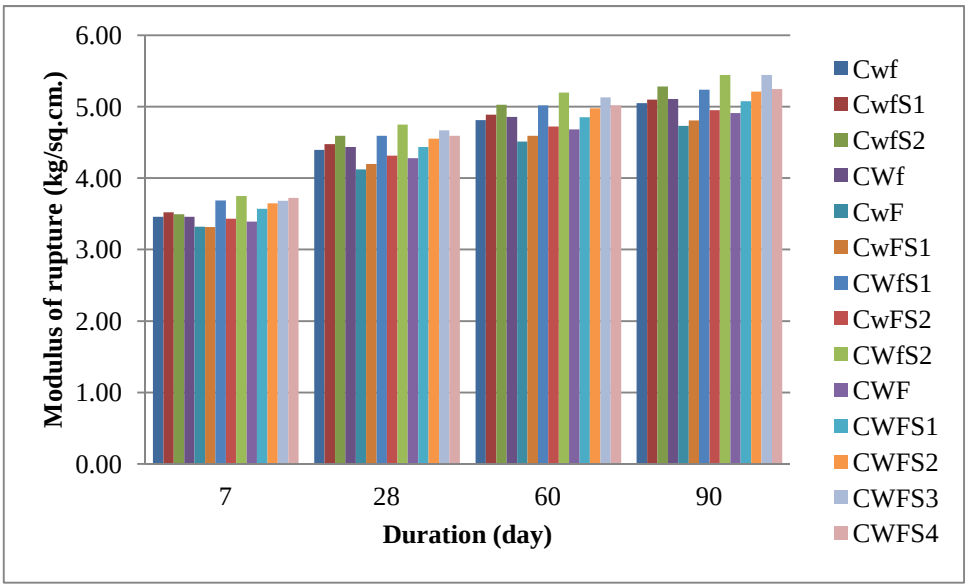

Fig 4.133 Flexural strength of combined concrete mixes

Inclusion of only wollastonite & flyash could not elevate flexural strength considerably particularly at the early age (7 day). However, there is an improvement in the flexural strength of WMF & flyash admixed concretes when they are moist cured for 28 days and above , that the rate of increment between 7 days and 28 days is more pronounced than concrete cured between 28 & 60 days, and 60 & 90 days. But after inclusion of microsilica into the cementitious system, on an average there were about 9.37% and 6.26%

increment in flexural strength for flyash-microsilica & WMF-microsilica admixed concrete at 28 days. The average percentage increase in flexural strength with inclusion of microsilica @ 5.0%, 7.5% & 10% at the age of 28 days, 60 days and 90 days with respect to 7 days moist curing for the same WMF & flyash content are (31.7, 43.9 & 50.6), (31.3, 43.7 & 51), (31.6, 46.2 & 60.7), (32.1, 44.4, & 51.1), (31.8, 46 & 59) and (31.5, 46.2 & 60.4) respectively.

4.5.5 Modulus of Elasticity

Modulus of elasticity depends on paste content as well as homogeneity of concrete/paste and not specifically on strength. For a concrete to be homogeneous, its interfaces should be cohesive and have good bond between them. These two things depend upon the gradation and proportions of various building elements of concrete/SCC. A concrete having higher percentage of paste has low elasticity because of the deforming capability of the paste under stresses. Same concrete having higher fraction of aggregates, loses its capability to hold the aggregates as a single building block under stresses, as a result of which the cracks easily develop in the thin pastes between the aggregates, and they get displaced.

Hence in both cases the modulus of elasticity could not be maintained. For a given mix design, and that too of a SCC, it is obvious that the volume of fine aggregates and paste would be higher than that of coarse aggregates. The higher binder content of SCC thus makes, it to inherit lesser modulus of elasticity with respect to a normal concrete. Although SCC has lower modulus of elasticity, but the use of admixtures in it could improve the bonding of the mortar with the aggregates as well as improving the stiffness of the paste (making it stiff as an aggregate) by improved hydration. Tables 4.24 & 4.25 show the modulus of elasticity variation for different mixes. Figs. 4.134- 4.139 show the comparison charts of the variation of modulus of elasticity in mortar and concrete mixes.

Table 4.24 Modulus of elasticity (GPa) of mortar mixes for different durations

Mix	Modulus of Elasticity (GPa)	Mix	Modulus of Elasticity (GPa)	Mix	Modulus of Elasticity (GPa)
C	26.60	CF1	23.95	CW1	20.75
Cwf	22.41	CF2	22.41	CW2	21.35
CwfS1	25.27	CF3	19.56	CW3	22.38
CwfS2	25.69	CFS1	20.75	CWS1	20.17
CWf	23.71	CFS2	21.61	CWS2	23.19
CwF	18.19	CFS3	22.33	CWS3	24.99
CwFS1	19.36	CFS4	22.67	CWS4	24.99
CWfS1	24.88	CFS5	20.73	CWS5	23.76
CwFS2	20.86	CFS6	20.70	CWS6	22.31
CWfS2	27.81	CFS7	20.93	CWS7	22.87
CWF	19.38	CFS8	22.11	CWS8	21.72
CWFS1	20.15	CFS9	21.24	CWS9	20.58
CWFS2	21.51	CFS10	20.50	CWS10	19.81
CWFS3	22.87	CFS11	19.50	CWS11	19.32
CWFS4	24.97	CFS12	17.55	CWS12	18.52

Table 4.25 Modulus of Elasticity of concrete mixes for different durations

Sr .No.	Mix	7 Days	28 Days	60 Days	90 Days
1	C	23.89	30.30	35.51	35.80
2	CF1	16.84	22.04	25.80	25.93
3	CF2	15.46	20.30	23.94	24.58
4	CF3	12.28	16.13	19.17	20.15
5	CW1	12.29	16.06	18.83	19.02
6	CW2	14.75	19.42	22.76	22.97
7	CW3	14.97	19.58	22.83	22.66
8	CFS1	12.72	16.76	19.62	19.72
9	CFS2	13.60	17.88	20.95	21.12
10	CFS3	15.28	20.14	23.54	23.53
11	CFS4	14.08	18.48	21.81	22.46
12	CFS5	10.35	13.55	15.91	16.14
13	CFS6	11.87	15.61	18.43	18.97
14	CFS7	12.59	16.53	19.82	21.43
15	CFS8	15.50	20.34	24.40	26.37
16	CFS9	11.58	15.20	17.94	18.48
17	CFS10	12.90	16.86	20.08	21.26
18	CFS11	11.61	15.25	18.19	19.33
19	CFS12	12.18	15.99	19.29	21.21
20	CWS1	14.17	18.63	21.93	22.41
21	CWS2	14.21	18.60	21.78	21.89
22	CWS3	22.28	29.28	34.34	34.68
23	CWS4	22.83	29.92	35.23	36.00
24	CWS5	15.59	20.43	24.07	24.66
25	CWS6	16.84	22.12	26.08	26.78
26	CWS7	23.81	30.85	36.07	36.08
27	CWS8	22.46	29.42	34.67	35.51
28	CWS9	15.95	20.97	24.69	25.23
29	CWS10	17.37	22.79	27.10	28.56
30	CWS11	20.37	26.59	31.83	34.20
31	CWS12	22.84	30.03	36.22	39.81
32	Cwf	15.31	19.21	22.57	22.93
33	CwfS1	21.87	27.41	32.12	32.38
34	CwfS2	10.98	14.37	16.89	17.19
35	CWf	17.68	22.43	26.37	26.86
36	CwF	10.41	12.68	14.90	15.13
37	CwFS1	8.40	10.50	12.32	12.48
38	CWfS1	9.91	12.12	14.22	14.35
39	CwFS2	10.23	12.68	14.89	15.10
40	CWfS2	15.12	18.89	22.18	22.49
41	CWF	12.41	15.44	18.14	18.42
42	CWFS1	13.34	16.26	19.08	19.33
43	CWFS2	9.86	12.10	14.20	14.38
44	CWFS3	15.76	19.71	23.27	23.97
45	CWFS4	15.10	18.24	21.40	21.63

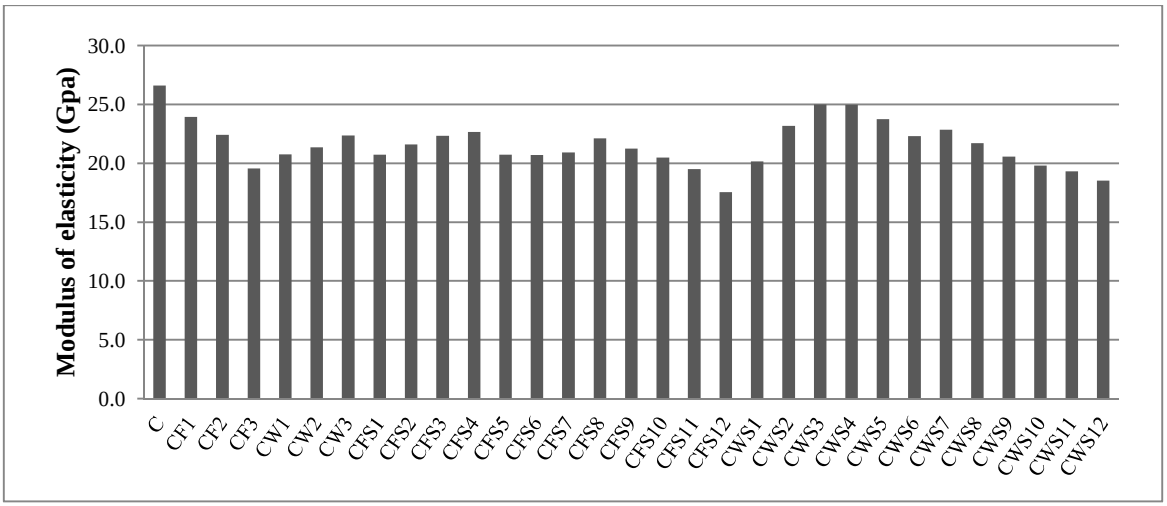

Fig 4.134 Modulus of elasticity of normal, binary and ternary mortar mixes

The modulus of elasticity is very sensitive to the increased paste content, as the higher volume of paste increase the tendency of the mortar to consolidate under loading increases. As can be seen from Fig. 4.134, the modulus of elasticity of mortar containing flyash is less than that of neat cement mortar. The percentage reductions in modulus of elasticity for CF1, CF2, and CF3 with respect to normal mortar are 9.96 %, 15.75%, and 26.47 % respectively.

The trend of decreasing in modulus of elasticity of flyash admixed mortar maintained linear relationship with fly ash contents.

But when WMF was incorporated @ 10%, 20% & 30% by weight of cement, modulus of elasticity of WMF admixed mortar increases. The increase of modulus of elasticity is more pronounced for higher dosage incorporation of WMF. However, the value of modulus of elasticity of WMF admixed mortar is lower than that of flyash admixed mortar. Present analysis strongly indicates that higher percentage replacement level of WMF would produce favourable results in comparison to flyash admixing. Incorporation of flyash in conjunction with microsilica doesn't show any sign of significant improvement in modulus of elasticity of mortar irrespective of replacement levels as may be seen from Fig.4.134. But when WMF and microsilica were incorporated together, to some extent modulus of elasticity was elevated at par with that of normal mortar's particularly CWS4 (Cement 80%; wollastonite 10 %; Microsilica 10 % & CWS3 (Cement 82.5%; wollastonite 10%, microsilica 7.5 % (Fig. 4.59). The main reason for reduction in modulus of elasticity

of flyash admixed mortar is due to reduction in compressive strength of the mortar on account of slower rate of hydration and dilution caused by flyash. Considerable enhancement in modulus of elasticity mortar system on admixing of WMF is by virtue of its higher modulus of elasticity and excellent reinforcing effect. The inclusion of microsilica in 20% flyash admixed mortars lead to a decrease in modulus of elasticity upto 22.18 %. From the present study, one thing is clearly depicted that microsilica plays a pivotal role in enhancing modulus of elasticity in both WMF and flyash cases. FIP commission on concrete in its report [39] also suggests, that the modulus of elasticity of concrete containing microsilica is somewhat higher, than is the case with Portland cement only concretes of similar W/C ratio.

If it is seen closely, then it could be noticed , that the total volume of the paste at 20% flyash and with increasing content of microsilica, increase the volume of the paste to a higher extent then the increased strength of the paste. Same case happens when WMF content is higher than 10%. Though there is densification of matrix, with increased microsilica content, but the increased WMF and flyash respective contents, also fill the voids within cement grains with some of their fine fractions, and thus microsilica is free to fill the voids between other admixtures. That portion of paste is not so stiffer in comparison to the paste containing cement grains and admixtures in between. In case of strength enhancement, this point has not been discussed because overall there was hydration taking place, wherever microsilica was situated, and the overall increased strength was more, whether it happened due to microsilica filling cement grains or outside in the WMF/flyash grains.

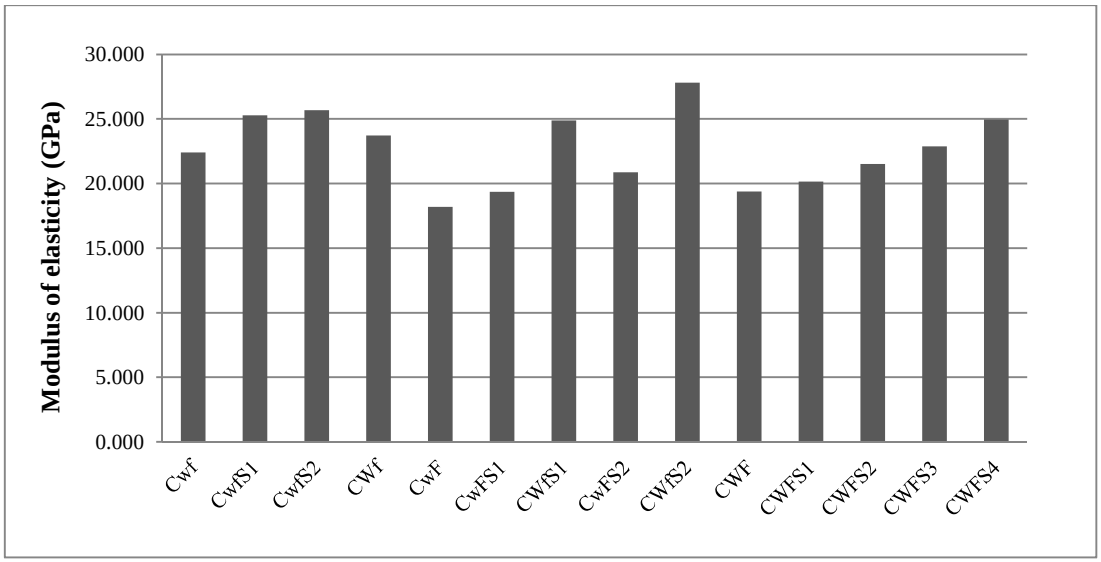

Fig 4.135 Modulus of elasticity of combined mortar mixes

In case of combined mixes the combined content of WMF-flyash in the mixes is quite low, and is not able to increase the paste content for most of the mixes. Hence, whether it is WMF or flyash, with the introduction of microsilica, the modulus of elasticity has increased. Flyash and WMF have played the same role in effecting modulus of elasticity as they did in binary or ternary mixes.

Even for mixes having combined WMF-flyash content of 20%, the matrix is so formed, that microsilica does not increase the paste content. Though, both WMF and flyash enter into the voids in cement grains, brings an increment in free microsilica content but, this free microsilica enters into the very fine voids created by the duo of WMF and flyash, which increased the paste stiffness in comparison to its volume.

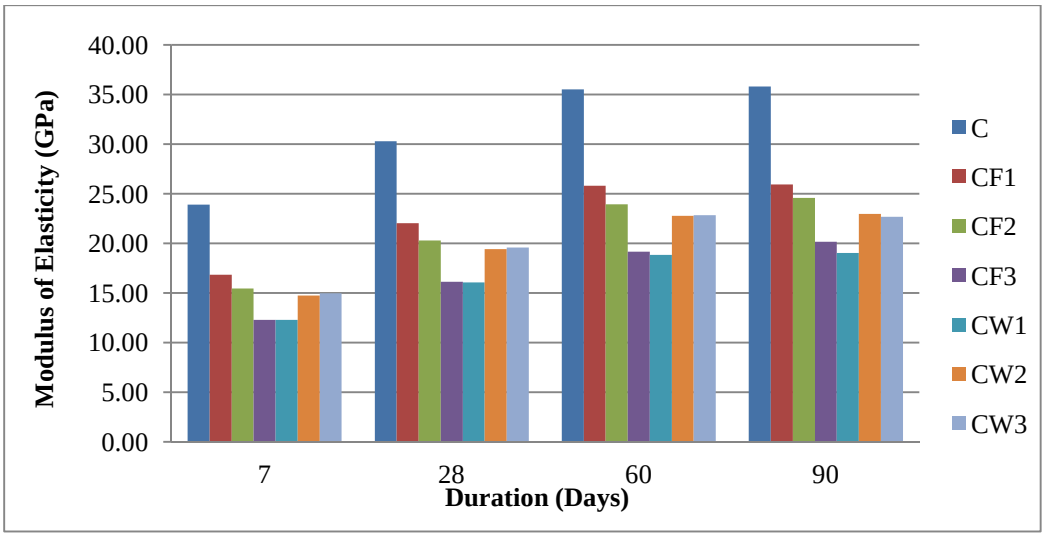

Fig 4.136 Modulus of elasticity of normal and binary concrete mixes

Alike mortars, the modulus of elasticity of normal concrete is higher than admixed SCC mixes. The present finding is in agreement with work done by Lomboy et al. [90]. They also suggested that the modulus of elasticity of semi flowable SCC concrete is lower than, that of normal concrete on account of higher paste content. Modulus of elasticity of SCC normal concrete increases with days of moist curing. Modulus of elasticity increases with an increase in the compressive strength of concrete but there is no agreement on the precise form of the relationship. This not surprising, given the fact that the modulus of elasticity of concrete is affected by the modulus of elasticity of the aggregate and by the volumetric proportion of aggregate in the concrete. In the present investigation, it is clearly depicted that modulus of elasticity of normal concrete at 7, 28 , 60 and 90 days are 23.89 GPa 30.3 GPa, 35.51 GPa, and 35.8 GPa respectively. The rate of increase of modulus of elasticity of concrete is approximately linear with days of moist curing as shown in Fig. 4.136.

But one thing is very clear about the modulus of elasticity of admixed concretes are less than that of normal concrete's irrespective of days of curing. However, it is also clearly visible from the Fig. 4.136 that modulus of elasticity of flyash admixed concrete showed decreasing order for respective age of curing i.e. 7, 28, 60 and 90 days. Modulus of elasticity of flyash admixed mortar approximately linear in decreasing order with the content of flyash. Whereas for WMF admixed concrete, modulus of elasticity increases with the

increase of WMF content in the cementitious system irrespective of days of moist curing. But modulus of elasticity of WMF admixed concrete showed less than modulus of elasticity of flyash admixed concrete. The reduction in modulus of elasticity of admixed concrete is mainly due to presence of higher paste volume in the SCC mix. This is not surprising, given the fact that the paste volume factor dominates strength improvement factors.

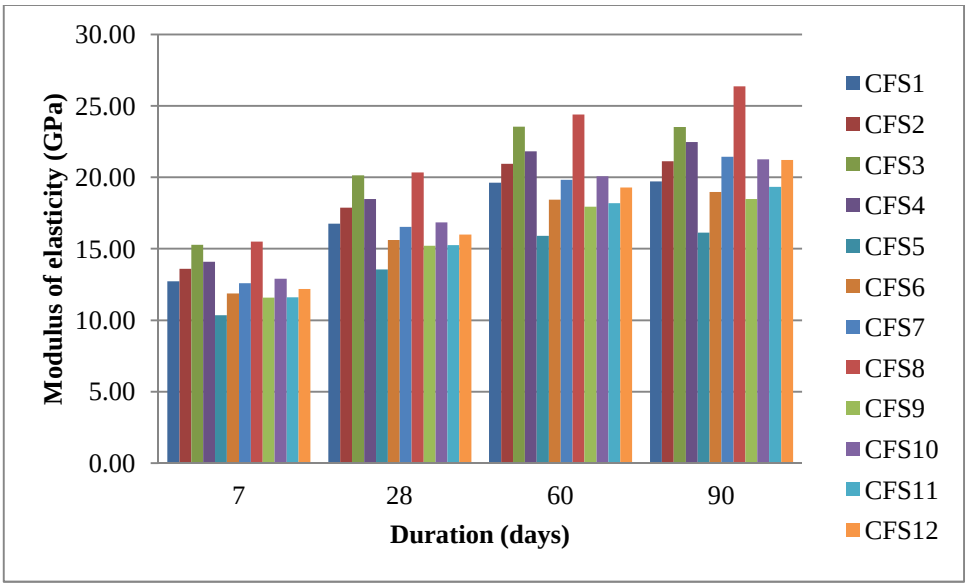

Fig 4.137 Modulus of elasticity of flyash admixed ternary concrete mixes

The potential of microsilica in improving the modulus of elasticity of flyash admixed concrete is clearly illustrated in Fig. 4.137. CFS4 and CFS8 offered the highest modulus of elasticity of flyash & microsilica admixed concretes at 7 & 28 day moist curing. But under prolonged moist curing condition i.e. at 60 & 90 days moist curing, CFS8 offered the highest modulus of elasticity. To draw maximum advantage for improving the modulus of elasticity of flyash admixed concrete, microsilica may be incorporated in the range of 7.5% to 10% by weight of cement as revealed by the present work. The improvement in modulus of elasticity is mainly due to improvement in the bond strength of aggregates and mortar at their interfacial zones by the action of flyash and microsilica. The improvement in modulus of elasticity is more pronounced by incorporation of microsilica to WMF admixed concretes irrespective of days of moist curing when compared to flyash admixed concretes. The better improvement observed in the modulus of elasticity of concrete when both WMF & microsilica were admixed is mainly attributed to higher stiffness property offered by WMF and secondary reaction between the CH present at the interface zone and microsilica.

For combined SCC concrete mixes, maximum modulus of elasticity is offered by CwfS1(C: 87.5%; w: 5%; f: 5 %; S: 2.5%) irrespective of days of moist curing. This value is comparable to the modulus of elasticity of normal concrete. It is also worth mentioning that second highest modulus of elasticity value is being offered by CWf (C: 85 %; W: 10%, and f: 5 %) as shown in Fig. 4.63. The considerable improvement in modulus of elasticity is attributed to better pore size refinement due to presence of micro fine materials i.e. WMF and flyash at the transition zone.

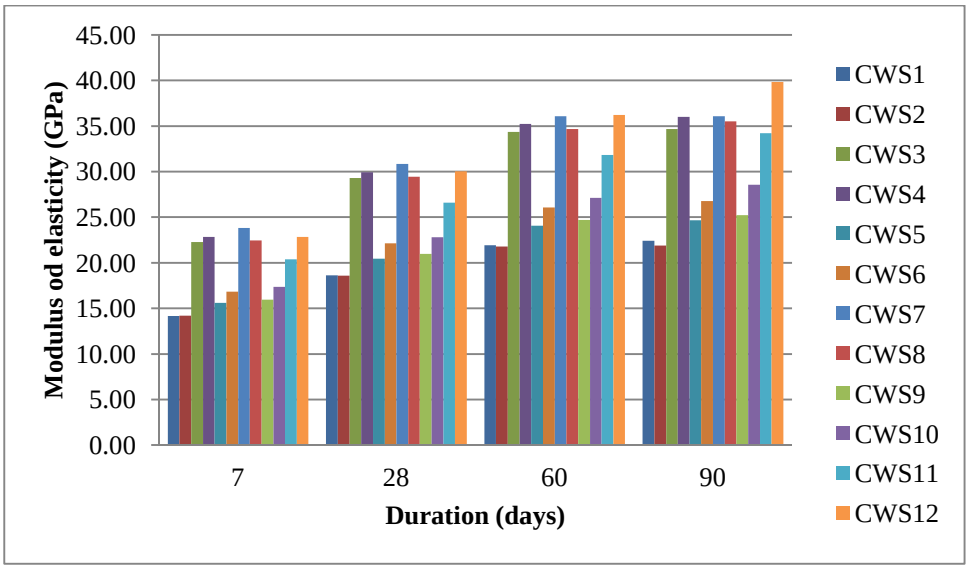

Fig 4.138 Modulus of elasticity of WMF admixed ternary concrete mixes

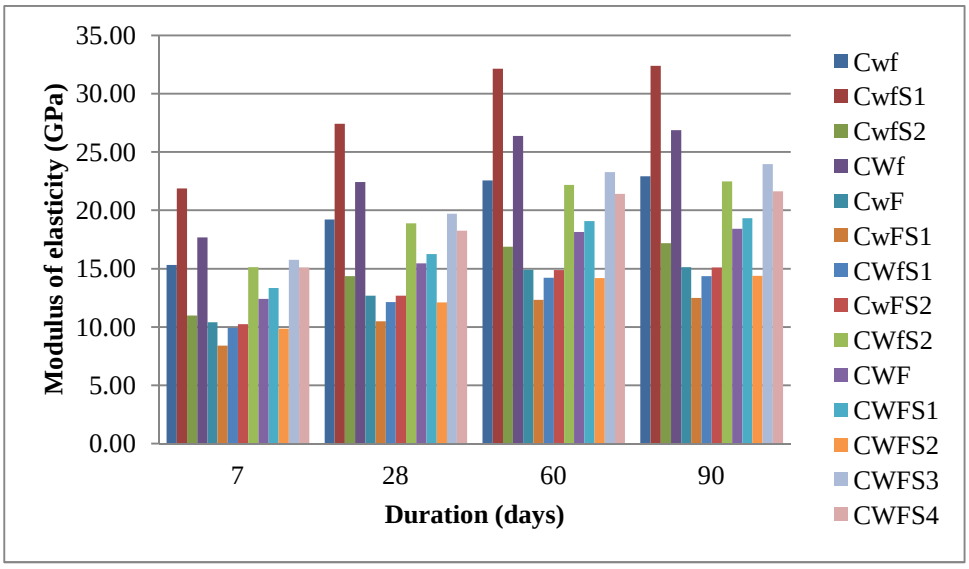

Fig 4.139 Modulus of elasticity of combined concrete mixes

4.5.6 Drying Shrinkage Resistance

Verbeck, G.J. [172] in his study on the pore structure of the hydrated cement paste clearly mentioned the effect of loss of humidity form the paste. It was stated that hydrated paste bears hydrophobic nature due to the presence of pores in it. Two types of pores namely: capillary pores/voids and gel pores exist in the hydrated paste. The loss of humidity up to 45 % causes loss of capillary water whereas water in the gel pores remain adsorbed on the paste even at very low humidities. Hence it could be deduced from this study, that the admixtures which could reduce the capillary voids into gel pores or could block them from losing the water may efficiently reduce the shrinkage of concrete. It would be obvious that finer admixtures would perform this function quite suitably, but a doubt still exists about the use of these types of fine admixtures. The doubt is based on the shrinkage increment capability of the admixtures on basis of its fine nature. It is known that fine admixtures adsorb more water than coarser ones and therefore when this water is lost; there is shrinkage in the hydrated paste. Including either fly ash or ground granulated blast furnace slag in the mix increases shrinkage. Specifically, at a constant water/cement ratio, a higher proportion of fly ash or slag in the blended cement leads to higher shrinkage by some 20 percent with the former material, and by up to 60 percent at very high contents of slag. E.J. Sellevold [155] found, that microsilica increases the long term shrinkage. Hence, it would not be wrong to presume that fine admixtures would try to promote more shrinkage.

F.H. Wittman [174] has also done an elaborative work in this area. The results from the study clearly distinguish between two types of shrinkage; plastic and drying. Plastic shrinkage occurs when water is lost from the surface of the hydrated paste and in the plastic state of mix, whereas drying shrinkage occurs in the semi hard consistency of the mix. Therefore the shrinkage depends upon the plasticity of the paste too. Fine admixtures like microsilica increase the surface area of the paste/mix and thus cause higher plastic shrinkage, whereas the same admixtures in the semi hard consistency decreases the drying shrinkage of the paste due to reduction of capillary voids and high rate of strength increment. Lesser fine admixture like fly ash has exactly opposite behaviour. It increase the drying shrinkage whereas decrease the plastic one.

Water reducing admixtures, per se, probably cause a small increase in shrinkage. Their main effect is indirect, in a way, that the use of an admixture may result in a change in the water content or in the cement content of the mix, or in both, and it is the combined effect of both the changes, that influences shrinkage. Super plasticizers have been found to increase shrinkage by some 10 to 20 percent. However, the changes in the observed shrinkage are too small to be accepted as reliable and generally valid [22].

Grzybowski [51] suggested, that no standard test exist to assess the cracking due to restrained shrinkage, but the use of ring shaped concrete specimen restrained by an internal steel ring can be informative, as far as comparative conclusions have to be made regarding the resistance of different concretes with respect to cracking.

This test corresponds to the behaviour of concrete in the period before 28 days, and thus the behaviour of concrete in the first seven days has more prominent effect on the drying shrinkage of concrete. Therefore, correlating drying shrinkage with compressive strength or tensile strength of 28 days makes no sense.

After hardening, concrete begins to shrink, as the water present in the capillary voids, and not consumed by cement hydration leaves the system. This is known as drying shrinkage. Water above that quantity, which is necessary to hydrate cement, is required for proper workability and finishability; this water is called “water of convenience.” In general, the higher the additional water content, the higher the shrinkage potential. If somehow, the water in capillary voids is also bound by adsorption, then the chances of its leaving the system are reduced, which reduces the drying shrinkage rate.

For small, unrestrained concrete specimens (prisms), a low ultimate shrinkage (strain) is considered to be less than 520 millionths (at 50% relative humidity and 73° Fahrenheit). Typical concrete shrinkage has been measured at 520 to 780 millionths. However, for some mixtures, shrinkage exceeding 1,100 millionths has been documented. Using concrete with a higher drying shrinkage increases the risk of problems with the floor performance. Fig 4.140-4.144 below, show the compressive strain data with respect to square root of elapsed time for different concrete mixes. Table 4.26 shows the cracking time and final stress rate for different mixes.

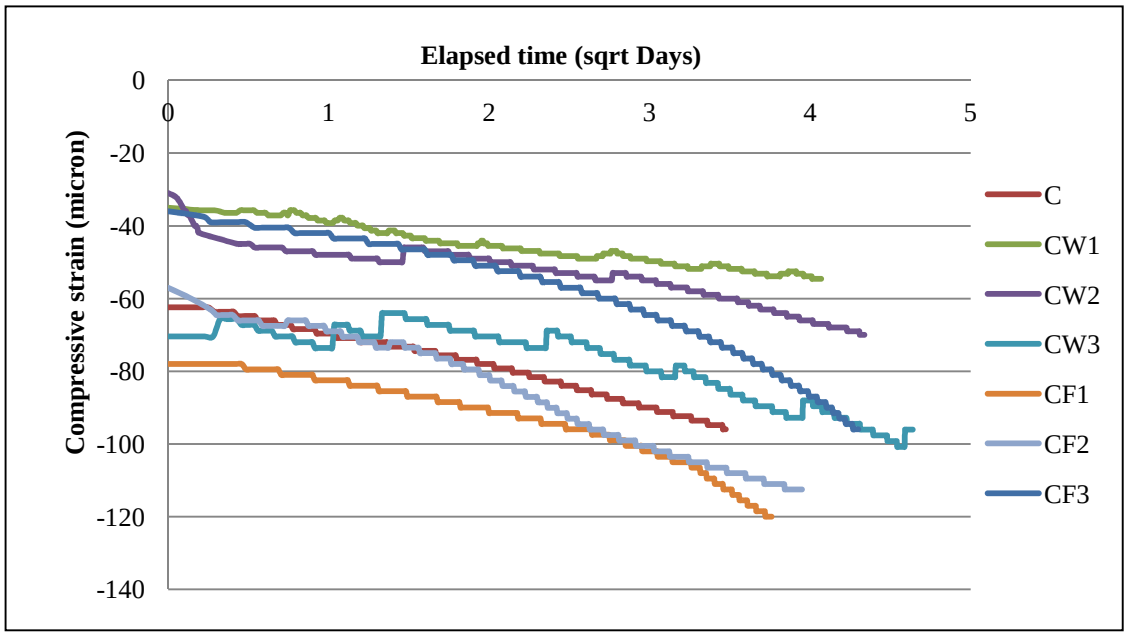

Fig. 4.140 Compressive strain v/s elapsed time for binary mixes

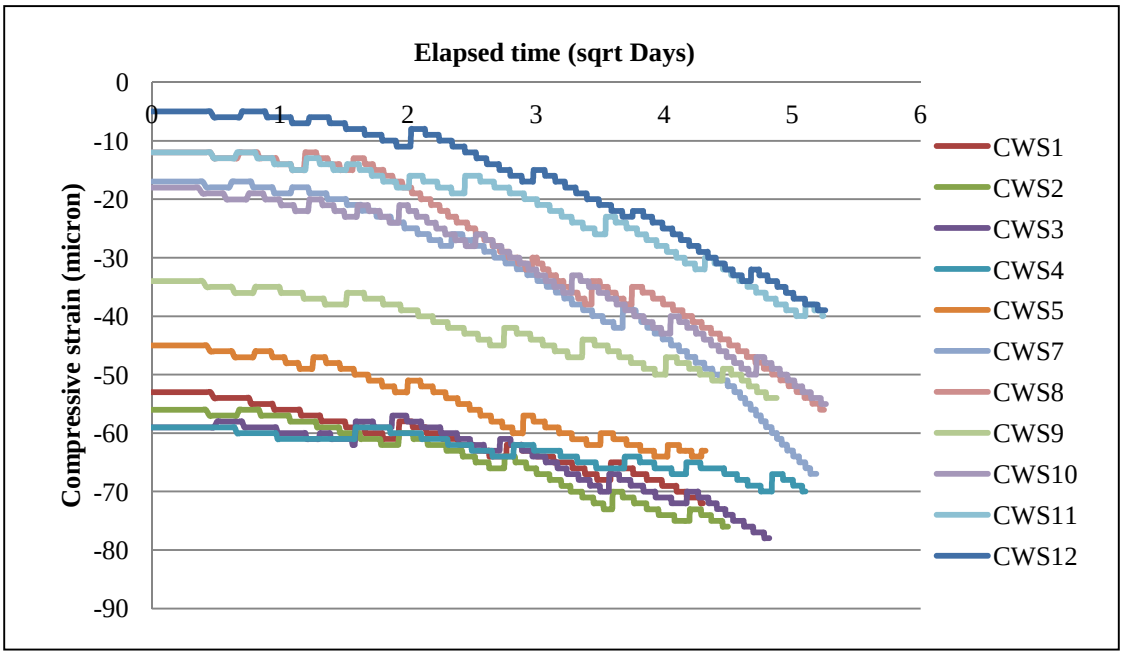

Fig. 4.141 Compressive strain v/s elapsed time for WMF reinforced ternary mixes

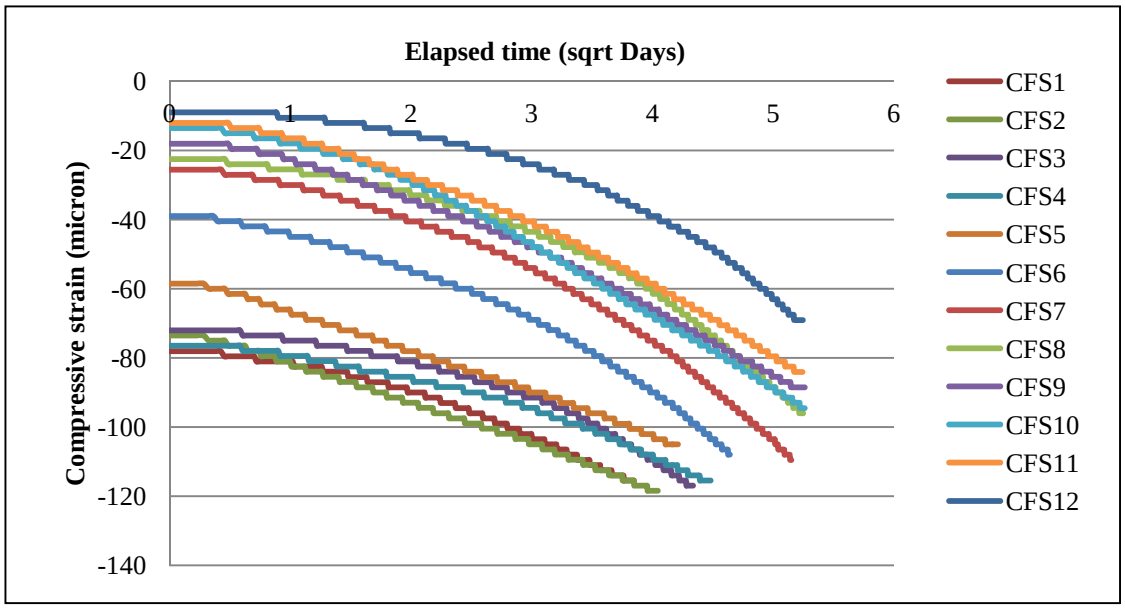

Fig. 4.142 Compressive strain v/s elapsed time for flyash reinforced ternary mixes

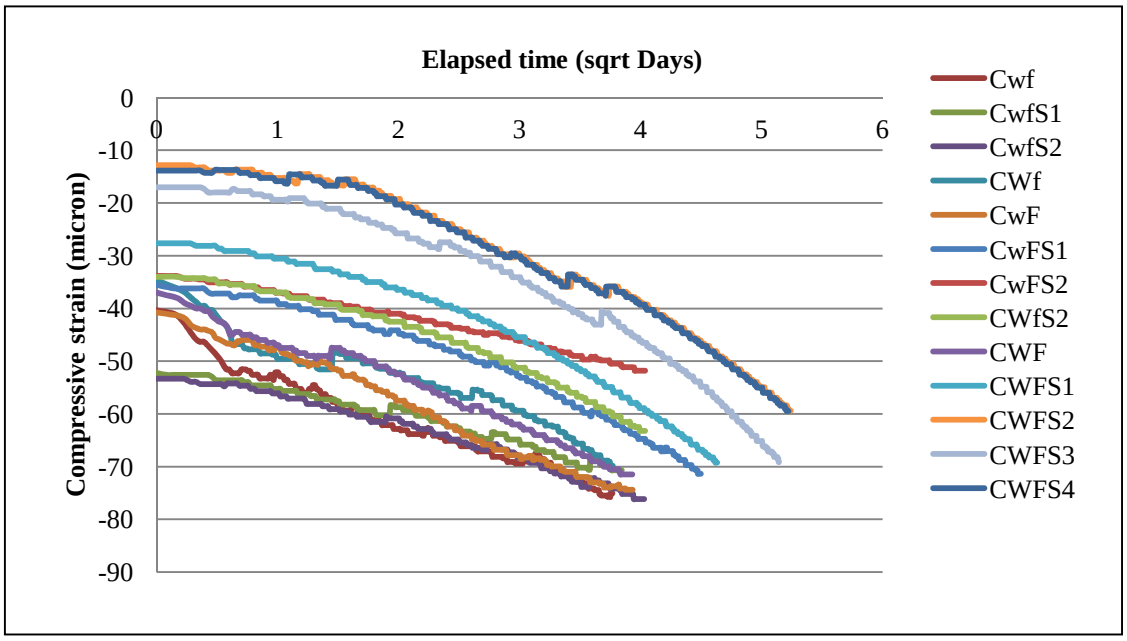

Fig. 4.143 Compressive strain v/s elapsed time for combined mixes

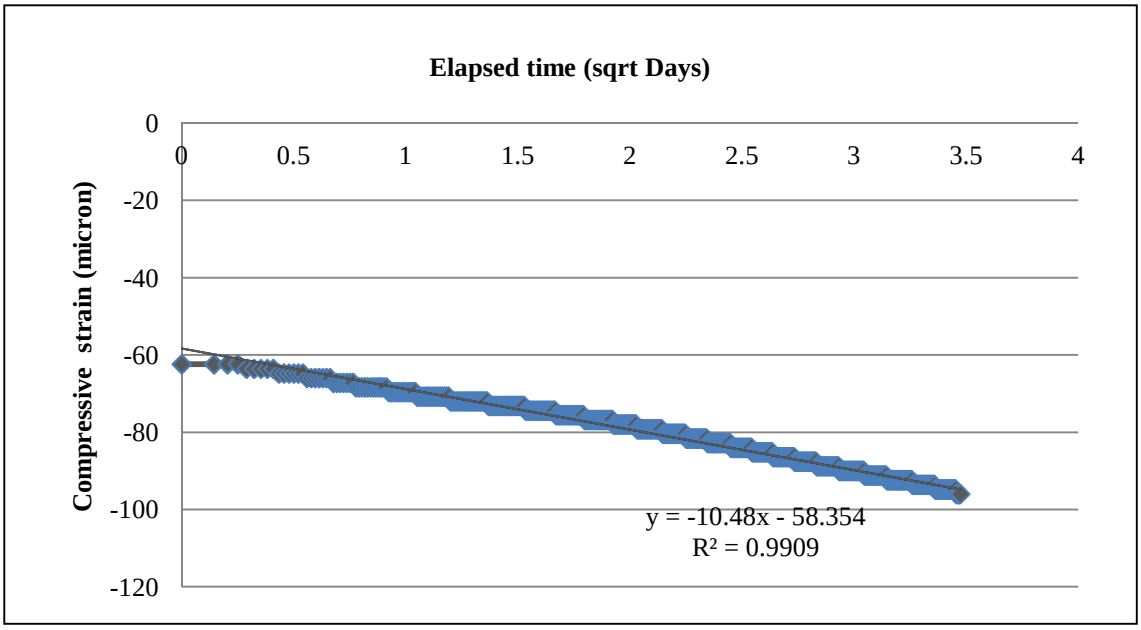

Fig 4.144 Equation relating Compressive strain v/s elapsed time for normal concrete

Table 4.26 Results obtained from the restrained shrinkage test

Mix	Max. Strain (μ)	Initial age in Days	Age at max. strain (Days)	Strain rate (ε) at elapsed time T (ε=α×T½+K)	Avg. strain rate (α)× (10^{-6})	Elapsed time at age of max. strain (Tr Days)	Stress rate (q) MPa at Tr	Potential for cracking
C	-96	0.24	12.31	Y=10.48X-58.35	10.48	12.06	0.109	Mod High
CW1	-70	0.03	18.85	Y= 6.872X-37.00	6.87	18.82	0.057	Mod Low
CW2	-55	0.25	16.81	Y= 4.836X-35.12	4.83	16.56	0.043	Mod Low
CW3	-96	0.24	23.69	Y= 9.069X-54.14	9.07	23.45	0.068	Mod Low
CWS1	-56	0.47	28.00	Y= 10.95X+0.280	10.95	27.52	0.075	Low
CWS2	-64	0.34	19.54	Y= 5.266X-42.20	5.27	19.19	0.043	Mod Low
CWS3	-68	0.34	22.51	Y= 9.956X-17.54	9.96	22.17	0.076	Mod Low
CWS4	-67	0.50	27.40	Y=11.13X-2.352	11.13	26.89	0.077	Low
CWS5	-72	0.26	18.78	Y= 4.316X-51.34	4.32	18.51	0.036	Mod Low
CWS6	-70	0.55	26.59	Y= 2.317X-56.68	2.32	26.03	0.016	Low
CWS7	-78	0.47	23.69	Y= 4.856X-51.09	4.86	23.21	0.036	Mod Low
CWS8	-76	0.27	20.50	Y= 5.390X-51.34	5.39	20.23	0.043	Mod Low
CWS9	-39	0.40	28.02	Y= 8.081X+6.033	8.08	27.63	0.056	Low
CWS10	-40	0.55	28.02	Y= 6.505X-3.328	6.51	27.47	0.045	Low
CWS11	-54	0.34	24.13	Y= 10.69X-1.725	10.69	23.79	0.079	Mod Low
CWS12	-55	0.34	28.02	Y= 12.36X+3.933	12.36	27.68	0.085	Low
CF1	-120	0.32	14.44	Y= 12.05X-68.02	12.05	14.13	0.116	Mod Low
CF2	-96	0.44	18.92	Y= 15.07X-22.94	15.07	18.49	0.127	Mod Low
CF3	-113	0.42	16.01	Y= 15.59X-52.78	15.59	15.59	0.143	Mod Low
CFS1	-117	0.37	19.17	Y= 12.09X-58.50	12.09	18.80	0.101	Mod Low

CFS2	-116	0.45	20.53	Y= 10.28X-66.31	10.28	20.08	0.083	Mod Low
CFS3	-119	0.29	16.64	Y= 12.05X-69.14	12.05	16.35	0.108	Mod Low
CFS4	-116	0.27	15.04	Y= 11.82X-67.93	11.82	14.77	0.111	Mod Low
CFS5	-84	0.55	28.02	Y= 16.22X+4.654	16.22	27.47	0.112	Mod Low
CFS6	-89	0.34	28.02	Y= 16.03X-2.588	16.03	27.68	0.110	Mod Low
CFS7	-69	0.53	28.02	Y= 13.61X+12.02	13.61	27.49	0.094	Low
CFS8	-95	0.34	28.02	Y= 18.55X+5.899	18.55	27.68	0.127	Mod Low
CFS9	-96	0.50	28.02	Y= 16.42X+0.420	16.42	27.52	0.113	Mod Low
CFS10	-105	0.29	18.02	Y= 11.88X-54.38	11.88	17.73	0.102	Mod Low
CFS11	-108	0.29	21.81	Y= 16.85X-22.19	16.85	21.52	0.131	Mod Low
CFS12	-110	0.45	26.95	Y= 18.88X-2.764	18.88	26.50	0.132	Mod Low
Cwf	-76	0.27	14.47	Y= 7.605X-46.21	7.61	14.20	0.073	Mod Low
CwfS1	-76	0.40	16.64	Y= 6.482X-49.37	6.48	16.24	0.058	Mod Low
CwfS2	-71	0.24	15.04	Y= 5.457X-49.47	5.46	14.81	0.051	Mod Low
CWf	-64	0.29	16.64	Y= 8.414X-28.14	8.41	16.35	0.075	Mod Low
CwF	-74	0.26	15.75	Y= 9.378X-39.02	9.38	15.49	0.086	Mod Low
CwFS1	-71	0.27	20.50	Y= 8.999X-27.76	9.00	20.23	0.072	Mod Low
CWfS1	-70	0.26	16.59	Y= 7.426X-38.48	7.43	16.32	0.066	Mod Low
CwFS2	-63	0.32	15.72	Y= 8.410X-27.03	8.41	15.41	0.077	Mod Low
CWfS2	-52	0.32	16.61	Y= 4.885X-31.74	4.89	16.29	0.044	Mod Low
CWF	-72	0.26	21.78	Y= 8.879X-36.05	8.88	21.52	0.069	Mod Low
CWFS1	-69	0.32	27.84	Y= 10.44X-16.57	10.44	27.52	0.072	Low
CWFS2	-59	0.55	27.84	Y= 10.26X-0.818	10.26	27.29	0.071	Low
CWFS3	-59	0.37	27.84	Y= 10.3X-0.398	10.30	27.47	0.071	Low
CWFS4	-69	0.47	26.93	Y= 11.56X-2.457	11.56	26.45	0.081	Low

While testing at a laboratory, shrinkage is measured by two parameters: stress rate due to shrinkage and time for crack development. Both of these parameters vary according to paste composition (fineness), which affects the continuity of pores in hardened paste as well as the rate of hydration. The rate of hydration in turns affects the tensile strength of concrete. The time for crack development directly depends on the tensile strength of concrete and indirectly on the stress rate and the factors causing it. Generally a concrete having higher stress rate develops crack early, because at a certain stage the shrinkage stresses in the concrete exceed its tensile strength. But in case of pozzolana and fiber reinforced concrete and that too, for a self-compacting concrete, the behaviour is quite complex, which depends upon the impact of microstructure and workability of concrete on the above mentioned parameters.

The Concrete develops cracks when the shrinkage of fine volumes on account of water reduction from their surface, is opposed by aggregates or reinforcement, which brings the mortar in tension and aggregates/reinforcement in compression. If the concrete is having lesser tensile strength in comparison to the stresses at that moment, the cracks start growing at the interface between paste and aggregates. Here an important thing to point out is , that the obstructer to shrinkage is not a fine material, and whether a material is inert or active, its shrinkage depends upon loss of water from its adjoining voids, which creates a surface tension force, bringing the fines together as if they are being compressed. Following paragraph provides the results obtained from the restrained shrinkage test in terms of the effect of addition of various admixtures in the SCC:

(i) WMF addition:

It is not sufficient enough to say that the shrinkage of a concrete would be higher, if it contains larger fraction of fine materials. This would be true to say only, if the water adsorbed by the particle at the capillary voids is not held strongly, if the particle is not able to convert the capillary voids into gel pores, and if the pores are continuous. All of these factors are dependent upon the size and reactivity of the particle. Soliman and Nehdi [160] have also suggested that there is a reduction in total shrinkage with increasing content and aspect ratio of wollastonite microfibers. In this study it was found, that as the microfiber content increased from 4 to 12%, the reduction in total shrinkage at 7 days increased from

11 to 16% for very fine microfibers and from 2 to 9% for medium fine microfibers with respect to that of the control mixture. Microfibers delay the coalescence and propagation of cracks at early age through better stress transfer at microcracks [11, 164]. On the other hand, the increase in the cracking age with increasing microfiber content implies a higher crack-bridging efficiency and ability of larger-size wollastonite microfibers to overcome the reduction in matrix strength induced by dilution effect.

Initially when WMF is added in lower quantity up to 20%, the cement particles are not far apart in the solution, and the voids in between them are easily filled or blocked by WMF due to its pore size or grain size refinement. Though the water is released when WMF enters into the cement voids, but this water only is used by in the accelerated hydration done by cement particles. As a result of which, the water is not able to escape from the pores (mainly gel pores) and shrinkage is reduced. With the increment in the content of WMF in the mix, the cement particles increase their distance and more and more WMF particles enter into the pore solution present in between their voids. As a result of which the number of capillary spaces increase whereas the gel pores reduce. Since the void space is larger, the initial hydration as well as insufficient capacity to block the voids, provided by WMF, is not sufficient to stop the water from escaping from these capillary voids. Therefore, an increased shrinkage stress was reported for WMF content greater than 20%.

As a reinforcer, WMF will increase the tensile strength of mortar, which would resist the crack development and also will delay the propagation of cracks by distributing the stresses over a local region. Thus, the overall effect observed for WMF addition, was the delay in crack development in spite of high stress rate. Since the time period of cracking also depends upon the stress rate development, therefore the variation trend for time period of cracking is similar to the stress development.

(ii) Flyash addition

Idorn & Thaulow [60] suggested, that coarser flyash particles act as micro aggregates which reduce the shrinkage, increase the packing of aggregates with the paste and thus increase the tensile strength, increase the density of the concrete thereby leading to reduction in crack propagation and porosity causing a direct increase in compressive strength and stiffness.

Also this portion of flyash, absorbs the water in capillary pores due to surface tension and holds it for long time hydration [60]. Hence, when microsilica is present, the unreacted coarser flyash at later ages avail the water to the microsilica, and cause its hydration, thereby increasing the strength of the concrete. An excessive flyash beyond 30% of total cementitious material has been found to reduce strength due to dilution of cement and increment in porosity cause by its coarser particles [118,119].

For flyash mixes, the hydration rate is higher than normal concrete uptil 7 days. The effect of this acceleration increases its crack development time in comparison to normal cement concrete. After 14 days the effect of acceleration diminishes and the samples start cracking. Though flyash contain alumina and lime, which promote ettringite formation in presence of sulphates, but the consumption of lime due to flyash hydration may hinder the formation of ettringite. Also, the reactivity of alumina depends upon, whether it is available in glass part of the compound or not [173]. If it is present in glass part than it provides a long term source of ettringite formation in presence of sulphates. the reactivity of flyash as noticed from the XRD test suggest, that ettringite formation is hindered in presence fo flyash. this suggests that flyash does not contain reactive alumina and highly neutralizes CH; if it did, then ettringite formation would have been promoted rather than hindered.

Thus, the stress rate is equal to or a bit higher than normal concrete because effect of pore refinement is nullified by presence of fine material (fraction of flyash much finer than cement) verified by particle size analysis. Hence with the increment in flyash content both the stress rate and the crack time increase to a small extent.

Form the results obtained it has been found that WMF mixes has the highest stress rate increment capacity and its crack development time is followed by microsilica. Microsilica has maximum stress rate reduction capacity. Flyash has lowest crack time increment capacity.

It has been assumed that whatever water of convenience has been required for maintaining workability of self-compacting concrete (which generally contains different kind of fine materials and viscosity modifying material), would be provided by superplasticizer action alone. That’s why the water to cement ratio has been kept at 0.36,

both for normal pump able concrete and all SCC mixes. The workability adjustments to the SCC mixes have been done by trials of superplasticizer addition to the normal mix. Even if some water in excess is present then that got minuted during plastic shrinkage and rest left would not be able to create capillary cavities. Hence the water contained in the interstitial voids or gel pores of SCC has only been considered as affecting the stress rate which only depends upon the paste composition. Fine aggregates' effect has not been considered as the CA/FA ratio is same in normal pump able concrete and SCC. This has been done to find out the differences caused, only due to effect of materials which make production of SCC possible.

(iii) Microsilica addition

In the present study with microsilica the stress rate decreased; and time for crack development also increased, this is due to higher paste strength imparted by high rate of hydration caused by microsilica.

Cohen et al. [29] studied the influence of silica fume on bulk paste modification and pressed, that excessive fine cement promotes rapid hydrations, which is further complemented by microsilica, and thus cause expansion of concrete. On the loss of water, this expanded concrete starts shrinking, but the restraint offered by concrete on account of high strength provided by microsilica, as well as the pore discontinuity provided through filler effect & pore refinement, controls the shrinkage.

The results of this study are thus, in agreement with their study.

4.5.7 Chloride Ion Penetration Resistance

This test is specifically for concrete as it tests the porosity of interfacial transition zone in a concrete mix. Basically it tests the continuity of voids or pores in the concrete mix.

Chlorides can be present in concrete because they have been incorporated in the mix through the use of contaminated aggregate, sea water, brackish water or by admixtures containing chlorides. But, according to ACI 318-89 (Revised 1992) approach is to be considered water-soluble chloride ions only.

In the present study, chloride ion penetration test has been conducted on self-compacting concrete mix. Being SCC mix, having more volume of mortar, it would have a lesser continuity of pores due to thicker paste as a result of which it would offer greater chloride ion penetration resistance in comparison to normal concrete. Table 4.27 presents the percentage chloride ion penetration noted at 30, 60 and 90 days ponding for concretes with or without admixtures.

The chloride ion penetration increases with the increase of ponding duration for all considered mixes irrespective of admixtures content and their combinations as can be seen from Figs. 4.70 & 4.71. But if we look at the best three individual mix performances for different ponding periods, the greatest resistance to chloride ion penetration is being offered by CWS12 (c: 60%, w: 30%, s: 10%,) followed by CWS11 (C: 62.5%, W: 30%, S: 7.5%) and CWS8 (C: 30%, W: 20%, S: 10%) respectively. Their average percentage reductions for all curing periods are about 91.71%, 88.53% & 83.16%, respectively, when compared to that of normal concrete. Fig.4.145 clearly depicted , that with the inclusions of flyash, WMF and microsilica, irrespective of their combinations, chloride ion penetrability resistance increases significantly. For the same part replacement level of flyash and WMF, the penetrability resistance of chloride ion is better for WMF admixed concrete in comparison to fly ash admixed concrete except for 20% part replacement level. Absurd results observed at 20% part replacement of WMF may be due to improper mixing of powdery materials as a result of which proper chemical reaction could not be achieved. Based on the present laboratory results, one thing is very clear that WMF has better potential to reduce the permeability of concrete in comparison to flyash. Inclusion of WMF 10% reduces the chloride ion penetration up to 10.87%, 16.42% and 9.86% for the ponding periods of 30, 60 & 90 days respectively with respect to counter part of flyash admixed concrete. Higher the percentage inclusion of WMF, higher the percentage reduction in chloride ion penetration. This reduction is even more if microsilica is incorporated along with WMF irrespective of their contents. WMF being microfine fiber, inclusion of the same refines the pore size considerably and imparts tight packing against the surface of the aggregate due to its excellent reinforcing effect therefore, the porosity in the interface zone is reduced considerably. Fly ash admixed concretes showed tremendous improvement particularly after 28 days as pore size refinement improves significantly due to latter pozzolanic action.

Fig.4.146 clearly illustrated that CWfS2 (C: 80%, W:10%, F: 5%, S: 5%) is the mix which offered maximum resistance against chloride ion ingression followed by CWFS4 (C: 70 %,W: 10%, F: 10%, S: 10%), CWf (C: 85%, W: 10%, F: 5%), CWfS1 (C: 82.5%, W: 10%,F: 5%, S: 2.5%), CwF (C: 85%, W: 5%, F: 10%), CWFS3 (C: 72.5%, W: 10%, F: 10%, S: 7.5%), CwfS2 (C: 85%, W: 5%, F: 5%, S: 5%), CWFS1 (C: 87.5%, W: 10%, F: 10%, S: 2.5%), CWF (C: 80%, W: 10%, F: 10%), CwfS1 (C: 87.5%, W: 5%, F: 5%, S: 2.5%), CwFS2 (C: 80%, W: 5%, F: 10%, S: 5%), CwFS1 (C: 82.5%, W: 5%, F: 10%, S: 2.5%) and Cwf (C: 90%, W: 5%, F: 5%) respectively. This analysis clearly shows that CWf is the best mix which offers the maximum resistance against Chloride ion ingression if only WMF and flyash are to be admixed into the normal SCC. Similar study has been conducted by Wittman [171] on normal concrete, and he has suggested that chloride ion penetrability drops highly when 8% microsilica is incorporated in control concrete, at the age of 28 days. For flyash, this level of improvement takes longer time i.e. at 120 days. But one thing is very clear from the present laboratory studies conducted, admixing of flyash, wollastonite microfiber and microsilica enhanced the resistance against the chloride ion penetration.

Table 4.27 Percentage Chloride Ion Penetration at Different Durations

Mix	30 days	60 days	90 days	Mix	30 days	60 days	90 days	Mix	30 days	60 days	90 days
C	0.42	0.68	0.82	CF1	0.46	0.67	0.71	CW1	0.41	0.56	0.64
Cwf	0.30	0.43	0.48	CF2	0.22	0.32	0.37	CW2	0.29	0.44	0.47
CwfS1	0.23	0.35	0.38	CF3	0.15	0.24	0.27	CW3	0.10	0.18	0.20
CwfS2	0.26	0.32	0.34	CFS1	0.40	0.56	0.63	CWS1	0.40	0.58	0.64
CWf	0.15	0.24	0.28	CFS2	0.33	0.50	0.50	CWS2	0.30	0.46	0.51
CwF	0.18	0.30	0.32	CFS3	0.29	0.42	0.48	CWS3	0.27	0.41	0.43
CwFS1	0.29	0.39	0.42	CFS4	0.20	0.30	0.33	CWS4	0.24	0.37	0.42
CWfS1	0.18	0.28	0.31	CFS5	0.29	0.43	0.45	CWS5	0.38	0.54	0.61
CwFS2	0.26	0.34	0.38	CFS6	0.28	0.43	0.45	CWS6	0.16	0.26	0.29
CWfS2	0.16	0.23	0.25	CFS7	0.26	0.37	0.39	CWS7	0.08	0.18	0.23
CWF	0.29	0.35	0.37	CFS8	0.15	0.24	0.25	CWS8	0.05	0.13	0.16
CWFS1	0.26	0.33	0.35	CFS9	0.31	0.47	0.48	CWS9	0.36	0.51	0.56
CWFS2	0.20	0.32	0.35	CFS10	0.30	0.45	0.46	CWS10	0.14	0.24	0.26
CWFS3	0.20	0.30	0.33	CFS11	0.27	0.39	0.44	CWS11	0.01	0.11	0.13
CWFS4	0.17	0.26	0.28	CFS12	0.09	0.16	0.17	CWS12	0.01	0.07	0.10

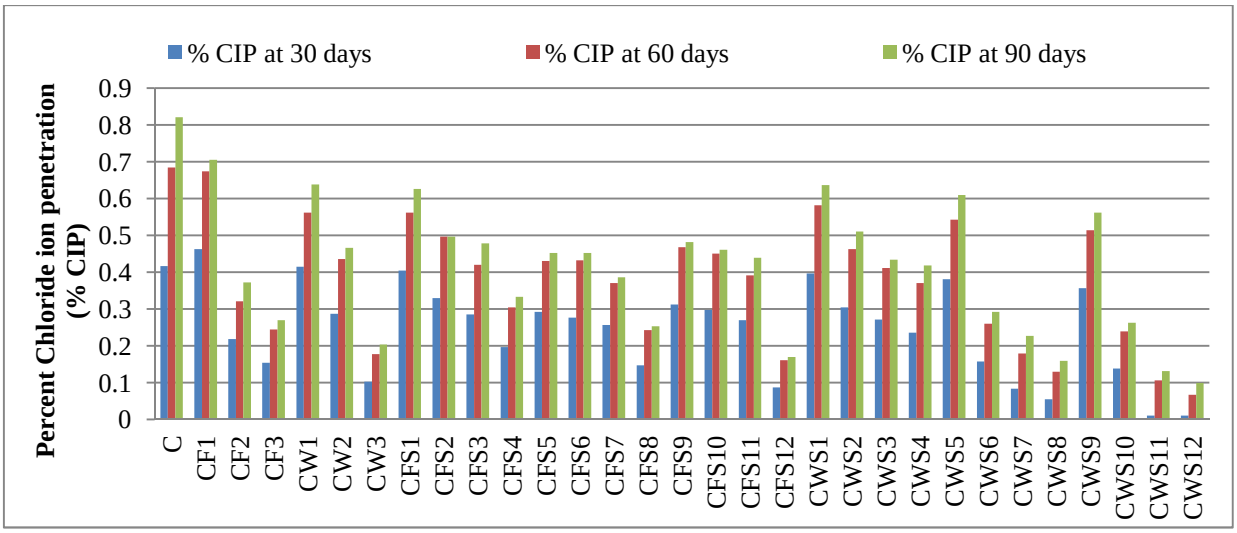

Fig 4.145 Chloride ion penetration of normal, binary, and ternary concrete mixes

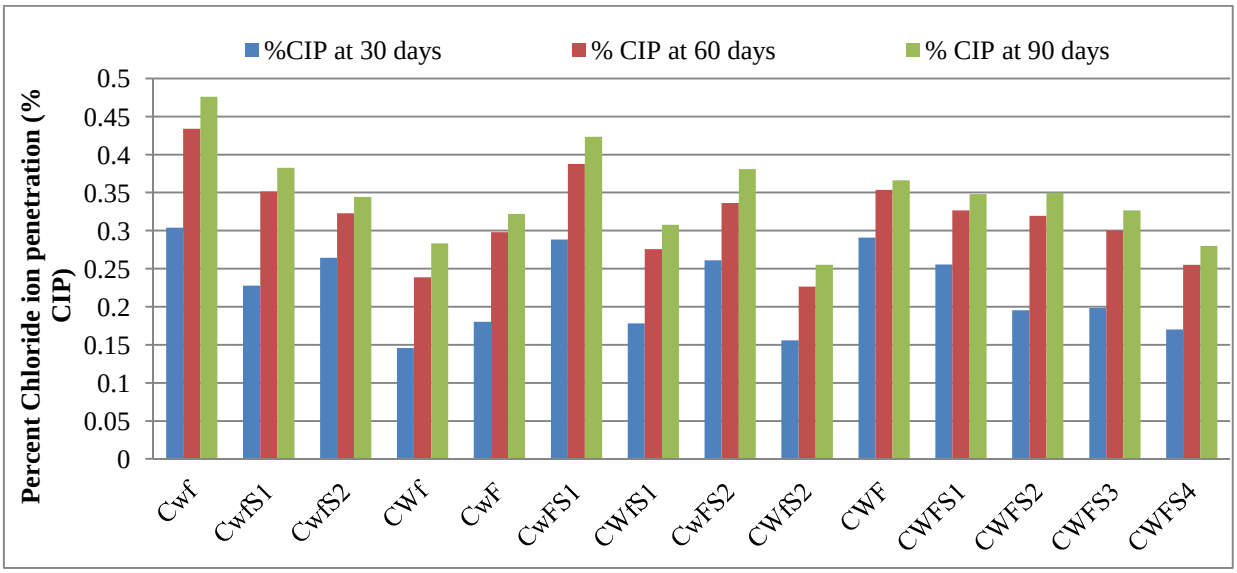

Fig 4.146 Chloride ion penetration of combined concrete mixes

4.5.8 Permeability

In concrete, the value of the coefficient of permeability decreases considerably with a decrease in the water-cement ratio: over the range of water-cement ratios of 0.75 to 0.26, the coefficient decreases by upto 4 orders of magnitude [175] and over the range of 0.75 to 0.45, by 2 orders of magnitude.

At a water-cement ratio of 0.45, the coefficient is typically 10^{-11} or 10^{-12} m/s; permeability of an order of magnitude lower than the last value is considered to represent

concretes with a very low permeability. There is a considerable increase in the permeability at water-cement ratios in excess of about 0.4. In the vicinity of this water-cement ratio, the capillaries become segmented so that there is a substantial difference in permeability between mature cement pastes with water cement ratio below 0.4 and those with higher water-cement ratios. This difference has implications for ingress of aggressive ions into concrete. As regard to the present study, SCC mixes were prepared at water-cement ratio of 0.36 with VMA to achieve desirable flow value suitable for old pavement quality concrete rehabilitation. In addition, present study incorporates three different admixtures into the normal SCC mix to judge their efficacy as a cementitious material. Therefore, it is quite obvious to note that incorporation of these microfine materials would affect the properties of normal cement paste considerably, efforts have been made to conduct permeability test to substantiate the chloride ion penetration test conducted. The observations made out of laboratory are presented in Table 4.28 and their relevant graphical representation are depicted in Figs. 4.147, 4.148 & 4.149 for normal & binary concretes, normal & ternary concretes and combined concrete mixes respectively. Fig. 4.147 clearly depicts that coefficient of permeability of concrete decrease as the percentage of flyash and WMF part replacement increases. The percentage reductions are 14.13%, 32.07% and 37.23% when flyash was admixed @ 10%, 20% & 30% respectively with respect to that of normal concrete. Similarly, for WMF admixed concretes they are 48.33%, 50.15% and 59.12% respectively with respect to normal concrete.

With time, the hydration of cement particles generate CH which increase the alkalinity of pore solution and flyash starts reacting at a higher rate. Generally the rate of flyash hydration is very low in comparison to that of cement and this rate keeps on fluctuating with solution alkalinity. Because of the reduction in permeability of concrete on maturity, there is lesser ingress of chloride ions into the concrete [25].

Khayat & Aitcin [67] had conducted durability study on concrete containing 5% microsilica and reported that coefficient of permeability reduces by three orders of magnitude w.r.t. normal concrete. Microsilica reduces the permeability of transition zone around the aggregate particles, as well as the permeability of the bulk paste. The reduced permeability also reduces the chloride ion ingress into the concrete. Also, Thomas et al. [167] have

suggested that group of admixtures taken together to form a ternary blend offered better resistance to permeability and penetration of chloride ions.

Least coefficient of permeability is being offered by CWS12 followed by CWS8 for wollastonite and microsilica admixed concrete. Similarly, CFS12 is the mix which offered the least coefficient of permeability, followed by CFS7, for flyash and microsilica admixed concrete. Their percentage reductions are 98.52%, and 89.24%, for concrete mixes containing both wollastonite and microsilica together, with respect to normal concrete. Similarly for flyash admixed concrete, these values are 88.09%, & 81.16% respectively for CFS12 & CFS7. But if we look at the combined concrete mixes performances shown in Fig. 4.57, maximum resistance against permeability of water is being offered by CWFS4 followed by CWfS2, CWFS3 and CWFS2; only four top mixes are considered. Their percentage reductions are 87.61%, 85.71%, 85.33% and 84.04%, respectively with respect to that of normal concrete. Out the present data analysis, it is learnt that inclusion of WMF altered the cement paste properties and hence could bring down the coefficient of permeability of concrete significantly as this material could reduce the lime content (manifested from XRD test) and hence better grain size & pore size refinement exhibits. Flyash showed less pozzolanic action than WMF as a result of which pore refinement takes placed in slower rate and hence the resistance against water permeability is also slightly inferior to WMF admixed concretes. But inclusion of microsilica brought down coefficient of permeability significantly in comparison to WMF and flyash. This was mainly due to its ultra fine particles and high pozzolanic reactivity, excellent reorientation of cementitious particles took place physically and chemically its impart to produce more amount of C-S-H gels by depleting CH compounds and created stronger bond at the interface of aggregates and cement paste as a result of which significance reduction in coefficient of permeability was noted.

Table 4.28 Permeability Values of Concrete Mixes after 28 Days

Mix	Permeability (cm/sec)	Mix	Permeability (cm/sec)	Mix	Permeability(cm/sec)
C	6.58E-09	CF1	5.65E-09	CW1	3.40E-09
Cwf	5.15E-09	CF2	4.47E-09	CW2	3.28E-09
CwfS1	4.59E-09	CF3	4.13E-09	CW3	2.69E-09
CwfS2	4.12E-09	CFS1	3.21E-09	CWS1	2.30E-09
CWf	3.29E-09	CFS2	2.74E-09	CWS2	1.67E-09
CwF	3.51E-09	CFS3	2.11E-09	CWS3	1.28E-09
CwFS1	2.79E-09	CFS4	1.86E-09	CWS4	9.95E-10
CWfS1	2.22E-09	CFS5	2.47E-09	CWS5	1.85E-09
CwFS2	2.20E-09	CFS6	1.52E-09	CWS6	1.28E-09
CWfS2	9.40E-10	CFS7	1.24E-09	CWS7	9.98E-10
CWF	2.18E-09	CFS8	8.37E-10	CWS8	7.08E-10
CWFS1	1.64E-09	CFS9	1.77E-09	CWS9	1.58E-09
CWFS2	1.05E-09	CFS10	1.15E-09	CWS10	9.92E-10
CWFS3	9.65E-10	CFS11	9.06E-10	CWS11	5.16E-10
CWFS4	8.15E-10	CFS12	7.84E-10	CWS12	9.75E-11

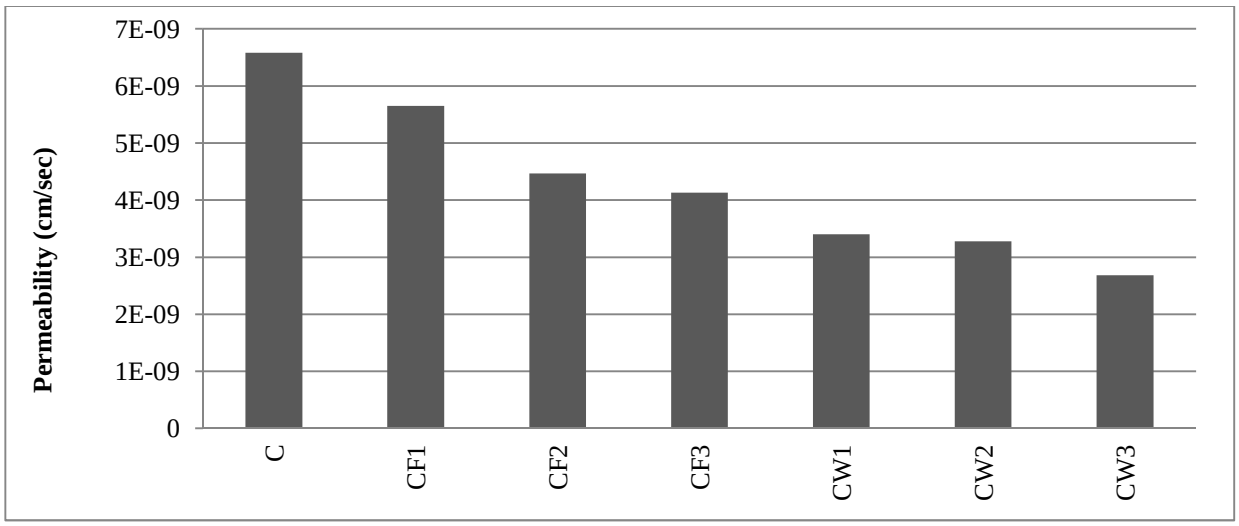

Fig 4.147 Permeability of normal and binary concrete mixes

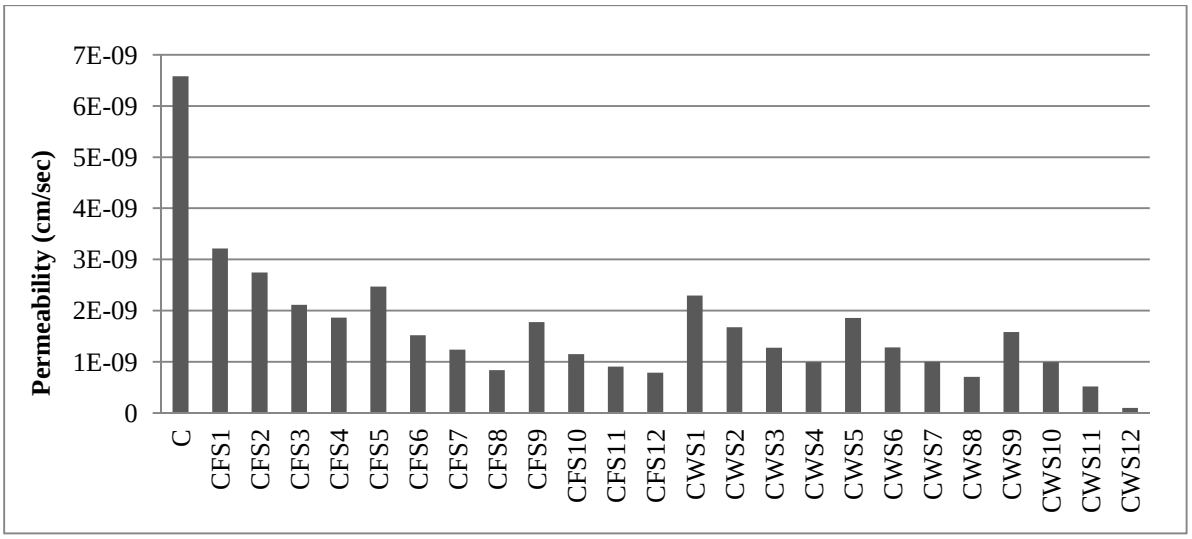

Fig. 4.148 Permeability of normal and ternary concrete mixes

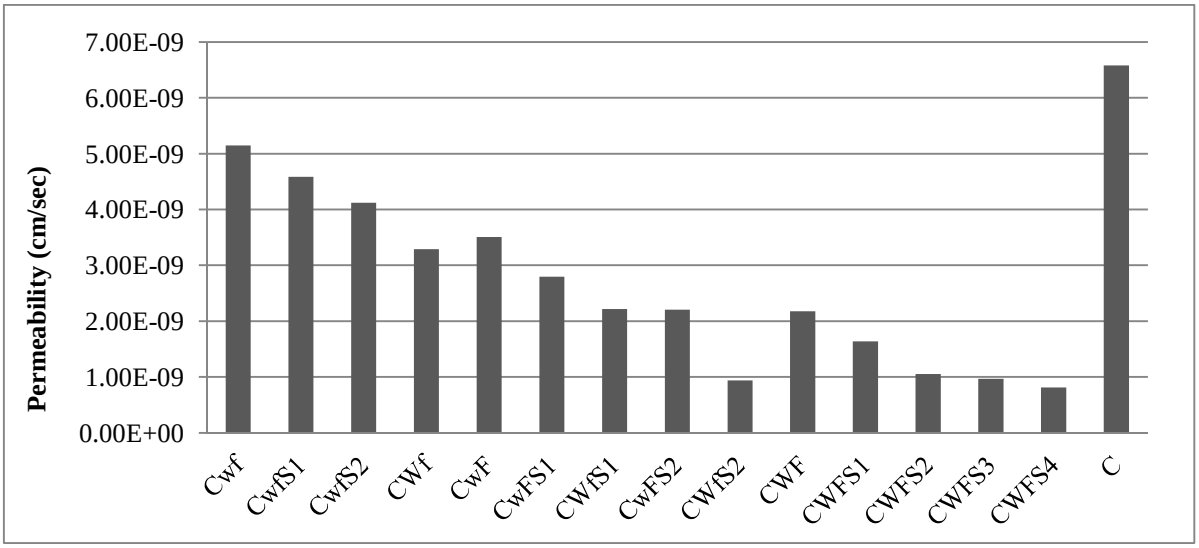

Fig. 4.149 Permeability of combined concrete mixes

4.6 RELATIONSHIP AMONGST PROPERTIES OF SCC

The relationship between the compressive strength & modulus of elasticity, and compressive strength & flexural strength were determined for the mixes. Since the 45 mixes were having different matrix compositions, establishing a general equation for all admixtures together was not possible.

Hence, in the present analysis, effort was made to establish the relationship for five cases: cement+ flyash, cement+WMF, cement+ flyash+ microsilica, cement+ WMF+ microsilica, and cement+ WMF+ flyash+ microsilica.

Since the binary mixes containing either flyash or WMF as an admixture did not have enough sample size, they were not taken into consideration as it would make no sense. Hence, those three cases were excluded.

The methods proposed by Noguchi et al. [115] and Arioglu et al. [7] were adopted for establishing the aforementioned relationships. The details of the relationship established for the mixes are presented in Table 4.29.

Table 4.29 Relationship between mechanical properties of SCC

Relationship	Modulus of elasticity (E) with Compressive strength (σ)	Compressive strength (σ) with Flexural strength (f_{cr})
Cement+Flyash+ microsilica	$E = 14.46\pm^{0.3} - 28.81$, R^2=0.99	$f_{cr} = 1.391\pm^{0.5} - 4.836$, R^2=0.99
Cement+WMF+ microsilica	$E = 27.93\pm^{0.4} - 107.2$, R^2=0.998	$f_{cr} = 1.462\pm^{0.5} - 5.602$, R^2=0.99
Cement+Flyash+ WMF+microsilica	Good correlation could not be achieved	$f_{cr} = 0.66\pm^{0.5} - 0.0129$, R^2=0.99

The relationship between modulus of elasticity and compressive strength of the mixes indicate , that both flyash-microsilica and WMF–microsilica admixed ternary mixes have lower modulus of elasticity than normal concrete. No correlation could be developed for combined mixes, as these mixes exhibit high variation of compressive strength with respect to modulus of elasticity. This variation was generated on account of variable stiffness of paste in different combined mixes, due to large amount of unreacted flyash in the mix.

The relationship between flexural strength and compressive strength exhibits good correlation for all the mixes, because both flexural and compressive strength were not significantly affected by the increased amount of non-stiff volume paste. They were more dependent on paste porosity and strength of interfacial transition zone.

4.7 RELATIONSHIP BETWEEN SCC AND MORTAR

4.7.1 Compressive Strength Relationship

Figs. 4.150-4.152 presents the relationship between compressive strength of fly ash admixed concrete and flyash admixed mortar obtained at the age of 28 days moist curing. Mathematical analysis of data shows a fair relationship between compressive strength of mortar and concrete as shown in Fig.4.150. But WMF admixed mortar and concrete maintained good relationship between them as can be seen from Fig.4.151. This was due to considerable improvement in the strength of mortar than the concrete imparted by WMF. But for combined mixes, both mortar and concrete do not exhibit good relationship (Fig.4.152).

The correlation curves between different corresponding concrete and mortar mixes obtained for 28 days strength compressive strength.

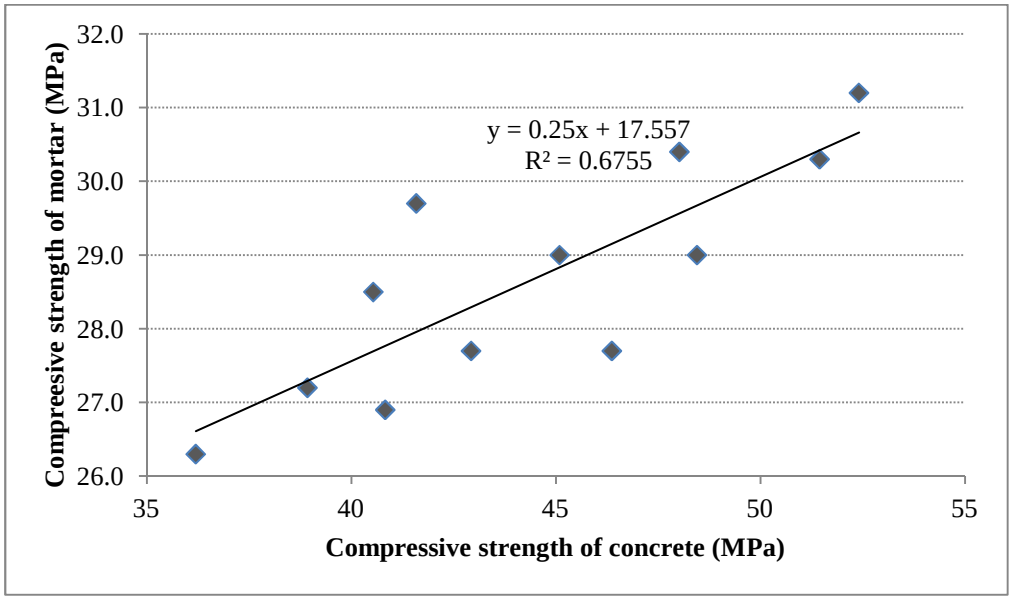

Fig. 4.150 Relationship between compressive strength of flyash-microsilica admixed concrete & mortar

A medium correlation in case of flyash-microsilica admixed mortar mixes is on account high improvement in ITZ, but a low improvement in paste strength. Since, both ITZ

and paste strength control the compressive strength, therefore in this case the correlation comes out to be average.

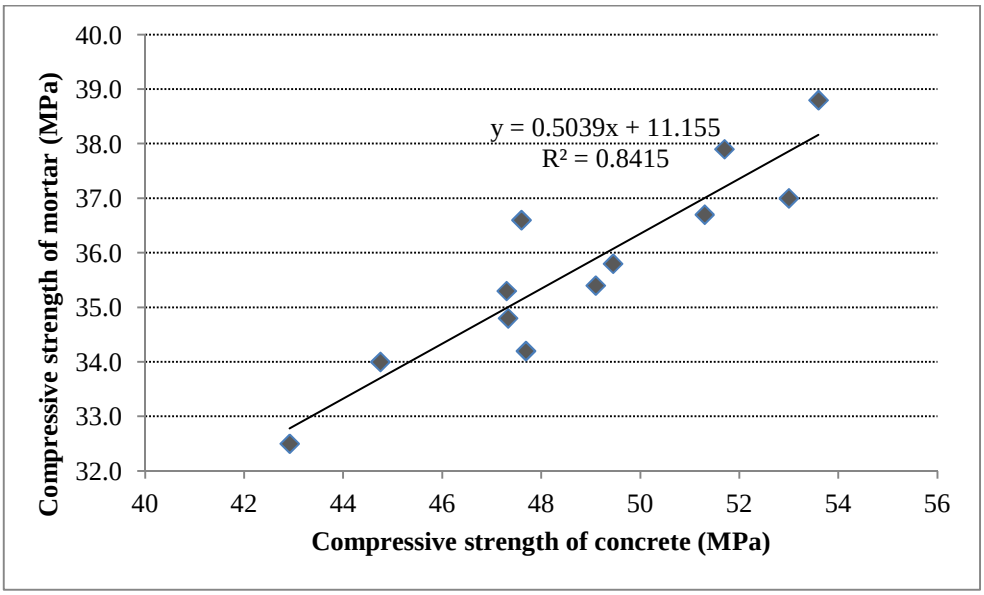

Fig 4.151 Relationship between compressive strength of WMF-microsilica admixed concrete & mortar

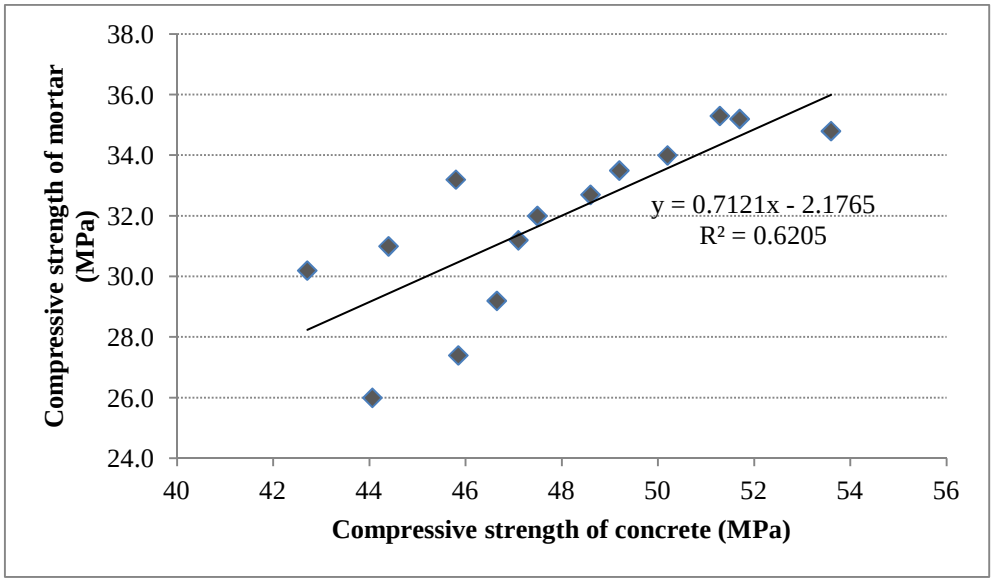

Fig 4.152 Relationship between compressive strength of combined concrete & mortar

4.7.2 Splitting Strength Relationship

Figs. 4.153-4.155 entails the mathematical relationship between splitting tensile strength of flyash admixed concrete and flyash admixed mortar. The splitting tensile strength of concrete and mortar maintained linear relationship and has good correlation between them indicating considerable improvement in the ITZ of the concrete. Whereas for WMF admixed concrete and WMF admixed mortar, coefficient of regression is very low hence considered no good correlation is exist between the aforesaid parameters (Fig.4.154). But for combined concrete mixes (cement:wollastonite:flyash:microsilica) the mathematical relationship shows that splitting tensile strength between mortar and concrete maintained a fair relationship as reasonable regression coefficient exhibits (Fig.4.155). This is caused mainly due to the improvement of ITZ, influenced by the presence of flyash as manifested from SEM study.

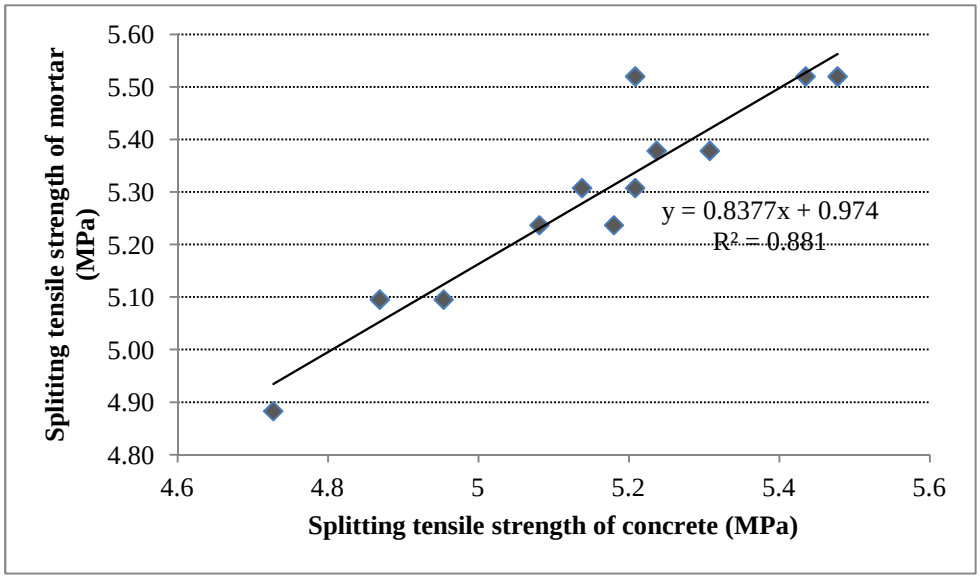

Fig 4.153 Relationship between splitting tensile strength of flyash-microsilica admixed concrete & mortar

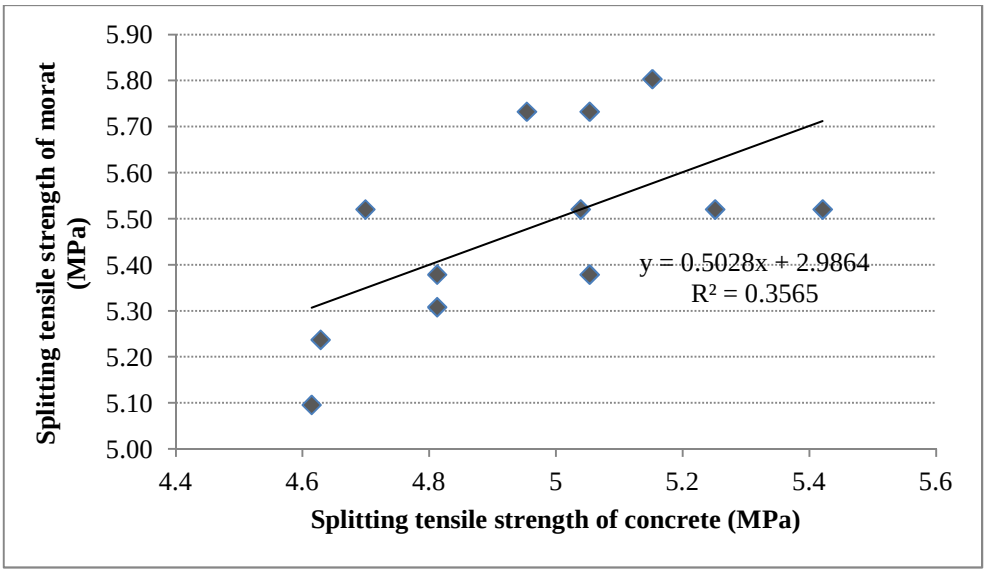

Fig 4.154 Relationship between splitting tensile strength of WMF-microsilica admixed concrete & mortar

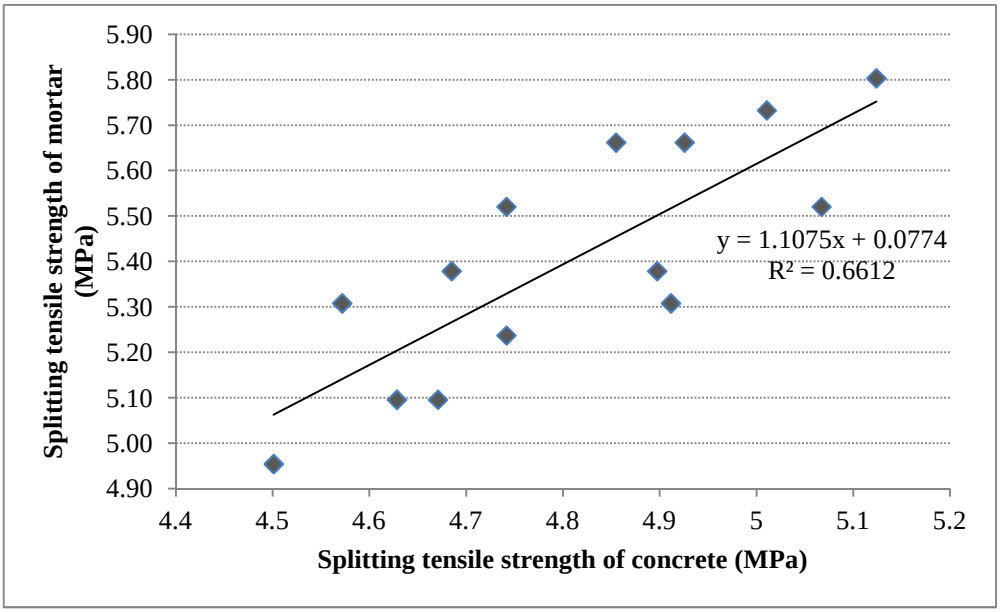

Fig 4.155 Relationship between splitting tensile strength of combined concrete & mortar

4.7.3 Flexural Strength Relationship

In reinforced concrete construction the strength of the concrete in compression is only taken into consideration. The tensile strength of concrete is generally not taken into consideration. But the design of pavement quality concrete (cement concrete pavement slab)

is often based on the flexural strength of concrete. It is imperative to assess the flexural strength of concrete either from compressive strength or independently. Also, in order to understand the influence of mortar in the development of flexural strength of concrete with or without admixtures, efforts have been made to establish correlation between this parameter. Figs. 4.156-4.158 present the mathematical analysis of flexural strength between the performances of mortar and concrete. Fig. 4.156 shows a strong linear relationship between mortar's flexural strength and concrete's flexural strength with a good coefficient of regression value indicating appreciable improvement in paste properties and ITZ due to presence of flyash. This is true for the case of WMF admixed concrete also as it maintains linear relationship with a strong coefficient of regression nearing to unity (Fig. 4.157). But Fig.4.158 strongly indicated that no good correlation exhibits between flexural strength of combined mix (C: W: F: S) concretes and mortar as revealed by the low regression coefficient.

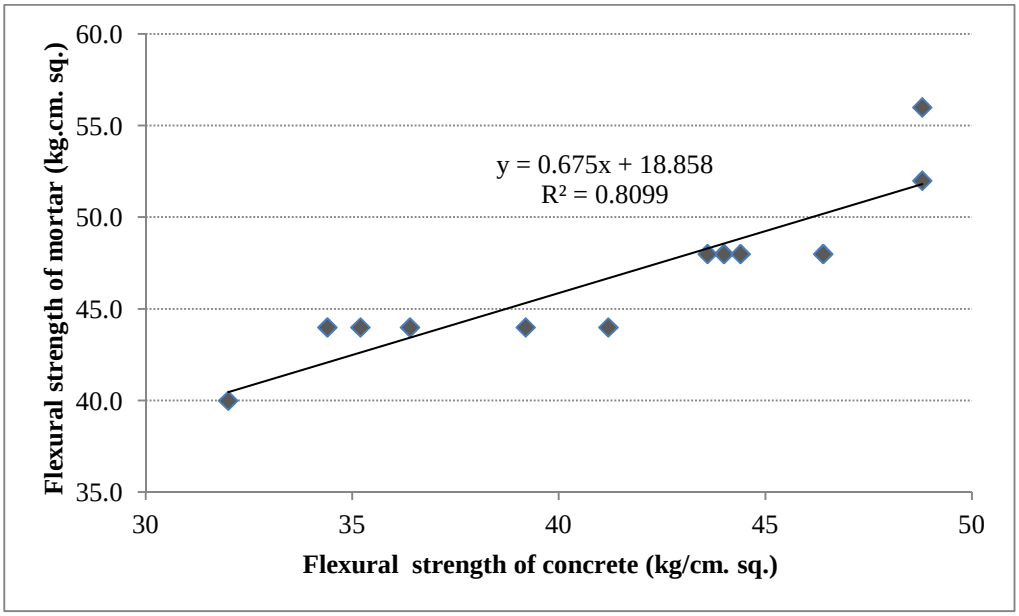

Fig 4.156 Relationship between flexural strength of flyash-microsilica admixed concrete and mortar

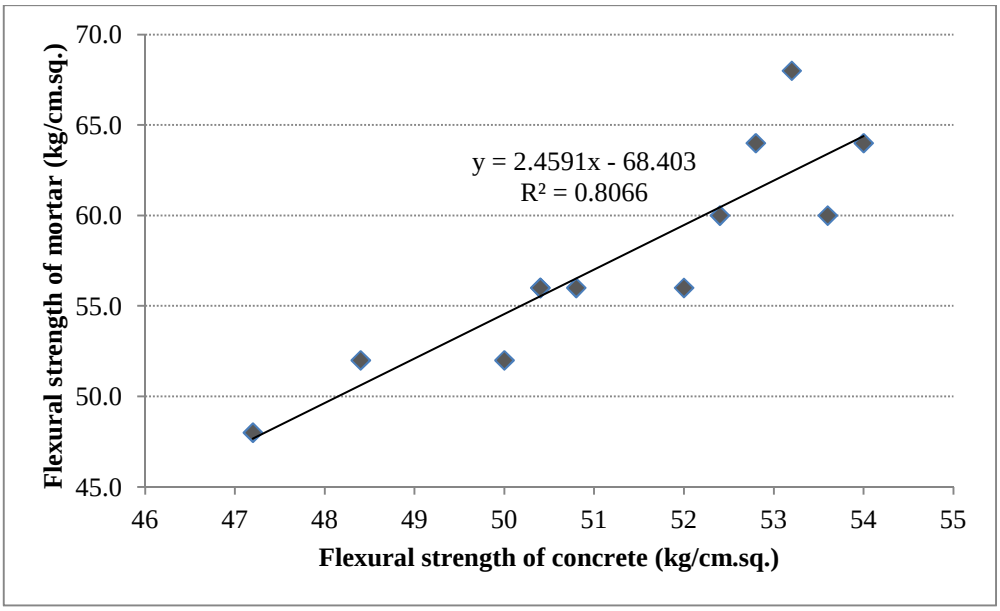

Fig 4.157 Relationship between flexural strength of WMF admixed concrete and mortar

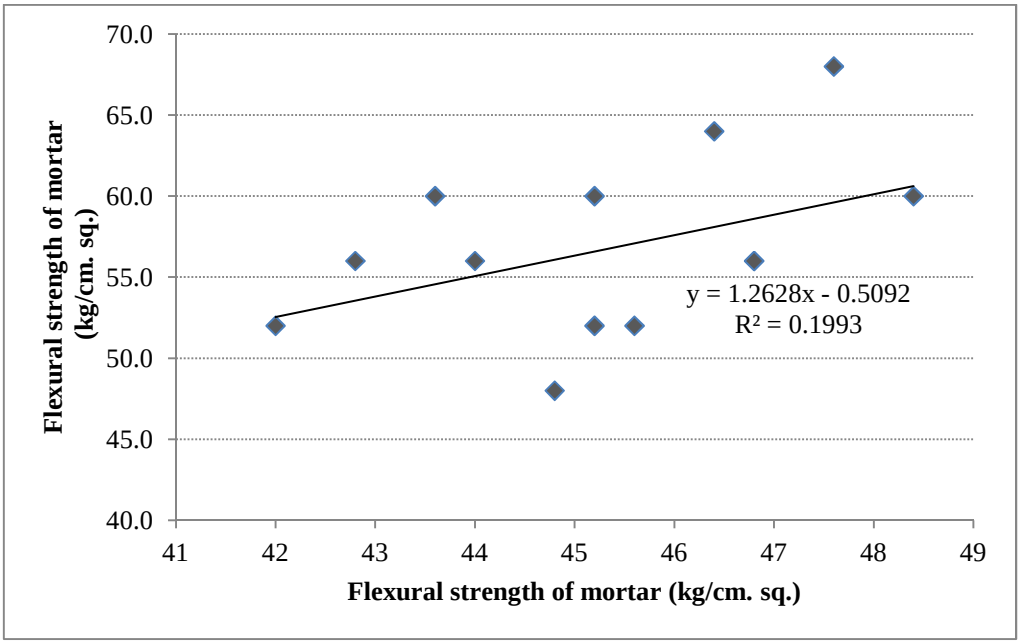

Fig 4.158 Relationship between flexural strength of combined concrete and mortar

4.7.4 Relationship in Modulus of Elasticity

There is no doubt that the modulus of elasticity increases with an increase in the compressive strength of concrete, but there is no agreement on the precise form of the

relationship. It has been well established that the modulus of elasticity of concrete is affected by the modulus of elasticity of the aggregate and by the volumetric proportion of aggregate in the concrete. But the present effort is to check closeness of modulus of elasticity of concrete and mortar with or without admixtures. Based on the mathematical relationship established between modulus of elasticity of mortar and concrete, it clearly indicates that no good correlation can be established between the modulus of elasticity of concrete and mortar irrespective of types of admixtures and their content as may be seen from Figs. 4.159-4.161. This may be due to creation of more ITZ, influenced by the higher surface area of admixtures, as a result of which affects the distribution of stresses. More is the ITZ, more irregular would be the distribution of the stresses and lesser would be the stiffness of the concrete.

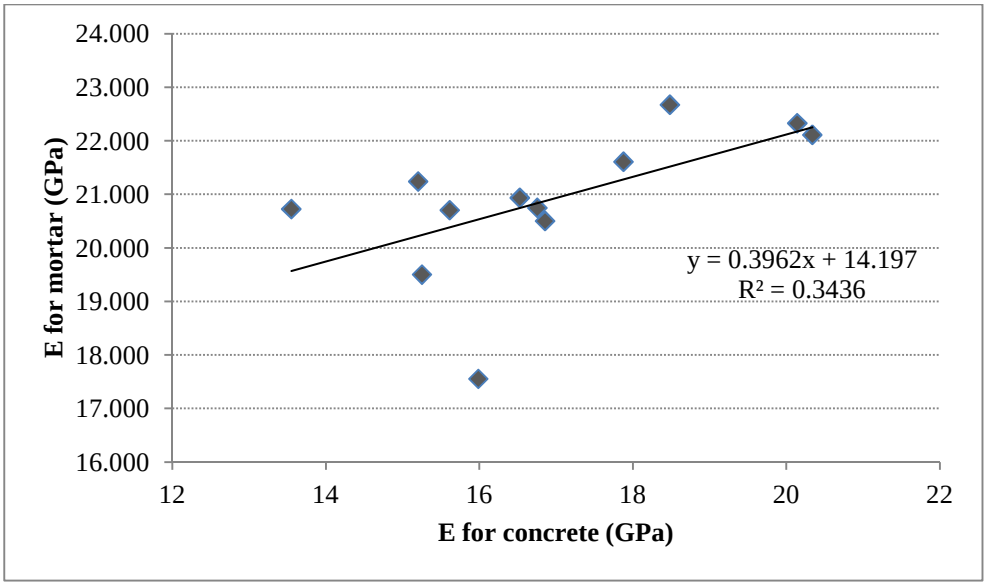

Fig 4.159 Relationship between modulus of elasticity of flyash-microsilica admixed concrete and mortar

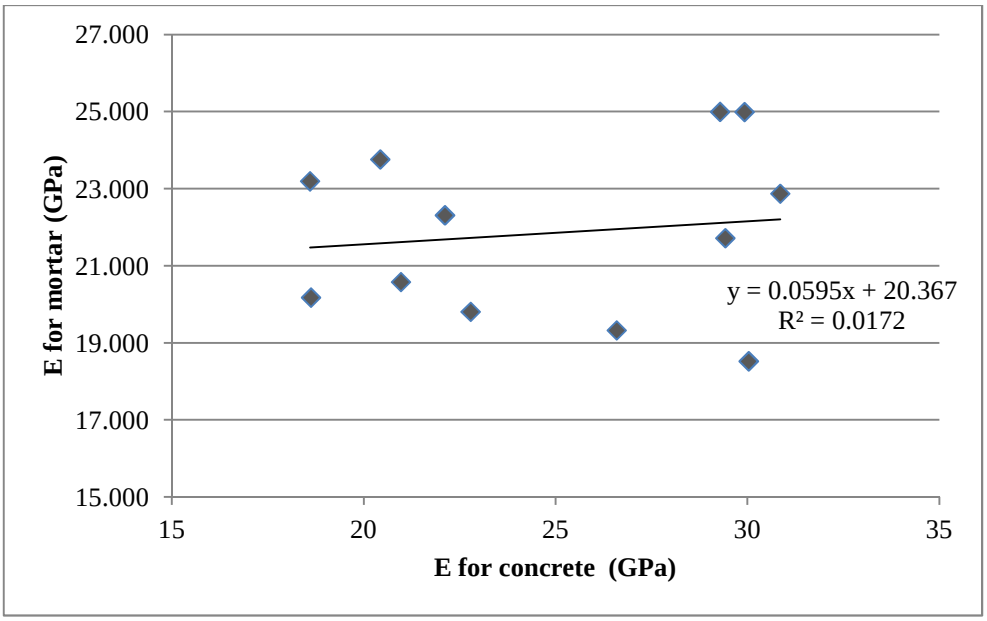

Fig 4.160 Relationship between modulus of elasticity of WMF-microsilica admixed concrete and mortar

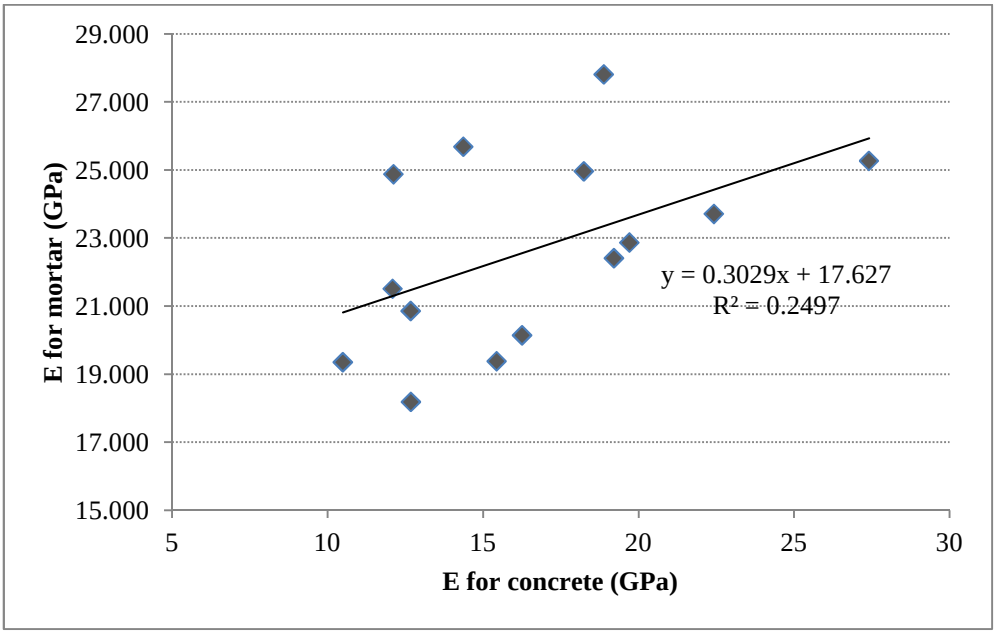

Fig 4.161 Relationship between modulus of elasticity of combined concrete and mortar

A very low value of correlation between the modulus of elasticity of concrete and mortar mixes, is on account of creation of more ITZ due to higher surface area of admixtures. even though the ITZ is developed with full bond strength caused by admixtures

like flyash and microsilica but, still it is the presence of the surface area of ITZ which affects the distribution of stresses. More is the ITZ, more irregular would be the distribution of the stresses and lesser would be the stiffness of the concrete.

5. FINITE ELEMENT MODELLING AND COST ANALYSIS

5.1 GENERAL

Efforts have been made to study the feasibility of using wollastonite micro fiber, flyash and microsilica for producing ideal SCC mix for PQC rehabilitation work. In the present laboratory study, total 45 (Forty five) concrete mixes were established including normal concrete to evaluate the efficacies of WMF, flyash and microsilica as a part of binder in SCC. After having a judicious examination of rheological & mechanical properties and durability properties of hardened SCC, it was found that SCC containing both WMF & microsilica produced favourable results. As there were 12 (twelve) different combinations of WMF and microsilica; the best combination i.e. CWS6 (Cement: 70%; WMF: 20%; S:5%) has been selected for the purpose of rehabilitation of PQC.

In this context, it was essential to create a pavement prototype in the pavement testing hall in order to evaluate the two important design parameters, i.e. load transfer efficiency and fatigue life consumption of the prototype. Deflections at top of the slab fiber and flexural stresses at the bottom fiber of PQC slab were observed under static loading condition using plate load test. The aforesaid tests were conducted for normal non-rehabilitate PQC, normal rehabilitate PQC and PQC rehabilitate with microfiber reinforced SCC. Sufficient numbers of dial gauges were employed for measuring the deflections at the top of the PQC slab under different loading conditions. The details of loading conditions and deflections measured at different points are presented in Table 5.1. At the interior of the slab, higher loadings were applied because the slab at this location sustains higher stress and hence to cause an appreciable deflection of the slab, it was mandatory to impose 11.25 tonnes at the initial stage of loading itself. Whereas, for edge and corner loading, the starting load chosen for the study were 5.0 tonnes and 2.5 tonnes respectively. Thus, the maximum load which could be applied at a certain location of the pavement was different for different locations, the minimum being at the corner.

Depending upon the maximum load which could be applied, the load intervals for gauging deflections were decided. Therefore, the load values at which the deflections were taken did not bear constant difference between each other.

As the existing laboratory set up does not permit us to measure the flexural stresses experienced by the PQC slab at the bottom fiber, it was unanimously decided to use the deflection data measured at the top fiber of the slab for validating the model from which flexural stresses of the PQC were established.

A finite element model (FEM) has been created using ABAQUS application. For obtaining flexural stresses at the bottom of the PQC slab, validation has been done considering only edge loading condition. The Chi-Square test was performed to check the goodness of fit between the prototype and the model. From the above check, it was found that the prototype and model bears good fitness for normal PQC and microfiber reinforced SCC. Whereas, for PQC rehabilitate with normal concrete mix could not be established goodness of fit between the model and prototype due to poor bonding at the interfaces of old normal PQC and newly laid normal PQC mix inspite of maintaining good quality control. This is also true for dowel bar system and newly laid PQC mix.

After the validation of the model, flexural stresses at the bottom of the PQC slab were found out for both normal concrete and microfiber reinforced SCC rehabilitated pavement. Accordingly, stress ratios were worked out for both the cases and their respective fatigue life consumption were determined. The full model of the prototype established and constructed in the pavement testing hall is depicted in Fig. 5.1.

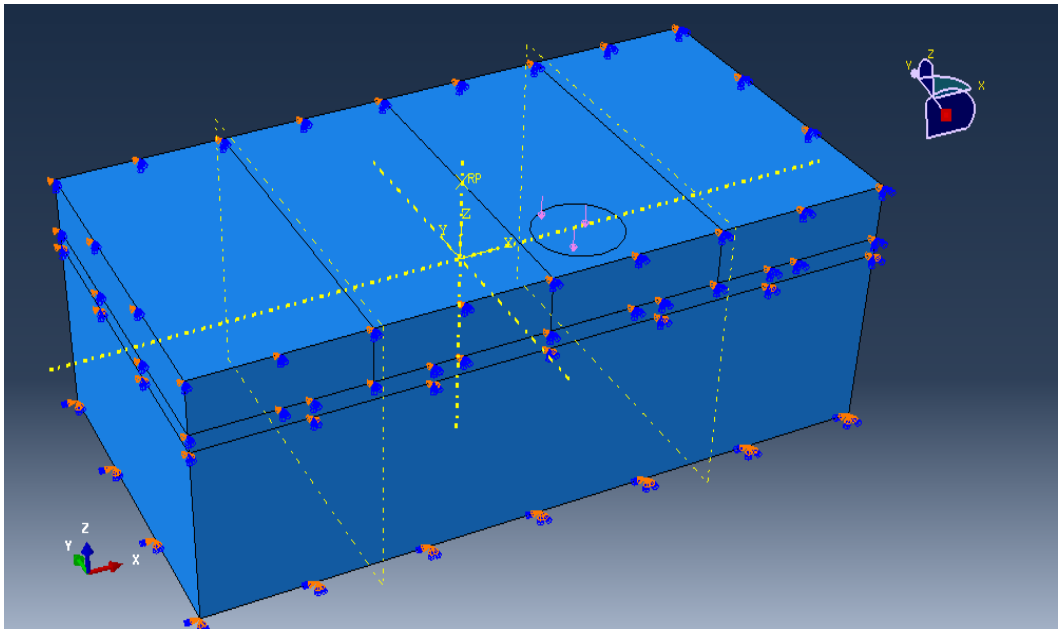

Fig 5.1 Full model of PQC

The model as well as prototype consists of two panels laid in the direction of traffic flow, having a contraction joint in between. The panel size is 1800×1800×300 mm^3, dowel bars of ϕ 35mm and 500mm length were embedded as wire elements in the model, and a dry lean concrete (DLC) layer of 100 mm thickness was sandwiched between PQC slab and properly compacted subgrade layer.

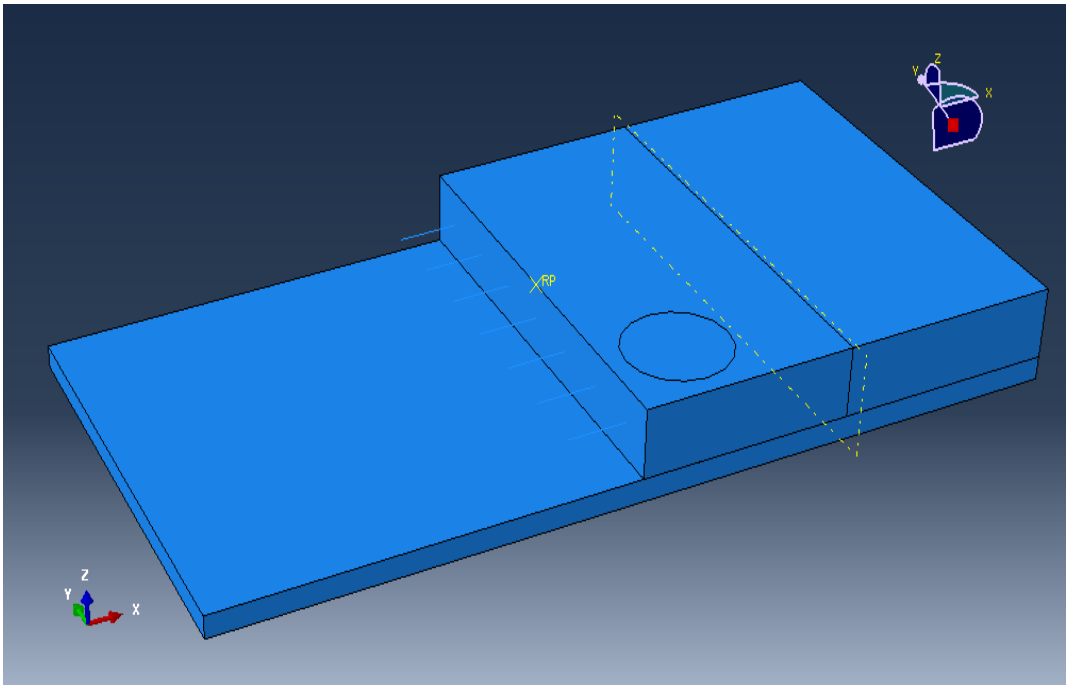

Fig 5.2 Model showing the DLC, one panel of PQC and dowel bars

Fig. 5.2 shows one panel of PQC wherein dowel bars are embedded within it, and dry lean concrete layer has been introduced beneath the PQC slab. The loading pattern at the edge of the slab is being shown in Fig. 5.2 which is in the form of circular ring having diameter of 45 cm spaced at a distance of 30 cm from both the edges of the panel. The loading was applied by means of circular bearing plate made of steel having 25.4 mm thickness in accordance with IS: 9412.

The division lines in the panel show the area earmarked for different mesh spacing. The half area where load was applied was provided with lesser mesh spacing (50mm inter nodal distance) for ease in converging to the solution, whereas the half panel area away from load was given larger mesh spacing (100mm).

5.2 PLATE LOAD TEST ON PROTOTYPE

Plate load test on three prototype structures was performed. Those were non-rehabilitated normal PQC (NRP), normal PQC rehabilitated pavement (NCRP) and fiber reinforced self-compacted concrete rehabilitated pavement (FRSCCRP).

As discussed in chapter-3, three loading locations i.e. interior, edge and corner have been selected and deflection of the slab was measured from seven different locations for corner loading. Similarly, deflections were noted from six different locations for interior and edge loading maintaining a distance of 300 mm from the edges of the panel. The details of the same are also clearly illustrated in Chapter 3 Fig. 3.12.

The details of numbering of the dial gauges for different locations are illustrated in Fig. 3.12, Chapter-3. Plates 5.1-5.3 entail the conduction of the plate load test.

Plate 5.1 Plate load test on non-rehabilitated normal PQC

Plate 5.2 Plate load test on normal concrete rehabilitated PQC

Plate 5.3 Plate load test on WMF reinforced rehabilitate PQC

In order to simulate better in-service condition, dowel bars system consisting dowel basket was embedded within the concrete mass and was allowed to cure for requisite number of days (28 days). After taking the details of deflections of the aforesaid PQC slab, one third portion of the panel was cut to a half depth of the total pavement thickness. The cutting was made in such a way that the dowel bars are completely separated out from the hardened concrete without disturbing the position of dowel basket so as to treat as a part of retrofitting of the dowel bars. Subsequently, cut portion was infilled with normal concrete mix and properly compacted with the help of vibrators to ensure proper bonding at the interfaces of old PQC slab and newly prepared concrete mix. In a very similar way, rehabilitation work was carried out for fiber reinforced SCC mix too. Deflection readings were obtained for both the cases for further analyses. The deflections measured using the plate load tests are presented in Tables 5.1, 5.2 and 5.3.

Table 5.1 Deflections for Plate load test on non rehabilitated pavement

Interior loading	Deflection in mm at location						
Load (N)	2	3	4	5	6	7	
112500	0.04	0.22	0.12	-0.04	-0.07	-0.05	
250000	0.23	0.43	0.3	-0.1	-0.19	-0.09	
387500	0.47	0.7	0.52	-0.2	-0.33	-0.14	
Edge loading	Deflection in mm at location						
Load (N)	2	3	4	5	6	7	
50000	0.23	0	0	-0.04	0	0	
85000	0.42	-0.05	0	-0.12	-0.02	0	
125000	0.69	-0.09	0	-0.24	-0.05	0	
175000	1.02	-0.16	0	-0.33	-0.14	0	
225000	1.33	-0.2	-0.02	-0.45	-0.25	-0.03	
Corner loading	Deflection in mm at location						
Load (N)	1	2	3	4	5	6	7
25000	0.17	-0.01	0	0	-0.01	0	0
50000	0.38	-0.06	-0.05	0	-0.01	0	0
70000	0.59	-0.12	-0.06	0.02	-0.01	0	0
92500	0.77	-0.18	-0.09	0.07	-0.04	0	0
117500	0.97	-0.27	-0.11	0.13	-0.07	0.02	0.01
145000	1.18	-0.36	-0.14	0.23	-0.08	0.08	0.03
162500	1.39	-0.45	-0.15	0.32	-0.09	0.12	0.06

Table 5.2 Deflections for Plate load test on normal concrete rehabilitated pavement

Interior loading	Deflection in mm at location						
Load (N)	2	3	4	5	6	7	
112500	0.06	0.3	0.15	-0.07	-0.13	-0.1	
250000	0.3	0.57	0.37	-0.2	-0.3	-0.16	
387500	0.59	0.88	0.66	-0.4	-0.55	-0.21	
Edge loading	Deflection in mm at location						
Load (N)	2	3	4	5	6	7	
50000	0.28	0	0	-0.07	0	0	
85000	0.53	-0.06	0	-0.19	-0.02	0	
125000	0.89	-0.13	0	-0.34	-0.07	0	
175000	1.28	-0.23	0	-0.45	-0.19	0	
225000	1.61	-0.26	-0.04	-0.58	-0.28	-0.04	
Corner loading	Deflection in mm at location						
Load (N)	1	2	3	4	5	6	7
25000	0.22	-0.01	-0.03	0	-0.01	0	0
50000	0.47	-0.08	-0.07	0.03	-0.02	0	0
70000	0.76	-0.15	-0.1	0.05	-0.03	0.01	0
92500	0.98	-0.23	-0.13	0.09	-0.06	0.03	0.02
117500	1.2	-0.35	-0.16	0.17	-0.09	0.05	0.04
145000	1.48	-0.48	-0.17	0.3	-0.1	0.14	0.06
162500	1.7	-0.59	-0.2	0.39	-0.12	0.19	0.09

Table 5.3 Deflections for Plate load test on FRSCC rehabilitated pavement

Interior loading	Deflection in mm at location					
Load (N)	2	3	4	5	6	7
112500	0.04	0.22	0.12	-0.04	-0.07	-0.05
250000	0.23	0.43	0.3	-0.1	-0.19	-0.09
387500	0.47	0.7	0.52	-0.2	-0.33	-0.14
Edge loading	Deflection in mm at location					
Load (N)	2	3	4	5	6	7
50000	0.23	0	0	-0.04	0	0
85000	0.42	-0.05	0	-0.12	-0.02	0
125000	0.69	-0.09	0	-0.24	-0.05	0
175000	1.02	-0.16	0	-0.33	-0.14	0
225000	1.33	-0.2	-0.02	-0.45	-0.25	-0.03

Corner loading	Deflection in mm at location						
Load (N)	1	2	3	4	5	6	7
25000	0.17	-0.01	0	0	-0.01	0	0
50000	0.38	-0.06	-0.05	0	-0.01	0	0
70000	0.59	-0.12	-0.06	0.02	-0.01	0	0
92500	0.77	-0.18	-0.09	0.07	-0.04	0	0
117500	0.97	-0.27	-0.11	0.13	-0.07	0.02	0.01
145000	1.18	-0.36	-0.14	0.23	-0.08	0.08	0.03
162500	1.39	-0.45	-0.15	0.32	-0.09	0.12	0.06

5.2.1 Load Transfer Efficiency

After obtaining the deflections from the pre-decided gauging locations, efforts have been made to establish equations to find out the load transfer efficiency of the dowel bars provided across the PQC slab for all considered three different cases, under three different loading conditions. This was done by determining the deflections obtained at both ends of the dowel bars. The established equations related to the load transfer efficiency are presented in Table 5.4.

The locations 2-5 signifies loading side edge bar; 3-6 signifies middle bar, and 4-7 signifies non-loading side edge bar as presented in Table 5.4. The ordinate Y in the equation was taken as the deflection on the opposite side of loading, whereas abscissa X was taken as the deflection on the loading side.

Afterwards, a set of deflections was chosen such that the deflections bear uniform difference with respect to each other. Taking these deflections' values as X in the equations, the corresponding Y values were determined, as shown in Tables 5.5 and 5.7. After obtaining the Y values, which are the deflections at the opposite side of loading, the difference between the deflections of the two cases i.e. non-rehabilitated & normal concrete rehabilitated pavement and, non-rehabilitated and fiber reinforced concrete rehabilitated pavement was determined. Tables 5.6 and 5.8 show the difference in the values of deflections between the two cases.

Table 5.4 Relationship between deflections on opposite end of dowel bars

Equations relating deflections for normal concrete rehabilitated pavement			
	Loading side edge bar (2-5)	Middle bar (3-6)	Non loading side edge bar (4-7)
Edge load near bar	$Y=0.059X^2-0.485X+0.056$	$Y=-4.102X^2-0.053X-0.003$	$Y=X$
Corner load	$Y=0.113X^2+0.266X-0.002$	$Y=11.25X^2+1.511X+0.041$	$Y=0.034X^2+0.221X-0.004$
Interior load near bar	$Y=-0.027X^2-0.441X-0.04$	$Y=-0.304X^2-0.364X+0.006$	$Y=0.196X^2-0.375X-0.048$
Equations relating deflections for FRSCC rehabilitated pavement			
	Loading side edge bar (2-5)	Middle bar (3-6)	Non loading side edge bar (4-7)
Edge load near bar	$Y=0.063X^2-0.476X+0.061$	$Y=-5.885X^2-0.167X-0.006$	$Y=2X$
Corner load	$Y=0.112X^2+0.274X+0.004$	$Y=11.19X^2+1.063X+0.008$	$Y=0.710X^2-0.032X$
Interior load near bar	$Y=-0.031X^2-0.217X-0.041$	$Y=0.052X^2-0.734X+0.090$	$Y=-0.032X^2-0.234X-0.038$
Equations relating deflections for Normal concrete pavement			
	Loading side edge bar (2-5)	Middle bar (3-6)	Non loading side edge bar (4-7)
Edge load near bar	$Y=0.055X^2-0.452X+0.058$	$Y=-6.603X^2-0.125X-0.003$	$Y=1.5X$
Corner load	$Y=0.049X^2+0.235X+.001$	$Y=10.64X^2+0.927X+0.006$	$Y=0.631X^2-0.013X$
Interior load near bar	$Y=-0.034X^2-0.200X-0.040$	$Y=0.110X^2-0.643X+0.066$	$Y=-0.012X^2-0.216X-0.023$

Table 5.5 Deflections on opposite end of dowel bars for NCRP and NRP

Deflection (mm)	0.3		0.6		1.05		1.2		1.5	
	Rehab.	Normal	Rehab.	Normal	Rehab.	Normal	Rehab.	Normal	Rehab.	Normal
Loading side edge bar										
Edge load near bar	-0.084	-0.073	-0.210	-0.193	-0.388	-0.356	-0.441	-0.405	-0.539	-0.496
Corner load	0.088	0.076	0.198	0.1596	0.402	0.3018	0.480	0.354	0.651	0.464
Interior load near bar	-0.177	-0.108	-0.320	-0.182	-0.535	-0.305	-0.610	-0.349	-0.764	-0.442
Middle bar										
Edge load near bar	-0.388	-0.635	-1.510	-2.455	-4.581	-7.414	-5.974	-9.661	-9.312	-15.047
Corner load	1.507	1.242	4.998	4.393	14.031	12.710	18.054	16.440	27.62	25.337
Interior load near bar	-0.131	-0.117	-0.320	-0.280	-0.711	-0.488	-0.869	-0.547	-1.224	-0.651
Non loading side edge bar										
Edge load near bar	0.300	0.450	0.600	0.900	1.050	1.575	1.200	1.800	1.500	2.250
Corner load	0.065	0.053	0.141	0.219	0.266	0.682	0.310	0.893	0.404	1.400
Interior load near bar	-0.143	-0.089	-0.2	-0.157	-0.226	-0.263	-0.216	-0.300	-0.170	-0.374

Table 5.6 Difference in the values of deflections for NCRP and NRP

	Loading side edge bar				
Edge load near bar	-15.880	-10.530	-9.057	-8.845	-8.564
Corner load	-15.890	-24.200	-33.174	-35.739	-40.431
Interior load near bar	-63.400	-73.380	-75.158	-74.628	-72.907
	Middle bar				
Edge load near bar	38.863	38.433	38.211	38.172	38.115
Corner load	-21.350	-13.770	-10.391	-9.819	-9.013
Interior load near bar	-11.590	-14.860	-45.808	-58.728	-88.018
	Non loading side edge bar				
Edge load near bar	33.333	33.333	33.333	33.333	33.333
Corner load	-23.580	35.795	61.067	65.269	71.148
Interior load near bar	-60.730	-29.010	14.208	27.955	54.679

Table 5.7 Deflections on opposite end of dowel bars for FRCRP and NRP

Deflection (mm)	0.3		0.6		1.05		1.2		1.5	
	Rehab.	Normal	Rehab.	Normal	Rehab.	Normal	Rehab.	Normal	Rehab.	Normal
Loading side edge bar										
Edge load near bar	-0.076	-0.073	-0.202	-0.193	-0.369	-0.356	-0.420	-0.405	-0.511	-0.496
Corner load	0.096	0.076	0.209	0.160	0.415	0.302	0.494	0.354	0.667	0.464
Interior load near bar	-0.109	-0.108	-0.182	-0.182	-0.303	-0.305	-0.346	-0.349	-0.436	-0.442
Middle bar										
Edge load near bar	-0.586	-0.635	-2.225	-2.455	-6.670	-7.414	-8.681	-9.661	-13.498	-15.047
Corner load	1.334	1.242	4.674	4.393	13.461	12.710	17.397	16.440	26.780	25.337
Interior load near bar	-0.126	-0.117	-0.332	-0.280	-0.623	-0.486	-0.716	-0.547	-0.894	-0.651
Non loading side edge bar										
Edge load near bar	0.600	0.450	1.200	0.900	2.100	1.575	2.400	1.800	3.000	2.250
Corner load	0.054	0.053	0.236	0.219	0.749	0.682	0.984	0.893	1.550	1.400
Interior load near bar	-0.111	-0.089	-0.19	-0.157	-0.319	-0.263	-0.365	-0.300	-0.461	-0.374

Table 5.8 Difference in the values of deflections for FRCRP and NRP

	Loading side edge bar				
Edge load near bar	-4.790	-4.405	-3.759	-3.524	-3.023
Corner load	-26.834	-30.744	-37.580	-39.744	-43.827
Interior load near bar	-0.675	0.044	0.756	0.950	1.301
	Middle bar				
Edge load near bar	7.722	9.380	10.042	10.149	10.298
Corner load	-7.433	-6.411	-5.910	-5.822	-5.697
Interior load near bar	-7.282	-18.373	-27.772	-30.833	-37.327
	Non loading side edge bar				
Edge load near bar	-33.333	-33.333	-33.333	-33.333	-33.333
Corner load	-2.666	-7.768	-9.845	-10.185	-10.659
Interior load near bar	-24.977	-21.030	-21.271	-21.838	-23.262

The difference in the deflections value so obtained, provided a data which could be statistically studied for finding out the reduction in load efficiency of the rehabilitated pavement. The results obtained suggested , that there is 85% probability, that load transfer efficiency is not reduced by more than 30% and 60% for WMF reinforced concrete rehabilitated pavement, and normal concrete rehabilitated pavement respectively. For the same probability, the fiber reinforced rehabilitated pavement yields more load transference than normal concrete rehabilitated pavement. Hence the use of fiber reinforced SCC, improved the load transference of rehabilitated pavement by two times.

5.3 VALIDATION OF THE MODEL

The model was validated from prototype, on the basis of chi square factor. With the use of chi square value, a comparison of the observed deflections from the model, and expected deflections from the prototype could be established. It was difficult for the model to differentiate between non rehabilitated pavement and normal concrete rehabilitated pavement, because in both the cases the concrete had same properties, and upon, that the application assumes ideal conditions of interaction between the old and new pavement.

Deflections under edge loading has only been considered, because this case is the most critical for load transferences as there is weak shoulder support at edge beyond the PQC slab, which proves as an inferior material with respect to concrete for load transference. The deflections in the model at the edge were determined by running the model for same load profile, as was done for prototype. Afterwards, the chi square (χ^2) values were determined for both of the cases as shown in Table 5.9.

Table 5.9 Chi square values for NRP, FRSCC and NCRP rehabilitated pavement

	Model		Prototype		χ^2 value		
Load (N)	Non rehab.	FRSCC rehab.	Non rehab.	FRSCC rehab.	χ^2 (Non rehab.)	χ^2 (FRSCC rehab.)	χ^2 (Normal concrete Rehab.)
50000	0.15	0.18	0.23	0.25	2.78	1.96	6.04
85000	0.34	0.39	0.42	0.47	1.52	1.36	6.81
125000	0.59	0.64	0.69	0.77	1.45	2.19	10.11
175000	0.9	1	1.02	1.13	1.41	1.50	11.28
225000	1.27	1.43	1.33	1.48	0.27	0.17	7.18
					$\Sigma\chi^2$ =7.44	$\Sigma\chi^2$ = 7.18	$\Sigma\chi^2$ =41.42

The value of χ^2 corresponding to 5% level of significance is 9.488 for 4 degree of freedom, which is higher than these values. Hence the model is assumed validated. The model assumes full quality control (all ideal conditions) for construction; therefore the deflections under load for normal concrete rehabilitated pavement obtained from the model are very low in comparison to those, observed from the rehabilitated prototype. Hence, chi square value for this case is greater than 9.488. Therefore, the model is validated only for non-rehabilitated and FRSCC rehabilitated pavements.

5.3.1 Stress Ratio and Fatigue Life Evaluation

Figs. 5.3-5.14 show the images of the stress contour charts of loaded panel of PQC subjected to a set of loads in the model. The loading has been applied on full PQC model; however, in the present analysis only top loaded panel has been shown to provide better clarity. The stress chart on the upper left hand side of the image shows the max and minimum values of the stresses experienced in the panel. The blue portion in the image indicates compression zone and red portion shows tension zone where maximum flexural tensile stresses developed. As may be seen from the chart an average 75% stress value has been shown in the charts. The application does automatically to avoid discontinuity of the contours in the chart. Actually, the stresses are evaluated only at nodal points, but in order to maintain continuity of the contours, smooth variation between contours is evaluated on basis of the condition that the adjacent stresses at the nodes do not vary by more than 25%. Results from two nodes have been averaged should the stress values lie within 75% of each other.

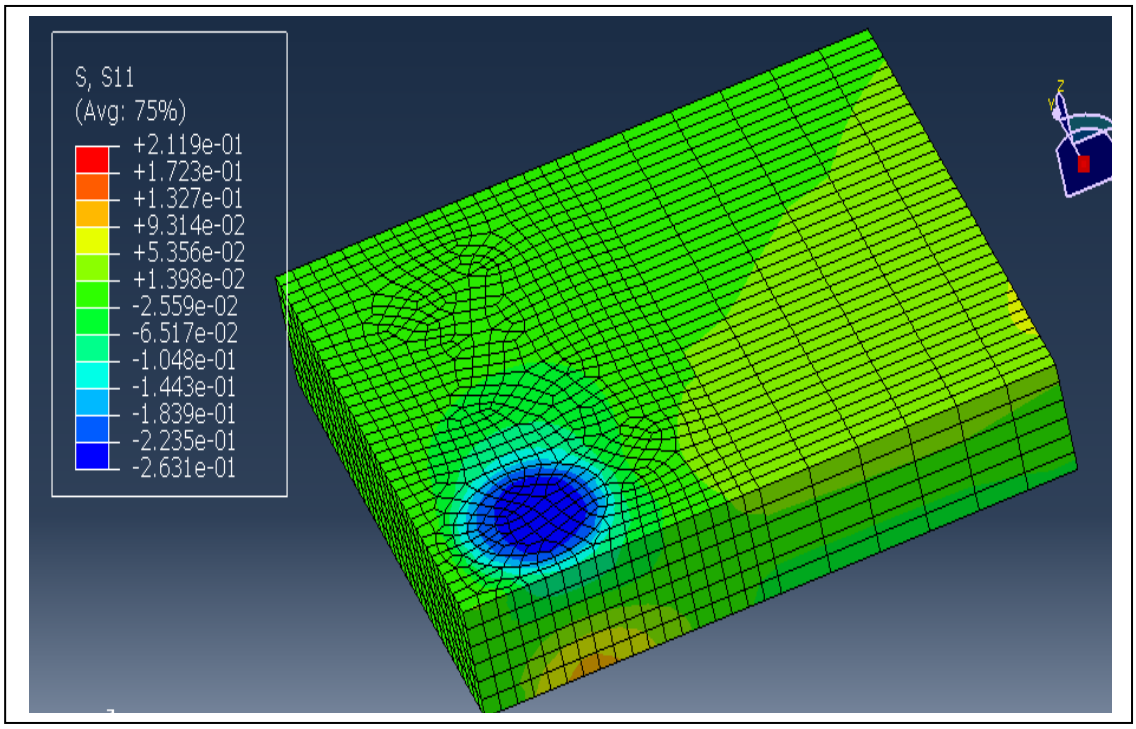

Fig 5.3 Flexural stress in FRSCC rehabilitated panel at 2 tonne load

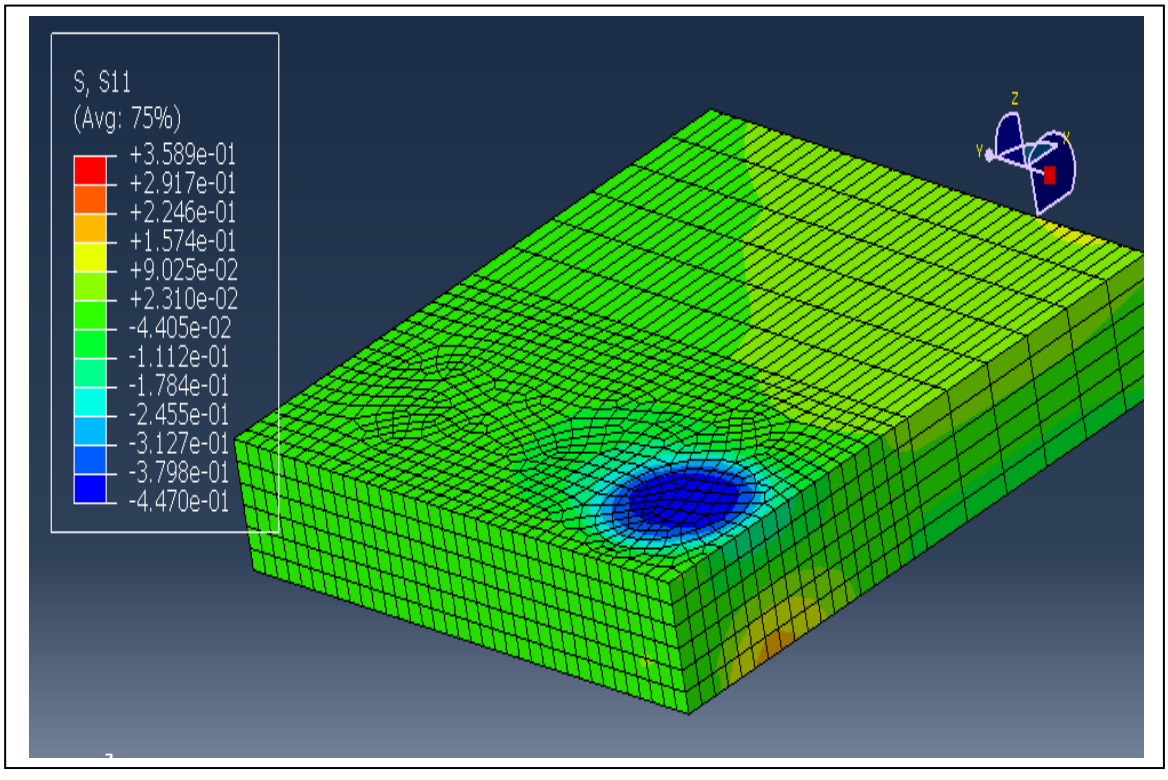

Fig 5.4 Flexural stress in FRSCC rehabilitated panel at 3.4 tonne load

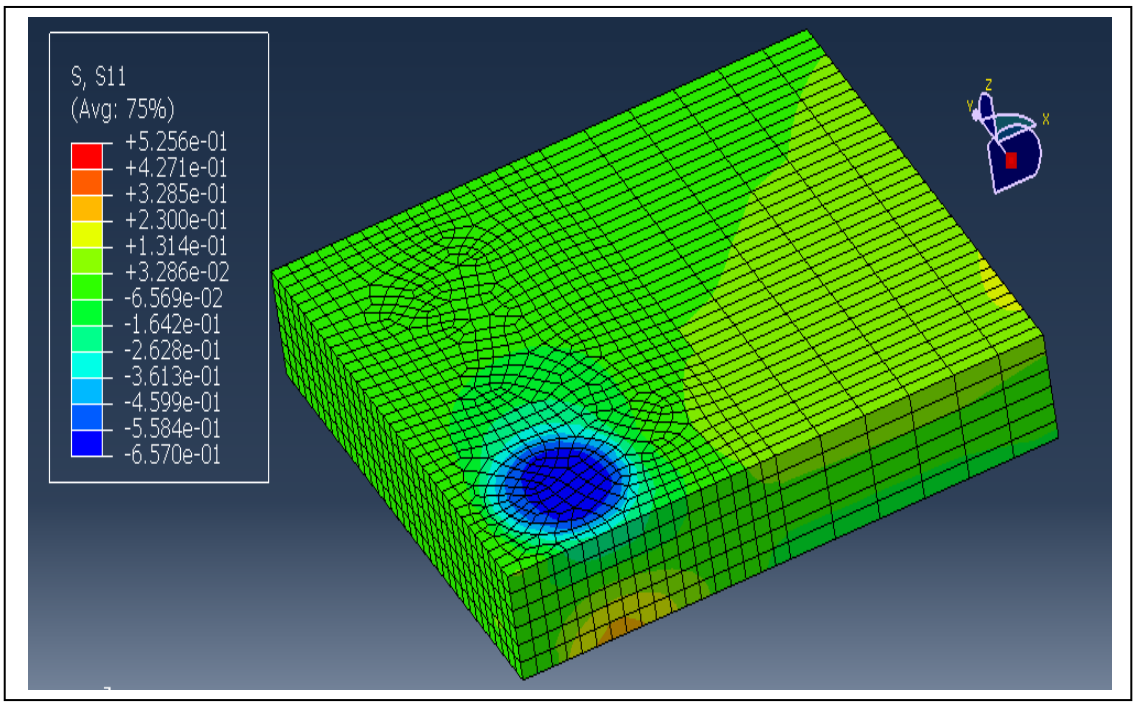

Fig 5.5 Flexural stress in FRSCC rehabilitated panel at 5 tonne load

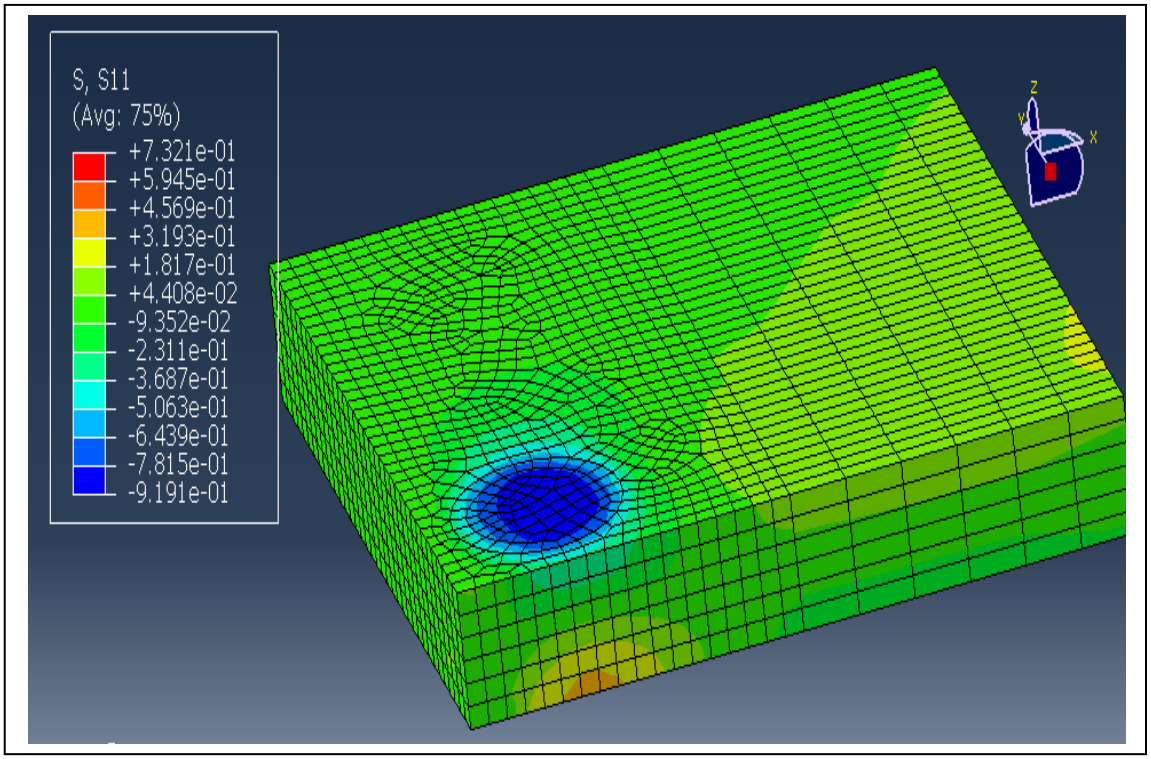

Fig 5.6 Flexural stress in FRSCC rehabilitated panel at 7 tonne load

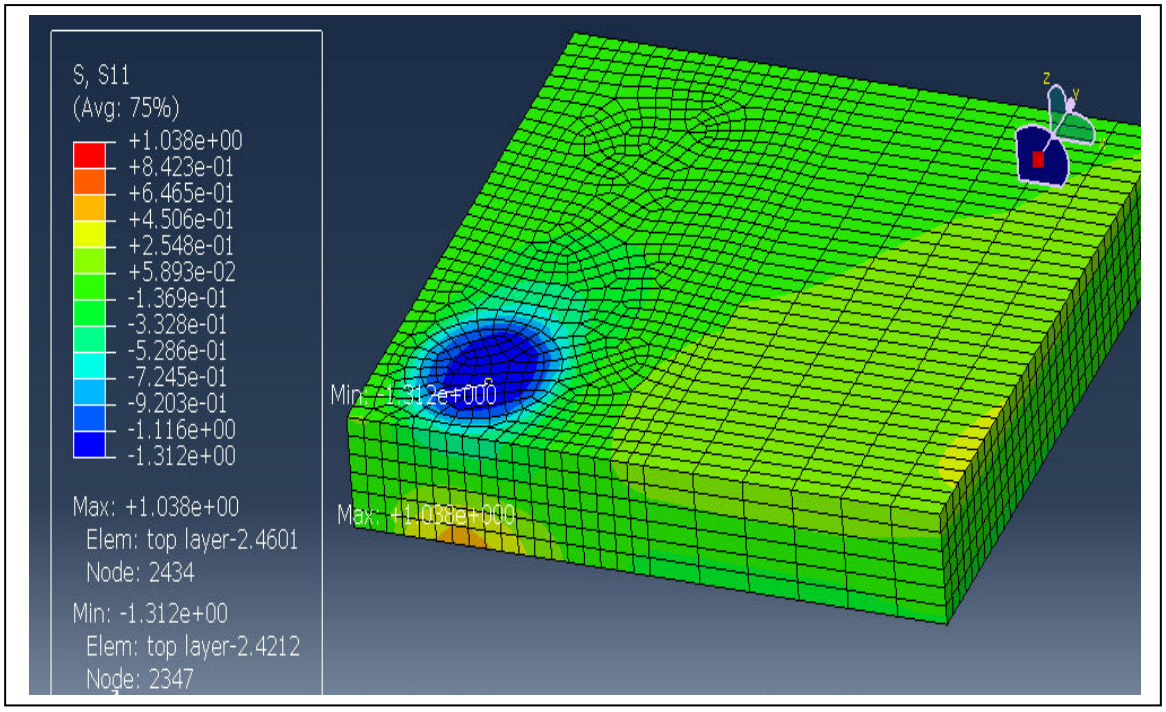

Fig 5.7 Flexural stress in FRSCC rehabilitated panel at 10 tonne load

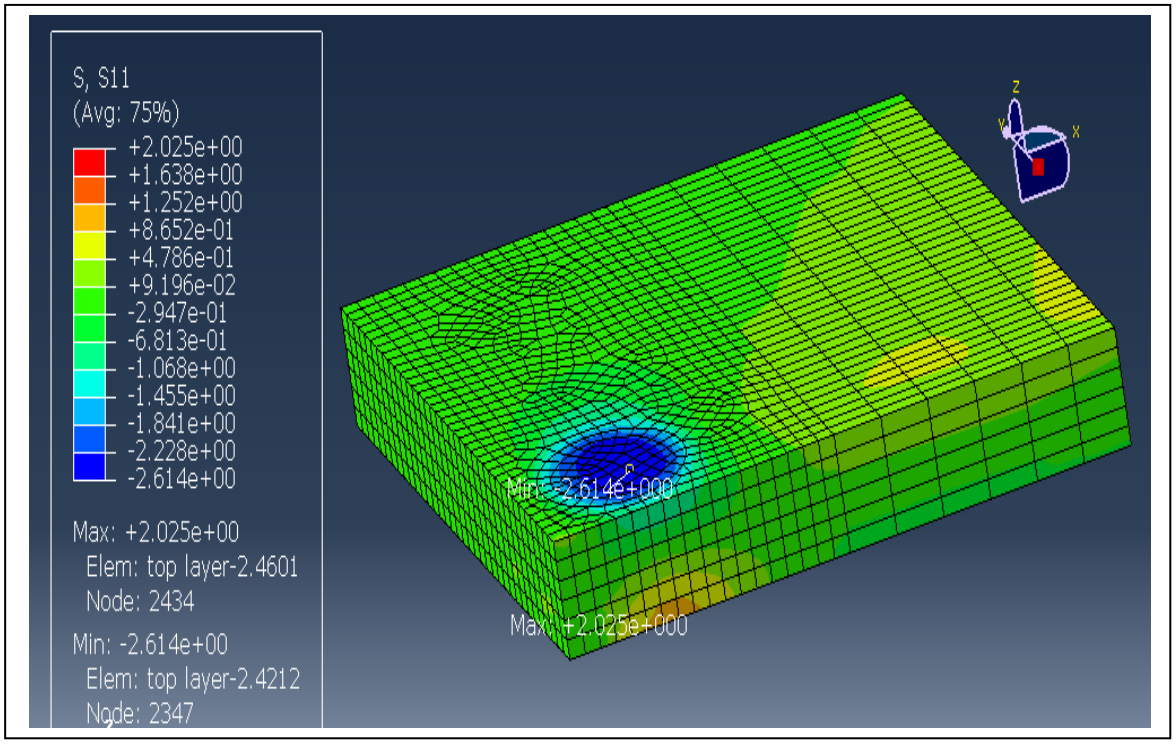

Fig 5.8 Flexural stress in FRSCC rehabilitated panel at 20 tonne load

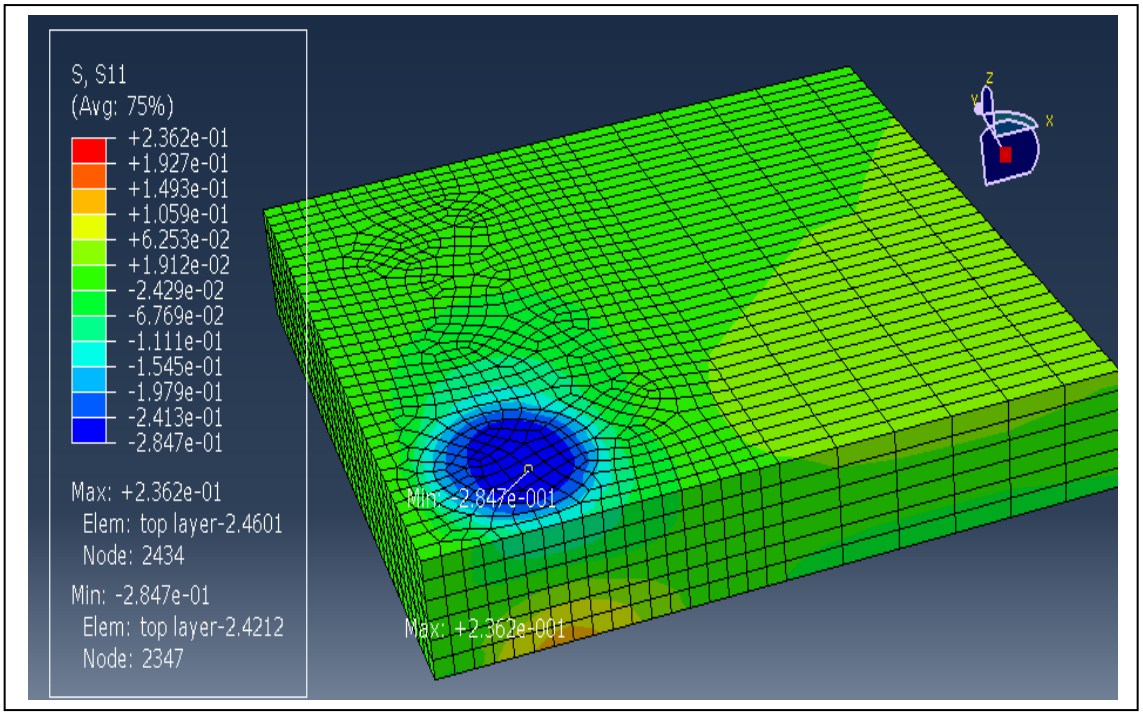

Fig 5.9 Flexural stress in normal PQC panel at 2 tonne load

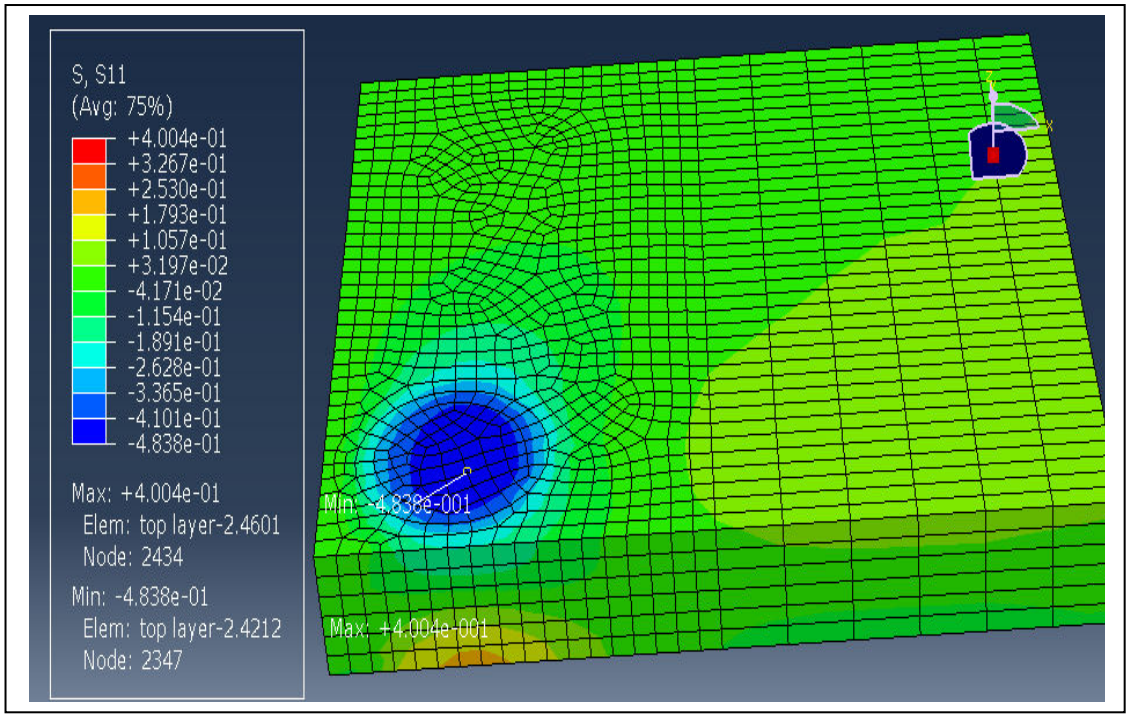

Fig 5.10 Flexural stress in normal PQC panel at 3.4 tonne load

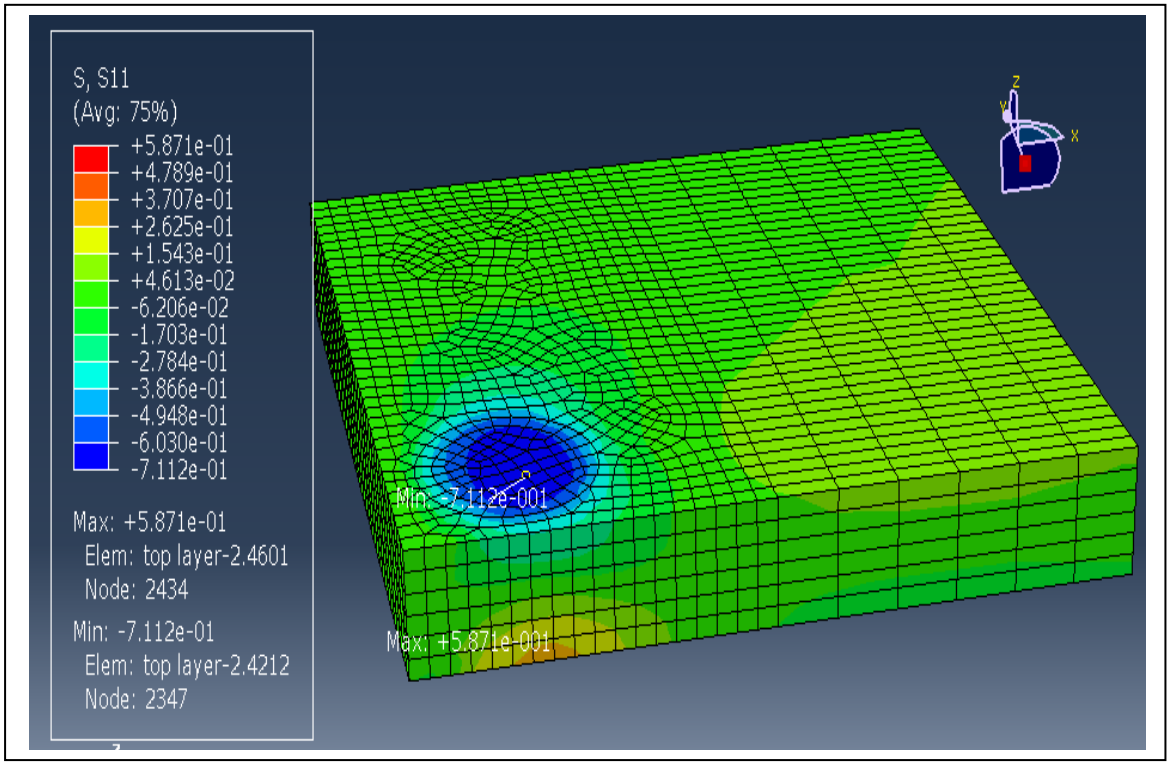

Fig 5.11 Flexural stress in normal PQC panel at 5 tonne load

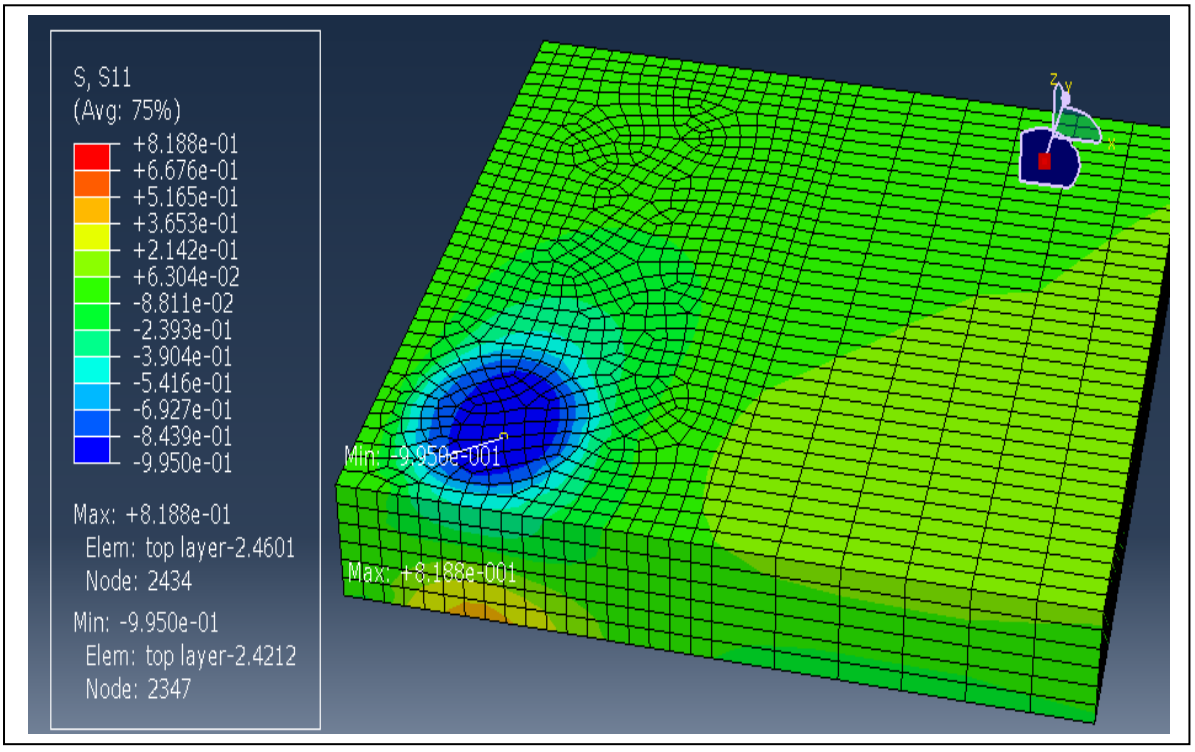

Fig 5.12 Flexural stress in normal PQC panel at 7 tonne load

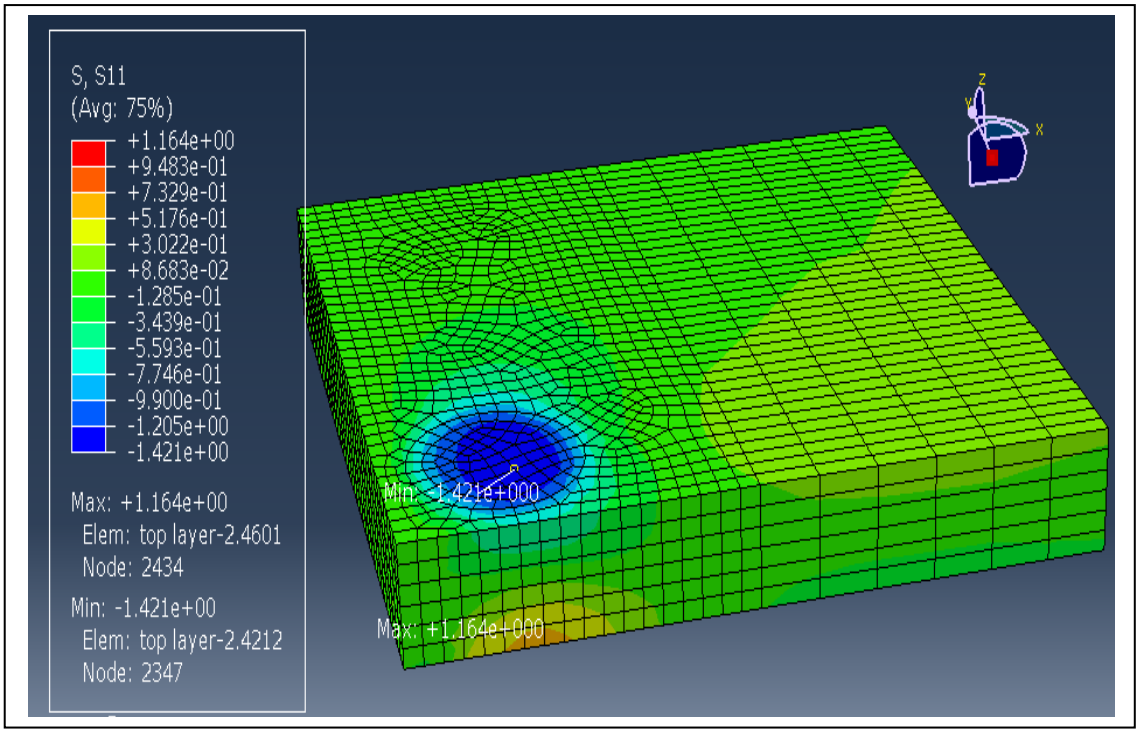

Fig 5.13 Flexural stress in normal PQC panel at 10 tonne load

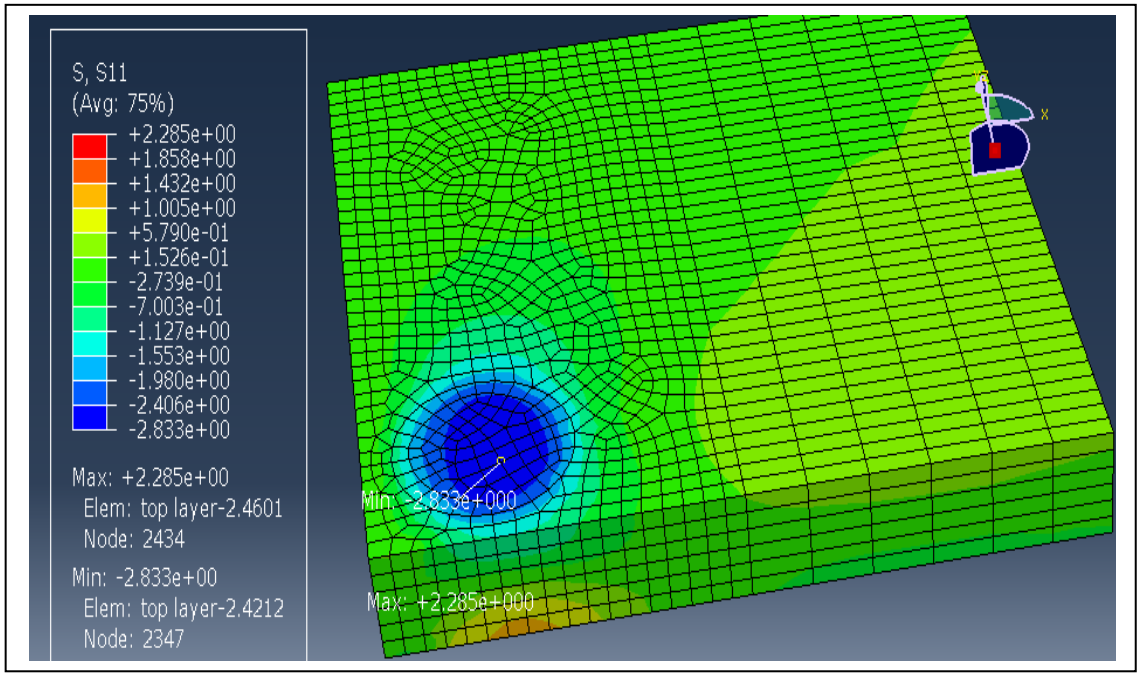

Fig 5.14 Flexural stress in normal PQC panel at 20 tonne load

In the present study, loading was done under static condition employing plate load test through a circular plate of diameter 450 mm as there was no arrangement for dynamic loading in the pavement testing hall. Though pattern of loading is done not exactly as similar

to in-service condition, it does provide reliable information about applied load and the magnitude of the load experienced by the slab through plate would be rather severe than the stresses under dual wheel assembly.

The flexural stress values obtained from the established model for FRSCC and normal concrete are presented in Table 5.10. The laboratory results revealed that FRSCC concrete has lower compressive strength & modulus of elasticity in comparison to normal concrete. But rehabilitation done with FRSCC imparts better load transfer efficiency and the cause of the same may be due to the following reasons:

(i) Better bonding effect developed at the interfaces of the slab and FRSCC mix.
(ii) More contact area of FRSCC with dowel bars by virtue of its excellent flow ability properties.
(iii) Stronger ITZ developed between mineral aggregates and cementitious paste thereby increasing the flexural strength.

As a result of improvements mentioned in (i) & (ii), flexural stresses of FRSCC rehabilitated PQC reduce considerably.

From the above data analyses, it is also strongly suggested that FRSCC having lower modulus of elasticity would impart better flexibility in comparison to normal concrete as can be seen from deflections patterns presented in Table 5.9. One of the interesting findings of the present study is that despite of having lower values of compressive strength and modulus of elasticity, FRSCC offers lesser flexural stresses as compared to normal PQC. The reduced stresses were complemented by high flexural strength of FRSCC, as a result of which the stress ratio came out to be quite low with respect to normal concrete and also it increased stress distribution at higher loads thereby structure would exhibit dual behaviour i.e. flexible at the initial loads and quasi ductile at higher loads.

Table 5.10 Variation of flexural stresses in PQC

	FRSCC	Normal concrete
Load (ton)	Flexural Stress (MPa)	Flexural Stress (MPa)
2	0.212	0.236
3.4	0.359	0.4
5	0.526	0.587
7	0.732	0.819
10	1.038	1.164
20	2.025	2.285
22.5	2.284	2.575

The stress ratio worked out against 20 tonne load came out to be less than 0.45 for FRSCC, whereas for normal concrete, this value was found to be 0.48. The later case clearly suggested, that FRSCC rehabilitated PQC would sustain infinite number of repetitions for the given 20 tonne load. In order to increase the stress ratio for the sake of comparison it was mandate to increase the load to 22.5 tonnes and the corresponding flexural stresses are 2.284 and 2.575 for FRSCC and normal concrete respectively. Accordingly, their stress ratios were found to be 0.45 and 0.53 respectively.

The fatigue life values, so calculated from equation 3.12 given in chapter are found to be 62790761 and 229127, for FRSCC and normal concrete, respectively. This strongly suggested, that there is a considerable improvement in fatigue life of rigid pavement when WMF was incorporated in SCC mix.

5.4 COST ANALYSIS

The cost analysis was an important part of the study, as it's the cost constraints, on the basis of which use of a certain admixture in the concrete could be decided. Following factors make it necessary to undergo the cost analysis of the construction work of rigid pavement:

(i) Part substitution of cement with admixtures like micro silica, which are dearer than cement.

(ii) The use of super plasticizer (PCE based) to reduce water demand for a required workability (flow in our case).

(iii) The preparation of SCC to be used in construction purpose which generally contains higher binder content.

(iv) The mitigating effect of self compacting concrete on the time of construction, requirement of machinery & labour.

(v) Improvement in fatigue life of pavement due to the use of fiber reinforced self compacting concrete, for construction and maintenance of rigid pavements.

Since the fatigue life comparison was done in the form of number of repetitions of load, therefore, making comparison on base of time scale is difficult enough. On the other hand, the cost analysis has only time and monetary terms involved in it. In the cost comparison, four life cycles of pavement, each of 15 years period, have been considered. Since the fatigue life of FRSCC pavement was found very high than normal concrete pavement, therefore only one life cycle of FRSCC constructed pavement has been considered with respect to four life cycles of normal concrete constructed rigid pavement.

Calculations for cost have been done on the basis of existing rate of material, machinery and workmanship in India. This has been done according to the Schedule of Rates 2011-12, finalised by Water Resources Department Government of Karnataka. Table 5.11 provides the cost calculation for a single panel of PQC made of normal concrete, and FRSCC. The cost of materials has been taken according to the expenses on buying and procuring these materials for performing laboratory tests. It was decided to find out the cost for constructing 1 km stretch of road. Therefore calculations have been performed in the following sequence:

(i) Firstly, the volume of concrete required for constructing 1 panel of PQC has been calculated.

(ii) Then, the materials required for preparing this much volume has been calculated.

(iii) Afterwards, the quantity of the materials has been multiplied with their respective costs per unit quantity, in order to find out the cost of materials for preparing one panel.

(iv) Final step is calculation of concrete panels required for one km stretch of road, and then finding out the cost for constructing 1 km stretch by multiplying the cost of one panel with the number of panels.

It was found that 444 panels of size (4.5×3.6×0.3) cum. were required for constructing 1 km stretch of road with a cost of 96,99224 INR for FRSCC, and 80,83245 INR for normal concrete PQC respectively.

Table 5.11 Cost for construction of single panel of rigid pavement

	Quantity/cum		Quantity per panel (4.86cum)		Cost (INR)/unit item	Cost of item per panel	
	PQC	CWS6	PQC	CWS6		PQC	CWS6
Cement (A) kg	414	337.5	2012.04	1640.25	7	14084.28	11481.75
C.A. (B) Kg	1033	884	5020.38	4296.24	0.1205	604.9558	517.69692
F.A.(C) Kg	730	884	3547.8	4296.24	0.1563	554.5211	671.50231
WMF (D) kg	0	90	0	437.4	2	0	874.8
Flyash (E) kg	0	0	0	0	1	0	0
Micro silica (F) kg	0	22.5	0	109.35	16	0	1749.6
S.P. (G) litre	0	2.46	0	11.96	300	0	3588
Steel (H) kg			53.85	53.85	55	2961.75	2961.75
			Total cost/panel=			18205.51	21845.10
			Total cost/km=			8083245.00	9699224.10

The laboratory work for constructing the prototype of the rigid pavement, helped significantly in making vivid observation regarding the necessity of equipment, manpower and time requirement. Following points describe the observations, made during the prototype construction:

(i) Before the start of construction, compaction of subgrade, installation of formwork, laying of dowel bars and post construction proper curing of the concrete pavement is required. For the following purposes apart from machinery, manpower is required. In the machinery item a rolling compactor is required. For installation of formwork and laying of dowel bars, a semi skilled light labourer/mazdoor is required. For curing and running the compactor an unskilled heavy labourer/ mazdoor is required.

(ii) Before laying and mixing of concrete, batching of various materials for a given volume of concrete mix, and then blending of binder material is required to be done. This necessitates a batch plant and a blending machine along with their respective crew. A special skilled labourer called as cement/asphalt handling labourer/mazdoor is required to handle and transport the cement, powder ingredients, and aggregates to the batching plant and blending machine.

(iii) A concrete mixer and its crew (handler) for mixing the water and super-plasticizer with dry concrete mix are required. The work of inputting the dry ingredients into the mixer is done by the unskilled labourer.

(iv) After mixing the concrete, the flowable concrete is transferred to the concrete paver manually, and then paved by it into the formwork. The crew handling the paver does this job.

(v) For PQC constructed with normal concrete, vibratory compaction is a must, whereas for SCC constructed PQC it's not. Hence for normal concrete PQC, a vibrating Plate compactor machine and its crew are required after the concrete is paved.

(vi) Then it's the job of mason to shoulder the edges and level the surface of concrete. In case of SCC the job of mason is easy, but his presence is inevitable, because proper levelling of the PQC surface and effective shoulder support is a

must. The mason also does the job of sawing the contraction joints within sawing window and forming the construction joints.

Hence, in all, two number of heavy unskilled labourers, one semi skilled light labourer, one specially skilled handling labourer and one mason is required, apart from the respective crew of batching plant, blending machine, mixers, pavers, and compacting machine. Table 5.12 provides the cost analysis of machine requirement and workmanship for constructing normal concrete PQC, and FRSCC PQC for 1 km stretch of road. From the construction of prototype, it was found, that for same volume of work i.e. laying a volume of 1.944 cum of PQC and FRSCPQC, 3 and, 2 hours respectively were required. Apart from this, construction of 100 mm thick DLC (0.648 cum) took 1 hour, whereas secondary works like; compaction of subgrade, installation of formwork, took 3 hours. On an average, if the rest period in between the laying of DLC and PQC is neglected, then, laying of rigid pavement of 3.6 m stretch took 7 and 6 hours respectively for normal PQC and FRSCPQC. Hence, for constructing 1 km stretch of road, 1945 and 1667 hours are required. Or in other words, 243 and 208 days are required for constructing 1 km stretch of road with normal PQC and FRSCPQC, assuming 8 hours/day of work.

Summing up the cost for construction material, machinery and workmanship, it was found that a sum of 1,26,69,846 INR and 1,35,48,004 INR are required for constructing 1km stretch of rigid pavement having a top surface constructed of normal PQC, and FRSCPQC respectively. This cost is quite less in comparison to the advantages which are received in form of greater serviceability due to considerably larger fatigue life and lesser maintenance requirements.

Table 5.12 Cost for machinery and workmanship

Machinery	Unit	Hire Charge	Fuel Charge	Crew Charge	Total charge for normal PQC	Total charge for FRSCPQC	PQC (243Days @ 8 Hours/Day)	FRSCC (208 Days @ 8 Hours/Day)
Road roller diesel (10 tonne)	Hr	235	577	77.9	889.9	889.9	1729966	1480794
Batching plant 6 cum/hour rated capacity	Hr	134	134	117	385	385	748440	640640
Blending machine	Hr	40	81	49.5		170.5	0	283712
Concrete mixer (600 / 400 litre) (electrical)	Hr	79	54	81	214	214	416016	356096
Vibrating Plate compactor	Hr	56	64	96.9	216.9	0	421653.6	0
Concrete paver 100 sq.m./hr	Hr	290	19	156	465	465	903960	773760
Workmanship		Basic Wage/Day	DA/Day	Total Wage/			0	0
Heavy mazdoor/labourer (2 No.)	Day	83.2	62.05	143.75	289	289	140454	120224
Light mazdoor /labourer	Day	81.7	62.05	143.75	287.5	287.5	69862.5	59810.4
MasonCl - I / Brick layer Cl- I	Day	111.7	62.05	173.75	347.5	347.5	84442.5	72280
Cement / Asphalt handling mazdoor/labourer	Day	85.7	62.05	147.75	295.5	295.5	71806.5	61464
Total cost (INR)							45,86601	38,48780

6. CONCLUSIONS AND RECOMMENDATIONS

6.1 GENERAL

The present study describes an experimental investigation of the effects of wollastonite microfiber, flyash and microsilica on the behaviour of self-consolidating concrete (SCC) in the fresh and hardened states for use in maintenance of old Pavement Quality Concrete (PQC). Various tests related to the performance of self-consolidating concrete were conducted in the laboratory for judging their suitability to use as a part of cement as well as to enhance the rheological properties of SCC mix. The present research work has been executed realizing the difficulty, lack of uniformity & bonding, and complete compaction of conventional concrete by vibration particularly while retrofitting dowel bars and full depth repairing of PQC. Concrete pavements in real situations suffer from one distress or many times with a combination of distresses. Some types of distress like depressions, heave, single crack, ravelling, loss of surface texture will only need repair and hence repairing of such minor distresses have not been taken into account in the present research proposal. The present research work confined to only with dowel retrofit or with full depth repair for extreme severity. Normally, total distressed and surrounding areas (to be repaired) are marked on the pavement in rectangular form with sides parallel and perpendicular to the centre line after sounding with a hand hammer, ensuring not less than 50 mm cutting beyond unsound concrete. Then concrete faces with tie bars or dowel bars are scrabbled/sandblasted to give a rough key to the new concrete to ensure proper bonding between old concrete surface and fresh concrete mix. Also, before concreting the bottom and sides of the pit are kept wet for few hours (not less than 4 hours) for ensuring proper tacking of fresh concrete mix and old concrete pavement. In addition, many times engineers use cement: sand 1:1 slurry with water-cement ratio not more than 0.62 to coat the sides and bottom of pit and fresh concrete mix is poured in the central portion of the pit first and then worked towards edges ensuring complete vibrations including the corners. In spite of putting painstaking efforts, it is very difficult to achieve a strong cross-stitching at the interface of the old slab and freshly laid concrete as normal concrete mix doesn’t possess enough flow

ability properties as a result of which numerous macro air voids formed at the perimeter of the area to be repaired particularly at the vicinity of corners of the slab. Also, the concrete material cannot flow forward along the entire dowel/tie embedment length due to insufficient presence of fines in the concrete mix. Therefore, special care is important to compact the concrete in the corners, along the patch perimeter and around the dowel bars; over and above more workers are required, more energy is invested and time is consumed.

Taking cognizance of the above difficulties, present research work has been taken up with a main motive to improve the rheological properties of SCC mix by incorporating wollastonite microfiber (WMF) which is abundantly available in the belt of Udaipur, Rajasthan, Tamil Nadu, Uttarakhand and Andhra Pradesh as a low cost material. For present work, wollastonite microfiber was obtained from the mines of Khera Tarla in Udaipur. The present level of extraction of WMF as per estimates is 250,000 MT/year from the mines of Khera and Belka Pahar. It has been reported that at the above extraction rate, WMF would be available for another 50 years from now. Wollastonite has unique chemistry that makes it a valuable source of CaO and SiO_2, both available in nearly equal proportions and it's a white silicate mineral of high modulus of elasticity. Taking the advantage of this excellent engineering property, efforts have been made to introduce WMF in the arena of cement concrete pavements construction particularly for retrofitting of dowel & tie bars. Cement requires high energy in its manufacturing process and production of every tone of cement emits carbon dioxide to the tune of about 0.87 tonne. It can be said that 7% of the world's carbon dioxide emission is attributable to cement industry alone. One of the practical solutions to economize cement is to replace it with supplementary cementitious materials like flyash, rice husk ash, rice straw ash, baggasse ash, microsilca and WMF etc. In this context, attempts have also been made to incorporate flyash, microsilica into SCC other than WMF; also the effects of these materials evaluated when they are admixed together to maximize their use. The research work therefore directed towards the part replacement of cement to strike a chord of economy in concrete road construction in the country in addition to enhancement of rheological properties of SCC.

The gist of the present experimental work conducted are as follows:

(i) Incorporating wollostonite microfiber improves mechanical and durability properties of SCC in comparison to normal concrete but no pro flow factor is present due to presence of larger frictional forces under larger weight. But its higher content by virtue of its micro fine size makes the mortar viscous. Incorporation of WMF upto 20% by weight of cement into normal concrete improved compressive strength at all ages considerably irrespective of days of moist curing. Such improvement is also observed for durability properties. However, the rate of improvement is more pronounced for prolonged curing. The increase in compressive strength is due to excellent water expelling capacity of WMF from the voids of the cement particles under filler effect. Addition of WMF beyond 20% doesn't provide any additional advantages on rheological properties of the SCC, strength and durability properties. For achieving good flowability in the SCC containing WMF, incorporation of 5-7.5% microsilica is mandatory irrespective of WMF content.

(ii) Inclusion of WMF & microsilica together improves both compressive & flexural strength of SCC considerably in comparison to normal SCC, cement-WMF SCC, cement-flyash SCC concretes. Laboratory results have clearly demonstrated that microsilica is a promising admixture to elevate compressive strength of SCC. It is also proven that inclusion of WMF highly improves flexural strength and modulus of elasticity with age. Whereas, flyash flyash improves compressive and splitting tensile strength with age. Higher flexural strength is a must for rigid pavements for enhancing the fatigue life of the concrete slab; therefore, WMF is the preferred admixture for cement concrete pavements/rigid pavements/pavement quality concrete among all chosen admixtures.

(iii) The fatigue life of pavement rehabilitated with WMF admixed SCC showed higher than that of pavement rehabilitated with normal concrete. This is mainly due to improved rheological properties of SCC mix in its fresh state on admixing of both WMF & microsilica as a result of which stronger bond developed at the interface of old wall and fresh SCC mix when its harden.

6.2 CONCLUSIONS

The broad conclusions drawn from the present investigation are presented below:

6.2.1 SCC Mix Design Parameters

For achieving good SCC mix for pavement quality concrete rehabilitation works particularly for dowel & tie bars retrofitting and full depth repairing, the following are the few essential points:

(i) Total powder in SCC mix should be between 160 to 240 litres (400-600 kg) per cubic meter. Based on the present study, water-cement ratio of 0.36 with VMA of 0.3 to 0.6 % by weight of cement could suffice the requirements of rheological properties as well as strength of concrete.

(ii) Typically water content does not exceed 200 liter/m^3.

(iii) Fine aggregate volume could be increased over and above the volume obtained from a normal concrete mix, in accordance with the volume of the binder. Whatever volume ratio of fine aggregate to binder is achieved in the mix design of normal concrete PQC, the increase in fine aggregate content should be done to maintain the same ratio. New volume of binder is obtained from the average surface areas of the admixtures and fibers. Fine aggregate volume could be increased with proportional increase in powder volume, such that the ratio of fine aggregate to mortar by volume should not be higher than 55:45 and lower than 50:50. In terms of the volume of the mix, fine aggregate content should not be higher than 38% and lower than 33%.

(iv) For WMF admixed SCC, lower volume coarse aggregate is preferred as it is very difficult to establish SCC with WMF for coarse aggregate to fine aggregate ratio either higher than 50:50 or lower than 45:55. But if it is expressed in terms of volume of the mix, coarse aggregates content should not be higher than 36% and also not lower than 29%.

(v) The additional increase in water demands due to increase in fine content could be met out by adding NFS type superplasticizer (0.3-0.6%).

6.2.2 Rheological Properties

(i) Flyash addition improves the flow ability and passability of SCC mixes irrespective of part replacement level with or without microsilica. Segregation resistance of SCC mix improves considerably with an increase in flyash content. However, inclusion of flyash alone into the normal SCC was not possible to achieve ideal SCC mix on account of this, it is necessary to incorporate cohesivity inducing admixture like microsilica. Higher content of flyash is possible for achieving ideal SCC provided the ratio of flyash to microsilica be maintained in the range of 4:1 to 3:1.

(ii) Alike fly ash, inclusion of WMF at higher dosage affects the rheological properties of SCC mix considerably. The maximum part replaceable level of WMF in presence of microsilica and VMA is 20% by weight of cement. For achieving good flowability and passability of the SCC, about 5 -7.5% microsilica inclusion would be essential. Admixing of WMF modifies the gel pores and density of the SCC mix significantly.

(iii) Part substitution of cement by both WMF and flyash together in presence of microsilica doesn't impart significant impact on the rheological properties of SCC. Effect of WMF in reducing the flow is more prominent than flyash. The right amount to add WMF and flyash together in presence of 5% microslilca is 15% for achieving ideal SCC mix. This analysis clearly infers that certain amount of microsilica should be incorporated for enhancing rheological properties of SCC if at all WMF and flyash are to be incorporated. Improvement in rheological properties of SCC on admixing of microsilica is attributed to micro-fine particles & spherical shape of microsilica which imparts better lubricating effect between cement grains and could conceived better degree of cohesion within the cementitious system and mortar matrix as a result of which it overcomes the bleeding, laitance formation and segregation.

6.2.3 Mechanical Properties

(i) Admixing of WMF improves flexural strength & modulus of elasticity of SCC significantly. This improvement is continuous with days of moist curing. Maximum flexural strength noted for WMF admixed concrete was 4.88 MPa which is

comparable to that of normal concrete. The maintenance of flexural strength even on replacement of cement with WMF admixed concrete is attributed to the high modulus of elasticity of WMF and its excellent reinforcing effect which enables to reorient the particles of the entire cementitious system physically leading to better densification of the SCC. This improvement is even better on admixing of microsilica in the range of 5%-7.5% by weight of cement. The percentages increased are 1.84, 4.72, 5.26 & 7.04 at 7, 28, 60 & 90 days moist curing respectively for 20% WMF admixed SCC with 5% microsilica. Beyond 20%, part replacement of cement by WMF doesn't improve flexural strength of SCC considerably on account of overlapping of mortar volume affected by fiber.

(ii) In contrary, flyash admixed SCC improves compressive and splitting tensile strength irrespective of replacement levels and days of moist curing. The increment of the aforesaid strength continuous with prolonged curing. Since, performance of cement concrete pavement or pavement quality concrete is being evaluated based on the fatigue life consumption and hence it is pertinent to select those mixes which produce higher flexural strength of concrete. In this context, WMF admixed SCC in presence of microsilica offered the highest flexural strength and it was about 3.5% higher than that of normal SCC in overall irrespective of WMF content. Whereas reductions of 17% and 8.5% in flexural strength were observed on an average for SCC containing both flyash & microsilica and quaternary blend respectively. While talking about inter mixes' behaviour, the mixes CWS2, CWS5, CWS6, CWS9, CWS10, CWFS1, and CWFS2 have flexural strength greater than 4.5 MPa, whereas for normal concrete it is nearing to 4.2 MPa.

(iii) Irrespective of amount and types of admixtures used, modulus of elasticity (E) was found to be lower in value in comparison to normal concrete. Reduction in E-value is mainly due to presence of higher paste volume for a given volume of concrete. If it is looked at the overall E-values, highest reduction is being offered by quaternary mixes (45.3%) irrespective of types of admixtures used followed by SCC concretes containing both flyash & microsilica (44.3%) and WMF-micsrosilica admixed concretes (17.6%) respectively. But prolong curing showed tremendous improvement in E-values for all considered SCC.

(iv) WMF admixed mortar offered higher flexural strength than WMF admixed SCC regardless of WMF content. This phenomenon is mainly due to presence of higher paste volume in mortar than SCC per unit volume.

(v) From the present laboratory studies conducted, efforts have also been made to establish relationship between the compressive strength and modulus of elasticity and compressive strength and flexural strength for cement+flyash+microsilica, cement+ WMF+microsilica and cement+flyash+WMF + microsilica SCC mixes. The following are the relationship established for the aforesaid mixes:

Relationship	Modulus of elasticity (E) with Compressive strength (σ)	Compressive strength (σ) with Flexural strength (f_{cr})
Cement+Flyash+ Micro silica	$E = 14.46\pm^{0.3} - 28.81$, R^2=0.99	$f_{cr} = 1.391\pm^{0.5} - 4.836$, R^2=0.99
Cement+WMF+ Micro silica	$E = 27.93\pm^{0.4} - 107.2$, R^2=0.998	$f_{cr} = 1.462\pm^{0.5} - 5.602$, R^2=0.99
Cement+Flyash+ WMF+Micro silica	Good correlation could not be achieved	$f_{cr} = 0.66\pm^{0.5} - 0.0129$, R^2=0.99

6.2.4 Durability Properties

(i) The principle of flow of water through concrete under pressure is taken into account in the present study so as to compare the coefficient of permeability of SCC with or without admixtures. Permeability of normal concrete was found to be 6.58E-09 cm/sec at 28- day age. But this value reduced to 3.40E-09 cm/sec on admixing of 10% WMF. This value further reduced to 2.69E-09 cm/sec when 20% WMF was admixed in normal SCC. This clearly infers that inclusion of WMF reduces permeability of SCC irrespective of WMF content. Higher reduction in permeability was observed for higher percentage inclusion of WMF. About 82% reduction in permeability value was observed on admixing of microsilica in presence of WMF in comparison to normal concrete followed by flyash-microsilica admixed SCC by having a reduction of 74% with respect to normal concrete. Based on the overall results of quaternary mixes, about 61.5% permeability is reduced with respect to

normal concrete. Laboratory results analysis strongly prompted that admixing of WMF, flyash & microsilica would not only improve the rheological properties of SCC, mechanical properties of SCC but also would improve durability of pavement by offering higher resistance against movement of moisture and harmful air within the mass of hardened SCC. In a mature paste, the permeability depends on size, shape and concentration of the gel particles and on whether or not the capillaries have become discontinuous. Reduction in permeability values of admixtures admixed concrete was mainly due to proper proportioning of the mixtures and presence of microsilica which enables to improve the pore structure of hardened cement paste and hence increases the resistivity.

(ii) The problem of chloride attack arises usually when chloride ions ingress from outside. The ingress of chloride into the concrete is strongly influenced by the exact sequence of wetting and drying. PQC slab installed near the sea shore in the tidal zone is vulnerable to chloride attack. Taking this factor into consideration, in the present study attempt has been made to determine the percentage of ingression of chloride ion into the hardened concrete slabs made with or without WMF, flyash and microsilica so as to check the potential of these admixtures to prevent the ion ingression. It is found that inclusion of WMF offers higher resistance against penetration of chloride ion followed by FA admixed SCC and normal concrete respectively irrespective of days of ponding. Similarly, for ternary mixes, higher resistance against chloride ion penetration (CIP) is offered by WMF-microsilica admixed SCC followed by FA-microsilica admixed SCC and normal SCC respectively. Higher resistance against CIP on admixing of admixtures is due to better densification caused by pore refinement. Chloride ion penetration values for the mixes CWS2, CWS5, CWS6, CWS9, CWS10, CWFS1, and CWFS2 were 0.3% by mass of concrete which is lower than that of normal concrete (0.41%). It is also noted that on an average, the permeability of mineral admixed SCC mixes has been reduced by 67% irrespective of the type of mineral admixture, and 74%, 82% & 62% respectively for flyash-silica fume, WMF-Silica fume and quaternary mixes. As far as shrinkage resistance is concerned CWS2, CWS5, CWS6, CWFS1, CWFS2 had stress rates nearly half of that shown by normal concrete. Their stress rate was ≤ 0.7

MPa at failure which occurred at duration of nearly 20 days for all mixes, except CWFS1 and CWFS2, which showed failure at 23 and 27 days. CWS9 and CWS10 gave larger stress rates. Hence maximum amount of cement substitution with admixtures could be made beneficially corresponding to mix CWS6 at 25%.

(iii) Resistance of concrete to abrasion is difficult to assess as the damaging action varies depending on the exact cause of wear, and no one test procedure is satisfactory in evaluating all the conditions: rubbing test, including rolling balls, dressing wheel, or sand blasting may each be appropriate in different cases. In the present research work, sandblasting method has been employed to find the relative volume loss of concrete prepared with or without WMF, FA and microsilica. Higher abrasion resistance was offered SCC containing WMF in presence of microsilica regardless of their content. From the statistical analysis, it is learnt that good correlation exhibits between abrasion resistance and compressive strength of SCC. Higher compressive strength leads to higher abrasion resistance.

(iv) It is noted that drying shrinkage stress rate of WMF-Silica fume admixed mixes is found to be lowest (49% lower than normal concrete) followed by quaternary mixes (36.6%). Flyash admixed mixes showed increment in stress rate by 1.25% in comparison to normal concrete. Also, increment in critical time is highest in WMF-Silica fume admixed mixes (100%), followed by flyash-silica fume (88%) and quaternary mixes (63%). Shrinkage resistance depends upon both stress rate development and tensile strength (indicated by critical time). WMF being pozzolan and finer than flyash (3 times), fills the gel pores (lime reduction) and refines the pore too. WMF also produces more ettringite which swells and causes reduction in shrinkage stresses. Flyash has nearly same surface area as cement grains. Although its pozzolanic activity is greater than WMF during the initial days, yet, due to factors discussed above, it increases the stress development. Higher percentage of both admixtures is observed to increase the stress rate due to creation of more voids by the extra volume of admixtures.

6.3 FATIGUE LIFE IMPROVEMENT

The fatigue life of pavement rehabilitated with WMF admixed SCC (CWS6) was way higher than that of normal concrete rehabilitated pavement. Apart from rehabilitation, for a period of 60 years, a WMF admixed SCC constructed pavement would have safely one life cycle in comparison to 4 life cycles of normal concrete pavement. For the construction of FRSCC PQC 96, 99224 INR would be required, as against 80, 83245 INR for normal concrete PQC respectively. This increase in cost is very less; if maintenance and retrofitting works are avoided and efficient working of pavement is considered.

Based on the study conducted on the prototype constructed in the laboratory, it was found that WMF admixed SCC offered appreciable load transfer efficiency with respect to normal concrete rehabilitated pavement. About 30% reduction in deflection on the adjoining slab was noted for WMF admixed SCC rehabilitated pavement for a given set of loadings. Whereas, for normal concrete rehabilitated pavement, the percentage reduction was 60% at a confidence level of 85% under the same working conditions.

6.4 RECOMMENDATIONS

Based on the studies carried out in the present research work, following recommendations are being made:

1. Admixing of WMF improves flexural strength & modulus of elasticity of SCC considerably. For achieving good flowability and passability of the SCC, the following combinations for cement: wollastonite microfiber: flyash: microsilica are recommended based on the present research work:
   (i) Cement : Wollastonite microfiber: Microsilica = 75% : 20% : 5%,
   (ii) Cement : Wollastonite microfiber: Flyash :Microsilica = 80% : 10% : 5%: 5%,
   (iii) Cement : Wollastonite microfiber : Flyash: Microsilica = 80% : 5% : 10%: 5%,
   (iv) Adding of PCE based superplasticizer in the range of 0.3- 0.6% by weight of cementitious materials is essential for all the above-mentioned mixes.

2. For satisfactory production of SCC, total powder content shall be maintained between 160-240 liters (400-600 kg) per cubic meter. New volume of binder is obtained from the average surface areas of the admixtures and fibers. Fine aggregate volume could be increased with proportional increase in powder volume, such that the ratio of fine aggregate to mortar by volume should not be either higher than 55:45 or lower than 50:50. In terms of the volume of the mix, fine aggregate content should not be either higher than 38% or lower than 33%.
3. Inclusion of wollastonite microfiber and flyash alone into the normal SCC was not possible to achieve ideal SCC. Thus, inclusion of at least 5% microsilica is strongly recommended.
4. Prolong curing is strongly suggested for admixed SCC as it improves both strength and durability properties of SCC tremendously.
5. Higher abrasion resistance was offered SCC containing WMF in presence of microsilica regardless of their content. Hence, wollastonite microfiber is the preferred additive over flyash for construction of Pavement Quality Concrete (PQC) as well as rehabilitation of old PQC (cement concrete pavements).

6.5 SCOPE OF FUTURE RESEARCH

1. The present study entails with the specific water-cement ratio of 0.36. Study for different water-cement ratios may be conducted for construction of PQC as well as for rehabilitation of old PQC.
2. Freezing and thawing properties of the SCC containing wollastonite microfiber, flyash and microsilica may be studied.

REFERENCES

1. ACI 223-93 (1994). “Standard practice for the use of shrinkage compensating concrete.” ACI Manual of concrete practice, Part 1: Materials and general properties of concrete, Detroit, Michigan, 29.
2. ACI 226.3R-87 (1994). “Use of flyash in concrete.” ACI manual of concrete practice, Part 1: Materials and general properties of concrete, Detroit, Michigan, 29.
3. ACI Committee 231 (2010). “Report on early-age cracking: causes, measurement, and mitigation.” Technical Committee Document No. 231R-10, ACI, Farmington Hills, USA.
4. ACI Committee 232-94 (1994). “Use of flyash in concrete.” ACI Publication, Farmington Hills, USA.
5. Aly, T., Sanjayan, J. G., and Collins, F. (2008). “Effect of polypropylene fibres on shrinkage and cracking of concretes.” J. of Mater. Struct., 41(10), 1741–1753.
6. Alford, N. McN, Groves, G.W. and Double, D.D.(1982). “Physical properties of high strength cement paste.” Cement and concrete research, 12 (3), 349-58.
7. Arioglu, N., Girgin Z. C., and Arioglu E. (2006). “Evaluation of ratio between splitting tensile strength and compressive strength for concretes up to 120 MPa and its application in strength criterion.” ACI Materials Journal, 103(1), 18-24.
8. Aveston, J., Copper, G. A., and Kelly, A. (1971). “Single and multiple fracture; Properties of fiber composites.” Conf. Proc., IPC Press, Guildford, U.K., 15–24.
9. Banthia, J., and Dubeau, S. (1994). “Carbon and steel microfiber-reinforced cement-based composites for thin repairs.” Journal of Materials in Civil Engineering, 6(1), 45-71.
10. Banthia, N., and Gupta, R. (2006). “Influence of polypropylene fiber geometry on plastic shrinkage cracking in concrete.” J. of Cement and Concrete Research, 36(7), 1263-1267.
11. Banthis, N, and Sheng, J. (1996). “Fracture toughness of microfiber reinforced cement composites.” Cement and Concrete Composites, Elsevier, 18(4), 251-269.
12. Banthia, N., and Trottier, J. F. (1994). “Concrete reinforced with deformed steel fibers, Part I: Bond-slip mechanisms. ACI Mat. J., 91(5), 435–446.

13. Banthia, N., Mindess S., and Trottier, J. F. (1996). “Impact resistance of steel fiber-reinforced concrete.” ACI Mat. J., 93(5), 472–479.
14. Banthia, N., Yan, N., Chan, C., Yan, C., and Bentur, A. (1995). “Bond slip mechanisms in steel micro-fiber reinforced cement composites.” J. of Comp., Materials Research Society, USA, 370, 529-537.
15. Bartos, P.J.M. (1998). “An appraisal of the Orimet test as a method for on site assessment of fresh SCC concrete.” Proceedings of the International Workshop on Self Compacting Concrete, Kochi, 121-135.
16. Bayasi, Z., and Zeng, J. (1993). “Properties of polypropylene fibre reinforced concrete.” ACI Mater. J., 90(6), 605–610.
17. Bentz, D. P., Sant, G., and Weiss, J. (2008). “Early-age properties of cement-based materials.” Part I: Influence of cement fineness. Journal of Materials in Civil Engineering, 20(7), 502-508.
18. Bentz, D.P. Stutzman, P.E., and Garboczi, E.J. (1992). “Experimental and simulation studies of the interfacial zone in concrete.” Cement and Concrete Research, 22 (5), 891-902.
19. Betancourt, G.H. (1988). “Admixtures, workability, vibration and segregation.” Journal of Materials and Structures, 21 (124), 286-288.
20. Boel, V., Audenaert, K., and Schutter, G.D. (2002). Pore structure of self compacting concrete. First north American conference on the design and use of self consolidating concrete, USA, November, 21-30.
21. Bouzoubaa, N., and Lachemi, M. (2001). “Self-compacting concrete incorporating high volumes of Class F fly ash preliminary results.” Cement and Concrete Research, 31, 413-420.
22. Brooks, J.J., and Neville, A.M. (1975). “Estimating long term creep and shrinkage from short term tests.” Magazine of Concrete Research, 27 (90), 3-12.
23. Bui, V.K., (2002). “Application of minimum paste volume method in designing cost effective self consolidating concrete- An experience in New Zealand.” First North American Conference on the Design and use of Self Consolidating Concrete, USA, November, 121-126.
24. Bui, V.K., Shah, S.P., and Akkaya, Y. (2002). “A new approach in mix design of self consolidating concrete.” First North American Conference on the Design and Use of Self Consolidating Concrete, USA, November, 69-74.

25. Cao, H.T., Bucea, L., Wortley, B., and Sirivivatnanon, V. (1994), “Corrosion behaviour of steel embedded in Flyash blended cements.” Durability of Concrete, Ed. V.M. Malhotra, Detroit, Michigan, ACI SP-145, 215-27.
26. Chen, W.F., and Carson, J.L. (1971). “Stress-strain properties of random wire reinforced concrete.” ACI Journal, 68 (12), 933-936.
27. Cheyrezy, M., Maret, V., and Frouin, L. (1995). “Micro-structural analysis of RPC (Reactive Powder Concrete).” Cement and Concrete Research, 25(7), 1491-1500.
28. Clark, P. (1998). “Future of automotive body materials: Steel, Aluminum & Polymer Corporation.” Massachusetts Institute of Technology, < http://readpdf.net/file/future-steel-vehicle.html>.
29. Cohen, M.D., Goldman, A., and Chen, W.F. (1994). “The role of Silica gel in mortar: transition zone versus bulk paste modification.” Cement and Concrete Research, 24(1), 95-98.
30. CUR Report (1991). “Fly ash as addition to concrete.” Centre for Civil Engineering Research and Codes, Report 144, Netherlands, pp. 99.
31. Cunha, V.M.C.F., Barros, J.A.O., and Sena-Cruz, J.M. (2010). “Pullout behavior of steel fibers in self-compacting concrete.” Journal of Materials in Civil Engineering, 22(1), 1-9.
32. Daczko, J.A., and Kurtz, M.A. (2001). “Development of high volume coarse aggregate self compacting concrete.” Proceedings of the Second International Symposium on Self Compacting Concrete, Tokyo, Japan, 403-412.
33. Dattatreya, J.K., Nellamegam, M., Rajemane, N.P., and Gopalakrishnan, S. (2003). Self compacting concretes with high volumes of cement replacement materials. Proceedings of Third Quinquennial International Symposium on Innovative World of Concrete, Pune, 45-46.
34. Diamond, S. (1976). “Cement paste microstructure- An overview at several levels.” Proc. Conf. Hydraulic Cement Pastes: Their Structure and Properties, Cement And Concrete Association, Sheffield, 2-30.
35. EFNARC (2002). “Specification and guidelines for self-compacting concrete.” Association House, 99 West Street, Farnham, Surrey, GU9 7EN, UK.
36. EFNARC (2005). “The European guidelines for self-compacting concrete: Specification, Production and Use”, EFNARC, www.efca.info or www.efnarc.org.
37. Felt, E. J. (1956). “Resurfacing and patching concrete pavements with bonded concrete.” Highway Res. Board Proc., 35, 444-469.

38. Felt, E. J. (1960). “Repair of concrete pavement.” J. American Concrete Inst. Proceedings, 57, 139-153.
39. FIP 1998. “Condensed silica fume in concrete, state of the art report.” FIP Commission on Concrete, Thomas Telford, London, 37.
40. Fraay, A.L.A., Bijen, J.M., and De Haan, Y.M. (1989). “The reaction of fly ash in concrete: a critical examination.” Cement and Concrete Research, 19 (2), 235-46.
41. Fornasier, G., Fava, C. and Zitzer, L. (2001). “Self compacting concrete in Argentina: The first experience.” Proceedings of the Second International Symposium on Self Compacting Concrete, Tokyo Japan, October, 309-318.
42. Fowler, D., (1980). “Guide for Repair of Concrete Superstructures.” ACI Committee 546, Concrete International, 2(9), 69-88.
43. Furlonge, R.L. (1996). “Road fatality modeling in Trinidad and Tobago.” West Indian Journal of Engineering, 19(1).
44. Fwa, T. F., and Paramasivam, P. (1990). “Thin steel fibre cement mortar overlay for concrete pavement.” Cement & Concrete Composites, 12, 175-184.
45. Ghezal, A., and Khayat, K.H. (2001). “Optimization of cost effective self consolidating concrete.” Proceedings of the Second International Symposium on Self Compacting Concrete, Tokyo, Japan, October, 329-338.
46. Ghugal, Y.M. (2003). “Effects of steel fibers on various strengths of concrete.” ICI Journal, 4(3), 23-29.
47. Gomes, P.C.C, Gettu, R., Agullo, L., and Bernard, C. (2001). “Experimental optimization of high strength self compacting concrete.” Proceedings of the Second International Symposium on Self Compacting Concrete, Tokyo, Japan, October, 377-386.
48. Griffith, A.A. (1920). “The phenomena of rupture and flow in solids.” Philosophical Transactions, Royal Society, London, Series A, 221, 163-98.
49. Grunewald, S., and Walraven, J. C. (2001). “Parameter-study on the influence of steel fibers and coarse aggregate content on the fresh properties of self-compacting concrete.” Cement and Concrete Research, 31(12), 1793-1798.
50. Grunewald, S., and Walraven, J. C. (2001). “Rheological study on the workability of fiber reinforced mortar.” Proceedings of the Second International Symposium on Self Compacting Concrete, Tokyo, Japan, 127-136.
51. Grzybowski, M., and Shah, S.P. (1990). “Shrinkage cracking of fiber reinforced concrete.” ACI Materials Journal, 87(2), 138-148.

52. Gupta, S., Kantarao, V.V.L., and Sengupta, J.B. (2008). “Evaluation of Polyester Fiber Reinforced Concrete for use in Cement Concrete Pavement Works.” Road Materials and Pavement Design, Lavoiser, Paris, 9(3).
53. Hammer, T.A., Johansen, K., and Bjontegaard, O. (2001). “Volume changes as driving forces to self induced cracking of Norwegian SCC.” Proceedings of the Second International Symposium on Self Compacting Concrete, Tokyo, Japan, October, 423-432.
54. Hannant, D.J., Buckley, K.J., and Croft. J. (1973). “ The effect of aggregate size on the use of the cylinder splitting test as a measure of tensile strength.” Materials and Structures, 6 (31), 15-21.
55. Helmuth, R. (1987). “Flyash in cement and concrete.” PCA, Skokie, III, 203.
56. Hooton, R.D. (1993). “Influence of Silica fume replacement of cement on physical properties and resistance to sulphate attack, freezing and thawing, and alkali-silica reactivity.” ACI Materials Journal, 90(2), 143-151.
57. Horikoshi, T., Ogawa, A., Saito, T., and Hoshiro, H (2006). “Properties of polyvinylalcohol fiber as reinforcing materials for cementitious composites.” Proceedings of the International RILEM Workshop on High Performance Fiber Reinforced Cementitious Composites in Structural Applications, RILEM Publications SARL, 145-153.
58. Hori, A., Kida T., Tamaki, T., and Hagivara, H. (1998). “Study on self compacting concrete with expansive additives.” Proceedings of the International Workshop on Self Compacting Concrete, Kochi, 218-227.
59. Hossain, K.M.A., Lachemi, M., Sammour, M., and Sonebi, M. (2012). “Influence of polyvinyl alcohol, steel and hybrid fibers on fresh and rheological properties of self-consolidating concrete.” Journal of Materials in Civil Engineering, 24(9), 1211–1220.
60. Idorn, G.M. and Thaulow, N. (1985). “Effectiveness of research on flyash in concrete.” Cement and Concrete Research, 15 (3), 535-44.
61. Jain, A.K. (2001). “Cement industry and future challenges.” Proceedings of SEC 2001 on Recent Developments in Structural Engineering. Indian institute of Technology, Roorkee. 129-136.
62. Johansen, K., and Busterud, L. (2001). “Low grade SCC with secondary natural sand rich in fines.” Proceedings of the Second International Symposium on Self Compacting Concrete, Tokyo, Japan, 303-308.

63. Kalla, P., Misra, A., and Sancheti, G. (2011) “Properties of Wollastonite and Flyash aided concrete.” Indian Highways, Journal of Indian Roads Congress, 39(12), 25-31.
64. Kaushik, S.K., Gupta, V.K., and Gupta, S. (1994). “Properties of fresh and hardened SFRC. Proceedings of the National Seminar on Fiber reinforced Comentitious Products, Roorkee, India, January, 247-257.
65. Kerr, P. Y. (1959). “Optical Mineralogy”. McGraw-Hill Book Co. Inc., New York, 3rd Ed., 442.
66. Khan, T.A.H., Laid, S.M., and Ramakrishna, B. (1987). “Experimental study of SFRC under compression, indirect and pure bending.” Proceedings of the international symposium on fiber reinforced concrete, Madras, India, 2.39-2.48.
67. Khayat, H.K., and Aitcin, P.C. (1992). “Silica fume in concrete- an overview.” Flyash, Silica fume, Slag and Natural Pozzolans in Concrete, Ed. V.M. Malhotra, ACI SP-132, Detroit, Michigan, 2, 835-72.
68. Khayat, H.K., Hu, C., Laye, J.M. (2002). “Importance of aggregate packing density on workability of self consolidating concrete.” First North American Conference on Design and Use of Self Consolidating Concrete, USA, November, 55-62.
69. Kim, J.K., Han, S.H., Park, Y.D., and Noh, J.H. (1998). “Material properties of self-flowing concrete.” Journal of Materials in Civil Engineering, 10(4), 244-249.
70. Konig, G., Dehn F., Ma, J., and Dietz, J. (2001). “Examinations for the production of self compacting concrete using lignite fly ashes.” Proceedings of the Second International Symposium on Self Compacting Concrete, Tokyo, Japan, October, 349-359.
71. Kovler, K., Sikuler, J., and Bentur, A. (1992). “Free and restrained shrinkage of fibre reinforced concrete with low polypropylene fibre content at early age.” Fourth Rilem Int. Symp. on Fibre Reinforced Cement and Concrete, International Union of Laboratories and Experts in Construction Materials, Systems and Structures, Sheffield, UK, 91–101.
72. Krishnadev, M. R., Berrada, S., Banthia, N. and Fortier, J. F. (1992). “Deformed steel fiber pull-out mechanics: Influence of steel properties.” Fibre Reinforced Cement and Concrete, R. N. Swamy, Ed., E & FN Spon., London, 390–399.
73. Krishnamoorthy, S., and Ahmad, R. (1994). “Behaviour of fiber and steel fiber reinforced flexural members.” Proceedings of the National Seminar on Fiber Reinforced Cementitious Products, Roorkee, India, January, 381-388.

74. Krishnamoorthy, T.S., and Kumar, B.H. (1994). “Influence of steel fibers on the compression and flexural behavior of concrete.” Proceedings of the National Seminar on fiber Reinforced Cementitious Products, Roorkee, India, Januray, 25-32.
75. Kukreja, C.B., and Chawla, S. (1989). “Flexural characteristics of steel fiber reinforced concrete.” The Indian Concrete Journal, March, 154-157.
76. Kumar, P., and Kaushik, S.K. (2003). “Can marginal materials be used to produce self compacting concrete.” Proceedings of Third Quinquennail International Symposium on Innovative World of Concrete, Pune, 116-119.
77. Kumar, P., and Kaushik, S.K. (2004). “Transition zone in self compacting concrete.” The Indian concrete journal, 78, (6), 39-43.
78. Langan, B.W., Weng, K., and Ward, M.A. (2002). “Effect of silica fume and Fly ash on heat of hydration of portland cement.” Cement and Concrete Research, 32(7), 1045–1051.
79. Larbi, L.A. (1993). “Microstructure of the interfacial zone around aggregate particles in concrete.” Heron Journal, 38(1), 5-69.
80. Lawler, J. S. (2001). “Hybrid fiber reinforcement in mortar and concrete.” Ph.D. Thesis, Northwestern Univ., Evanston.
81. Lawler, J. S., Zampini, D., and Shah, S. P. (2002). “Permeability of cracked hybrid fiber-reinforced mortar under load.” ACI Mater. J., 99(4), 379–385.
82. Lawler, J.S., Zampini, D. and Shah, S. P. (2005). “Microfiber and macrofiber hybrid fiber-reinforced concrete.” Journal of Materials in Civil Engineering, 17(5), 595-604.
83. Leung, C. K. Y. (1992). “Fracture-based two-way debonding model for discontinuous fibers in elastic matrix.” J. Engg. Mech., ASCE, 118(11), 2298-2318.
84. Leung, C. K. Y., and Chi, J. (1995). “Crack bridging force in random ductile fiber brittle matrix composites.” J. Engg. Mech., ASCE, 121(12), 1315–1324.
85. Lewandowski, R. (1983). “Effect of different flyash qualities and quantities on the properties of concrete.” Betonwerk & Fertigteil, (1, 2, 3), 18.
86. Li, V. C., and Leung, C. K. Y. (1992). “Tensile failure modes of random discontinuous fiber reinforced brittle matrix composites.” J. Engg. Mech., ASCE, 118(11), 2246–2264.
87. Li, V. C., and Wu, H. C. (1992). “Conditions for pseudo strain-hardening in fiber reinforced brittle matrix composites.” Appl. Mech. Rev., 45(8), 390–398.

88. Li, V. C., and Wu, H. C. (1992). “Micromechanics based design for pseudo strain-hardening in cementitious composites.” Proc., 9th ASCE Conf. on Engg. Mech., L. D. Lutes and J. M. Niedzwecki, Eds., ASCE, Reston, Va., 740–743.
89. Li, V. C., Wu, H. C., and Chan, Y. W. (1996). “Effect of plasma treatment of polyethylene fibers on interface and cementitious composites properties.” J. American Ceramic Soc., 79(3), 700–704.
90. Lomboy, G., Wang, K., and Ouyang, C. (2011). “Shrinkage and Fracture Properties of Semiflowable Self-Consolidating Concrete.” J. Mater. Civil Engineering- Energy Efficient and Environmentally Friendly Paving Materials, 23, Special Issue, 1514-1524.
91. Low, N.M.P., and Beaudoin, J. J. (1992). “Mechanical properties of high performance cement binders reinforced with Wollastonite micro-fibres.” Cement and Concrete Research, 22(5), 981-989.
92. Low, N.M.P., and Beaudoin, J.J. (1993). “The effect of Wollastonite micro-fibre aspect ratio on reinforcement of portland cement-based binders.” Cement and Concrete Research, 23, 1467-1479.
93. Mac Donald, K.A., and Lukkarila, M.R. (2002). “Impact of production and proportioning on microstructure and properties of self compacting concrete.” First North American Conference on the Design and Use of Self Consolidating Concrete, USA, 15-19.
94. Massazza, F. (1993). “Pozzolanic Cements.” Cement & Concrete Composites, 15, 185-214.
95. Madasamy, C., Harik, I.E., Allen, D.L. and Fleckenstein, L.J. (1999). “Laboratory testing and analysis of joints for rigid pavements.” Research Report, KTC-99-22, Kentucky Transportation Centre, College of Engineering, University of Kentucky, Lexington, Kentucky.
96. Maeyama, A., Maruyama, K., Midorikawa, T., and Skata, N. (1998). “Characterization of powder for self compacting concrete.” Proceedings of the international workshop on self compacting concrete, Kochi, 191-200.
97. Mahesh, Y.V.S.S.U., and Santhanam, M. (2004). “Simple test methods to characterize the rheology of self compacting concrete.” The Indian Concrete Journal, 78 (6), 39-43.
98. Makishima, O., Tanaka, H., Itoh, Y., Komada, K. and Satoh F. (2001). “Evaluation of mechanical properties and durability of super quality concrete.” Proceedings of the Second International Symposium on Self Compacting Concrete., Tokyo, Japan, October, 475-482.

99. Malhotra, V.M. (2000). “Role of supplementary cementing materials in reducing green house gas emissions.” Concrete Technology for a Sustainiable Development in the 21st Century, Edited by Gjorv, O.E., and Sakai, K.E. & F.N. Spon, New York.
100. Marquardt, I., Vala J., and Diederichs, U. (2001). “Optimization of self compacting concrete mixes.” Proceedings of the Second International Symposium on Self Compacting Concrete, Tokyo, Japan, October, 295-302.
101. Mathur, R., Mishra, A.K., and Goel, P. (2007). “Influence of Wollastonite on mechanical properties of concrete.” Journal of Scientific and Industrial Research, 66, 1029-1034.
102. Mehta, P.K. (1985). “Influence of Flyash characteristics on the strength of Portland-Flyash mixtures.” Cement and Concrete Research, 15(4), 669-674.
103. Mehta, P.K., and Monterio, P.J.M. (1997). “Concrete- microstructure, properties and materials.” Indian Edition, Indian Concrete Institute, Chennai.
104. Midorikawa, T., Pelova, G.I., and Walraven, J.C. (2001). “Application of the water layer model to self compacting mortar with different size distribution of fine aggregate.” Proceedings of the Second International Symposium on Self Compacting Concrete, Tokyo, Japan, 237-246.
105. Mortsell, E., and Rodum, E. (2001). “Mechanical and durability aspects of SCC for road structures.” Proceedings of the second international symposium on self compacting concrete, Tokyo, Japan, 459-468.
106. Mueller, H.S., Mechtchrine, V. and Haist, M. (2001). “Development of self compacting light weight aggregate concrete.” Proceedings of the Second International Symposium on Self Compacting Concrete, Tokyo, Japan, 737-742.
107. Murata, J., Ogihara, Y., Koshikawa, S., and Itoh, Y. (2004). “Study on water tightness of concrete.” ACI Materials Journal, 101 (2), 107-116.
108. Myers, D., Kang, T.H.K., and Ramseyer, C. (2008). “Early-age properties of polymer fibre-reinforced concrete.” Int. J. Concr. Struct. Materials, 2(1), 9–14.
109. Naaman, A. E., and Shah, S. P. (1976). “Pull-out mechanism in steel fiber-reinforced concrete.” J. Struct. Div., ASCE, 102(8), 1537–1548.
110. Nawa T., Izumi T., and Edmatsu, Y. (1998). “State of the art report on materials and design of self compacting concrete.” Proceedings of the International Workshop on Self Compacting Concrete, Kochi, 160-190.

111. Nelson, P. K., Li, V. C., and Kamada, T. (2002). “Fracture toughness of microfiber reinforced cement composites.” Journal of Materials in Civil Engineering, 14(5), 384–391.
112. Neville, A.M. (1959). “Some aspects of the strength of concrete.” Civil engineering (London), 54, Part1, Oct. 1959, 1153-1156; Part 2, Nov 1959, 1308-1310; Part3, Dec. 1959, 1435-1438.
113. Neville, A.M. (1959). “The influence of the direction of loading on the strength of concrete test cubes.” ASTM Bulletin, 239, 63-65.
114. Nezamian, A., Setunge, S., Kumar, A., & Fenwick, J. (2004). “Decision support in using fibre reinforced polymer (FRP) composites in rehabilitation of concrete bridge structures.” 1st International Conference on Innovative Materials and Technologies for Construction, Lecce, Italy.
115. Noguchi, T., and Mori, H. (1998). “State of the art report: evaluation of fresh properties of self compacting concrete in laboratory and on site.” Proceedings of the International Workshop on Self Compacting Concrete, Kochi, 97-110.
116. Noguchi, T., Tomosawa, F., Nemati, K.M., Chiaia, B.M., and Fantilli, A.P. (2009). “A practical equation for elastic modulus of concrete.” ACI Structural Journal, 106(5), 690-696.
117. Oberai, R., and Veeraragavan, A. (2013). “Rehabilitation and upgradation of an existing airfield runway pavement for operation of next generation aircrafts.” Highway Research Journal, Indian Roads Congress, 74(3), 269-288.
118. Odler, I., and Rossler, M. (1985). “Investigations on the relationship between porosity, structure and strength of hydrated portland cement pastes. I. Effect of porosity.” Cement and Concrete Research, 15(2), 320-330.
119. Odler, I., and Rossler, M. (1985). “Investigations on the relationship between porosity, structure and strength of hydrated portland cement pastes. II. Effect of pore structure.” Cement and Concrete Research, 15(2), 320-330.
120. Olek, J., and Diamond, S., (1989). “Proportioning of constant paste composition Flyash concrete mixtures” ACI Materials Journal, American Concrete Institute, 86(2), 159-166.
121. Otter, D.E., and Naaman, A.E. (1987). “Strain rate effects on the compressive properties of fiber reinforced concrete.” Proceedings of the international symposium on fiber reinforced concrete, Madras, India, 2.225-2.235.

122. Ouchi, M. (1998). “History of development and applications of self compacting concrete in Japan.” Proceedings of the International Workshop on Self Compacting Concrete, Kochi, 1-10.
123. Ozawa, K., Maekawa, K., Kunishima, M. and Okamura, H. (1989). “Development of high performance concrete based on the durability design of concrete structures.” Proceedings of the Second East Asia and Pacific Conference on Structural Engineering and Construction (EASEC-2), Chaing-Mai, 1, 445-450.
124. Paillere, A.M., and Serrano, J.J. (1978). “Use of metal fibers in lightweight aggregate concrete.” Proceedings of RILEM Symposium on Testing and Test Methods of Fiber Cement Composites, The Construction Press, Lancaster, 205-222.
125. Parra, C., Valcuende, M., and Gomez, F. (2011). “Splitting tensile strength and modulus of elasticity of self-compacting concrete.” Construction and Building Materials, 25(1), 201-207.
126. Pateriya, I.K. (2009). “Performance Evaluation of Glass Fibre Reinforced Concrete.” Civil Engineering and Construction Review, 22(10).
127. Pedersen, B., and Mortensen, E. (2001). “Characterization of fillers for SCC.” Proceedings of the Second International Symposium on Self Compacting Concrete, Tokyo, Japan, October, 257-266.
128. Pendyala, R., Mendis, P. and Patnaikuni, I. (1996). “Full range behavior of high strength concrete flexural members: comparison of ductility parameters of high and normal strength concrete members.” ACI Structural Journal, 93(1), 30-35.
129. Pareira, E.N.B., Barros, J.A.O., and Camoes, A. (2008). “Steel fiber-reinforced self-compacting concrete: experimental research and numerical simulation.” Journal of Structural Engineering, 134 (8), 1310–1321.
130. Peterssen, O. (2001). “Limestone powder as filler in self compacting concrete- Frost resistance strength and compressive strength.” Proceedings of the Second International Symposium on Self Compacting Concrete, Tokyo, Japan, 277-284.
131. Petrov, N., Khayat, K.H., and Hamou, A.T. (2001). “Effect of stability of self consolidating concrete on the distribution of steel- corrosion characteristics along experimental wall elements.” Proceedings of the Second International Symposium on Self Compacting Concrete, Tokyo, Japan, 441-450.
132. Pfyl, T., and Marti, P. (2001). “Versuche an stahlfaserverstärkten Stahlbetonelementen.” Institute for Structural Engineering, ETH Zürich, Zürich, Switzerland.

133. Pierre, P., Pleau, R., and Pigeon, M. (1999). “Mechanical properties of steel microfiber reinforced cement pastes and mortars.” Journal of Materials in Civil Engineering, 11 (4), 317-324.
134. Pradhan, B., and Bhattacharjee, B. (2007). “Role of steel and cement type on chloride induced corrosion in concrete.” ACI Materials Journal, 104 (6), 612-619.
135. Rajkumar, C., (2001). “Provisions for cement and mineral admixtures.” The Indian Concrete Journal, 105-112.
136. Ramakrishnan, R. (1993). “Recent advancement in concrete fiber composites.” Proceedings of the International Symposium on Innovative World of Concrete (ICI-IWC-93), Madras, India, 163-192.
137. Ramalingam, N., Paramasivan, P., Mansur, M.A. and Madlej, M. (2001). “Flexural behaviour of hybrid fiber reinforced cement composites containing high volume fly ash.” Seventh Canmet/ ACI international Conference on Flyash, Silica Fume, Slag and Natural Pozzolanas in Concrete. SP-199,1, Ed. V.M. Malhotra, 147-161.
138. Ramey, G. E., Moore, R. K., Parker, Jr. F. and Strickland, A.M. (1988). “Laboratory evaluation of four rapid-setting concrete patching materials.” Transp. Res. Rec., 104(1), 47-52.
139. Ransinchung, G. D., and Kumar, B. (2010). “Investigations on pastes and mortars of ordinary portland cement admixed with Wollastonite and Microsilica.” J. Mat. Civ. Engg., 22(4), 305-313.
140. Ransinchung, G.D., Kumar, B., and Kumar, V. (2009). “Assessment of water absorption and chloride ion penetration of pavement quality concrete admixed with Wollastonite and Microsilica.” International Journal of Construction & Building Materials, Elsevier, 23(2), 1168-1177.
141. Rapoport, J., Aldea, C.M., Shah S.P., Ankenman, B. and Karr, A. (2001). “Permeability of cracked steel fiber-reinforced concrete.” Technical Report National Institute of Statistical Sciences, No. 115, USA, January, 1-10.
142. Ravindrarajah, R., Siladyi, D. and Adamopoulas, B. (2003). “Development of high strength self compacting concrete with reduced segregation potential.” Proceedings of the 3rd International RILEM Symposium, Iceland, 1, 1048.
143. Reknes, K. (2001). “Particle matrix model based of self compacting concrete with lignosulfonate water reducer.” Proceedings of the Second International Symposium on Self Compacting Concrete, Tokyo, Japan, 247-256.

144. Ribeiro, A.B., and Goncalves, A. (2001). “A low cost self compacting concrete.” Proceedings of the Second International Symposium on Self Compacting Concrete, Tokyo, Japan, October, 339-348.
145. Rooney, J.M., and Bartos, P.J.M., (2001). “Development of the settlement column segregation test for fresh self compacting concrete (SCC).” Proceedings of the Second international Symposium on Self Compacting Concrete, Tokyo, Japan, 109-116.
146. Roy, D.M. (1987). “Hydration of blended cements containing slag, Flyash or Silica fume.” Proceedings of Meeting -Institute of Concrete Technology, Coventry, UK, 29.
147. Roy, D.M., and Idorn, G.M. (1992). “The effect of blast furnace slag and related materials on the hydration and durability of related concrete.” Durability of Concrete-Int. Symposium, Detroit, Michigan, ACI SP-131, 195-208.
148. Saak, A.W., Jennings, H.M. and Shah, S.P. (2001). “New methodology for designing self compacting concrete.” ACI Materials Journal, 98(6), 429-439.
149. Saje, D., Bandelj, B., Sustersic, J., Lopatic, J. and Saje, F. (2011). “Shrinkage of polypropylene fiber-reinforced high-performance concrete.” Journal of Materials in Civil Engineering, 23(7), 941–952.
150. Sasturkar, P.J., and Kaushik, S.K. (1994). “Flexural behavior of fiber reinforced concrete beams.” Proceedings of the National Seminar on Fiber Reinforced Cementitious Products, 177-183.
151. Schmidt, M., and Fehling, E. (2005). “Ultra-high-performance concrete: Research, development and application in Europe.” Proc., 7th Int. Symp. on Utilization of High-Strength/ High Performance Concrete, Washington D.C., 1, 51-77.
152. Scrivener, K.L., Bentur, A., and Pratt, P.L. (1988). “Quantitative characterization of the transition zone in high strength concretes.” Advances in Cement Research, 1(4), 230-7.
153. Scrivener, K.L., and Gariner, E.M. (1988). “Microstructural gradients in cement paste around aggregate particles.” Materials Research Symposium Proceedings, 114, 77-85.
154. Shah S,P, and Naaman, A.E.. (1976). “Mechanical properties of glass and steel fiber reinforced mortar.” ACI Journal, 73(1), January, 50-53.
155. Sellevold, E.J. (1992) “Shrinkage of concrete: effect of binder composition and aggregate volume fraction from 0 to 60%.” Nordic concrete Research, The Nordic Concrete Federation, Oslo Publication, 11, 139-152.
156. Singh, G., and Madan, S.K. (1994). “Shear resistance of steel fiber reinforced concrete.” Proceedings of the National Seminar on Fiber Reinforced Cementitious Products, Roorkee, India, 15-23.

157. Singhal, D., Gupta, V.K., Kumar, V., and Nautiyal, B.D. (1994). “Ductility of steel fiber concrete beams with equal conventional reinforcement on both faces.” Proceedings of the National Seminar on Fiber Reinforced Cementitious Products, Roorkee, India, January, 57-62.
158. Skarp, U., Engstrand, J. and Jasson, I. (2002). “A concept for enhancing early strength development in self consolidating and normal concrete by means of increased stability and homogeneity.” First North American Conference on the Design and Use of Self Consolidating Concrete, USA, 325-330.
159. Smith, F.L. (1958). “Effect of aggregate quality on resistance of concrete to abrasion.” ASTM Sp. Tech. Publication, 205, 91-105.
160. Soliman, A.M., and Nehdi, M.L. (2012). “Effect of natural Wollastonite microfibers on early-age behavior of UHPC”, Journal of Materials in Civil Engineering, 24(7), 816–824.
161. Song, H.W., Byun, K.J., Kim, S.H., and Choi, D.H. (2001). “Early age creep and shrinkage in self compacting concrete incorporating GGBFS.” Proceedings of the Second International Symposium on self Compacting Concrete, Tokyo, Japan, 413-422.
162. Sorelli, L., Davila, R., Ulm, F.J., Perry, V. and Seibert, P. (2008). “Risk analysis of early-age cracking in UHPC structures.” Proc., 2nd Int. Symp. on UHPC, Germany, 331-338.
163. Subsompon, W. (1997). “Development of Performance-Based Specifications for Pavement Overlays.” Chulalongkorn University Journal of Engineering, 12(2), 13-18.
164. Swamy, R. N., and Stavrides, H. (1979). “Influence of fibre reinforcement on restrained shrinkage and cracking.” J. of American Concrete Inst., 76(3), 443–460.
165. Tayebali, A. A., Malpass, G. A., & Khosla, N. P. (1998). “Effect of mineral filler type and amount on design and performance of asphalt concrete mixtures.” Superpave: Binder Specifications, Mixture Design and Construction, Transportation Research Record, Washington, D.C., 1609, 36-43.
166. Termkhajornkit P., Nawa T., and Ohnuma, H. (2002). “Role of flyash and naphthalene sulphonate superplasticizer on fluidity of paste.” First North American Conference on the Design and Use of Self Consolidating Concrete, USA, November, 43-47.
167. Thomas, M.D.A., Shehata, M.H., Shashiprakash, S.G., Hopkins, D.S. and Cailb, K. (1999). “Use of ternary cementitious systems containing silica fume and Flyash in concrete.” Cement and Concrete Research, 29, 1207–1214.

168. Tikalsky, P., and Carasquillo, R.L. (1991). “Flyash evaluation and selection for use in sulphate resistant concrete.” ACI Materials Journal, 90 (6), 545-51.
169. Turcry, P., Loukili, A., Haidar, K., Pijaudier-Cabot, G., and Belarbi, A. (2006). “Cracking tendency of self-compacting concrete subjected to restrained shrinkage: experimental study and modeling.” Journal of Materials in Civil Engineering, 18(1), 46–54.
170. Vaysburd, A.M., Emmons, P.H., and Sabnis, G.M. (1997). “Minimising cracking- the key to durable concrete repairs.” The Indian concrete journal, 71, (12), 652-658.
171. Vengala, J., Sudarshan, M.S., and Ranganath, R.V.(2003). “Experimental study for obtaining self compacting concrete.” The Indian concrete journal, 1261-1266.
172. Verbeck, G.J. (1955). “Hardened concrete-pore structure.” ASTM Sp. Tech. Publication, 169, 136-142.
173. Wesche, K. (Ed.) (1991). “Flyash in concrete.” RILEM report of technical committee 67-FAB, section 3.2.5 by J. Bijen, 103, E & FN Spon, London.
174. Wittman, F.H. (1976) “On the action of capillary pressure”, Cement and Concrete Research, 6(1), 49-56.
175. Whiting, D. (1998). “Permeability of selected concretes.” Permeability of Concrete, ACI SP-108, Detroit, Michigan, pp. 195-221.
176. Wu, H. C., and Li, V. C. (1995). “Stochastic process of multiple cracking in discontinuous random fiber reinforced brittle matrix composites.” Int. J. Damage Mech., 1(4), 83–102.
177. Wu, H.C. (2001). “Discussion on mechanical properties of steel microfiber reinforced cement pastes and mortars.” Journal of Materials in Civil Engineering, 13(3), 240 -241.
178. Xie, Y., Liu, B., Yin, J., and Zhou, S. (2002). “Optimum mix parameters of high-strength self-compacting concrete with ultra-pulverized Flyash.” Cement and Concrete Research, 32(3), 477–480.
179. Zhu, W., and Bartos, P.J.M. (2003). “Permeation properties of self-compacting concrete.” Cement and Concrete Research, 33(6), 921–926.
180. Zhu, W., Quinn, J. and Bartos, P.J.M. (2001). “Transport properties and durability of self compacting concrete.” Proceedings of the Second International Symposium on Self Compacting Concrete, Tokyo, Japan, 451-458.
181. Zollo, R. F. (1984). “Collated fibrillated polypropylene fibres in Fibre Reinforced Concrete.”, American Concrete Institute, Detroit, ACI SP-81, 397–409.

182. Zollo, R. F., Ilter, J. A., and Bouchacourt, G. B. (1986). “Plastic and drying shrinkage in concrete containing collated fibrillated polypropylene fibres.” 3rd Int. Symp. on Developments in Fibre, 86(1), RILEM Technical Committee 49-TFR, Cachan, France.
183. Zongjin, L. (2011). “Advanced concrete technology.” J. Wiley& Sons Inc., Hoboken, New Jersey.

****